ANALYTICA CHIMICA ACTA
Vol. 71 (1974)

ANALYTICA CHIMICA ACTA

International monthly devoted to all branches of analytical chemistry
Revue mensuelle internationale consacrée à tous les domaines de la chimie analytique
Internationale Monatsschrift für alle Gebiete der analytischen Chemie

ELSEVIER SCIENTIFIC PUBLISHING COMPANY
AMSTERDAM

Anal. Chim. Acta, Vol. 71 (1974)

PRINTED IN THE NETHERLANDS

Analytica Chimica Acta, 71 (1974) 1–16

A COMPUTER-BASED STUDY OF THE EFFECT OF pH AND TEMPERATURE ON THE ELECTRONIC ABSORPTION SPECTRA OF ACID–BASE INDICATOR SOLUTIONS

TREVOR R. GRIFFITHS and PHILIP J. POTTS*

Department of Inorganic and Structural Chemistry, The University, Leeds LS2 9JT (England)

(Received 2nd January 1974)

Aqueous solutions of acid-base indicators are usually considered to exist as an equilibrium between two species, an acid form and a basic form. Such equilibria are shifted by changing the hydrogen ion concentration (pH) of the solution. However, few reports have described the effect of temperature on the spectra of indicator solutions[1]. A study was therefore undertaken to determine the effect of changes in both pH and temperature on the spectra of some common acid–base indicator solutions. The spectra of such solutions usually exhibit one or more isosbestic points and their presence is commonly taken as evidence for a two-species equilibrium. It has been shown that this conclusion is not always valid[2,3], and that a linear relationship between the spectra should be established at all wavelengths over the wavelength range where the two species absorb[3]. Brynestad *et al.*[4] described this as a test for internal linearity relationships between spectra, and while normally time-consuming, it is readily performed in a computer. These workers examined a two-species equilibrium, at constant temperature, in a molten salt system, as a function of composition; we have applied their test as a function of pH and of temperature. Several other parameters can influence equilibria, including pressure and time, and these effects may also be monitored by this technique.

The application of computer techniques to spectra is a currently popular topic and several books and reviews have been written[5,6]. However, the term spectra has been confined almost exclusively to mass spectrometry and infrared spectra; electronic spectra have received little attention. Further, the available papers on this topic do not contain sufficient information for other workers to be able to reproduce reported techniques and computer programmes without considerable difficulty and wasteful employment of computer and research time. In this paper, the techniques used, and their applications and limitations, are described in some detail, so that their possibilities in other fields may be appraised.

EXPERIMENTAL

Stock solutions of sodium hydroxide and hydrochloric acid (both 0.01 *M*) were prepared by diluting accurately standard solutions (0.1 *M*; B.D.H.). Stock

* Present address: Department of Earth Sciences, The Open University, Walton Hall, Milton Keynes, Bucks. MK7 6AA, England.

solutions of the indicators methyl red, methyl orange and phenolphthalein, dissolved in alcohol, were used as supplied (B.D.H.; 0.01%, 0.04% and 1% (w/v), respectively). Solutions of potassium nitrate or chloride (0.1 *M*; Fisons, analytical grade reagent) were used to maintain the ionic strength of the indicator solutions constant.

Sample and reference solutions were prepared by mixing the ionic background solution of potassium nitrate or chloride (5 ml pipetted) and sodium hydroxide (appropriate volume, 0.01 *M* from a 10-ml microburette) in 10-ml graduated flasks. A suitable volume of indicator solution (maximum 0.25 ml) was added to the sample solution only and the solutions were made up to 10 ml with distilled water.

Spectra were recorded on an Applied Physics Cary 14H spectrophotometer in 1-cm cells. The effect of pH changes on the spectra of indicator solutions was measured by adding all the 10 ml of sample solution to a dry 1-cm cell with a 25-cm neck attached[7]. In this way, the initial volume of solution was known and dilution factors could be accurately calculated. Spectra were recorded relative to air as reference, after aliquots of hydrochloric acid solution had been added dropwise from a 5-ml microburette. Solutions were shaken thoroughly and allowed to equilibrate for 2 min. The heat of neutralization was detected even at the high dilutions employed; temperature rises in the sample solutions, typically 2–3°C, were observed during the titration.

Temperature effects were measured by studying solutions contained in 1-cm stoppered cells. Thermostatted water was circulated around the sample cell and an identical reference cell containing solvent in the reference beam, over the temperature range 15–75°C (within ± 0.5°C).

Digitization of spectra

Digitization may be described as the process by which a physically continuous function, such as an absorption spectrum, is transformed into an array of numbers which represents accurately the original function. A spectrum is most simply digitized by recording both the absorbance and the wavelength (or wavenumber as appropriate) at suitable, though not necessarily equal, intervals of wavelength; each digitized point is thus accurately defined on the ordinate and abscissa. The digitizing process may be related to the gradient of the spectrum: the larger the gradient, the closer the wavelength interval of digitization. In this way, any sharp discontinuities in a spectrum are recorded accurately.

A more useful procedure is to digitize a spectrum at equal intervals of wavelength. The bulk of data required to represent a spectrum is then approximately halved, as the wavelength corresponding to every digitized absorbance need not be stored. If the initial wavelength of digitization, the wavelength interval, and the total number of digitized absorbances are all known, the wavelength corresponding to any sequentially digitized absorbance can be calculated. (Unfortunately, this method can be prone to error because, should one absorbance be missed during the digitizing process, the following digitized absorbances will be offset by one wavelength interval.) Perhaps the most important advantage of digitizing spectra at equal wavelength intervals is the simplicity with which a variety of mathematical procedures may then be applied to such data.

Various systems for digitizing spectra have been described[2, 3, 8–11]. At the present time, there is an emphasis on real-time computer utilization. This is expensive

and the user is rarely able to monitor the recording process. The data are generally only suitable for Fourier transformations or for re-plotting on preferred sizes and types of ordinates and abscissae; they are not readily suitable for the procedures used here to produce chemical information. Here, spectra are digitized at suitable equal wavelength intervals, and recorded automatically on paper-tape, which is subsequently edited as necessary. Instrumental details of the system will be published elsewhere.

Some of the research described here, and to be presented in subsequent papers, was commenced before the above digitizing equipment was fully operational. Some spectra were therefore digitized by hand, absorbance values being read off chart-paper at 5-nm intervals and transposed on to paper-tape. Most of the computer programmes were tested, corrected and developed with such spectra. Nevertheless, the chemical information that emerges is most valuable; the hand digitizing process, while somewhat tedious, is not particularly time-consuming if applied correctly to selected spectra. However, some of the techniques described here are better suited to less than 5-nm sampling intervals and automatic digitizing is therefore recommended wherever possible.

ISOSBESTIC POINTS

The theory of the origins of isosbestic points in a set of spectra, and the chemical conclusions that may be drawn from their presence, have been considered by several groups of workers[2–4, 12–23]. A simplified summary of the nature of those systems which give rise to isosbestic points is outlined below.

(a) Unequivocal conclusions may not be drawn from spectra in which isosbestic points are observed without first examining internal linearity relationships between spectra.

(b) Provided that the spectra of component species are invariant with respect to the external parameter, the concentrations of absorbing species from an internally linear system are linearly related to a single reaction parameter, which may be, for example, pH, temperature, pressure, *etc.* Usually this dependence means that a two-species equilibrium exists within the system. In other cases, changes in spectra can frequently be interpreted in terms of a pseudo-two-species equilibrium. However, additional chemical evidence is always required before a definite interpretation can be proposed.

(c) Great care is required in interpreting internally linear spectra recorded at different temperatures. The spectra of component species are not usually invariant with respect to temperature changes. However, it will be shown, in a later section, that over limited ranges, internally linear spectra can be recorded for a system in which the equilibrium between two species is shifted by changes in temperature. Similar studies have produced this phenomenon[15, 24]. Other experimental studies suggest that internal linearity relationships can result from the effect of temperature on the spectrum of a single absorbing species[2, 4, 25]. Independent chemical evidence is thus required to characterize the system under study.

INTERNAL LINEARITY FUNCTIONS: MATHEMATICAL REPRESENTATION

Two procedures have been proposed for establishing internal linearity rela-

tionships between a set of spectra. The first, formalized mathematically by Chylewski[23], involves plotting the absorbances, at any two wavelengths in a set of spectra, against each other. Internally linear spectra show a linear dependence in such plots. A more rigorous procedure has been briefly described by Brynestad *et al.*[4]. The relationships between spectra are determined over as large a wavelength range as possible. Any one spectrum in an internally linear set is a linear combination of any two other spectra from that set. This may be expressed mathematically by the equation

$$\varepsilon_3 = (1-\beta)\varepsilon_1 + \beta\varepsilon_2 \tag{1}$$

which is valid at any wavelength in the internally linear range. ε_1, ε_2, and ε_3 are the formal absorbances of the three spectra at any given wavelength; β is the constant of internal linearity relative to the spectra ε_1 and ε_2. The formal absorbance is calculated relative to the total concentration of absorbing species, and β is a monotonous function[3,4] of the external parameters at which the three spectra were recorded; β is independent of wavelength. Stylized spectra of a typical internally linear system are shown in Fig. 1.

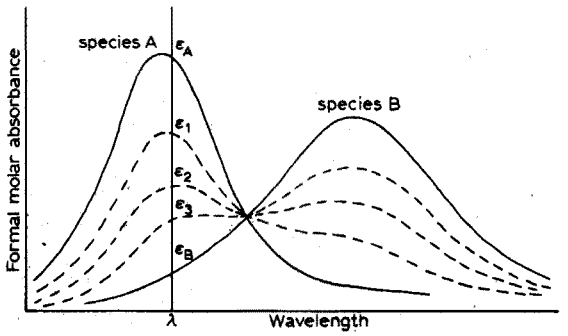

Fig. 1. Internally linear spectra of a stylized two-species equilibrium. The terminal spectra of A and B are shown with three spectra of an equilibrium mixture, A⇌B, where [A]+[B]=constant, nominally recorded at three different values of the external parameter that influences the position of the equlibrium.

The symbol β is an abbreviation of $\beta_{(3,2,1)}$, which specifies the order in which spectra appear in eqn. (1). For reasons which will become apparent, the spectra represented by ε_1 and ε_2 in eqn. (1) are termed the reference spectra. Rearrangement of eqn. (1) gives

$$(\varepsilon_3 - \varepsilon_1) = \beta(\varepsilon_2 - \varepsilon_1) \tag{2}$$

This expression defines the statement of internal linearity given by McKay and Scargill[19], that the difference spectra of an internally linear set are identical apart from scaling factors (β).

A computer programme has been developed to determine internal linearity relationships between sets of spectra. A set of three digitized spectra is first read by the programme and checked for compatibility. The constant of internal linearity (β) is computed at each digitized wavelength from

$$\beta_\lambda = (\varepsilon_3 - \varepsilon_1)/(\varepsilon_2 - \varepsilon_1) \tag{3}$$

The computer then attempts to calculate an average value ($\bar{\beta}$) from the array of β_λ values determined at each wavelength. If a meaningful $\bar{\beta}$ is found, the deviation (Δ_λ) from ideal linearity ($\Delta_\lambda \rightarrow 0$) is computed at each wavelength from

$$\Delta_\lambda = (1-\bar{\beta})\varepsilon_1 + \bar{\beta}\varepsilon_2 - \varepsilon_3 \quad (4)$$

A plot of this deviation against wavelength will establish to what degree, and over what wavelength range, the set of spectra can be considered internally linear. Examples of Δ functions for indicator solutions will be discussed later.

RESULTS AND DISCUSSION

Spectrophotometric titration curves

One aspect of the effect of pH on the spectra of methyl red, methyl orange and phenolphthalein is shown in Fig. 2. The absorbance at the wavelength maximum of the basic or acidic forms of these indicators follows a spectrophotometric titration curve as the concentration of 0.01 *M* hydrochloric acid is increased.

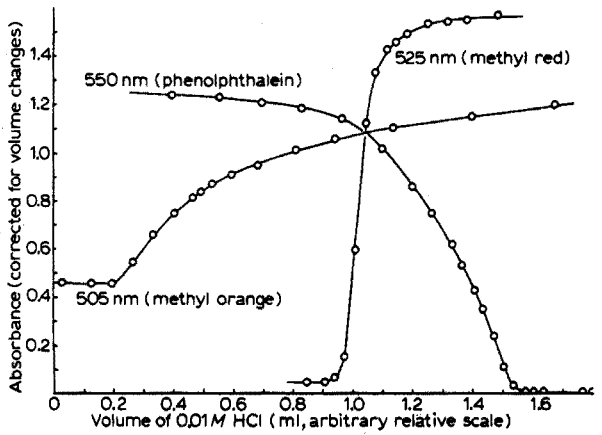

Fig. 2. Effect of pH on indicator solutions. Variation of absorbance, with HCl increase, at the peak maximum of the acid form of methyl red (A, $\lambda_{max} = 525$ nm), methyl orange (B, $\lambda_{max} = 505$ nm) and of the basic form of phenolphthalein (C, $\lambda_{max} = 550$ nm).

Phenolphthalein is not a simple indicator, several ionic species appearing in solution as the pH is increased in the range 8.3–10.0 (ref. 1). It was not possible to add sufficient 0.01 *M* acid to convert methyl orange entirely into its orange-red acidic form, which is found in solutions of pH below 3.1. Methyl red changes colour from red to yellow as the pH is increased from 4.2 to 6.3; the titration curve of this indicator clearly demonstrates that this material is most suited to further spectrophotometric study with 0.01 *M* reagents.

Methyl red—pH effects

The effect of pH on the spectrum of an aqueous solution of methyl red in a background solution of potassium nitrate or chloride is illustrated in Fig. 3. The two sets of data are presented in order to identify all the spectra used in the subsequent computations, as the pH of most of the spectrophotometric solutions was not

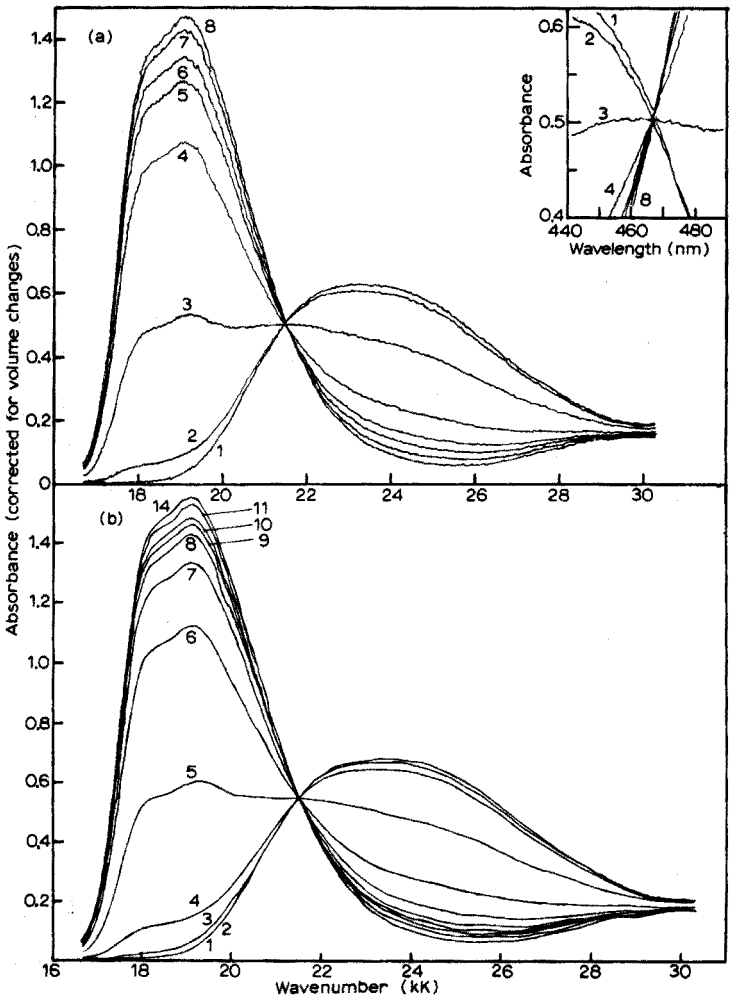

Fig. 3. (a) Spectrum of methyl red (solution A) in KCl solution (0.05 *M*) containing NaOH (0.009 *M*), and after the addition of aliquots of HCl (0.01 *M*). Digital sampling interval 1 nm, recorded automatically. Curves drawn on graph-plotter, connecting each data point by a straight line. Spectra: (1) 0.0, (2) 0.102, (3) 0.139, (4) 0.173, (5) 0.209, (6) 0.242, (7) 0.333 and (8) 0.602 ml HCl added. Insert: spectra as recorded on chart-paper.

(b) Spectrum of methyl red (solution B) in KNO_3 solution (0.1 *M*) containing NaOH (0.0095 *M*), and after the addition of aliquots of HCl (0.01 *M*). Digital sampling interval 5 nm, transposed manually from chart-paper. Curves drawn on graph-plotter after the data had been smoothed by a 5-point convolute. Spectra: (1) 0.0, (2) 0.061, (3) 0.092, (4) 0.129, (5) 0.161, (6) 0.199, (7) 0.231, (8) 0.266, (9) 0.300, (10) 0.337, (11) 0.403 and (14) 0.638 ml HCl added.

measured, for to do so would result in the introduction of small and unknown amounts of water, thereby affecting concentrations. At low pH, the acid species forms an intense red solution with a principal absorption maximum at about 19.0 kK (525 nm). The paler yellow basic form has a spectrum with a broad maximum centred at 23.3 kK (430 nm). In the pH range 4.2–6.3, rapid changes occur, absor-

bances of one form increasing in intensity at the expense of absorbances of the other. A well defined isosbestic point is observed at 21.4 kK (467 nm).

The effect of such pH changes may be interpreted *a priori*, as resulting from a shift in an equilibrium between two species only, the red acid form and the yellow basic form of methyl red. Further evidence to support this proposition may be obtained from an internal linearity analysis of the spectra.

Internal linearity analysis—pH effects

A graphical analysis, based on the method of Chylewski[23], is shown in Fig. 4. The absorbance at 430 nm, the maximum of the basic species, is plotted against the absorbance at 525 nm for the acid species, from the data plotted in Fig. 3b. Over most of the pH range the plot is linear and of negative slope. The small deviations at the ends of the line are real and will be considered in the next section. A more detailed investigation of the relationships between these spectra requires an analysis of internal linearity functions between sets of spectra over the entire range of wavelengths.

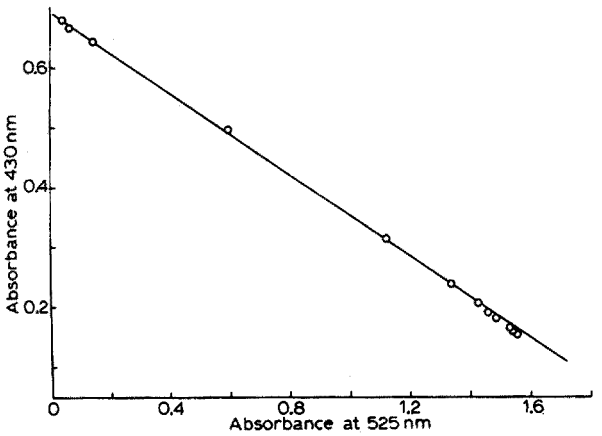

Fig. 4. Graphical analysis, after Chylewski[23], for internal linearity for methyl red spectra (from Fig. 3b). Variation of absorbance of basic form (at 430 nm) with that of acidic form (at 525 nm).

Two runs, A and B, recording the effect of pH on the spectrum of methyl red, were digitized automatically at 1-nm intervals (Fig. 3a) and by hand at 5-nm intervals (Fig. 3b). Internal linearity constants were computed for both sets of spectra to determine the accuracy with which the spectra conformed to internal linearity. A comparison was made between analyses of spectra digitized at 1- and 5-nm intervals. The effect of correcting spectra for volume changes resulting from the titration was also examined. The internal linearity analyses of the automatic and hand digitized spectra are given in Tables I and II, respectively; the quantities listed require some explanation.

In Table I, the spectra numbered 2 and 4 (Fig. 3a) were chosen as reference spectra and the *Order of spectra* refers to the order in which spectra were used to calculate the internal linearity constant. Thus $\beta_n = \beta_{n,4,2} = (\varepsilon_n - \varepsilon_2)/(\varepsilon_4 - \varepsilon_2)$ at any wavelength. The internal linearity programme attempts to average the β_λ values

TABLE I

INTERNAL LINEARITY ANALYSIS: EFFECT OF pH CHANGE ON METHYL RED SOLUTION A

(Total no. of digitized points, 271; temperature, 20°C; ionic strength, 0.05 *M* KCl.)

Order of spectra[a]			β_n	*R.m.s. deviation*		*Rejected points*		*R.m.s. deviation* Δ*(absorbance)*
n	*Reference*			*From* β_n	*% of* β_n	*Threshold*[b]	*Total*	
1	4	2	−0.059	0.003	4.6	139	166	0.002
2	4	2	0.0	—	—	—	—	—
3	4	2	0.443	0.007	1.5	24	92	0.005
4	4	2	1.0	—	—	—	—	—
5	4	2	1.207	0.013	1.1	3	30	0.007
6	4	2	1.290	0.019	1.5	3	37	0.011
7	4	2	1.374	0.026	1.9	3	51	0.016
8	4	2	1.426	0.044	3.1	3	56	0.026
Mean[c] volume corrected				0.018	2.3	29	72	0.011
Mean volume uncorrected[d]				0.022	4.4	24	73	0.016

[a] Numbers refer to Fig. 3(a); spectra digitized at 1-nm intervals; absorbances corrected for dilution effects.
[b] Threshold differences between spectra: 0.02 absorbance units.
[c] Mean parameters from above 8 analyses.
[d] Mean of analyses identical to [c] but uncorrected for dilution effects.

TABLE II

INTERNAL LINEARITY ANALYSIS: EFFECT OF pH CHANGE ON METHYL RED SOLUTION B

(Total no. of digitized points, 55; temperature, 20°C; ionic strength, 0.1 *M* KNO_3)

Order of spectra [a]			β_n	*R.m.s. deviation*		*Rejected points*		*R.m.s. deviation*
n	*Reference*			*From* β_n	*% of* β_n	*Threshold*[b]	*Total*	
1	6	5	−1.016	0.041	4.0	3	16	0.015
2	6	5	−1.001	0.046	4.6	3	17	0.018
3	6	5	−0.964	0.047	4.8	3	17	0.018
4	6	5	−0.827	0.035	4.3	4	14	0.012
5	6	5	0.0	—	—	–	—	—
6	6	5	1.0	—	—	–	—	—
7	6	5	1.414	0.019	1.4	1	11	0.005
8	6	5	1.591	0.022	1.4	1	14	0.007
9	6	5	1.668	0.024	1.5	1	13	0.008
10	6	5	1.722	0.032	1.8	1	8	0.010
11	6	5	1.796	0.040	2.2	1	13	0.012
14	6	5	1.871	0.056	3.0	1	11	0.018
Mean[c]				0.036		2	13	0.012

[a] Numbers refer to Fig. 3(b); spectra digitized at 5-nm intervals; absorbances corrected for dilution effects.
[b] Threshold differences between spectra: 0.01 absorbance units.
[c] Mean parameters from above 12 analyses.

calculated at each wavelength from a group of three spectra, as indicated earlier, but if the differences between spectra at any wavelength are less than a threshold value, the corresponding value β_λ is considered to be insufficiently accurate to warrant further averaging, and is rejected.

Other β_λ values are rejected if they lie outside a range defined about a preliminary averaged β_n value, determined as follows. A value of $\bar{\beta}$ is calculated for the data points remaining after passing the threshold value "gate" and its r.m.s. (root mean square) deviation value is also found. Any β_λ value then lying outside the range $\bar{\beta} \pm$ r.m.s.$(\bar{\beta})$ is rejected and from the remaining data the mean β_n is determined, together with its r.m.s. deviation. The numbers of points rejected on the threshold criterion and the total number rejected are given in the Tables.

The root mean square deviation from β_n, calculated at all digitized wavelengths not rejected, is listed next to the appropriate value of β_n. This deviation has also been computed as a percentage of β_n. Clearly, the number of rejected points will affect the r.m.s. deviation from β_n. The intention of the rejection "gate" is to eliminate spurious values of β_λ, which were found when the absorbance was excessively noisy and where the differences between spectra were small. To include these β_λ values leads to an unrepresentative mean value of β_n and an excessively large r.m.s. deviation from internal linearity (Δ), calculated from eqn. (4). Δ was computed over all digitized wavelengths, whether or not they were rejected in the averaging process. The computed Δ-function was not observed to be offset from a mean value of zero (Fig. 5) and it is therefore concluded that a representative mean β_n is calculated by the averaging procedure.

Criteria for internal linearity

The experimental uncertainty in absorbances recorded on the Cary 14H

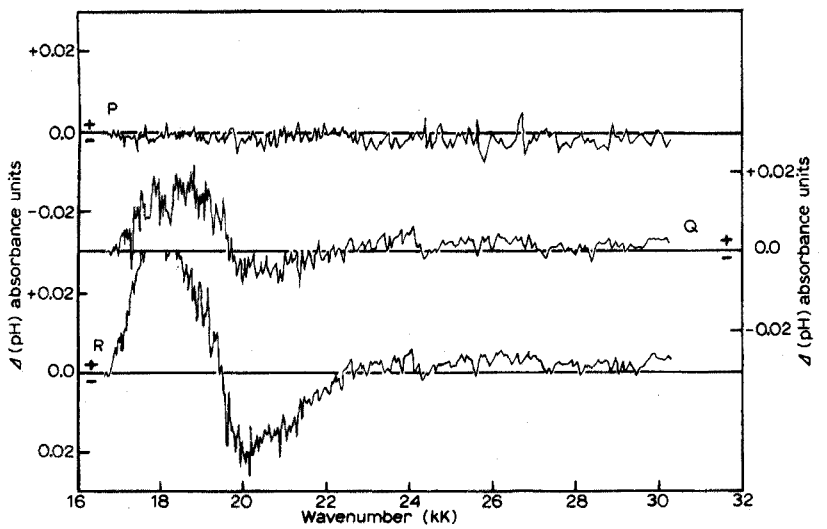

Fig. 5. Wavenumber dependence of internal linearity function Δ, for sets of pH-dependent spectra defined in Fig. 3a. P, Q and R Δ-functions computed from $\Delta = \{[(1-\beta_n)\varepsilon_2] + \beta_n\varepsilon_4 - \varepsilon_n\}$, where n represents the spectra 1, 5 and 7, respectively. The r.m.s. deviations of Δ are 0.002 (P), 0.006 (Q) and 0.016 (R).

spectrophotometer is ± 0.003 units. Comparison of this figure with the deviations listed in Tables I and II indicates that experimental noise in a group of three internally linear spectra may cause r.m.s. deviations in Δ of up to 0.015 absorbance units or its molar equivalent. This deviation is independent of the maximum molar absorbance of the spectra, contrary to ref. (4). The largest values of Δ occur in those regions of the spectra where the absorbance is changing rapidly; an increase in the number of data points taken in these regions, or a very slow scan speed, would ameliorate this effect. Also, if variations of less than 2% are obtained for the r.m.s. deviations from β_n, for a reasonable number of groups of three spectra from a set, then the entire set is considered to be internally linear. These criteria appear to be more useful than those proposed by Brynestad *et al.*[4].

The analyses for the sets of data digitized at both 1-nm and 5-nm wavelength intervals show that these sets of spectra are internally linear over almost all the pH range studied. Root mean square deviations of both β_n and Δ lie within the above-mentioned limit of 2% and 0.015 absorbance units, respectively, for many of the groups of spectra analysed in the Tables. The wavenumber dependence of the Δ-function for three sets of spectra taken from Fig. 3a and analysed in Table I is plotted in Fig. 5. No systematic drift away from $\Delta = 0$ can be detected in these plots and deviations from Δ are in accord with the r.m.s. value calculated in Table I.

Larger deviations from internal linearity than those just specifed can be seen in Tables I and II and Fig. 5, particularly for analyses of groups including a spectrum recorded at high pH (*e.g.*, Table I, set 1; Table II, sets 1, 2, 3 and 4). These analyses involve a spectrum consisting largely of the basic species of methyl red. This will be discussed in a later section in terms of a breakdown in the two-species equilibrium at high pH.

The slightly larger deviations calculated from groups of spectra which include one recorded at low pH (*e.g.*, Table I set 8; Table II, sets 11 and 14), may be attributed to a long extrapolation of the differences in absorbance between these spectra and the reference spectra. A small error in the dilution factor may have the same result.

Before these internal linearity analyses are related to the chemistry of the system, a further piece of evidence must be considered. A close inspection of the isosbestic point formed at 21.4 kK (Fig. 3) shows that this is a common crossing point for all spectra except those recorded at high pH. This small discrepancy is magnified in the insert to Fig. 3. Three attempts were made at recording the spectra of these pH titrations: in each case, the phenomenon just described was reproduced.

It may be concluded from this isosbestic point evidence, and the larger deviations from internal linearity noted earlier, that, in the context of this sytem, the spectra recorded at high pH are not internally linear with the remaining spectra analysed in Tables I and II. The implications of this conclusion for methyl red indicator solutions are considered below.

The ionization of methyl red solutions

The simple theory of acid–base indicators postulates that the acid form of the indicator is ionized to a basic species as the pH of the solution is increased. This is an over-simplification. Indicators generally exist in two or more tautomeric forms, each having a different colour[26]. One species is usually a non-electrolyte (pseudo-acid or pseudo-base), the other forms being the acid or basic species.

Methyl red is the sodium salt of 2-[4-(dimethylamine)phenylazo]-benzoic acid. Walton[1] has discussed some aspects of the ionization of azo indicators and, by analogy with the equilibria reported for the related indicator methyl orange[27], three structures are here proposed for methyl red.

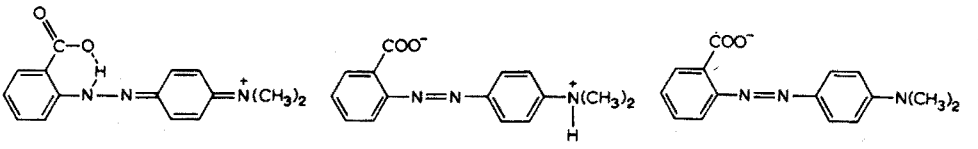

I acid form (red) II pseudo-acid form (yellow) III basic form (yellow)

At low pH the indicator exists in the red acid form (I) which changes to the yellow basic species (III). However, this species has two sites at which protonation can occur and at intermediate values of pH, significant proportions of the pseudo-acid species (II) can be formed in solution. Nevertheless, species (I) is the most stable acid form because in this complex the added proton is stabilized by the adjacent carboxylic group, a six-membered ring being formed.

The electron conjugation in species (II) and (III) is similar, with little difference in the length of the delocalized π-bonds. Thus species (II) will be yellow and is expected to have a spectral profile very similar to that of structure (III).

The spectral changes observed in this study may be explained by assuming that, at high pH, only species (III) is present in solution. However, as the hydrogen ion concentration of such a solution is increased, protonation can, and does, occur at both available sites in the methyl red molecule. Over the pH range around the titration end-point, significant proportions of all three species are present in solution. The concentration of the intermediate species (II) is always low and in constant proportion with the concentration of the other yellow form (III). The equilibrium is effectively a pseudo-two-species equilibrium.

Internal linearity breaks down at high pH when the spectral concentration of species (I) falls to zero. Subsequent increases in pH cause a change in the constant ratio between species (II) and (III) as methyl red is then progressively ionized to (III). Spectra recorded at these high pH values are not internally linear with those from the lower pH range, because the concentrations of species (II) and (III) are no longer in the same constant proportion as they were when species (I) was present in solution. However, only small discrepancies are detected in the spectra because the concentration of species (II) is low and it has a very similar absorption profile to species (III). Without computer-based interval linearity checks, the experimental measured, for to do so would result in the introduction of small and unknown findings, including deviations from the isosbestic point, would probably have been ascribed to experimental error and an entirely different chemical explanation proposed.

Small changes in the relative concentrations of species (II) and (III) may occur in the lower pH range but, because this only causes a small difference in their combined spectrum compared with changes caused by pH, only a small decrease in the accuracy of the internal linearity function, *i.e.* a small increase in the associated r.m.s. value, will result from this discrepancy.

Further findings from computed data

No direct comparison can be made between the analyses of spectra digitized at 1-nm and 5-nm intervals, as there is no correlation between their respective pH values. However, overall, there is little significant difference between the deviations of β_n and Δ computed from the two sets of data, and thus it may be concluded that manually digitized data have yielded a profitable return for the effort involved.

As might be expected, mean deviations for spectra which have been corrected for small volume changes are significantly smaller than those for the same data which were not so corrected (Table I). It is thus essential to make these corrections, and this may readily be performed on digitized spectra before re-drawing on a graph-plotter. The noise that is inherent in all spectroscopic measurements may also be reduced before re-drawing. The simple moving average of Savitzky and Golay[28] was used to convolute the spectral data. This involves multiplying a sequential set of 5, 7, 9... data points by a corresponding number of convolution coefficients*. The sum of this set of products is divided by a normalizing factor. The result is an exact, least squares-fitted, smoothed value of the central data point of the set. By continually moving the data set on by one point, the whole spectrum may be smoothed. Care must however be exercised in choosing the size of the sequential set; the size must be small if the number of points describing any peak in the spectral profile is small. Figure 3b shows the effect of a 5-data point convolute on the spectra. Figure 3a has all the data points, unsmoothed, connected by straight lines. For other data, *e.g.*

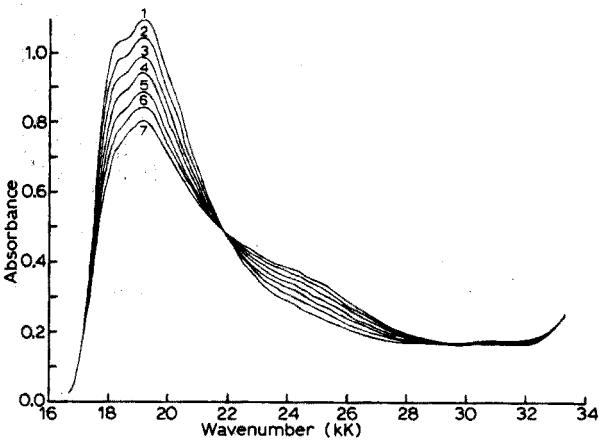

Fig. 6. Effect of temperature on the spectrum of methyl red (Solution C) in KCl solution (0.05 *M*); pH adjusted to 4.84 at 25°C. Absorbances were not corrected for thermal expansion. Spectra: (1) 15.3, (2) 25.6, (3) 35.4, (4) 44.5, (5) 55.3, (6) 64.7 and (7) 73.4°C.

Fig. 6, the graph-plotter was programmed to draw a smooth continuous curve through all defined points. This, too, had to be used with care, as the programme could not cope adequately with large gradient changes, producing rather bizarre curves in such cases.

* Unfortunately, some of the coefficients given in ref. 28 are in error. Corrected values are available from the present authors.

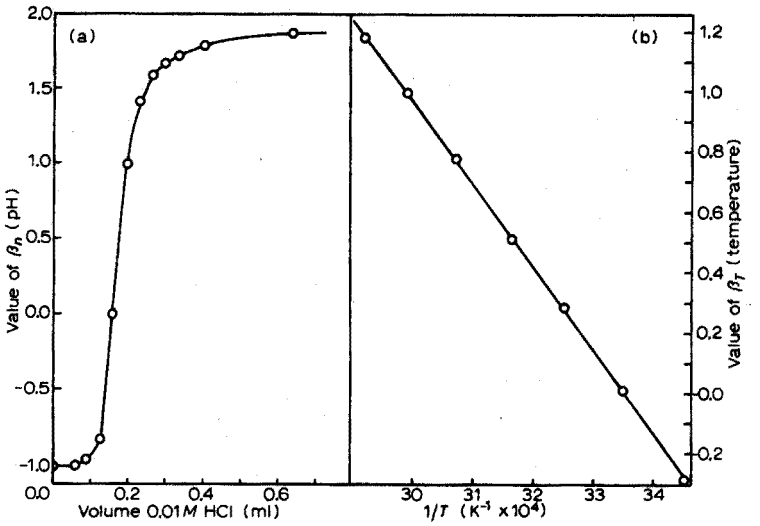

Fig. 7. (a) Dependence of internal linearity constant β_n (Table II) on corresponding volume of HCl added to methyl red solution B (Fig. 3b). (b) Dependence of β_T (Table III) on the reciprocal temperature of methyl red solution C (Fig. 6).

No interpretation has been placed on the relationship between the pH of the solution and the corresponding β_n value calculated relative to the reference spectra. However, a plot of β_n against added hydrochloric acid (Fig. 7a) follows very closely the shape of the end-point titration curve described by the changes in absorbance (Fig. 2). This will be considered in a wider context in a later publication.

Methyl red—temperature effects

The spectra of solutions containing predominantly the yellow basic form of methyl red were found to be rather insensitive to changes in temperature. However, larger spectral changes were observed when a significant proportion of the red species was also present.

A set of spectra recorded between 15 and 73°C for a methyl red solution of pH 4.84 at 25°C is shown in Fig. 6. These spectra were digitized by hand at 5-nm intervals. The absorbance in the region of the yellow species (23–26 kK) increases as the temperature increases, whereas that of the red form, around 19 kK, decreases in intensity. A well-defined isosbestic point is observed at 21.9 kK (457 nm). Similar changes were recorded when solutions of pH 5.47 and 5.90 were studied. Isosbestic points were then measured at 22.1 kK (453 nm) and, less well-defined, between 22.4 and 23.0 kK (435–445 nm), respectively.

An internal linearity analysis of the data in Fig. 6, is given in Table III; on comparison with the analyses in the first two Tables, it may be seen that here the r.m.s. deviations from the internal linearity constant, now designated β_T, are, on average, slightly larger for spectra recorded at different temperatures. By contrast, the r.m.s. deviations of A are smaller. Both these observations may be attributed in part to the small differences between spectra recorded at successive temperatures, as demonstrated by the large number of digitized absorbances rejected because the

TABLE III

INTERNAL LINEARITY ANALYSIS: EFFECT OF TEMPERATURE ON METHYL RED SOLUTION C

(Total no. of digitized points, 61; pH, 4.84 at 25°C; ionic strength 0.05 *M* KCl.)

Order of spectra[a]			β_T	*R.m.s. deviation*		*Rejected points*		*R.m.s. deviation* Δ*(absorbance)*
n	*Reference*			*From* β_n	*% of* β_n	*Threshold*[b]	*Total*	
1	6	2	−0.297	0.029	9.66	36	42	0.005
2	6	2	0.0	—	—	—	—	—
3	6	2	0.282	0.015	5.33	41	47	0.003
4	6	2	0.521	0.012	2.32	25	36	0.002
5	6	2	0.787	0.015	1.91	21	32	0.002
6	6	2	1.0	—	—	—	—	—
7	6	2	1.186	0.019	1.64	19	30	0.003
Mean[c] volume uncorrected				0.018	4.2	28	37	0.003
Mean volume corrected[d]				0.021	4.8	27	35	0.003

[a] Numbers refer to Fig. 6; spectra digitized at 5-nm intervals; absorbances not corrected for volume expansion.
[b] Threshold differences between spectra: 0.02 absorbance units.
[c] Mean parameters from above 7 analyses.
[d] Mean of analyses identical to [c] but corrected for thermal expansion of solutions.

differences between spectra did not exceed 0.020 absorbance units. (The threshold difference was here increased from the earlier value of 0.010 absorbance units because the maximum absorbance recorded was less and the spectra were much closer together over a much wider wavelength range.) The spectra plotted in Fig. 6 were not corrected for thermal expansion of the solution. When such a correction was applied the mean internal linearity deviations increased, compared with those for the uncorrected spectra (Table III).

Errors in internal linearity analyses of spectra recorded at different temperatures are accentuated by two facts. Firstly, only small changes in spectra result from the shift in any equilibria in solution caused by temperature changes. Secondly, the spectra of the individual species are almost always dependent to some extent upon temperature. Both these factors result in a loss in the precision of the internal linearity analyses of spectra recorded over a range of temperatures. It can therefore be considered that, for temperature-sensitive equilibria, the set is internally linear if the r.m.s. deviation from β_T does not exceed 5% for such spectra. This percentage must only be regarded as a guide, and the extent of the broadening and shifting of the spectrum of each constituent species over the temperature range studied must be considered. For some molten salt systems over wide temperature ranges, higher percentage deviations have been found among internally linear spectra[29].

The spectra in Fig. 6 are thus taken as internally linear with respect to temperature. On comparison with the effects deduced on varying pH, it is concluded that there is a shift in the equilibrium between the red (I) and the yellow (II+III) forms of methyl red, the yellow species being favoured at high temperatures. The wavenumber dependence of the Δ-function is shown for a selection of spectra in Fig. 8.

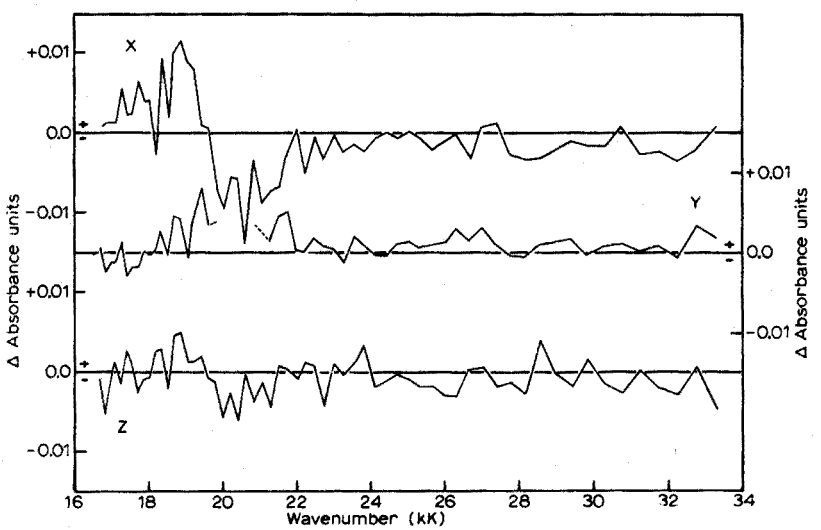

Fig. 8. Wavenumber dependence of internal linearity function Δ, for sets of temperature dependent spectra defined in Fig. 6. X, Y and Z Δ-functions computed from $\Delta = \{[(1-\beta_T)\varepsilon_2] + \beta_T\varepsilon_6 - \varepsilon_T\}$, where T represents the spectra 1, 4 and 7, respectively. The r.m.s. deviations of Δ are 0.005 (X), 0.003 (Y) and 0.002 (Z).

Walton[1] has discussed the effect of temperature on indicator solutions. Azo indicators show a considerable increase in dissociation as the temperature is increased, which can be attributed mainly to a corresponding reduction in the dielectric constant of water[1]. Walton estimated that the end-point pH at 70°C for methyl red solution differed from that at 18°C by −0.2 pH units.

The variation of β_T (Table III) with temperature is shown in Fig. 7b. The linear relationship found between β_T and the reciprocal of the absolute temperature parallels that between log K (K being the formation constant) and $1/T$ in ΔH determinations. A theoretical relationship between β_T and log K for an equilibrium in a molten salt system has been established[29].

A full examination of the effect of temperature on methyl red solutions was not undertaken, and thus the temperature dependence of the spectra of individual species cannot be assessed. However, one further point from this study merits attention. According to "classical" isosbestic point theory, if a two-species equilibrium is shifted by any constraint, any isosbestic points observed in the spectra of the system occur at a unique wavelength characteristic of the two species[2]. The position of the isosbestic point recorded here as the temperature was varied is dependent on the pH of the solution. This is not readily understood but may arise from the temperature dependence of the spectra of the individual species. Hence, for this system, the relationship between β_T and K cannot be a simple one. Thus at the present time there is insufficient experimental evidence to develop this relationship further.

We thank the Science Research Council for a Research Studentship to P.J.P. and for the Cary 14H spectrophotometer. The digitizing equipment was purchased out of an E.M.R. contract with the United Kingdom Atomic Energy Authority, Harwell.

SUMMARY

Analysis by computer of a series of spectra of some indicator solutions as a function of pH has shown that, for methyl red, three, rather than two, species are present in solution. The basic form and the pseudo-acid form occur in a constant ratio to each other, except at high pH when the pseudo-acid form, never in large concentrations, is lost. The isosbestic points observed are shown, by internal linearity analyses, to relate to a pseudo-two-species equilibrium. At intermediate pH values an increase in temperature produces an isosbestic point and thus temperature does not here alter the relative concentrations of the basic and pseudo-acid forms. The merits of and procedures for digitizing and analysing spectra are discussed.

REFERENCES

1 H. F. Walton, *Principles and Methods of Chemical Analysis*, Prentice-Hall, Englewood, N.J, 2nd edn., 1964, p. 290.
2 J. R. Morrey, *J. Phys. Chem.*, 66 (1962) 2169; 67 (1963) 1569.
3 J. Brynestad and G. P. Smith, *J. Phys. Chem.*, 72 (1968) 296.
4 J. Brynestad, C. R. Boston and G. P. Smith, *J. Phys. Chem.*, 47 (1967) 3179.
5 In J. S. Mattson, H. B. Mark and H. C. MacDonald (Eds.), *Computers in Chemistry and Instrumentation, Vol. 3, Spectroscopy and Kinetics*, Marcel Dekker, New York, 1973.
6 S. P. Perone and D. O. Jones, *Digital Computers in Scientific Instrumentation: Applications to Chemistry*, McGraw-Hill, New York, 1973.
7 T. R. Griffiths and R. K. Scarrow, *Trans. Faraday Soc.*, 65 (1969) 2567.
8 F. R. Lipsett, G. Bechthold, F. D. Blair, F. V. Cairns and D. H. O'Hara, *Appl. Opt.*, 9 (1970) 1312.
9 R. N. Jones, *Pure Appl. Chem.*, 18 (1969) 303.
10 W. L. Butler and D. W. Hopkins, *Photochem. Photobiol.*, 12 (1970) 439.
11 V. R. Sakalys, *Internat. Lab.*, March/April 1972, 11.
12 T. R. Griffiths and R. K. Scarrow, *J. Chem. Soc. A*, (1970) 827.
13 M. D. Cohen and E. Fischer, *J. Chem. Soc., London*, (1962) 3044.
14 W. Brügel, *Einführung in die Ultrarotspectroskopie*, Steinkopff, Darmstadt, 1957, p. 292.
15 C. A. Angell and D. M. Gruen, *J. Amer. Chem. Soc.*, 88 (1966) 5192.
16 H. A. C. McKay and J. L. Woodhead, *J. Chem. Soc., London*, (1964) 717.
17 C. F. Timberlake and P. Bridle, *Spectrochim. Acta, Part A*, 23 (1967) 313.
18 T. Nowicka-Jankowska, *J. Inorg. Nucl. Chem.*, 33 (1971) 2043.
19 H. A. C. McKay and D. Scargill, *J. Inorg. Nucl. Chem.*, 30 (1968) 3095.
20 R. A. Reinhardt and J. S. Coe, *Inorg. Chim. Acta*, 3 (1969) 438.
21 L. Skulski and J. M. Kanabus, *Bull. Acad. Pol. Sci., Ser. Sci. Chim.*, 17 (1969) 311.
22 M. J. Blandamer, M. C. R. Symons and M. J. Wootten, *J. Chem. Soc. D*, (1970) 366.
23 C. Chylewski, *Angew. Chem., Int. Ed. Engl.*, 10 (1971) 195.
24 E. W. Smith, J. Brynestad and G. P. Smith, *J. Chem. Phys.*, 52 (1970) 3890.
25 G. P. Smith, C. R. Boston and J. Brynestad, *J. Chem. Phys.*, 45 (1966) 829.
26 A. I. Vogel, *A Text-book of Quantitative Inorganic Analysis: Theory and Practice*, Longmans Green, London, 3rd edn., 1964, p. 53.
27 I. M. Kolthoff, E. B. Sandell, E. J. Meeham and S. Bruckenstein, *Quantitative Chemical Analysis*, MacMillan, London, 4th edn., 1969, p. 695.
28 A. Savitzky and M. J. E. Golay, *Anal. Chem.*, 36 (1964) 1627.
29 T. R. Griffiths and P. J. Potts, unpublished results.

Analytica Chimica Acta, 71 (1974) 17–34

A COMPUTER-BASED STORAGE AND RETRIEVAL SYSTEM FOR ELECTRONIC ABSORPTION SPECTRA

ARNT GERHARD SCHÖNING
Billeruds AB, S-661 00 Säffle (Sweden)
(Received 2nd January 1974)

Absorption spectrophotometry is one of the classical methods in analytical and physical chemistry. The method has, through the decades, been of increasing value in evaluation of chemical structure and in identification of unknown compounds. As an increasing number of correlations are discovered, both empirically and theoretically, between chemical composition and light absorption, the absorptiometric method seems to be of continuously increasing importance. This is verified by the development of the instrumentation. Today, instruments of increasing capacity and performance, higher resolution and greater automation are commercially available, thus making this classical method a modern instrumental one.

The literature on the subject is vast and growing; the number of published spectra in the ultraviolet and visible region is of the magnitude of 10^5. These spectra are classified or organized only to a small extent, which is a serious drawback for an effective usage of existing spectral information. There are some collections as graphs[1–3] covering this region, which makes information available, at least for some group of substances.

The use of spectra falls into three categories, *viz.* quantitative analysis, structure elucidation and identification. Of these, identification, or the problems of identification, was the prime interest in the present work. For identification purposes, the above-mentioned catalogued spectra or spectral data are of great value, since identical compounds have identical spectra. The comparison, however, of the spectrum of an unknown compound, and that of many thousands of known compounds is time-consuming and cumbersome. The goal was therefore set, to develop a computer system which could automatically make the comparison and present the result. Consideration was also given to the fact that different absorption curves may be partially identical if there is a partial structure identity between the corresponding compounds, and such information should also be available. This would undoubtedly enhance the value of the computer system, as it also would bring it into the region of structure elucidation.

Existing data systems

In the literature, some data systems which exist for the ultraviolet and visible region are mechanically oriented and based on card sorting, such as the European DMS system and the American ASTM system[4]. In the infrared region, however, more computer-oriented systems have been developed (refs. 5, 6 and refs. therein).

The currently used computer systems for handling spectral data contain selected information, such as the position of absorption maxima, number of maxima, absorption at maximum, *etc.*, but none of these systems retrieve the whole absorption curve. Thus, existing systems can not replace visual comparison and examination of absorption curves, for only by such means can maximum information be obtained from the absorption. One should, however, bear in mind that the demand for investigating the entire absorption curve is more pronounced for electronic spectra than for i.r. spectra. For the latter, sufficient information is obtained from the position of the maxima and their intensities, as very characteristic group frequencies are found here; electronic spectra are more related to the gross molecular structure and hence not only the positions of the maxima but also the shapes of the curves are of interest.

Demands on new system

If a structural elucidation based on spectra is to be optimal, or an identification is to be made, the complete absorption curve for the actual region should be used. The following demands were set up:

(1) The entire absorption curve should be stored and retrieved.

(2) If there is only partial identity between the observed (unknown) spectrum and a stored (reference) spectrum, information about this should also be given, stating in what wavelength regions identity is found.

(3) There should be allowance for displacements of the curves, necessary to obtain identity, arising from hypo-, hyper-, hypso-, and batho-chromic effects.

(4) For spectra using absorbance, differences in concentration between absorbing solutions used for observed and reference (stored) spectra should be automatically compensated, thus making the comparisons independent of concentration.

It can be seen that a system considering all the above-mentioned points should do the same thing as is done when two absorption spectra, each drawn on transparent paper, are compared. By such a comparison the spectra (or the paper sheets) are displaced horizontally and vertically until in some region identity is found. Then further displacements are carried out, looking for identity in other regions, and so on. When identity is found, the formation is memorized or written down. Then another reference curve is taken, and the same procedure repeated. A data system, such as proposed, should do this much more effectively for several reasons. The comparison is made systematically point by point, with exactly defined displacements if wanted, and identities found in preselected regions are stored in the computer's memory for as many spectra as wanted. The computer will not tire, or lose information. Computer retrieval is also very fast compared with visual or manual retrieval. After the search, all the stored detailed information can immediately be written out and identical curves can be displayed, *etc.* Finally, absorbance spectra belonging to the same chemical system, but different in shape owing to differences in concentration, are regarded as identical by the computer.

PRINCIPLES OF THE NEW SYSTEM

Regions and units

Guided by the demands mentioned above, the basic principles for the new

system were set up. The first thing to be decided was the best wavelength region. The whole absorption curve should be stored, and later retrieved, hence the curve should not be too complicated or contain too many details, as this could make identification difficult.

Absorption curves in the infrared region are very rich in detail. It was therefore natural to select the ultraviolet and visible region, where the curves are simpler (in a graphical sense), provided that they are not developed under extreme conditions causing fine (vibrational) structure bands. This region was also selected because of the important correlations between molecular structure and ultraviolet and visible absorption which have been proved in recent decades and on which the literature now contains a large amount of information[7–11]. The proposed data system may promote the use of this information and also contribute to the further development of this topic.

The units to be used for wavelength and for intensity had also to be decided. For a computerized identification, it seemed unimportant whether wavelength or some function of it, *e.g.* wavenumber, was used. Programs for both wavelength and wavenumber were constructed. With regard to intensity, the choice between different units is more critical. There are two main units to select between, the absorbance (extinction) and the absorptivity (extinction coefficient). The absorbance is directly measured, without any conversion, whereas for the absorptivity, it is necessary to adjust the output signal with knowledge of concentration or molecular weight. When molecular absorptivity is used, curves cannot be produced unless the molecular weight is known. These considerations would favour the use of absorbance. For structure determinations, however, a detailed comparison of spectra should preferably be carried out with spectra as independent as possible of extensive factors. As concentration is such a factor, absorbance spectra are in this respect inferior to absorptivity spectra.

Absorbance spectra should not, however, be discarded. First, many catalogued spectra, even comprehensive and important collections[3], are given in absorbance. In order to transfer these directly into a computer register, absorbance must be used as the independent variable. A computer program could, of course, handle the problems of conversion between all the different units in use, but this does not seem a good solution to the problem. Computer storage and retrieval of spectra should, preferably, be done with units internationally adopted for such a purpose. A second reason for the retention of absorbance spectra is that the composition as well as the molecular weight is often not known or cannot be determined exactly. This is true for many technical and biological compounds of high complexity.

It was therefore desirable to develop two systems, one for absorbance and one for absorptivity. In the first case wavelength, and in the second case wavenumber, was taken as the independent variable. In this part of the work, the system based on absorbance is presented. The work was also restricted initially to a system functioning in the u.v. region.

Basic increments

The wavelength increments selected were based on three considerations, *viz.* the form of existing catalogued spectra, (from which the system would get its first input values), the resolution power of commercial instruments, and the graphical

presentation of spectra by means of the computer. For a computer system such as that proposed, the first of these points was of greatest importance. The entire absorption curves were to be stored and available spectra, presented graphically, had to be used; moreover, for existing spectra it is inconvenient to make steps smaller than 2 nm. Therefore, a wavelength increment of 2 nm was selected.

The resolution power of many commercial instruments has a magnitude of 1 nm, or in some advanced cases 0.01 nm. With regard to presentation of spectra, or plotting by means of the computer, it seems best to use increments of 1 nm, to obtain good visual information. These two points indicate that, for further development, the incremental value selected may be diminished. (It should be noted that this also is a question of computer capacity).

It was only for the wavelength that increments were chosen; for absorbance, the observed (read) value was taken. In the latter case, however, the accuracy of the input values had to be decided. This decision was based almost solely on what can be observed from catalogued absorption curves. It was decided to present to the system absorbance values correct to two decimal places, thus making 0.01 in absorbance the smallest difference detectable for the computer. This accuracy should suffice even for fine structure studies.

Subregions

The next point to study was how to satisfy the second demand, namely that of retrieving partial identity. This partial identity of two spectra of two compounds can be formally thought of as of two kinds, namely, that which exists in a narrow region, arising from common small groups, *e.g.* carbonyl and amino groups, and that existing in a much broader region, resulting from identities in gross structure between major parts of the molecules. When electronic spectra are used for structural elucidation, both these kinds of identities are used, although the second kind predominates, owing to the nature of electronic spectra. It was therefore decided to use two kinds of subdivisions, one relatively broad, called a subregion, and one narrow, called an identity zone (see below). The subregion is regarded by the computer as an independent entity, in which the retrieval procedure is performed from start to finish.

A study of absorption spectra of different classes of compounds showed that characteristic parts of the spectra were found within a wavelength range of 50 nm. The magnitude of this range is of course strongly influenced by all those factors which determine the molecular structure, and to establish this magnitude on purely physico-chemical grounds is not easy. Moreover, the magnitude of the region also depends on the other demands or restrictions placed on the system, so that the scope of the system must be considered also. As the main purpose of the system is identification, a searching region or a subregion of 50 nm must be regarded as very convenient, at least as a starting point. Accordingly, four subregions are considered: 200–250 nm, 250–300 nm, 300–350 nm and 350–400 nm, designated subregions 1–4, respectively. The identification of subregions is treated below in the 'Retrieval Procedure' section.

The identity zone

It should be emphasized that a subregion represents a fixed range within which

a retrieval procedure is started and ended. If some identity is found within a region, information is written out, which states in which subregion identity was found. This message does not give information about the magnitude of the zone in which identity was found. This zone, here called the identity zone, can be made equal to, or smaller than, a subregion. The value of the identity zone can be selected when the program is loaded, as described later.

Experience gathered so far with retrieval of spectra has proved the great importance of this identity zone. It can be thought of as an 'eye', moving continuously from one end of the spectrum to the other, critically examining two superimposed spectral curves. Displacement parameters, described below, automatically centre this 'eye' to the midpoint of that part of the (observed) spectral curve which is under observation.

Displacements

It is well-known that small changes in a molecule, *e.g.* the introduction of a substituent, usually cause a systematic displacement of the spectrum. Also changes in environmental conditions, *e.g.* pH, temperature, solvent, *etc.*, may cause spectral displacements. These displacements are of two kinds: those resulting in a wavelength change at a characteristic absorption maximum or some other part of the curve, and those resulting in an absorbance change at a characteristic wavelength or wavelength region. The former changes are known as batho- and hypsochromic effects, and the latter as hyper- and hypochromic effects. Such effects must be considered in developing the retrieval system, so that displacements can be allowed for, and compounds which differ only in a small and systematic manner from the original (observed) spectrum can be identified. This procedure is obviously of great informative value, and also compensates for errors in wavelength setting, as well as in absorbance.

When these displacement values are selected, some consideration must be given to the magnitude of the subregion, which covers a range of 50 nm. If a maximal wavelength displacement of 10 nm is allowed in each direction, the maximum total displacement would be nearly equal to half the range of a subregion. This must be regarded as a maximum displacement if the retrieval is to be meaningful. If a greater displacement value were chosen, the identification would perhaps not be restricted enough. Should the user of the system only be interested in seeking compounds (spectra) which are entirely identical in all or some wavelength regions, he may choose to make this shift equal to zero. As described later, the displacement is a parameter, the value of which can be chosen when the program is loaded. In this way, the user can, if he does not find any identical spectrum with zero displacement, allow for successive displacements to retrieve all those spectra which have some identity with that observed. The displacement of the absorbance value at a fixed wavelength is also constructed as a program parameter, the value of which can be selected when the program is loaded. The value can be set from 0.01 upwards with no limit.

When the absorbance value is allowed to lie within a given range, this should virtually coincide with the automatic concentration correction, described in the next section. If, however, two spectra differ in shape only to a small extent, this would not be detected through a concentration correction alone. This is verified by means

of test curves, described below under 'Test Curves and Test Results'. It is very important to have simultaneous access to several spectra differing only to a small extent in shape, especially when several possible structures have to be distinguished.

Correction for differences in concentration

According to the equation:

$$A = abc$$

where A = absorbance, a = absorptivity, b = cell length, and c = concentration, the absorbance is linearly related to the concentration.

If, therefore, several absorbance spectra (from solutions) are to be compared in order to study identity in some wavelength region, the spectra must be compared at the same concentration of solute. One cannot, however, demand that all the spectra to be stored in an information system shall be produced at exactly the same concentration. This would be impracticable, for in many cases the concentration is chosen so as to give the most convenient spectrum. Most important, existing catalogued spectra are presented with quite different concentrations. To solve this problem, it was decided to let the computer compensate for differences in concentration.

Two spectra, each from two different solutions of the same solute, differing only in concentration, will be linearly displaced (along the absorbance axis) by the same relative amount at all wavelengths, as shown in Fig. 1. Thus, the proportion between two absorbance values at a fixed wavelength is constant over the whole wavelength range. This can also be deduced from the equations:

$A1 = a1\,b\,c1$ (absorbance at wavelength 1 and concentration $c1$)
$A2 = a1\,b\,c2$ (absorbance at wavelength 1 and concentration $c2$)
$A3 = a2\,b\,c1$ (absorbance at wavelength 2 and concentration $c1$)
$A4 = a2\,b\,c2$ (absorbance at wavelength 2 and concentration $c2$)

The letters above are also shown in Fig. 1.

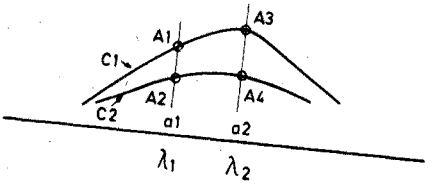

Fig. 1. Absorbance (A) for one compound at two different concentrations $c1$ and $c2$.

From these four equations it easily follows that:

$$A1/A2 = A3/A4$$

or

$$An/Am = \text{constant}$$

where An and Am are the absorbances at concentrations cn and cm respectively.

If one of the absorbance values, say Am, is taken as the absorbance at maximum for a reference (stored) spectrum, and the other absorbance value, An, is

taken as the absorbance for the observed (unknown) spectrum at the same wavelength, a correction factor (CORR) can be computed according to the equation:

$$\text{CORR} = \frac{\text{Absorbance (observed)}}{\text{Absorbance (reference)}}$$

This correction factor is valid for the entire wavelength region. If each absorbance value in the reference spectrum is multiplied by the correction factor CORR, the reference spectrum will coincide with the observed spectrum, provided that the two spectra belong to the same compound.

This procedure is performed by the computer as follows. When spectra are stored, the maximal absorbance and the corresponding wavelength are calculated for each of the four subregions and stored together with the spectrum. When the file is searched for an observed spectrum, the absorbance of this at the same wavelength as the maximum for the reference spectrum is first found, and the correction factor calculated. Then the absorbance values in the reference spectrum are adjusted by means of CORR to the corrected concentration, and the comparison between the observed and the reference spectrum is carried out. The procedure is performed separately for each subregion.

This principle makes it possible to compare absorption spectra even if these are produced at different concentrations. One need not even know the concentration when a spectrum is produced, whether the purpose is for storing or for retrieval. This has the advantage that a spectrum can be produced at such a concentration that characteristic absorption takes place. The concentration must, however, be constant within the entire wavelength range selected. (If wavelength displacements are not used, this restriction is unnecessary.)

FILES DESCRIPTION

Input

The punched card was chosen as input medium. This is the most convenient input medium to use in transferring catalogued spectra to computer storage.
The card layout is shown in Fig. 2 and further explained below. The first card in a series is used for identification. If an increment of 2 nm is used for the wavelength region 200–400 nm, a further five cards suffice to punch all the absorbance values.

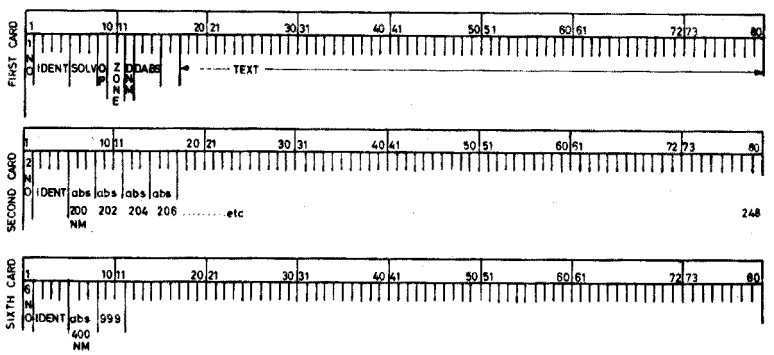

Fig. 2. Card layout (input).

First card:
(Identification card)

Column 1 Card number. (1)
The card number is a control key used to ensure the correct order of absorbance values.

Columns 2–5 Identification field.
Every compound is identified with a numerical or alpha-numerical code. Together with the name of the compound, which also is punched, the identification code strengthens the control of storing and retrieving. The identification code has also another important function, *i.e.* to prevent mixing of cards, and thus absorbance values belonging to different compounds. If only numerical codes are used, the field allows identification of 10,000 compounds.

Columns 6–8 Solvent code.
As the absorption spectrum may be strongly influenced by the solvent, this must be identified. The number of solvents used in electronic absorption, is restricted, thus three positions should suffice for identification purposes. Other external factors which influence the absorption, such as pH, temperature, pressure, *etc.*, are not coded in this system. The pH (for aqueous media) should be incorporated in the code. With regard to temperature, the absorption is nearly always measured at 20°C (or 25°C), and only relatively large deviations from these values affect the spectrum; in such cases, this should be incorporated in the code.

Column 9 Operation code.
The operation code decides if the computer will store or retrieve the compound. Three codes are used:
1 for storing,
2 for searching for identical compound,
3 for comparing with all stored spectra.

Columns 10, 11 Zone.
The identity zone in nm.

Column 12 DNM value.
Displacement along the wavelength axis. This value is a whole number in the range 0–5. The displacement in nm is equal to twice the DNM value. Thus, for a DNM value of zero no displacement takes place, and a DNM value of 5 results in the maximal displacement of 10 nm in each direction.

Columns 13–15 DABS value.
Displacement along the absorbance axis. This field consists of three positions of which the last two are the decimal fraction. No point

is punched. A punched value of, for example, 010 allows for a displacement in absorbance of 0.10 in both directions.

Column 16 Blank.

Columns 17–80 Text.
This field is optional. The name of the compound should be punched, as this text field is stored and also printed in the terminal output list, which gives the result of the retrieval procedure.

Second card:

Column 1 Card number. (2).

Columns 2–5 Identification field.
(Same as in first card).

Columns 6–80 Absorbance values.
Each absorbance value has a field of three positions. The two last are the decimal fraction, no point is punched. The first field represents the absorbance value at 200 nm, the second at 202 nm and so on, and the last field, columns 78–80, gives the absorbance value at 248 nm.

Third to fifth card:

Same structure as the second card.

Sixth card:

Column 1 Card number. (6).

Columns 2–5 Identification field.
(Same as in previous cards).

Columns 6–8 Absorbance value at 400 nm.

Columns 9–11 End of series indication.
In this field the number 999 is punched, which indicates the end of data for a series, *i.e.* for a compound in a certain solvent. When this number is observed, no more cards are read for this series, and the program continues with its operations according to the operation code.

Job file

The card package for the job file is shown in Fig. 3. As many spectra as wanted can be operated on in the same batch. The spectra must be either for storage or for retrieval. In the retrieval mode, the two kinds of operation can be mixed. Originally the program was constructed for both storage and retrieval in the same job, but this procedure seemed to have no great advantage. If such a possibility is wanted, it can easily be included by minor changes in the program. An end of spectra card follows the cards for the last series.

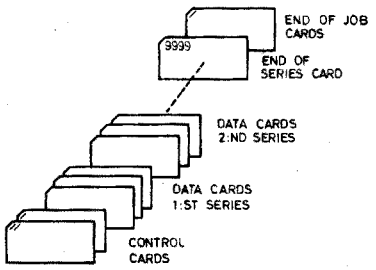

Fig. 3. Card package.

Storage layout

Of the variables read into the core memory from the above-described data cards, the identification number, the solvent code, the absorbance values and the text field are also permanently stored on an external memory device. The other input variables, such as card number, operation code, DNM and DABS values, are used only during execution. Some derived variables are also permanently stored. These are, for each subregion, the maximal absorbance values and their corresponding wavelength. A disk package is used as external storage device.

With regard to the mode of storage, a choice must be made between sequential and direct access files. For the system (program) developed here, the spectra stored are inspected in turn; they are thus read as well as written sequentially. The reading and writing instructions, however, are given in the direct access mode which can be used also for sequential performance. The thought behind this is that it should be possible to have random access to the spectra in case one seeks (or stores) spectra with special characteristics, *e.g.* spectra belonging to special groups of chemical compounds or spectra with special structural details. In such cases, every spectrum should be stored with a record key, and the file structure should be organized in blocks, each block containing spectra with a common characteristic. This is a very interesting possibility for further development of the program, and could be performed with minor alterations.

The layout of the external file is shown in Fig. 4. The record is composed of words, each word representing a variable.

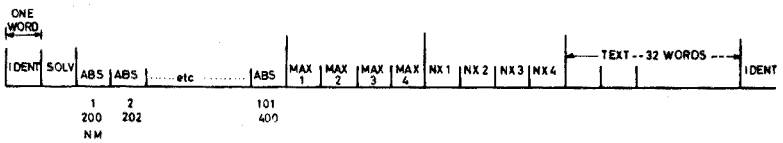

Fig. 4. Disk record.

In the proposed system, numerical values are packed to two bytes per word, and characters to one byte each, each byte consisting of eight bits. The two first words represent the identification number and the solvent code, and the following 101 words contain the absorbance values from 200 to 400 nm. After these, comes a field consisting of four words containing the four maximal values in the four subregions, followed by another four-word field containing the corresponding wavelength values. The last field in the record is a text-field of 32 words containing the name of the compound and additional information (optional).

For the disk file, there is no special end of record mark, as the disk is initialized before use. This initialization procedure is machine-dependent and is not described here. An end-of-file mark is, however, used in the system. This is equal to the value 9999 and is placed in the first word in the last record. It will therefore be equivalent to an identification number of 9999. When spectra are stored, an identification number of 9999 is first sought. Storage then begins at this record and the identification number replaces the end of file mark. When storage is completed, a new end of file mark is inserted. This is accomplished by writing the first variable read from the last input card (end of data card).

In the retrieval procedure, the searching is ended if an end of file mark is encountered, and a message is written out, stating that no more spectra are stored. The counting of records is made automatically when direct access read and write statements are used.

RETRIEVAL PROCEDURE

In searching for identity (retrieval), each subregion is investigated separately and in turn, starting with subregion no. 1 (200–250 nm). The first statements to be made are those connected with the calculation of the correction factor CORR, as previously described. All the comparisons performed between a stored (reference) spectrum and an observed spectrum and described in the following, are done after this correction has taken place.

In Fig. 5 the records of two spectra are shown, one reference (stored) and one observed spectrum. The records are positioned as they virtually would be at

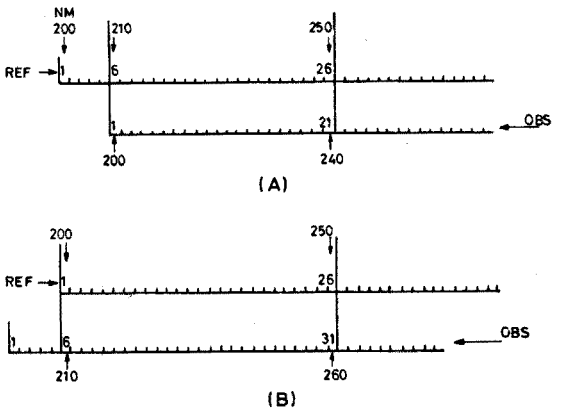

Fig. 5. Configuration of stored (REF) and observed (OBS) spectra records during comparison.

some moment in the comparison procedure during the search for identity. In the upper part (A) in Fig. 5 the observed spectrum is in the farthest right position to the reference spectrum. This configuration is obtained when the DNM value is set at its highest value, *i.e.* 5. Then the first position in the observed spectrum, representing the absorbance value at 200 nm, is compared with the absorbance value in the sixth position in the reference spectrum, containing the absorbance value at 210 nm. For this comparison a difference in the two absorbance values is allowed for, corresponding to the DABS value given. If this difference is within the accepted interval, the two absorbance values are regarded as identical. As it would be meaningless to assume identity when there is no absorption, values equal to or lower than 0.01 are disregarded. Then comparison is continued for the next cell and so on. If identity for this subregion is not revealed in this configuration, the observed spectrum is displaced one unit to the left, and new comparisons between the cells are carried out. If identity is obtained for one configuration, the comparison procedure for this subregion is terminated and the comparison started for subregion no. 2. If identity is not revealed, these displacements may continue until the observed spectrum has reached the farthest left position, as shown in Fig. 5B.

During the comparison procedure, two counters are in operation, one for identical events, and one for non-identical events. This is to minimize the searching time, since the searching is stopped as soon as the prescribed number of identical cells is obtained, or as soon as the number of non-identical cells is past, whichever is first.

When no wavelength displacement takes place, the number of cells is the same in all subregions. With displacements, however, this number is diminished for the two subregions at each end of the spectrum, as comparison cannot be made outside these regions. The number of positions or cells which cover each other is for the end regions a function of the DNM value and of the actual configuration. This variation in the number of identical values obtainable is considered by the program. Each time the demanded number of identical values is obtained, identity is confirmed by setting a program switch on, one switch for each region. As long as a subregion switch is off, identity is not found within that region. It is by controlling the state of these switches that the program determines in which part of the spectrum identity is found.

PROGRAM LOGIC FLOWCHART

The program logic flowchart is shown in Fig. 6. This gives only the principal steps in the program, and is not a detailed presentation. Some program details have been described in the previous sections. The complete program is available in IBM FORTRAN IV from the author.

The first input values in a series, *i.e.* for a spectrum, given in card no. 1, serves as an identification for that series and as information to the system about the operations to be performed. These values are first checked, so that they are in accordance with the rules set up for the corresponding parameters. Then the data cards, containing all the absorbance values are read and also checked for consistency. If something is wrong in some of the input cards, a message is written

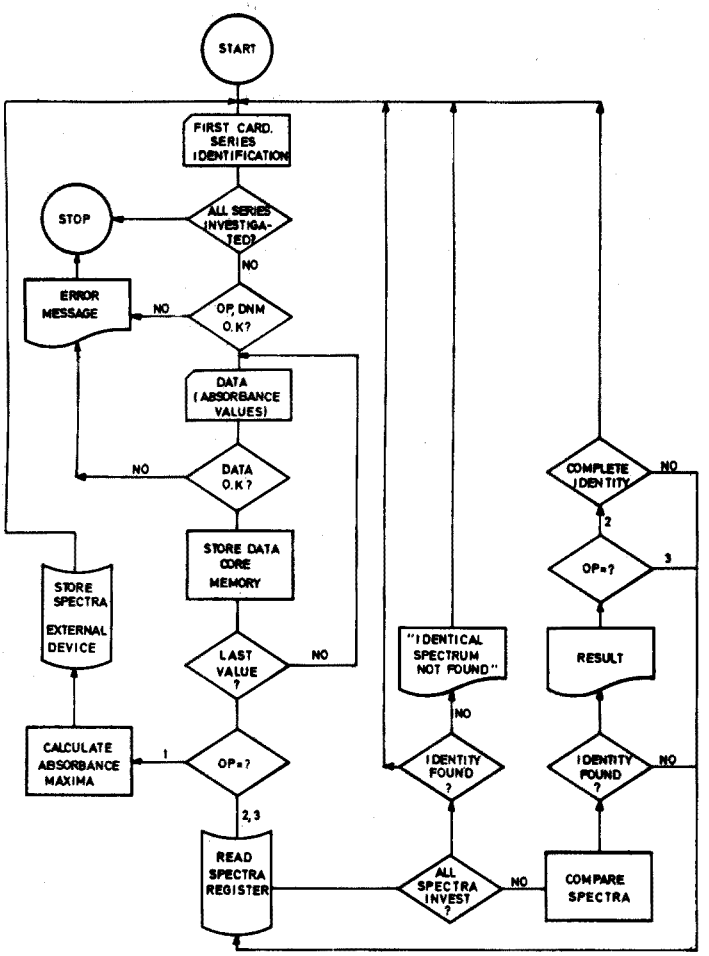

Fig. 6. Program logic flowchart.

out, indicating the kind of error and in what series, and execution is terminated. The actual cards are then taken from the card package and corrected. All the spectra (series) operated on before the error are unaffected, both in the storage and in the retrieval mode of the program, so that the execution can be continued with the remaining cards. When all the data for one series have been read in and checked, and consecutively stored in the core memory, the input phase is terminated.

Depending upon the value of the operation code (OP), the execution of the program is now continued with storage or retrieval. For OP equal to 1, the absorbance maxima is first found. Then the spectrum, together with these maxima, and its identifying parameters, is stored on an external device. After storage, the next series is read into the memory and so on. If the operation code is not equal to 1, the retrieval procedure is started. Reading is first performed on the register containing all the stored spectra. At this stage, each output record consists of one stored spectrum, and this is compared with one observed spectrum. If identity

is not found, the next stored spectrum is read from the register into the core memory and compared with the same observed spectrum. When identity, partial or total, is found, the result is written out. If the operation code after the execution of the write statement is equal to 3, the next stored spectrum is retrieved and investigated. This procedure is continued until all stored spectra have been investigated.

If OP is equal to 2 after execution of the above-mentioned write statement, execution is terminated when total identity between stored and observed spectrum is found. Should identity not be found between one observed spectrum and all the stored spectra, a statement about this is written.

TEST CURVES AND TEST RESULTS

To investigate if the program was functioning in all details, test curves were constructed. These are shown in Figs. 7–10, and are called Alfa, Beta, Gamma, Delta-1, Delta-2, Lambda and Kappa.

The first operation carried out was the storage of the spectra Alfa, Beta, Delta-1, Gamma and Kappa. Then the retrieval procedure (operation code 3) with these spectra was performed. The result is given in Fig. 11. It can be seen

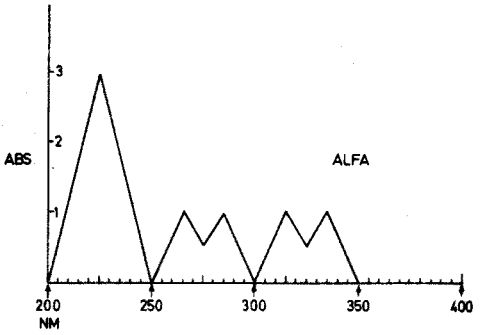

Fig. 7. Test curve, Alfa.

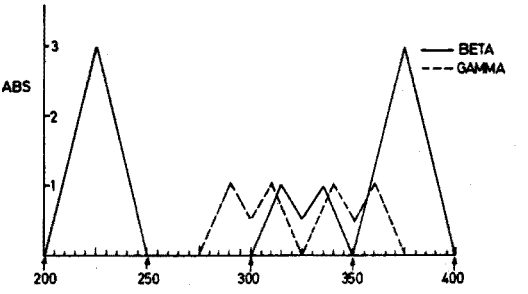

Fig. 8. Test curves, Beta and Gamma.

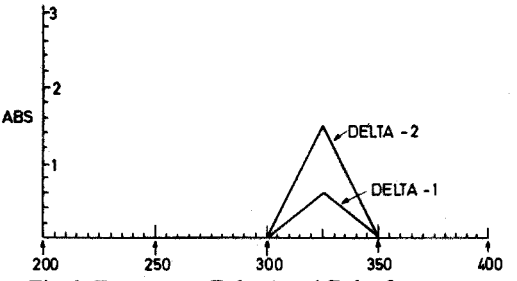

Fig. 9. Test curves, Delta-1 and Delta-2.

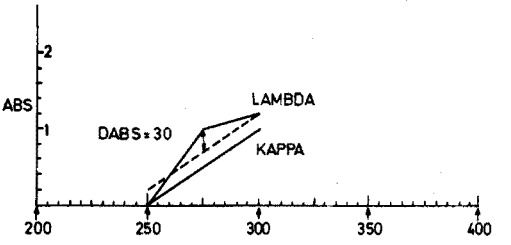

Fig. 10. Test curves, Kappa and Lambda.

```
TEST ALFA                                                          IDENT =   1 *
IDENTICAL WITH TEST ALFA                                           IDENT =   1
IN THE REGION 200 - 350 NM
IDENTICAL WITH TEST BETA                                           IDENT =   2
IN THE REGION 200 - 250 NM AND IN THE REGION 300 - 350 NM

TEST BETA                                                          IDENT =   2 *
IDENTICAL WITH TEST ALFA                                           IDENT =   1
IN THE REGION 200 - 250 NM AND IN THE REGION 300 - 350 NM
IDENTICAL WITH TEST BETA                                           IDENT =   2
IN THE REGION 200 - 250 NM AND IN THE REGION 300 - 400 NM

 TEST DELTA-1                                                      IDENT =   8 *
IDENTICAL WITH  TEST DELTA-1                                       IDENT =   8
IN THE REGION 300 - 350 NM

TEST GAMMA                                                         IDENT =   3 *
IDENTICAL WITH TEST GAMMA                                          IDENT =   3
IN THE REGION 250 - 400 NM

 TEST KAPPA                                                        IDENT =  10 *
IDENTICAL WITH  TEST KAPPA                                         IDENT =  10
IN THE REGION 250 - 300 NM

     RETRIEVAL TERMINATED
```

Fig. 11. Spectra retrieval.

```
TEST DELTA-2                                                    IDENT =   9 *
IDENTICAL WITH  TEST DELTA-1                                    IDENT =   8
IN THE REGION 300 - 350 NM

TEST GAMMA                      DNM=5                           IDENT =   3 *
IDENTICAL WITH TEST ALFA                                        IDENT =   1
IN THE REGION 250 - 350 NM
IDENTICAL WITH TEST BETA                                        IDENT =   2
IN THE REGION 300 - 350 NM
IDENTICAL WITH TEST GAMMA                                       IDENT =   3
IN THE REGION 250 - 400 NM

TEST LAMBDA                                                     IDENT =  11 *

     IDENTICAL SPECTRUM NOT FOUND

TEST LAMBDA  DABS = 20                                          IDENT =  11 *

     IDENTICAL SPECTRUM NOT FOUND

TEST LAMBDA  DABS = 35                                          IDENT =  11 *
IDENTICAL WITH  TEST KAPPA                SEPTEMBER 1972        IDENT =  10
IN THE REGION 250 - 300 NM

     RETRIEVAL TERMINATED
```

Fig. 12. Spectra retrieval.

that all the spectra were found, and it is also stated in what wavelength region (subregion) they were identical. Further, it can be seen that Alfa was found to be identical with Beta in the region 200–250 nm and in the region 300–350 nm, and that Beta was found to be identical with Alfa in the same regions, in accordance with the form of the spectra.

To facilitate the identification of compounds, the identification number is also given, as can be seen on the right side of Fig. 11. The identification numbers of observed spectra are followed by an asterisk.

Further checks of the program were performed in a second retrieval procedure. The results of this, which should be compared with the corresponding Figures, is given in Fig. 12. Delta-2 was found to be identical with Delta-1 in the region 300–350 nm. In accordance with the form of these spectra, their difference could have arisen from a difference in concentration only. Thus they are regarded as identical, in agreement with the program instructions.

When the Gamma spectrum, with an allowable wavelength shift of 5 nm in both directions was used as the observed spectrum, identity was also found with the Alfa- and Beta-spectrum in the regions set out in the Figure. This is in complete agreement with the form of these spectra. For Lambda identical spectra were not found. This spectrum is given together with the spectrum for Kappa in Fig. 10; this shows that these two spectra are nearly of the same form, but not so much that a concentration correction would make them identical. If, however, a minimal difference in absorbance of 0.30 were allowed in both directions, they would be regarded as identical. Thus, if the range of absorbance is set equal to 0.35 in both directions, identity is obtained, as can be seen from Fig. 12. From this Figure it can also be seen that a range of 0.20 in absorbance does not suffice for identity.

The results from these test curves prove that the computer program operated as expected. It remained, however, to show the system at work with real spectra. This was done for some benzene derivatives in an Appendix which is available from the author on request.

CONCLUSION

The study of spectral curves plays an important role in chemistry and physics. This is true for many types of spectra, such as Raman spectra, light absorption spectra, fluorescence spectra and mass spectra. For continuous spectra, such comparisons very often are carried out by comparing the observed spectrum with several reference spectra. Often this procedure is performed stepwise in smaller parts of the spectral range, and the curves may be displaced in horizontal and vertical directions to investigate if there should be any kind of identity. As such a process may be time-consuming and in most cases inaccurate, a computer-based system has been constructed which simulates this comparative process, thus making it faster, easier and more reliable.

The author is greatly indebted to Professor David Dyrssen and to Dr. Torbjörn Anfält and Dr. Daniel Jagner at the Department of Analytical Chemistry, University of Gothenburg for their help and advice in carrying through this project.

SUMMARY

A computer-based system for storage and retrieval of spectra in the ultraviolet region, with absorbance as the observed variable, is described. Differences in concentration between solutions relating to observed and stored spectra are automatically adjusted. The entire spectral curve is stored, not only selected points such as maxima *etc.*; this makes it possible to investigate the spectral range continuously during the retrieval procedure. The increment between two observations (absorbance values) is 2 nm on the wavelength axis.

The input medium is punched cards containing values taken directly from observed (catalogued) spectra. The output is a printed list, giving information about observed and retrieved spectra, system parameters used during the retrieval procedure, *etc.* An important feature of the system is that displacements between observed and stored spectra are allowed for, in two dimensions during comparison, thus taking into account 'chromic' effects. Information about partial identity between observed and stored (retrieved) spectra is given, even if this partial identity exists in dislocated wavelength regions. To test the program, constructed (test) curves as well as real spectra were used. The system is capable of collecting in groups substances with common spectral characteristics, and thus substances belonging to the same class of chemical compounds. This makes the system a valuable tool not only for identification work but also for the study of spectral behaviour in general.

REFERENCES

1 *International Critical Tables*, Vol. V, McGrawHill, 1929.
2 *Sadtler Standard Spectra, Ultraviolet (1959)*, Sadtler Research Laboratories, Pasadena, Calif.
3 *Catalog of Ultraviolet Spectral Data, American Petroleum Institute Research Project 44 (1945–1958)*, Chemical and Petroleum Research Laboratory, Pittsburgh, Pa.
4 L. E. Kuentzel, *Anal. Chem.*, 23 (1951) 1413.
5 P. C. Jurs, B. R. Kowalski and T. L. Isenhour, *Anal. Chem.*, 41 (1969) 21.
6 R. W. Sebesta and G. G. Johnson, *Anal. Chem.*, 44 (1972) 260.
7 A. E. Gillam and E. S. Stern, *Electronic Absorption Spectroscopy*, Arnold, London, 1957.
8 C. N. R. Rao, *Ultraviolet and Visible Spectroscopy*, Butterworths, London, 1961.
9 A. I. Scott, *Interpretation of the Ultraviolet Spectra of Natural Products*, Pergamon, Oxford, 1964.
10 L. Lang, *Absorption Spectra in the Ultraviolet and Visible Region*, Vol. VIII, Akademiai Kiado, Budapest, 1967.
11 *Annu. Rev. Anal. Chem.*, 42 (1970) 239R, 240R.

Analytica Chimica Acta, 71 (1974) 35–42

ATOMIC ABSORPTION SPECTROMETRIC DETERMINATION OF CADMIUM, LEAD, SILVER, THALLIUM AND ZINC IN SILICATE ROCKS BY DIRECT ATOMIZATION FROM THE SOLID STATE

F. J. LANGMYHR, J. R. STUBERGH, Y. THOMASSEN, J. E. HANSSEN and JAN DOLEŽAL*
Department of Chemistry, University of Oslo, Oslo 3 (Norway)
(Received 15th January 1974)

The furnace techniques of atomic absorption spectrometry have proved very useful in geochemical analysis. Trace elements may now be determined by direct atomization from the solid state, so that tedious and time-consuming decompositions are no longer required, and analysis can be made without addition of reagents and without any separation or preconcentration steps.

In a previous paper[1], direct-atomization methods were described for the determination of rubidium and cesium in silicate rocks. The present paper contains methods for the determination of cadmium, lead, silver, thallium and zinc; the methods were tested by analyzing various reference and other rocks.

A survey of the literature showed that Belyaev *et al.*[2,3] have determined cadmium and silver in silicate rocks by direct atomization from a small graphite crucible heated either by a high current or by an arc. The method was used in the analysis of some international reference rocks; however, the agreement with earlier data was not very satisfactory.

Talmi and Morrison[4] describe the use of an induction furnace for the micro-analysis of solids by atomic absorption and emission spectrometry; the equipment was used for the determination of zinc in two international reference rocks, and cadmium, lead, silver and zinc in a synthetic mixture of the oxides in a silica matrix. The construction of the furnace of Talmi and Morrison differs considerably from that of the present furnace, and there are also other significant differences.

The content of the elements discussed here may vary from about 1 p.p.b. up to about 100 p.p.m. in silicate rocks. The geochemistry of some of these elements, *e.g.* cadmium and silver, is not well known.

EXPERIMENTAL

Apparatus

The measurements were made with a Perkin–Elmer 303 atomic absorption spectrophotometer equipped with a deuterium arc source background corrector. The construction of the graphite furnace (heated by a high-frequency induction generator) is described elsewhere[1]. The signals were registered with a 2-channel recorder; one of the channels plotted the peak (in percent absorption), after trans-

* On leave from Department of Analytical Chemistry, Charles University, Prague, Czechoslovakia.

formation of the percent absorption signals into absorbance by a logarithmic amplifier and integration with a laboratory-made electronic integrator; the second channel recorded the integrated peak area.

Weighings were made with semi-micro or micro balances.

Reagents

Standard solutions were prepared from high-purity metals (purity 99.99% or better), and the acids were of Suprapur quality (Merck). The argon used for purging the furnace was of purity 99.9% (by volume). Graphite of the quality used in the furnace was finely pulverized in an agate mortar and employed as a dispersing agent.

Standard solutions

Separate primary standard solutions of cadmium and zinc (1000 p.p.m.) were prepared by dissolving 1 g of the metals in 100 ml of sulphuric acid (1+5) and diluting to 1 l. A silver standard solution of the same concentration was prepared by dissolving 1 g in 100 ml of nitric acid (1+9) and diluting to 1 l. In the preparation of secondary diluted solutions, a great excess of sulphuric acid was added, so that the element would be present as the sulphate before atomization in the furnace.

Sample preparation

The present method requires sample amounts ranging from less than 1 mg up to about 20 mg. In order to avoid serious sampling errors, it is necessary to grind the samples to a very fine state of sub-division. The samples were normally ground to pass a 270-mesh (53 μm) sieve (it may be difficult to reduce the particle size of certain minerals, such as mica, to pass this sieve).

Preliminary experiments confirmed the observations made by previous authors[2], *viz.* that, for some elements, sharper signals were obtained from samples mixed with graphite. The beneficial effects of graphite were pronounced for silver and zinc; for lead no satisfactory signals could be obtained without adding graphite. The two former metals were determined in mixtures of equal amounts of sample and graphite; in the analysis of lead, a 1:3 ratio of graphite to sample was found sufficient.

For cadmium and thallium, satisfactory signals were obtained without addition of graphite.

Decompositions

Six 0.5-g portions of the Nordic reference sample ASK schist (a carbonaceous Ordovician schist) were transferred to platinum dishes and moistened with water; 15 ml of 40% hydrofluoric and 2.0 ml of 60% perchloric acids were added, and the mixtures were heated to dryness on the boiling water bath and hot plate. The evaporation was repeated with 10 ml of hydrofluoric and 1.0 ml of perchloric acids; after the second evaporation most of the carbon had been removed by oxidation. The perchlorates were finally transformed to sulphates by adding 2.0 ml of concentrated sulphuric acid and evaporating to dryness; during this operation all remaining carbon was oxidized. The residues were moistened with 3.0 ml of sulphuric acid (1+9) and water was added; the solutions were finally diluted to

50 ml and transferred to plastic bottles. A blank solution was prepared. The series of solutions was used in the determination of cadmium by the furnace technique.

For the determination of zinc in the ASK schist by the conventional flame technique, four 0.2-g portions were transferred to platinum dishes, 5.0 ml of 40% hydrofluoric and 1.0 ml of 60% perchloric acid were added, and the mixtures were evaporated to dryness. The residues were then evaporated twice to dryness in the presence of 1.0 ml of concentrated sulphuric acid. The salts were moistened with 1.5 ml of sulphuric acid (1+9) and dissolved by adding water and heating. The solutions were finally diluted to 50 ml and transferred to plastic bottles. A blank solution was prepared.

In the analysis of zinc by the direct atomization technique, the U.S. Geological Survey reference rock BCR-1 was used as the solid standard. The content of zinc in this standard was redetermined by the conventional flame technique. Six 0.2-g portions of BCR-1 were transferred to 100-ml polyethylene bottles with screw caps, 5.0 ml of 40% hydrofluoric acid were added by pipette and the tightly closed bottles were heated in a drying oven for 30 min at 70°C. After cooling, the bottles were opened, 50 ml of saturated boric acid solution were added by pipette, and the closed bottles were reheated in the oven until the solutions were clear. The solutions were diluted to 100 ml by adding 45 ml of water by pipette. A blank solution was prepared.

Five 0.2-g portions of the reference rock W-1 were decomposed as described above for the rock BCR-1.

Procedure

Before starting the measurements with the furnace, the hollow-cathode and deuterium lamps were heated for about 1 h. Atomizations in the flame were made without use of the deuterium lamp. The measurements were made at the following wavelengths: cadmium, 228.8 nm; lead, 283.3 nm; silver, 328.1 nm; thallium, 276.8 nm; zinc: in the furnace, 307.6 nm (the concentration of zinc in silicate minerals and rocks is normally too high to permit the use of the most sensitive zinc line at 213.9 nm), and in the flame, 213.9 nm. The flow of argon was adjusted to 6 ml s^{-1}.

Suitable amounts (1–20 mg) of solid samples or standards with or without added graphite were weighed in small tantalum scoops (Perkin–Elmer) and placed in the middle of the furnace by means of a laboratory-made adjustable inserting device (a commercial type is produced by Perkin–Elmer). The scoops were reweighed.

It is recommended that analyses of liquid samples or standards in the furnace should be based on adding a constant volume, which should not exceed 25 μl. Syringes were used to insert liquids through the radial opening of the furnace.

After having established by some preliminary measurements the amounts of solid or liquid samples or standards suitable for use, these were weighed out or pipetted. The measurements were normally made in the following order: standard 1—sample 1—standard 2—sample 2, *etc.* The amounts of standard were varied in such a way that a calibration curve could be plotted, and that signals below and above those of the samples were obtained.

Elements giving very sharp peaks can often be analyzed by measuring the peak heights, but, in the present investigation, all determinations were based on measuring the integrated peak areas.

Cadmium was determined as follows. Sample or standard solutions were

evaporated in the furnace at 80°C for 45 s, the residues were heated at 130°C for 45 s and atomized at 1700°C for 45 s. The furnace was cleaned by 60-s heating at maximum voltage (1950°C).

Solid samples (without added graphite) were dried at 130°C for 45 s; the further procedure was the same as described above for solutions. Preliminary experiments had shown that cadmium in solid samples could be determined by measurements with liquid standards; these were evaporated, dried and atomized as described above.

The contents of cadmium in the present samples were too low to permit determinations by the conventional flame technique.

Preliminary studies had demonstrated that liquid standards could not be used in the determinations of lead, silver and zinc by the direct atomization technique. As solid natural standards in these analyses, the following U.S. Geological Survey reference samples were selected: for lead, W-1 (content 8.1 p.p.m. according to analyses—*vide infra*—in the furnace); for silver, AGV-1 (content 0.11 p.p.m. according to Flanagan[5]); for zinc BCR-1 (content 113 p.p.m. according to analyses by the conventional flame technique, see Table IV below).

The mixtures of the solid samples or standards with graphite were prepared by mixing and pulverizing intimately 0.1000 g of the sample or standard with the proper amount of graphite (0.1000 g for silver and zinc, 0.0333 g for lead) in an agate mortar.

The drying procedure for lead, silver and zinc was the same as for cadmium (*vide supra*); the subsequent 60-s atomizations were made at 1750°C for lead, 1700°C for silver and 1800°C for zinc. Every run was finished by a 60-s heating at 260 V (1950°C).

Zinc could also be determined by the conventional flame technique, but the concentrations of silver were below the detection limit of this method.

The content of lead in W-1 was established by measurements with the glass issued by the National Bureau of Standards. A 3-mm wafer no. 612 was pulverized finely in an agate mortar; 75.0 mg of the powder were mixed intimately with 25.0 mg of graphite powder. Five portions of the glass and of W-1 were atomized, as described below, in the furnace. From the certificate value of lead (38.57 ± 0.2 p.p.m.) in the glass, the content of lead in W-1 was found to be 8.1 p.p.m. (the average value listed by Flanagan[5] is 7.8 p.p.m.)

Thallium was determined without the addition of graphite; as the natural solid standard in these analyses, the U.S. Geological Survey reference rock GSP-1 was selected. The content of thallium in this sample is not exactly known, but, according to Flanagan[5], it is 1.3 p.p.m. In a recent compilation, Flanagan[5] has tabulated the 1972 values for international geochemical reference samples; from this list it appears that for thallium no recommended values—only averages or magnitudes—can be indicated; for a number of samples, no thallium values have been published.

It was found desirable to carry out a redetermination of thallium in GSP-1. The low concentration prevented analyses of solutions in the flame or in the furnace. However, the standard addition technique, based on adding a constant volume (10 μl) of a series of thallium(I) solutions (as the sulphate) to 10.0-mg portions of GSP-1, was successful, and the mixtures gave a single sharp peak. By the method

of least squares, the content of thallium in GSP-1 was found to be 1.3 p.p.m., *i.e.* of the magnitude listed by Flanagan[5]; consequently, the value 1.3 p.p.m. was chosen as the content of thallium in GSP-1. The mixtures of solid sample and thallium standard solution were first heated at 105°C for 60 s and then at 450°C for 60 s; they were then atomized at 1750°C for 60 s. Solid samples without added solution were given the same treatment, but without the heating at 450°C.

RESULTS AND DISCUSSION

Tables I–IV contain the results obtained by the direct-atomization technique; as is apparent from the Tables, some samples were also analyzed by atomizing sample solutions in the furnace or in the flame. The present data have not been corrected for the content of hygroscopic water. For the international and Nordic reference rocks, some recently published values are also tabulated.

TABLE I

ANALYTICAL RESULTS FOR CADMIUM

Results are expressed as p.p.m. Cd.)

Sample and type of rock	Sample specifications	Atomizing solid sample in furnace				Atomizing sample solution in furnace				Previous data	
		N^a	$\bar{X}$	s	s_r	N	$\bar{X}$	s	s_r	$\bar{X}$	Reference
W-1 Diabase	—	3	0.16	0.03	17	—	—	—	—	0.164	6
										0.151	7
										0.3	8
BCR-1 Basalt	Split/position 77/4	4	0.14	0.01	7	—	—	—	—	0.12	5
										0.154	6
GSP-1 Granodiorite	Split/position 15/22	6	0.052	0.003	6	—	—	—	—	0.06	5
										0.068	6
										0.050	7
ASK Schist	Series 1 Bottle no. 037	16	0.88	0.10	12	6	0.86	0.17	20	0.75	9

N denotes the number of analyses: X, average; s, standard deviation; s_r, relative standard deviation.

Table I lists the data for cadmium. The data obtained compare favourably with recent analyses by the absorption tube technique[6] and with activation analysis[7]. The latest data for cadmium in W-1 indicate that the value (0.3 p.p.m.) listed by Fleischer[8] is somewhat high. The detection limit (defined as the amount giving a recorder deflection twice that of the average maximum noise) for cadmium by the proposed direct-atomization method was found to be approximately $3 \cdot 10^{-11}$ g.

The proposed method was applied to the determination of lead in a series of samples previously analyzed by X-ray spectrography. In Table II, the present and X-ray[10] data are listed. For most samples the agreement between the results is satisfactory. Considering the low levels of lead, the proposed method can be classified as moderately precise. Unfortunately, there were not sufficient data from

TABLE II

ANALYTICAL RESULTS FOR LEAD AND THALLIUM

(Unless otherwise stated, 5 analyses of each sample were made; results are expressed as p.p.m. Pb or Tl.)

Sample and type of rock		*Content of lead*				*Content of thallium by atomizing solid sample in furnace*		
		Atomizing solid sample in furnace			*X-ray spectrography*			
		$\bar{X}$[a]	s	s_r	($\bar{X}$) (ref. 10)	$\bar{X}$	s	s_r
Gneiss	1/66	23	2.2	10	26.7	2.4	0.35	15
Gneiss	3/66	12	2.4	20	14.5	1.4	0.21	16
Gneiss	7/66	8	2.4	32	6.0	< 0.1[b]	—	—
Gneiss	11/66	43	2.6	6	36.2	0.71	0.08	11
Mangerite	39/66	16	1.8	11	15.3	$\leqslant 0.1$[b]	—	—
Mangerite	45/66	40	3.0	8	41.2	< 0.1[b]	—	—
Mangerite	92/66	16	1.2	7	15.8	< 0.1[b]	—	—
Mangerite	99/66	19	2.3	13	20.2	0.19	0.09	47
Granulite (banded)	16/66	17	1.5	9	16.7	0.22	0.05	23
Granulite (banded)	50/66	25	2.9	12	22.2	0.19	0.02	11
Granulite (banded)	103/66	11	3.5	33	11.8	< 0.1[b]	—	—
Anorthosite	94/66	2	0.4	20	4.6	< 0.1[b]	—	—

[a] Symbols as in Table I.
[b] Only 3 analyses were made.

the X-ray spectrographical investigation to compare the results by statistical methods. The detection limit for lead by the proposed technique, and measurements at the wavelength 283.3 nm, was found to be approximately 10^{-9} g.

The analytical results for silver are listed in Table III, which also gives some recent values from the literature. The content of silver in silicate rocks is normally well below 1 p.p.m., which made it difficult to employ methods based on atomizing sample solutions in the flame or in the furnace. From the literature it appears that the methods which have been employed in the determination of silver in rocks are limited to optical spectrography, mass spectrometry, neutron activation analysis and atomization from the solid state.

The number of determinations of silver in W-1, BCR-1 and GSP-1 is rather small, and the agreement between the values is not very satisfactory. More work is required before any recommended values can be indicated. For the ASK schist, only one other analysis (by emission spectrography) had been performed. The detection limit for silver by the proposed technique was found to be about $6 \cdot 10^{-11}$ g.

The method developed for thallium was used in the analysis of the samples in which lead was also determined. The results are listed in Table II; no previous data were available for comparison. The detection limit for thallium was calculated to be about 10^{-9} g.

In Table IV, the results for zinc are given together with some recent values from the literature. The present data for zinc in W-1 are in good agreement with

TABLE III

ANALYTICAL RESULTS FOR SILVER

(5 analyses of each sample were made; results are expressed as p.p.m. Ag.)

Sample and type of rock	*Sample specifications*	*Atomizing solid sample in furnace*			*Previous data*	
		$\bar{X}$[a]	s	s_r	$\bar{X}$	*Reference*
W-1 Diabase	—	0.079	0.005	6	0.05	8
					0.068	11
					0.029	3
BCR-1 Basalt	Split/position 77/4	0.050	0.009	20	0.036	5
GSP-1 Granodiorite	Split/position 15/22	0.12	0.01	8	0.10	5
ASK Schist	Series 1 bottle no. 037	0.43	0.04	9	0.3	12

[a] Symbols as in Table I.

TABLE IV

ANALYTICAL RESULTS FOR ZINC

Results are expressed as p.p.m. Zn.)

Sample and type of rock	*Sample specifications*	*Atomizing solid sample in furnace*				*Atomizing sample solution in flame*				*Previous data*	
		N[a]	$\bar{X}$	s	s_r	N	$\bar{X}$	s	s_r	$\bar{X}$	*Reference*
W-1 Diabase	—	10	78	14	18	5	82	3	3.3	82	8
BCR-1 Basalt	Split/position 77/4	—	—	—	—	6	113	3	2.7	120	5
GSP-1 Granodiorite	Split/position 15/22	10	95	13	14	—	—	—	—	98	5
ASK Schist	Series 1 bottle no. 37	5	164	11	7	4	158	10	6	166	12

Symbols as in Table I.

the value recommended by Fleischer[8]. The present determinations of zinc in BCR-1 by the flame method gave the average 113 p.p.m.; this result was chosen as the standard value in the analyses by the direct-atomization technique. The value 113 p.p.m. of zinc is somewhat lower than the latest value—120 p.p.m.—recommended by Flanagan[5] (in 1969 the average value for zinc in BCR-1 was 132 p.p.m.[5]). The present value for zinc in GSP-1 (95 p.p.m.) is in good agreement with the latest recommended value[5] (98 p.p.m.). For the Nordic reference sample ASK schist, the values 164 and 158 p.p.m. of zinc were obtained by atomizing solid samples and sample solutions, respectively; these results compare favourably with the average

166 p.p.m. obtained by various techniques[12]. The detection limit for zinc by the present measurements at the wavelength 307.6 nm was calculated to be about $1.5 \cdot 10^{-7}$ g.

SUMMARY

Atomic absorption spectrometric methods are described for the determination of cadmium, lead, silver, thallium and zinc in some international and other silicate rocks. The metals are atomized directly from the solid samples in a graphite furnace. The data are compared with results obtained by atomizing solutions in the flame, in the graphite furnace, and with earlier data.

REFERENCES

1 F. J. Langmyhr and Y. Thomassen, *Z. Anal. Chem.*, 264 (1973) 122.
2 Y. J. Belyaev, A. M. Pchelintsev, N. F. Zvereva and B. J. Kostin, *Zh. Anal. Khim.*, 26 (1971) 492.
3 Y. J. Belyaev, A. M. Pchelintsev and N. F. Zvereva, *Zh. Anal. Khim.*, 26 (1971) 1295.
4 Y. Talmi and G. H. Morrison, *Anal. Chem.*, 44 (1972) 1455.
5 F. J. Flanagan, *Geochim. Cosmochim. Acta*, 37 (1973) 1189.
6 J. Yamada, C. Iida and K. Yamasaki, *Jap. Anal.*, 19 (1970) 1259.
7 S. Marowsky, *Z. Anal. Chem.*, 253 (1971) 267.
8 M. Fleischer, *Geochim. Cosmochim. Acta*, 33 (1969) 65.
9 E. Steinnes, Private communication.
10 K. S. Heier, Private communication.
11 A. O. Brunfelt and E. Steinnes, *Radiochem. Radioanal. Lett.*, 1 (1969) 219.
12 Results from a cooperative Nordic investigation, to be published.

C.S.I.R.-R.F.is 679

Analytica Chimica Acta, 71 (1974) 43–51

FURTHER INVESTIGATIONS OF THE SPECTROMETRIC ANALYSIS OF RAW GOLD BY GLOW DISCHARGE EXCITATION

H. JÄGER

National Physical Research Laboratory, C.S.I.R., Pretoria (South Africa)

(Received 20th November 1973)

The glow discharge lamp was first introduced into spectrochemistry by Grimm[1]. It has found wide application in the analysis of both conductive and non-conductive materials. Several studies on the properties of this lamp have been reported[2–5]. The glow discharge lamp has also been used for the analysis of raw gold (80–90% Au) and refined gold (99.6% Au), based on one set of analytical lines and the same mathematical treatment of the raw intensity data[6,7].

Raw gold was considered as the ternary system gold–silver–copper with additional impurities such as lead, iron, nickel, *etc.* All three major elements were shown to cause serious interelement interferences. A brief explanation of these third-partner effects has been given[6], but a more detailed explanation is reported here.

In practice, lead proved to be present in relatively high concentrations thus causing additional interference. It therefore seemed necessary to reconsider the previously established system for the analysis of raw gold, and to learn more about the nature of the interferences with the aim of improving the analyses.

EXPERIMENTAL

Samples and apparatus

The lack of standards for the system Au–Ag–Cu–Pb required an approach to the problem in two steps. The interferences were studied with available standards of the type Au–Ag–Cu. The analytical system was then tested with accurately analysed samples containing lead, taken from the production runs. These samples then served as standards.

The glow discharge lamp used was a commercial light source (RSV, Germany). The measuring system used was a 2-m grating spectrometer (Ebert mount, RSV) with an on-line computer (Data General Corporation, Nova).

The tests carried out consisted of the simultaneous recording of spectral lines of the elements of the sample and the discharge gas, the recording of the discharge parameters, and the determination of the absolute sputtering rates of the samples. Table I shows the spectral lines investigated (the Cu 324.32-nm line could not be recorded simultaneously with the other lines because of its proximity to the Cu 324,75-nm line). Table II shows the concentrations of the investigated samples.

TABLE I

SPECTRAL LINES

Element	*Line*	*Wavelength (nm)*	*Excitation energy (eV)*
Gold	Au I	312.28	5.10
	Au I	264.15	5.82
Silver	Ag I	338.29	3.66 (Resonance)
	Ag I	381.09	7.02
Copper	Cu I	324.75	3.82 (Resonance)
	Cu I	324.32	8.92
Argon	Ar I	420.07	14.50
	Ar II	434.81	19.49

TABLE II

CONCENTRATION OF STANDARDS (%)

Au	*Ag*	*Cu*	*Au*	*Ag*	*Cu*
100	—	—	84	15	1
99	1	—	83.5	15	1.5
97	3	—	83	15	2
95	5	—	80	15	5
90	10	—	90	5	5
85	15	—	85	10	5
84.5	15	0.5			

Non-linear calibration curves

Thus far, only non-linear calibration curves have been reported when the glow discharge lamp has been used for the analysis of raw gold[6]. Usually linearity up to very high concentrations is claimed.

Figure 1 depicts the comparison of calibration curves of two silver lines obtained under various discharge conditions. The Ag 338.29-nm line is a resonance line; the Ag 381.09-nm line emits to a level 3.77 eV above the ground level. The non-resonance line produced linear calibration curves from 0 to 15% under all conditions. The resonance line showed varying curvature depending on the discharge conditions. Measurements of the absolute sputtering rates (mg min^{-1}) showed that the highest sputtering rates were obtained under conditions which caused maximal curvature of the calibration curves.

Both copper lines produced non-linear calibration curves, the resonance Cu 324.75-nm line being more affected. The reason for the slight non-linearity of the Cu 324.32-nm calibration curve will be discussed later. Both gold lines investigated showed linear intensity increases from 85 to 100% gold.

It can therefore be concluded that the non-linearity of calibration curves is caused by self-absorption. Since the self-absorption depends on the density of atoms in the plasma and therefore on the amount of sputtered material, discharge conditions can be chosen, as is shown in Fig. 1, which suppress self-absorption to a

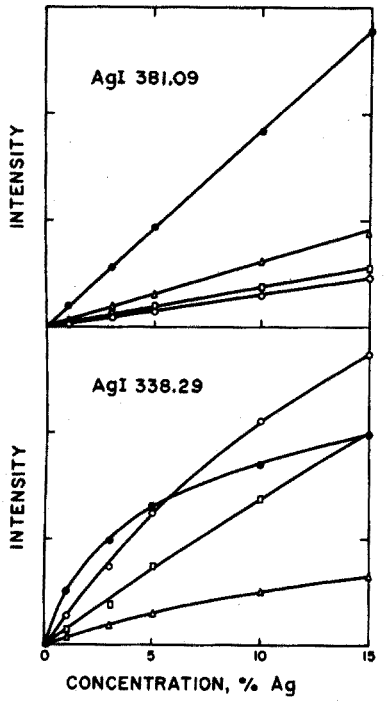

Fig. 1. The influence of varying discharge parameters on the emission of a non-resonance and a resonance silver line. (●) const. 1 kV, ≈100 mA, 7.5 Torr; (○) const. 1 kV, ≈55 mA, 5 Torr; (□) const. 1.5 kV, ≈50 mA, 4 Torr; (△) const. 2 kV, ≈50 mA, 2.5 Torr.

certain degree. In the case of trace analysis, however, considerably higher sputtering rates are required and self-absorption then is unavoidable.

Splitting of calibration curves

Besides the non-linearity, a third partner effect causes serious splitting of the calibration curves[6]. A comparison of sputtering rates (expressed in particles per time unit, n min^{-1}) to measured intensities of gold, silver, and copper lines is shown in Fig. 2. As can be seen in the lower part of the graph, the presence of copper caused a splitting of the gold and silver calibration curves, and the presence of silver split the copper calibration curve. Similarly, in the upper part of the graph, the presence of copper and silver reduced the sputtering. The sputtering rates shown in Fig. 2 are based on the total sputtering rates measured on each sample (three determinations); the individual rates were then calculated.

There is a linear relationship between the respective sputtering rates S and the intensities I of the Au 264.15, Ag 381.09 and Cu 324.32-nm lines:

$$I = k \cdot S \tag{1}$$

where k is a constant, and the intensities can be calculated, if the sputtering rates are known. In the case of the Ag 338.29-nm and Cu 324.75-nm lines, self-absorption causes a marked deviation from linearity. At the Au 312.28-nm line, there is a slight deviation from linearity.

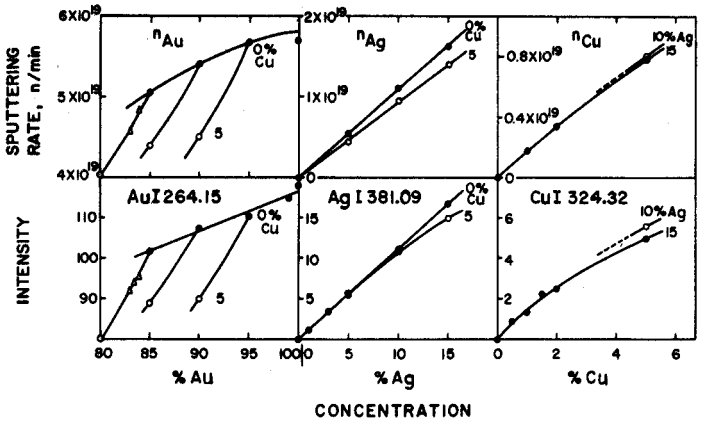

Fig. 2. Sputtering rates and line intensities of gold, silver and copper in Au–Ag–Cu alloys. Discharge conditions: const. 1 kV, 100–110 mA, 7.5 Torr.

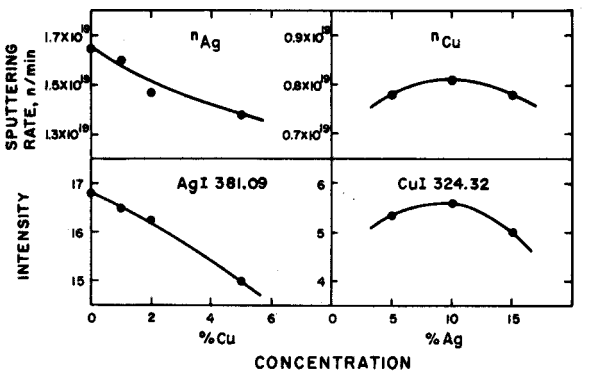

Fig. 3. Effect of copper concentration on silver emission (15% Ag) and silver concentration on copper emission (5% Cu) compared with the individual sputtering rates of the elements in Au–Ag–Cu alloys. Discharge conditions: const. 1 kV, 100–110 mA, 7.5 Torr.

Figure 3 shows the influence of varying copper and silver concentrations on the silver and copper intensities. Increasing copper content causes a steady decrease in the silver intensity (15% Ag), whereas the copper intensity (5% Cu) reaches a maximum if 10% silver is present.

DISCUSSION

The interferences can be explained as follows.

(i) Self-absorption causes a non-linear relationship between intensity and concentration in the case of resonance lines.

(ii) The presence of copper in a gold sample reduces the sputtering rate and therefore reduces the intensities of all emitted lines. This leads to splitting of the calibration curves for gold and silver as a function of the copper concentration. Varying silver concentrations in the sample influence the sputtering to a lesser degree,

but also cause splitting (copper calibration). It can be assumed that lead would also contribute to this type of interference.

(iii) It follows from (ii) that a linear calibration curve for copper in gold cannot exist even if a non-resonance line is used, because the increase of copper in the sample leads to a non-linear reduction of the sputtering rate (Fig. 2).

Discharge characteristics

It has already been reported that the current at constant voltage and pressure shows strong variations from sample to sample[6]. Figure 4 shows a comparison of four quantities which represent the lamp system as a whole, namely the total sputtering rate, the discharge current and the emission of the argon I and II lines at 420.07 and 434.81-nm, respectively. These four quantities are depicted as functions of the gold concentration. They show very good agreement.

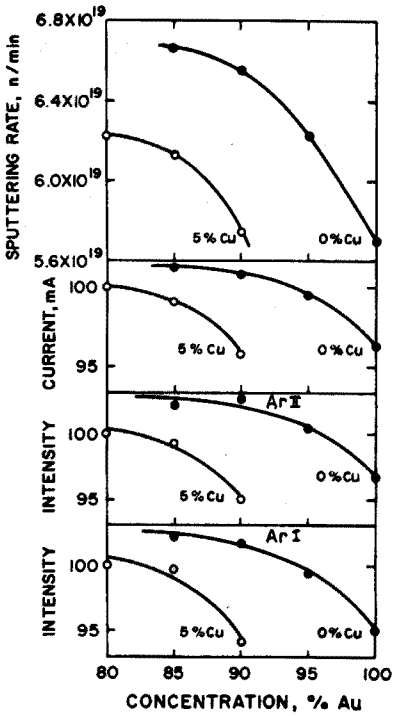

Fig. 4. Intensities of argon I and II lines, discharge current and sputtering rate related to gold concentration. (●) Au–Ag alloys, (○) Au–Ag–Cu alloys with 5% Cu. Discharge conditions: const. 1 kV, 100–110 mA, 7.5 Torr.

Obviously the current is a function of the total sputtering rate. An increase in copper concentration from 0 to 5% causes a decrease in both the total sputtering rate and the current. There is a general increase in the total sputtering rate with decreasing gold concentration (at constant copper concentration), which results in increasing current. At constant discharge voltage and pressure, the total sputtering rate is determined by the magnitudes of these two parameters. The

discharge current is then a function of the conductivity of the plasma which consists of atoms and ions of both the discharge gas and the sample and of electrons. Since there is a difference in ionization energies for metal atoms of the sample and for gas atoms (Cu 7.72, Ag 7.57, Au 9.22, and Ar 15.76 eV), an increase in metal atoms in the plasma must lead to an increase in the current.

Owing to the low gas pressure, an excitation mechanism of the argon atoms by collisions of the first kind can be assumed. An increase in the electron density must therefore influence the emission of the argon lines. This is confirmed by the very good agreement between current and intensities of argon lines (Fig. 4).

The variations of the electron pressure should also influence the emission of the sample atoms in spite of the good agreement found between sputtering rate and intensity (Fig. 2), but the influence is not as marked as in the argon lines. There is a greater probability for an electron to collide with an argon atom or ion than with a metal atom, because the electrical field quickly transports the electrons out of the metal vapour, which is concentrated in front of the cathode. The metal vapour does not penetrate very deeply into the gas atmosphere of the discharge chamber, because the gas stream is directed towards the cathode and is quickly sucked away through a small gap surrounding it. Side-on observations of the line emission in the glow-discharge lamp show that argon lines are emitted over a longer distance from the cathode than are the lines of the metals of the sample[2].

The variations of the electron pressure seem to be the reason for the splitting of the calibration curves in Fig. 5 (upper curves).

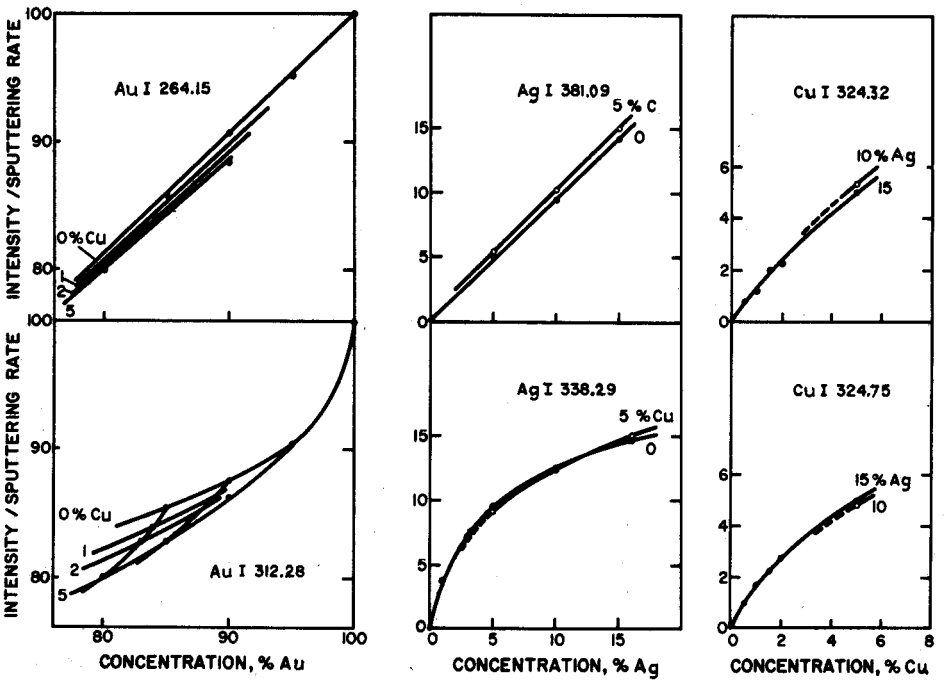

Fig. 5. Gold, silver and copper calibration curves at const. 1 kV, 100–110 mA, 7.5 Torr.

Analytical aspects

The above findings should make improved gold analyses possible, if non-resonance lines are employed, because of the steeper slopes of the calibration curves. To prove this, two line groups—Au 312.28, Ag 338.29, Cu 324.75 nm, and Au 264.15, Ag 381.09, Cu 324.32 nm—were compared. The raw intensity data were treated as reported previously[6]:

The raw intensity data I are normalized so that

$$I'_{Au} : I'_{Ag} : I'_{Cu} \ldots = c_{Au} : c_{Ag} : c_{Cu} \ldots \quad (2)$$

where c is the concentration in the sample, and I' is referred to the relative sputtering rate S of the sample, which is given as

$$S = I'_{Au} + I'_{Ag} + I'_{Cu} + \ldots \quad (3)$$

The normalized intensities

$$J = I'/S \quad (4)$$

are then plotted against concentration to establish calibration curves.

Figure 5 shows the sets of calibration curves thus obtained. There is marked improvement in the interference effects if the second (in the graph the upper) set of spectral lines is used: the calibration curves are almost linear and the slopes are close to 45°.

In practice, as already mentioned, lead plays an important role and the system Au–Ag–Cu–Pb has to be considered. With the aid of 47 standards (accurately analysed samples containing all four elements taken from the production runs), calibration curves were established. In the case of lead, only the Pb 405.78-nm line was recorded. No alternative line, as in the case of silver or copper, could be found in the glow discharge spectrum.

The excitation conditions were chosen after a careful study of burn-off curves; those chosen allow constant intensity ratios during the integration period: constant 1 kV. 100–110 mA, 7.5 Torr, 20-s preburn time, 15-s integration time. Three measurements, taken at random, were averaged. For the two sets of spectral lines investigated in this report (the Cu 402.27-nm line was used instead of the 324.32-nm line to allow the simultaneous recording of two copper lines), plus the lead line, two curve-fitting calculations were carried out to eliminate the four element interferences; second and third order polynomials of the following type were applied:

$$\left.\begin{aligned} c = {} & x_1 + x_2 J_1 + x_3 J_2 + x_4 J_3 + \\ & x_5 J_1^2 + x_6 J_2^2 + x_7 J_3^2 + x_8 J_1 J_2 + x_9 J_1 J_3 + x_{10} J_2 J_3 + \end{aligned}\right] (5) \quad \left.\begin{aligned} & \text{2nd order} \\ & \text{polynomial} \end{aligned}\right.$$

$$\left.\begin{aligned} & x_{11} J_1^3 + x_{12} J_2^3 + x_{13} J_3^3 + x_{14} J_1^2 J_2 + x_{15} J_1^2 J_3 + x_{16} J_2^2 J_1 + \\ & x_{17} J_2^2 J_3 + x_{18} J_3^2 J_1 + x_{19} J_3^2 J_2 + x_{20} J_1 J_2 J_3 \end{aligned}\right] (6) \quad \left.\begin{aligned} & \text{3rd order} \\ & \text{polynomial} \end{aligned}\right.$$

where c = concentration, J = normalized intensity/sputtering rate, 1, 2, 3 being Au, Ag and Cu, respectively, x = coefficients.

One set of coefficients was calculated for each of the four major elements gold, silver, copper and lead. The calculations were carried out on an IBM 360/65 computer.

Several samples were analysed and concentrations were obtained for both line groups and both types of curve fitting.

The results were as follows.

(i) The line group containing the resonance lines required a third-order curve fitting, while for the second line group a second-order curve fitting sufficed. Accuracy of curve fitting was improved when the second line group was used.

(ii) The precision of the determination of gold and silver was improved when the second line group was applied (relative standard deviation for gold was 0.1% instead of 0.5%, and for silver 1.3% instead of 3.3%).

(iii) The accuracy of the analysis was also improved when the second line group was used. Table III shows a comparison of spectrometric analyses and accepted values for several samples.

TABLE III

ACCURACY OF SPECTROMETRIC GOLD ANALYSIS

Spectrometric values (%)[a,b]				*Accepted values (%)*[c]			
Au	*Ag*	*Cu*	*Pb*	*Au*	*Ag*	*Cu*	*Pb*
80.17	12.19	4.96	2.41	80.12	12.09	5.03	2.52
87.81	9.39	2.47	0.25	87.88	9.36	2.51	0.19
89.17	8.96	1.69	0.07	89.33	8.72	1.70	0.03
88.38	9.63	1.84	0.09	88.53	9.52	1.84	0.03
86.00	9.41	2.34	2.13	86.05	9.39	2.32	2.08
85.89	11.13	2.20	0.59	85.94	10.94	2.26	0.76
85.04	12.39	2.36	0.07	85.06	12.31	2.34	0.07
84.21	12.48	3.17	0.00	84.30	12.48	3.23	0.02

[a] Non-resonance lines; second order curve fitting.

[b] Average of three determinations: the s_r values of the single determinations were 0.1% for Au, 1.3% for Ag, 1.7% for Cu, and 3.5% for Pb.

[c] Determined by fire assay, a.a.s. and wet chemical methods at the Rand Refinery, Ltd.

The author wishes to thank the Rand Refinery Limited, South Africa, for the support received.

SUMMARY

Studies leading to an explanation for interference effects found in the analysis of raw gold by the glow discharge method are reported. Splitting of the calibration curves is caused by changes in the sputtering rate, which are mainly caused by varying copper contents of the sample. Non-linearity of calibration curves is caused by self-absorption, and is observed when resonance lines are used. An improvement in the analysis of raw gold has been achieved with the use of non-resonance lines and by the application of a four-element-interference correction by computer.

REFERENCES

1 W. Grimm, *Spectrochim. Acta*, 23B (1968) 443.

2 M. Dogan, K. Laqua and H. Massmann, *Spectrochim. Acta*, 26B (1971) 631.
3 M. Dogan, K. Laqua and H. Massmann, *Spectrochim. Acta*, 27B (1972) 65.
4 S. El Alfy; K. Laqua and H. Massmann, *Z. Anal. Chem.*, 263 (1973) 1.
5 P. W. J. M. Boumans, *Anal. Chem.*, 44 (1972) 1219.
6 H. Jäger, *Anal. Chim. Acta*, 58 (1972) 57.
7 H. Jäger, *Anal. Chim. Acta*, 60 (1972) 303.
8 H. Jäger and J. H. J. Coetzee, *J.S.A. Chem. Inst.*, 25 (1972) 103.

Analytica Chimica Acta, 71 (1974) 53–65

DETERMINATION OF SILICON AND OXYGEN IN COAL AND COAL ASH BY 14-MeV NEUTRON ACTIVATION

C. BLOCK* and R. DAMS

Institute for Nuclear Sciences, Rijksuniversiteit Gent, Proeftuinstraat 86, B-9000 Gent (Belgium)

(Received 2nd January 1974)

The combustion of coal is still considered as one of the major sources of air pollution, especially through the production of aerosols. Therefore, a knowledge of the inorganic impurity content of coal and the composition of its ash is useful in order to elucidate some problems associated with atmospheric pollution.

Since silicon is a major constituent of coal ash, it seems likely that, during combustion, large amounts of it become airborne; this may explain the high silicon concentrations encountered in atmospheric aerosols. Van Grieken and Dams[1] found silicon concentrations ranging from 4 to 14 $\mu g\ m^{-3}$ in aerosols collected in the industrial zone and the urban environment of Ghent. Henry and Bloser[2], also mention high silicon concentrations in air samples collected above different towns in the U.S.A. The determination of oxygen, although not of immediate importance to environmental pollution, can give information useful towards accounting for the total mass of coal ash.

Within the framework of a detailed study of atmospheric air pollution by aerosols in Belgium, the influence of the combustion of fossil fuels is being studied, mainly by thermal neutron activation analysis[3]. Silicon and oxygen are the only major constituents of coal ash that cannot be determined by reactor neutron activation; the use of 14-MeV neutrons for the determination of these components was therefore investigated. Activation analysis of silicon and oxygen with 14-MeV neutrons has the advantages of being instrumental, fast and non-destructive, leaving the sample available for further analyses. A few authors[4,5] have already described the analysis of silicon and oxygen in coal and coal ash by this technique. In the present work, the accuracy and reproducibility of their simultaneous determination by 14-MeV neutron activation are critically studied.

Nuclear data

Irradiation with 14-MeV neutrons of silicon and oxygen in coal and coal ash gives rise to several nuclear reactions, the most important of which are summarized in Table I. The most widely used nuclide for the determination of oxygen is ^{16}N, whose highly energetic γ-rays can be counted almost without interference above 4.5 MeV. Of the three isotopes produced from silicon, ^{28}Al is the most abundant and therefore most commonly used.

*Research fellow of the I.W.O.N.L.

TABLE I

IMPORTANT NUCLEAR REACTIONS ON 14-MeV NEUTRON IRRADIATION

Element	*Nuclear reaction*	*Isotopic abundance (%)*	*Cross section (mb)*	*Half-life*	*γ-Energy (MeV) (Abundance %)*
O	$^{16}O(n, p)\,^{16}N$	99.76	35.1	7.13 s	6.13(68); 7.12(5)
	$^{16}O(p, \alpha)\,^{13}N$	99.76	—	10.0 min	0.511(100)
Si	$^{28}Si(n, p)^{28}Al$	92.21	250	2.24 min	1.78(100)
	$^{29}Si(n, p)^{29}Al$	4.7	101	6.6 min	1.27(94); 2.43(6)
	$^{30}Si(n, \alpha)\,^{27}Mg$	3.1	80	9.5 min	0.84(69); 1.01(30)
F	$^{19}F(n, \alpha)\,^{16}N$	100	57	7.13 s	6.13(68); 7.12(5)
B	$^{11}B(n, p)\,^{11}Be$	80.39	3.3	13.7 s	6.81(4.4); 7.99(1.7)
P	$^{31}P(n, \alpha)\,^{28}Al$	100	140	2.24 min	1.78(100)
Al	$^{27}Al(n, \alpha)\,^{24}Na$	100	120	15.00 h	1.37(47); 2.75(52)
	$^{27}Al(n, \alpha)\,^{28}Al$	100	0.53	2.24 min	1.78(100)
Fe	$^{56}Fe(n, p)^{56}Mn$	91.66	115	2.582 h	0.85(100); 1.81(29)
Mg	$^{24}Mg(n, p)^{24}Na$	78.70	200	15.00 h	1.37(47); 2.75(52)
C	$^{13}C(p, n)^{13}N$	1.11	—	10.0 min	0.511(100)
N	$^{14}N(n, 2n)^{13}N$	99.60	—	10.0 min	0.511(100)

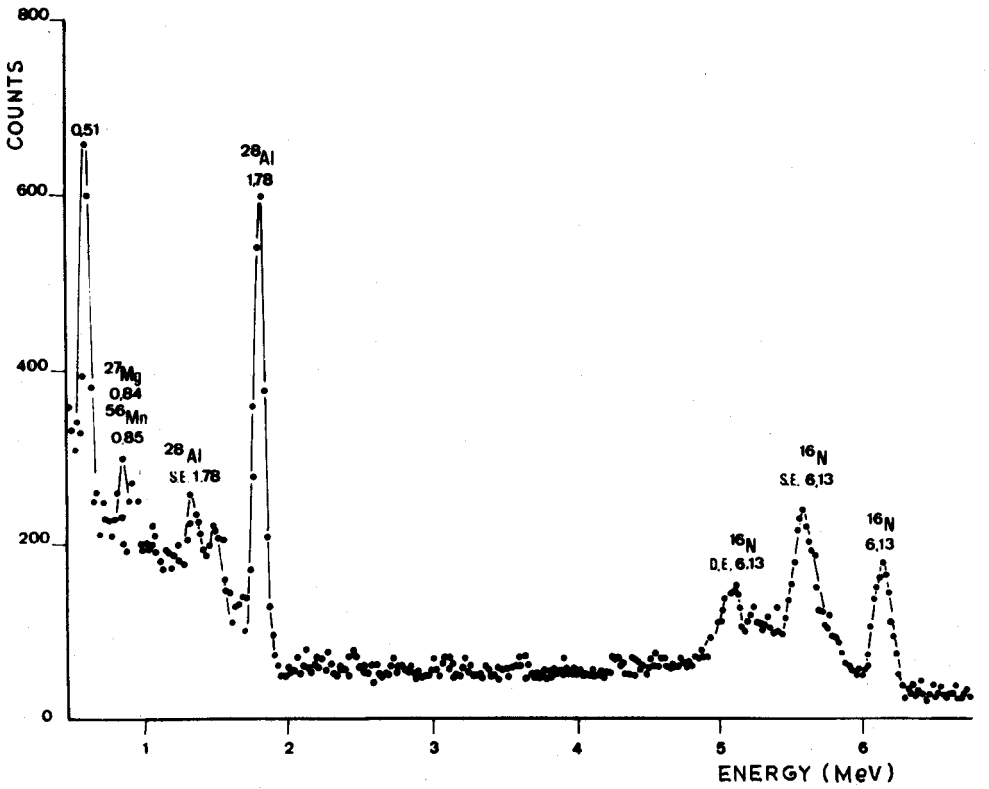

Fig. 1. ^{16}N spectrum recorded after irradiation of a coal sample; $T_{irr} = 15$ s, $T_{cool} = 5$ s, $T_{meas} = 15$ s.

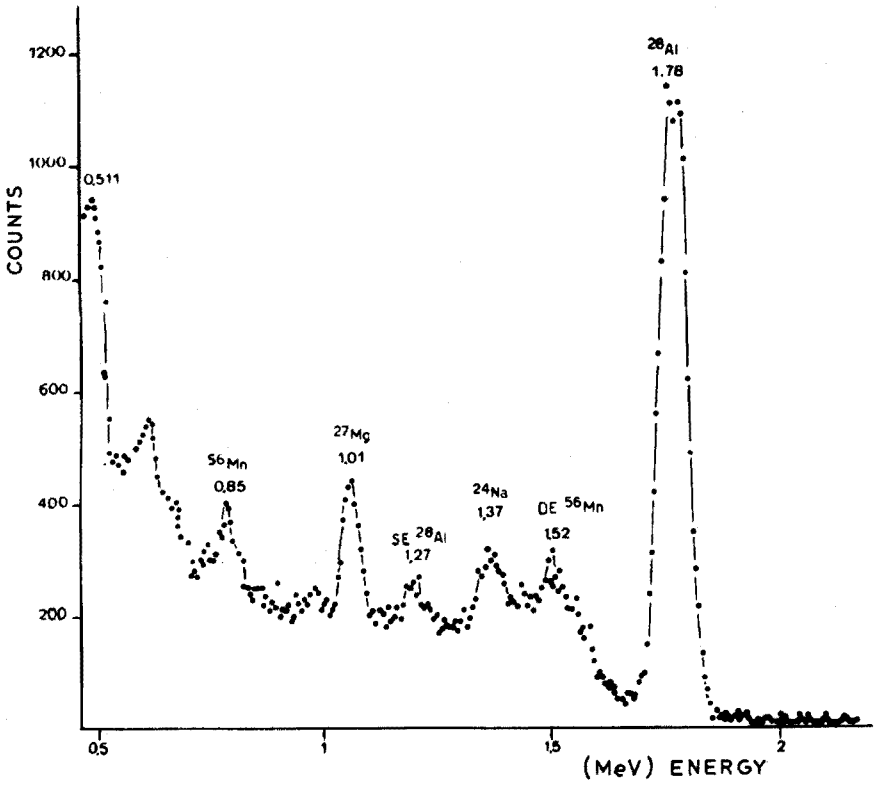

Fig. 2. ^{28}Al spectrum recorded after irradiation of a coal sample; $T_{irr} = 15$ s, $T_{cool} = 75$ s, $T_{meas} = 2$ min.

When a NaI detector is used, the ^{28}Al photopeak area may contain contributions of other γ-rays from isotopes such as ^{24}Na and ^{56}Mn. Nuclear interferences of aluminium and phosphorus must also be taken into account.

Figures 1 and 2 show ^{16}N and ^{28}Al spectra recorded after a 15-s irradiation of a coal sample at a mean neutron flux of $6 \cdot 10^8$ n s^{-1} cm^{-2}. The oxygen was counted for 15 s, after a decay time of 5 s, whereas the silicon was counted for 2 min after a 75-s waiting time.

EXPERIMENTAL

Apparatus

A Sames Type J (150 keV, 2.5 mA) 14-MeV neutron generator with a 80 MHz–60 W r.f. ion source was used. The 14-MeV neutrons were produced by the ^{3}H(d, n)^{4}He reactions from a rotating 90-Ci tritium target. The neutron production was controlled by means of a pneumatically operated removable, water-cooled tantalum screen. The pneumatic transport system consisted of a pair of rectangular aluminium tubes (internal section 9.5 mm × 26.5 mm). The neutron generator transfer system and counting equipment have been described in detail elsewhere[6, 7].

γ-Spectrometry of silicon and oxygen was performed with a 7.6×7.6 cm NaI(Tl) detector (resolution *ca.* 8%). The photomultiplier signal passed through a preamplifier and an amplifier coupled to two single-channel analysers. The first of these discriminated all signals below 4.5 MeV for the ^{16}N measurement, and the second selected an energy region between 1.68 and 1.88 MeV for the ^{28}Al measurement. Irradiation, waiting and counting times were selected automatically with electronic timers.

The output signal of the amplifier could also be fed into the convertor of an Intertechnique SA 40B 400-channel analyser. The neutron flux was monitored with a low-geometry BF_3 counter.

A diagram of the counting system is given in Fig. 3.

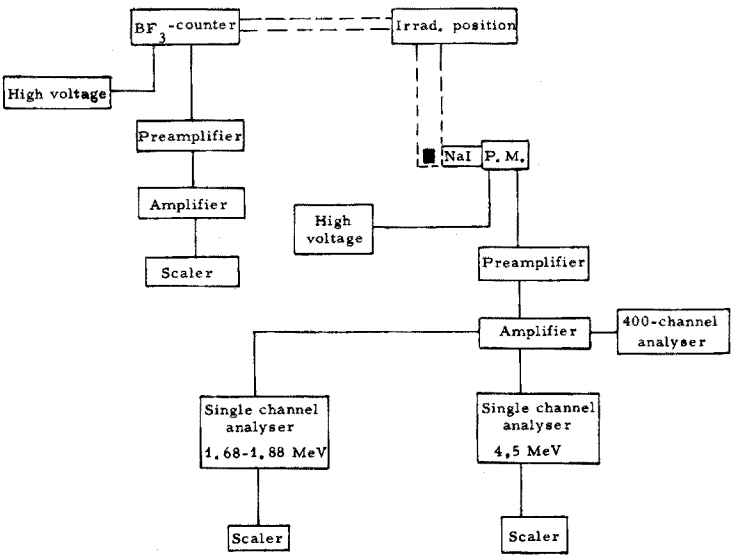

Fig. 3. Schematic diagram of counting equipment.

Preparation of standards and samples

Coal samples were ground in an agate mortar, dried at 105°C, and homogenized by shaking for 3 h. Samples with a low ash content (for home heating, coke) were packed, as such, in polyethylene cylindrical transfer rabbits with inner dimensions of 7 mm × 22 mm and outer dimensions of 9 mm × 26 mm, thus fitting into the transport system. Coal samples with high ash content (for power stations) were mixed with an equal weight of pure graphite. The mixture was homogenized by shaking for 5 h. In both cases the total sample weight amounted to about 1.5 g.

For the determination of oxygen and silicon in coal ash, 130–300 mg of ash were mixed with graphite and treated as above. Five oxygen and silicon standards were prepared from silica (Quartz feinkörnig, E. Merck). The silica powder was ground to pass through a 150-mesh sieve, homogenized by tumbling for 2 h and ignited at 1000°C. About 350 mg was weighed, mixed with spectrally pure graphite, homogenized by shaking for 5 h and packed in rabbits with the same dimensions as those used for the coal and coal ash samples.

Procedure

Oxygen and silicon can be determined after a single irradiation, when appropriate irradiation, waiting and counting times are selected, because of the difference between the half-lives of ^{16}N and ^{28}Al. An analysis cycle consisted of the following steps. Standards and samples were irradiated separately for 15 s at a beam intensity of 150 μA, *i.e.* an average neutron flux of *ca.* $6 \cdot 10^8$ neutron s^{-1} cm^{-2}.

Five s after irradiation, a 15-s measurement of ^{16}N was automatically started. The ^{16}N activity was counted integrally above 4.5 MeV.

After a cooling time of 75 s, a second measurement of 2 min was started for the silicon determination. The single-channel analyser was adjusted to measure the ^{28}Al photopeak at 1.78 MeV in the energy region between 1.68 and 1.88 MeV.

An analysis sequence consisted of the consecutive irradiation and measurement of a standard, 3–5 samples and a second standard. The average activity of both standards was used for the calculation of silicon and oxygen concentrations. All countings were normalized for neutron flux differences by means of the BF_3 long counter. Flux differences were usually quite small (*ca.* 2%).

The oxygen content of the polyethylene irradiation rabbits was 6 mg. The blank value was determined by irradiation and counting of empty sample holders in the same way as the standards and samples. This blank value did not increase significantly when the rabbit was filled with graphite. Since no significant silicon blank was found (< 0.5 mg/rabbit), only a background subtraction had to be performed.

Interferences

Oxygen. Owing to the short irradiation time and high discrimination energy, few interferences are expected. Some authors[6,8] point out that only fluorine and boron can cause substantial interference. According to Hoste *et al.*[6], an error of 100% in the oxygen determination corresponds to a F:O or B:O ratio of 2.5 or 1.2, respectively. In coal samples, such interferences are negligible, since these ratios are at least two orders of magnitude smaller.

Silicon. The elements phosphorus and aluminium may interfere with the silicon determination owing to their nuclear reactions $^{31}P(n, \alpha)^{28}Al$ and $^{27}Al(n, \gamma)^{28}Al$. The (n, p) reaction on ^{56}Fe produces the isotope ^{56}Mn; the 1.81-MeV photopeak of this isotope cannot be distinguished from the 1.78-MeV photopeak of ^{28}Al with a NaI(Tl) detector. Moreover, part of the Compton continuum of ^{24}Na formed by the (n, α) reaction of ^{27}Al and the (n, p) reaction on ^{27}Mg, contributes to the total number of counts under the 1.78-MeV photopeak of ^{28}Al.

Correction factors were determined by irradiating known quantities of Fe_2O_3, Al_2O_3, MgO and P_2O_5 under the same conditions as the standards and samples.

It was found experimentally that 1 mg of aluminium or phosphorus, respectively, produces apparent silicon contents of 0.0033 mg or 0.52 mg. Iron (1 mg) corresponds to 0.010 mg of silicon, and 1 mg of magnesium to 0.0052 mg of silicon. Since the Si:Al ratio in coal and coal ash is about 1.1, a correction was performed for the aluminium contribution. The aluminium content was known from reactor neutron activation analyses[3]. The relative correction was smaller than 0.3%. The contribution of ^{31}P to the ^{28}Al activity was also corrected for. The phosphorus

content of coal ash was determined chemically for a few samples; for the others it was estimated. The phosphorus concentration in coal was derived from its ash content. As the Si:P ratio in coal and coal ash is about 80, the correction was small. The contributions of other elements appeared to be negligible in the concentration ranges normally occurring in coal[3].

Neutron, gamma and beta attenuation

If weight, density and composition of samples and standards are not equal, differences in neutron-, γ- and β-attenuation may introduce systematic errors.

These problems have been studied by several authors[9–11]. Correction factors for neutron and γ-attenuation were calculated, according to the formulae given previously[11], for a standard and two samples, one with maximal and one with minimal density. Differences were found to be smaller than 0.1% and could consequently be neglected.

Possible systematic errors, owing to varying degrees of self-absorption of β-radiation in standard and samples of different density, were avoided by shielding the detector with a copper absorber[11]. Indeed, besides γ-radiation, ^{16}N also emits β^--radiation with a maximum energy of 10.3 MeV.

RESULTS AND DISCUSSION

Reproducibility and accuracy

The reproducibility (σ_{repr}) of the analysis can be considered as built up from different contributions, *i.e.* those determined by counting statistics σ_{stat}, which are the most obvious, and a residual contribution σ_{res}, given by $(\sigma_{repr}^2 - \sigma_{stat}^2)^{\frac{1}{2}}$. This σ_{res} can further be divided into a first contribution σ_i (arising from vatiations in positioning of standard and sample during irradiation and measurement and from the instability of the counting system a second contribution σ_h, which is due to sample inhomogeneity. Consequently σ_{res} can also be given as $(\sigma_i^2 + \sigma_h^2)^{\frac{1}{2}}$.

The coal sample itself may be inhomogeneous, and dilution with graphite and packing in the polyethylene rabbits may also lead to irreproducible results. To investigate the latter contribution, two samples—coal, and coal diluted with graphite, respectively—were analysed 5 times, with each side alternately facing the target; the results are summarized in Table II. The t-test (95% confidence level) applied to the results obtained for both sides, did not reveal a significant difference; thus σ_h was not significant, and σ_{res} nearly equalled σ_i. Table II shows that the mean reproducibility (σ_{repr}) was 2.2% with, for the present samples, σ_{stat} being 1.3%; a mean value of 1.8% was found for σ_i.

The homogeneity of the coal samples was checked by analysing five different batches of the same coal. These batches were of the same weight and were not diluted. This experiment was repeated for a second, different coal sample. A reproducibility of 3–3.5% was found (Table III); σ_{res} was calculated and found to be 2.5–3.0%, which is larger than the value for the previous test. This additional contribution was probably due to the inhomogeneity of the coal samples. σ_h was calculated from $(\sigma_{res}^2 - \sigma_i^2)^{\frac{1}{2}}$, in which a σ_i value of 1.8% (see previous experiment) was substituted. A mean σ_h value of 2.1% was found.

TABLE II

STUDY OF THE HOMOGENEITY OF THE RABBIT PACKING

Sample	*O content (%)*	*Rel. diff. (%)*	σ_{repr} *(%)*	σ_{stat} *(%)*	$\sigma_{res}=\sigma_i$ *(%)*	*Si content (%)*	*Rel. diff. (%)*	σ_{repr} *(%)*	σ_{stat} *(%)*	$\sigma_{res}=\sigma_i$ *(%)*
(1) Coal										
S_1	7.34 ± 0.06^a	0.14	1.9	1.3	1.4	1.72 ± 0.01^a	1.8	1.7	1.3	1.1
S_2	7.33 ± 0.08		2.4		2.0	1.69 ± 0.02		2.3		1.9
(2) Coal + graphite										
S_1	29.24 ± 0.33	1.20	2.6	1.4	2.2	6.07 ± 0.05	0.5	2.1	1.3	1.6
S_2	29.61 ± 0.32		2.4		1.9	6.10 ± 0.06		2.2		1.8
Mean			2.3	1.35	1.9			2.1	1.3	1.6

[a] Standard deviation on the mean.

TABLE III

STUDY OF THE HOMOGENEITY OF THE COAL SAMPLES

Sample	*O content* (%)	σ_{repr} (%)	σ_{stat} (%)	σ_{res} (%)	σ_h (%)	*Si content* (%)	σ_{repr} (%)	σ_{stat} (%)	σ_{res} (%)	σ_h (%)
Coal 1	10.09±0.14[a]	3.1	1.5	2.7	2.0	1.56±0.05[a]	3.2	1.9	2.6	1.9
Coal 2	7.42±0.25	3.3	1.5	2.9	2.3	1.70±0.06	3.5	1.3	3.2	2.6
Mean		3.2	1.5	2.8	2.2		3.3	1.6	2.9	2.2

[a] Standard deviation on the mean.

TABLE IV

DETERMINATION OF OXYGEN AND SILICON IN SYNTHETIC SAMPLES

Sample	*O added* (mg)	*O found* (mg)	*Rel. diff.* (%)	σ_{repr} (%)	σ_{stat} (%)	$\sigma_{res}=\sigma_i$ (%)	*Si added* (mg)	*Si found* (mg)	*Rel. diff.* (%)	σ_{repr} (%)	σ_{stat} (%)	$\sigma_{res}=\sigma_i$
S_1	21.0	20.7±0.3[a]	−1.4	4.1	2.4	3.3	18.5	18.2±0.2[a]	−1.6	2.8	1.5	2.3
S_2	42.1	40.6±0.6	−3.5	2.6	1.8	1.9	36.9	35.4±0.2	−4.0	1.4	1.2	0.7
S_3	112.2	110.2±1.3	−1.8	3.4	1.4	3.1	98.6	98.4±0.9	−0.2	2.6	0.9	2.4
S_4	141.8	141.4±1.2	−0.5	2.6	1.3	2.2	124.5	124.4±0.7	0.08	1.7	0.8	1.5
S_5	206.1	204.9±2.5	−0.6	3.4	1.3	3.1	180.9	182.0±1.1	0.6	1.9	0.8	1.7
S_6	261.3	265.7±1.7	1.7	1.9	1.2	1.5	229.3	229.5±0.8	0.09	1.0	0.7	0.7
S_7	288.7	288.8±1.7	0.04	1.7	1.2	1.2	253.4	254.5±1.1	0.4	1.4	0.7	1.2
S_8	341.2	347.0±1.8	1.7	1.6	1.2	1.1	300.5	304.4±2.4	1.3	2.2	0.7	2.1
S_9	360.6	361.3±1.7	0.5	1.4	1.1	0.9	316.5	318.5±1.1	0.6	0.9	0.7	0.6
S_{10}	463.1	465.2±2.1	0.5	1.4	1.1	0.9	406.4	405.7±1.4	−0.2	1.0	0.7	0.7
Mean			1.2	2.6	1.5	2.1			0.9	1.8	0.9	1.5

[a] Standard deviation on the mean.

The accuracy of the method was checked by preparing and analysing ten synthetic samples (graphite) with different silica contents (Table IV); as can be seen, the mean differences are very similar to the reproducibilities σ_{repr}, *i.e. ca.* 1%. Table IV also lists the percentage standard deviation expected from counting statistics σ_{stat} and the residual percentage standard deviation σ_{res}. If standards are assumed to be homogeneous, σ_{res} equals σ_i; an average σ_i of 1.8% was again found.

A relation $y=a+bx$ between added and determined concentrations was found; the constants a and b were calculated, by the method of the weighted least squares, and were found to be -1.02 ± 1.13 and 1.008 ± 0.008, respectively, for oxygen; and -0.63 ± 0.73 and 1.006 ± 0.003, respectively for silicon. Since the slopes of both regression lines were nearly 1, no systematic errors were present. The standard deviation on the slopes were below 1%, indicating the high reproducibility of the method.

From these experiments it may be concluded that the overall reproducibility is 2.5–3.5% for the oxygen and silicon determinations in coal and coal ash. These standard deviations consist of contributions from counting statistics (σ_{stat} 1–2%), instrumental errors (σ_i 1.0–2.2%) and inhomogeneity of the coal (σ_h 1.5–2.5%).

Applications

The applicability of the method was tested by analysing 40 coal samples and 20 coal ash samples originating from different Belgian coal mines. Table V contains some results for oxygen and silicon. Mean reproducibilities for the oxygen and silicon determinations were found to be, respectively, 2.9% and 2.8%; this is in agreement with the values given above. The coal samples are classified according to the mining region Campine (Kempen) or Wallonia (Wallonië), and their intended use, such as home heating, electric power or coke. The large concentration differences between the different samples, both for oxygen and silicon, are striking. Even in a defined group (same origin, same use), large differences are apparent. In the coal ash, however, where silicon and oxygen are major constituents, the spread between the concentrations in different samples is small. The oxygen concentration amounts to 40–50% and the silicon concentration to 20–25%.

In combination with activation analysis by thermal neutrons[3], the use of 14-MeV neutrons allows a complete and accurate analysis of the chemical composition of coal ash (Table VI). A determination of the major inorganic constituents in coal is also possible.

Loska and Gorski[12] observed a correlation between the total ash content and the silicon concentration for a series of Upper Silesian coal samples, which can be expressed as $y=ax^b$, where x and y are the percentage silicon and ash contents, and a and b are constants. It seemed interesting to verify whether this relation holds for the Belgian coal samples. The results for 31 coal samples analysed for silicon and ashed by combustion[13] are shown in Fig. 4. The constants a and b were computed by the method of the least squares; values of 4.78 ± 0.20 and 0.930 ± 0.025, respectively, were found. When these constants are used in the above equation, the ash content of the coal samples investigated can be predicted within 8% of the true value. The given equation also indicates that as a first approximation, the total ash content for Belgian coal samples is about 5 times their silicon content

TABLE V

SILICON AND OXYGEN CONCENTRATIONS IN COAL AND COAL ASH

Sample	Coal				Coal ash			
	Si conc. (%)	σ_{repr} (%)	*O conc.* (%)	σ_{repr} (%)	*Si conc.* (%)	σ_{repr} (%)	*O conc.* (%)	σ_{repr} (%)
Wa_3[a]	0.72±0.01[b]	2.8	5.39±0.10	3.1	20.30±0.18	1.6	45.92±0.69	2.6
Wi_3[a]	0.74±0.01	2.8	6.16±0.11	3.2	21.26±0.16	3.3	46.30±0.82	3.0
Z_3[a]	1.26±0.02	3.2	10.49±0.18	3.0	19.40±0.25	2.2	47.20±0.74	2.7
E[c]	0.62±0.01	3.2	4.11±0.08	3.4	20.18±0.40	3.1	45.40±0.87	3.3
F[c]	0.57±0.01	3.5	3.79±0.08	3.7	20.00±0.26	2.2	44.72±0.21	2.1
MF_1[c]	2.03±0.03	2.9	9.22±0.16	3.1	14.20±0.29	3.5	41.52±0.87	3.6
MF_3[c]	0.85±0.01	2.3	4.77±0.07	2.1	21.50±0.38	3.0	46.96±0.98	3.6
MF_9[c]	0.72±0.01	2.8	3.94±0.08	3.3	21.80±0.43	3.4	47.24±0.72	2.6
MF_{14}[c]	0.92±0.02	3.2	4.86±0.08	2.9	21.30±0.32	2.5	48.25±0.88	3.1
C[d]	1.66±0.03	3.6	9.95±0.09	2.5	21.70±0.42	3.3	46.83±0.66	2.4
B[d]	0.51±0.01	3.9	5.49±0.07	2.3	19.00±0.25	2.2	45.80±0.55	2.1
Wi_2[d]	0.74±0.01	2.7	6.59±0.10	2.8	21.97±0.32	2.5	45.69±0.79	3.0
E_2[d]	1.49±0.02	2.0	8.86±0.18	3.5	22.60±0.40	3.0	44.70±0.89	3.4
Wa_4[e]	11.24±0.29	3.5	27.90±0.37	2.3	24.45±0.28	2.0	47.00±0.55	2.0
Z_4[e]	9.50±0.18	3.1	26.00±0.43	2.9	25.20±0.39	2.7	45.90±0.93	3.4
B_1[e]	5.44±0.07	2.2	20.41±0.37	3.2	22.26±0.34	2.6	46.85±0.77	2.8
E_1[e]	6.78±0.12	2.9	18.28±0.26	2.5	26.17±0.40	2.6	46.53±0.69	2.6
MF_3[f]	5.80±0.07	2.0	15.63±0.26	2.9	25.80±0.43	2.9	46.00±0.78	2.9
MF_{10}[f]	9.90±0.14	2.4	22.56±0.46	3.5	26.16±0.54	3.5	47.72±1.05	3.8
MF_{13}[f]	7.96±0.15	3.2	18.41±0.29	2.1	26.38±0.38	2.5	46.50±0.82	3.1

[a] Home heating coal (Campine).
[b] Standard deviation on the mean (3 determinations).
[c] Home heating coal (Wallonia).
[d] Coke (Campine).
[e] Electric power (Campine).
[f] Electric power (Wallonia).

TABLE VI

DETERMINATION OF THE CHEMICAL COMPOSITION OF COAL ASH

Element	*Conc. (%)*	*Element*	*Conc. (%)*
Si	21.3 ± 0.3	S	1.21 ± 0.08
O	48.3 ± 0.9	P	0.23 ± 0.04
Al	17.3 ± 0.4	Ni	0.07 ± 0.02
Fe	1.47 ± 0.03	Ba	0.09 ± 0.02
Mg	4.7 ± 0.4	Mn	0.032 ± 0.003
Ca	3.8 ± 0.4	V	0.042 ± 0.001
K	0.11 ± 0.01	Cu	0.052 ± 0.002
Na	0.48 ± 0.07	Zn	0.03 ± 0.01
Ti	0.23 ± 0.05	Cr	0.035 ± 0.001
Other elements	0.14		
Total:	99.54%		

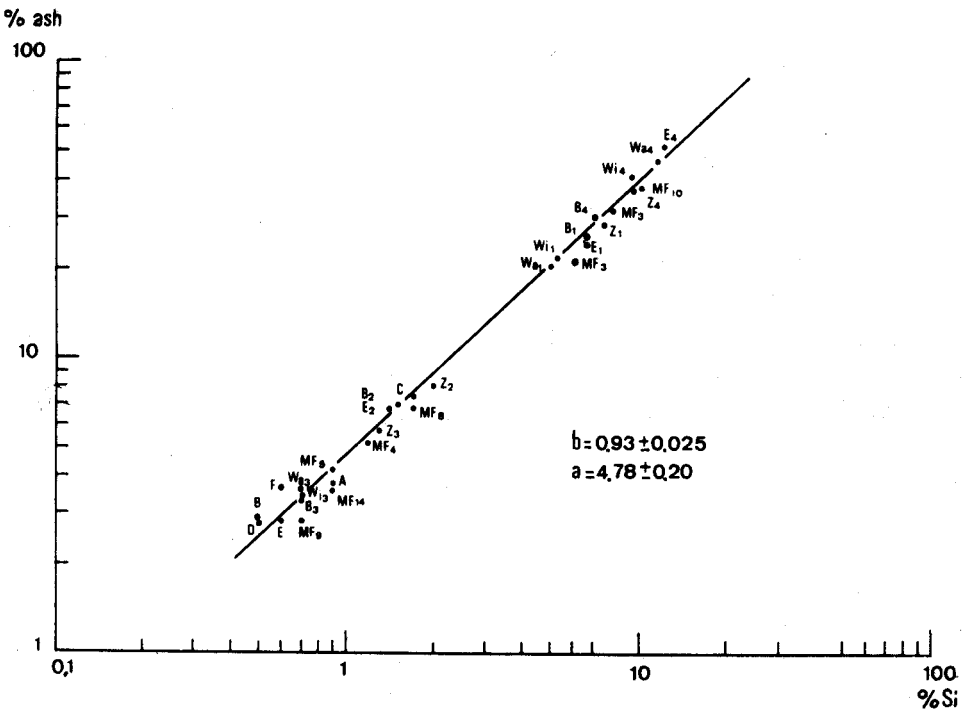

Fig. 4. Ash content of coal as a function of the silicon content.

The correlation between oxygen concentration in coal and ash content was also investigated (Fig. 5). Values of 0.30 ± 0.07 and 1.48 ± 0.10 for *a* and *b*, respectively, were found. When these constants were used in the equation, relative differences between calculated and real ash content of about 15% were found. As expected,

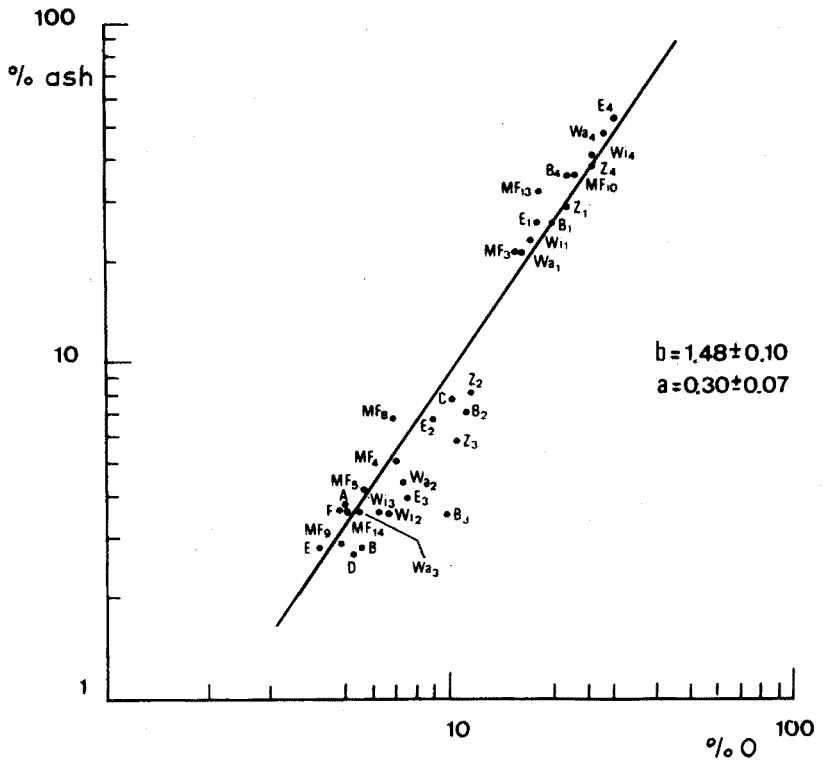

Fig. 5. Ash content of coal as a function of the oxygen content.

this correlation is less close than that with silicon, since oxygen in coal can be organic as well as inorganic. However, if only a rough estimate of ash content is required, a fast oxygen determination may suffice.

Conclusion

This investigation shows that instrumental neutron activation analysis with 14-MeV neutrons is well suited for the simultaneous determination of silicon and oxygen in coal and coal ash samples.

The complete analysis cycle takes about 4 min and, because the samples remain intact, they are available for further analyses. Combination of activation analysis with thermal neutrons[3] and 14-MeV neutrons allows a complete analysis of the chemical composition of coal ash, besides the determination of the major constituents of coal.

An estimate of the ash content is possible from the silicon content within 8% of the true value.

Thanks are due to Prof. Dr. J. Hoste for his interest. This research was sponsored in part by the "Nationaal Centrum voor de Studie van de Lucht-verontreiniging door Verbranding". One of us (C.B.) expresses her gratitude to the I.W.O.N.L. for financial support.

SUMMARY

Oxygen and silicon were simultaneously determined in 40 coal samples and 20 coal ash samples, by means of a 15-s 14-MeV neutron irradiation, followed by 15-s and 2-min measurements of the induced ^{16}N and ^{28}Al activities after decay periods of 5 and 75 s, respectively. The standards consisted of silica mixed with spectrally pure graphite. Possible interferences were checked. Only aluminium and phosphorus interfere although slightly, and corrections are possible. The instrumental error (1.8–2.2%) and the inhomogeneity of the coal samples (1.5–2.5%) contribute to the overall reproducibility (2.5–3.5%). Silicon can be a measure of the ash content of coal.

REFERENCES

1 R. Van Grieken and R. Dams, *Anal. Chim. Acta*, 63 (1973) 369.
2 W. H. Henry and E. R. Bloser, *Identification and estimation of ions, molecules and compounds in particulate matter collected from ambient air, Final report, CPA-70-15B*, Battelle Columbus Laboratories, July 1971.
3 C. Block and R. Dams, *Anal. Chim. Acta*, 68 (1973) 11.
4 T. C. Martin, S. C. Mathur and I. L. Morgan, *Int. J. Appl. Radiat. Isotop.*, 15 (1964) 334.
5 D. E. Wood, *Nucl. News*, 9 (9) (1966) 12.
6 J. Hoste, D. De Soete and A. Speecke, *Euratom report EUR-3565e*, 1967.
7 R. Gijbels, A. Speecke and J. Hoste, *Anal. Chim. Acta*, 43 (1968) 133.
8 J. R. Vogt and W. D. Ehmann, *Radiochim. Acta*, 4 (1965) 24.
9 R. Gijbels, A. Speecke and J. Hoste, *Modern Trends in Activation Analysis*, N.B.S. special publication 312, Vol. II, 1968, p. 1298.
10 S. S. Nargolwalla, M. R. Crambes and J. E. Suddueth, *Anal. Chim. Acta*, 49 (1970) 425.
11 C. Vandecasteele, R. Van Grieken, R. Gijbels and A. Speecke, *Anal. Chim. Acta*, 65 (1973) 1.
12 L. Loska and L. Gorski, *Radiochem. Radioanal. Lett.*, 10 (1972) 315.
13 F. J. Welcher, *Standard Methods of Chemical Analysis*, Vol. II, Van Nostrand, New York, 1966, p. 1159.

Analytica Chimica Acta, 71 (1974) 67–77

THE DETERMINATION OF OXYGEN IN SILICON BY ALPHA AND HELIUM-3 ACTIVATION ANALYSIS

C. VANDECASTEELE*, F. ADAMS and J. HOSTE

Institute for Nuclear Sciences, Rijksuniversiteit Gent, Proeftuinstraat 86, 9000 Ghent (Belgium)

(Received 15th January 1974)

Charged particle activation analysis is known to be very suitable for the determination of oxygen in silicon. Helium-3[1–3] and α-particles[4–7] have already been applied by several authors. The oxygen content is an important characteristic in determining the quality of starting silicon[8]. Nuclear methods such as 14-MeV neutron activation[9] cannot determine the low oxygen contents found in commercially important samples. Techniques such as infrared spectrometry[10,11] and spark-source mass spectrometry are essentially relative methods, which require careful standardization against another independent method. Therefore, charged particle activation analysis for oxygen in silicon is of considerable importance, and a thorough study of the accuracy and the precision of this technique seemed appropriate. To date, most determinations have provided a standard deviation of 20–40%, or even more for samples with an oxygen content as high as several $\mu g\ g^{-1}$. Moreover, uncertainty exists about the applied standardization methods as well as about possible interferences from the matrix.

In the present paper, results of repeated analyses of a large number of samples, containing widely varying oxygen concentrations, obtained by both helium-3 and α-particle activation are reported, and factors that can influence the precision and accuracy of the method are investigated. The results are further compared to values obtained by infrared spectrometry, in an attempt to select the optimal calibration factors for the latter technique.

Alpha and helium-3 activation analyses for oxygen are based, respectively, on the $O(\alpha,nx)^{18}F$ and the $O(^3He,nx)^{18}F$ reactions. The isotope ^{18}F is a pure positron emitter with a 109.8-min half-life. As shown by Engelmann[12], the most important interferences are F(20), Na(25) in 15-MeV helium-3 activation and F(0.40), Na(70), N(170) in 35-MeV α-activation. (The figures in parentheses give the concentration ratio of the indicated element to oxygen that results in a 100% error on the oxygen concentration.) The ratios of all the indicated elements are believed to be well below these values. In any case, activation with two different particles at largely different energies would yield different systematic errors from interfering reactions, if they occur at all.

It has been shown[13] that the α-energy should be chosen below 37 MeV, otherwise spallation of silicon can occur, yielding ^{18}F.

---

* Aspirant of the N.F.W.O.

The problem is less severe for ^{3}He activation, where ^{18}F production cannot be expected below about 20 MeV (ref. 1). The energy chosen was, however, 14 MeV, as no substantial increase in sensitivity can be expected above this level.

EXPERIMENTAL

Irradiation

Irradiations were carried out with the isochronous variable energy cyclotron at Louvain-La-Neuve, Belgium. The nominal energy was 40 MeV for α-particles and 20 MeV for helium-3 particles. The energy resolution was about 0.3%. Beam intensities up to 2 μA were used. The samples were irradiated under vacuum ($< 10^{-4}$ Torr) in the external beam facility. They were placed in a water-cooled copper target holder and were irradiated with a defocussed beam of 16-mm diameter for 5–40 min, depending on the oxygen content. The position and homogeneity of the beam could be observed on a quartz target. During the irradiation, the incident current on the sample was read from a digital voltmeter, or integrated with a current digitizer.

Standards and samples

To eliminate possible uncertainties in beam intensity, a relative method was applied whereby the sample and some standard foils were irradiated one behind the other.

Muscovite foils (20-mm diameter, 10–20-μm thick) were used as standards. Their oxygen content was 47.4% ± 0.3% as determined by 14-MeV neutron activation analysis. Standard foils (3–6) were placed in front of the sample as shown in Fig. 1. In order to avoid errors from ^{18}F recoil, the first foil was never used as a standard.

Different samples of mono- and polycrystalline silicon were analysed. Two varieties of monocrystalline samples were obtained: czochralski, and floating zone

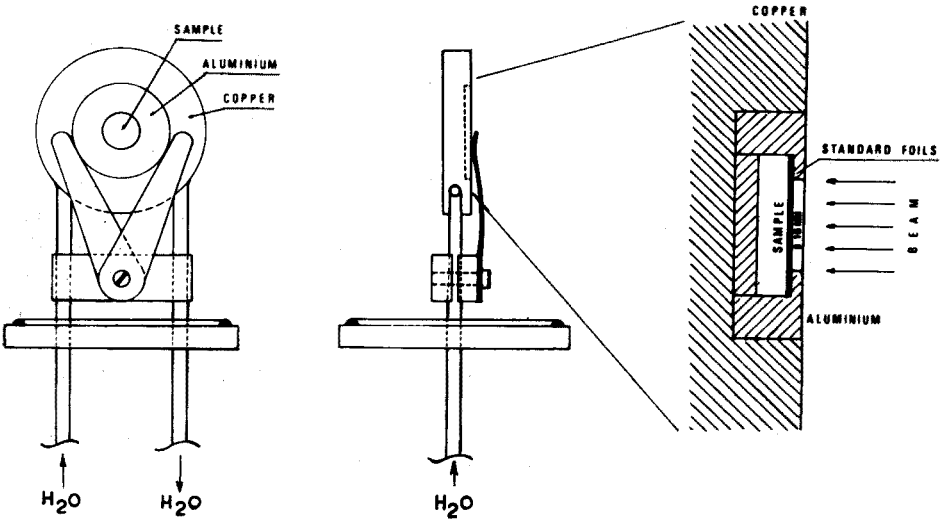

Fig. 1. Experimental configuration during the irradiation.

crystals purified under different atmospheres. Before activation, the sample surface was mechanically polished and etched for 20 min in a nitric–hydrofluoric–acetic acid mixture.

Post-irradiation treatment

To overcome surface and recoil contamination, a post-irradiation chemical etch was applied. The etching solution contained 68% (by volume) concentrated nitric acid, 9% hydrofluoric acid (50%) and 23% acetic acid. At room temperature, the resulting etching rate was about 1 μm min^{-1}. Although it could be shown that an etching thickness of 20 μm is sufficient (see below) to overcome contamination effects, a surface layer of at least 40 μm was removed. In order to avoid deposition of ^{18}F from the solution onto the etched surface[14], the samples were successively etched in four different solutions.

Measurements

The photons at 511 keV, resulting from the annihilation of the ^{18}F positron emission, were measured by placing the sample directly between two 7.5 × 7.5 cm NaI(Tl) detectors. To assure complete positron annihilation and to stop β-rays from other radionuclides, the samples were sandwiched between two 3-mm thick lucite adsorbers. Each detector was coupled to a preamplifier NE 5288, an amplifier Canberra 1418 and a timing discriminator NE 4616. The timing discriminators were triggered by a single-channel analyser Canberra 1431, which selected the 400–600-keV energy region. The signals from both timing discriminators were fed to a time-to-amplitude converter NE 4645 which was connected to a single-channel analyser and a scaler NE 4612. The resolving time of this coincidence unit was set at 200 ns. The entire counting and waiting cycle was automatically controlled by two NE 4624 clocks. The results were printed by a Kienzle printer. The background of the counting system was about 6 c.p.m.

Measurements of the samples were started about 1 h after irradiation and the decay was followed for about 6 h. The standard foils were then measured. If these activities were too high, the detectors were placed 40 cm apart, thus reducing the count rate to 5% of its original value. This factor was determined with a ^{64}Cu source of the same form and dimension as the standard foils.

Determination of the activation curves

Stacks of mylar (average thickness, 12 μm), and mica foils (average thickness, 13 μm) were irradiated with α-particles ($E = 40$ MeV; intensity = 30 nA). The decay of each foil was followed over a period of at least 6 h and the results were analysed by the CLSQ decay curve analysis program[15], with weighted least squares. The measurements for the mylar foils were started 4 h after irradiation to allow for the decay of ^{13}N and ^{11}C activities. Ge(Li) spectrometry of the irradiated mica foils showed the presence of ^{44}Sc ($T_{\frac{1}{2}} = 3.9$ h) and ^{43}Sc ($T_{\frac{1}{2}} = 3.9$ h) activities from ^{41}K(α, n)^{44}Sc and ^{41}K(α, 2n)^{43}Sc or ^{40}K(α, n)^{43}Sc, mainly in the last foils of the stack. This interference was corrected for by taking a 3.9-h half-life component into account in the analysis of the decay curve. After iteration, a mean half-life of 111 min was found for the activity attributed to ^{18}F.

For the helium-3 activation, similar mylar (thickness decreasing gradually

from 25 to 8 μm) and mica (average thickness, 13 μm) stacks were irradiated with 20-MeV particles at 20 nA intensity for 20 min. Measurements were started 4 h after irradiation for the mica foils and 36 min after irradiation for the mylar foils. The ^{18}F activity in the mylar foils was resolved from ^{11}C and ^{13}N activities by means of the CLSQ-program, so as to obtain the activation curves for ^{18}F and ^{11}C. The mean experimental half-life for the activity attributed to ^{18}F was 111 min in the experiment with mica, and 107 min in the experiment with mylar. The component of the decay curve due to ^{11}C provided a half-life of 19.5 min.

Calculation of the results

The decay data for each sample were analysed with the CLSQ program. In α-activation, a good fit to the experimental decay data was obtained when the least-squares iterative analysis was started, with half-lives of 10.0 min (^{13}N), 109.8 min (^{18}F) and 15 h (^{24}Na). The presence of ^{24}Na was confirmed by Ge(Li) spectrometry. As a qualitative criterion for ^{18}F, iterations were performed for its half-life, the other half-lives being kept constant.

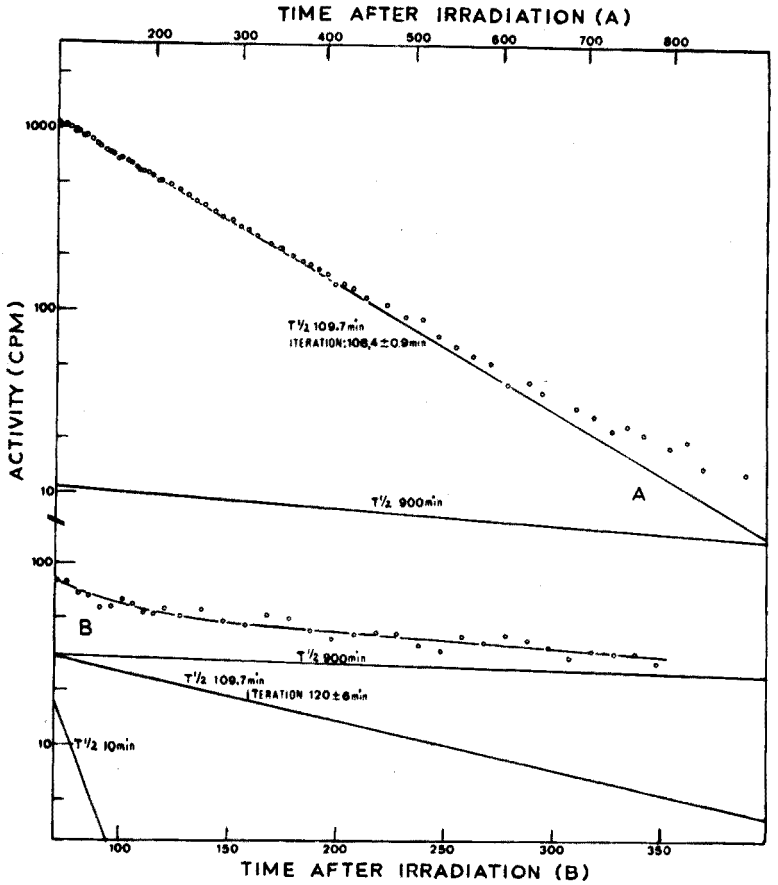

Fig. 2. Decay curves for α-particle irradiated samples. (A) Sample 4 containing 3.9 p.p.m. of oxygen. $T_{irr} = 30$ min; 1.0 μA intensity. (B) Sample 2 containing 56 p.p.b. of oxygen. $T_{irr} = 40$ min; 1.3 μA intensity.

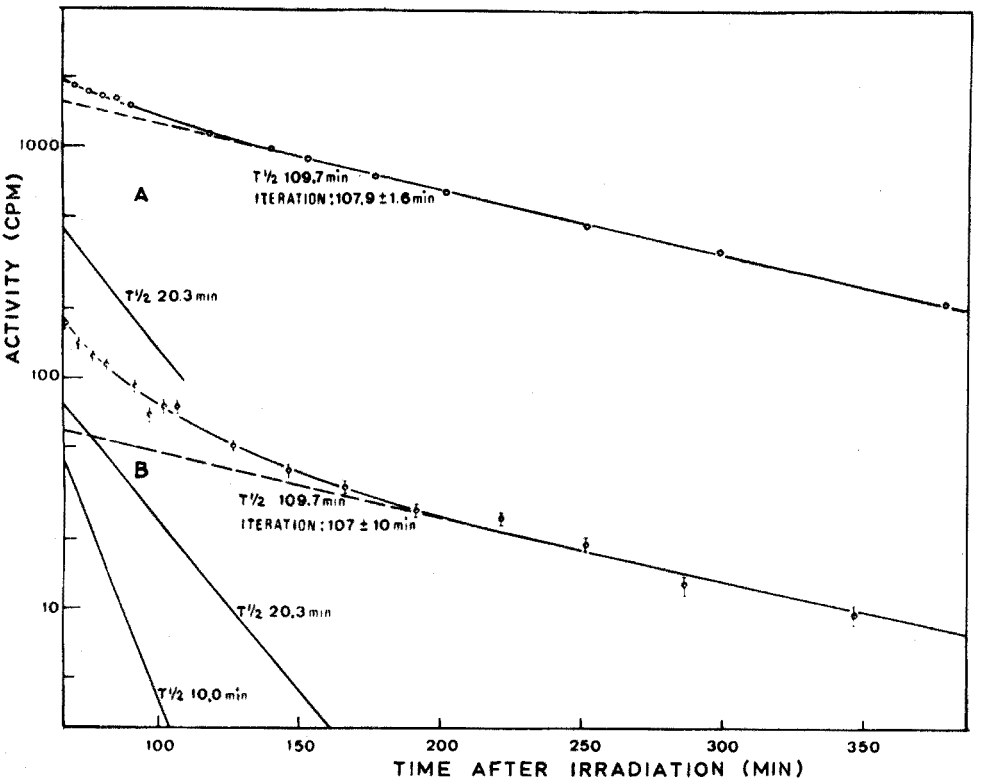

Fig. 3. Decay curves for helium-3 irradiated samples. (A) Sample 2B containing 10.0 p.p.m. of oxygen. $T_{irr} = 10$ min; 0.7 μA intensity. (B) Sample 2 containing 56 p.p.b. of oxygen. $T_{irr} = 30$ min; 1.5 μA intensity.

In helium-3 activation the same procedure was applied, but half-lives of 10.0 min (^{13}N), 20.3 min (^{11}C) and 109.8 min (^{18}F) were used. This is illustrated by the decay curves given in Figs. 2 and 3.

The so-called equivalent thickness method was used for quantitation. The entire calculation procedure was performed with a FORTRAN program OCCAL, which used as input values the initial ^{18}F activity in the sample obtained from the CLSQ-program, the activity and thickness of the standard mica foils, the etched thickness, the geometry reduction factor, and the time between the start of the measurements on the sample and on the standards. As a separate input, the equivalent thickness as a function of energy, the range energy data for mica and silicon, and the experimental activation curve in mica, were read in.

For each sample, the energy is calculated at a depth corresponding to the surface layer removed by etching (*ca.* 40 μm) and the corresponding equivalent thickness is determined by interpolation. A correction is applied if the particle energy in the foils chosen as standards does not correspond exactly to the energy relative to which the equivalent thickness is calculated. Finally, the oxygen concentration is calculated from the equation:

$$p.p.m._x = p.p.m._s \frac{A_x}{A_s} \frac{t_s}{e}, \qquad (1)$$

where $p.p.m._x$ denotes the oxygen content in the sample, $p.p.m._s$ the oxygen content in the standard, A_x the ^{18}F activity in the sample, A_s the ^{18}F activity in the standard corrected for decay and dead-time losses, t_s the thickness of the standard foil (mg cm^{-2}), and e the equivalent thickness (mg cm^{-2}).

RESULTS AND DISCUSSION

The entire procedure is based on the equivalent thicknesses, which are deduced from the experimental activation curves in mica and mylar. For this purpose, a modified version of the computer program RET[16] was used. The ranges in mica and mylar were calculated from the range–energy data for the pure elements[17] by the equation:

$$\frac{1}{R} = \sum_i \frac{f_i}{R_i} \tag{2}$$

where R and R_i are the charged particle ranges in mylar or mica and in the pure element i, and f_i is the weight fraction of element i.

The two experimental activation curves transformed to silicon are given in Figs. 4 and 5. As follows from Fig. 6, the equivalent thicknesses deduced from the curves in mica and mylar agree within 4% for 35-MeV α-activation, and within 7% for 14-MeV helium-3 activation. This may be considered as a check of the validity of the range transformation procedure. Because of the greater similarity in composition

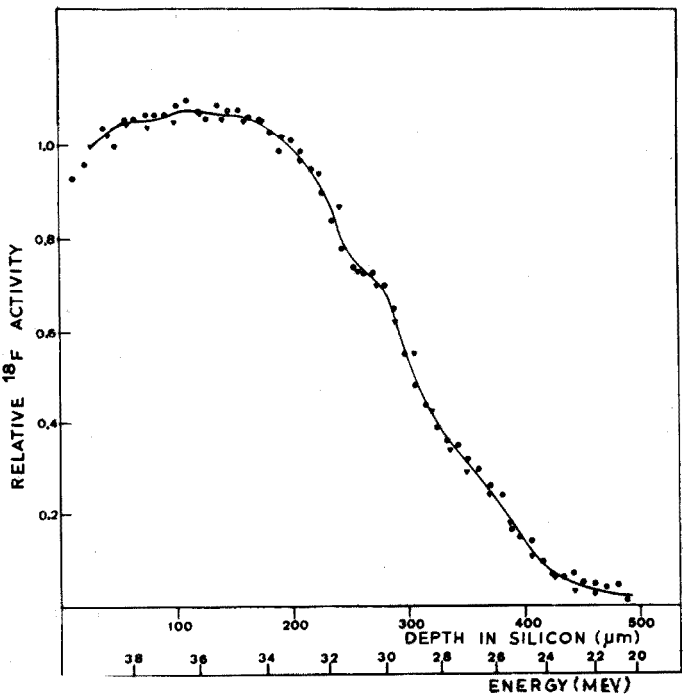

Fig. 4. Activation curve for the O(α, nx) ^{18}F reactions in silicon. (○) Mylar, (▽) mica.

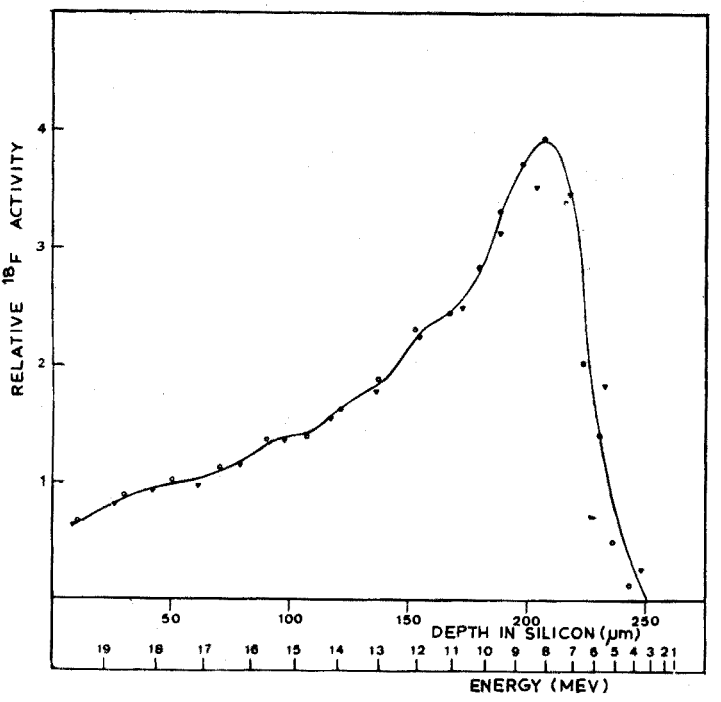

Fig. 5. Activation curve for the O(^{3}He, nx) ^{18}F reactions in silicon. (○) Mylar, (▽) mica.

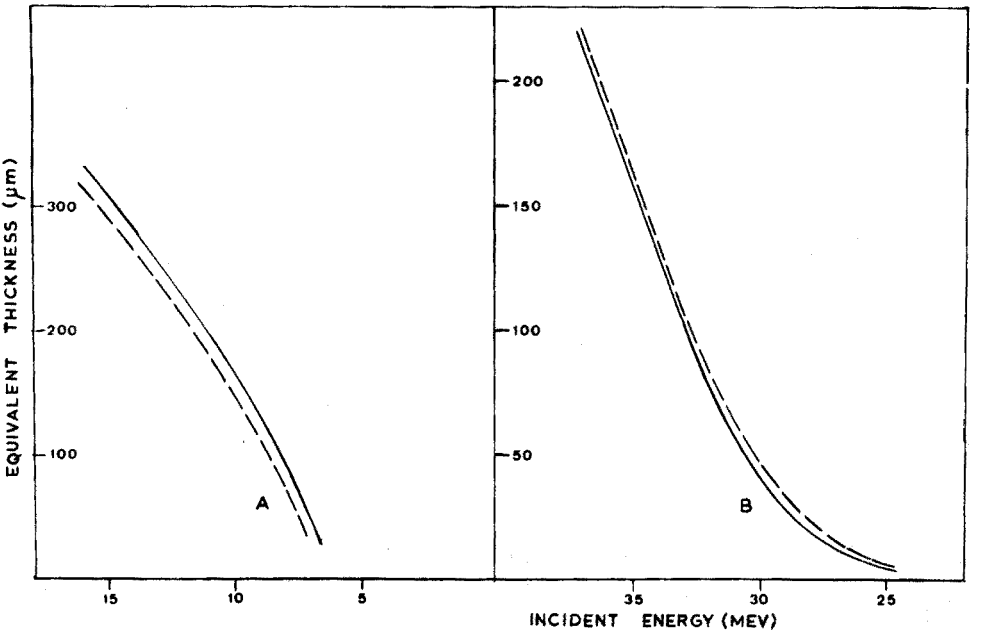

Fig. 6. Equivalent thicknesses for O(^{3}He, nx) ^{18}F (A) and O(α, nx) ^{18}F (B) as a function of particle energy. (---) Mylar, (——) mica.

between mica and silicon, all results were calculated with the equivalent thicknesses deduced from the mica curves, rather than those obtained from mylar. To evaluate further the validity of the standardization method, the α-activation curve in mica was determined three times over a period of several months. Results obtained for equivalent thicknesses agreed within 5%. The differences reflect the overall precision obtainable with the present standardization method. The equivalent thicknesses in Fig. 6 are the mean value of the three determinations.

The thickness that should be etched from a sample after irradiation, to remove surface and recoil contamination, was determined experimentally. A silicon sample containing 180 p.p.b. oxygen was irradiated, and successive layers were removed by etching its front. After each etching, the sample was counted, and the apparent oxygen content was calculated. The oxygen content was found to remain constant, within experimental error, as soon as a surface layer of about 20 μm had been removed as shown in Fig. 7.

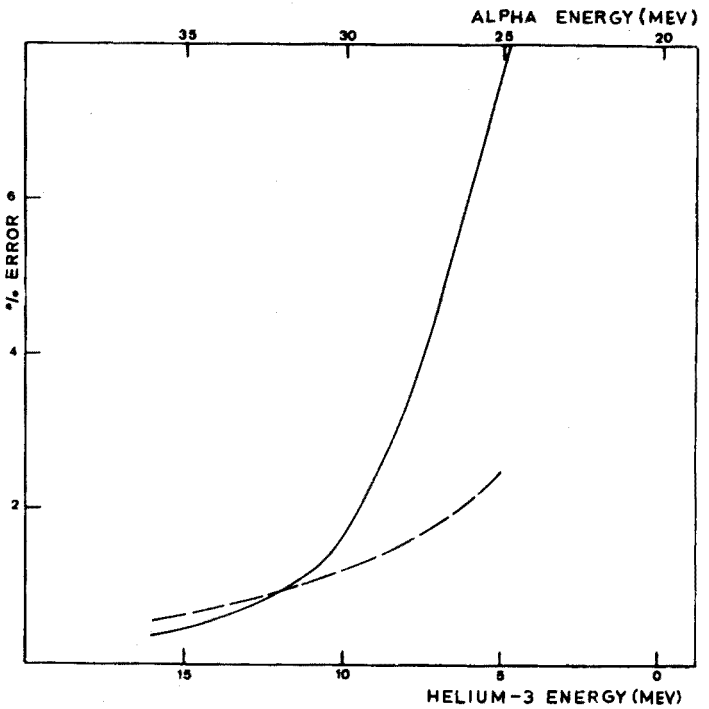

Fig. 7. Relative error on the oxygen determination if an error of 1 μm on the thickness is assumed. (——) ^{3}H, (– – – –) α-irradiation.

The activity induced in the standard mica foils was very high. Even after the geometry had been reduced, as explained previously, activities of the order of 3500 and 3000 c.p.s. were obtained after a 30-min irradiation, at 2 μA and an 8-h decay period, with α- and helium-3 particles, respectively. Considerable errors may thus be introduced, as a consequence of counting losses in the measuring equipment.

Therefore, the experimental dead-time was determined by following the decay of the ^{18}F activity in an α-irradiated quartz sample for 11 h, starting with an activity of about 4000 c.p.s. From a comparison of the high activity in the first part of the decay curve with the low activity in the second part, the dead time per pulse was calculated. A value of 26.5 ± 2 μs per pulse was found. This value was then used for a precise determination of the half-life. A value of $109.8^4 \pm 0.08$ min was obtained.

TABLE I

DETERMINATION OF OXYGEN IN SILICON IN THE CONCENTRATION RANGE ABOVE 1 P.P.M.

(Czochralski samples)

Sample	*Oxygen concentration (p.p.m.)*							
	α-activation				*^{3}He activation*			*I.r.*
1	11.5	10.4	10.9	10.9 ± 0.5[a]	11.9	10.9	11.4 ± 0.7	10.5[b]
2A	8.4	7.7	—	8.0 ± 0.5				
2B	7.8	8.4	—	8.1 ± 0.4	9.9	10.2	10.0 ± 0.4	9.3
2C	8.2	8.6	8.0	8.3 ± 0.3				
2D	9.9	8.3	9.0	9.1 ± 0.8				
3	5.6	5.5	6.1	5.7 ± 0.3	6.2	4.1	5.2 ± 1.5	7.4
4	3.6	4.1	—	3.9 ± 0.3	5.6	—		

[a] Standard deviation on 1 measurement.

[b] Analyses based on ASTM calibration curve.

Table I shows some results of repeated analyses by both helium-3 and α-activation analysis on a selected number of samples containing oxygen concentrations above 1 p.p.m. In this concentration range, the precision of the α-activation analysis is, on average, about 6%. Samples 2A–2D were cut from the same rod, which was expected to have oxygen homogeneously distributed. The coefficient of variation for one determination was 7%. For helium-3 activation, a coefficient of variation of 13% was obtained. The higher dispersion is due to the low value (4.1 p.p.m.) obtained for sample 3. It was calculated that, on average, the results with helium-3 are 8% higher than those with α-particles. Since for these high oxygen samples, errors from interferences and counting statistics are minimized, the results can be considered as a further test of the method. The observed difference (8%) seems reasonable, in view of the errors on the equivalent thicknesses and of the precision of the results.

The spread of the experimental results can partly be attributed to uncertainties in the sample thickness. From the silicon activation curves one can calculate the error corresponding to a precision of 1 μm in the thickness measurement. The results are given in Fig. 7. If the total uncertainty for the two thickness measurements is assumed to be 4 μm (*i.e.* 2 μm per measurement), an error of about 3% occurs both for 34-MeV α-particles and 13-MeV helium-3.

The results in Table I were compared with values obtained by an ASTM i.r. spectrometric method[11]. The overall agreement seems satisfactory. It should be

mentioned that several calibration factors have been proposed for i.r. analysis for oxygen, differing by as much as a factor of three.

Table II presents results for polycrystalline silicon samples and for floating zone crystals with an oxygen content lower than 1 p.p.m. The fair agreement between α-particle and helium-3 activation analysis for oxygen contents below 100 p.p.b. is illustrated by an average coefficient of variation for one measurement, calculated for samples 2–4, amounting to about 19%. This indicates that the interferences of both impurity elements, such as fluorine and sodium, and the matrix itself through spallation, are negligible at the oxygen concentrations determined.

TABLE II

DETERMINATION OF OXYGEN IN SILICON IN THE SUB-P.P.M. CONCENTRATION RANGE

Sample	*Particle (energy)*	*Oxygen concentration (p.p.b.)*	
Polycrystalline	α (34.7 MeV)	160	183 ± 40[a]
	α (33.9 MeV)	230	
	α (34.4 MeV)	160	
Monocrystalline			
1. Floating zone	α (33.1 MeV)	250	280 ± 40
	α (34.2 MeV)	310	
2. Floating zone under argon + 0.5% H_2	α (33.3 MeV)	63	56 ± 14
	α (32.7 MeV)	39	
	^{3}He (13.7 MeV)	72	
	^{3}He (13.9 MeV)	52	
3. Floating zone under argon	α (32.0 MeV)	74	70 ± 5
	^{3}He (14.2 MeV)	67	
4. Floating zone under vacuum	α (32.2 MeV)	59	69 ± 14
	^{3}He (13.1 MeV)	79	
5. Floating zone under argon	α (32.5 MeV)	81	

[a] Standard deviation on one determination.

It is clear that these concentrations are not at the sensitivity limit of the determination, since irradiations lasting longer than 40 min were never carried out. For a 2-μA irradiation with 14-MeV helium-3 particles lasting one half-life, one can calculate[18] a detection limit of 0.7 p.p.b. and a determination limit of 4 p.p.b. This corresponds to an activity of 3.6 counts min^{-1} $p.p.b.^{-1}$, 1 h after irradiation. For this calculation, a 10-min counting time was assumed, as longer countings would prevent control of the half-life.

For the same conditions, 34-MeV α-particles give a detection limit of 6 p.p.b. and a determination limit of 22 p.p.b. This is based on an activity of 1.8 counts min^{-1} $p.p.b.^{-1}$, 1 h after irradiation, and on an induced ^{24}Na activity of 109 counts min^{-1}. The poorer detection limits are mainly due to this increase in the blank value.

Grateful acknowledgement is made to R. Kieffer for valuable technical assistance, to the "comité de gestion du cyclotron" of Louvain-La-Neuve (U.C.L.) for the

use of the cyclotron, to the operating staff of the cyclotron and the scientists of the "laboratoire de chimie nucléaire" for their kind cooperation, to Dr. L. De Laet (Metallurgy Hoboken) for providing samples, to W. Van Hove for the i.r. analyses, and to the N.F.W.O. and the I.I.K.W. for financial support.

SUMMARY

A non-destructive analytical method for oxygen in silicon by both helium-3 and α-particle activation analysis was applied to different samples, containing 0.05–10 p.p.m. of oxygen. The accuracy and precision of the method were studied. For concentrations above 1 p.p.m., the average coefficient of variation is about 6% for α-activation and 13% for helium-3 activation. For concentrations of about 60 p.p.b., the corresponding figure is about 20%. The results of both methods, which agree within 8%, are compared to infrared analysis. The determination limit of the method is 4 p.p.b. for helium-3 activation and 22 p.p.b. for α-activation.

REFERENCES

1 T. Nozaki, Y. Yatsurugi and N. Akiyama, *J. Radioanal. Chem.*, 4 (1970) 87.
2 C. Kim, *Anal. Chim. Acta*, 54 (1971) 407.
3 G. Aleksandrova, A. Demidov, G. Kotelnikov, G. Plashakova, G. Sukhov, K. Choporov and G. Shmanenkova, *Sov. At. Energy*, 23 (1967) 797.
4 H. Rook and E. Schweikert, *Anal. Chem.*, 41 (1969) 958.
5 J. Giroux, M. Talvat, J. Thomas and J. Tousset, *Bull. Soc. Chim. Fr.*, (1971) 706.
6 C. Engelmann, Y. Gosset, M. Loeuillet, A. Marschal, P. Ossart and M. Boissier, *Proc. Int. Conf. Mod. Trends Activ. Anal., NBS Spec. Publ., 312*, Vol. II, 1969, p. 819.
7 E. Schweikert and H. Rook, *Anal. Chem.*, 42 (1970) 1525.
8 A. Mayer, *Solid State Technol.*, April 1972, 38.
9 H. Nass, *J. Inorg. Nucl. Chem.*, 33 (1971) 617.
10 W. Kaiser and P. Keck, *J. Appl. Phys.*, 28 (1957) 882.
11 *ASTM No. F 121-70 T.*
12 C. Engelmann, *J. Radioanal. Chem.*, 7 (1971) 281.
13 J. Giroux, M. Talvat, J. Thomas and J. Tousset, *J. Radioanal. Chem.*, 6 (1970) 423.
14 H. Rook, E. Schweikert and R. Wainerdi, *Anal. Chem.*, 40 (1968) 1194.
15 J. Cumming, *BNL Report 6470.*
16 H. Rook, *Dissertation*, Texas A & M University, 1969.
17 C. Williamson, J. Boujot and J. Picard, *Rapport CEA-R 3042*, 1966.
18 L. Currie, *Anal. Chem.*, 40 (1968) 586.

Analytica Chimica Acta, 71 (1974) 79–84

RAPID DETERMINATION OF PRIMARY AMINO GROUPS ON SOLUBLE POLYMERS

K. SCHMIDT and K. GECKELER

Lehrstuhl für Organische Chemie der Universität Tübingen, Auf der Morgenstelle, D-7400 Tübingen 1 (Germany)

(Received 2nd January 1974)

The determination of amino groups on polymers is very important for the characterization of macromolecules. For instance, the composition of copolymers can be determined if one of the monomers has amino groups. This method makes it possible to determine the capacity, if the amino groups are used as reactive groups for forming complexes or for fixation of a compound to the polymer.

For the determination of amino groups on synthetic polymers, the literature usually refers to analytical methods for monomers (*e.g.* van Slyke)[1,2]. But these methods often have disadvantages when used for macromolecular compounds (long reaction times, loss of sensitivity, *etc.*). Elemental analysis of polymers is a possible method in this case, but there is then no possibility of distinguishing the different types of nitrogen binding.

A reagent which reacts in a highly selective manner with primary amino groups is fluorescamine (4-phenyl-spiro(furan-2(3H),1′-phthalan)-1,3-dione)[3–5].

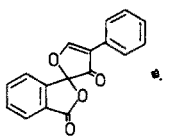

Fluorescamine

The reaction product of fluorescamine with primary amino groups is a strongly fluorescent compound, whereas fluorescamine itself does not fluoresce. The reaction proceeds rapidly and quantitatively, so that an effortless determination of amino groups is possible, after determination of the calibration curve.

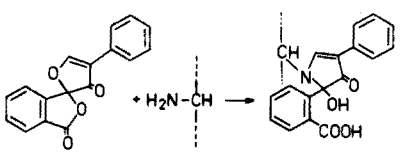

For calibration, a compound of known structure is first fixed to the polymer; the derivative is then cleaved, and the content of this compound is determined by the usual analytical methods.

In the present work, two copolymers with known contents of primary amino groups were used: Polymer I is a copolymer of 1-vinyl-2-pyrrolidinone and alanine vinylester; Polymer II is a copolymer of 1-vinyl-2-pyrrolidinone and allylamine.

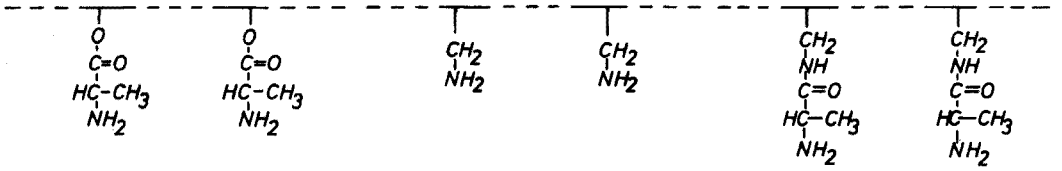

Polymer I Polymer II Polymer II with bound alanine

EXPERIMENTAL

Apparatus

A Perkin–Elmer MPF 3 fluorescence spectrophotometer equipped with two monochromators, a high-pressure xenon source, and quartz microcuvettes, was used to obtain the fluorescence spectra. The fluorescence calibration curves were obtained with an excitation wavelength of 390 nm and an emission wavelength of 475 nm. Excitation and emission slits were both 7.5 nm. All pH measurements were made with a WTW Digitalmeter Digi 610 equipped with a combination glass/reference electrode.

Chemicals and reagents

Fluorescamine was obtained from Hoffmann–La Roche AG, Basel, Switzerland. The copolymers were prepared as described elsewhere[6]. For the separation from monomers and low-molecular-weight substances, the polymers were ultrafiltered[7]. The solvent for all fluorescence measurements was a (1 + 1) mixture of acetone and water. The water, distilled in a quartz apparatus, had a negligible fluorescence blank. The acetone was of analytical grade (Merck). The pH was adjusted to 8 with hydrochloric acid or sodium hydroxide (Merck).

Coupling

Dissolve 0.5 g of polymer II in 7 ml of dichloromethane, and then add 0.2 g of tert-butyloxycarbonyl–alanine and the equivalent amount of dicyclohexylcarbodiimide[8]. After stirring for 24 h, evaporate the solvent, add distilled water, and filter off the precipitated dicyclohexylurea. Then ultrafilter the solution through a membrane, type UM 10 (Amicon N.V., Oosterhout, Netherlands)[9], until there is no positive reaction with ninhydrin.

Determine the content of alanine by amino acid analysis[6,10]. The cleavage of alanine is done by hydrolysis in 6 *M* hydrochloric acid for 24 h at 110°C. Afterwards, the solvent is evaporated and an aliquot amount is used for analysis.

Cleavage of the tert-butyloxycarbonyl group

Dissolve the copolymer in 1.2 *M* hydrogen chloride in glacial acetic acid, stir for 20 min and then evaporate the solvent. After repeating this operation,

dissolve the polymer in 0.5 *M* sodium hydrogencarbonate solution for neutralization. Ultrafilter through a membrane, type UM 10. The completeness of the cleavage is checked by thin-layer chromatography on silica gel plates (60 F_{254}, Merck) with 3:1:1 n-butanol–acetic acid–water as eluent[11].

Analytical procedure

Dissolve 1–10 mg of polymer in 5 ml of distilled water and add a five-fold molar excess of fluorescamine (related to the estimated content of primary amino groups) dissolved in 5 ml of acetone. Then dilute the solution with (1+1) acetone–water, until the relative fluorescence of the sample is in the linear part of the calibration curve. After measurement against a water blank, evaluate the concentration of primary amino groups from the calibration curve (see below).

RESULTS

In order to measure the fluorescence of polymer I, a concentrated solution of the polymer was prepared in a mixture of water and acetone, and the emission spectrum was recorded, at high sensitivity, between 350 and 500 nm (spectrum I, Fig. 1). There is an intense Rayleigh scatter peak at 390 nm and a Raman scatter peak at 453 nm. Both peaks originate from the solvent; no fluorescence peak of the polymer can be discerned. Afterwards the solution of the polymer was diluted (1+99) with the same solvent and the reaction with a 5-fold molar excess of fluorescamine was carried out. Then the emission spectrum II (Fig. 1) was recorded at an amplifier sensitivity reduced by a factor of 100. The spectrum shows an intense fluorescence peak at 475 nm, whereas the solvent peaks have virtually disappeared. This minimal solvent fluorescence makes it possible to draw the calibration curve through zero. Measurements of polymer II showed the same results.

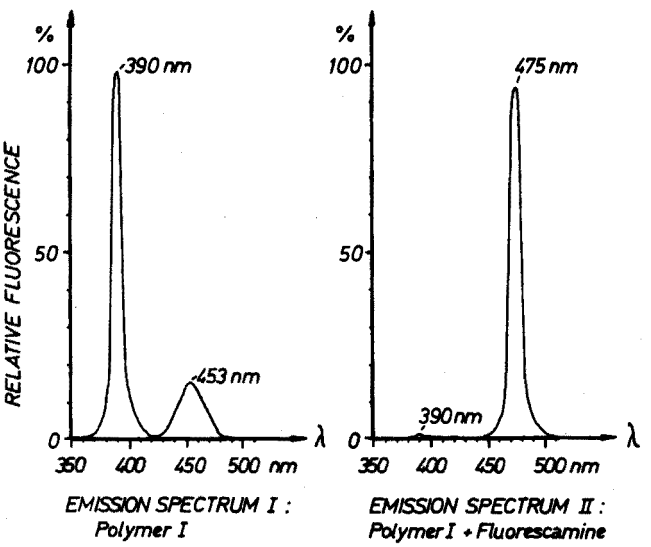

Fig. 1. Emission spectra of polymer I and the reaction product of polymer I with fluorescamine. $\lambda_{exc.} = 390$ nm.

Dilution series of both polymers were made, and the relative fluorescences measured after the reaction with fluorescamine. During all determinations, reaction time (15 min), temperature and pH were kept constant. Figure 2 shows the calibration curves of the polymers after conversion of the polymer concentration to the content of amino groups by amino acid analysis.

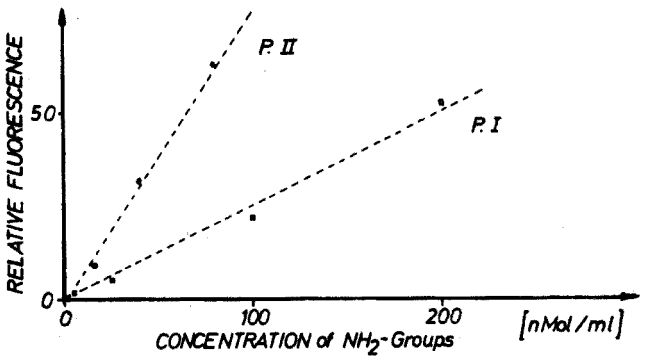

Fig. 2. Fluorescence calibration curves of the two polymers after reaction with fluorescamine.

DISCUSSION

The determination of amino groups on soluble polymers is very important for several reasons:

(1) for checking the product during polymer synthesis;

(2) for determining the composition of copolymers if only one comonomer bears amino groups;

(3) for determining the capacity of polymers to bind compounds to the amino groups;

(4) for checking the completeness of coupling reactions in liquid-phase peptide synthesis[1,2].

The usual method for determination of functional groups involves (a) fixation of a low-molecular compound, (b) separation of the excess from the polymer, (c) cleavage of the coupled compound, and (d) determination of the cleaved compound; this is time-consuming and includes many sources of error. Moreover, large quantities of the precious polymer are often necessary. The direct determination of amino groups bound to the polymer, by measurement of the fluorescence after reaction with fluorescamine, has the great advantage of rapidity and sensitivity.

The reproducibility of the measurements depends essentially on standardization of the conditions during reaction and measurement. As already described for monomers[3], there is also a direct relationship between pH and fluorescence for polymers. Therefore it is necessary to adjust the pH to a constant value before measurement. The optimal pH can be determined easily for any polymer by simple measurements.

In order to account for the influence of the structure of the polymer and of side groups on the fluorescence, it is necessary to record a calibration curve for

every polymer. This might make the checking, during synthesis with polymer carriers, difficult, as new side-groups may be formed after each reaction step. The proposed rapid and simple method is most suitable for application in series analysis where only one calibration is necessary.

Supplementary measurements showed a strong relationship between relative fluorescence and reaction time. The $t_{\frac{1}{2}}$ of 100–500 ms which has been mentioned in the literature for monomers[3] is significantly greater for the reaction of fluorescamine with soluble polymers. Therefore, the period of time between addition of the reagent and measurement was kept constant at 15 min.

The linearity of the calibration curve allows the application of fluorescence measurements for determination of NH_2-groups on soluble polymers.

CONCLUSIONS

The content of primary amino groups of two soluble polymers was determined by fluorescence measurements, with fluorescamine as the reagent. The primary amino groups of the polymer-bound alanine of polymer I were treated with fluorescamine, and the relative fluorescence of the reaction product was measured for various concentrations of the polymer. On comparison with the capacity determined by analysis with ninhydrin after cleavage of alanine, a linear relationship between the content of amino groups and the relative fluorescence was found.

As another example, fluorescence was measured after reaction of fluorescamine with amino groups directly bound to the polymer chain of polymer II. The primary amino groups of polymer II were also coupled with alanine by dicyclohexylcarbodiimide. After cleavage of the alanine, the content of amino groups was determined by analysis of the cleaved alanine with ninhydrin. In this case the relative fluorescence was also a linear function of the concentration of the amino groups. A highly sensitive, rapid and simple determination of primary amino groups on soluble polymers is therefore possible by measuring the relative fluorescence after reaction with fluorescamine. The calibration to absolute values can be carried out with ninhydrin or any other method which is usual for monomers.

SUMMARY

A method for the rapid determination of primary amino groups on soluble polymers is described and discussed. After reaction of the amino groups with fluorescamine, the relative fluorescence is measured. The calibration and application of the procedure in practice is demonstrated for two copolymers of 1-vinyl-2-pyrrolidinone with alanine vinylester or allylamine.

REFERENCES

1 Houben, Weyl, Müller, *Methoden der Organischen Chemie, 14/2*, Verlag, Stuttgart, 1963, p. 926.
2 D. Braun, H. Cherdron and W. Kern, *Praktikum der makromolekularen Chemie*, Dr. Alfred Hüthig Verlag, Heidelberg, 1966, p. 85.

3 S. Udenfriend, S. Stein, P. Böhlen, W. Dairman, W. Leimgruber and M. Weigele, *Science*, 178 (1972) 871.
4 M. Weigele, J. F. Blount, J. P. Tengi, R. C. Czaijkowski and W. Leimgruber, *J. Amer. Chem. Soc.*, 94 (1972) 4052.
5 M. Weigele, S. L. DeBernhardo, J. P. Tengi and W. Leimgruber, *J. Amer. Chem. Soc.*, 94 (1972) 5927.
6 K. Geckeler and E. Bayer, *Makromolekulare Chemie*, in press.
7 H. Strathmann, *Chem. Ing. Tech.*, 42 (1970) 1095.
8 J. C. Sheehan and G. P. Hess, *J. Amer. Chem. Soc.*, 77 (1955) 1067.
9 *Catalogue, Ultrafiltration with Diaflo-Membranes, Publ. NV 400*, Amicon N.V., Oosterhout, Netherlands.
10 J. M. Stewart and J. D. Young, *Solid-phase Peptide Synthesis*, Freeman, San Francisco, 1969.
11 R. A. Fahmy, A. Niederwieser, G. Pataki and M. Brenner, *Helv. Chim. Acta*, 44 (1961) 2022.
12 E. Bayer and M. Mutter, *Nature (London)*, 237 (1972) 512.

Analytica Chimica Acta, 71 (1974) 85–96

SPECTROPHOTOMETRIC STUDIES ON THE REACTION OF COBALT WITH 4-(2-PYRIDYLAZO)-1,3-DIAMINOBENZENE AND ITS HALOGEN DERIVATIVES

SHOZO SHIBATA, MASAMICHI FURUKAWA and KAZUO GOTO

Government Industrial Research Institute, Nagoya Hirate-machi, Kita-ku, Nagoya (Japan)

(Received 2nd January 1974)

Recently, the analytical application of *o*-aminoazo compounds has been studied extensively[1–7]. The authors have already reported on the preparation of 4-(2-pyridylazo)-1,3-diaminobenzene (PADAB) and its halogen-substituted compounds, and their analytical application to the determination of cobalt[1,3] and palladium[6]. These cobalt complexes have extremely high molar absorptivities; for example, those values of PADAB, 4-[(5-chloro-2-pyridyl)azo]-1,3-diaminobenzene (5-Cl-PADAB) and 4-[(5-bromo-2-pyridyl)azo]-1,3-diaminobenzene (5-Br-PADAB) are 1.07, 1.12 and $1.17 \cdot 10^5$ l mol^{-1} cm^{-1}, respectively. The other main advantages in the use of these reagents are as follows: the bathochromic shifts caused by chelation are very large, so that in practice water can be used for blank solutions; the complexes are not decomposed even by addition of concentrated hydrochloric acid or other mineral acids; the selectivity is excellent; one of these cobalt complexes, CoL_2, is quantitatively extracted into organic solvents such as 3-methyl-1-butanol and tributylphosphate; both the reagents themselves and their complexes are very stable.

At the present time, these reagents for the spectrophotometric determination of small amounts of cobalt have received considerable attention owing to their unusual sensitivity and selectivity in comparison with others. Therefore, this work centered on the establishment of the mechanisms of complex formation between PADAB and its halogen derivatives and cobalt, in order to explain these characteristics.

EXPERIMENTAL

Reagents

PADAB, 5-Cl-PADAB and 5-Br-PADAB solution. The reagents were prepared by coupling *m*-phenylenediamine with 2-pyridyldiazotate in ethanolic or ethanolic aqueous solution[1]. The diazotate was prepared by Chichibabin's method. Purification was done by repeated reprecipitation–dissolution cycles from a (1 + 1) ethanol–water mixture; the reagents were finally purified by sublimation under vacuum if necessary. An ethanolic 10^{-3} *M* solution was prepared from the pure materials. The solutions were stable for several months if stored in an amber bottle.

Cobalt(II) solution. A 10^{-2} *M* stock solution was prepared from 99.99% pure cobalt metal as chloride.

Buffer solutions. 0.2 *M* Acetic acid–0.2 *M* sodium acetate, 0.2 *M* ammonia–

0.2 *M* ammonium chloride, and dilute hydrochloric acid, were used for pH adjustment. Sulfuric acid was used for $-H_0$ (Hammett's acidity function) adjustment.

Organic solvents were purified by the usual methods. All other reagents used were made from high-purity materials or purified reagents, and all solutions were prepared with redistilled water.

Apparatus

Absorbance curves were measured with a Model 300 Hitachi recording spectrophotometer with 1-cm cells. A Hitachi M5 type pH meter was used.

General procedures

Determination of acid-dissociation constants. The reagent stock solutions were pipetted into a 25-ml volumetric flask and appropriate buffers were added to adjust the pH. The ionic strength was adjusted to 0.2 by adding potassium chloride, and the solution was diluted to the mark with distilled water. The absorbance spectra were measured in a 1-cm cell at $20 \pm 0.5°C$, and the pH was measured using another portion of the solution.

Measurement of absorption spectra of cobalt complexes. The cobalt solution was pipetted into a 25-ml volumetric flask and suitable amounts of ethanolic reagent solution were added. Then the pH was adjusted to above 5 with dilute alkali or buffer. After a few minutes, the pH was adjusted to the required pH or $-H_0$ with buffer solution or concentrated sulfuric acid. However, in the case of the determination of the initial conditions for full colour development, the pH of the solution was adjusted to the required pH before addition of reagent (See Figs 5 and 13).

RESULTS AND DISCUSSION

Protonation behaviour of the reagents

All the reagents were sparingly soluble in water, but soluble in various organic solvents, including alcohol, dioxane, 3-methyl-butanol and tributyl phosphate. Four species of these reagents, H_3L^{3+}, H_2L^{2+}, HL^+ and L, are involved in the acid-dissociation behaviour. These four forms are related by the following equilibria (resonance and tautomeric forms omitted):

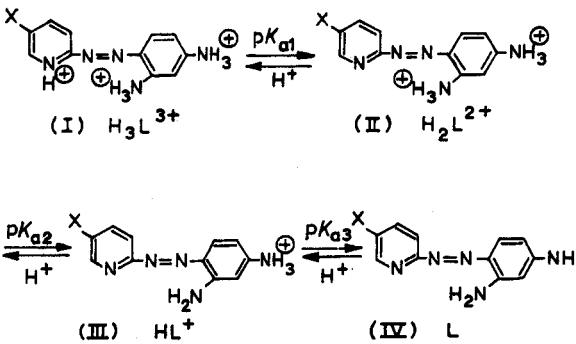

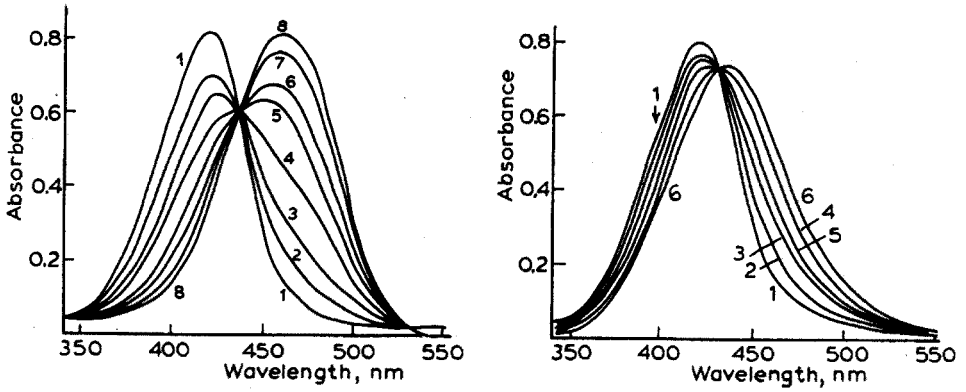

Fig. 1. Absorption spectra of 5-Cl-PADAB in aqueous solution, $2 \cdot 10^{-5}$ *M*, 1-cm cell. $-H_0$: (1) 0.53, (2) 4.44, (3) 4.84, (4) 5.23, (5) 5.61, (6) 6.00, (7) 7.47, (8) 8.14.

Fig. 2. Absorption spectra of 5-Cl-PADAB in aqueous solution, $2 \cdot 10^{-5}$ *M*, $\mu = 0.2$ *M* KCl, 20°C, 1-cm cell. pH: (1) 0.21, (2) 0.78, (3) 1.09, (4) 1.40, (5) 1.69, (6) 3.00.

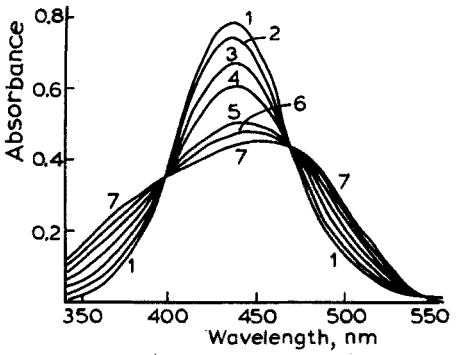

Fig. 3. Absorption spectra of 5-Cl-PADAB in aqueous solution, $2 \cdot 10^{-5}$ *M*, $\mu = 0.2$ *M* KCl, 20°C, 1-cm cell. pH: (1) 2.95, (2) 4.46, (3) 4.88, (4) 5.30, (5) 5.91, (6) 6.30, (7) 7.50.

where X = H, Cl and Br. The equilibria are marked by the isosbestic points on the absorption spectra of the reagents (See Figs. 1–3).

The dissociation equilibria of reagents may be formulated:

$$H_3L^{3+} \overset{K_{a1}}{\rightleftharpoons} H_2L^{2+} + H^+ \tag{1}$$

$$H_2L^{2+} \overset{K_{a2}}{\rightleftharpoons} HL^+ + H^+ \tag{2}$$

$$HL^+ \overset{K_{a3}}{\rightleftharpoons} L + H^+ \tag{3}$$

If simple relationships are assumed for the dissociation constants, then:

$$K_{a1} = \frac{[H_2L^{2+}][H^+]}{[H_3L^{3+}]} \tag{4}$$

$$K_{a2} = \frac{[HL^+][H^+]}{[H_2L^{2+}]} \tag{5}$$

and

$$K_{a3} = \frac{[L][H^+]}{[HL^+]} \tag{6}$$

These dissociation equilibria can be calculated independently because the steps are sufficiently separated. The following equation may be written for the first equilibrium in sulfuric acid

$$pK_{a1} = H_0 + \log \frac{A - A_{H_3L^{3+}}}{A_{H_2L^{2+}} - A} \tag{7}$$

where H_0 is Hammett's acidity function for the sulfuric acid solution; $A_{H_3L^{3+}}$, $A_{H_2L^{2+}}$ and A are the absorbances of a solution containing the two protonated species and a mixture of the two species, respectively. The acidity function of Paul and Long[8], and Jorgenson and Hartler[9] is used here. The following equations may be written for the second and third equilibria:

$$pK_{a2} = pH + \log \frac{A - A_{H_2L^{2+}}}{A_{HL^+} - A} \tag{8}$$

$$pK_{a3} = pH + \log \frac{A - A_{HL^+}}{A_L - A} \tag{9}$$

where the suffixes have the same meanings as those in eqn. (7). In Fig. 4 are shown the plots of absorbance *versus* pH for the calculation of the molar absorptivities of each particular form and the dissociation constants.

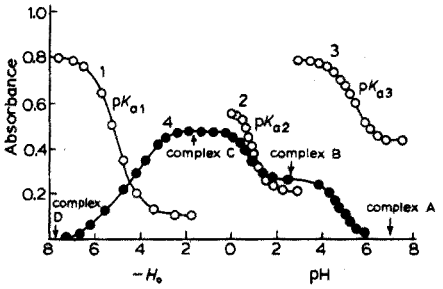

Fig. 4. Absorbance *vs.* pH curves for 5-Cl-PADAB and its cobalt complexes in aqueous solution 1-cm cell, 20°C. Reagent $2 \cdot 10^{-5}$ *M*, at (1) 470 nm, (2) 460 nm, (3) 435 nm. (4) Reagent $1 \cdot 10^{-5}$ *M* with a large excess of cobalt(II), at 570 nm.

The optical characteristics of the dissociated forms, the isosbestic points, and the dissociation constants found are listed in Tables I and II. According to the colour properties of the protonated forms and the known acidity constants of several 2-pyridylazo compounds and *m*-phenylenediamine[10], it may be assumed that the values of pK_{a1} correspond to the protonation of the pyridine nitrogen, and the values of pK_{a2} and pK_{a3} to the protonation of the two amino groups.

The reaction of cobalt ion with the reagents

Cobalt(II) reacts with the reagents from about pH 2 gradually upwards as shown in Fig. 5; the complex formation is accompanied by a decrease in the

TABLE I

ABSORPTION MAXIMA, MOLAR ABSORPTIVITIES AND ISOSBESTIC POINTS OF REAGENTS[a]

Form	*PADAB*		*5-Cl-PADAB*		*5-Br-PADAB*	
	λ_{max}	ε	λ_{max}	ε	λ_{max}	ε
H_3L^{3+}	458	4.2	462	4.1	464	4.1
↓↑	(430)		(438)		(442)	
H_2L^{2+}	417	4.0	422	4.1	424	4.2
↓↑	(436)		(430.5)		(432)	
HL^+	436	3.0	436	3.75	438	3.88
↓↑	(409)		(396, 469)		(396, 470)	
L	445	2.1	458	2.3	460	2.3

[a] λ_{max} and isosbestic points (in parentheses) are given in nm. All molar absorptivities (ε) are given as $\cdot 10^4$ l mol^{-1} cm^{-1}.

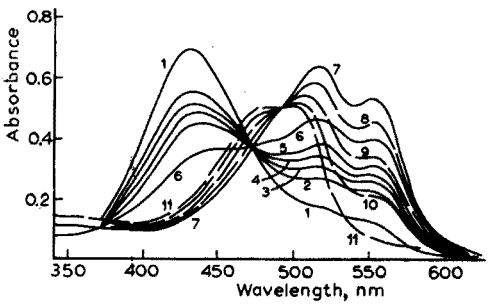

Fig. 5. Absorption spectra of 5-Cl-PADAB–cobalt complexes in aqueous solution, $1 \cdot 10^{-5}$ *M* reagent, cobalt in large excess, water as blank, 1-cm cell, 20°C. pH: (1) 1.50, (2) 2.34, (3) 2.58, (4) 2.90, (5) 3.08, (6) 3.40, (7) 3.98, (8) 4.42, (9) 4.82, (10) 5.29, (11) 7.50.

absorbance maximum at 436 nm and the appearance of two new absorbance peaks at about 520 and 560 nm. The formation of the cobalt complex starts immediately after the reactants have been mixed, and is complete within minutes. Above pH 4, the absorption maximum shifts to shorter wavelength with decreasing molar absorptivity; above pH 7 a definite complex (Complex A) is formed finally.

As mentioned above, cobalt and the reagents in acidic solution, below pH 1–1.5, do not form complexes (see Figs. 5 and 13). However, once the complex has been formed, it can be changed into another deeply coloured stable species (Complex C) via an intermediate (Complex B), which possesses increased absorptivity, by addition of mineral acid, such as hydrochloric, nitric, perchloric or sulfuric. Complex C is the most suitable for analytical purposes. It can also be changed into a final yellowish form (Complex D) by the addition of concentrated sulfuric acid. The absorption spectra of the cobalt complexes of 5-Cl-PADAB and 5-Br-PADAB are shown in Figs. 6–9.

The shape of the absorption spectra and the pH dependency of the cobalt complexes suggest that cobalt forms four types of complex with these reagents, and

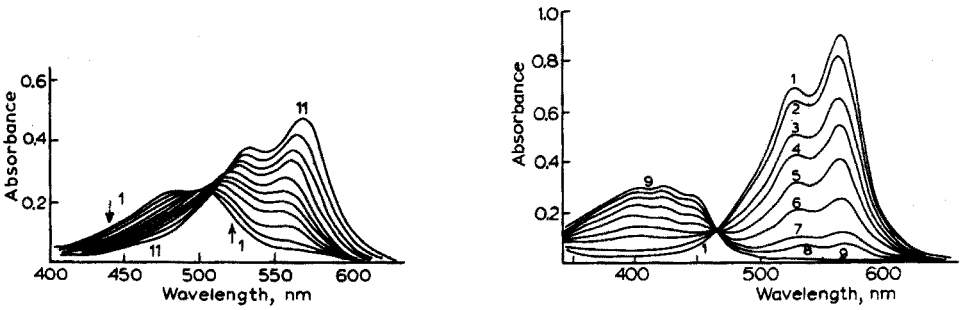

Fig. 6. Absorption spectra of 5-Cl-PADAB–cobalt complexes in aqueous solution. 10^{-5} *M* reagent, cobalt in large excess. Initial pH for full colour development is 6.0. pH: (1) 5.75, (2) 5.37, (3) 5.05, (4) 4.59, (5) 4.31, (6) 3.97, (7) 2.55, (8) 1.22, (9) 0.77, (10) 0.42, (11) $-H_0$ 0.43.

Fig. 7. Absorption spectra of 5-Cl-PADAB–cobalt complexes in aqueous solution, $1.6 \cdot 10^{-5}$ *M* reagent, cobalt in large excess, water as blank, 1-cm cell, 20°C. Initial pH for full colour development is 6.0. $-H_0$: (1) 1.35, (2) 3.61, (3) 4.44, (4) 4.84, (5) 5.23, (6) 5.61, (7) 6.00, (8) 6.39, (9) 7.47.

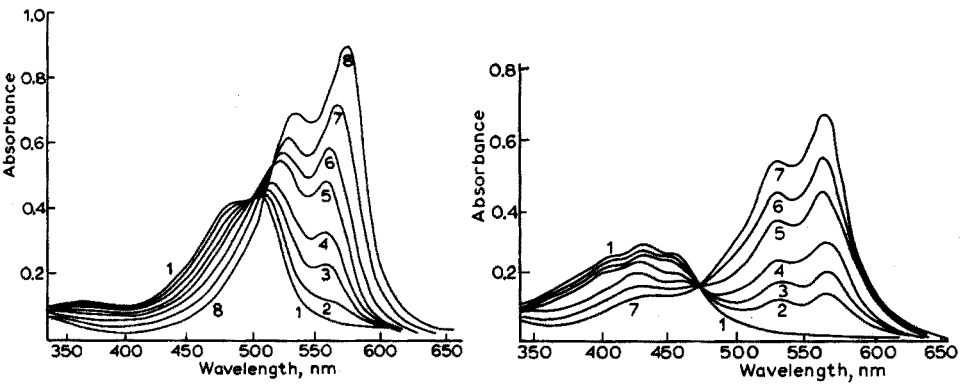

Fig. 8. Absorption spectra of 5-Br-PADAB–cobalt complexes in aqueous solution. $2 \cdot 10^{-5}$ *M* reagent, cobalt in large excess, water as blank, 1-cm cell, 20°C. Initial pH for full colour development is 7.5. pH: (1) 5.49, (2) 4.82, (3) 4.18, (4) 3.74, (5) 2.95, (6) 0.65, (7) 0.28, (8) $-H_0$ 0.59.

Fig. 9. Absorption spectra of 5-Br-PADAB–cobalt complexes, $2 \cdot 10^{-5}$ *M* reagent, cobalt in large excess, water as blank, 1-cm cell, 20°C. Initial pH for full colour development is 7.5. $-H_0$: (1) 7.89, (2) 5.86, (3) 5.62, (4) 5.38, (5) 4.64, (6) 4.13, (7) 3.00.

that the equilibria between the four complexes are completely reversible against pH or the Hammet's acidity function. In Fig. 4 is shown the plot of absorbance against pH for 5-Cl-PADAB complexes, and Figs. 10–12 show the plots of log $(A - A_{\text{complex A}})/(A_{\text{complex B}} - A)$ against pH for 5-Br-PADAB, which is a straight line of slope 1.0. The optical characteristics of the complexes, with the isosbestic points, are shown in Table III.

The initial pH of colour development for 5-Cl-PADAB in practical analysis is shown in Fig. 13. For these studies, the initial pH was as stated, but the absorbance was measured finally in 2.4 *M* hydrochloric acid media. The absorbance increases steeply in the pH range 2–3, but there is no change in absorbance

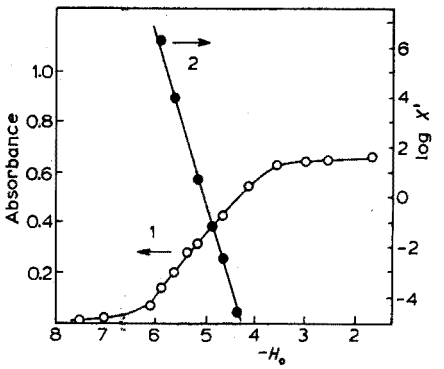

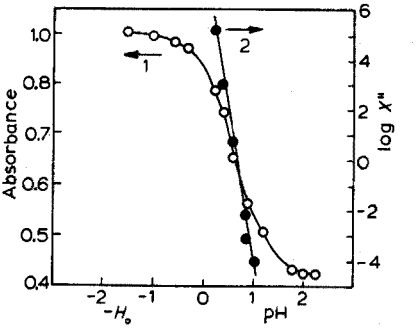

Fig. 10. The plots of the absorbance *vs.* pH and *vs.* log X', where $X'=[(A_{\text{complex C}}-A)/(A-A_{\text{complex D}})]$, for 5-Br-PADAB–cobalt complexes at 568 nm in 1-cm cells. (1) Absorbance *vs.* pH; (2) log X^1 *vs.* pH.

Fig. 11. The plots of the absorbance *vs.* pH and log X'', where $X''=[(A-A_{\text{complex B}})/(A_{\text{complex C}}-A)]$, for 5-Br-PADAB–cobalt complexes at 570 nm in 1-cm cells. (1) Absorbance *vs.* pH; (2) log X'' *vs.* pH.

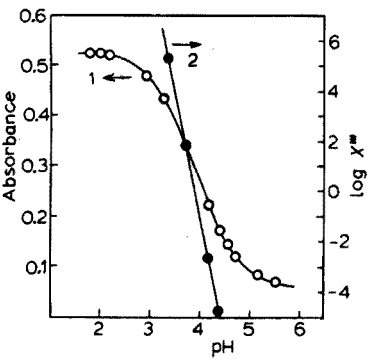

Fig. 12. The plots of the absorbance *vs.* pH and log X''', where $X'''=[(A-A_{\text{complex A}})/(A_{\text{complex B}}-A)]$ of 5-Br-PADAB cobalt complexes at 560 nm in 1-cm cells. (1) Absorbance *vs.* pH; (2) log X''' *vs.* pH.

TABLE II

ACID DISSOCIATION CONSTANTS OF REAGENTS IN AQUEOUS SOLUTION ($\mu=0.2$, KCl, 20 ± 0.5°C.)

Reagent	pK_{a1}[a]	pK_{a2}	pK_{a3}
PADAB	5.0	3.1	6.1
5-Cl-PADAB	5.4	1.3	5.4
5-Br-PADAB	4.9	1.3	5.5

[a] Hammett's acidity function in sulfuric acid.

over the pH range 3.5–11.5. The results show that all the cobalt ions are complexed with reagent in this pH region; this complex then changes to another deeply coloured species on addition of hydrochloric acid.

TABLE III

ABSORPTION MAXIMA OF COBALT COMPLEXES WITH MOLAR ABSORPTIVITIES[a]

Complex	*PADAB*		*5-Cl-PADAB*		*5-Br-PADAB*	
	λ_{max}	ε	λ_{max}	ε	λ_{max}	ε
CoL_2	469.5	5.4	480	4.9	484	5.4
↓↑	490	5.2	504	5.0	507	5.8
	(473.5)		(494)		(500)	
CoL_2H^+	507	6.6	520	6.2	522	7.3
↓↑	540	5.3	558	5.3	560	6.7
	(501.5)		(515)		(519)	
CoL_3H^{2+}	519	8.3	530	8.7	533	8.5
	555	10.7	568	11.4	572	11.7
↓↑	(440)		(464)		(474)	
$CoL_2H_n^{n+}$[b]	384	4.0	404	3.0	410	3.1
	400	4.1	424	3.1	433	3.7
	427	3.4	448	2.7	456	3.3

[a] λ_{max} and isosbestic points (in parenthesis) are given in nm. All molar absorptivities ε are given as $\cdot 10^4$ l mol^{-1} cm^{-1}.

[b] n is probably 3 (see text).

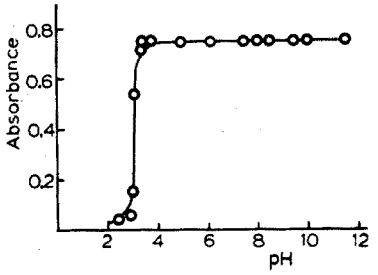

Fig. 13. Initial pH for full colour development of the 5-Cl-PADAB–cobalt complex, with reagent in large excess. Co, 0.4 p.p.m., 570 nm.

Composition of the cobalt complex

In order to establish the structure of each complex, the continuous variations and slope ratio methods were applied at pH 7.5, pH 2, 2.4 *M* hydrochloric acid and concentrated sulfuric acid. In every case one mole of cobalt reacts with two moles of reagent. The complexes contain the same molar ratio of cobalt to ligand, regardless of whether excess of cobalt or reagent is present.

The formation of protonated cobalt complex

As mentioned above, although cobalt ion reacts with the reagents to form several different complexes, the metal: ligand ratio of their complexes are the same. The explanation of this phenomenon probably lies in the formation of some protonated cobalt complexes which have high stability in acidic solution. Therefore, the following protonation steps are proposed for each equilibrium (charge for cobalt omitted).

$$CoL_2 \underset{pK_{a3}}{\overset{H^+}{\rightleftharpoons}} CoL_2H^+ \underset{pK_{a2}}{\overset{H^+}{\rightleftharpoons}} CoL_2H_2^{2+} \underset{pK_{a1}}{\overset{H^+}{\rightleftharpoons}} CoL_2H_3^{3+} \quad (10)$$

The protonation constant pK_a was calculated from the modified eqn. (1). The protonation constants determined are reported in Table IV.

The reaction of cobalt(II) with benzeneazo-m-phenylenediamine and pyridine-2-azo-p-dimethylaniline

Benzeneazo-*m*-phenylenediamine(V), *i.e.* chrysoidine, does not react with cobalt in aqueous solution. Therefore, the nitrogen of the pyridine ring must be very important for chelation.

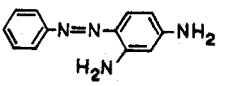

(V)

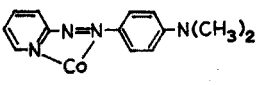

(VI)

On the other hand, pyridine-2-azo-*p*-dimethylaniline(VI) reacts with cobalt, and several physicochemical data have been reported by Klotz and Ming[11]. However, the cobalt complex is less stable than those of PADAB; an amino group in the *o*-position to the azo group is also co-ordinated to metals. Therefore, it appears that PADAB acts as a tridentate ligand, forming two stable 5-membered chelate rings by the use of the *o*-amino group, the heterocyclic nitrogen and the azo group. The structure of the cobalt complexes can be considered as follows (cobalt charge omitted):

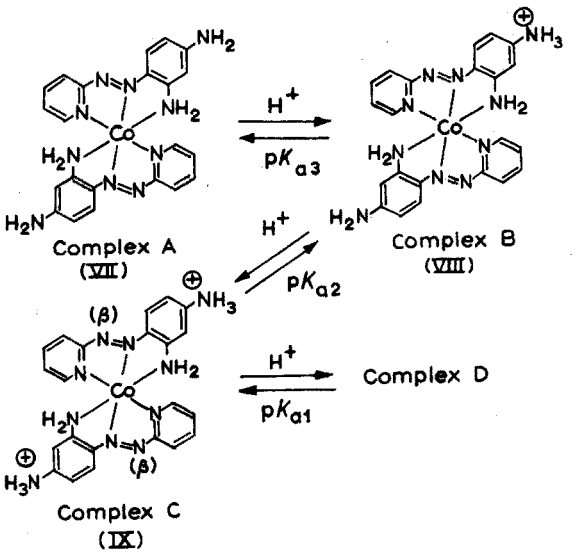

Distribution diagrams for the four species of the 5-Cl-PADAB–cobalt complex as a function of pH or $-H_0$ are shown in Fig. 14.

TABLE IV

PROTONATION CONSTANTS OF COMPLEXES IN AQUEOUS SOLUTION (20±0.5°C)

Reagent	pK_{a1}[a]	pK_{a2}	pK_{a3}
PADAB	4.2	1.4	5.3
5-Cl-PADAB	5.1	0.9	4.8
5-Br-PADAB	5.05	0.75	3.9

[a] Hammett acidity function in sulfuric acid.

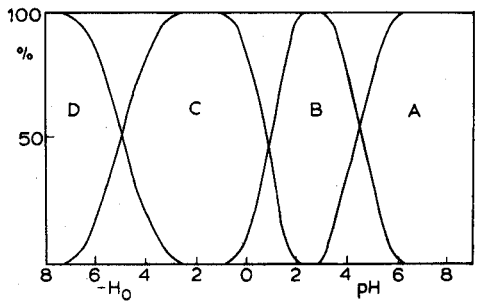

Fig. 14. Distribution diagram of the four cobalt–5-Cl-PADAB complexes as a function of pH.

At the present time, any decision on the composition of complex D is rather difficult because it is in chemical equilibrium in concentrated sulfuric acid. However, the considerable decrease in the molar absorptivity and the hypsochromic shifts of the absorption spectrum may be due to protonation on the β-nitrogen of the azo groups. In connection with this problem, it should be noted that the results of Fig. 10 for the pK_{a1} value of the 5-Br-PADAB cobalt complexes are appropriate to two protonation steps, that is to give $CoL_2H_4^{4+}$. In any event, complex D is not so important as an analytical species.

As mentioned before, many metals, *e.g.*, iron, nickel, copper, cobalt, palladium and mercury, react with these reagents under normal pH conditions (pH 2–10). But, in strongly acidic media, only the cobalt complexes are stable, and even in moderately acidic media (pH 2–2.4 *M* hydrochloric acid), only the cobalt and palladium complexes are stable. This stability of the cobalt and palladium complexes may be explained by the formation of an inner-orbital type complex. Other complexes probably contain bonds between the metal and the donor groups which are at least only partially covalent in nature or primarily ionic. Therefore, these complexes are not stable compared with those of cobalt and palladium. Further study of these cobalt and palladium complexes from the standpoint of chelate chemistry is necessary.

Valency state of cobalt in complex

The absorption spectra of the cobalt complex are virtually unaffected by the presence of ascorbic acid, hydrogen peroxide and potassium periodate; cobalt(II) and reagents react instantaneously, and the colour is not changed. The absorption spectra in 2.4 *M* hydrochloric acid medium was not recorded because of oxidation

of the reagents by potassium periodate. From these results, cobalt seems to be stabilized in the cobalt(II) state. Generally, the cobalt(III) state can be stabilized by complex formation. In the present case, stabilization of cobalt(II) may be due to a relatively low oxidation potential of the dyestuffs; the oxidation of cobalt(II) to cobalt(III) by oxygen is probably inhibited by the free amino groups of the complex and the large excess of reagents.

Extractable species of the cobalt complex

It was found, as expected from the proposed composition, that only CoL_2 (correctly written as $[CoL_2]2X$; X = univalent anion) can be completely extracted by 3-methyl-1-butanol or tributylphosphate (see Fig. 15). The cobalt can then be quantitatively back-extracted into a volume of acidic aqueous phase as its protonated complex $CoL_2H_2^{2+}$, since its distribution ratio into the acidic aqueous phase is high. This procedure should be very useful for the determination of small amounts of cobalt. Further investigations of solvent extraction are now in progress.

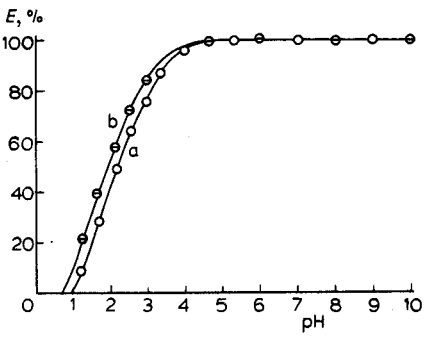

Fig. 15. Extraction of cobalt with 5-Cl-PADAB (a) and 5-Br-PADAB (b) in 3-methyl-1-butanol. Reagents in large excess. Initial pH of aqueous phase for full colour development is 5.

Further study with these reagents, particularly of their application to practical analysis, should be quite fruitful.

SUMMARY

Cobalt reacts with 4-(2-pyridylazo)-1,3-diaminobenzene (PADAB) and its halogen derivatives to form CoL_2 complexes. These complexes are changed into other deeply coloured monoprotonated complexes, CoL_2H^+, and diprotonated complexes, $CoL_2H_2^{2+}$, by the addition of hydrochloric or other mineral acids. The diprotonated complexes have extremely high molar absorptivities; the values for PADAB and 4-[(5-bromo-2-pyridyl)azo]-1,3-diaminobenzene (5-Br-PADAB) are 1.07 and $1.17 \cdot 10^5$ l mol^{-1} cm^{-1}, respectively. The CoL_2 complexes can be extracted quantitatively by 3-methyl-1-butanol or tributylphosphate, and then cobalt can be back-extracted into an acidic aqueous phase as its diprotonated complexes $CoL_2H_2^{2+}$. The acid dissociation constants of the ligand, composition of the complexes, protonation constants of the complexes, and valency state of cobalt, are described in detail.

REFERENCES

1 S. Shibata, M. Furukawa, Y. Ishiguro and S. Sasaki, *Anal. Chim. Acta*, 55 (1971) 231.
2 S. Shibata, in H. Flaschka and A. J. Barnard Jr. (Eds.), *Chelates in Analytical Chemistry*, Vol. IV. Marcel Dekker, New York, 1972, p. 220.
3 S. Shibata, *Bunseki Kagaku*, 21 (1972) 551.
4 S. Shibata, M. Furukawa and K. Goto, *Colloq. Spectrosc. Int. XVI*, preprints Vol. I, Heidelberg, 1971, p. 114.
5 S. Shibata, E. Kamata and M. Furukawa, *Int. Congress Analyt. Chem.*, I.U.P.A.C., Kyoto, April 1972, Abstracts p. 393.
6 S. Shibata, Y. Ishiguro and R. Nakashima, *Anal. Chim. Acta*, 64 (1973) 305.
7 S. Shibata, M. Furukawa and K. Goto, *Talanta*, 20 (1973) 426.
8 M. A. Paul and F. A. Long, *Chem. Rev.*, 57 (1957) 1.
9 M. J. Jorgenson and D. R. Hartter, *J. Amer. Chem. Soc.*, 85 (1963) 878.
10 A. Albert and E. P. Serjeant, *Ionization Constants of Acids and Bases*, Methuen, London, 1962, Table 8.12.
11 I. M. Klotz and W. C. Loh Ming, *J. Amer. Chem. Soc.*, 75 (1953) 4159.

Analytica Chimica Acta, 71 (1974) 97–105

NOUVELLE MÉTHODE DE DOSAGE PHOTOMÉTRIQUE AUTOMATIQUE DES PROTÉINES DANS LE LAIT ENTIER

PARTIE II. LINÉARITÉ, SÉLECTIVITÉ, SPÉCIFICITÉ*

J. BOSSET et B. BLANC

Station fédérale de recherches laitières de Liebefeld–Bern (Suisse)

E. PLATTNER

Institut de génie chimique de l'Ecole Polytechnique Fédérale de Lausanne (Suisse)

(Reçu le 2 janvier 1974)

ÉTUDE DE LA LINÉARITÉ

Il est reconnu depuis longtemps que la réaction du biuret sous sa forme classique suit la loi de Lambert–Beer dans un domaine assez vaste. La présence d'un second complexant du cuivre(II), la n-butylamine, amène à vérifier la validité de cette loi pour les conditions expérimentales proposées[1]. Ce point a été étudié de la manière suivante: on ajoute, comme pour les précédents essais, 5 ml du mélange des réactifs (2 ml d'une solution de Cu–EDTA–$Na_2 \cdot 2\ H_2O$ à 9,6 g l^{-1} en milieu NaOH 0,2 *M* et 3 ml de n-butylamine pure) à 0,1 ml de lait entier dont la concentration, après une série de dilutions avec de l'eau, varie de 0% (≡référence) à 100% (lait tel quel). On fait à nouveau abstraction de l'influence du lactose. Les mesures sont effectuées avec le PMQII, à 535 nm, contre de l'eau, après 15 min de développement à température ambiante. Les résultats obtenus sont présentés par le Tableau I.

Dans les conditions expérimentales ainsi définies, la loi de Lambert–Beer est

TABLEAU I

VÉRIFICATION DE LA LOI DE LAMBERT–BEER EN PRÉSENCE DE n-BUTYLAMINE

Conc. du lait (%)	E_{535}[a]	ΔE[a] *(apparent)*	*Conc. du lait (%)*	E_{535}[a]	ΔE[a] *(apparent)*
0	0,061	0,000	20	0,096	0,035
1	0,062	0,001	40	0,134	0,073
2	0,065	0,004	60	0,164	0,103
5	0,070	0,009	80	0,201	0,140
10	0,080	0,019	100	0,233	0,172

[a] Y compris la composante cuivre(II)–lactose omise en première approximation, qui intervient elle aussi proportionnellement avec la concentration.

* Extrait d'une thèse de doctorat menée sous la conduite des Prof. B. Blanc et E. Plattner.

donc vérifiée, en tous cas jusqu'à 80 ou 90% (v/v de lait dans l'eau). Au delà de cette concentration, la réponse photométrique obtenue s'écarte progressivement de la droite de proportionnalité (*cf.* Partie I[1]). C'est ce que montre le schéma de principe de la figure 1, lorsque le rapport Q (concentration en protéines/concentration en cuivre(II)) tend vers 1. Une augmentation de 25% à 50% de la teneur en cuivre(II) du réactif est donc souhaitable pour atteindre un excès suffisant.

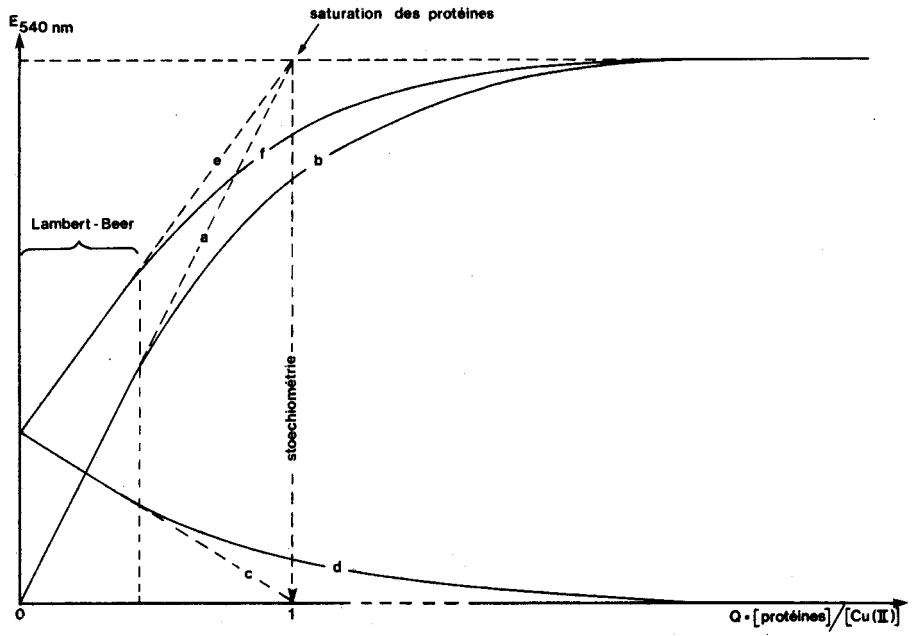

Fig. 1. Variation de la coloration en fonction de la concentration en protéines pour une concentration en cuivre(II) donnée (schéma de principe). a, Réponse (réelle, en négligeant la coloration du cuivre(II) en l'absence de protéine et de BTA) en l'absence de BTA; b, réponse (virtuelle) en présence de BTA (équilibre); c, réponse (virtuelle) de la BTA; d, réponse (virtuelle), différence de f−b (équilibre); e, réponse (virtuelle), somme de a+c; f, réponse (réelle), en présence de BTA (équilibre).

La loi de Lambert–Beer a encore été vérifiée avec d'autres "polypeptides" que les protéines du lait, notamment avec un standard proposé en chimie clinique pour étalonner les dosages de protéines du sérum sanguin (Standard à 5 g/100 ml, Diagnostica de F. Hoffmann–La Roche et Co., AG.).

SPÉCIFICITÉ ET SÉLECTIVITÉ

Si l'on définit la spécificité de la méthode comme la propriété de cette dernière de ne réagir qu'avec les protéines, dans leur ensemble (à l'exception de toute autre classe de substances), on peut définir la sélectivité de la méthode comme sa propriété de réagir différemment avec chaque type de protéine. L'idéal dans le cas présent est de disposer d'une méthode hautement spécifique, mais peu sélective.

De façon générale, on peut dire que la réaction est spécifique aux protéines, exception faite du lactose. Salwin[2] indique que ce dernier est le seul composant non protéique du lactosérum qui contribue à la réaction de coloration. Schober et coll.[3] parviennent à la même conclusion dans leur étude de l'influence des sels anorganiques sur le dosage de la caséine: ces derniers n'interviennent qu'à des concentrations beaucoup plus élevées (fractionnement des protéines[4]). Certains acides aminés libres peuvent donner une réaction positive avec le cuivre(II)[5], mais de façon générale, on peut considérer leur effet comme négligeable ou constant dans un lait frais et propre.

Quant à sa sélectivité vis à vis de protéines différentes, on trouve dans la littérature les avis les plus divergents[4-6]. C'est la raison pour laquelle les coefficients d'extinction ont fait l'objet de mesures particulières dans les conditions expérimentales propres à ce travail. L'étude a été effectuée avec les principales protéines lactiques*, à savoir avec le l'α- (41%), de la β- (27%) et de la κ- (12%) caséine, isolées, purifiées et lyophilisées, avec de la caséine native (mélange des trois, isolé par ultracentrifugation et dialyse) et avec de la caséine selon Hammarsten (mélange légèrement dénaturé, précipité à pH 4.6). Pour les protéines lactosériques, il a été retenu la β-lactoglobuline (9%) et l'α-lactalbumine (3%).

Après une semaine de dessiccation sur P_2O_5 jusqu'à poids constants, on dissout ou met en suspension environ 100 mg de protéines (4,5 mg pour l'α-lactalbumine vu sa rareté) dans 4 ml de soude 0.4 *M*. Au moyen d'une micropipette Eppendorf, 200 µl de solution sont mélangés au 5 ml de réactifs indiqués au paragraphe précédent. Après environ 30 min de reaction à température ambiante, les solutions ainsi obtenues sont mesurées à 540 nm, contre de l'eau. Les résultats obtenus sont consignés dans le tableau II. Le même essai, effectué avec 100 µl de

TABLEAU II

VALEURS DES $\varepsilon_{540\,nm}$ OBTENUES POUR LES PRINCIPALES PROTÉINES LACTIQUES[a]

Type	*ΔE (100 µl)*[b]	*Conc. engagée (mg/100 µl)*	ε_{540} *par g de protéine dans 100 µl*[c]	ε_{540} *par mole de protéine dans 100 µl*[c] *(·10³)*	ε_{540} *par pont peptidique*[c] *(·10³)*
α-Caséine	0,103	$2{,}584_5$	39,9	941	4,75
β-Caséine	0,105	$2{,}384_5$	44,0	1.056	5,08
κ-Caséine	0,083	$2{,}040_0$	40,7		
Caséine (pH 4.6)	0,100	$2{,}364_5$	42,3	—	—
Caséine (native)	0,106	$2{,}483_5$	42,7	—	—
β-Lactoglobuline	0,131	$2{,}341_5$	55,9	1.027	6,38
α-Lactalbumine	0,109	$2{,}229_0$	48,9	693	5,68

[a] Toutes les valeurs de ε_{540} indiquées sont entachées d'une erreur de l'ordre de ±3% qui est due aux erreurs de pesées, de pipetage et de photométrie.

[b] 100 µl = Volume de solution ou de suspension de protéine dans NaOH 0,4 *M* engagé pour l'essai.

[c] Apparent, car le E_R mesuré et soustrait (pour obtenir ΔE) est en fait plus grand que le E_R vrai, comme le montre la figure 1.

* Entre paranthèses est indiqué le pourcentage pondéral moyen de chaque type de protéines dans le mélange naturel complet.

solution, donne des valeurs égales à la moitié, ce qui confirme d'une part que l'excès de cuivre(II) engagé est suffisant, d'autre part que la loi de Lambert–Beer est également respectée pour chaque protéine prise individuellement.

L'enregistrement des spectres d'absorption de ces différentes protéines contre le réactif, à savoir ΔE (apparent), indique que leurs λ_{max} se situent tous entre 530–540 nm. Les sommets des pics sont suffisamment plats pour que les petites différences de leurs λ_{max} puissent être négligées.

Si l'on calcule la moyenne pondérée pour le mélange d'α-, β- et κ-caséines (en considérant que leurs poids sont approximativement dans le rapport 3:2:1), on obtient un ε_{540} voisin de 41,4 qui correspond assez bien aux valeurs mesurées de 42,3 pour la caséine selon Hammarsten et de 42,7 pour la caséine native. En conclusion, les différences des ε_{540} par gramme de protéine(s) sèche(s) pour les différentes caséines sont relativement faibles: −5,7% pour l'α-, −4,0% pour la β-, et −3,8% pour la κ-caséine par rapport à la valeur obtenue pour le mélange selon Hammarsten. Par contre, la différence est relativement plus importante en ce qui concerne les protéines lactosériques: +32,2% pour la β-lactoglobuline et +15,6% pour l'α-lactalbumine (toujours par rapport à la caséine selon Hammarsten, purifiée, considérée comme référence vu son importance quantitative). Si l'on fait la moyenne pondérée totale des valeurs obtenues pour la caséine (*ca.* 42,5 en moyenne) et les protéines du lactosérum, on trouve une valeur de ε_{540} proche de 44,0.

Sur la base d'une comparaison avec la méthode de Kjeldahl, Johnson et Swanson[4] ont déjà observé qu'il existe un écart appréciable entre la coloration due aux caséines et celle due aux protéines du lactosérum lors de la réaction du biuret. En chimie clinique, Sizer[7] note que non seulement le pourcentage de transmission à une longueur d'onde donnée, mais également la forme du pic est fonction de la nature et de la concentration des protéines, ce qui n'empêche pas de trouver chez Lieben et Jesserer[8] de même que chez Robinson et Hogden[9] l'affirmation du contraire.

Aucune théorie satisfaisante ne semble avoir été proposée jusqu'ici pour expliquer les différences de ε*. La connaissance de la structure primaire de chacune de ces protéines[10–13] permet de conclure que ces différences ne proviennent en aucun cas de la seule "densité" des liaisons peptidiques (nombre de ponts peptidiques/poids moléculaire) qui ne varie que très peu d'une protéine à l'autre: $8{,}384 \cdot 10^{-3}$ pour l'α-, $8{,}673 \cdot 10^{-3}$ pour la β-, $8{,}836 \cdot 10^{-3}$ pour la κ-caséine, $8{,}768 \cdot 10^{-3}$ pour la β-lactoglobuline et $8{,}606 \cdot 10^{-3}$ pour l'α-lactalbumine. Le calcul du nombre de sites actifs (atomes d'azote et d'oxygène) capables de fixer du cuivre(II) ne permet pas non plus d'expliquer à lui seul ces différences. Mehl et coll.[14] pensent qu'il faut les attribuer à la nature des acides aminés qui forment les ponts peptidiques. La composition en acides aminés intervient certainement, mais également leur séquence (structure primaire). Ce type d'interprétation n'est pas sans fondement théorique, puisque en un milieu aussi alcalin, surtout en présence de n-butylamine, les structures quaternaires et tertiaires sont détruites (protéines dissoutes par dénaturation), la structure secondaire étant selon toute vraisemblance elle aussi altérée;

* Il s'agit de ε apparents puisque calculés à partir d'un $\Delta E = E_A - E_R$ apparent. Si leurs valeurs absolues sont vraisemblablement un peu faibles, leurs valeurs relatives—qui sont intéressantes—sont certainement correctes.

cela n'exclut pourtant la possibilité que d'autres structures plus simples se reforment. Sans tenter de donner une explication irréfutable de la différence des extinctions dues aux protéines lactosériques et aux caséines, on peut formuler quelques hypothèses quant à ses origines. Intervient sans doute le degré d'"accessibilité" aux ligands, variable d'une protéine à l'autre en raison de la solubilité, de la polarité et de l'encombrement stérique de ces dernières. Les stoechiométries cuivre(II)–protéines et les constantes de dissociation ne sont peut-être pas les mêmes pour toutes les protéines et pour les différentes parties d'une même protéine (la stoechiométrie 1 Cu/4 N ne serait alors qu'une valeur moyenne). En résumé, il semble, que ces différences d'extinctions (pondérales, molaires, *etc.*) résultent de la somme de petites mais nombreuses différences de réaction, dont l'effet global devient sensible.

Influence du lactose

Jusqu'ici, l'influence du lactose sur la réaction dite du biuret n'a été que mentionnée. Pour la mise au point générale de la méthode, il est en effet possible, en première approximation, de la négliger ou de la considérer comme constante, mais il vaut la peine d'étudier son influence sur la réaction.

Le lactose peut intervenir comme réducteur et comme complexant. La réaction du biuret n'ayant lieu qu'avec le cuivre(II), il faut prévenir la réduction du cuivre(II). La dissolution du lait se réalisant en moins d'une minute de chauffage à 60°C et la formation du complexe cuivre(II)–protéines se formant en 15–30 min à température ambiante, il est aisé de travailler de façon à minimiser la formation de cuivre(I): il suffit de ne pas dépasser ce temps de chauffage, puis de laisser la réaction se développer à température ambiante. Par contre, la formation du complexe cuivre(II)–lactose est beaucoup plus génante, parce que impossible à éviter complètement sans gêner celle du complexe cuivre(II)–protéines.

L'étude du complexe cuivre(II)/lactose a été effectuée de la manière suivante. Expérimentalement, on effectue la même réaction que précédemment avec 100 μl d'une solution aqueuse ne contenant que du lactose (monohydraté) dont la concentration croît successivement de 0% à 10% (p/v)*. Les mesures sont effectuées comme précédemment à 540 nm, contre de l'eau, après 30 min de développement de réaction à température ambiante. Comme pour les protéines, la coloration se développe très rapidement pendant les premières minutes pour se stabiliser environ vers 15 à 30 min. Dans le domaine de concentration 0% à 10% (ΔE 0,000 à 0,037), la loi de Lambert–Beer est donc vérifiée, malgré la présence de n-butylamine. Ce chélateur du cuivre(II), bien qu'en grand excès par rapport au lactose, ne peut à lui seul totalement empêcher la formation du complexe cuivre(II)–ose. Les essais précédents montrent pourtant que l'extinction (apparente) due au complexe cuivre(II)–protéines est heureusement bien supérieure à celle due au complexe cuivre(II)–lactose: le rapport de ces extinctions apparentes (calcul pour des concentrations en lactose et en protéines normales dans un lait frais) est de l'ordre 7 à 8, ce qui signifie que l'extinction due au complexe cuivre(II)–lactose représente environ 11 à 13% de l'extinction totale (protéines + lactose du lait).

Une telle proportion n'est pas négligeable pour une analyse de précision (ε_{540} = 4/g de lactose monohydraté engagé dans les 100 μl de solution).

* Le lait frais contient approximativement 5% de lactose.

L'enregistrement du spectre d'absorption du complexe cuivre(II)–lactose au moyen du spectrophotomètre à double faisceau P.E.-124/165, contre une solution de référence (blanc) contenant tous les réactifs à l'exception du lactose ($\Delta E_{apparent}$), indique que le maximum se situe à 550–560 nm, au lieu de 535–540 nm pour les protéines. Les pics d'absorption des complexes que forme le cuivre(II) avec les protéines et avec le lactose sont donc presque superposés dans le visible, à la différence près de leur ε (amplitude différente). Enregistrés contre de l'eau, les spectres E_A montrent des maxima situés à *ca.* 695 nm en présence de lactose au lieu de *ca.* 685 nm en présence de protéines (pour le réactif seul: 705 nm). Une telle similitude dans les spectres d'absorption indique une similitude dans la structure des complexes formés.

La quasi superposition des pics d'absorption obtenus rend très difficile l'élimination de l'influence du lactose lors du dosage des protéines selon cette méthode. Si les maxima d'absorption se trouvaient être suffisamment distants l'un de l'autre, il serait possible d'effectuer deux mesures d'extinction aux deux λ_{max} correspondantes, et de corriger les résultats par le calcul. Mais le si faible décalage des pics (env. 10 nm aux λ_{max}) rend inopérante une telle solution. Une destruction chimique ou bactériologique du lactose n'entre pas en ligne de compte parce que ou trop lente ou trop agressive pour les protéines (hydrolyse, solubilité, *etc.*). On peut par contre envisager les quatre possibilités suivantes, qui présentent chacune avantages et inconvénients:

(a) négliger l'influence des variations de la teneur en lactose (et non la teneur en lactose elle-même) sur la détermination des protéines. Cette approximation est encore admissible pour des laits frais normaux ou bien conservés, vu que les variations de la teneur en glucides sont bien inférieures à $\pm 10\%$ relatifs (généralement $\pm 5\%$ relatifs). Si l'on considère de plus la faible contribution du lactose à l'extinction totale (*ca.* 11–13%), on obtient une erreur finale inférieure à $\pm 1\%$ relatif sur le dosage des protéines.

(b) doser parallèlement la teneur en lactose par une autre méthode insensible à la présence des protéines et des graisses, et corriger mathématiquement les résultats obtenus.

(c) engager du lactose ou une substance analogue en quantité telle qu'on sorte du domaine de Lambert–Beer avec la coloration "parasite". La pente de la courbe de réponse extinction/concentration tendant vers zéro, une variation de la teneur en lactose devient alors imperceptible. La glycérine, par exemple, donne un complexe analogue ($\lambda_{max} \simeq 560$ nm), sans présenter un pouvoir aussi réducteur. De plus, elle ne semble pas diminuer la dissolution ou la solubilité des divers composants du mélange. Cette substance a fait l'objet de l'essai suivant: au mélange de réactifs utilisés jusqu'ici, on ajoute encore 1 ml d'une solution de glycérine dont la concentration varie successivement de 0% à 100% (v/v) (les 100 μl d'eau ou de lait ne sont pas engagés). La figure 2 présente les résultats obtenus. Le grand désavantage de cette solution est l'énorme affaiblissement du signal photométrique donné par les protéines. En raison du déplacement des divers équilibres, la pente de la réponse extinction/concentration est réduit de plus des deux tiers. Il serait éventuellement possible de compenser cette perte par une expansion d'échelle ou par amplification par un facteur constant, mais les signaux dus au lactose et au bruit de fond en général sont également amplifiés.

(d) choisir une autre longueur d'onde, par exemple 342 nm, pour laquelle la différence des coefficients d'extinction des complexes cuivre(II)–protéines et cuivre(II)–lactose est plus grande qu'à 535 nm (le ΔE apparent des protéines est environ 2,5 fois plus grand à 342 nm qu'à 540 nm, contre environ 1,4 fois plus grand pour la lactose).

Influence de la matière grasse

On ne trouve dans la littérature aucune indication concernant l'influence des lipides. Cela est dû au fait que ces derniers sont normalement absents (pour le sérum sanguin) ou qu'on les élimine lors d'une étape antérieure (pour les protéines lactiques) puisqu'ils gènent en raison de la diffusion lumineuse qu'ils engendrent. Dans le cas d'une dissolution totale du lait entier, il est nécessaire de connaître leur influence. Cet essai a été effectué comme les précédents, mais avec 100 μl de différents esters (ester éthylique de l'acide acétique, ester méthylique de l'acide laurique, *etc.*), en l'absence de protéines et de lactose. On observe une légère diminution de la coloration finale. Ceci peut s'expliquer par le fait que l'ester (les triglycérides pour le lait) est lentement hydrolysé par le milieu. L'acide ainsi libéré est saponifié, abaissant légèrement le pH du milieu dont dépendent étroitement les constantes d'équilibre des complexes colorés. Comme pour le lactose, on ne peut négliger l'influence totale de la matière grasse—lors d'une analyse de précision—mais l'influence des variations de la concentration de celle-ci ($\leqslant \pm 1\%$ relatif sur la teneur en protéines). De plus, l'accroissement de la coloration dû à la glycérine

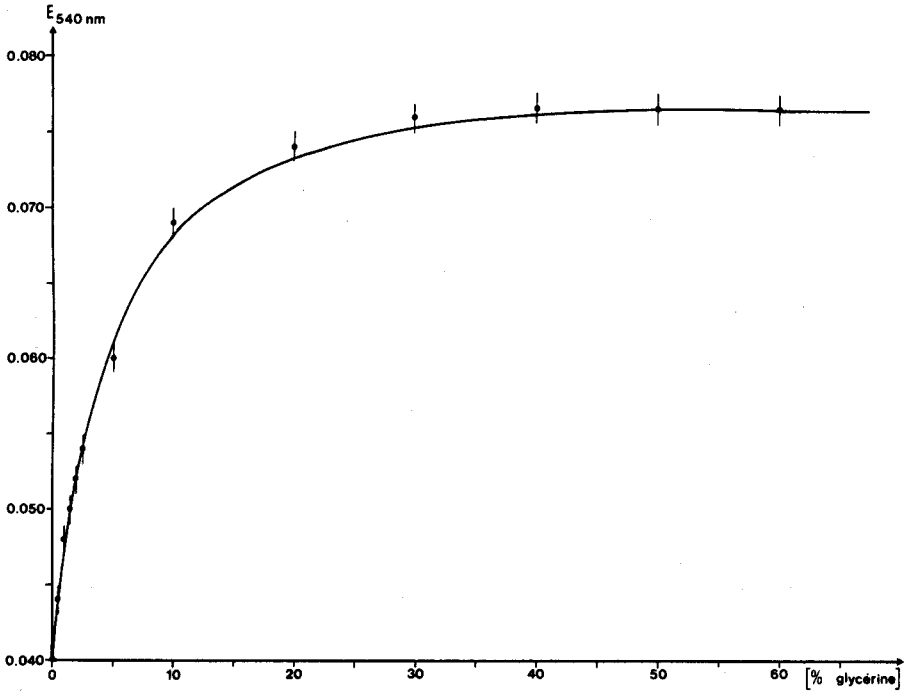

Fig. 2. Influence d'une éventuelle adjonction de glycérine.

libérée simultanément par l'hydrolyse des triglycérides lactiques compense encore l'effet de cette légère acidification. En travaillant à un pH plus élevé, on peut non diminuer la vitesse d'hydrolyse, mais l'influence de cette saponification sur le pH final.

CONCLUSION

A condition de disposer d'un excès de cuivre(II) suffisant (à cause de la n-butylamine), la coloration obtenue suit la loi de Lambert–Beer. Les résultats obtenus ont indiqué que l'extinction finale (mesurée) est fonction dans une certaine mesure de la composition en protéines (les protéines lactosériques ayant un coefficient d'extinction un peu plus élevé que les caséines) et, dans une moindre mesure, de la teneur en lactose et même en matière grasse. De plus, la méthode est relative. Ces considérations suggèrent que le meilleur système d'étalonnage est de prendre comme références (pour établir une droite d'étalonnage) un certain nombre de laits entiers frais analysés (parallèlement) par une autre méthode, absolue, par exemple par un Kjeldahl (PN = TN − NPN). Ainsi est-il possible de compenser dans une très large mesure tous les facteurs qui peuvent influencer le dosage des seules protéines.

Des essais manuels de reproductibilité ont montré que pour des mesures effectuées avec soin on peut atteindre un écart $\leqslant \pm 1\%$ relatif. Ce point sera repris lors de l'application entièrement automatisée de cette méthode, de même que l'étude du coefficient de corrélation avec la méthode de Kjeldahl qui indiquera en définitive dans quelle mesure les petites mais nombreuses approximations proposées dans ce travail sont acceptables, leur effet d'ensemble étant difficile à prévoir.

RÉSUMÉ

Cette deuxième partie indique que, même en présence de n-butylamine, les mesures des extinctions obtenues avec le complexe dit du biuret (pour différentes concentrations en protéines) suivent la loi de Lambert–Beer, à condition que l'excès de cuivre(II) engagé soit suffisant. Les interactions possibles entre les divers complexes colorés entrant en compétition y sont discutées. Une autre étude porte sur la sélectivité de la méthode en comparant les coefficients d'extinction que montre isolément chacune des principales protéines lactiques dans les conditions expérimentales définies précédemment. Une dernière étude est consacrée à la spécificité de la méthode, notamment à l'influence du lactose et des triglycérides présents lors de l'analyse.

SUMMARY

Absorbance measurements of the so-called "biuret complex" at different concentrations of milk proteins obey Beer's law, if copper(II) is used in sufficient excess, even in presence of n-butylamine. The possible interactions between the different coloured complexes are discussed. The selectivity of the method is studied by comparing the absorptivities of each isolated main protein under defined experimental conditions. The effects of lactose and triglycerides, which are the two main interfering compounds of fresh milk, are described and means of overcoming the interferences are discussed.

BIBLIOGRAPHIE

1 J. Bosset, B. Blanc et E. Plattner, *Anal. Chim. Acta*, 70 (1974) 327 (Partie I).
2 H. Salwin, *Food Res.*, 19 (1954) 235.
3 R. Schober, W. Niclaus et W. Christ, *Milchwissenschaft*, 10 (1955) 238.
4 B. C. Johnson et A. M. Swanson, *J. Dairy Sci.*, 35 (1952) 823.
5 P. Baudet et C. Giddey, *Helv. Chim. Acta*, 31 (1948) 1879.
6 E. Renner et S. Ömeroglu, *Z. Lebensm. Unters.-Forsch.*, 149 (1972) 335.
7 I. W. Sizer, *Soc. Exp. Biol. Med.*, 37 (1937) 107.
8 F. Lieben et H. Jesserer, *Biochem. Z.*, 285 (1936) 36.
9 H. W. Robinson et C. G. Hogden, *J. Biol. Chem.*, 135 (1940) 707.
10 R. L. J. Lyster, *J. Dairy Res.*, 39 (1972) 279.
11 J. C. Mercier, F. Grosclaude et B. Ribadeau-Dumas, *Milchwissenschaft*, 27 (1972) 402.
12 J. Jolles, F. Schoentgen, Ch. Alais et P. Jolles, *Chimia*, 26 (1972) 645.
13 H. A. McKenzie, *Milk proteins; Chemistry and Molecular Biology*, Vol. II, Academic Press, New York, 1971, pp. 117–215, 255–365.
14 J. W. Mehl, E. Pakovska et R. J. Winzler, *J. Biol. Chem.*, 177 (1949) 13.

Analytica Chimica Acta, 71 (1974) 107–111

EXTRACTION–SPECTROPHOTOMETRIC DETERMINATION OF DI(2-ETHYLHEXYL)PHOSPHORIC ACID WITH RHODAMINE B

K. BHATTACHARYYA and T. K. S. MURTHY

Chemical Engineering Division, Bhabha Atomic Research Centre, Trombay, Bombay-400085 (India)

(Received 10th December 1973)

Di(2-ethylhexyl)phosphoric acid (DEHPA) is used for the liquid–liquid extraction of uranium from sulphuric acid leach liquors obtained from ores[1, 2]. Hurst *et al.*[3] recently employed this extractant in synergic combination with trioctyl phosphine oxide (TOPO) for concentration of uranium from wet-process phosphoric acid. It also finds application in the recovery of many other metals[4–6]. In all these solvent extraction processes, there is a need for the determination of small amounts of extractant carried in the raffinates. As pointed out by Ashbrook[7], this is necessary not only from an economic point of view but also from the need to control environmental pollution. Ashbrook was also the first to report a spectrophotometric method for this purpose, based on the extraction of $Fe(SCN)^{2+}$, in association with DEHPA (anion) with carbon tetrachloride. In the work described here, the possibility of utilizing highly coloured cationic dyes to increase the sensitivity of the method is investigated. This paper gives the results with rhodamine B for the determination of traces of DEHPA in raffinates from sulphate leach liquors and wet-process phosphoric acid.

In acidic aqueous solutions and in polar organic solvents, rhodamine B (RB) exists predominantly in the protonated, highly coloured cationic form RBH^+. In the presence of a hydrophobic anion (A^-), it can form an ion-pair (RBH^+A^-), which is extractable by an organic solvent[8, 9]. The anion of DEHPA, in view of its structure, is well suited for such an ion-pair extraction. This is the basis of the present method. Since any other anion (inorganic or organic) present in the solution can, in principle, be extracted by the same mechanism, the success of the method lies in finding a solvent and aqueous phase conditions which can make the extraction of DEHPA selective.

EXPERIMENTAL

Reagents

Rhodamine B. B.D.H. Laboratory reagent-grade dye was purified[10] and a 0.2% solution made. The molar absorptivity in 1 *M* potassium chloride–0.03 *M* ammonia was found to be $9.9 \cdot 10^4$ as against $1.1 \cdot 10^5$ reported[8].

DEHPA solution. Prepare a 10 $\mu g\ ml^{-1}$ solution by dissolving a weighed amount of B.D.H. Laboratory reagent-grade DEHPA in 1,2-dichloroethane. When other solvents were to be tested, a known aliquot was evaporated and the residue dissolved in that solvent.

Phosphate mixture. Adjust 0.1 *M* potassium dihydrogenphosphate to pH 4 by adding phosphoric acid.

Solvents. Reagent-grade solvents were used after washing with 5% sodium carbonate and water.

Apparatus

For spectrophotometric measurements a Beckman Model B spectrophotometer with 10-mm glass cells was used.

Recommended procedure

Pipette 1–5 ml of the sample (sulphate liquor or wet-process phosphoric acid) into a separating funnel and dilute to 10 ml with 0.1 *M* sulphuric acid. Add 10 ml of 1,2-dichloroethane and shake for 2–3 min. Allow the phases to separate for 15 min. Collect the lower organic layer. Transfer an aliquot of this extract, containing 5–25 μg of DEHPA, along with enough fresh solvent to make the total volume 10.0 ml, to another separating funnel. Add 9 ml of phosphate mixture (pH 4) and 1.0 ml of rhodamine B (0.2%) solution and mix the contents for 2 min. After allowing to stand for 20 min, collect the coloured organic layer and measure its absorbance at 560 nm against 1,2-dichloroethane, as blank.

Determine the amount of DEHPA from a calibration curve obtained with known amounts (including a blank with zero DEHPA) added to 9 ml of phosphate mixture and 1 ml of rhodamine B solution and extracted into 10 ml of solvent.

RESULTS

Choice of solvent for extraction

For extraction of the coloured complex, the following solvents were tried: n-heptane (I), benzene (II), chlorobenzene (III), carbon tetrachloride (IV), chloroform (V), 1,2-dichloroethane (VI), methyl isobutyl ketone (VII), isobutanol (VIII), ethyl acetate (IX), and diisopropyl ether (X). Solvents I, II, III, IV, V and X showed low colour formation in the organic phase, while VII, VIII and IX showed high blanks by extracting the dye appreciably, even in the absence of DEHPA, presumably in association with other anions like $H_2PO_4^-$. 1,2-Dichloroethane (VI) showed the required property of low blank and high extraction of the complex. With this solvent, the aqueous phase became almost colourless, apparently because the dye was mostly transferred to the organic phase in the colourless lactone form.

Absorption spectrum of the extracted species

The spectrum of the DEHPA–rhodamine B complex in 1,2-dichloroethane is shown in Fig. 1. Maximal absorption occurs at 560 nm, while for the blank it occurs at 553 nm.

Effect of pH and dye concentration

To 10 ml of 0.1 *M* potassium dihydrogenphosphate adjusted to different pH values by addition of phosphoric acid or potassium hydroxide, were added 20 μg of DEHPA and 1 ml of dye solution. The complex was extracted into 10.0 ml of 1,2-dichloroethane and the absorbance of the organic layer was measured. A similar

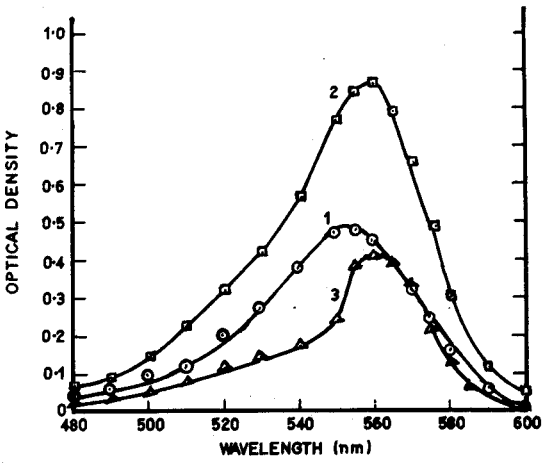

Fig. 1. Absorption spectra in dichloroethane. (I) Blank, (1) 20 μg DEHPA, (3) difference.

TABLE I

EFFECT OF pH ON THE DEHPA–RHODAMINE B COMPLEX

pH	*Absorbance (560 nm)*		
	Blank	*Sample*	*Difference (20 μg DEHPA)*
2.0	0.800	1.26	0.460
3.0	0.490	0.990	0.500
4.0	0.420	0.940	0.520
5.0	0.380	0.800	0.420
6.0	0.370	0.640	0.270

set (blank) of extractions was carried out in the absence of DEHPA. The results (Table I) show that at pH 4 the colour was maximal and this pH was adopted for all subsequent work. It was found that when acetate buffer was used, the blank readings were higher. Extractions from phosphate solution of pH 4 to which varying amounts of 0.2% rhodamine B were added, showed that the blank reading increased almost linearly with dye concentration. The absorbance of the standard became almost constant beyond 2 ml of dye. However, to keep the blank reasonably low, the addition of only 1.0 ml of dye solution was preferred.

The absorbances of the blank and sample (40 μg DEHPA) extracts did not vary up to 3 h of standing.

Calibration graph

The calibration graphs were linear up to 4 p.p.m. of DEHPA in 1,2-dichloroethane and beyond that there was a negative deviation. From the linear portion of the graph, the molar absorptivity was calculated as 75,000 (after correcting for blank).

Effect of additives in the solvent

Tri-n-butylphosphate, dibutyl-butylphosphonate and trioctylphosphine oxide

(TOPO) are generally added to the DEHPA–kerosene mixture as synergic agents[10], and primary alcohols like isodecanol and 2-ethylhexanol as modifiers. It was found that none of these reagents caused interference when added in a DEHPA: additive ratio of 1:200, while normally the ratio did not exceed 1:1.

Separation and determination of DEHPA from acid solutions

Since the method was to be applied for the determination of DEHPA in raffinates from solvent extraction runs of commercial wet-process phosphoric acid with DEHPA and TOPO, the effect of phosphoric acid on the recovery of DEHPA was studied. To 10 ml of 1.5–8 *M* phosphoric acid (reagent grade), 0.1 ml of an ethanolic solution of DEHPA was added and mixed well. DEHPA was then separated and determined by the recommended procedure. The results (Table II) showed that the recovery was not affected by acid concentration. Different salts were separately added to 6 *M* phosphoric acid to give 10 g Fe(II) l^{-1}, 10 g Fe(III) l^{-1}, 0.5 g U(VI) l^{-1}, 6 g Al(III) l^{-1}, 0.5 g Cr(III) l^{-1}, 30 g SiF_6^{2-} l^{-1} and 40 g SO_4^{2-} l^{-1}, and the recovery of 5 p.p.m. of added DEHPA was found to be unaffected.

TABLE II

DETERMINATION OF DEHPA IN PHOSPHORIC ACID

H_3PO_4(M)	1.6	3.2	4.8	6.4	8.0
DEHPA (μg) added	10	5	20	10	10
DEHPA (μg) found	10.6	4.8	19.1	10.0	9.5

In order to examine the determination of DEHPA in sulphate solutions, a synthetic solution containing 5 g Fe(III) l^{-1}, 3 g Al(III) l^{-1}, 1 g Ni(II) l^{-1}, 1 g Cu(II) l^{-1}, 2.5 g Mn(II) l^{-1}, and 50 g SO_4^{2-} l^{-1} at pH 1.5 was prepared, by mixing the sulphates; to 10-ml aliquots, 10, 20 and 30 μg of DEHPA was added. The separation and determination were carried out by the procedure given above. The experimentally determined values were within ±2 μg of the added amounts.

DISCUSSION

The method for the determination of DEHPA presented here is based on the formation of a highly coloured ion-pair (RBH^+A^-) (where $A^- = (C_8H_{17}O)_2\text{-}PO\cdot O^-$) which is soluble in dichloroethane. The dye is extracted almost completely into the organic phase in a colourless lactone form from phosphate solution of pH 4 in the absence of DEHPA, whereas in its presence the colour of the organic phase intensifies. Thus the following equilibria probably predominate.

$$\underset{\text{(coloured, quinonoid form)}}{RBH^+H_2PO_4^-} \overset{pH_4}{\rightleftharpoons} \underset{\text{(colourless, lactone form)}}{(RB)_{org} + H_3PO_4} \quad (1)$$

$$(RB)_{org} + (HA)_{org} \rightleftharpoons \underset{\text{coloured}}{(RBH^+A^-)_{org}} \quad (2)$$

Equilibrium (1) depends on the pH of the aqueous solution and the nature of the organic solvent. At low pH and with polar solvents, more of the dye is extracted as coloured ion-pairs, ($RBH^+ H_2PO_4^-$). DEHPA is known to exist as a dimer[11] in organic solvents, the extent of dimerization depending on the nature of the solvent. Many of the solvents tested did not lead to sufficient colour formation, perhaps because of the high stability of the dimer in these solvents.

For the determination of DEHPA in sulphate liquors and phosphoric acid raffinates, a preliminary extraction with 1,2-dichloroethane is recommended. This is mainly to avoid the effect of the precipitate formed when the solution is neutralized to pH 4 in the presence of phosphate; the precipitate tends to adsorb traces of DEHPA causing 5–20% negative errors. The dissolved and suspended DEHPA in actual raffinates was of the order of 10–25 p.p.m., so that a 1–2 ml aliquot should be sufficient for analysis and the adverse effect of precipitate formed should be negligible. However, a practical difficulty is experienced in sampling such raffinates, owing to adsorption of traces of extractant on the surface of pipettes, *etc.* To overcome this effect, it is recommended that a larger volume of raffinate, say 10–20 ml, be taken and the DEHPA extracted into a known volume of 1,2-dichloroethane. Other precautions for the same purpose were suggested by Ashbrook[12]. As mentioned earlier, the only other spectrophotometric method reported for this purpose is that of Ashbrook[7]. The sensitivity of the proposed method appears to be about 200 times greater.

SUMMARY

A spectrophotometric method for the determination of traces of di(2-ethylhexyl)phosphoric acid (DEHPA) in raffinates from solvent extraction processes is described. The two types of aqueous solutions considered are sulphate leach liquors from uranium ores, and wet-process phosphoric acid (6 *M*) which originally contained uranium. The method is based on the formation of a strongly coloured ion-pair between the rhodamine B cation and the DEHPA anion in 1,2-dichloroethane. DEHPA is extracted from the aqueous solution by dichloroethane, and the organic layer is contacted with an aqueous solution containing rhodamine B and phosphate buffer pH 4. The effective molar absorptivity of the coloured complex is about 75,000.

REFERENCES

1 C. A. Blake, K. B. Brown and C. F. Coleman, *Report ORNL-1903* (1955).
2 K. B. Brown, C. F. Coleman, D. J. Crouse, C. A. Blake and A. D. Ryon, *Int. Conf. Peaceful Uses At. Energy, Geneva*, 3 (1958) 478.
3 F. J. Hurst, D. J. Crouse and K. B. Brown, *Report ORNL-TM-2522* (1969).
4 C. A. Blake Jr., C. F. Baes Jr., K. B. Brown, C. F. Coleman and J. C. White, *Int. Conf. Peaceful Uses At. Energy, Geneva*, 28 (1958) 296.
5 G. M. Ritcey and A. W. Ashbrook, *Trans. Instn. Mining Met.*, C, 78 (1969) 57.
6 T. C. Owens and M. Smutz, *J. Inorg. Nucl. Chem.*, 30 (1968) 1617.
7 A. W. Ashbrook, *Anal. Chim. Acta*, 58 (1972) 123.
8 R. W. Ramette and E. B. Sandell, *J. Amer. Chem. Soc.*, 78 (1956) 4873.
9 I. M. Korenman, F. R. Sheyanova and A. A. Kalugin, *Chem. Abstr.*, 17 (1969) 64138d.
10 C. A. Blake Jr., C. F. Baes Jr., K. B. Brown, C. F. Coleman and J. C. White, *Int. Conf. Peaceful Uses At. Energy, Geneva*, 28 (1958) 294.
11 T. Sato, *J. Inorg. Nucl. Chem.*, 27 (1965) 1402.
12 A. W. Ashbrook, Dept. of Energy, Mines and Resources, Mines Branch, Canada. *Inf. Circular IC, 284* (1972) 23.

Analytica Chimica Acta, 71 (1974) 113–121

DETERMINATION OF URANIUM IN NATURAL WATERS AFTER ANION-EXCHANGE SEPARATION

J. KORKISCH and L. GÖDL

Analytical Institute, Analysis of Nuclear Raw Materials Division, University of Vienna, Währingerstrasse 38, A-1090 Vienna (Austria)

(Received 15th January 1974)

The uranium content of non-saline natural waters is usually lower than that of sea water, hence highly sensitive methods are required for the determination of uranium in water samples which are collected for prospecting purposes. Canadian experience[1,2] in hydrogeochemical prospecting shows that the detection limit must be better than a few tenth of 1 p.p.b., because uranium contents of land waters in excess of 1 p.p.b. (1 $\mu g\ l^{-1}$) are regarded as an anomaly.

Besides showing high sensitivity, any method employed for the determination of uranium in waters should also be applicable on a routine basis, so that the large number of samples required for uranium prospecting can be analysed effectively. Of the methods in use, the commonest is based on measuring the fluorescence of uranium in an alkali metal fluoride flux[3]. In many cases, however, this fluorimetric method cannot be applied directly, *i.e.* without preliminary enrichment and separation of uranium from the water matrix, because of the presence of elements such as iron which quench the uranium fluorescence. For this reason, and also to increase the detection limit and the accuracy of the fluorimetric determination of uranium, this method is best used in combination with anion-exchange separation procedures[4–7]. In this paper, a combination of these methods is described.

EXPERIMENTAL

Solutions and reagents

Ion-exchange resin. The strongly basic anion-exchange resin Dowex 1 (Bio-Rad AG 1-X8; 100–200 mesh; chloride form) was used. Slurry the resin (4 g) with a few ml of the pretreatment solution (see below) and after about 15 min pour into an ion-exchange column. Subsequently, wash the resin bed with 50 ml of the pretreatment solution to convert the resin to the thiocyanate form.

Uranium standard solutions. Dilute aliquots of a stock solution, containing 500 μg of uranium (as uranyl chloride) per ml of 6 *M* hydrochloric acid, with 6 *M* hydrochloric acid to obtain standard solutions containing 0.025–10 p.p.m. of uranium.

Pretreatment solution. This solution is prepared a few hours before its use. Acidify 100 ml of distilled water with 1 ml of concentrated hydrochloric acid and dissolve in it 0.5 g of ascorbic acid and 1 g of potassium thiocyanate. Solutions older than about 2–3 days are less effective for pretreatment of the resin.

THF–MG–HCl mixture. Prepare a mixture of 50 vol.% tetrahydrofuran

(THF), 40 vol.% methyl glycol (MG, monomethyl ether of ethylene glycol) and 10 vol.% 6 *M* hydrochloric acid. In order to prevent the formation of air bubbles in the resin bed, prepare the mixture several hours before use. This solution can be stored indefinitely without loss of effectiveness as eluent.

Reagent solution. Prepare an aqueous 0.1% solution of arsenazo III (ref. 3, p. 174).

Other reagents. Zinc metal was used in the form of zinc dust or finely granulated zinc. Fluorbase (200 mg) pellets consisting of 95% sodium fluoride and 5% lithium fluoride (Nordrhein-Chemie, Wolfgang Zeh jun., 41 Duisburg 12, Western Germany) are also needed.

Apparatus

The uranium separations were performed in ion-exchange columns of the same type and dimensions as described earlier[8].

The fluorimetric determinations were carried out with a Galvanek–Morrison fluorimeter, Mark V (Jarrell-Ash).

A Beckman spectrophotometer model B, with 1-cm cells, was also employed.

Ion-exchange procedure

Acidify 1 l of the water sample with 10 ml of concentrated hydrochloric acid. (If a larger or smaller volume of sample is required for analysis, the amounts of reagents to be added have to be varied accordingly.) Filter through a dense filter and to the filtrate add 5 g of ascorbic acid and 10 g of potassium thiocyanate. Mix thoroughly until the reagents have dissolved, and after 5–6 h pass the mixture (sorption solution) through an ion-exchange column containing 4 g of the pretreated anion-exchange resin using a flow rate which corresponds to the back-pressure of the resin bed (about 70–80 ml h^{-1}). Afterwards, wash the resin bed with 100 ml of the THF–MG–HCl mixture (or 200 ml for water samples containing large amounts of iron) and then with 100 ml of 6 *M* hydrochloric acid. Subsequently elute the uranium with 50 ml of 1 *M* hydrochloric acid (uranium eluate).

Determination of uranium

Fluorimetric method. Evaporate the uranium eluate to dryness on a steam-bath and take the residue up in 2 ml of 6 *M* hydrochloric acid. Evaporate an aliquot (*e.g.* 0.1 ml) of this solution in a small platinum dish[8] and after addition of a Fluorbase pellet, prepare a melt by fusion, under strictly controlled conditions[3]. Measure the fluorescence intensity of the cold flux and compare with the intensities of fluxes of known uranium concentrations.

Spectrophotometric method[9]. Evaporate the uranium eluate to dryness on a steam-bath and transfer the residue to a 50-ml wide-neck Erlenmeyer flask by taking it up in 5 ml of 9 *M* hydrochloric acid added in portions. To this solution, add an exactly weighed amount of 0.550 g of zinc and cover the flask loosely with a stopper. During this reduction process, shake the flask carefully until all the zinc has dissolved. Immediately afterwards, add 0.15 g of oxalic acid and 0.50 ml of the arsenazo III solution and measure the absorbance of the solution at 665 nm against a reagent blank solution prepared in the same way. Obtain the uranium content by comparison with a calibration curve (in the concentration range 1–10

μg of uranium) which is constructed by using the reduction procedure described above. The absorbance remains constant for at least 30 min and for 5 μg of uranium its value is 0.20.

RESULTS AND DISCUSSION

Anion-exchange separation of uranium

The anion-exchange separation procedure described is based on the fact that uranium forms an anionic thiocyanate complex which is strongly retained by strongly basic anion-exchange resins[10–17]. A batch equilibrium study showed that the weight distribution coefficient of uranium(VI) has a value of 6970 in the presence of 10 g of potassium thiocyanate per litre of water sample (acidified with 10 ml of concentrated hydrochloric acid and containing 5 g of ascorbic acid). However, in the presence of 1 g and 5 g of thiocyanate, the distribution coefficients of uranium have the much lower values of 8.46 and 78, respectively, whereas a value of 85,000 was measured when the thiocyanate concentration was increased to 20 g l^{-1}.

When a thiocyanate concentration of 10 g l^{-1} or higher is used, it is possible to adsorb uranium quantitatively on the resin even if its concentration is as high as 1000 μg l^{-1}. This is illustrated by the results (Table I), which were obtained by applying the recommended procedure to the analysis of deionized water samples to which known amounts of uranium had been added.

To investigate the effect of the volume of water sample on the recovery and accuracy of the uranium determination, varying volumes of tap water were analysed for its natural uranium content. The results are shown in Table II. It can be seen that the volume of water has no effect on the recovery of uranium, because of the high distribution coefficient (6970). However, the volume has a decided influence of 85,000 was measured when the thiocyanate concentration was increased to 20

TABLE I

RECOVERY OF URANIUM FROM 1-l SAMPLES OF DEIONIZED WATER CONTAINING KNOWN AMOUNTS OF URANIUM

U added (μg)	1	5	10	50	100	500	1000
U recovered (μg)	1.16	5.15	9.45	58.25	105.5	539	989

TABLE II

FLUORIMETRIC DETERMINATION OF URANIUM IN VIENNA TAP WATER AFTER SEPARATION BY ANION-EXCHANGE

Tap water taken (l)	0.1	0.5	1	2	5
U content found (μg l^{-1})	0.1	0.30	0.31	0.37	0.31
	0.1[a]	0.31[b]	0.26[c]	0.37[c]	0.31[c]

[a] Uranium content after deduction of 0.025 μg of uranium which was added as a spike before the anion-exchange separation.

[b] Uranium content after deduction of 0.125 μg of uranium which was added as a spike before the anion-exchange separation.

[c] Uranium content after deduction of 0.25 μg of uranium spike which was added per litre of sample before the anion-exchange separation.

on the accuracy of the fluorimetric uranium determination when sample volumes of less than 0.5 l are analysed; the uranium content is then too low to allow accurate determinations. From the results of uranium determinations in the tap water samples, 0.5–5 l (Table II), an arithmetic mean value of 0.317 μg U l^{-1} was calculated.

Effects of other metal ions

The addition of ascorbic acid to the acidified water sample serves to reduce iron(III) to iron(II) and thus to prevent the coadsorption of the deep-red anionic iron(III)–thiocyanate complex. This reduction, however, is not complete in the presence of thiocyanate, so that part of the iron is coadsorbed with the uranium; this is clearly indicated by a more or less red coloration of the resin bed after passage of the water sample. A more complete reduction of iron is obtained if the water sample is not passed immediately after addition of ascorbic acid and thiocyanate, but 5–6 h later.

Also retained by the resin are the anionic thiocyanate complexes of the following metals: vanadium[10,18], molybdenum[19,20], copper[10], cobalt[10,21], zinc[10,21], cadmium[10,21], mercury[10,21], and silver[10,21]. However, these elements are not likely to interfere with the adsorption of uranium because their contents in natural waters are usually also in the p.p.b.-range, so that they cannot displace uranium from the resin.

On washing the resin bed with the THF–MG–HCl mixture, the portion of iron which was adsorbed as thiocyanate complex is quantitatively removed from the resin. With this mixture, the thiocyanate complexes of iron, uranium, cobalt, copper and of other coadsorbed metal ions are effectively destroyed, and chloride complexes are formed which are strongly retained by the resin (in the THF–MG–HCl mixture, the distribution coefficient of uranium has a value of 3630), except for vanadium, iron and most of the molybdenum, which are eluted owing to the CIESE effect[6]. This elution of iron and molybdenum is clearly indicated by the removal of the red thiocyanate band, which moves down the resin bed soon after washing with the THF–MG–HCl mixture has been started. By means of this mixture, the last traces of ascorbic acid and potassium thiocyanate are also removed from the resin bed

The washing step, involving treatment of the resin with pure aqueous 6 *M* hydrochloric acid, serves to separate uranium from copper, silver and cobalt which have low distribution coefficients in this acid[6] and hence pass into the effluent. Further adsorbed on the resin from this 6 *M* acid are uranium (distribution coefficient, 283), molybdenum (the residual amount which was not removed with the THF–MG–HCl mixture), zinc, cadmium and mercury; of these, only molybdenum passes into the eluate when uranium is eluted with 1 *M* hydrochloric acid.

Investigations of the suitability of various eluents for uranium after its adsorption as the thiocyanate complex gave the results summarized in Table III. It can be seen that uranium can be eluted very effectively by means of eluent systems 1 and 2, while on application of the other media only 50% (elution with perchloric acid[12]) or practically no uranium at all is detectable in the eluate. The eluent system 2, as well as concentrated hydrochloric acid followed by water as recommended by other authors[10], has the disadvantage that it elutes not only uranium but also iron[10,21]

TABLE III

SUITABILITY OF VARIOUS ELUENTS FOR THE QUANTITATIVE ELUTION OF THE URANIUM THIOCYANATE COMPLEX

(100 μg uranium[a]; 4 g column of Dowex 1)

Eluent system	*Uranium content of eluate (μg)*
1 100 ml THF–MG–HCl mixture followed by 100 ml 6 *M* HCl and 50 ml 1 *M* HCl	100
2 50 ml concentrated HCl followed by 50 ml 1 *M* HCl	97
3 50 ml 1 *M* $HClO_4$	50.5
4 50 ml 6 *M* HCl followed by 50 ml 1 *M* HCl	0.08
5 50 ml 1 *M* HNO_3	0.00
6 50 ml 2 *M* H_2SO_4	0.00

[a] This amount of uranium was added to 1-l samples of deionized water and the solutions were treated by the recommended procedure.

which interferes with the determination of uranium by quenching its fluorescence. An effective separation of uranium from iron (and also from most of the molybdenum), after these elements have been adsorbed as thiocyanate complexes, is possible only by a combination of an aqueous–organic solvent mixture with pure aqueous hydrochloric acid solutions (eluent system 1).

Although it is expected that not more than p.p.b.-quantities of the coadsorbable elements (except iron and molybdenum, of which p.p.m.-amounts are contained in some samples) are present in natural waters, experiments were carried out to investigate the effect of varying concentrations of these metal ions on the anion-exchange separation and determination of uranium. The results (Table IV) show that the accuracy of both the fluorimetric and spectrophotometric methods for uranium is very much dependent on the amount of coadsorbed metal ion and on the washing procedure which is used for its removal from the resin. Thus, when the washing technique described in the Procedure section is employed, quantitative separation of uranium from all metal ions is obtained, provided that their concentrations do not exceed 500 $\mu g\ l^{-1}$. At higher concentrations of iron (5 or 50 $mg\ l^{-1}$; see Table IV), 100 ml of the THF–MG–HCl mixture is not sufficient to elute the coadsorbed iron quantitatively, so that a portion of this element passes into the uranium eluate where it causes a quenching of the uranium fluorescence and also interferes with the spectrophotometric uranium determination. Thus, when uranium is to be determined in water samples containing very large amounts of iron, the resin bed should be washed with 200 ml of the THF–MG–HCl mixture.

When uranium is determined by the spectrophotometric arsenazo III method, special attention must be paid to the fact that incomplete removal of coadsorbed molybdenum may cause serious interferences (see Table IV). The molybdenum which is coeluted with uranium can either lead to a relatively small positive error or to a very large negative error if its concentration exceeds 100 μg in the measuring solution (see Table V); in the presence of 200–500 μg of molybdenum, zero recovery of uranium was obtained. Therefore, the spectrophotometric arsenazo III method

TABLE IV

EFFECT OF COADSORBED METAL IONS ON ANION-EXCHANGE SEPARATION AND DETERMINATION OF URANIUM

Metal tested	*Amount (μg) added to 1 l Vienna tap water spiked with 5 μg U*	*Washing procedure before elution of U with 50 ml 1 M HCl*	*Uranium content (μg l⁻¹)*	
			Fluori-metry	*Spectro-photo-metry*
Fe(III)	50	50 ml THF–MG–HCl + 50 ml 6 *M* HCl	5.25	5.35
	500	50 ml THF–MG–HCl + 50 ml 6 *M* HCl	4.87	5.20
	5000	50 ml THF–MG–HCl + 50 ml 6 *M* HCl	4.55	3.94
	50000	50 ml THF–MG–HCl + 50 ml 6 *M* HCl	2.14	0.85
	500	100 ml THF–MG–HCl + 100 ml 6 *M* HCl	4.95	5.00
	5000	100 ml THF–MG–HCl + 100 ml 6 *M* HCl	3.37	4.82
	50000	100 ml THF–MG–HCl + 100 ml 6 *M* HCl	2.74	4.56
	500	50 ml 5% aq. ascorbic acid soln. + 100 ml THF–MG–HCl + 100 ml 6 *M* HCl	5.25	5.10
	5000	50 ml 5% aq. ascorbic acid soln. + 100 ml THF–MG–HCl + 100 ml 6 *M* HCl	4.85	4.55
	50000	50 ml 5% aq. ascorbic acid soln. + 100 ml THF–MG–HCl + 100 ml 6 *M* HCl	4.70	4.45
	5000	100 ml 5% aq. ascorbic acid soln. + 200 ml THF–MG–HCl + 100 ml 6 *M* HCl	5.27	4.50
	50000	100 ml 5% aq. ascorbic acid soln. + 200 ml THF–MG–HCl + 100 ml 6 *M* HCl	5.15	5.00
	5000	100 ml 0.1 *M* HCl containing 5 g of ascorbic acid + 200 ml THF–MG–HCl + 100 ml 6 *M* HCl	5.35	4.65
	50000	100 ml 0.1 *M* HCl containing 5 g of ascorbic acid + 200 ml THF–MG–HCl + 100 ml 6 *M* HCl	4.86	4.40
	5000	100 ml 1.0 *M* HCl containing 5 g of ascorbic acid + 200 ml THF–MG–HCl + 100 ml 6 *M* HCl	5.00	5.35
	50000	100 ml 1.0 *M* HCl containing 5 g of ascorbic acid + 200 ml THF–MG–HCl + 100 ml 6 *M* HCl	5.00	4.45
	50000	200 ml THF–MG–HCl + 100 ml 6 *M* HCl	5.20	4.25
Mo(VI)	0.5	50 ml THF–MG–HCl + 50 ml 6 *M* HCl	5.0	4.62
	5.0	50 ml THF–MG–HCl + 50 ml 6 *M* HCl	4.95	4.70
	50	50 ml THF–MG–HCl + 50 ml 6 *M* HCl	5.0	5.0
	500	50 ml THF–MG–HCl + 50 ml 6 *M* HCl	4.75	5.5
	5000	50 ml THF–MG–HCl + 50 ml 6 *M* HCl	4.70	0.0
	500	100 ml THF–MG–HCl + 100 ml 6 *M* HCl	5.25	5.5
	5000	100 ml THF–MG–HCl + 100 ml 6 *M* HCl	5.0	5.35
V(V)	0.5	50 ml THF–MG–HCl + 50 ml 6 *M* HCl	5.20	5.0
	5.0	50 ml THF–MG–HCl + 50 ml 6 *M* HCl	5.36	4.9
	50	50 ml THF–MG–HCl + 50 ml 6 *M* HCl	5.20	4.9
	500	50 ml THF–MG–HCl + 50 ml 6 *M* HCl	5.36	5.0
	5000	50 ml THF–MG–HCl + 50 ml 6 *M* HCl	5.20	5.1

(continued on p. 119)

Metal tested	*Amount (μg) added to 1 l Vienna tap water spiked with 5 μg U*	*Washing procedure before elution of U with 50 ml 1 M HCl*	*Uranium content (μg l⁻¹)*	
			Fluori-metry	*Spectro-photo-metry*
Cu(II)	50	50 ml THF–MG–HCl + 50 ml 6 *M* HCl	5.12	5.1
	500	50 ml THF–MG–HCl + 50 ml 6 *M* HCl	4.70	4.75
	5000	50 ml THF–MG–HCl + 50 ml 6 *M* HCl	4.55	4.90
	500	100 ml THF–MG–HCl + 100 ml 6 *M* HCl	5.0	5.0
	5000	100 ml THF–MG–HCl + 100 ml 6 *M* HCl	4.5	4.91
Co(II)	50	50 ml THF–MG–HCl + 50 ml 6 *M* HCl	5.1	4.9
	500	50 ml THF–MG–HCl + 50 ml 6 *M* HCl	4.9	4.8
	5000	50 ml THF–MG–HCl + 50 ml 6 *M* HCl	4.2	5.25
	500	100 ml THF–MG–HCl + 100 ml 6 *M* HCl	5.0	5.1
	5000	100 ml THF–MG–HCl + 100 ml 6 *M* HCl	5.0	5.2
Zn(II)	50	50 ml THF–MG–HCl + 50 ml 6 *M* HCl	4.85	4.9
	500	50 ml THF–MG–HCl + 50 ml 6 *M* HCl	5.0	5.1
	5000	50 ml THF–MG–HCl + 50 ml 6 *M* HCl	5.0	5.0
Cd(II)	500	50 ml THF–MG–HCl + 50 ml 6 *M* HCl	5.0	5.1
Hg(II)	500	50 ml THF–MG–HCl + 50 ml 6 *M* HCl	5.25	4.95
Ag(I)	500	50 ml THF–MG–HCl + 50 ml 6 *M* HCl	4.20	4.82
	500	100 ml THF–MG–HCl + 100 ml 6 *M* HCl	5.25	5.0

TABLE V

EFFECT OF MOLYBDENUM ON THE SPECTROPHOTOMETRIC DETERMINATION OF URANIUM WITH ARSENAZO III

(5 μg U taken)

Mo present (μg)	0	5	50	100	200	300	400	500
U found (μg)	4.92	5.30	5.90	4.55	0.00	0.00	0.00	0.00
	5.25	5.52	5.65	4.46	0.00	0.00	0.00	0.00

which has been recommended by several investigators[22–25] for the determination of uranium in natural waters, can only be used after separation of uranium from molybdenum and also iron.

Application to natural waters

In Table VI, data are presented which show that the procedure recommended here gives practically the same results as the much more time-consuming THF–MG–HCl method described earlier[6]. This latter technique is based on the anion-exchange separation of uranium in a THF–MG–HCl system after complete evaporation of the water sample.

TABLE VI

RESULTS OF FLUORIMETRIC URANIUM DETERMINATIONS IN SAMPLES OF AUSTRIAN WATERS FROM WHICH URANIUM WAS ISOLATED BY TWO DIFFERENT ANION-EXCHANGE METHODS

Samples no., geographical origin and sampling data	*U content ($\mu g\ l^{-1}$)*	
	This method	*THF–MG–HCl method*[6]
95/1; Zinkenbach, Salzkammergut; 21.6.1973	0.16	0.20
95/4; Russbach, Salzkammergut; 21.6.1973	0.33	0.32
95/5; Lammer, Salzkammergut; 21.6.1973	0.33	0.32
73/17/2; Moosbach, Lower Austria; 17.8.1973	0.47	0.50

TABLE VII

RESULTS OF FLUORIMETRIC AND SPECTROPHOTOMETRIC URANIUM DETERMINATIONS IN SAMPLES OF AUSTRIAN WATERS CONTAINING MORE THAN 1 P.P.B. OF URANIUM

Sample no., geographical origin and sampling date	*U content ($\mu g\ l^{-1}$)*	
	Fluorimetry	*Spectrophotometry*
199/1; Gailwaldbach, Carinthia; 6.8.1973	1.20	—
199/2; Klausenbach, Carinthia; 6.8.1973	1.39	—
199/3; Förolacherbach, Carinthia; 6.8.1973	2.40	3.23
198/2; Gösseringbach, Carinthia; 6.8.1973	1.26	—
198/3; Močnik Graben, Carinthia; 6.8.1973	1.02	—
196/2; Gärberbach, Tyrol; 7.8.1973	1.24	—
197/3; Podlanigbach, Carinthia; 7.8.1973	2.20	2.67
197/6; Sittmooserbach, Carinthia; 7.8.1973	1.06	—
197/7; Mayengraben, Carinthia; 7.8.1973	1.64	—
197/8; Dellacherbach, Carinthia; 7.8.1973	1.63	—
179/1; Sturzelbach, Tyrol; 10.8.1973	3.52	4.62
179/2; Gamsbach; Tyrol; 10.8.1973	4.30	4.62
179/3; Leisacher Almbach, Tyrol; 10.8.1973	2.22	2.46
145/2; Himmelswiesbergbach, Tyrol; 26.8.1973	2.19	2.56
145/3; Breithaslachbach, Tyrol; 26.8.1973	2.52	2.68
196/5; Quelle bei Tuffbad; Tyrol; 26.8.1973	5.00	6.67

In Table VII results are shown of uranium determinations in Austrian water samples by the recommended procedure. These results clearly show that the spectrophotometric method gives results which are invariably higher than those obtained by fluorimetry. This is most probably due to incomplete removal of molybdenum from the resin bed before elution of the uranium.

In most other samples collected at more than 100 different locations in Austria, uranium contents of less than 1 p.p.b. (mostly in the range 0.1–0.5 p.p.b.) were found by the fluorimetric procedure.

Because the anion-exchange separation can be performed more or less automatically, numerous samples can be analysed simultaneously, *i.e.* the procedure is very well suited for the routine determination of uranium in natural waters.

This research was sponsored by the Fonds zur Förderung der wissenschaftlichen Forschung, Vienna, Austria. The generous support from this Fund is gratefully acknowledged.

SUMMARY

A method is described for the determination of uranium by fluorimetry and spectrophotometry in samples of natural non-saline waters. After acidification with hydrochloric acid, the water sample is filtered and, following the addition of ascorbic acid and potassium thiocyanate, passed through a column of the strongly basic anion-exchange resin Dowex 1-X8 (thiocyanate form). On this exchanger uranium is adsorbed as an anionic thiocyanate complex. After removal of iron and other coadsorbed elements by washing first with a mixture consisting of 50 vol.% tetrahydrofuran, 40 vol.% methyl glycol and 10 vol.% 6 *M* hydrochloric acid, and then with pure aqueous 6 *M* hydrochloric acid, the uranium is eluted with 1 *M* hydrochloric acid. In the eluate, uranium is determined fluorimetrically or by means of the spectrophotometric arsenazo III method. The procedure was used for the routine determination of uranium in water samples collected in Austria.

REFERENCES

1 J. A. MacDonald, *Can. Mining J.*, 89 (1968) 89.
2 A. Y. Smith and J. J. Lynch, *Geol. Surv. Can., Pap., 69-40*, 1969.
3 J. Korkisch and F. Hecht, *Handbook of Analytical Chemistry, Third Part; Quantitative Analysis*, Vol. VI, b; β, Springer-Verlag, Berlin–Heidelberg, 1972.
4 R. E. Shoaf, H. L. Galloway and F. S. Voss, *Rept. GAT-L-197*, Goodyear Atomic Corporation, Cincinnati, Ohio, May 18, 1956.
5 I. Hazan, J. Korkisch and G. Arrhenius, *Z. Anal. Chem.*, 213 (1965) 182.
6 J. Korkisch and I. Steffan, *Mikrochim. Acta*, (1972) 837.
7 J. Korkisch and W. Koch, *Mikrochim. Acta*, (1973) 157.
8 W. Koch and J. Korkisch, *Mikrochim. Acta*, (1972) 687.
9 H. Onishi, *Jap. Anal.*, 18 (1969) 1134.
10 A. K. Majumdar and B. K. Mitra, *Z. Anal. Chem.*, 208 (1965) 1.
11 I. A. Kuzin and V. P. Taushkanov, *Zh. Prikl. Khim. (Leningrad)*, 37 (1964) 764.
12 H. Hamaguchi, K. Ishida and R. Kuroda, *Anal. Chim. Acta*, 33 (1965) 91.
13 D. L. Kiser, Thesis, University of Iowa, Ames, U.S.A., 1965.
14 D. J. Pietrzyk and D. L. Kiser, *Anal. Chem.*, 37 (1965) 1578.
15 J. H. Pannell, S. B. Michal, D. F. Thorpe, G. W. Lower and F. W. Bloecher, *USAEC Topical Rept. ACCO-12*, 1953.
16 P. McGlone and G. L. Wilward, *Scientific Rept. C.R.L./A.E. 94*, The Chemical Research Laboratory, Teddington, England, 1952.
17 J. D. Harbutt and G. L. Wilward, *Scientific Rept. C.R.L./A.E. 80*, The Chemical Research Laboratory, Teddington, England, 1951.
18 T. Kiriyama and R. Kuroda, *Anal. Chim. Acta*, 62 (1972) 464.
19 K. Kawabuchi, *Jap. Anal.*, 14 (1965) 52.
20 K. Kawabuchi, *J. Chem. Soc. Japan, Pure Chem. Sect.*, 87 (1966) 262.
21 J. B. Turner, R. H. Philp and R. A. Day, *Anal. Chim. Acta*, 26 (1962) 94.
22 E. Singer and J. Mareček, *Z. Anal. Chem.*, 196 (1963) 321.
23 A. A. Nemodruk and R. Yu. Deberdeeva, *Radiokhimiya*, 8 (1966) 248.
24 Z. Šulcek and P. Povondra, *Collect. Czech. Chem. Commun.*, 32 (1967) 3140.
25 Z. Šulcek and V. Sixta, *Anal. Chim. Acta*, 53 (1971) 335.

Analytica Chimica Acta, 71 (1974) 123–132

SEPARATION OF LITHIUM FROM SODIUM, BERYLLIUM AND OTHER ELEMENTS BY CATION-EXCHANGE CHROMATOGRAPHY IN NITRIC ACID–METHANOL

F. W. E. STRELOW, C. H. S. W. WEINERT and T. N. VAN DER WALT
National Chemical Research Laboratory, P.O. Box 395, Pretoria (Republic of South Africa)
(Received 28th January 1974)

The separation of lithium from sodium by cation-exchange chromatography on sulphonated polystyrene resins, using aqueous inorganic acids, such as HCl, HNO_3, H_2SO_4 or $HClO_4$, as eluting agents, involves separation factors of only about 1.5–2.0 (refs. 1–3). Fairly large columns are required to separate mmole amounts of these elements quantitatively. Okuno *et al.*[4] have improved the separation by using 0.2 *M* hydrochloric acid containing 30% methanol, in which case sodium is retained; this increases the separation factor to about 3, and reasonably good separations can be obtained provided that the amounts of sodium and other more strongly retained cations are not excessive. The method has been applied to the determination of lithium in water samples[5,6]. Davies and Owen[7] have eluted lithium with 0.7 *M* hydrochloric acid in 80% acetone to give separation from sodium; the separation factor is again about 3. Nevoral[8] has used hydrochloric acid–ethanol mixtures for the successful separation of lithium, sodium and potassium, and has shown that the free volume between the elution peaks increases with increasing ethanol concentration. The eluting agent, 0.6 *M* hydrochloric acid–60% ethanol, which he uses for the elution of lithium, again provides a separation factor of about 3 for the lithium–sodium pair. It has been stated by Šulcek *et al.*[9] that the largest separation factor for the lithium–sodium pair in mixtures of aqueous hydrochloric acid and methanol is obtained at 80–90% methanol, and a method has been described for the separation of lithium from sodium and other elements occurring in rock samples by its selective elution with 0.5 *M* hydrochloric acid in 80% methanol[9,10] Though not given by Šulcek *et al.*, the separation factor for the lithium–sodium pair in this case is about 5, when AG50W-X8 resin is used (Table II), and is considerably larger than the factors applicable to the previous methods. A separation factor of 4–5 can also be obtained by eluting lithium with 1.0 *M* hydrochloric acid in 80% ethanol from BioRex 40, a condensed phenol–formaldehyde resin with $-CH_2SO_3H$ exchange groups[11]. A solution of 2.4 *M* hydrochloric acid in 80% methanol has been suggested for the elution of lithium and its separation from sodium with Duolite C-3 resin[12], but the distribution coefficient for sodium is rather low under these conditions, and an early breakthrough occurs when fairly large amounts are present.

One would prefer the sulphonated polystyrene resins in cases where large amounts of sodium and more strongly retained ions are present, because these resins have larger capacities. The method described by Šulcek *et al.*[9,10] uses a

polystyrene resin and operates with a sufficiently large separation factor, but it has the disadvantage that under the experimental conditions used, the distribution coefficient of lithium, with a value of about 19, is rather high. In order to avoid too large elution volumes, the authors, therefore, had to work with rather small columns which limited the sample size to about 0.2 g of rock material[10]. To accommodate larger samples, a larger column would be preferred, and in order to obtain smaller elution volumes, the concentration of hydrochloric acid might be increased. Unfortunately, iron(III) forms chloride complexes in about 1 *M* hydrochloric acid when 80% methanol is present, and an early breakthrough will occur with larger amounts of iron(III).

Since the most important factor responsible for increasing the selectivity between lithium and sodium seems to be the selective destruction of the outer hydration shell of cations in the external solution phase with increasing concentration of the organic solvent, there seems to be no reason why another strongly dissociated inorganic acid could not be substituted for hydrochloric acid without causing large changes in the distribution coefficients and the separation factor of lithium and sodium. Nitric acid was selected for this purpose because its tendency to form complexes with iron(III) and almost all other elements is negligible. It was preferred to perchloric acid because of its lower boiling point. No systematic information about the ion-exchange distribution coefficients of lithium, sodium and some other rock-forming elements in nitric acid–methanol mixtures seems to be available in the literature. Some relevant coefficients, therefore, were determined. From these, a method for the separation of lithium from sodium and other elements in 1.0 *M* nitric acid containing 80% methanol was developed, and employed for the separation and determination of lithium in some standard rock samples. Since coefficients for the alkali metals in hydrochloric acid–methanol mixtures also do not seem to be available, their determination was included for comparative purposes and they are presented together with the coefficients in nitric acid–methanol media.

EXPERIMENTAL

Reagents and apparatus

Only analytical reagent-grade chemicals were used. The resin was AG50W-X8 sulphonated polystyrene cation exchanger (BioRad Richmond, California). Resin of 100–200 mesh particle size was used for batch equilibrium, and of 200–400 mesh for column experiments. Borosilicate glass tubes of 2.1-cm inner diameter fitted with B19 ground joints at the top, and glass sinter plates of No. 2 porosity and burette taps at the bottom, were used as columns. A Perkin–Elmer 303 and a Zeiss PMQ II instrument were used for atomic absorption spectrometry and optical spectrophotometry, respectively.

Equilibrium distribution coefficients

Dry resin (2.500 g) in the H^+-form was equilibrated with 5 exchange milliequivalents of the cation in 250 ml of solution, containing either nitric or hydrochloric acid and methanol of the desired concentration, by shaking for 24 h at 25°C. The mixture, designated as 250 ml of 1 *M* nitric acid–80% methanol, is equivalent to 25 ml of 10 *M* nitric acid mixed with 25 ml of water or aqueous

solution of the cation and 200 ml of methanol. Volume changes on mixing were disregarded. After shaking, the resin was separated from the aqueous–organic phase, and the amounts of the elements in both phases were determined by suitable analytical methods. From the results, the equilibrium distribution coefficients

$$D = \frac{\text{moles on resin}}{\text{moles in solution}} \cdot \frac{\text{ml solution}}{\text{g dry resin}}$$

were calculated. Coefficients in nitric acid–methanol for some relevant elements are presented in Table I, while Table II shows some coefficients in hydrochloric acid–methanol, for comparative purposes.

Elution curves

From the distribution coefficients in Table I it appears that 1.00 *M* nitric

TABLE I

DISTRIBUTION COEFFICIENTS IN NITRIC ACID–METHANOL

Molarity of HNO_3	*Element*	*% Methanol*					
		0	*20*	*40*	*60*	*70*	*80*
0.50	Fe(III)	491	620	1150	2980	4570	8360
	Bi(III)	490	516	617	727	593	498
	Pb(II)	174	217	341	577	739	841
	Hg(II)	122	147	214	331	360	301
	Mg	82	96	142	258	327	536
	U(VI)	73	87	129	225	305	424
	Be	52	55	68	101	124	156
	Na	12.2	15.6	22.8	38.8	63	78
	Li	7.6	8.7	10.2	15.0	18.7	21.1
1.00	Fe(III)	100	131	224	538	910	2010
	Bi(III)	63	64	71	73	66	47.6
	Pb(II)	36.0	45.0	67	103	129	170
	Hg(II)	31.2	38.4	52	67	76	82
	U(VI)	26.5	31.4	48.1	81	102	143
	Mg	26.3	32.8	46.4	86	124	184
	Be	15.6	16.9	20.3	31.6	40.7	57
	Na	5.9	7.5	10.9	20.3	30.4	42.7
	Li	3.8	4.0	5.0	8.0	9.6	11.3
2.00	Fe(III)	21.8	31.0	56	129	241	—
	Bi(III)	7.0	7.3	8.6	8.2	6.6	—
	Pb(II)	6.0	6.4	8.8	19.8	18.4	—
	Hg(II)	8.5	12.2	15.6	17.8	19.3	—
	U(VI)	10.6	14.0	20.8	34.0	42.4	—
	Mg	9.1	11.0	17.9	28.8	49.6	—
	Be	4.1	5.5	6.2	10.5	14.6	—
	Na	2.6	3.0	4.5	8.4	12.5	—
	Li	1.8	2.0	2.4	3.4	5.3	—

TABLE II

DISTRIBUTION COEFFICIENTS IN HYDROCHLORIC ACID–METHANOL[a]

Molarity of HCl	*Element*	*% Methanol*					
		0	*20*	*40*	*60*	*70*	*80*
0.50	Fe(III)	237	213	213	236	184	108
	Na	12.7	17.2	26.4	52	74	92
	Li	7.4	8.0	9.3	14.6	17.2	18.9
1.00	Fe(III)	34.2	27.4	30.2	31.4	21.4	9.3
	Na	6.0	7.7	10.9	20.7	35.7	52
	Li	3.6	3.9	4.4	7.2	8.8	9.7
2.00	Fe(III)	3.6	2.8	4.3	5.4	4.0	
	Na	2.6	3.4	5.5	9.0	15.2	
	Li	1.5	1.7	2.2	2.7	2.8	

[a] At all stated concentrations of acid and methanol, the distribution coefficient for mercury(II) was < 0.5.

acid–80% methanol gives the most favourable conditions for the separation of lithium from sodium and other elements. An elution curve with this agent was therefore prepared. About 50 ml of a solution, containing about 5 mmoles each of lithium and sodium in 0.1 *M* nitric acid–50% methanol, was passed through a column containing 60 ml (20 g) of AG50W-X8 resin. The column was 19 cm in length and 2.1 cm in diameter and had been equilibrated with 0.1 *M* nitric acid–50% methanol. The ions were washed onto the resin with this solution, and then eluted with 1.00 *M* nitric acid–80% methanol at a flow rate of 3.0 ± 0.3 ml min^{-1}. Fractions of 25-ml volume were taken with an automatic fractionator, and the amounts of lithium and sodium in the fractions were determined by atomic absorption spectrometry at the 670.8 and 589.0 nm lines, respectively. The experimental elution curve is shown in Fig. 1. For comparative purposes, Fig. 2 shows

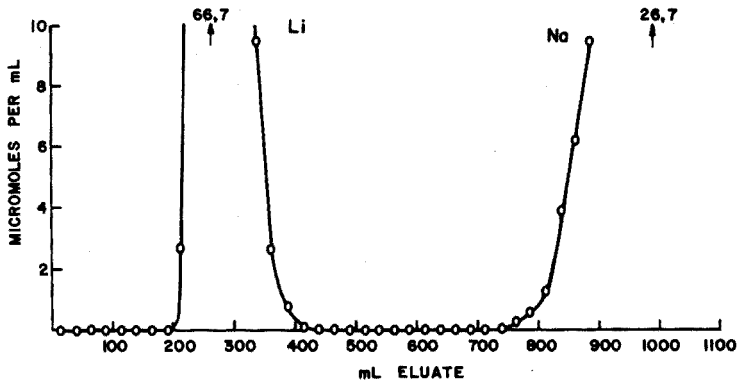

Fig. 1. Elution curve for Li–Na with 1.00 *M* HNO_3–80% methanol. 60 ml [19 × 2.1 cm] AG50W-X8 resin, 200–400 mesh. Flow rate 3.0 ± 0.3 ml min^{-1}. 5 mmol of each element.

an elution curve obtained with 1.00 *M* hydrochloric acid–80% methanol as eluting agent, with all other experimental conditions as described above. Figures 3 and 4 present elution curves for the Li–Be and Li–Bi(III) pairs with 1.00 *M* nitric acid–80%

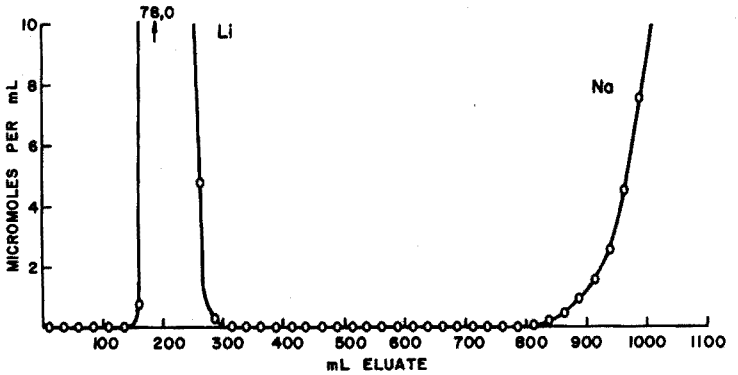

Fig. 2. Elution curve for Li–Na with 1.00 *M* HCl–80% methanol. Column and conditions as for Fig. 1.

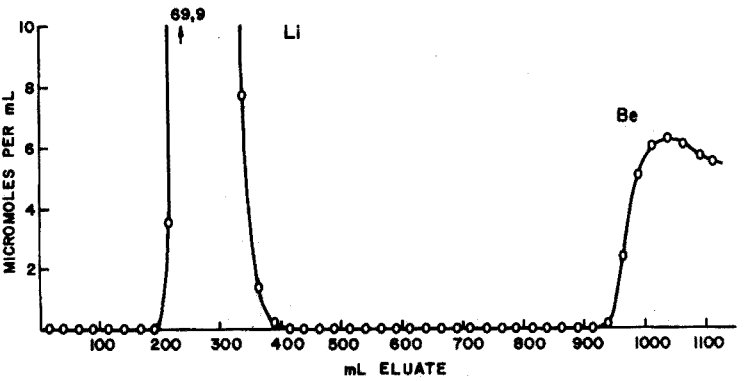

Fig. 3. Elution curve for Li–Be with 1.00 *M* HNO_3–80% methanol. Column and flow rate as for Fig. 1. 5 mmol Li + 2.5 mmol Be.

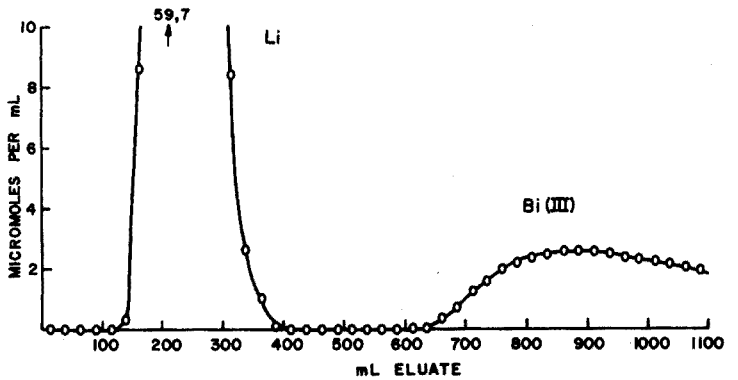

Fig. 4. Elution curve for Li–Bi(III) with 1.00 *M* HNO_3–80% methanol. Column and flow rate as for Fig. 1. 5 mmol Li + 1.67 mmol Bi(III).

methanol under the same conditions. No Fe(III), Ti(IV), Mg or Al could be found in the first 1000 ml of 1.00 *M* nitric acid–80% methanol when similar elution experiments were made with binary mixtures of lithium and these elements. The brown iron(III) band remained at the head of the column almost without movement while the orange band of the titanium(IV)–peroxide complex had moved about 40% of the column length after 1000 ml of eluting agent had been passed through.

Quantitative separation of synthetic mixtures

Volumes of standard solutions of lithium and one other element in 0.1 *M* nitric acid were measured out in triplicate and mixed. An equal amount of methanol was added to each mixture and the solutions were adsorbed on columns containing 60 ml of AG50W-X8 resin (200–400 mesh). The resin columns, 19 cm in length and 2.1 cm in diameter in water, had been equilibrated with 0.1 *M* nitric acid–50% methanol. The ions were washed onto the resin with 0.1 *M* nitric acid–50% methanol. Lithium was then eluted with 500 ml of 1.00 *M* nitric acid–80% methanol. After the methanol had been washed from the column by passage of about 60 ml of 0.1 *M* nitric acid, the other element was eluted with 300 ml of 3.0 *M* hydrochloric acid, except in the case of lead(II) and bismuth(III) which were eluted with 300 ml of 3.0 *M* nitric acid to simplify their determination, and sodium which was eluted with 300 ml of 1.00 *M* nitric acid. A flow rate of about 3.0 ± 0.5 ml min^{-1} was used throughout. In the case of trace amounts of sodium, only 250 ml of 1.00 *M* nitric acid were used, and the eluate was received in a 250-ml volumetric flask and made up to volume; the concentration of sodium was determined by comparison with standards also made up to 250 ml with 1.00 *M* nitric acid. All the other eluates were evaporated to dryness and the amounts of the elements were determined by suitable analytical methods. The results of the analyses are presented in Table III, and the analytical methods used are summarized in Table IV.

Determination of lithium in rock material

About 1 g of sample material was weighed out accurately and dissolved by heating with a mixture of hydrofluoric, hydrochloric and perchloric acids in a 100-ml teflon beaker with a temperature-controlled air-bath which enclosed the beakers to three-quarters of their height. Care was taken to remove all the hydrofluoric acid, and the solutions were finally fumed until only about 1 ml of perchloric acid remained. After dilution, any remaining insoluble residue was separated by filtration, and the filtrate was kept for the column separation. The residue was dissolved by heating with a hydrofluoric–perchloric–phosphoric acid mixture in a platinum crucible until a viscous transparent mass of polyphosphoric acid had been formed. The melt was dissolved in 5 ml of 1 *M* hydrochloric acid containing 0.3% hydrogen peroxide and diluted to 50 ml of 0.1 *M* hydrochloric acid containing 50% methanol and 0.03% hydrogen peroxide. This solution was then passed through a column of 60 ml of AG50W-X8 resin as described above, but the column was equilibrated with 0.1 *M* hydrochloric acid–50% methanol. The residue solution was followed by 50 ml of 0.01 *M* hydrochloric acid–50% methanol and then by the main filtrate which had been diluted to about 100 ml of 0.1 *M* hydrochloric acid–50% methanol. The ions were washed onto the resin and phosphoric acid was eluted from the resin with 100 ml of 0.01 *M* hydrochloric

TABLE III

RESULTS FOR QUANTITATIVE SEPARATIONS OF SYNTHETIC MIXTURES

Taken			*Found*	
Li (mg)	*Other element (mg)*		*Li (mg)*	*Other element (mg)*
35.43	Na	114.6	35.45 ± 0.04	114.6 ± 0.2
0.177	Na	114.6	0.176 ± 0.002	114.7 ± 0.2
0.0354	Na	114.6	0.0355 ± 0.0003	114.7 ± 0.2
70.86	Na	0.115	70.85 ± 0.07	0.114 ± 0.002
35.43	Be	22.46	35.44 ± 0.05	22.43 ± 0.05
35.43	Mg	58.20	35.43 ± 0.04	58.20 ± 0.04
35.43	Ca	100.2	35.41 ± 0.04	100.2 ± 0.1
35.43	Mn(II)	138.0	35.44 ± 0.03	138.1 ± 0.1
35.43	Fe(III)	139.6	35.42 ± 0.04	139.5 ± 0.1
35.43	Al	44.79	35.43 ± 0.05	44.78 ± 0.03
34.66	Ti(IV)	118.1	35.65 ± 0.04	118.1 ± 0.2
34.66	Pb(II)	521.7	34.67 ± 0.05	521.6 ± 0.3
34.66	Bi(III)	209.9	34.64 ± 0.04	209.9 ± 0.1
34.66	Zn(II)	163.1	34.66 ± 0.04	163.1 ± 0.1
34.66	Cd(II)	280.3	34.65 ± 0.03	280.2 ± 0.2
34.66	U(VI)	603.1	34.67 ± 0.04	602.9 ± 0.3
34.66	In(III)	190.6	34.64 ± 0.04	190.5 ± 0.2

TABLE IV

ANALYTICAL PROCEDURES

Element	*Method*
Li, Na	Gravimetrically as the sulphate; small amounts and elution curves by atomic absorption spectrometry
Be	Gravimetrically as precipitate with ammonium nitrosophenylhydroxylamine (Cupferron)
U(VI)	Gravimetrically as U_3O_8 after precipitation with CO_2-free ammonia solution
Mg	Complexim etrically with EDTA; eriochrome blue black B at pH 10 as indicator
Cd, Ca, Mn(II)	Complexim etrically with EDTA in slight excess of ammonia; methylthymol blue as indicator
Bi	Complexim etrically with EDTA at pH 1; xylenol orange as indicator
Pb(II), Zn	Complexim etrically with EDTA at pH 5.5; xylenol orange as indicator
Fe(III), Al, In	Complexim etrically with DCyTA; back-titration with $ZnSO_4$ at pH 5.5; xylenol orange as indicator
Ti(IV)	Differential spectrophotometry as peroxide complex at high absorbance

acid–50% methanol. Then the lithium was eluted with 500 ml of 1.00 *M* nitric acid–80% methanol at a flow rate of 3.0 ± 0.5 ml min^{-1}. The eluate was evaporated on the water-bath and the lithium salts were dissolved in a few ml of deionized water and made up to a volume of 10 ml in a volumetric flask. Two blanks, containing all the reagents used, were taken through the whole procedure. The concentration of the lithium was then determined by atomic absorption spectrometry with an acetylene–air flame at the 670.8-nm line.

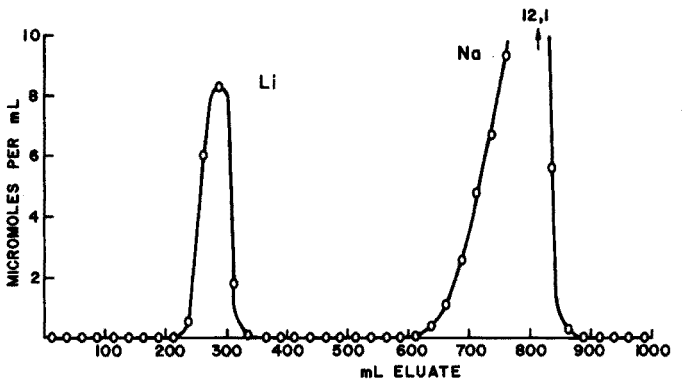

Fig. 5. Elution curve for 1 g of G2 standard granite doped with 0.5 mmol Li. Eluent 1.00 *M* HNO_3–80% methanol. Column and flow rate as for Fig. 1.

TABLE V

RESULTS FOR DETERMINATION OF LITHIUM IN ROCK SAMPLES

Sample	*Origin*	*Number of analyses*	*Average result (p.p.m. Li)*[a]
Granite G-2	U.S. Geological Survey	6	34.3±0.3
Granite NIM-G	NIM[b]	4	12.3±0.3
Syenite NIM-S	NIM	4	1.35±0.05
Lujavrite NIM-L	NIM	4	43.4±0.6
Norite NIM-N	NIM	4	5.1±0.3
Pyroxenite NIM-P	NIM	4	4.3±0.3
Dunite NIM-D	NIM	4	3.5±0.2

[a] Average of determinations with calculated standard deviations.
[b] National Institute for Metallurgy, Republic of South Africa.

A typical elution curve obtained for 1 g of the G2 standard granite of the U.S. Geological Survey, spiked with 0.5 mmol of lithium, is shown in Fig. 5. Only the sodium peak is indicated for the retained elements, because sodium is the first element to appear after lithium. Table V shows the results for the determination of lithium in the standard granite G2 and several other rock samples.

DISCUSSION

The described method is excellent for the selective separation of milligram as well as microgram amounts of lithium from practically all other elements. The separation factor for the Li–Na pair in 1 *M* nitric acid–80% methanol is somewhat smaller than in 1 *M* hydrochloric acid–80% methanol (Tables I and II), but with a value of about 4 is still quite satisfactory, and larger than the separation factors applicable to most of the other suggested procedures in hydrochloric acid–organic solvent mixtures[4–8]. The selectivity in 1 *M* nitric acid–80% methanol is much higher than in the hydrochloric acid–methanol mixture, and elements such as Zn, Cd, In, Pb(II), Bi(III) and Fe(III), which would accompany lithium during elution with

1 *M* hydrochloric acid–80% methanol, are clearly separated in the nitric acid–methanol mixture. Separations of lithium from Na, Be, Mg, Ca, Mn(II), Fe(III), Al, Ti(IV), Pb(II), Zn(II), Cd, U(VI), In(III) and Bi(III) are quantitative under the experimental conditions described, and as much as 5 mmole or more of these elements, may be present. The only exception is bismuth(III), which has a very wide and flat elution peak; only up to about 1 mmole (*ca.* 200 mg) of the element may be present for quantitative recovery ($\geqslant 99.9\%$). As little as 35.4 μg of lithium can be separated from 114.6 mg, and even larger amounts of sodium and other elements, and recovered quantitatively. Elements such as K, Rb, Cs, Sr, Ba, Cu(II), Co(II), Ni(II), Zr, Hf, Th, Sc, Y, La and the lanthanides, have not been investigated in detail; but, because these elements are considerably more strongly absorbed than either sodium (for monovalent) or beryllium (for di- and multivalent) elements, their separation should offer no problems. Elements forming oxy-anions such as V(V), Mo(VI), W(VI), Nb(V), Ta(V) and also phosphate, can be eluted by 0.01 *M* hydrochloric acid or nitric acid in 50% methanol containing hydrogen peroxide, before the elution of lithium is started. When hydrochloric acid is used, this should also elute elements such as Hg(II), Au(III) and the platinum metals which form very stable chloride complexes.

Figure 5 indicates that for high column loads and small amounts of lithium, as encountered in the analysis of rock samples, a smaller fraction of the eluate could be used for the determination of lithium. For safety purposes, the whole 500 ml of the eluate were used nevertheless. In a six-fold analysis of the G2 standard granite, a mean of 34.3 p.p.m. of lithium was obtained with a standard deviation of 0.28 p.p.m. and a coefficient of variation of 0.82%. Reagents and procedure blanks were run in duplicate and gave values of 0.08 and 0.08 p.p.m. of lithium; results were corrected accordingly. Flanagan[13] gives the average literature value for the G2 standard rock as 42.7 p.p.m. lithium. If one excludes the very high value of Mays (63 p.p.m.), all the other values are between 25 and 42 p.p.m. and give a mean of 32.8 p.p.m. which seems to be in reasonably good agreement with the value obtained by the method described above.

SUMMARY

Lithium can be separated from sodium, beryllium and many other elements by eluting lithium with 1 *M* nitric acid in 80% methanol from a column of AG50W-X8 sulphonated polystyrene cation-exchange resin. The separation factor is not quite as large as that in 1 *M* hydrochloric acid in 80% methanol, but many elements, such as Zn, Cd, In, Pb(II), Bi(III) and Fe(III), which form chloride complexes in 1 *M* HCl–80% methanol are retained quantitatively together with Na, Be, Mg, Ca, Mn(II), Al, Ti(IV), U(VI), and many other elements, when 1 *M* HNO_3–80% methanol is used for elution of lithium. A method for the accurate determination of traces of lithium in rock samples is described, and some results obtained are presented together with relevant distribution coefficients, elution curves and results for the analysis of synthetic mixtures.

REFERENCES

1 F. W. E. Strelow, *Anal. Chem.*, 32 (1960) 1185.

2 F. W. E. Strelow, R. Rethemeyer and C. J. C. Bothma, *Anal. Chem.*, 37 (1965) 106.
3 F. W. E. Strelow and H. Sondorp, *Talanta*, 19 (1972) 1113.
4 H. Okuno, M. Honda and T. Ishimori, *Jap. Anal.*, 2 (1953) 428.
5 Y. Mashiko and Y. Kanvoji, *J. Pharm. Soc. Japan*, 76 (1956) 441.
6 G. Bradford and P. F. Pratt, *Soil Sci.*, 91 (1961) 184.
7 C. W. Davies and B. D. R. Owen, *J. Chem. Soc., London*, (1956) 1676.
8 V. Nevoral, *Z. Anal. Chem.*, 195 (1963) 332.
9 Z. Šulcek, P. Povondra and R. Štangl, *Collect. Czech. Chem. Commun.*, 30 (1965) 380.
10 Z. Šulcek and J. Rubeška, *Collect. Czech. Chem. Commun.*, 34 (1969) 2048.
11 F. W. E. Strelow, C. J. Liebenberg and F. von S. Toerien, *Anal. Chim. Acta*, 43 (1968) 465.
12 F. Nelson, D. C. Michelson, H. O. Phillips and K. A. Kraus, *J. Chromatogr.*, 20 (1965) 107.
13 F. J. Flanagan, *Geochim. Cosmochim. Acta*, 33 (1969) 81.

Analytica Chimica Acta, 71 (1974) 133–140

PLASTICIZED OPEN-CELL POLYURETHANE FOAM AS A UNIVERSAL MATRIX FOR ORGANIC REAGENTS IN TRACE ELEMENT PRECONCENTRATION

PART II. COLLECTION OF MERCURY TRACES ON DITHIZONE AND DIETHYLDITHIOCARBAMATE FOAMS

T. BRAUN and A. B. FARAG

Institute of Inorganic and Analytical Chemistry, L. Eötvös University, P.O. Box 123, 1443 Budapest (Hungary)

(Received 28th January 1974)

The extensive literature[1,2] on the application of dithizone in liquid–liquid extractions for the separation of mercury at trace level concentrations is evidence of the importance of this chelating agent and also of the need for a simple method for the rapid collection of this dangerous inorganic pollutant[3]. In a recent publication, Sekizuka *et al.*[4] prepared two types of hydrophobic gels containing dithizone and examined their application in column operation. They claimed that mercury(II) can be selectively concentrated from large volumes of dilute aqueous solutions on gel-packed columns. However, as with all other granular supports, mass transport processes in the gel granules are slow.

Mazurski *et al.*[5] studied the collection of mercury(II) chloride and methylmercury(II) chloride from aqueous solution on polyurethane foam, previously treated in an electrical discharge with hydrogen sulphide to anchor SH groups on the foam. Although this method was successful, at relatively high flow-rates, in collecting mercury from large volumes of aqueous solution, it suffers from the following disadvantages: the preparation of the SH-treated polyurethane foam is quite complicated; the capacity of the SH-foam is very low; and the recovery of mercury from the foam material was possible only by soxhleting the foam with hydrochloric acid.

In a previous paper[6], a new general method was suggested for the physical immobilization of organic reagents on or in flexible polyether-type polyurethane foam, in an attempt to combine the well-known advantages of the multistage column operation with the high selectivity of some organic reagents in trace element preconcentration. Plasticized zinc dithizonate foam was prepared by allowing polyurethane foam to swell in contact with a zinc dithizonate solution in various plasticizers. The successful use of the proposed plasticized dithizone foam for simple, rapid and selective collection and preconcentration of silver suggested that an examination for the collection of trace amounts of mercury might be useful.

In the present work a detailed study of the use of dithizone foam for the collection and preconcentration of mercury was undertaken. Important experimental parameters were critically evaluated. The preparation and possible application of zinc diethyldithiocarbamate foam for the same purpose was also briefly examined.

EXPERIMENTAL

Reagents and materials

Analytical reagent-grade chemicals were used whenever possible. Tri-n-butyl phosphate (TBP) was purified as described by Hamlin *et al.*[7] α-Dinonyl phthalate, di-n-octyl phthalate and dibutyl adipate (pure grade) were used without further purification. Polyurethane foam, a polyether of open-cell type, was supplied by the North Hungarian Chemical Works, Sajóbábony, Hungary. Zinc dithizonate solutions (1%), in various plasticizers, were prepared as previously described[6]. Zinc diethyldithiocarbamate solution was prepared by shaking a saturated TBP solution of sodium diethyldithiocarbamate with an aqueous solution of zinc sulphate. Mercury(II) nitrate solutions were spiked with radioactive mercury-203 (Institute of Isotopes, Budapest).

Instrumentation

For activity measurement a NaI(Tl) well-crystal and an energy-selective counting device (type NK-107/B, Gamma, Budapest) were employed.

Preparation of dithizone and diethyldithiocarbamate foams

Dithizone foam was prepared as described previously[6]. Diethyldithiocarbamate foam was prepared by equilibration of the washed, dried foam cubes (edge *ca.* 5 mm) with a saturated solution of zinc diethyldithiocarbamate in TBP. The loaded foam material was then dried, as usual, between two sheets of filter paper to remove the excess of zinc diethyldithiocarbamate solution.

Column preparation

Glass columns of 25-mm diameter and 12-cm length were used; 5 g of the dried loaded foam was packed in the column, by the procedure previously described[6,8].

RESULTS AND DISCUSSION

To determine the feasibility of using dithizone foam for the rapid collection of traces of mercury from aqueous solutions, a detailed study of various factors was carried out.

Effect of acidity on the collection of mercury(II) with TBP-plasticized and unplasticized zinc dithizonate foam

In separate experiments, 10-ml aliquots of aqueous solution containing 0.72 μg of mercury(II) were shaken for 1 h with 0.1 g of zinc dithizonate foam at different nitric acid concentrations. As can be seen from the curves of Fig. 1, mercury(II) is more or less completely collected from nitric acid solution, of concentrations up to 2 *M*, with TBP-plasticized foam. At acid concentrations higher than 2 *M*, the percentage collection of mercury sharply decreased. A similar effect was observed in the case of the unplasticized zinc dithizonate foam (chloroform). Generally, the results in the latter case were slightly lower than in the case of the plasticized foam (Fig. 1).

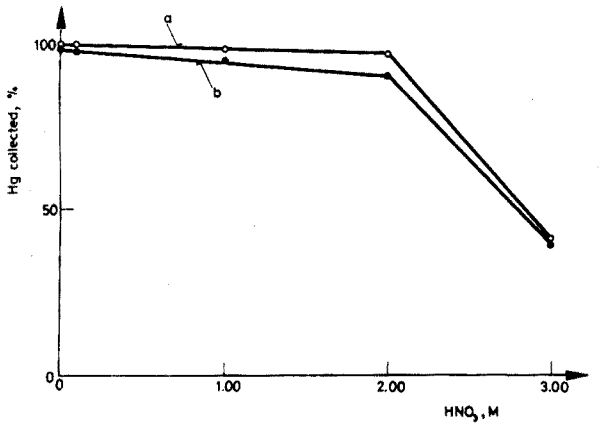

Fig. 1. Effect of acidity on the collection rate of mercury(II) with TBP-plasticized (a) and unplasticized (b) zinc dithizonate foam (chloroform solvent in unplasticized foam).

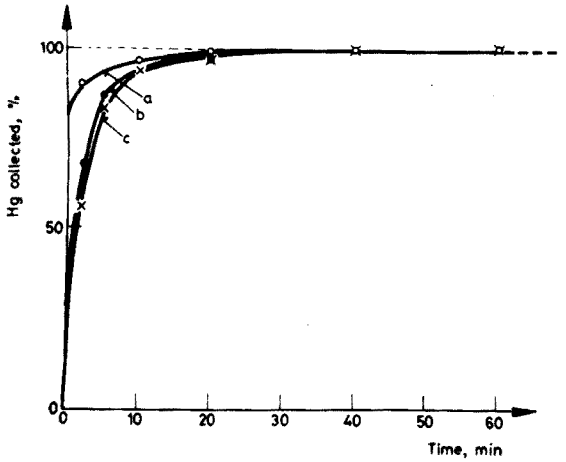

Fig. 2. Effect of pH on the collection rate of mercury(II) with TBP-plasticized zinc dithizonate foam. (a) Zinc dithizonate foam (pH 6); (b) zinc dithizonate foam (pH 0.2); (c) free dithizone foam (pH 6).

The effect of pH on the rate of collection of mercury(II) with TBP-plasticized zinc dithizonate foam was also investigated. Plots of the percentage collection of 0.72 μg of mercury(II) from neutral (pH 6) and acidic solutions (pH 0.2) with 0.1 g of zinc dithizonate foam are shown in Fig. 2 (curves (a) and (b), respectively). As can be seen, the collection of mercury(II) from neutral solution is faster than from acidic solution. The rate of collection of mercury(II) from neutral aqueous solution with free dithizone foam was also measured under the same experimental conditions. As is clear from the results obtained (Fig. 2, curve (c)), the rate of collection of mercury(II) from neutral aqueous solution with the free dithizone foam is almost identical to that obtained with the zinc dithizonate foam from acidic solution (pH 0.2).

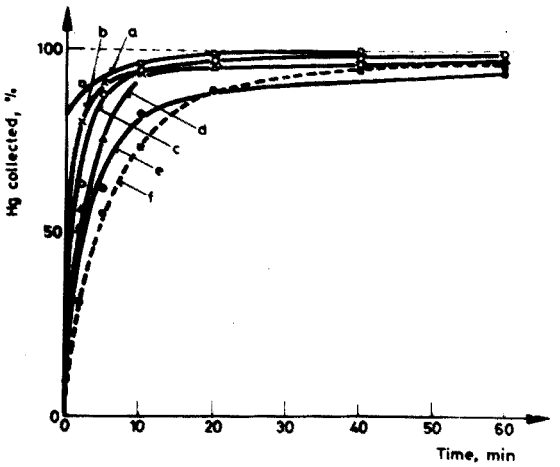

Fig. 3. Effect of plasticizer on the collection rate of mercury(II). (a) TBP; (b) dibutyl adipate; (c) α-dinonyl phthalate; (d) di-n-octyl phthalate; (e) CCl_4; (f) $CHCl_3$; (*) TBP-loaded foam alone (in the absence of dithizone).

Effect of plasticizers on the collection rate of mercury(II)

The curves of Fig. 3 represent the results obtained for the percentage collection of 0.72 μg of mercury(II) from 10 ml of aqueous solution (pH 6) with 0.1 g of polyurethane foam, which had been previously loaded with zinc dithizonate solutions in various plasticizers, carbon tetrachloride and chloroform, as a function of shaking time. It is obvious from these curves that the collection rates of mercury(II) with the plasticized foam materials are generally higher than with the unplasticized ones (chloroform or carbon tetrachloride). These results are in agreement with those previously reported[6] in the case of silver.

The highest collection rate was obtained with TBP-plasticized foam. Therefore, this foam material was selected for further investigation. It is worth mentioning that, as in the case of silver, the collection of mercury from aqueous solutions on TBP-plasticized foam, in the absence of dithizone, was found to be negligible under the experimental conditions used.

Effect of dithizone concentration on the collection rate of mercury(II) with TBP-plasticized polyurethane foam

The collection rate of mercury(II) from neutral aqueous solution (pH 6) with TBP-plasticized foam was examined as a function of zinc dithizonate concentration. The results obtained (Fig. 4) show that the rate of collection increased as the reagent concentration decreased. These results are in disagreement with the results generally reported[9] in liquid–liquid extraction, where the rate of extraction is decreased by decreasing the reagent concentration, most probably due to the presence of the plasticizer. Consequently, the same set of experiments was repeated, under the same experimental conditions, with unplasticized zinc dithizonate foam (chloroform). The results, plotted in Fig. 5, show that the collection rate of mercury decreased as the reagent concentration decreased which agrees with the liquid–liquid extraction behaviour.

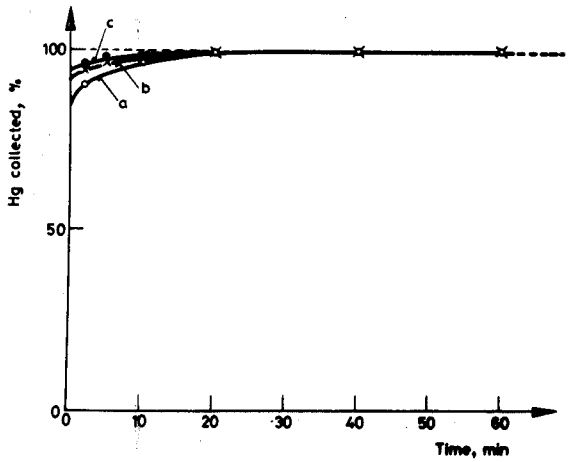

Fig. 4. Effect of zinc dithizonate concentration on the collection rate of mercury(II) with TBP-plasticized foam. (a) 1%; (b) 0.1%; (c) 0.01%.

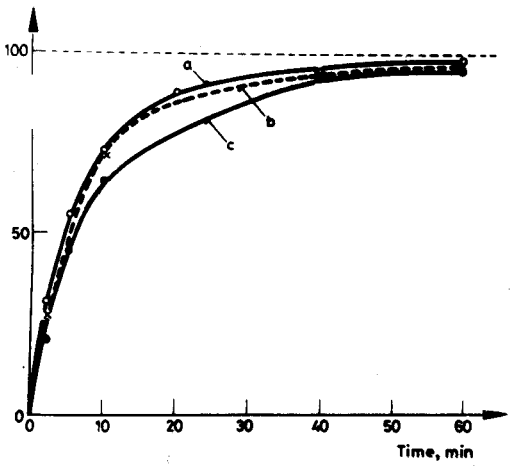

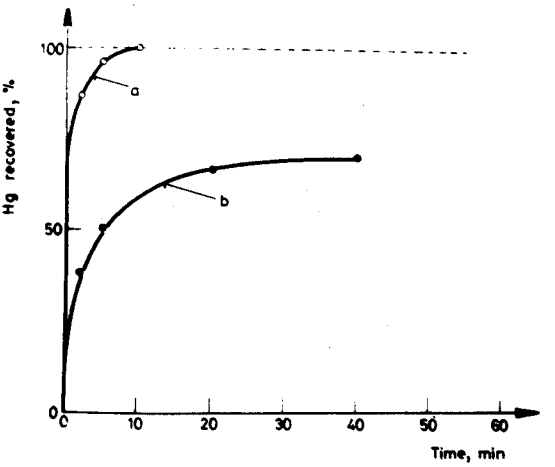

Fig. 5. Effect of zinc dithizonate concentration on the collection rate of mercury(II) with unplasticized foam (chloroform). (a) 1%; (b) 0.1%; (c) 0.01%.

Fig. 6. Effect of plasticizer on the recovery of mercury(II) from zinc dithizonate foam. (a) TBP-plasticized foam; (b) unplasticized foam ($CHCl_3$).

Effect of plasticizer on the recovery of mercury(II) from zinc dithizonate foam

The recovery of mercury(II) from zinc dithizonate foam with sodium thiosulphate solution was investigated for TBP-plasticized and unplasticized foam (chloroform). The curves obtained on plotting the percentage recovery of mercury(II) against the shaking time for TBP-plasticized polyurethane foam, loaded with various concentrations of zinc dithizonate (1, 0.1 and 0.01% solutions), and treated with 20 ml of 0.5 *M* sodium thiosulphate solution, were all similar in characteristics; consequently, only the percentage recovery of mercury(II) *vs.* shaking time for the

loaded foam containing the highest concentrations (1%) of zinc dithizonate are presented in Fig. 6 (curve (a)). Curve (b) of this Figure shows the results obtained with the unplasticized zinc dithizonate foam under identical experimental conditions. From these two curves the effect of the plasticizer on the rate of recovery of mercury(II) is quite clear. As can be seen from Fig. 6 (curve (a)), quantitative recovery of mercury is obtained after a shaking time of less than 10 min, while in the case of the unplasticized foam (curve (b)), 70% recovery is reached only after shaking for 40 min.

Isotherm for the retention of mercury(II) on TBP-plasticized zinc dithizonate foam

In batch experiments, mercury(II) nitrate at different concentrations (pH 6) was shaken with TBP-plasticized zinc dithizonate foam, with all other parameters constant. After a shaking time of 30 min, the radioactivity of 2 ml of the aqueous solution was measured, and the amount of mercury extracted was calculated. The results obtained are represented in Fig. 7. The isotherm shows that a good linear dependency was maintained between the concentration of mercury on the foam and its concentration in the aqueous solution over a relatively wide range of mercury concentrations.

Capacity

The total capacity of TBP-plasticized zinc dithizonate foam (1% dithizone solution) was determined by the batch technique with various concentrations of aqueous mercury(II) nitrate solution (pH *ca.* 6). The results showed that the equilibrium capacity is 23.4 μeq per 1 g of the loaded foam. This capacity is higher than those previously reported in the literature with various dithizone-loaded sup-

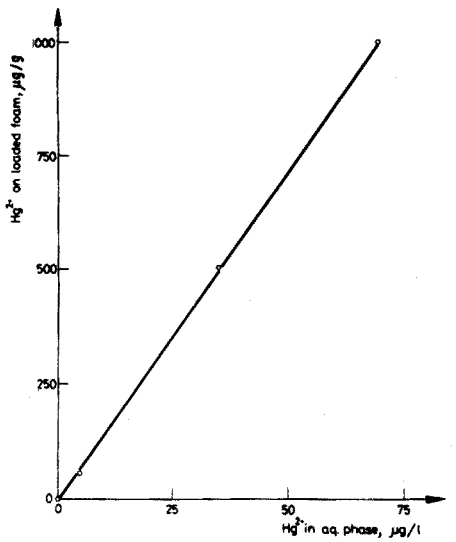

Fig. 7. Isotherm for the retention of mercury(II) on TBP-plasticized zinc dithizonate foam.

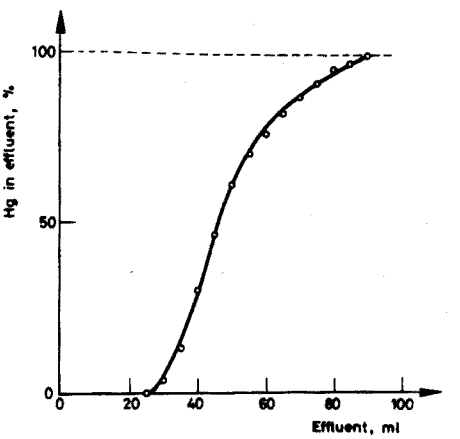

Fig. 8. Break-through curve of mercury(II) on TBP-plasticized zinc dithizonate foam column.

ports[10–12] and is still several times higher than that recently claimed[4,13] with dithizone in granular hydrophobic gel media. In further tests, the break-through capacity of a column packed with 1 g of TBP-plasticized zinc dithizonate foam was determined with a mercury solution containing 101 μg Hg^{2+} ml^{-1} at a flow-rate of 2 ml min^{-1}. The results (Fig. 8) show that the break-through capacity is 11 μeq g^{-1} and the overall capacity as calculated from this curve (dynamic method) is 22.3 μeq g^{-1}, which is quite near to the equilibrium value obtained in the batch method.

The break-through capacity of a column packed with TBP-plasticized zinc dithizonate foam was significantly decreased by washing the foam column with 1 l of distilled water before the capacity determination. As expected, this is due to leaching of the organic reagent because of the slight solubility in distilled water of the TBP containing the zinc dithizonate. It is worth mentioning that no such decrease was observed on percolating a solution previously saturated with TBP through the column.

Preconcentration of small amounts of mercury(II) with TBP-plasticized zinc dithizonate foam columns

The preconcentration of small amounts of mercury(II) from dilute solutions was examined for short columns, packed with polyurethane foam loaded with 0.1% zinc dithizonate solution in TBP. More than 94% of 0.72 μg of mercury(II) in 1 l of aqueous solution (previously saturated with TBP) was rapidly collected by percolating it through the foam columns at a flow-rate of about 40 ml min^{-1}.

The use of TBP-plasticized zinc diethyldithiocarbamate foam

Finally, the possibility of using TBP-plasticized zinc diethyldithiocarbamate foam (ZnDDTC foam) for the collection of mercury(II) from aqueous solutions (pH *ca.* 6) was investigated. In batch experiments, 10-ml aliquots of aqueous solution containing 0.72 μg of mercury(II) were shaken with 0.1 g of loaded foam in 25-ml stoppered flasks for varying times (1–60 min). The activity of 2 ml of the aqueous

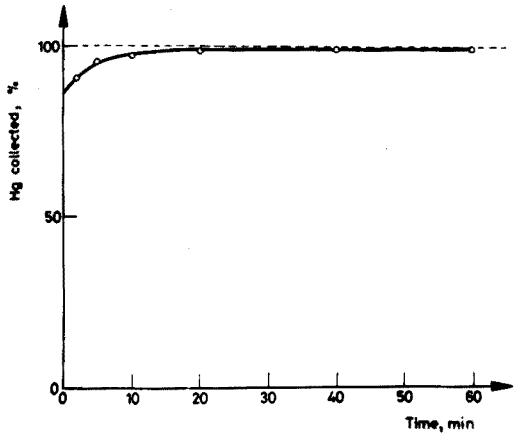

Fig. 9. Effect of shaking time on the percentage collection of mercury(II) with TBP-plasticized zinc diethyldithiocarbamate foam.

solution was then measured, and the amount of mercury collected was calculated. The results are given in Fig. 9. The curve indicates that the collection rate of mercury(II) with ZnDDTC foam was quite fast. More than 97% of mercury was collected after *ca.* 10 min. These results are considered to be promising and a detailed study on the application of the ZnDDTC foam for the rapid collection of mercury and other elements is now under consideration.

SUMMARY

The analytical suitability of zinc dithizonate foam for the collection and preconcentration of traces of mercury(II) has been examined. The effect of pH, plasticizer and chelating agent concentration on the collection rate of mercury has been critically investigated. The capacity for mercury(II) of a TBP-plasticized zinc dithizonate foam at pH 6 is 23.4 μeq g^{-1}. The effect of plasticizer on the rate of recovery of mercury with sodium thiosulphate solution is also discussed. The preparation of zinc diethyldithiocarbamate foam is described. Traces of mercury(II) can also be collected rapidly and quantitatively by this foam.

REFERENCES

1 A. K. De, S. M. Khopkar and R. A. Chalmers, *Solvent Extraction of Metals*, Van Nostrand–Reinhold, London, 1970.
2 G. Iwantscheff, *Das Dithizon und seine Anwendung in der Mikro- und Spurenanalyse*, Verlag Chemie, Weinheim, 2. Auflage, 1972.
3 *Mercury Contamination of Man and His Environment, Proc. Symp. 1972*, IAEA Vienna, Technical Reports Series No. 137, 1972.
4 Y. Sekizuka, T. Kojima, T. Yano and K. Ueno, *Talanta*, 20 (1973) 979.
5 M. A. J. Mazurski, A. Chow and H. D. Gesser, *Anal. Chim. Acta*, 65 (1973) 99.
6 T. Braun and A. B. Farag, *Anal. Chim. Acta*, 69 (1974) 85.
7 A. G. Hamlin, B. J. Roberts, W. Laughlin and S. G. Walker, *Anal. Chem.*, 33 (1961) 1547.
8 T. Braun and A. B. Farag, *Anal. Chim. Acta*, 61 (1972) 265.
9 Yu. A. Zolotov and I. M. Kuzmin, *Ekstraktsionnoe kontsentrirovannie*, Izd. Khimia, Moscow, 1971.
10 T. B. Pierce, *Anal. Chim. Acta*, 24 (1961) 146.
11 T. B. Pierce, and P. F. Peck, *Anal. Chim. Acta*, 26 (1962) 557.
12 H. Woidich and W. Pfannhauser, *Z. Anal. Chem.*, 261 (1972) 261.
13 K. Ueno, T. Yano and T. Kojima, *Anal. Lett.*, 5 (1972) 439.

Analytica Chimica Acta, 71 (1974) 141–150

GAS CHROMATOGRAPHY OF METAL CHELATES WITH CARRIER GAS CONTAINING LIGAND VAPOUR THORIUM(IV) TRIFLUOROACETYLACETONATE

T. FUJINAGA, T. KUWAMOTO and S. MURAI*

Chemistry Institute, Faculty of Science, Kyoto University, Sakyoku, Kyoto-shi (Japan)

(Received 2nd January 1974)

The gas chromatography of metal chelates has been extensively studied[1]. Recently, new chelating reagents have been synthesized in order to obtain more volatile chelates, but the perfect elution of chelates is not easily obtained, even when their volatility is comparable to that of organic compounds. Furthermore, other chromatographic properties of metal chelates, *e.g.* peak symmetry, base-line stability, and column efficiency, are not always satisfactory. Quantitative analytical applications are therefore limited.

These undesirable characteristics of metal chelates in gas chromatography are assumed to be mainly due to adsorption of the chelate on the solid supports, and/or breakdown of the chelate in the column and the injection port[2]. In order to avoid adsorption, the material for the stationary phases must be properly selected, and the metal chelate injected repeatedly until the peak area indicates quantitative elution.

In 1971, the authors[3] proposed a new method to improve the gas chromatographic separation of metal chelates, in which a constant amount of ligand vapour was contained in the carrier gas. The addition of ligand vapour is effective not only in suppressing the decomposition of metal chelates in the column, but also in scavenging chelates from the stationary phase.

Trifluoroacetylacetone (H-TFA) is well known as a reagent which forms volatile chelates with various metal ions, *e.g.* aluminium(III), beryllium(II), chromium(III), scandium(III), gallium(III), cobalt(III), rhodium(III), indium(III) and ruthenium(III); these chelates are easily eluted from gas chromatographic columns[4–9]. However, the chelates of iron(III), copper(II), manganese(III), zirconium(IV), hafnium(IV), zinc(II), thorium(IV), *etc.*, are apt to decompose on the column and are not quantitatively eluted.

With regard to thorium(IV) trifluoroacetylacetonate ($Th(TFA)_4$), it has been reported briefly that the chelate can be eluted and detected by gas chromatography[8], and also that it cannot be eluted[4]. In the present work, the gas chromatography of $Th(TFA)_4$ with H-TFA vapour as a carrier-gas additive, was studied fundamentally, and compared with the conventional method, helium being used as carrier gas.

* Present address: R & D Group, Sumitomo Electric Industries Co. Ltd., Osaka (Japan).

EXPERIMENTAL

Instrumentation

A Shimadzu model GC-IB gas chromatograph equipped with a vapour generator for supplying carrier-gas additive was used as described previously[3]. The vapour generator was controlled at a definite temperature in the range 20–35°C.

A Shimadzu model TM-2 thermobalance was used to obtain the thermogravimetric curves of metal chelates. A programmed heating rate (10°C min^{-1}) was used with a nitrogen gas flow rate of 50 ml min^{-1}.

Reagents

All reagents were of reagent grade unless otherwise specified.

Trifluoroacetylacetone (1,1,1-trifluoropentane-2,4-dione; H-TFA; Dojindo Co. Ltd. Research Laboratories) was distilled, and the 106–107°C fraction was collected and used immediately.

Samples

Trifluoroacetylacetone chelates of thorium(IV), uranium(IV), iron(III), chromium(III), aluminium(III) and beryllium(II) were prepared as suggested by Berg *et al.*[10,11], and purified by sublimation in vacuo (10^{-3} Torr). The elemental analyses for the purified metal chelates are shown in Table I. The sample was dissolved in acetone or isobutyl methyl ketone at a concentration of 10–20% (w/v). Generally, 10 μl of the sample solution were injected into the gas chromatograph.

TABLE I

ELEMENTAL ANALYSIS AND MELTING POINTS OF METAL TRIFLUOROACETYLACETONATES

	M.p. (°C)	*H(%)*		*C(%)*	
		Found	*Calcd.*	*Found*	*Calcd.*
$Th(TFA)_4$	128	2.1	1.9	28.4	28.4
$U(TFA)_4$	105	2.3	1.9	30.25	28.2
$Fe(TFA)_4$	117	2.5	2.3	35.1	34.95
$Cr(TFA)_4$	121	2.3	2.35	35.4	35.2
$Al(TFA)_4$	121	2.6	2.5	36.9	37.0
$Be(TFA)_4$	112	2.7	2.5	37.9	38.1

Gas chromatography

In the study of the conventional method with helium as carrier gas, many columns were used (Table II). For each column, the column temperature, the injection-port temperature and other chromatographic conditions were investigated in order to obtain good chromatograms of $Th(TFA)_4$. In the comparison of the various conditions, the following conditions were generally used: the column temperature was held at 180°C, the temperatures of the injection port and the detector were held at 250°C and 260°C, respectively and the helium flow was 35–60 ml min^{-1}; columns were made from 75 × 0.4 cm i.d. stainless steel tubing;

TABLE II

RETENTION VOLUME AND THEORETICAL PLATE NUMBER OF $Th(TFA)_4$ FOR VARIOUS COLUMNS[a]

Column no.[b]	*Stationary phase*	*Coating weight (%)*	*Retention volume (ml)*	*Number of theor. plates*	*Peak shape*[c]	*Solid support*	*Mesh size*	*Column size (mm × cm)*
1	Silicone DC-550	10	584	359	L	Gas Chrom-CLH	80/100	4 × 150
2*		10	90	12	T	Chromosorb-W	60/80	5 × 100
3		5	263	324	T	Gas Chrom-CLH	80/100	4 × 75
4*		0.2	102	25	T	Glass beads	60/80	5 × 100
5	Silicone XE-60	5	259	1140	T	Gas Chrom-CLH	80/100	4 × 150
6		2.5	75	196	T	Gas Chrom-CLH	80/100	4 × 75
7		0.5	26	400	T	Gas Chrom-CLH	80/100	4 × 150
8	Silicone SE-30	10	282	144	L	Gas Chrom-CLH	80/100	4 × 150
9	Silicone KF-96 oil	10	265	191	L	Gas Chrom-CLH	80/100	4 × 150
10	Silicone HV grease	10	247	167	L	Gas Chrom-CLH	80/100	4 × 150
11	Kel-F wax	10	224	121	L	Gas Chrom-CLH	80/100	4 × 150
12	Apiezon-L	10	157	235	T	Gas Chrom-CLH	80/100	4 × 150
13*		5	125	7	T	Gas Chrom-CLH	60/80	5 × 100
14		1	62	63	T	Gas Chrom-CLH	80/100	4 × 150
15*		1	90	16	T	Glass beads	60/80	5 × 100
16		0.5	33	64	T	Neosorb-NQ	40/80	4 × 150
17	PEG-1500	10	—	—	—	Gas Chrom-CLH	80/100	4 × 150
18	PEG-6000	0.5	66	671	T	Gas Chrom-CLH	80/100	4 × 150

[a] Sample: 10–20 μl of 20% (w/v) solution of $Th(TFA)_4$ in acetone.
[b] Column temperature: 180°C except for the asterisked columns which were maintained at 190°C.
[c] L: leading; T: tailing.

the detector was of the thermal-conductivity type with a cell current of 150 mA; the recorder f.s.d. was 2 mV.

In the study of the modified method with H-TFA vapour as carrier-gas additive, the chromatographic conditions were almost the same as those described above, except for the carrier gas. The carrier gas, containing H-TFA vapour, was prepared with the vapour generator, which was placed in the flow path before the injection port; a 50-ml glass bottle, containing 10–20 ml of H-TFA, placed in a thermostatted water bath at 30°C, was used as the generator.

GAS CHROMATOGRAPHY OF $Th(TFA)_4$

The conventional method with helium alone as carrier

Figure 1 shows the thermogravimetric curve of $Th(TFA)_4$. The chelate gradually sublimes above 110°C, and 95% of the chelate has sublimed at 180°C. Therefore, it would be expected that $Th(TFA)_4$ could be eluted from the gas chromatographic column at a temperature of about 160°C.

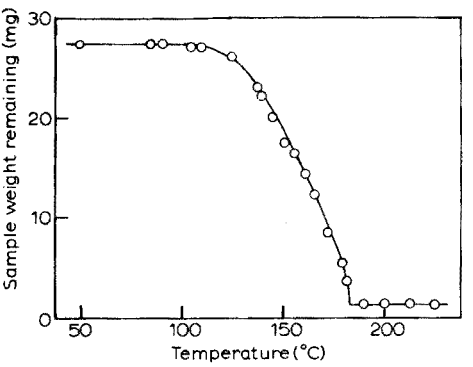

Fig. 1. Thermogravimetric curve of $Th(TFA)_4$.

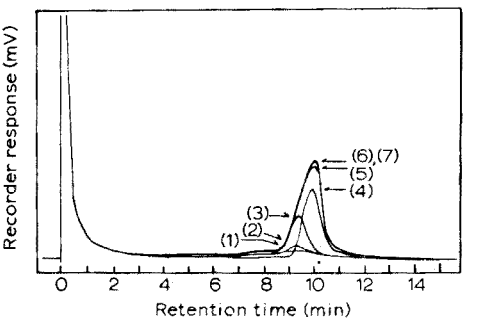

Fig. 2. Chromatograms of $Th(TFA)_4$ obtained by the conventional method. Column no. 1 in Table II; sample size 20 μl; carrier gas helium. (1) 0.5, (2) 1.0, (3) 2.0, (4), (5), (6) and (7), 4.0 mg $Th(TFA)_4$.

Various stationary phases were examined for the gas chromatography of $Th(TFA)_4$. Table II shows the retention volume, the number of theoretical plates and the peak shape for each stationary phase. It can be seen that large retention volumes and large numbers of theoretical plates were obtained by using silicone XE-60, DC-550 and SE-30 as the stationary phase. Actually, the best chromatogram was obtained with silicone DC-550 (see Fig. 2); however, $Th(TFA)_4$ was not quantitatively eluted, although the chromatogram seemed similar in shape to those obtained with the silicones as the liquid phase. The plot of chelate peak area against sample size did not pass through the origin (Fig. 3); the peak area of $Th(TFA)_4$ was not reproducible for samples of the same size, and no chelate peak could be obtained below about 0.5 mg of $Th(TFA)_4$.

Figure 4 shows a typical anomalous chromatogram. This net elution curve (3) shows two peaks composed of a broad front peak and a sharp main peak.

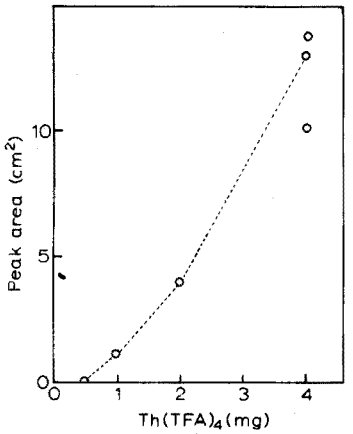

Fig. 3. Plot of the chelate peak area against the sample size. Chromatographic conditions as for Fig. 2.

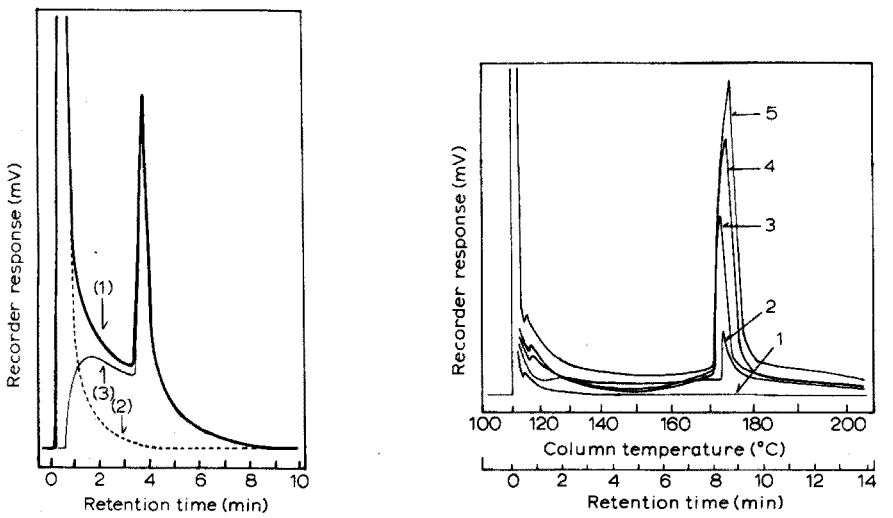

Fig. 4. Chromatogram of $Th(TFA)_4$ obtained by the conventional method. Column no. 6 in Table II; carrier gas helium. (1) 10 μl of 20% (w/v) solution of $Th(TFA)_4$ in acetone, (2) 10 μl of acetone, (3) the net elution curve of $Th(TFA)_4$ obtained from the difference between curves (1) and (2).

Fig. 5. Chromatograms of $Th(TFA)_4$ obtained by the programmed temperature method. Column no. 7 in Table II; carrier gas, helium. The rate of the programmed temperature was about 7.2°C min^{-1}; (1) 0.4, (2) 0.8, (3) 1.2, (4) 1.6, (5) 2.0 mg $Th(TFA)_4$.

The broad front peak is attributed to the successive decomposition of $Th(TFA)_4$ in the column, and not to decomposition in the injection-port. One of the eluted decomposition products is thought to be H-TFA, since the H-TFA molecule formed by the decomposition of $Th(TFA)_4$ is more volatile than $Th(TFA)_4$ itself.

The programmed-temperature method was examined to separate the decomposition products from the chelate peak. As shown in Fig. 5, an apparently

good separation of $Th(TFA)_4$ from the solvent was obtained, but the anomalous effluent was not isolated. In further tests H-TFA was injected into the same column after $Th(TFA)_4$ had been examined. As a result, part of the metal chelate left in the column was eluted. Therefore, it became clear that part of the sample was always retained in the column and that quantitative elution could not be achieved with the conventional method.

The new method with ligand vapour as carrier-gas additive

In the gas chromatographic separation of some metal chelates, it was clearly demonstrated that ligand vapour was extremely effective in obtaining quantitative elution[3]. Similar improvement is reported here for the determination of thorium. Figure 6 shows the chromatograms of $Th(TFA)_4$ which were obtained with helium alone and containing H-TFA vapour, as carrier gas; other chromatographic conditions were the same in both cases. In the chromatogram obtained with H-TFA as carrier-gas additive, the anomalous elution curve was not observed and the plotted curve of peak area *versus* sample size passed through the origin (Fig. 7).

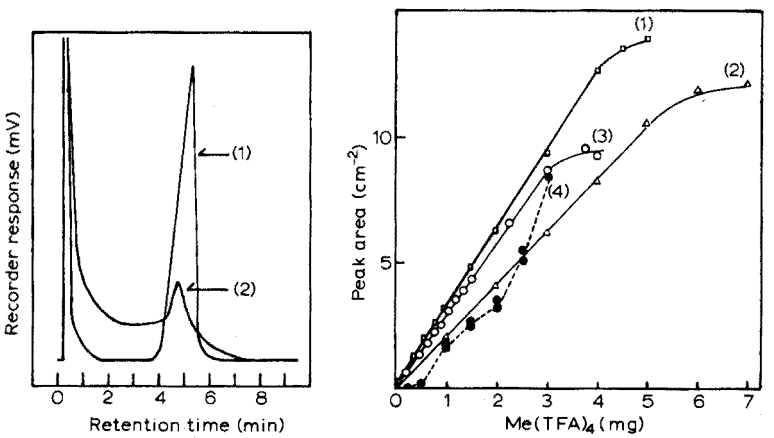

Fig. 6. Chromatogram of $Th(TFA)_4$ obtained with H-TFA vapour as carrier-gas additive. Column, no. 3 in Table II: (1) with the proposed method, (2) with the conventional method.

Fig. 7. Plot of the chelate peak area against sample weight of $Th(TFA)_4$ and $U(TFA)_4$. (1), (3) and (4) $Th(TFA)_4$, (2) $U(TFA)_4$. (1), (2) and (3) with the proposed method, (4) with the conventional method. Other chromatograph ic conditions: (1) and (2) as for Fig. 6: (3) and (4) as for Fig. 4.

The relationship between column temperature and retention volume. Figure 8 shows the retention volumes of $Th(TFA)_4$ at various column temperatures. The retention volume V_r of $Th(TFA)_4$ obtained by the proposed method agrees well with that obtained by the conventional method at the same temperature.

In the theory of gas–liquid chromatography, the relationship between the column temperature (T°K) and the retention volume (V_r) is represented by the following equation.

$$\ln V_r = [-\Delta H/(RT)] + \text{const.}$$

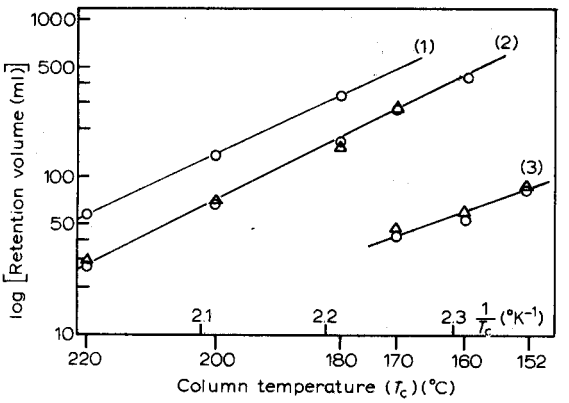

Fig. 8. Relationships between retention volume and column temperature; (1) and (2) $Th(TFA)_4$, (3) $U(TFA)_4$. (○) with the proposed method, (△) with the conventional method. Coating weight of the stationary liquid: (1) 10%, (2) and (3) 5%. Other chromatographic conditions as for Fig. 6.

where R is the gas constant, and ΔH is the differential molar heat of evaporation from the stationary liquid.

Figure 8 shows that the ΔH of the proposed method is almost the same as the ΔH of the conventional method, *i.e.* the distribution mechanism of $Th(TFA)_4$ between gas and liquid phases is not affected by the addition of H-TFA to helium. The addition of H-TFA is thought to be effective in suppressing the anomalous behaviour of a part of the $Th(TFA)_4$, and the number of theoretical plates was not changed by the presence of H-TFA vapour.

The choice of stationary liquid phases. In the various stationary liquids, the retention volumes and the numbers of theoretical plates of the proposed method, were almost the same as those of the conventional method. But, the effectiveness of the H-TFA additive for the quantitative elution of $Th(TFA)_4$ is greatly dependent on the polarity of the stationary phases.

The present method was found especially useful when silicone SE-30, DC-550 or XE-60 was used as the stationary phase. With such slightly polar liquids, quantitative elution of $Th(TFA)_4$ was observed, even when the liquid phase was loaded as high as 10% (w/w). But, with liquids of much stronger polarity, such as polyethyleneglycol (PEG)-6000, the H-TFA additive was not effective. except in the case of a lightly loaded column of PEG-6000. In non-polar liquids, such as Apiezon-L, H-TFA additive was not expected to be effective.

The amount of H-TFA additive in the column. The amount of H-TFA additive in the column was measured by the method of Green and Pust[12]. The amount of H-TFA carried in the column was found to be 1.7 mg min^{-1}, the amount of H-TFA retained in the liquid-loaded column was 0.7 mg, and the amount of H-TFA in the uncoated column was 0.6 mg at a flow rate of 21.6 ml min^{-1}. On the other hand, the maximal sample size, which still allowed quantitative elution of $Th(TFA)_4$, was about 4 mg of $Th(TFA)_4$. From these results, it appears that, if the amount of H-TFA present in the column is at least equivalent to the amount of $Th(TFA)_4$, the H-TFA vapour is sufficient to suppress the decomposition of $Th(TFA)_4$.

Other organic vapours as carrier-gas additive. Organic vapours, such as isobutyl methyl ketone, cyclohexane and benzene, were examined as the carrier-gas additive. However, all of them showed little effect in suppressing the anomalous elution of $Th(TFA)_4$.

GAS CHROMATOGRAPHY OF OTHER METAL TRIFLUOROACETYLACETONATES AND OF ACETYLACETONATES

The gas chromatography of trifluoroacetylacetonates of beryllium(II), aluminium(III), chromium(III), iron(III) and uranium(IV) were also examined with H-TFA vapour as carrier-gas additive. It was found that the trifluoroacetylacetonates of beryllium, aluminium, and chromium were quantitatively eluted in the proposed method and in the conventional method. On the other hand, the iron and uranium chelates were eluted quantitatively only in the presence of ligand vapour. The improved chromatograms are shown in Figs. 9 and 10.

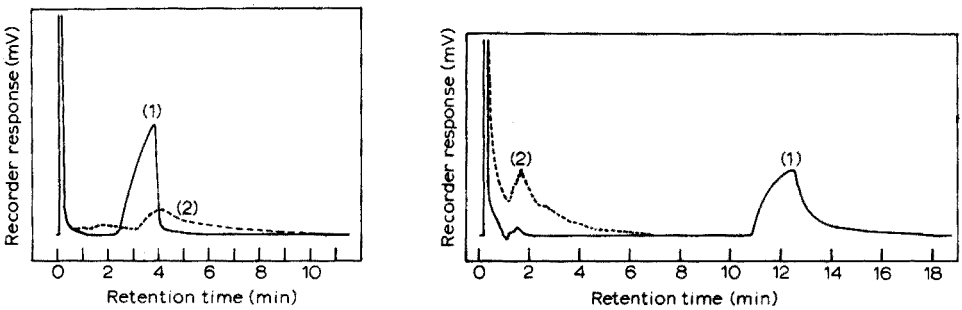

Fig. 9. Chromatograms of iron(III) trifluoroacetylacetonate; (1) with the proposed method, (2) with the conventional method (irreproducible). Chromatographic conditions as for Fig. 6 except for column temp. which was 140°C.

Fig. 10. Chromatograms of uranium(IV) trifluoroacetylacetonate; (1) with the proposed method, (2) with the conventional method (irreproducible). Chromatographic conditions as for Fig. 6 except for column temp. which was 140°C.

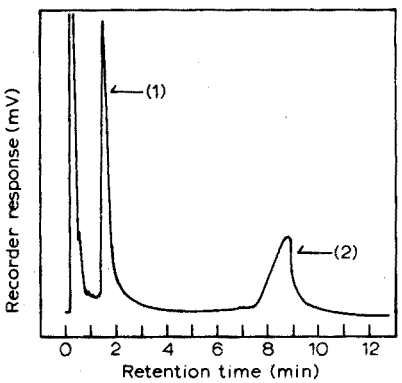

Fig. 11. Separation of $Th(TFA)_4$ and $U(TFA)_4$, Chromatographic conditions as for Fig. 6 except for column temp. which was 170°C. Sample: 10 μl of a solution containing 5% (w/v) $Th(TFA)_4$ and 5% (w/v) $U(TFA)_4$ in isobutyl methyl ketone.

The retention volume of uranium(IV) trifluoroacetylacetonate is smaller than that of $Th(TFA)_4$ as shown in Fig. 8. Therefore the separation of uranium from thorium is possible by the proposed method (Fig. 11).

Acetylacetonates of beryllium(II), copper(II), aluminium(III), chromium-(III), iron(III), thorium(IV), cobalt(III) and zinc(II) were examined with acetylacetone (H-AA) vapour as carrier-gas additive. The chromatographic conditions were the same as those in the case of trifluoroacetylacetonates, except for the column temperature. It was found that beryllium, copper, aluminium, chromium, iron and thorium were eluted quantitatively, but cobalt and zinc were not eluted under the chromatographic conditions examined. But, when the conventional method was used, only beryllium and copper acetylacetonates were quantitatively eluted. Therefore, the method with ligand vapour as carrier-gas additive was found effective for the acetylacetonates of aluminium, chromium, iron and thorium, as well as in the gas chromatography of trifluoroacetylacetonates.

CONCLUSION

It was found by thermogravimetric analysis that $Th(TFA)_4$ sublimes at 180°C. In conventional gas chromatography, $Th(TFA)_4$ is eluted at about 160°C and above, but the elution is not quantitative. The present work has shown that, when H-TFA vapour is used as carrier-gas additive, $Th(TFA)_4$ can be quantitatively eluted and the chromatographic elution pattern of the chelate greatly improved. The retention volumes and the number of theoretical plates of $Th(TFA)_4$ are not changed by addition of the H-TFA to the carrier gas. Slightly polar liquids (silicone XE-60, DC-550, SE-30 *etc.*) are the most useful for quantitative elution of $Th(TFA)_4$. For quantitative elution, the amount of H-TFA retained in the column must be at least equivalent to the amount of $Th(TFA)_4$ in the sample. From the results obtained, it can be concluded that the H-TFA in the column acts as a suppressor against the decomposition of $Th(TFA)_4$, relating to the polarity of the stationary liquid.

The gas chromatography of other metal trifluoroacetylacetonates and metal acetylacetonates was also examined by the proposed method, which was compared with the conventional method. The trifluoroacetylacetonates of iron(III) and uranium(IV), and the acetylacetonates of aluminium(III), chromium(III), iron(III) and thorium(IV) were quantitatively eluted and their chromatograms improved.

SUMMARY

When the conventional gas chromatographic method with helium as carrier gas is used, thorium(IV) trifluoroacetylacetonate shows an anomalous peak and the chelate is not eluted quantitatively. But, by using trifluoroacetylacetone vapour as a carrier-gas additive, the anomalous peak can be improved. The technique of using a carrier gas containing ligand vapour was studied fundamentally, and was found to be extremely useful in obtaining more reliable chromatographic peaks than those obtained in the absence of ligand vapour. The proposed method furnishes similar quantitative results in the determinations of uranium(IV) and

iron(III), as their trifluoroacetylacetonates, and aluminium(III), chromium(III), iron(III) and thorium(IV) as their acetylacetonates.

REFERENCES

1 See, *e.g.*, R. W. Moshier and R. E. Sievers, *Gas Chromatography of Metal Chelates*, Pergamon, Oxford, 1965.
2 P. C. Uden and C. R. Jenkins, *Talanta*, 16 (1969) 893.
3 T. Fujinaga, T. Kuwamoto and S. Murai, *Talanta*, 18 (1971) 429.
4 J. E. Schwarberg, R. W. Moshier and J. H. Walsh, *Talanta*, 11 (1964) 1213.
5 W. D. Ross, R. E. Sievers and G. Wheeler, Jr., *Anal. Chem.*, 37 (1965) 598.
6 H. Veening, W. E. Bachman and D. M. Wilkinson, *J. Gas Chromatogr.*, 5 (1967) 248.
7 W. D. Ross and R. E. Sievers, *Anal. Chem.*, 41 (1969) 1109.
8 K. Tanikawa, K. Hirano and K. Arakawa, *Chem. Pharm. Bull.*, 15 (1967) 915.
9 T. Fujinaga, T. Kuwamoto and Y. Ono, *Nippon Kagaku Zasshi*, 86 (1965) 1294.
10 E. W. Berg and J. J. C. Acosta, *Anal. Chim. Acta*, 40 (1968) 101.
11 E. W. Berg and J. T. Truemper, *J. Phys. Chem.*, 64 (1960) 487.
12 S. A. Green and H. Pust, *J. Phys. Chem.*, 62 (1958) 55.

Analytica Chimica Acta, 71 (1974) 151–156

ELECTROCHEMICAL INVESTIGATIONS IN NON-AQUEOUS MEDIA

PART I. INVESTIGATION OF THE DISSOCIATION OF DIBASIC ACIDS

T. TU AN, K. TÓTH and E. PUNGOR

Institute for General and Analytical Chemistry, Technical University, Budapest (Hungary)

(Received 2nd January 1974)

The importance of non-aqueous solvents has increased recently, and it is therefore desirable to study the electrochemical behaviour of various compounds in different non-aqueous solvents. In this series of papers, some investigations in this field will be reported.

The dissociation constants of dibasic acids in aqueous solutions can be determined by potentiometric[1–4], colorimetric[5] and spectrophotometric[6–12] methods. The search for methods applicable in non-aqueous media has been carried out from different points of view. In the literature, there are numerous data concerning the dissociation constants of monobasic acids measured in non-aqueous solvents[13–17], but for the dibasic acids only Kreskov *et al.*[18] have published data (without a detailed description of the method).

The aim of the work described here was to elaborate methods for measuring the dissociation constants of some dibasic acids in non-aqueous media. The results of investigations made in alcoholic media are reported here.

THEORETICAL PART

The dissociation constants of acids were determined by the potentiometric method. The measurements were carried out in the following cell:

glass electrode	dibasic acid,	R_4NCl, AgCl, Ag
e_2	non-aqueous solvent	e_r

e_j

At the first end-point of the titration, eqn. (1) is valid, while at the second end-point eqn. (2) is valid:

$$E_1 = e_r + e_j - e'_2 \quad (1)$$

$$E_2 = e_r + e_j - e''_2 \quad (2)$$

where e_r is the potential of the reference electrode, e'_2, e''_2 are the potentials of the indicator electrode, e_j is the liquid junction potential which can be considered constant, and E_1, E_2 are the measured e.m.f. values of the cell.

If it is assumed that the indicator electrode potential can be described by the Nernst equation, that the neutral acidic salts dissociate completely in alcohols, and that the two dissociation constants of the acid differ considerably, then the

following equations can be written:

$$E_1 = e_r + e_j - 0.059 \log \frac{K_1 \cdot c_{H_2A} \cdot f_{H_2A}}{c_{HA^-} \cdot f_{HA^-}} \quad (3)$$

$$E_2 = e_r + e_j - 0.059 \log \frac{K_2 \cdot c_{HA^-} \cdot f_{HA^-}}{c_{A^{2-}} \cdot f_{A^{2-}}} \quad (4)$$

If $f_{H_2A} \approx f_{HA^-}$ and $f_{HA^-} \approx f_{A^{2-}}$, then:

$$pK_1 = \frac{E_1 - (e_r + e_j)}{0.059} + \log \frac{c_{H_2A}}{c_{HA^-}} \quad (5)$$

$$pK_2 = \frac{E_2 - (e_r + e_j)}{0.059} + \log \frac{c_{HA^-}}{c_{A^{2-}}} \quad (6)$$

For the determination of $(e_r + e_j)$, it is necessary to use an acid, the dissociation constant of which is known or can be measured by another method:

$$e_r + e_j = E + 0.059 \log \frac{K_a \cdot c_a}{c_b} \quad (7)$$

where K_a is the dissociation constant of the standard acid, and c_a, c_b are the concentrations of the acid and salt, respectively.

EXPERIMENTAL

Chemicals

Solvents. Iso-propanol, n-butanol, iso-butanol and sec-butanol (p.a.) were used. The water content of the solvents was 0.1% (Karl-Fischer titration).

Dibasic acids. Malonic acid, oxalic acid, succinic acid, fumaric acid, citraconic acid and itaconic acid (p.a.) were recrystallized and stored in a desiccator.

Titrants. Tetraethylammonium hydroxide was prepared from the TEA iodide, sodium hydroxide and silver nitrate[19]. The titrant was prepared from tetraethylammonium hydroxide in methanol which was diluted (1+4) with the appropriate solvent. The concentration of the titrant was determined by potentiometric titration[20].

Methods

A conductivity meter (Type OK-102, Radelkis, Budapest) and a pH meter (Type OP-204, Radelkis) were used. The glass electrode (Type OP-700; Radelkis, Budapest) was soaked in the appropriate solvent before and between measurements. The reference electrode was Ag/AgCl, NaCl crystal, $(C_2H_5)_4NCl$.

The measurements were carried out at room temperature in solutions mixed with nitrogen gas. The cell constant was measured with 0.01 *M* KCl solution.

RESULTS AND DISCUSSION

Comparative investigations were carried out with picric acid, as its dissociation constant can be determined conductometrically. The calculation is made by means of the following equation[21]:

$$\frac{1}{\Lambda} = \frac{c_a \cdot \Lambda}{K_a \cdot \Lambda_0^2} + \frac{1}{\Lambda_0} \quad (8)$$

TABLE I

(e_r+e_j) VALUES MEASURED IN ISO-BUTANOL

0.0488 N TEAOH (ml)	*E (mV)*	e_r+e_j *(mV)*
0.40	−476.5	−683
0.60	−468.5	−690
0.80	−464.0	−695
0.90	−460.0	−696
1.00	−456.0	−697
1.10	−451.5	−698
1.20	−447.0	−698
1.30	−441.0	−697
1.40	−434.5	−697
1.50	−428.0	−696
1.60	−420.0	−695
1.70	−408.0	−691
		Mean value: −694

TABLE II

pK_{HPi} AND (e_r+e_j) VALUES IN DIFFERENT ALCOHOLS

Solvent	pK_{HPi} $(M\ l^{-1})$	e_r+e_j *(mV)*
iso-Propanol	3.73	−632
n-Butanol	4.03	−631
iso-Butanol	4.11	−694
sec-Butanol	4.22	−662

where Λ is the equivalent conductivity, Λ_0 is the equivalent conductivity at infinite dilution, and c_a, K_a are the concentration and the dissociation constant of picric acid, respectively.

The straight lines relevant to the measuring points were determined by the method of least squares[22]. The value of (e_r+e_j) in iso-butanol was determined in the potentiometric cell shown above. The related data are shown in Table I.

Table II contains pK data for picric acid measured by conductometry and (e_r+e_j) values determined potentiometrically in different alcohols.

With eqns. (5) and (6), the relative pK values of seven organic dibasic acids (oxalic acid, malonic acid, succinic acid, maleic acid, fumaric acid, citraconic acid and itaconic acid) were determined in four alcohols (iso-propanol, n-butanol, iso-butanol and sec-butanol). In Table III these values as well as those measured in tert-butanol by Kreskov *et al.*[18] are shown.

The results obtained for dibasic acids are presented in Fig. 1 in the way usually applied for monoacids.

An empirical equation was derived not only for monobasic acids[23, 24] but also for both dissociation steps of dibasic acids. This equation gives a correlation

TABLE III

pK VALUES FOR DIBASIC ACIDS IN VARIOUS SOLVENTS

Acid	*Water*	*iso-Propanol*		*n-Butanol*		*iso-Butanol*		*sec-Butanol*		*tert-Butanol*[18]
		Measured	*Calcd.*	*Measured*	*Calcd.*	*Measured*	*Calcd.*	*Measured*	*Calcd.*	
Oxalic acid	1.27	6.90	—	7.50	—	7.42	—	—	—	9.72
	4.27	12.7	—	12.3	—	12.9	—	—	—	15.62
Malonic acid	2.86	7.08	6.95	7.52	7.57	7.84	7.67	7.98	8.21	10.06
	5.70	14.9	14.5	14.3	14.0	14.9	14.6	15.9	15.9	18.38
Succinic acid	4.21	9.13	9.18	9.82	9.82	9.80	9.80	10.6	10.5	12.37
	5.64	13.9	14.3	13.5	13.8	14.2	14.5	15.5	15.7	17.49
Glutaric acid	4.34	—	9.39	-	10.0	—	10.0	—	10.7	13.57
	5.27	—	13.0	-	12.8	—	13.6	—	14.6	16.06
Fumaric acid	3.02	8.93	—	9.52	—	9.59	—	-	—	—
	4.38	11.7	—	11.7	—	12.3	—	-	—	—
Maleic acid	1.92	5.36	5.38	5.92	6.01	6.12	6.18	6.73	6.63	8.26
	6.23	16.2	16.3	15.3	15.4	15.8	15.9	17.4	17.4	19.72
Citraconic acid	2.29	5.93	6.00	6.76	6.62	6.74	6.77	7.30	7.25	—
	6.15	16.1	16.0	15.3	15.5	15.7	15.7	17.2	17.2	—
Itaconic acid	3.84		8.56	—	9.20	9.14	9.22	9.80	9.85	11.62
	5.55		14.0	—	13.5	14.3	14.3	15.6	15.4	17.43

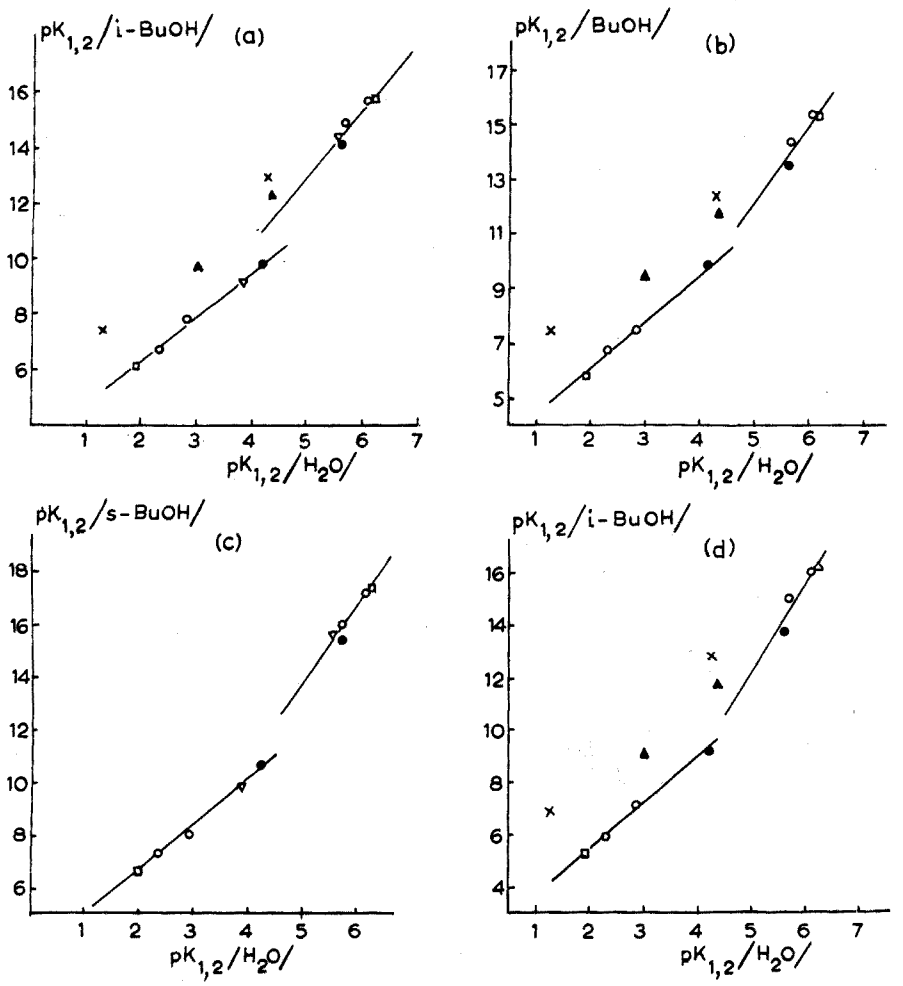

Fig. 1. Correlations between $pK_{1,2}$ values in water and in alcohol: (a) iso-butanol (i-BuOH), (b) n-butanol (BuOH), (c) sec-butanol (s-BuOH), (d) iso-propanol (i-PrOH). (×) Oxalic acid, (▲) fumaric acid, (○) malonic acid, (◒) citraconic acid, (●) succinic acid, (▽) itaconic acid and (□) maleic acid.

between the pK values measured in aqueous medium and the pK values measured in the solvents studied. Oxalic acid and the fumaric acid were the only exceptions, since their data did not lie on the straight line described by the following empirical equation:

$$pK_{R-OH} = a \cdot pK_{H_2O} + b \tag{9}$$

The constants of eqn. (9) in different solvents are shown in Table IV. In Table III the data measured and calculated by eqn. (9) are compared.

The differentiating effects of various alcohols on the same acid are different, while the slope of the $pK_{1_{R-OH}}$ *vs.* $pK_{1_{H_2O}}$ plot is the same in almost all the alcohols studied. Tert-butanol and iso-propanol have greater differentiating effects on pK_2 than the other alcohols studied.

TABLE IV

CONSTANTS OF THE EMPIRICAL EQUATION (9)

Solvent	*Acid examined*	*Dissociation step*	*a*	*b*
iso-Propanol	dibasic acids	pK_1	1.66	2.21
		pK_2	3.47	−5.31
n-Butanol	dibasic acids	pK_1	1.67	2.81
		pK_2	2.77	−1.83
iso-Butanol	dibasic acids	pK_1	1.58	3.15
		pK_2	2.33	1.31
sec-Butanol	dibasic acids	pK_1	1.68	3.41
		pK_2	2.93	−0.84
tert-Butanol[18]	dibasic acids	pK_1	2.25	3.42
		pK_2	5.21	−11.5

SUMMARY

The stoichiometric dissociation constants of seven dibasic acids were determined in four alcohols by potentiometric titration; it was assumed that the acidic and neutral salts dissociate completely. A linear relationship was found between the $pK_{1,2}$ values of dibasic acids in water and those in alcohols.

REFERENCES

1 H. I. Britton, *Hydrogen Ions*, Vol. I, Chapman and Hall, London, 1955, pp. 217, 218.
2 I. C. Speakman, *J. Chem. Soc.*, (1940) 855.
3 W. L. German and A. I. Vogel, *J. Amer. Chem. Soc.*, 58 (1936) 1546.
4 R. G. Bates, *J. Amer. Chem. Soc.*, 70 (1948) 1579.
5 R. H. Jones and D. I. Stock, *J. Chem. Soc.*, (1960) 102.
6 B. J. Thamer and A. F. Voigt, *J. Phys. Chem.*, 56 (1952) 225.
7 Kok-Peng-Ang, *J. Phys. Chem.*, 62 (1958) 1109.
8 T. Anno and A. Sado, *Bull. Chem. Soc. Japan*, 29 (1956) 620.
9 R. A. Robinson and A. K. Kiang, *Trans. Faraday Soc.*, 52 (1956) 327.
10 B. J. Thamer, *J. Phys. Chem.*, 59 (1955) 450.
11 G. Heys, H. Kinns and D. D. Perrin, *Analyst*, 97 (1972) 52.
12 B. Roth and J. F. Bunnet, *J. Amer. Chem. Soc.*, 87 (1965) 334.
13 J. Juillard, *Bull. Soc. Chim.*, (1966) 2150.
14 I. M. Kolthoff, S. Bruckenstein and M. K. Chantooni, *J. Amer. Chem. Soc.*, 83 (1961) 3927.
15 I. M. Kolthoff and T. B. Reddy, *Inorg. Chem.*, 1 (1962) 189.
16 I. M. Kolthoff and M. K. Chantooni, *J. Amer. Chem. Soc.*, 87 (1965) 4428.
17 M. Bos and E. A. M. F. Dahmen, *Anal. Chim. Acta*, 53 (1971) 39; 57 (1971) 361.
18 A. P. Kreskov, N. T. Smolova, N. S. Aldarova and N. A. Gabidulina, *Zh. Anal. Khim.*, 26 (1971) 2456.
19 R. H. Cundiff and P. C. Markunas, *Anal. Chem.*, 34 (1962) 584.
20 A. P. Kreskov, L. N. Bikova and N. A. Kazarjan, *Kislotno-Osnovnoe Titrovanije v Nevodnikh Rastvorakh*, Khimija, Moscow, 1967, p. 47.
21 C. A. Kraus and W. C. Bray, *J. Amer. Chem. Soc.*, 35 (1913) 1315.
22 L. M. Batuner and M. E. Pozin, *Matematicheskije Metodi v Khim. Technike*, Khimija, Moscow, 1971, p. 665.
23 S. M. Petrov and J. I. Umanskij, *Zh. Fiz. Khim.*, 41 (1967) 1374.
24 A. P. Kreskov, N. S. Aldarova and N. T. Smolova, *Zh. Obsh. Khim.*, 39 (1969) 1390.

Analytica Chimica Acta, 71 (1974) 157–163

POLAROGRAPHIC DETERMINATION OF CHLORPHENIRAMINE MALEATE IN PHARMACEUTICALS

EINAR JACOBSEN and KNUT HØGBERG

Department of Pharmacy, University of Oslo, Blindern, Oslo 3 (Norway)

(Received 12th January 1974)

The pyridine-derived antihistamine, chlorpheniramine maleate, is marketed in a variety of pharmaceutical preparations. The drug has been determined by spectrophotometry[1–4], by gas chromatography[5] and by non-aqueous titration[6]. However, most of these methods are not very sensitive, and time-consuming separations of the drug from complex mixtures are usually required before the determination.

The polarographic behaviour of chlorpheniramine maleate has not so far been investigated; the object of the present work was to study the electroreduction of the drug in detail and to investigate the application of polarography to a rapid determination of the drug in pharmaceuticals.

EXPERIMENTAL

The instruments and equipment used for polarographic, voltammetric and coulometric experiments have been described previously[7]. The capillary characteristics of the dropping mercury electrode, measured in 0.1 *M* potassium nitrate (open circuit) at a mercury height of 38.3 cm were $m = 2.652$ mg s^{-1} and $t = 2.78$ s.

Chlorpheniramine maleate (pharmaceutical grade) and tablets containing 4 mg of chlorpheniramine maleate were obtained from A/S Apothekernes Laboratorium for Specialpræparater, Oslo. A 10^{-3} *M* stock solution was prepared by dissolving the appropriate amount of the commercial product in 0.2 *M* sulphuric acid. The remaining chemicals were of reagent grade and were used without further purification.

ELECTROREDUCTION OF CHLORPHENIRAMINE MALEATE

Preliminary experiments showed that polarograms of chlorpheniramine maleate exhibit a single well-defined wave when strong acidic solutions are used as supporting electrolyte. The d.c. polarographic step is followed by an a.c. polarographic wave with a peak potential (E_p) slightly more negative than the half-wave potential (Fig. 1). The effect of pH on the polarographic wave was investigated by recording a.c. and d.c. polarograms in various supporting electrolytes. The reversibility of the electrode reaction was tested by determining the value $E_{\frac{1}{4}} - E_{\frac{1}{4}}$ for each d.c. wave and the width of the a.c. wave at half-height, $E_{p/2}$. The results are given in Table I. The polarogram recorded at pH 9.1 was

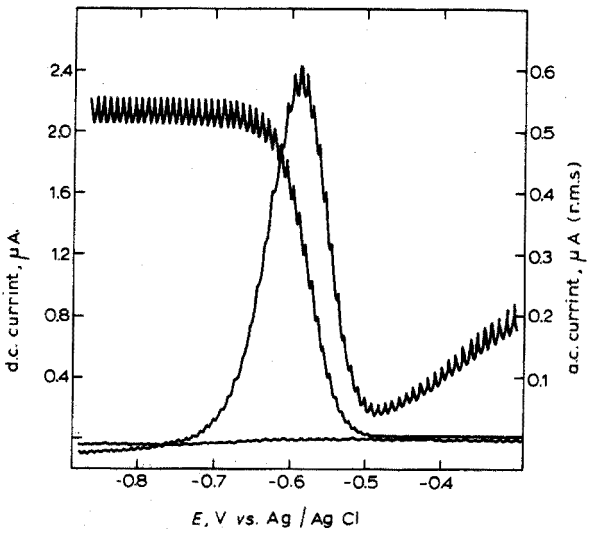

Fig. 1. A.c. and d.c. polarograms of 0.25 m*M* chlorpheniramine maleate in 0.2 *M* sulphuric acid.

TABLE I

POLAROGRAPHIC DATA OF 0.25 m*M* CHLORPHENIRAMINE MALEATE IN VARIOUS SUPPORTING ELECTROLYTES

Supporting electrolyte	*pH*	i_d *(μA)*	$-E_{\frac{1}{4}}$ *(V)*	$-(E_{\frac{1}{4}}-E_{\frac{1}{4}})$ *(mV)*	i_p *(μA r.m.s.)*	$-E_{p/2}$ *(V)*	$\Delta E_{p/2}$ *(mV)*
H_2SO_4	0.2	2.07	0.55	48	0.60	0.57	80
H_2SO_4	0.7	2.10	0.58	50	0.60	0.59	80
H_2SO_4	1.8	2.12	0.65	54	0.58	0.67	126
Citrate	3.0	2.12	0.80	64	0.49	0.83	130
Citrate	3.9	2.07	0.94	70	0.43	0.99	140
Acetate	4.4	1.98	0.98	72	0.41	1.01	166
Citrate	5.0	1.84	1.06	64	0.40	1.12	162
Citrate	5.9	1.61	1.16	66	0.41	1.23	156
Phosphate	6.5	1.45	1.22	63	0.41	1.26	130
Phosphate	7.3	1.40	1.28	56	0.40	1.32	130
Phosphate	7.8	1.35	1.30	57	0.38	1.33	125
NH_3/NH_4Cl	9.1	1.35	1.57		0.37	1.70	

ill-defined and the reduction occurred close to the reduction wave of the supporting electrolyte. In the pH range 3–6.5, a second reduction wave was observed. The half-wave potential of this wave was almost independent of pH ($E_{\frac{1}{4}} \approx 1.3$ V) and the current–voltage curve was ill-defined. This wave was obviously of no analytical value.

As indicated in Table I, the most reversible waves were obtained from strongly acidic electrolytes. Moreover, the limiting current as well as the a.c. polarographic peak current decreased markedly with increasing pH of the electrolyte. Consequently, 0.2 *M* sulphuric acid (pH 0.7) was chosen as supporting electrolyte

in the following experiments. The $(E_{\frac{1}{4}}-E_{\frac{1}{2}})$ value of -50 mV in this medium indicates an irreversible 2-electron reduction, but the appearance of an a.c. polarographic wave indicates that a fast electron transfer is involved in the overall electron reaction.

The effect of drop time was investigated by recording polarograms of 0.15 m*M* chlorpheniramine maleate in 0.2 *M* sulphuric acid at various heights of the mercury column. The value $ih^{-\frac{1}{2}}$, where h is the height of the column after correction for the "back pressure", was constant (Table II), indicating that the current is diffusion-controlled. The height of the a.c. wave increased slightly with the height of the column which implies that the a.c. current is partly controlled by the rate of adsorption[8]. The temperature coefficient (determined in the range 18–48°C) of the d.c. wave was $+1.4\%$ per degree, and that of the a.c. wave $+1.1\%$ per degree; this again implies that the current is controlled essentially by diffusion.

TABLE II

EFFECT OF PRESSURE OF MERCURY ON THE HEIGHTS OF THE POLAROGRAPHIC WAVES OF 0.15 m*M* CHLORPHENIRAMINE MALEATE IN 0.2 *M* SULPHURIC ACID

h_{corr} (cm)	i_d (μA)	i_p (μA r.m.s.)	$i_d h_{corr}^{-\frac{1}{2}}$ (μA cm$^{-\frac{1}{2}}$)
26.7	1.04	0.38	0.202
31.7	1.16	0.39	0.207
36.7	1.25	0.40	0.206
41.7	1.34	0.42	0.207
46.7	1.39	0.43	0.203
57.7	1.48	0.44	0.206

Polarograms recorded from 0.2 *M* sulphuric acid with various amounts of chlorpheniramine present, showed that the d.c. current increases linearly with concentration. As indicated in Table III, the a.c. current is much lower than the corresponding d.c. current and below 10^{-5} *M* no a.c. wave was observed on the polarograms. The data in Table III are perfectly reproducible, and suggest that chlorpheniramine maleate can be determined by d.c. polarography in the entire concentration range 10^{-6} to 10^{-3} *M* (0.3–400 μg ml^{-1}). Moreover, the drug is very stable in 0.2 *M* sulphuric acid. No decrease in diffusion current was observed 2 weeks after mixing the solution. The diffusion current constant, $I=i_d/cm^{\frac{2}{3}}t^{\frac{1}{6}}$, calculated from the data in Table III, is $I=3.70$.

In strong acidic media, the half-wave potential of chlorpheniramine maleate is shifted -63 mV per pH unit to more negative values with increasing pH. The number of hydrogen ions, Z, consumed in the electron reaction is given by

$$\Delta E_{\frac{1}{2}}/\mathrm{pH} = -0.059\ Z/\alpha n_a$$

where α is the transfer coefficient. The value αn_a calculated from the equation

$$E = E_{\frac{1}{2}} - (0.059/\alpha n_a)\cdot\log(i/i_d - i)$$

was 1.29, which gives the value $Z=1.38$. Consequently, two hydrogen ions are probably consumed in the electrode reaction.

TABLE III

POLAROGRAPHIC DATA FOR THE REDUCTION OF VARIOUS AMOUNTS OF CHLORPHENIRAMINE MALEATE IN 0.2 *M* SULPHURIC ACID

Conc. (*mM*)	i_d (*μA*)	$-E_{\frac{1}{2}}$ (*V*)	i_d/c (*μA mM*$^{-1}$)	i_p (*μA*)	$-E_p$ (*V*)	i_p/c (*μA mM*$^{-1}$)
1.000	8.36	0.57	8.36	2.35	0.59	2.35
0.800	6.70	0.57	8.38	1.91	0.59	2.39
0.500	4.20	0.57	8.40	1.21	0.59	2.43
0.250	2.09	0.57	8.36	0.605	0.59	2.42
0.100	0.839	0.58	8.39	0.242	0.59	2.42
0.075	0.630	0.58	8.40	0.176	0.59	2.35
0.050	0.419	0.58	8.38	0.118	0.59	2.36
0.030	0.252	0.58	8.40	0.072	0.60	2.40
0.013	0.110	0.59	8.42			
0.0050	0.042	0.59	8.40			
0.0025	0.021	0.59	8.40			
0.00100	0.0085	0.59	8.50			
0.00075	0.0066	0.59	8.80			

Coulometry

Coulometric reduction at controlled potential of chlorpheniramine maleate in 0.2 *M* sulphuric acid was performed to determine the number of electrons involved in the overall electron-transfer reaction. The experiments were performed in the absence of air in a small electrolysis cell with a mercury pool as the cathode. The potential of the working electrode was controlled at −0.7 V. 4.8 Coulombs were consumed in the reduction of $2.5 \cdot 10^{-5}$ *M* chlorpheniramine maleate which yields the value $n = 1.92$ and clearly demonstrate that 2 electrons are involved in the overall reaction.

Cyclic voltammetry

Voltammetric experiments were performed at a hanging mercury drop. Reproducible waves were obtained provided that the mercury drop was exchanged between each potential sweep. Voltammograms recorded from 0.2 *M* sulphuric acid exhibited one cathodic peak at potentials corresponding to the polarographic step (Fig. 2). No anodic peak resulting from reoxidation of the reduction product was observed at any scan rate, indicating an irreversible reduction. At high bulk concentration, the current function, $i_p/cv^{\frac{1}{2}}$, was fairly constant and independent of the scan rate, which implies that the electrode reaction is a simple electron-transfer and that it is neither preceded nor followed by a slow chemical reaction[9]. However, at low bulk concentration, the current function was not independent of the scan rate (Table IV), and the voltammograms showed an increase in symmetry with increased scan rate and decreased bulk concentration. This is probably the result of adsorption of the depolarizer on the electrode surface[10]. The adsorption of chlorpheniramine maleate and its reduction product was verified by drop-time measurements. As indicated in Fig. 3, the presence of the drug causes a large decrease in the drop time over a considerable potential range. This adsorption process is probably responsible for the *h*-dependence of the a.c. wave. No prewave

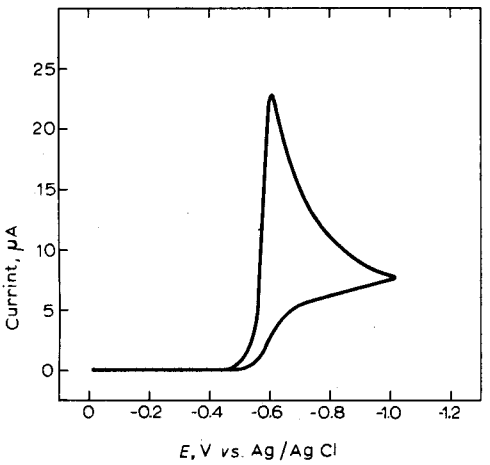

Fig. 2. Cyclic voltammogram of 1 m*M* chlorpheniramine maleate in 0.2 *M* sulphuric acid. Scan rate 0.1 V s^{-1}.

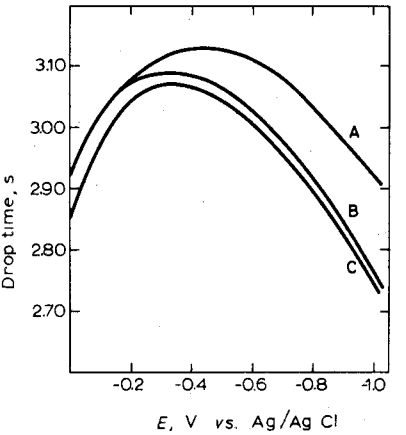

Fig. 3. Electrocapillary curves of 0.2 *M* sulphuric acid in the absence (curve A) and in the presence of 0.25 m*M* chlorpheniramine maleate (curve B) and in the presence of 0.25 m*M* of the reduction product of the drug (curve C).

TABLE IV

VOLTAMMETRIC DATA FOR THE REDUCTION OF CHLORPHENIRAMINE MALEATE IN 0.2 *M* SULPHURIC ACID

Scan rate ($V\ s^{-1}$)	*Conc. 1 mM*			*Conc. 0.01 mM*		
	i_p (μA)	$-E_p$ (*V*)	$i_p/cv^{\frac{1}{2}}$ ($\times 10^{-4}$)	i_p (μA)	$-E_p$ (*V*)	$i_p/cv^{\frac{1}{2}}$ ($\times 10^{-4}$)
0.5	50.70	0.65	7.17	0.532	0.64	7.52
0.2	32.40	0.61	7.25	0.337	0.64	7.54
0.1	22.70	0.60	7.18	0.248	0.63	7.84
0.05	16.10	0.60	7.20	0.183	0.63	8.18
0.02	10.22	0.60	7.23	0.123	0.62	8.70
0.01	7.22	0.60	7.22	0.094	0.62	9.40
0.005	5.15	0.60	7.28	0.071	0.62	10.04
0.002	3.58	0.60	8.01	0.053	0.62	11.85

or postwave was observed on the cyclic voltammograms at any sweep rate. Hence, the adsorption must be relatively weak. Furthermore, the adsorption must be very fast, because the d.c. current is controlled by the rate of diffusion of the depolarizer to the electrode.

Conclusion

It is evident from the experimental results that chlorpheniramine maleate is irreversibly reduced in a 2-electron step, and that two hydrogen ions are consumed in the reaction. The half-wave potential at various pH values, as well as the

decrease in diffusion current with increasing pH, are very similar to the data previously reported for reduction of maleic acid to succinic acid[11]. Hence, the reduction wave of chlorpheniramine maleate is probably due to the reaction:

$$R\cdot\begin{matrix}CHCOOH\\ \|\\ CHCOOH\end{matrix} + 2H^+ + 2e \rightarrow R\cdot\begin{matrix}CH_2COOH\\ |\\ CH_2COOH\end{matrix}$$

The poorly defined second wave at high negative potentials is probably due to reduction of the halogen:

$$R\cdot Cl + 2e \rightarrow R^- + Cl^-$$

ANALYTICAL APPLICATION

Experiments showed that the insoluble constituents in chlorpheniramine tablets do not cause any interference and need not be removed before the polarographic determination of the drug. Furthermore, the tablet disintegrates very rapidly in dilute sulphuric acid, and the drug is quantitatively released after shaking for 2–3 min. Based on the above experiments, the following procedure was outlined.

Recommended procedure

Transfer one tablet (equivalent to 2.5 mg of chlorpheniramine maleate) to a 100-ml volumetric flask and add 25 ml of 0.5 *M* sulphuric acid. Shake the flask for 2–3 min, and dilute to the mark with distilled water. Transfer a suitable amount of the suspension to a polarographic cell, deaerate with pure nitrogen, and record a d.c. polarogram in the potential range −0.4 to −0.8 V. Measure the diffusion current at −0.7 V and determine the amount of chlorpheniramine maleate from a standard curve prepared by the same procedure.

RESULTS

The results of a few determinations of chlorpheniramine maleate in tablets

TABLE V

DETERMINATION OF CHLORPHENIRAMINE MALEATE IN CHLORPHENIRAMINE MALEATE TABLETS

(Batch 29.5.70., declared amount 4 mg.)

Tablet no.	*Current (μA)*	*Found (mg)*	*Tablet no.*	*Current (μA)*	*Found (mg)*
1	0.86	4.00	9	0.85	3.95
2	0.87	4.05	10	0.86	4.00
3	0.85	3.95	11	0.86	4.00
4	0.88	4.10	12	0.87	4.05
5	0.87	4.05	13	0.86	4.00
6	0.86	4.00	14	0.85	3.95
7	0.84	3.90	15	0.87	4.05
8	0.85	3.95	16	0.85	3.95

are given in Table V. The proposed method is very sensitive and simple, and it has given satisfactory accuracy in the determination of chlorpheniramine maleate in tablets. Moreover, because removal of insoluble matter is omitted, the method is also much faster than spectrophotometric procedures.

The authors wish to thank cand. pharm. R. Gjermundsen and cand. pharm. V. Holm, Pharmaceutical Research Laboratory, A/S Apothekernes Laboratorium for Spesialpraeparater, for their kind interest in this work and for supply of the drugs used.

SUMMARY

The electroreduction of chlorpheniramine maleate has been investigated by a.c. and d.c. polarography, coulometry and cyclic voltammetry. Polarograms recorded from 0.2 *M* sulphuric acid exhibit a single well-defined 2-electron wave. The current is diffusion-controlled and proportional to the concentration in the entire range 0.3–400 μg ml^{-1}. A simple and rapid method for the determination of chlorpheniramine maleate in tablets is described.

REFERENCES

1 H. M. Jones and E. S. Brady, *J. Pharm. Sci.*, 38 (1949) 579.
2 J. Hudanick, *J. Pharm. Sci.*, 53 (1964) 332.
3 R. Hyatt, *J. Assoc. Offic. Agr. Chem.*, 48 (1965) 594.
4 D. J. Smith, *J. Assoc. Offic. Agr. Chem.*, 49 (1966) 536.
5 C. Hishta and R. G. Lauback, *J. Pharm. Sci.*, 58 (1969) 745.
6 E. G. Clair and L. G. Chatten, *J. Pharm. Sci.*, 50 (1961) 848.
7 K. Fossdal and E. Jacobsen, *Anal. Chim. Acta*, 56 (1971) 105.
8 E. Jacobsen, *Anal. Chim. Acta*, 35 (1966) 447.
9 R. S. Nicholson and I. Shain, *Anal. Chem.*, 36 (1964) 706.
10 R. H. Wopschall and I. Shain, *Anal. Chem.*, 39 (1967) 1514.
11 P. J. Elving and C. Teitelbaum, *J. Amer. Chem. Soc.*, 71 (1949) 3916.

Analytica Chimica Acta, 71 (1974) 165–174

CONTRIBUTION A L'ÉLECTROCHIMIE DES THIOLS ET DISULFURES PARTIE I. CYSTÉINE ET CYSTINE

C. A. MAIRESSE-DUCARMOIS, G. J. PATRIARCHE et J. L. VANDENBALCK

Institut de Pharmacie, Université Libre de Bruxelles, 50, Avenue F. D. Roosevelt, 1050 Bruxelles (Belgium)

(Reçu le 29 Novembre 1973)

Lors d'une étude consacrée à la coulométrie des thiols et disulfures, il nous a été permis d'envisager le dosage de ces divers constituants à l'aide de l'ion mercure(II) électrogénéré, soit en opérant directement, soit après réduction préalable sur cathode de mercure[1].

Le but du présent travail est d'étudier le comportement et le mécanisme électrochimique de ces composés et plus particulièrement de deux acides aminés: l'acide 1-amino-2-mercaptopropionique (cystéine) et l'acide 3,3′-dithiobis(2-amino-propanoïque) (cystine).

L'utilisation de techniques telles que la polarographie classique (d.c.), la polarographie à tension sinusoïdale surimposée (a.c.), la méthode impulsionnelle différentielle (p.p.) et les coulométries à intensité constante et à potentiel contrôlé nous ont permis de déterminer diverses caractéristiques électrochimiques et également de réaliser la séparation de ces deux acides aminés.

APPAREILLAGES ET RÉACTIFS

Les polarographies directes (d.c.), alternatives (a.c.) et impulsionnelles différentielles (p.p.) ont été effectuées à l'aide d'un polarographe Tacussel type PRG 34; la coulométrie à intensité constante se fait à l'aide de l'appareillage décrit précédemment[1,2] et les réductions électrolytiques sur cathode de mercure sont réalisées en maintenant le potentiel constant à l'aide d'un potentiostat Tacussel type PRT 20.

La cystéine et la cystine (Merck M2838 et M2837) ont été utilisés sans purification préalable. Les solutions sont préparées extemporanément avant chaque série d'opérations en dissolvant directement une certaine quantité de produit dans l'electrolyte de support préalablement désoxygéné par un courant d'azote prolongé. Les tampons utilisés sont de type Clark et Lubs jusqu'à pH 8 et Bates et Bower pour les pH supérieurs à 8[3].

RÉSULTATS ET DISCUSSION

Le comportement en milieu alcalin des thiols, disulfures et plus particulièrement de la cystéine et de la cystine ont fait l'objet de nombreuses investigations, le mécanisme de réduction de même que leur dégradation progressive en fonction

du temps n'étant pas encore totalement clarifiés[5–10]. C'est pourquoi nous avons effectué une étude approfondie de ces composés en fonction de la concentration, du pH, de l'électrolyte de support et en utilisant des techniques voltamétriques élaborées.

Le choix de l'électrolyte de support et de sa concentration a fait l'objet d'une étude particulière. C'est en milieu alcalin que la séparation est la plus nette et que les vagues sont les mieux développées et les plus reproductibles. Un mélange constitué de 0,05 *M* de borate de sodium et de 0,5 *M* de nitrate de potassium (pH 9,2) nous est apparu particulièrement adéquat pour réaliser cette séparation et le milieu alcalin nous a permis de mettre en évidence certains phénomènes que nous décrirons dans la suite du travail.

Étude de la cystéine

Étude en fonction de la concentration. La cystéine présente un tracé polarographique qui varie fortement avec la concentration en composé électroactif (Tableau I). C'est ainsi qu'à des concentrations comprises entre $1 \cdot 10^{-2}$ *M* et $5 \cdot 10^{-3}$ *M*, on observe deux vagues bien définies, respectivement vers $-0{,}450$ V et $-0{,}490$ V *vs.* ECS, tandis qu'à une concentration de $1 \cdot 10^{-3}$ *M*, il n'y a plus qu'une seule vague qui apparaît vers $-0{,}530$ V *vs.* ECS.

TABLEAU I

COMPORTEMENT POLAROGRAPHIQUE DE LA CYSTÉINE

Concentration (mol l^{-1})	*Nombre de vagues*	$E_{\frac{1}{2}}$ *(V vs. ECS)*	$E_{\frac{1}{2}} - E_{\frac{1}{2}}$ *(mV)*	E_{pic} *(V vs. ECS), a.c.*
$1 \cdot 10^{-2}$	2	$-0{,}457$		$-0{,}670$
		$-0{,}495$	15	
$5 \cdot 10^{-3}$	2	$-0{,}485$	10	$-0{,}585$
		$-0{,}587$	15	
$1 \cdot 10^{-3}$	1	$-0{,}525$	40	$-0{,}580$
$5 \cdot 10^{-4}$	1	$-0{,}530$	60	$-0{,}575$
$1 \cdot 10^{-4}$	1	$-0{,}540$	50	$-0{,}565$

L'origine de la première vague est due à un composé intermercuriel et l'onde qui en résulte a un potentiel de demi palier qui se situe vers des valeurs plus positives (Fig. 1). Kolthoff et coll.[6–8] interprètent ce phénomène par formation de constituants dans lesquels le mercure est lié fortement en tant que mercaptans sous forme de $Hg(RS)_2$, de $Hg_2(RS)_2$ ou de $Hg_3(RS)_3$. En présence d'ions chlorures, $Hg_2(RS)_2$ et $Hg_3(RS)_3$ ne se formeraient pas, étant supplantés par la formation du complexe tetrachlorure de mercure(II), $HgCl_4^{2-}$, qui est plus stable.

La réaction d'électrode pour ce composé intermercuriel peut s'écrire:

$$Hg \rightleftharpoons Hg^{2+} + 2e^-$$

$$Hg^{2+} + 2RSH \rightleftharpoons Hg(SR)_2 + 2H^+$$

ou encore

$$Hg + RSH \rightleftharpoons Hg(SR) + H^+ + e^-$$

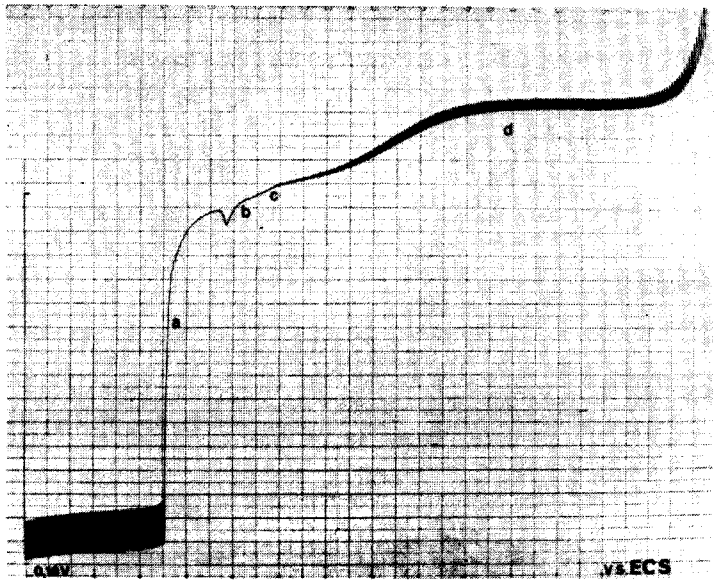

Fig. 1. Polarographie d.c. d'une solution de cystéine $1 \cdot 10^{-2}$ *M* oxydée à l'air durant 2 h. Sensibilité 12,5 μA, temps de chute de goutte 0,9 s (a) Composé intermercuriel, (b) vague anodique de la cystéine, (c) prévague de la cystine, (d) vague de réduction du disulfure.

tandis que la réaction d'oxydation de la cystéine peut s'écrire

$$2\,RSH \rightleftharpoons RSSR + 2\,H^+ + 2\,e^-$$

Par contre, à des concentrations inférieures à $2{,}5 \cdot 10^{-3}$ *M*, seule la vague anodique d'oxydation subsiste. Ce phénomène a pu être confirmé par des mesures a.c. et p.p.

Étude en fonction du pH. L'étude du comportement polarographique de la cystéine en fonction du pH a été réalisée pour des valeurs de pH comprises entre 1,8 et 11,6 et pour des concentrations de l'ordre de 10^{-3} *M* (Tableau II). Aux pH acides, seule la vague anodique apparaît et son potentiel de demi palier varie linéairement en fonction du pH. Par contre, au dessus de pH 6, une inflexion se marque au sommet de l'onde polarographique correspondant à la prévague d'adsorption du composé disulfure. La réversibilité de la réaction d'électrode évolue, elle aussi, fortement en fonction du pH si l'on en juge par les valeurs de $E_{\frac{3}{4}} - E_{\frac{1}{4}}$; celles-ci passent de 75 mV en milieu acide à 15 mV vers pH 8,9.

Les tracés polarographiques obtenus en utilisant la méthode a.c. reflètent les phénomènes observés en d.c. En effet, on observe un pic unique jusqu'à une valeur de pH égale à 5, mais celui-ci se déforme fortement dès qu'apparaît la prévague à pH 6 et se dédouble vers pH 9 (Fig. 2).

La Figure 3 représentant la courbe des potentiels de demi palier en fonction du pH montre une linéarité parfaite entre pH 1,8 et pH 7, mais s'incurve progressivement aux pH alcalins.

En milieu basique, la stabilité des solutions de cystéine laissées en contact avec l'oxygène de l'air s'altère fortement, comme le montrent les résultats du

TABLEAU II

COMPORTEMENT POLAROGRAPHIQUE DE LA CYSTÉINE EN FONCTION DU pH

(Solution 10^{-3} *M* en cystéine)

pH	$E_{\frac{1}{2}}$ *(V vs. ECS)*	$E_{\frac{3}{4}} - E_{\frac{1}{4}}$ *(mV)*	E_{pic} *(V), a.c.*
1,82	−0,105	75	−0,170
2,40	−0,135	55	−0,175
3,54	−0,235	20	−0,260
5,10	−0,350	15	−0,370
6,09	−0,415	15	−0,470
7,12	−0,470	25	−0,530
7,92	−0,515	20	−0,565
8,92	−0,550	15	−0,605
9,95	−0,560	50	−0,620
10,68	−0,590	50	−0,635
11,60	−0,595	45	−0,645

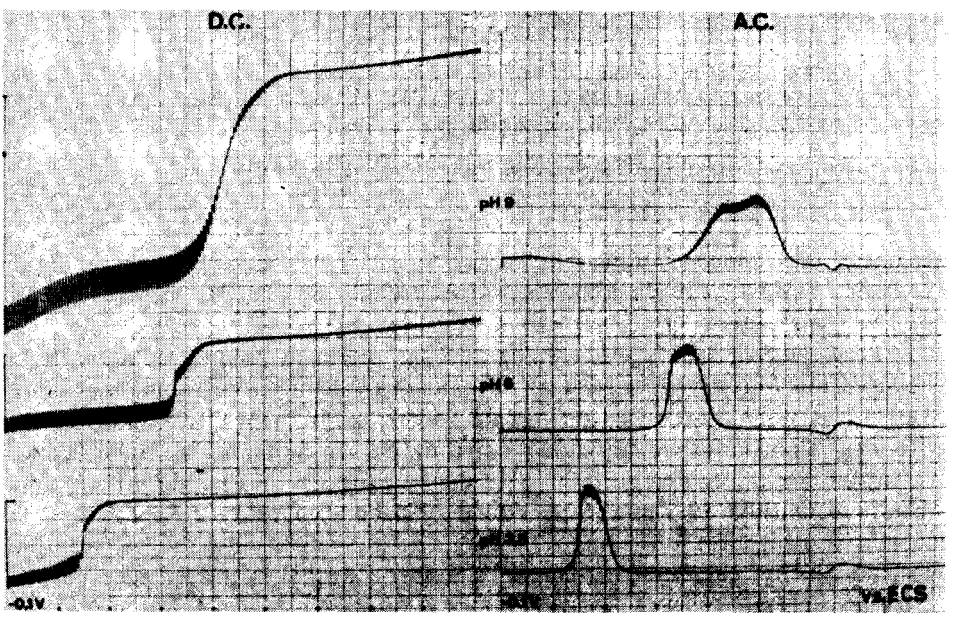

Fig. 2. Polarogrammes d.c. et a.c. d'une solution $1 \cdot 10^{-3}$ *M* en cystéine (pH 3,5, 6 et 9). (1) D.c. sensibilité 2,5 μA, (2) a.c. sensibilité 12,5 μA. Temps de chute de goutte 0,9 s.

Tableau III. Ce phénomène est en parfaite concordance avec ce que nous avions déjà décrit antérieurement[1].

Stabilité de la cystéine en solution aqueuse. Il est indéniable que lorsqu'on dissout un thiol tel que la cystéine en solution aqueuse une partie de celle-ci se transforme en disulfure et l'on assiste à une auto-oxydation rapide. Une prévague d'adsorption, dont le potentiel de demi palier est voisin de −0.60 V *vs.* ECS se dessine, de même qu'apparaît la vague de réduction du disulfure

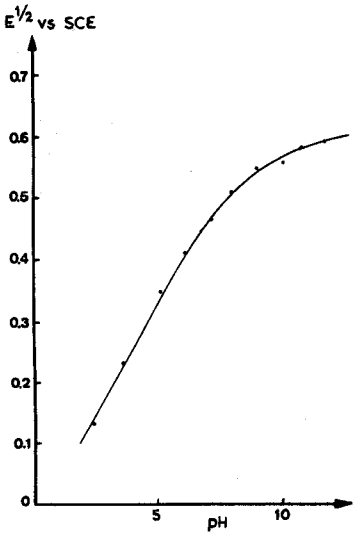

Fig. 3. Courbe $E_{\frac{1}{2}}$ en fonction du pH ($1 \cdot 10^{-3}$ *M* cystéine).

TABLEAU III

DIMINUTION DE LA TENEUR EN CYSTÉINE AU COURS DU TEMPS

(Cystéine: 40,32 mg %; tampon pH 9,2)

Temps (h)	*i_d de la cystéine (μA)*	*i_d de la cystine (μA)*	*Cystéine (%)*
0	4,68	0,36	—
1.5	4,16	0,70	−11,1
4	3,66	0,96	−21,8
6	3,04	1,84	−35,0
24	0,36	4,12	−92,3

progressivement formé ($E_{\frac{1}{2}} = -1{,}1$ V *vs.* ECS) (Fig. 4). Nous avons pu mettre en évidence la nature du courant de cette prévague par des mesures de courbes électrocapillaires (Fig. 5) et par d'autres techniques que nous décrivons lors de l'étude de la cystine.

Il est intéressant de noter que cette prévague d'adsorption du disulfure est toujours présente quelle que soit la concentration du thiol à réduire. Ceci est en parfaite concordance de vue avec la théorie émise au sujet des vagues d'adsorption de ce type[4].

Étude de la cystine

Kůta *et al.*[11] et d'autres auteurs[12–14] travaillant dans un tampon ammoniaque–chlorure d'ammonium de pH égal à 10 ont prouvé que l'allure des courbes à intensité-potentiel de la cystine varie de manière importante en fonction du vieillissement des solutions. Ces auteurs ont observé deux vagues sur des solutions

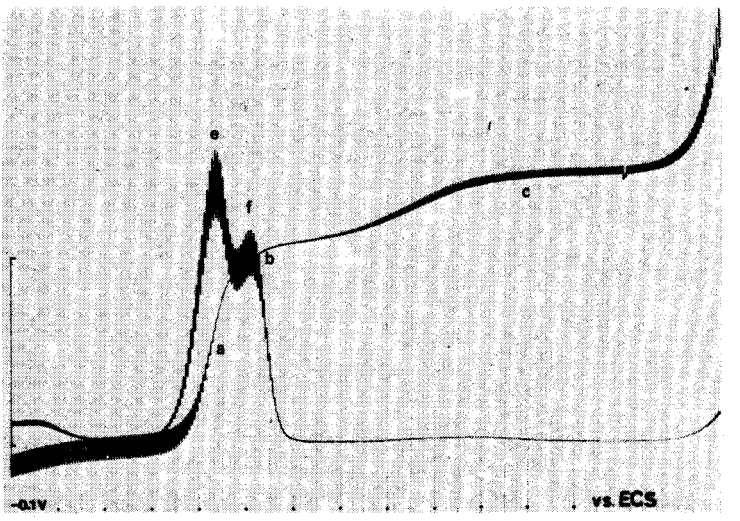

Fig. 4. Polarographies directe et alternative d'une solution de cystéine $2{,}5 \cdot 10^{-4}$ *M* oxydée à l'air durant 2 h. Sensibilité 500 nA; temps de chute de goutte 0,9 s. (a) Vague anodique de la cystéine, (b) prévague de la cystine, (c) vague cathodique de la cystine, (e) pic correspondant à la cystéine, (f) pic correspondant à la prévague d'adsorption de la cystine.

fraîches, trois, voire quatre vagues de réduction avec les mêmes solutions conservées durant plusieurs mois.

La cystine réduite à l'électrode à goutte de mercure présente en polarographie d.c. et surtout en a.c. un comportement beaucoup plus irréversible que celui de la cystéine (valeurs de $E_{\frac{1}{4}}-E_{\frac{1}{4}}$: mV; pente de la droite log $i/(i_d-i)$ par rapport au potentiel: 140 mV).

Lors de l'étude réalisée à différents pH (entre 2,5 et 11,6), nous avons pu mettre en évidence l'existence de cette vague de réduction très irréversible et d'une prévague d'adsorption se manifestant exclusivement entre pH 6,2 et 9,5 (Tableau IV).

TABLEAU IV

ÉTUDE DES $E_{\frac{1}{4}}$ ET DE LA RÉVERSIBILITÉ EN FONCTION DU pH

(Solution 10^{-3} *M* en cystine)

pH	$E_{\frac{1}{4}}$ *prévague V vs. ECS*	$E_{\frac{1}{4}}-E_{\frac{1}{4}}$ *(mV)*	$E_{\frac{1}{4}}$ *de la vague V vs. ECS*	$E_{\frac{1}{4}}-E_{\frac{1}{4}}$ *(mV)*
2,50	—	—	−0,690	125
3,66	—	—	−0,715	115
5,14	—	—	−0,820	165
6,22	−0,440	45	−0,860	200
7,17	−0,495	45	−0,850	165
8,07	−0,545	50	−0,905	180
8,98	−0,550	50	−1,100	140
10,07	—	—	−1,235	185
11,01	—	—	−1,480	175
11,64	—	—	−1,525	140

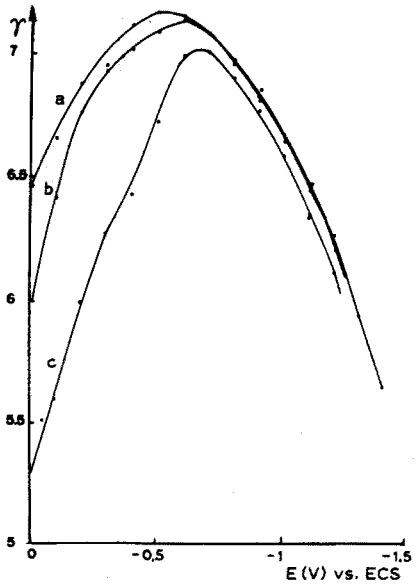

Fig. 5. Courbes électrocapillaires. (a) Electrolyte de support seul (0,05 *M* de borate de sodium et 0,5 *M* KNO_3), (b) électrolyte de support additionné de 10^{-3} *M* de cystine, (c) électrolyte de support additionné de 10^{-3} *M* de cystéine.

Cette prévague est particulièrement bien développée à pH 8: son potentiel de demi palier est alors de $-0{,}54$ V *vs.* ECS et la valeur de $E_{\frac{3}{4}} - E_{\frac{1}{4}}$ est égale à 45 mV. La méthode à tension sinusoïdale surimposée montre également un pic très aigu pour ce qui concerne la prévague, tandis que la deuxième vague, qui est celle de réduction, se présente sous forme d'un arrondi peu développé parfaitement symétrique; ce comportement a.c. est normal étant donné l'irréversibilité manifeste de la réduction du groupement disulfure.

L'importante variation de l'intensité du premier pic en fonction de la valeur de la fréquence (Fig. 6) tend à prouver que l'origine de ce courant est bien due à des phénomènes d'adsorption à l'électrode de mercure, comme nous l'avons déjà montré lors de l'auto-oxydation de la cystéine. Nous constatons en effet que si nous triplons la valeur de la fréquence surimposée, les intensités de pic passent de 180 à 384 nA. Par contre, la hauteur de la vague due à la réduction du disulfure reste quasi stationnaire en fonction de cette même variation de fréquence.

Étude de la séparation du mélange des deux constituants

Si nous considérons le mélange de ces deux acides aminés à pH 9,2, nous pouvons voir immédiatement que la séparation cystéine–cystine est réalisable (Fig. 7 (1)). Il est même possible de les doser séparément par les techniques polarographiques étant donné que les vagues étudiées répondent parfaitement aux critères de diffusion et que les courants mesurés varient linéairement avec la concentration. D'autre part, comme nous l'avons déjà montré[1], si nous soumettons le mélange à une électrolyse à potentiel contrôlé à une tension située dans le palier de diffusion du disulfure ($E = -1{,}45$ V *vs.* ECS) il est possible de transformer com-

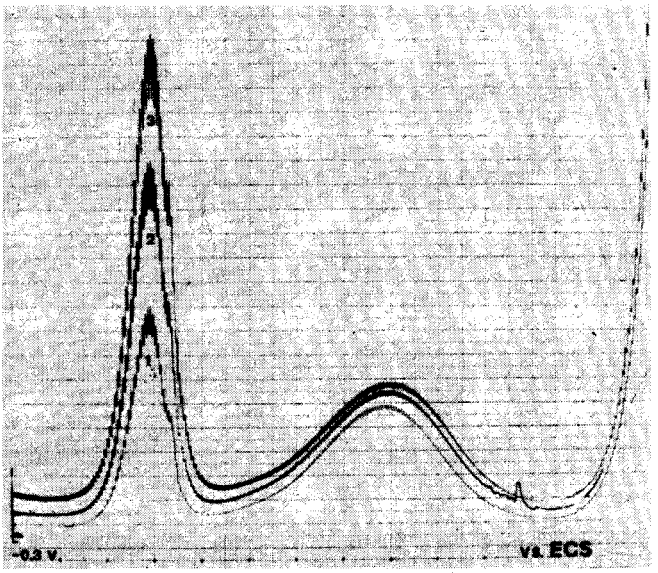

Fig. 6. Influence de la fréquence surimposée sur la courbe a.c. d'une solution 10^{-3} *M* de cystine (pH 9,2). Sensibilité 500 nA; amplitude surimposée 10 mV; Temps de chute de goutte 0,9 s. Fréquences: (1) 90 Hz, (2) 180 Hz, (3) 270 Hz.

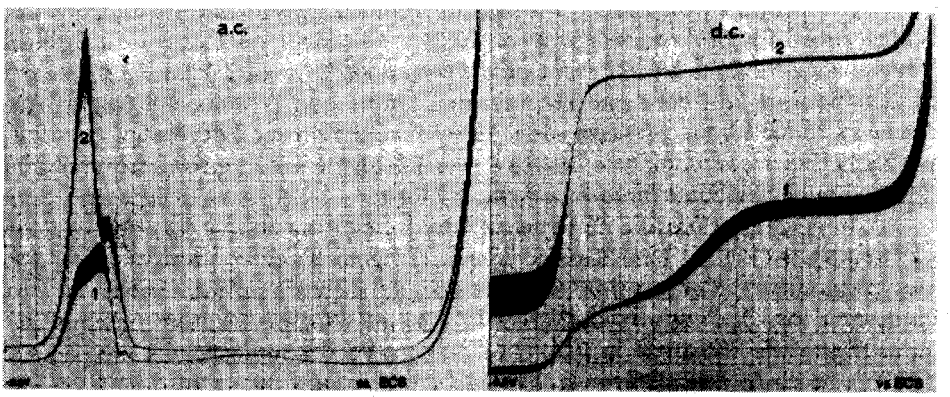

Fig. 7. Polarogrammes a.c. et d.c. d'une solution $1 \cdot 10^{-3}$ *M* de cystine et $1 \cdot 10^{-3}$ *M* de cystéine (pH: 9,2). (1) Avant réduction potentiostatique, (2) après réduction potentiostatique à $-1{,}45$ V *vs.* ECS. Sensibilité a.c. 5 μA, sensibilité d.c. 2,5 μA.

plètement tout le disulfure en thiols correspondants et de doser l'ensemble des thiols formés, soit polarographiquement, soit coulométriquement par le mercure(II) électrogénéré (Fig. 7(2)). La réduction s'effectue alors sur nappe de mercure et nécessite plus ou moins 6 h. La durée anormalement longue de l'opération s'expliquerait par des phénomènes d'adsorption au niveau de la nappe, par suite de la formation de composés intermercuriels. Lors d'une telle réduction, le courant mesuré au départ de l'opération est de l'ordre de 10 mA et en fin d'opération

ce courant (background current) atteint des valeurs approximativement égales à 0,2 mA, pour des concentrations de cystine à réduire de l'ordre de $1{,}75 \cdot 10^{-3}$ *M*. Le graphique de la Fig. 7 montre le tracé polarographique d.c. et a.c. du mélange de ces deux constituants avant et après 6 h de réduction potentiostatique.

Polarographie différentielle à impulsions du mélange cystéine–cystine

Cette méthode récente, particulièrement sensible et à grand pouvoir de résolution, a été utilisée pour réaliser la séparation de ces deux acides aminés soufrés et pour en déterminer les limites de détection.

La Figure 8, correspondant au tracé obtenu en réalisant la polarographie impulsionnelle du mélange de $0{,}5 \cdot 10^{-3}$ *M* de cystéine et de $0{,}5 \cdot 10^{-3}$ *M* de cystine à un pH de 9,2, montre trois pics bien développés respectivement à $-0{,}535$ V, $-0{,}625$ V et $-0{,}91$ V *vs.* ECS. Le premier de ceux-ci correspond à la cystéine, tandis que les deux autres concernent la réduction de la cystine.

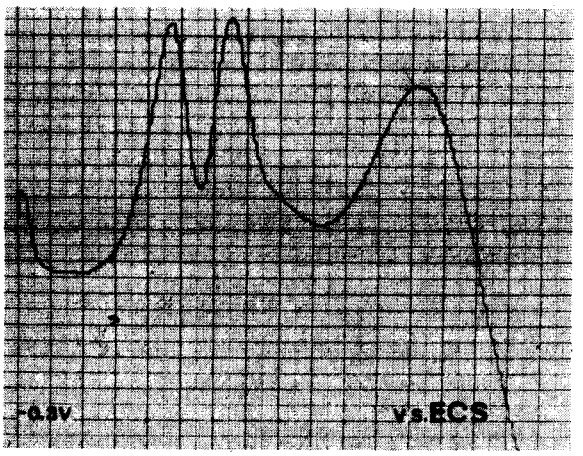

Fig. 8. Polarographie impulsionnelle différentielle d'un mélange de $5 \cdot 10^{-4}$ *M* de cystéine et $5 \cdot 10^{-4}$ *M* de cystine (pH: 9,2). Temps de chute de goutte 3 s; retard 2 s 60; durée de l'impulsion 40 ms; sensibilité 25 nA; amplitude surimposée 1 mV; vitesse de déroulement 2 mV s^{-1}.

Si l'on compare ce tracé à celui de la Fig. 7 qui reprend l'allure de la courbe obtenue en opérant sur la même solution par la technique alternative, on peut constater que le pouvoir séparateur de la polarographie impulsionnelle est nettement supérieur à celui des autres méthodes. Il en va de même du pouvoir de détection de cette technique. Alors qu'en polarographie classique nous sommes liés au courant de charge de la double couche qui nous empêche de détecter correctement au-delà de $5 \cdot 10^{-4}$ *M*, la polarographie impulsionnelle permet de mesurer des concentrations atteignant $1 \cdot 10^{-6}$ *M* avec une reproductibilité très bonne. Exprimées en mg, ces concentrations correspondent à 0,12 mg de cystéine et à 0,24 mg de cystine par litre.

Nos remerciements vont au Fonds National de la Recherche Scientifique pour l'aide apportée à l'un d'entre nous (G.J.P.).

RÉSUMÉ

L'étude des caractéristiques électrochimiques de la cystéine et de la cystine est réalisée par les polarographies conventionnelle, alternative et impulsionnelle.

Les modifications observées sur les tracés polarographiques en fonction de la concentration et du pH nous ont permis de mettre en évidence une, deux ou trois vagues dont le type de courant a été déterminé. La séparation de ces deux acides aminés est réalisée en tampon borate de pH 9,2. La polarographie impulsionnelle différentielle permet de séparer et de doser 0,12 mg de cystéine et 0,24 mg de cystine par litre.

SUMMARY

A study of the electrochemical characteristics of cysteine and cystine was carried out by d.c., a.c. and differential pulse polarography. Up to three waves were observed depending on the concentration and pH. The waves of the two amino acids could be separated in a borate buffer of pH 9.2. Differential pulse polarography made it possible to determine as little 0.12 mg of cysteine and 0.24 mg of cystine per litre.

BIBLIOGRAPHIE

1 C. A. Mairesse-Ducarmois, J. L. Vandenbalck et G. J. Patriarche, *J. Pharm. Belg.*, 28 (1973) 300.
2 G. J. Patriarche, *Contribution à l'Analyse Coulométrique*, Ed. Arscia-Maloine, Paris, 1964, p. 31.
3 L. Meites, *Handbook of Analytical Chemistry*, McGraw Hill, 1963, Sects. 11–6, 11–7.
4 J. Heyrovský et J. Kůta, *Principles of Polarography*, Academic Press, New York, 1966, p. 288.
5 D. B. Coult, *Analyst (London)*, 83 (1958) 422.
6 W. Stricks et I. M. Kolthoff, *J. Amer. Chem. Soc.*, 75 (1953) 5673.
7 I. M. Kolthoff, W. Stricks et R. C. Kapoor, *J. Amer. Chem. Soc.*, 77 (1955) 4733.
8 I. M. Kolthoff et C. Barnum, *J. Amer. Chem. Soc.*, 62 (1940) 3061.
9 Z. Kováčová et I. Žežula, *Collect. Czech. Chem. Commun.*, 37 (1972) 935.
10 J. H. Karchmer, *The Analytical Chemistry of Sulphur and its Compounds, Vols. 1 et 2*, Wiley-Interscience, New York, 1973.
11 P. Mader, J. Volke et J. Kůta, *Collect. Czech. Chem. Commun.*, 35 (1970) 552.
12 J. M. Swan, *Nature (London)*, 179 (1957) 965.
13 C. Demarco, M. Coletta et D. Cavallini, *Arch. Biochem. Biophys.*, 100 (1963) 151.
14 J. R. Dann, G. L. Oliver et J. W. Gates, *J. Amer. Chem. Soc.*, 79 (1957) 1944.

Analytica Chimica Acta, 71 (1974) 175–184

ELECTROREDUCTION AND PULSE-POLAROGRAPHIC DETERMINATION OF NICOTINAMIDE IN MULTIVITAMIN TABLETS

EINAR JACOBSEN and KNUD B. THORGERSEN
Department of Pharmacy, University of Oslo, Blindern, Oslo 3 (Norway)
(Received 12th January 1974)

The most widely accepted method for the determination of nicotinamide is based on the Kønig reaction[1]. This method utilizes the reaction of pyridine derivatives with a cyanogen salt and an aromatic amine, and the product is determined by spectrophotometry. Several variations of this method, as well as u.v. spectrophotometry have been recommended for the determination of nicotinamide[2,3]. However, these methods are very time-consuming, and separation from complex preparations is usually required before the determination.

Polarograms of nicotinamide recorded from alkaline media exhibit a single well-defined d.c. polarographic wave[4–8]. Because the reduction occurs at high negative potentials ($E_{\frac{1}{2}} = -1.75$ V *vs.* SCE in 0.1 *M* sodium hydroxide), the nicotinamide must be separated from other vitamins which are reduced at lower potentials[9]. Hence, the d.c. polarographic method is also very time-consuming and not suitable for routine analysis.

The object of the present work was to study the electroreduction of nicotinamide in detail and to investigate the application of a.c. and pulse polarography to rapid analysis of nicotinamide in multivitamin tablets.

EXPERIMENTAL

A.c. and d.c. polarograms were recorded with a Metrohm E 261 Polarecord connected to a Metrohm E 393 a.c. modulator. An Ag/AgCl/saturated KCl electrode served as reference electrode and a tungsten electrode was employed as auxiliary electrode. All a.c. polarograms were obtained with an amplitude of 10 mV r.m.s. The capillary characteristics of the dropping mercury electrode, measured in 2 *M* sulphuric acid at an applied potential of −0.90 V and a mercury height of 58.3 cm (corrected for the back pressure), were $m = 2.313$ mg s^{-1} and $t = 3.790$ s. Pulse polarograms were recorded with a PAR polarographic analyzer model 174, in the differential pulse mode.

Cyclic voltammetry, chronopotentiometry and coulometry were performed with a versatile solid-state instrument constructed in this laboratory to the design of Goolsby and Sawyer[10]. A Moseley 7030 AM X–Y recorder and a Honeywell Electronic 194 strip-chart recorder were used in conjunction with the instrument. A three-electrode assembly was used for all measurements. A Metrohm E 410 hanging mercury drop was used as working electrode for the cyclic voltammetric and chronopotentiometric experiments, and a mercury pool was employed for the

controlled potential coulometric experiments. The reference electrode and the auxiliary electrode (platinum coil) were isolated in glass tubes with fine-porosity fritted glass discs. The shield tubes were filled with the supporting electrolyte used in the sample solution.

All experiments were performed at 25 ± 0.1°C. Dissolved air was removed from the solutions by bubbling oxygen-free nitrogen through the cell for 10 min and passing it over the solution during the electrolysis.

Nicotinamide (pharmaceutical grade) and the multivitamin tablets "Vitaplex" and "B-Viplex" were obtained from Apothekernes Laboratorium for Special-praeparater, Oslo, Norway. Stock solutions of nicotinamide were prepared by dissolving the appropriate amount of the commercial product in 2 *M* sulphuric acid, 0.1 *M* sodium hydroxide or 0.1 *M* tetraethylammonium hydroxide. Only freshly prepared stock solutions were used throughout this work. A stock solution of the surfactant "Benax" (sodium dodecyldiphenyletherdisulphonate; Dow Chemical Co., Midland, Mich.) was prepared by simple dissolution in distilled water. All other chemicals were of reagent grade and were used without further purification.

ELECTROREDUCTION OF NICOTINAMIDE

Preliminary experiments showed that d.c. polarograms of nicotinamide recorded from acidic media exhibit a large maximum. The maximum was easily depressed by small amounts of the anionic surfactant Benax. Moreover, the height of the a.c. polarographic wave increased in the presence of this surfactant, indicating

TABLE I

EFFECT OF pH ON POLAROGRAMS OF 0.2 m*M* NICOTINAMIDE

(0.0025% Benax was used as maximum suppressor in acidic media.)

Buffer	*pH*	$-E_{\frac{1}{2}}$ *(mV)*	$-(E_{\frac{1}{2}}-E_{\frac{1}{4}})$ *(mV)*	i_d *(μA)*	$-E_p$ *(mV)*	i_p *(μA r.m.s.)*	$\Delta E_{p/2}$ *(mV)*
H_2SO_4	4 *M*	868	42	1.33	916	0.32	100
	2 *M*	882	40	1.36	926	0.43	92
HCl	0	889	46	1.50	940	0.46	96
Citrate buffer	0.42	930	48	1.56	986	0.47	96
	1.17	1010	104	3.26	1062	0.45	104
	1.51	1058	98	3.30	1114	0.44	102
	2.52	1160	112	3.50	1178	0.32	108
	3.96	poorly defined wave					
	4.80	poorly defined wave					
	7.60	1492	76	1.60	1531	0.50	107
NH_3/NH_4Cl	8.54	1530	50	1.15	1574	0.31	104
	9.15	1578	50	1.21	1620	0.33	102
NH_3	11.0	1662	44	1.37	1702	0.36	84
NaOH	13.0	1730	38	1.32	1765	0.36	88

a more reversible electrode reaction. The peak potential and the peak current were not affected even when the amount of Benax was increased to 0.003%. Consequently, 0.0025% Benax was added to all acidic supporting electrolytes. In neutral and alkaline media, no maximum was observed and no surfactant was added to these electrolytes.

The effect of pH on the current–voltage curve was investigated by recording polarograms of 0.2 m*M* nicotinamide in various supporting electrolytes. As indicated in Table I, the most reversible waves were obtained in strong acidic and in alkaline media. Only poorly developed waves were obtained from electrolytes of intermediate pH values. Moreover, in this pH region, the limiting current increased considerably and was not diffusion-controlled. The increase in limiting current in slightly acidic media is probably due to catalytic evolution of hydrogen as previously suggested by Knobloch[5]. Hence, only 2 *M* sulphuric acid and 0.1 *M* sodium hydroxide appear to be useful supporting electrolytes for the determination of nicotinamide.

A.c. and d.c. polarograms of nicotinamide recorded from 2 *M* sulphuric acid are given in Fig. 1. The effect of drop time was investigated by recording polarograms of 1 m*M* nicotinamide in 2 *M* sulphuric acid at various heights of the mercury column. The value $ih^{-\frac{1}{2}}$, where h is height of the column after correction for the "back-pressure", was constant, indicating that the d.c. current was diffusion-controlled. However, the height of the a.c. wave increased linearly with increasing height of the column, which implies that the concentration of the

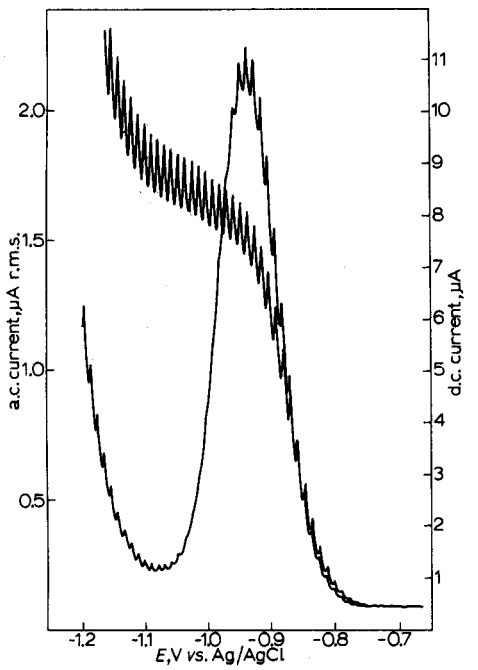

Fig. 1. A.c. and d.c. polarograms of 1 m*M* nicotinamide in 2 *M* sulphuric acid.

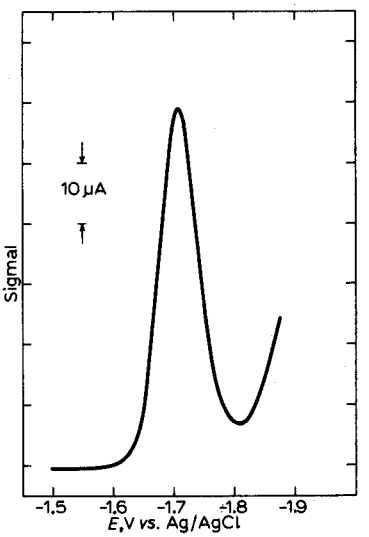

Fig. 2. Differential pulse polarogram of nicotinamide (0.083 mg ml^{-1}) in 0.1 *M* sodium hydroxide. Drop time 0.5 s, scan rate 2 mV s^{-1} and pulse amplitude 50 mV.

depolarizer responsible for the a.c. current is time-dependent, and that the a.c. current is partly controlled by the rate of a slow reaction[11,12]. The temperature coefficient (determined in the range 25–45°) of the d.c. current, 1.54% per degree, and that of the a.c. peak current, 1.05% per degree, indicate that the current is controlled essentially by diffusion.

Polarograms recorded from 2 *M* sulphuric acid with various amounts of nicotinamide present, showed that the d.c. current as well as the a.c. peak current increased linearly with concentration. 0.025% Benax was used as maximum supressor.

The a.c. polarographic peak height was more reproducible and gave more accurate results than the d.c. current. The results (Table II) indicate that nicotinamide can be determined in the entire concentration range $3 \cdot 10^{-5}$–10^{-3} *M* (3–120 μg ml^{-1}) by a.c. polarography. The diffusion current constant, $I = i_d/cm^{\frac{2}{3}}t^{\frac{1}{6}}$, calculated from the data in Table II, is $I = 3.13$. The same diffusion current constant was obtained when 0.1 *M* sodium hydroxide was used as supporting electrolyte.

TABLE II

POLAROGRAPHIC DATA FOR THE REDUCTION OF VARIOUS AMOUNTS OF NICOTINAMIDE IN 2 *M* SULPHURIC ACID

Conc. c (mM)	i_d *(μA)*	$-E_{\frac{1}{2}}$ *(mV)*	i_d/c *(μA mM^{-1})*	i_p *(μA r.m.s.)*	$-E_p$ *(mV)*	i_p/c *(μA mM^{-1})*
1.00	6.80	900	6.80	2.08	950	2.08
0.80	5.50	898	6.87	1.67	944	2.09
0.65	4.45	896	6.84	1.39	944	2.14
0.50	3.41	886	6.82	1.07	942	2.14
0.35	2.39	886	6.83	0.745	940	2.13
0.20	1.36	882	6.80	0.430	926	2.15
0.10	0.630	876	6.30	0.215	924	2.15
0.08	0.520	874	6.50	0.172	926	2.15
0.06	0.380	874	6.33	0.129	934	2.15
0.05	0.315	870	6.30	0.107	934	2.14
0.03	—	—	—	0.065	940	2.16

The plateau on the d.c. wave recorded from 0.1 *M* sodium hydroxide is very small, and the reduction wave of sodium interferes at low concentrations of nicotinamide. Hence, tetraethylammonium hydroxide is a more useful supporting electrolyte. However, differential pulse polarograms (Fig. 2) recorded from 0.1 *M* sodium hydroxide are well defined even at low concentrations of nicotinamide. As indicated in Table III, the peak current increases almost linearly with the concentration in the entire range $5 \cdot 10^{-6}$–10^{-3} *M* (0.6–120 μg ml^{-1}) nicotinamide.

Strong acidic solutions of nicotinamide are not stable. The diffusion current of 10^{-3} *M* nicotinamide in 2 *M* sulphuric acid decreased gradually with time and after ten days the current was only 50% of its original value. At the same time a new wave appeared at more negative potentials (Fig. 3), and the height of this wave increased with time at the expense of the nicotinamide wave. The peak potential of the new wave coincided with that of nicotinic acid, which indicates that the decrease in current is the result of hydrolysis of nicotinamide to nicotinic acid.

TABLE III

DIFFERENTIAL PULSE POLAROGRAPHIC DATA FOR THE REDUCTION OF VARIOUS AMOUNTS OF NICOTINAMIDE IN 0.1 *M* SODIUM HYDROXIDE

(Drop time 0.5 s, pulse amplitude 50 mV and scan rate 2 mV s^{-1}.)

Conc., c *(mM)*	$\Delta i/E_p$ *(μA)*	$(\Delta i/\Delta E_p)/c$ *(μA mM^{-1})*
1.00	89.50	89.50
0.80	71.50	89.38
0.65	58.25	89.61
0.50	44.50	89.00
0.25	22.25	89.00
0.10	8.85	88.50
0.08	7.00	87.50
0.05	4.35	87.00
0.01	0.870	87.00
0.005	0.435	87.00

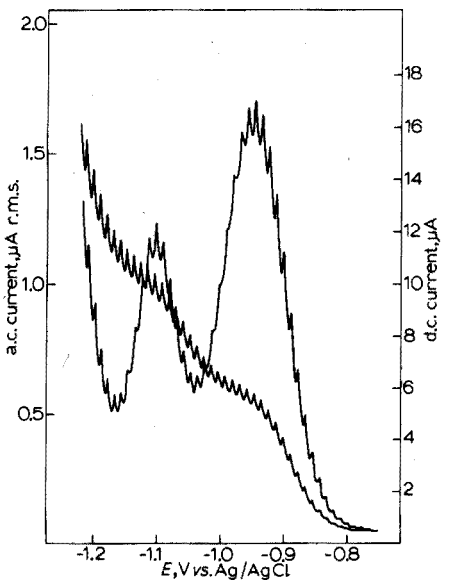

Fig. 3. A.c. and d.c. polarograms of 1 m*M* nicotinamide in 2 *M* sulphuric acid recorded one week after mixing the solution.

Consequently, only freshly prepared standard solutions of nicotinamide in 2 *M* sulphuric acid should be used.

The above experiments show that nicotinamide and nicotinic acid can be determined in the presence of each other by a.c. polarography. Hence, a few experiments were performed in order to study the polarographic behaviour of nicotinic acid. The limiting current of nicotinic acid is not diffusion-controlled. The height of the d.c. wave increased with increasing height of the mercury column but much less rapidly than the square root relationship would predict. This is a

characteristic feature of kinetic waves. Furthermore, the limiting current of nicotinic acid decreased with increasing pH of the electrolyte, and above pH 10 no reduction wave was observed. These experiments indicate that the anion of nicotinic acid is not reduced at the dropping mercury electrode and that the kinetic behaviour of the reduction wave of nicotinic acid is due to the reaction:

$$R{\cdot}COO^- + H^+ \xrightarrow{\text{slow}} RCOOH$$

Coulometry

Coulometric reductions at controlled potential of nicotinamide in 0.1 *M* tetraethylammonium hydroxide were performed to determine the number of electrons involved in the overall electron-transfer reaction. The experiments were carried out in the absence of air with a small electrolysis cell and a mercury pool as working electrode. The potential of the mercury pool was controlled at a potential slightly more negative than the half-wave potential. 4.56 Coulombs were consumed in the reduction of $2.5 \cdot 10^{-5}$ mole of nicotinamide which yields the value $n = 1.89$, and clearly demonstrates that 2 electrons are involved in the overall reaction. Coulometric experiments in 2 *M* sulphuric acid did not give reproducible results, because reduction of hydrogen ions interfered at low concentrations of nicotinamide. However, the same diffusion current and the same height of the a.c. wave were observed for nicotinamide recorded from 2 *M* sulphuric acid and from 0.1 *M* tetraethylammonium hydroxide, which suggests that 2 electrons are also involved in the electrode reaction in acidic media.

Cyclic voltammetry

Voltammetric experiments were performed at a hanging mercury drop electrode. Voltammograms recorded from 2 *M* sulphuric acid and from 0.1 *M* tetraethylammonium hydroxide exhibited one cathodic peak at potentials corresponding to the polarographic step (Fig. 4). No anodic peak resulting from reoxidation of the reduction product was observed at any scan rate.indicating an irreversible reduction. Some voltammetric data are given in Table IV.

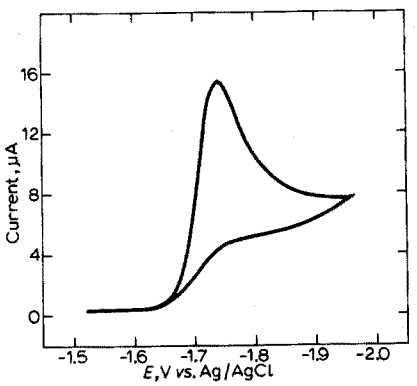

Fig. 4. Cyclic voltammogram of 1 m*M* nicotinamide in 0.1 *M* tetraethylammonium hydroxide. Scan rate 0.05 V s^{-1}.

TABLE IV

VOLTAMMETRIC DATA FOR THE REDUCTION OF NICOTINAMIDE IN 0.1 *M* TETRAETHYLAMMONIUM HYDROXIDE

Conc. *(mM)*	*Scan rate* *($V\ s^{-1}$)*	i_p *(μA)*	$-E_p$ *(mV)*	$i_p/cv^{\frac{1}{2}}$ *($\mu A\ mM^{-1}\ V^{-\frac{1}{2}}\ s^{\frac{1}{2}}$)*	αn_a
1.0	0.2	22.0	1775	49.17	—
	0.1	19.0	1755	60.08	—
	0.05	15.0	1740	67.03	—
	0.02	9.9	1725	70.00	0.77
	0.01	7.3	1719	73.00	1.46
	0.005	5.3	1713	74.92	1.46
0.1	0.2	2.18	1773	48.75	—
	0.1	1.92	1750	60.72	—
	0.05	1.70	1735	76.00	—
	0.02	1.15	1725	81.32	1.17
	0.01	0.82	1718	82.00	1.46
	0.005	0.58	1712	82.00	1.46

Values of αn_a may be calculated from cyclic voltammetric data relating peak potential and the logarithm of the scan rate in the relationship:

$$(E_p)_2 - (E_p)_1 = (0.059/2\alpha n_a) \log (v_1/v_2)$$

where $(E_p)_1$ and $(E_p)_2$ are the two peak potentials for a given reaction, v_1 and v_2 the appropriate scan rates, and n_a the number of electrons in the rate-determining step. The value of αn_a calculated at scan rates less than 0.01 V s^{-1} (a time scale comparable to the polarographic data) was $\alpha n_a = 1.46$, which is close to the value calculated from the d.c. polarographic wave ($\alpha n_a = 1.37$) by means of the equation: $E_{\frac{1}{4}} - E_{\frac{3}{4}} = -0.0517/\alpha n_a$. Exactly the same results were obtained when 2 *M* sulphuric acid was used as supporting electrolyte. However, the value αn_a calculated from faster sweep rates decreased with increasing sweep rate, which indicates that a slow one-electron transfer is involved in the overall reaction. This result was confirmed by chronopotentiometric experiments. The number of electrons involved in the fast electron-transfer step was calculated from the width of the a.c. wave at half height[13] by means of the equation $\Delta E_{p/2} = 90.5/n$. The values $n = 0.98$ and $n = 1.08$ for a.c. waves recorded from 2 *M* sulphuric acid and from 0.1 *M* tetraethylammonium hydroxide, respectively, indicate that a fast one-electron step is involved in the overall electrode reaction.

Conclusion

It is evident from the experimental results that nicotinamide is irreversibly reduced at mercury electrodes. Two electrons are consumed in the overall electrode reaction and one electron in the rate-determining step. The shift in half-wave potential with increasing pH indicates that three hydrogen ions are consumed in the reaction in strong acidic medium, and that two hydrogen ions are consumed in alkaline medium. The effect of the anionic surfactant Benax on the a.c. polarographic waves shows that nicotinamide is positively charged in acidic medium[12,14].

Hence, the following reduction mechanisms may be postulated:
Strong acidic medium:

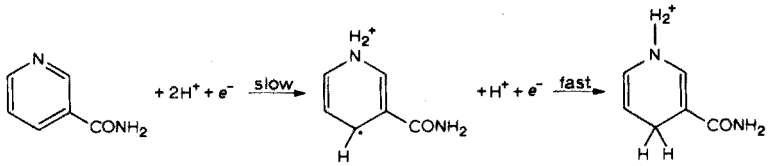

Strong alkaline medium:

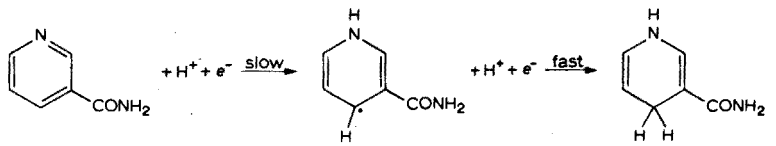

The second electron transfer is fast and must be responsible for the a.c. polarographic step. The first electron transfer is slow, and explains the *h*-dependence of the a.c. peak current.

ANALYTICAL APPLICATIONS

As stated above very well-defined a.c. polarograms of nicotinamide are obtained from 2 *M* sulphuric acid. Unfortunately, strong acid solutions are not suitable for the determination of nicotinamide in tablets. Experiments showed that in acidic media riboflavin is strongly adsorbed on the electrode surface, and that the adsorbed layer inhibits the reduction of nicotinamide.

However, polarograms of nicotinamide recorded from strong alkaline media are not affected by even large amounts of riboflavin. Moreover, insoluble constituents in the tablets do not cause any interference and need not be removed before the polarogram is recorded. Nicotinamide is reduced at high negative potentials ($E_p = -1.7$ V). Hence, small amounts of nicotinamide are best determined with tetraethylammonium hydroxide as supporting electrolyte. In most tablets, the nicotinamide content is relatively high (10–20 mg) and in such determinations 0.1 *M* sodium hydroxide may also be used as supporting electrolyte. The tablets disintegrate very quickly in strong alkaline media, and nicotinamide is quantitatively released in a couple of minutes. Most other vitamins are polarographically active, but they are reduced at potentials less negative than nicotinamide. Hence, differential pulse polarography is without doubt the best method for the determination of nicotinamide in complex mixtures.

Based on the above experiments the following procedure is suggested.

Recommended procedure

Transfer one tablet (equivalent to 10–30 mg of nicotinamide) to a 250-ml volumetric flask and add 200 ml of 0.1 *M* sodium hydroxide. Crush the tablet with a glass rod, shake the flask for 5 min, and dilute to the mark with 0.1 *M* sodium hydroxide. Transfer a suitable amount of the suspension to a polarographic cell. Remove dissolved air with pure nitrogen, and record a differential pulse polaro-

gram with drop time 0.5 s, pulse amplitude 50 mV and scan rate 2 mV s^{-1} in the potential range 1.5–1.9 V. Measure the peak current and determine the amount of nicotinamide from a standard curve prepared by the same procedure or by the standard addition method. Because nicotinamide is not stable in strong alkaline medium the polarogram should be recorded within 2–3 h after mixing the solution.

Results

The results of a few determinations of nicotinamide in multivitamin tablets are given in Table V. The Vitaplex tablets contain in addition to the vitamins A, B_1, B_2, B_6, C, D and calcium pantothenate, also starch, talcum, methylcellulose, sugar, calcium carbonate etc. The B-Viplex tablets contain only the vitamins B_1, B_2, B_6, calcium pantothenate, yeast and similar insoluble constituents.

TABLE V

DIFFERENTIAL PULSE POLAROGRAPHIC DETERMINATION OF NICOTINAMIDE IN VITAPLEX AND B-VIPLEX TABLETS

Vitaplex tablets[a]			*B-Viplex tablets*[b]		
Tablet	*Current* $\Delta i/\Delta E_p$ *(μA)*	*Nicotinamide found (mg)*	*Tablet*	*Current* $\Delta i/\Delta E_p$ *(μA)*	*Nicotinamide found (mg)*
1	58.00	20.57	1	37.00	15.69
2	58.30	20.67	2	36.00	15.27
3	60.00	21.27	3	39.00	16.55
4	59.00	20.92	4	38.75	16.43
5	61.35	21.75	5	35.88	15.21
6	62.25	22.07	6	38.75	16.43
7	59.25	21.01	7	38.38	16.27
8	56.30	19.96	8	36.75	15.60
9	58.60	20.78	9	39.13	16.64
10	58.25	20.65	10	38.38	16.27
11	59.70	21.17	11	37.00	15.69
12	58.50	20.74	12	38.00	16.12
13	57.00	20.21	13	37.00	15.63
14	58.60	20.78	14	35.75	15.17
15	60.00	21.27	15	35.75	16.00
16	56.00	19.86			
17	60.10	21.31		Mean	15.93
18	57.50	20.39			
19	61.90	21.95			
20	59.40	21.06			
	Mean	20.92			

[a] Declared amount of nicotinamide 20 mg + 5% excess = 21 mg.
[b] Declared amount of nicotinamide 15 mg + 5% excess = 15.75 mg.

The proposed method is very simple and has given satisfactory accuracy in determinations of nicotinamide in multivitamin tablets. Moreover, because the removal of insoluble matter and the separation from other vitamins are omitted, the present method is also much faster than previous methods.

The authors wish to thank cand. pharm. R. Gjermundsen and cand. pharm. V. Holm, Pharmaceutical Research Laboratory, A/S Apothekernes Laboratorium for Specialpraeparater for their kind interest in this work and for supply of the vitamins and tablets used.

SUMMARY

The electroreduction of nicotinamide has been investigated by d.c., a.c. and pulse polarography, cyclic voltammetry and coulometry. A single well-defined polarographic wave is obtained from 2 *M* sulphuric acid and from 0.1 *M* sodium hydroxide. In both media, nicotinamide undergoes an irreversible 2-electron reduction; 3 hydrogen ions are consumed in acidic medium and two hydrogen ions in alkaline medium. The current is diffusion-controlled and proportional to the concentration in the range 0.6–120 $\mu g\ ml^{-1}$. Reduction mechanisms are proposed. A simple and rapid method for the determination of nicotinamide in multivitamin tablets by differential pulse polarography is described.

REFERENCES

1 W. Kønig, *J. Prakt. Chem.*, 69 (1904) 105; 70 (1904) 19.
2 O. Pelletier and J. A. Campbell, *J. Pharm. Sci.*, 50 (1961) 926.
3 R. Strohecker and H. M. Henning, *Vitamin Assay-Tested Methods*, Verlag Chemie, G.m.b.H., Weinheim/Bergstr., Germany, 1965, pp. 193–195.
4 P. C. Tompkins and C. L. Schmidt, *Univ. Calif., Berkeley, Publ. Physiol.*, 8 (1943) 247.
5 E. Knobloch, *Chem. Listy*, 39 (1945) 54; *Collection Czech. Chem. Commun.*, 12 (1947) 581.
6 J. J. Lingane and O. L. Davis, *J. Biol. Chem.*, 137 (1941) 567.
7 Y. Asahi, *J. Vitaminol. (Kyoto)*, 4 (1958) 118.
8 M. E. Schertel and A. J. Sheppard, *J. Pharm. Sci.*, 60 (1971) 1070.
9 J. M. Moore, *J. Pharm. Sci.*, 58 (1969) 1117.
10 A. D. Goolsby and D. T. Sawyer, *Anal. Chem.*, 39 (1967) 411.
11 C. H. Aylward and J. W. Hayes, *J. Electroanal. Chem.*, 8 (1964) 442.
12 E. Jacobsen, *Anal. Chim. Acta*, 35 (1966) 447.
13 B. Breyer and H. Bauer, *Alternating Current Polarography and Tensammetry*, Interscience, New York, 1963, p. 50.
14 N. Gundersen and E. Jacobsen, *Anal. Chim. Acta*, 45 (1969) 346.

Analytica Chimica Acta, 71 (1974) 185–191

DETERMINATION DU TELLURE(IV) EN MILIEU ACIDE PAR POLAROGRAPHIE À TENSION ALTERNATIVE IMPULSIONNELLE ET PAR VOLTAMMÉTRIE À BALAYAGE LINÉAIRE

M. VOLAIRE, O. VITTORI et M. PORTHAULT

Laboratoire de chimie analytique III de l'Université Claude Bernard Lyon I, 43 Boulevard du Onze Novembre 1918, 69100-Villeurbanne (France)

(Reçu le 14 janvier 1974)

A la suite de nos travaux[1] sur le tellure(IV) en milieu acide nous avons appliqué les conditions expérimentales et les résultats que nous avions obtenus au dosage de traces de cet élément, dont la toxicité est bien connue.

Nous avons opéré en milieu acide perchlorique molaire. Les techniques employées ont été la polarographie à tension alternative surimposée (PTAS), la polarographie à impulsion mode dérivé (PID) et la voltammétrie cyclique, à balayage linéaire. Notre étude se décompose en deux parties: l'une est consacrée aux limites de détection, l'autre aux interférences de dosage provoquées par le cuivre(II), l'arsenic(III) et le selenium(IV).

L'étude par polarographie à courant continu du tellure(IV) a été primitivement présentée par Lingane et Niedrach[2,3]. Il ressort de ces travaux ainsi que de ceux de Shinagawa *et coll.*[4], pour ne citer que les plus importants, que la réduction en milieu acide du tellure(IV) se fait en deux étapes. La première consiste en la réduction de Te(IV) en tellure élémentaire, adsorbé sur la goutte de mercure, et la seconde est due à la réduction finale du tellure élémentaire en Te^{2-}. Cette dernière étape fournit en polarographie classique un maximum très important situé sur le plateau de la vague de réduction de Te(IV) en tellure élémentaire. Ce maximum apparait dans tous les milieux sauf dans la soude, et il est admis que celui-ci est lié à une réduction catalytique de l'hydrogène[2].

Ainsi nous pouvons schématiquement écrire:

1° étape $Te(IV) + 4e \rightarrow Te(0)$

2° étape $Te(0)_{ads} + 2H \rightarrow HTe^-_{ads} + H^+$

$$HTe^-_{ads} + e \rightarrow \tfrac{1}{2}H_2 + Te^{2-}_{ads}$$

$$Te^{2-}_{ads} + H^+ \rightarrow HTe^-_{ads}$$

En fait, comme nous l'avons souligné par ailleurs[1], il est peu probable que la première étape soit aussi simple qu'un échange rapide de quatre électrons quoique globalement elle apparaisse comme unique et très irréversible. Cependant pour des fins analytiques il semble plus intéressant de considérer la seconde étape qui fournit un courant environ vingt fois plus élevé que celui de la vague dans l'étape 1 (Fig. 1). En PTAS, comme en PID, cette seconde étape montre un pic

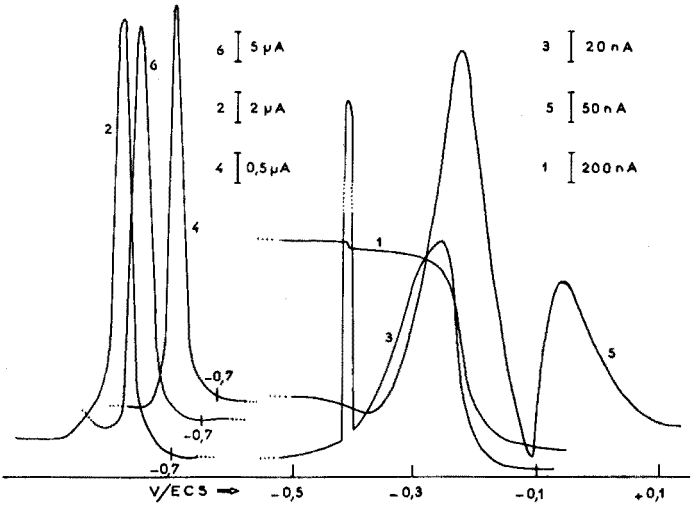

Fig. 1. Polarogrammes du tellure(IV) en milieu acide perchlorique *M*. Courbes 1 et 2, polarographie classique; courbes 3 et 4, PTAS; courbes 5 et 6, PID.

très sensible par rapport aux pics de la première étape, d'ailleurs dédoublés en PID (Fig. 1).

Sur le plan analytique la détermination du tellure a été nettement plus développée que l'aspect théorique de la réduction. Un grand nombre de travaux a porté sur les milieux les plus divers, caractérisés de plus par une gamme de pH non moins large. Dans les milieux de pH élevé, la vague de réduction est déplacée vers les potentiels cathodiques (entre $-0{,}6$ et $-0{,}8$ V/ECS) et correspond à l'étape 1[5,6]. Assez souvent les milieux contiennent NH_4Cl–NH_4NO_3 et NH_4OH entre les pH 6 et 10[6–11]. Lorsque le tellure est dosé en présence d'autres éléments, l'addition d'agents complexants comme l'EDTA ou l'hydrazine en favorise la détermination. Dans la majorité des cas la polarographie classique est utilisée, mais nous notons certains travaux en PTAS[8,12–14], en PID[12] et en oscillopolarographie[15].

Le pic très intense qui apparait vers $-0{,}80$ V/ECS a été utilisé pour déterminer du tellure dans les acides chlorhydrique et sulfurique[16]. D'autres milieux ont également été essayés et nous renvoyons à l'ouvrage de Nazarenko et Ermakov qui fait le point sur l'état actuel des travaux[17].

Pour notre part nous nous sommes proposés de déterminer le tellure en milieu perchlorique (*M*) par PTAS, PID et voltammétrie cyclique en mettant l'accent sur les possibilités de haute sensibilité offertes par le pic à $-0{,}80$ V/ECS qui correspond au maximum présenté par la vague de réduction du tellure(IV) en polarographie classique.

PARTIE EXPÉRIMENTALE

Nous avons utilisé les ensembles polarographiques PRG 3 et PRG 4 de marque Solea–Tacussel. Chaque ensemble a en commun un potentiostat PRT 30-01 de haute stabilité, un enregistreur EPL 2 muni d'un tiroir TV 11 GD et asservi

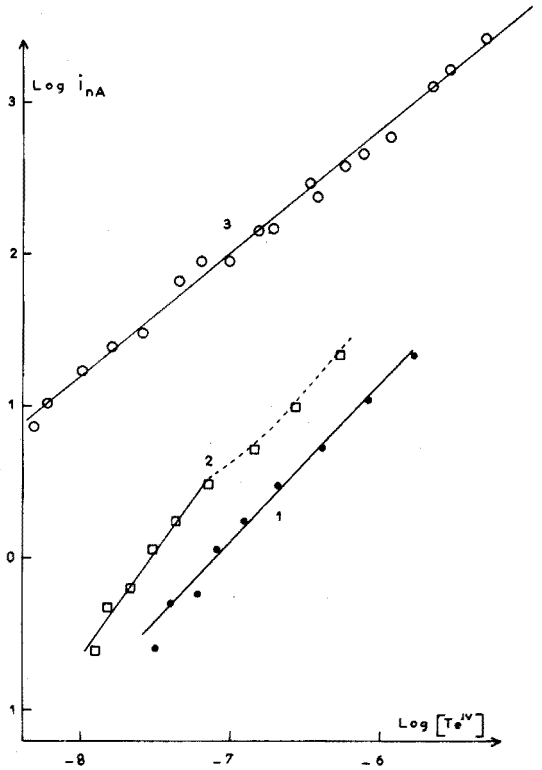

Fig. 2. Droites d'étalonnage en fonction de la concentration. Courbe 1, PTAS; courbe 2, PID (goutte normale); courbe 3, PID (goutte pendante).

au tiroir polarographique UAP 3 (polarographie à tension alternative surimposée) et UAP 4 (polarographie impulsionnelle).

Pour les essais sur goutte pendante nous disposions du dipositif Metrohm à piston dont la reproductibilité est satisfaisante. Les solutions de tellure(IV) ont été réalisées à partir de l'oxyde TeO_2. Les autres produits: $HClO_4$, $CuSO_4 \cdot 5H_2O$, As_2O_3, SeO_2 étaient de qualité analytique, ultra-purs.

Les conditions opératoires générales étaient celles que requiert usuellement la polarographie dans le dosage des traces. Toutes les solutions plus diluées que 10^{-4} *M* étaient préparées fraichement pour éliminer toutes contaminations et adsorptions parasites.

RÉSULTATS

Utilisation de la PTAS

Nous avons effectué les mesures par la technique des ajouts d'une solution connue de tellure(IV) en milieu $HClO_4$ dans un volume initial d'acide à la même normalité, en cellule, sur lequel le blanc était effectué. Les premières additions sont faites avec des seringues Hamilton de 20 μl.

Le pic étant situé vers $-0{,}75$ V/ECS, les enregistrement ont été effectués de

$-0{,}50$ à $-0{,}95$ V/ECS. Les valeurs des paramétres sont usuelles: $t = 4$s, $N = 60$ Hz, $E = 10$ mV, angle de déphasage, nul. Nous avons vérifié que le pic était proportionnel à la concentration en tellure(IV) initial dans une gamme allant de 10^{-8} à 10^{-6} M (Fig. 2).

Utilisation de la PID

Nous avons conduit de façon analogue deux séries d'essais sur la goutte de mercure habituelle (débit de 0,533 mg s^{-1}) et sur goutte pendante. Les paramètres utilisés sont: retard à l'impulsion 2s, durée de l'impulsion 150 ms, échantillonnage 50–70%, $\Delta E = 50$ mV, mode PID à impulsions surimposées. Le choix de telles valeurs des paramètres est inhabituel mais il s'imposait pour les raisons suivantes: avec un temps de vie de goutte court la capacité de double-couche et son courant de charge lors de l'impulsion demeurent modérés. L'impulsion longue de 150 ms avec échantillonnage de 75 à 105 ms permet d'éliminer correctement ce courant capacitif. Une amplitude d'impulsion de 50 mV augmente le courant de réponse donc la sensibilité à la réaction faradique.

La goutte pendante a une surface de 2,99 mm^2 (6 divisions du vernier). Les limites de détection sont voisines de 10^{-8} M (soit 1,6 p.p.b.) pour la goutte normale et $6.5 \cdot 10^{-9}$ M (soit 1 p.p.b.) pour la goutte pendante (Fig. 2).

Voltammétrie cyclique à balayage linéaire

Nous avons opéré sur goutte pendante dans les mêmes conditions que précédement. La surface était à nouveau fixée à 2,99 mm^2. La vitesse maximale de balayage qu'autorisait notre appareillage était 100 mV s^{-1}.

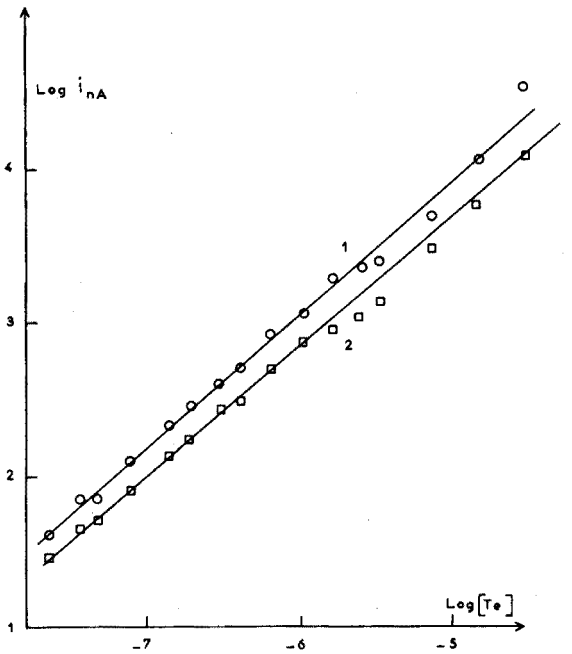

Fig. 3. Droites d'étalonnages en fonction de la concentration par voltammétrie cyclique. Courbe 1, au 2° balayage; courbe 2, au 10° balayage.

Nous avons constaté que le premier balayage était impropre aux déterminations car le pic se confondait avec le front du solvant. Par contre au cours des balayages successifs suivants (du 2° au 10°) le pic dû à la réduction du tellure élémentaire est situé à $-0{,}74$ V/ECS et permet le dosage. En fait le second balayage fournit une intensité de pic que nous ne retrouvons pas ensuite aux balayages suivants car il y a une décroissance assez marquée au cours des cycles. Cependant si pour les cinq premiers cycles la diminution est nette, elle est peu marquée au dela. Nous avons donc tracé les droites d'étalonnage pour les second et dixième balayages (Fig. 3).

Les limites de détection ont toujours été estimées pour la concentration à laquelle la largeur à mi-hauteur de pic est égale à la hauteur totale du pic. Pour cette condition satisfaite il est alors possible d'identifier le tellure. Les résultats sont donnés dans le tableau I. De ce tableau il ressort que les quatres méthodes sont assez voisines dans leurs performances. Nous pensons que l'accumulation de tellure élémentaire à la surface de la goutte rend aussitôt disponible une quantité de tellure élémentaire trés supérieure à ce qu'aurait apporté un processus classique de diffusion. Ceci explique la forte intensité due à cette réduction, qui implique, de plus, une réduction catalytique de l'hydrogène.

TABLEAU I

LES LIMITES DE DÉTECTION

Mode polarographique	*Électrode*	*Limites de détection*	
		Concentration (mole l^{-1})	*Limite (p.p.b.)*
PTAS	Goutte normale $t=4$s	$1.5\cdot10^{-8}$	2
PID	Goutte normale retard 2s	$1.0\cdot10^{-8}$	1,6
PID	Goutte pendante $A=2{,}99$ mm^2	$6{,}5\cdot10^{-9}$	1
Voltammétrie cyclique	Goutte pendante $A=2{,}99$ mm^2	$3{,}0\cdot10^{-8}$	4

Interférences du cuivre(II), de l'arsenic(III) et du selenium(IV)

Nous avons testé l'influence de quelques éléments fréquement rencontrés avec le tellure. Nous nous sommes fixés volontairement des concentrations assez élevées car nous avions été confrontés à des dosages de catalyseurs au tellure, où la proportion de ce dernier était importante. Nous n'avons utilisé que la PID avec les réglages suivants: $E=50$ mV, retard à l'impulsion 2s, largeur de l'impulsion 50 ms, échantillonnage 50 à 70%, goutte de mercure lentement croissante. La solution initiale est $10^{-4}M$ en tellure à laquelle sont ajoutés le cuivre(II) et l'arsenic(III) en quantités croissantes. Pour maintenir constante la concentration en tellure(IV), des

ajouts sont également effectués à l'aide d'une solution concentrée de cet élément. Nous voyons que l'influence de Cu(II) et As(III) se manifeste par une baisse sensible de l'intensité du pic de détection du tellure au-dessus de $2{,}5 \cdot 10^{-6}$ et $4.0 \cdot 10^{-5}$ M respectivement. Dans le cas du sélénium nous opérons de la même façon sur une solution initialement 10^{-5} M en tellure(IV). L'influence de cet élément apparait dés 10^{-5} M. Néanmoins dans les trois cas la détection du tellure demeure très sensible et moyennant un étalonnage ou une technique d'ajouts il est encore possible d'atteindre la concentration initiale en tellure(IV) (Fig. 4).

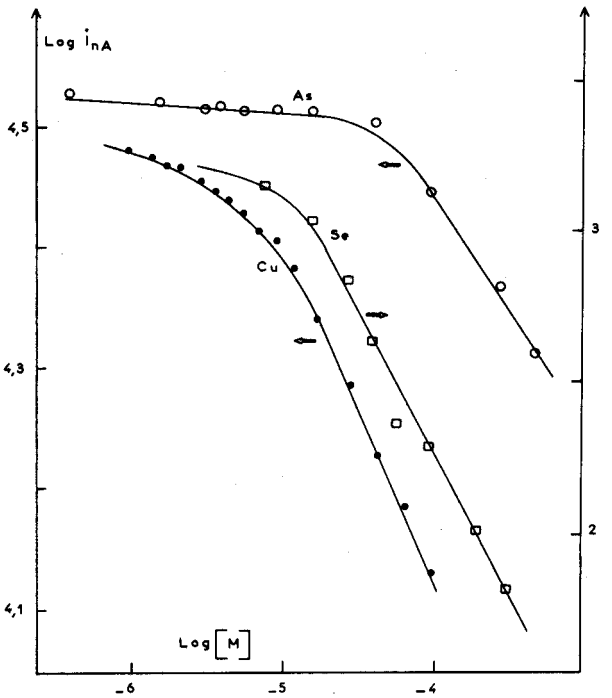

Fig. 4. Courbes d'interférences de Cu(II), As(III) et Se(IV) sur le détection du tellure(IV).

Ces interférences peuvent être provoquées par les adsorptions simultannées de l'arsenic élémentaire et du selenium élémentaire déjà décrites, qui seront concurrentes avec celle du tellure élémentaire[3,18]. Dans le cas du cuivre il a été également envisagé la possibilité de formation d'un composé intermétallique[3].

CONCLUSIONS

Les dosages du tellure(IV) en milieu acide perchlorique se sont révélés facilités par la réduction catalytique des ions hydrogène, qui provoque un fort courant de pic attribué à la réaction: $Te^0_{ads} \rightarrow Te^{2-}$. La linéarité de la variation de l'intensité avec la concentration a été établie de 10^{-8} à 10^{-5} M environ par les trois méthodes: polarographie impulsionnelle et à tension alternative surimposée, et voltammétrie cyclique. Les études sur goutte pendante se sont révélées les plus

sensibles. Les interférences de Cu(II), As(III) et Se(IV) ont été constatées dans des solutions 10^{-4} et 10^{-5} *M* en Te(IV). Elles semblent dans ce milieu, et pour le pic à $-0{,}75$ et à $-0{,}80$ V/ECS, plus importantes que dans l'acide iodhydrique[17].

RÉSUMÉ

Les auteurs ont soulignés l'intérêt analytique de la réduction $Te^0_{ds} \rightarrow Te^{2-}$ en milieu acide perchlorique molaire par sa haute sensibilité au dosage de traces. Ils ont montré que la polarographie impulsionnelle, à tension alternative surimposée et la voltammétrie cyclique permettaient d'atteindre quelques p.p.b. Les interférences de Cu(II), As(III) et Se(IV) sont décrites.

SUMMARY

Tellurium can be determined polarographically in the range 10^{-5}–10^{-8} *M* by means of the $Te^0_{ads} \rightarrow Te^{2-}$ reduction in 1 *M* perchloric acid as supporting electrolyte. Pulse polarography, a.c. polarography and linear sweep cyclic voltammetry can be used to determine tellurium in the p.p.b. range. Copper(II), arsenic(III) and selenium(IV) interfere, but the interferences can be overcome by a standard addition method.

BIBLIOGRAPHIE

1 M. Volaire, *Thèse no. 306*, Lyon, 1973.
2 J. J. Lingane et L. W. Niedrach, *J. Amer. Chem. Soc.*, 70 (1948) 4115.
3 J. J. Lingane et L. W. Niedrach, *J. Amer. Chem. Soc.*, 71 (1949) 196.
4 M. Shinagawa, N. Yano et T. Kurosu, *Talanta*, 19 (1972) 439.
5 Wu Kuo Hui et Hua Hsueh Ch' Ingchien, *Zh. Fiz. Khim.*, (1958) 39389.
6 G. S. Deshmukh et V. S. Sankara Rao, *Z. Anal. Chem.*, 240 (1968) 322.
7 A. I. Alekperov, *Azerb. Khim. Zh.*, (1961) 133; (1963) 73.
8 R. G. Pats, L. N. Vasil'Eva et T. V. Semochkina, *Zh. Anal. Khim.*, 23 (1968) 241.
9 M. Suzuki, *J. Electrochem. Soc. Jap.*, 23 (1955) 544.
10 L. V. Zolotareva et P. N. Kovalenko, *Zh. Anal. Khim.*, 19 (1964) 731.
11 K. J. Cathro, *Aust. J. Appl. Sci.*, 9 (1958) 255.
12 Y. S. Lyalikov et L. S. Kopanskaya, *Ukr. Khim. Zh.*, 30 (1964) 91.
13 R. G. Pats et T. V. Semochkina, *Tr. Gintsvetmet.*, 27 (1967) 50.
14 R. G. Pats, S. B. Tsfasman et T. V. Semochkina, *Zavod. Lab.*, 30 (1964) 140.
15 G. L. Whitnack, T. M. Donovan et M. H. Ritchie, *Zh. Fiz. Khim.*, 24 G (1967) 150.
16 E. T. Chikryzova et L. S. Kopanskaya, *Zh. Anal. Khim.*, 23 (1968) 394.
17 I. I. Nazarenko et A. N. Ermakov, *Selenium and Tellurium*, Wiley, New York, 1972.
18 J. P. Arnold et R. M. Johnson, *Talanta*, 16 (1969) 1191.

Analytica Chimica Acta, 71 (1974) 192–195

SHORT COMMUNICATION

The fluorimetric determination of triphenyltin compounds

F. VERNON

Department of Chemistry and Applied Chemistry, University of Salford, Salford M5 4WT, Lancs. (England)

(Received 30th September 1973)

Organotin compounds are widely used as catalysts and poly(vinyl chloride) stabilizers and have proved to be effective fungicides. However, their fungicidal applications, particularly efficient in the control of potato blight, are restricted by their high mammalian toxicity.

The toxicity of triphenyltin compounds has been investigated by Stoner[1], who concluded that "very little triphenyltin could be permitted in food". For the use of triphenyltin compounds as potato fungicides, Stoner[2] has said that from the results of animal experiments, the acceptable daily intake of triphenyltin for man would be less than 1 μg per kg of bodyweight. Present chemical methods cannot detect a residue which would be toxicologically significant, and this has resulted in several countries imposing a ban on the use of triphenyltin fungicides for potato crops.

The analytical method suggested here is sufficiently sensitive and involves the fluorimetric measurement of the triphenyltin moiety after complex formation with 3-hydroxyflavone, a reagent which has been used by Coyle and White[3] for the fluorimetric determination of inorganic tin. For the determination of the triphenyltin content of potatoes, the extraction sequence recommended by Thomas and Tann[4] has been used with minor modification.

Experimental

Reagents and organotin compounds. 3-Hydroxyflavone (Eastman Organic Chemicals), tetraphenyltin and triphenyltin chloride (Alpha Inorganics), triphenyltin acetate (Pure Chemicals), diphenyltin dichloride (B.D.H.), tin(IV) chloride (Hopkin and Williams). Monophenyltin trichloride was prepared by the disproportionation of diphenyltin dichloride with tin(IV) chloride in a sealed tube at 180 °C (ref. 5).

Instrumental. All fluorimetric measurements were made with 1-cm quartz cells and an Aminco–Bowman Spectrofluorimeter.

Method for triphenyltin residues in potatoes. Macerate a 500-g potato sample with 20 ml of 1 *M* sulphuric acid and 300 ml of acetone and filter. Macerate the pulp once with 200 ml of acetone and filter, and then macerate twice with 200-ml portions of dichloromethane and filter. Combine the aqueous acetone and dichloromethane extracts in a separating funnel, adjust the pH of the upper (aqueous) layer to 7–8 by addition of 2 *M* potassium hydroxide, add 2 g of

EDTA (disodium salt), shake for 1 min and allow to separate. Remove the organic layer and wash the aqueous layer by shaking with two 50-ml portions of dichloromethane. Bulk the dichloromethane extracts, dry by shaking with 10 g of anhydrous sodium sulphate and filter. Remove most of the dichloromethane by means of a rotary evaporator; when the residual volume is 5–10 ml, add 100 ml of sulphur-free, redistilled benzene and again reduce the volume to 5–10 ml. Transfer this solution quantitatively to a 30-ml glass vial and evaporate almost to dryness in a warm air-bath. Remove the vial from the bath when the volume of benzene becomes negligible but without drying completely. Add 5.0 ml of 0.01 %(w/v) solution of 3-hydroxyflavone in benzene followed by 1 ml of saturated sodium acetate solution. Stopper the vial and shake on a mechanical shaker for 30 min. After separation, transfer a quantity of the benzene layer to a 1-cm fluorimeter cell and measure the fluorescence intensity at 497 nm using 415-nm excitation.

Calibration. Satisfactory instrument calibration can be obtained by placing a solvent blank, 0.5 and 1.0-ml samples of a 0.00025% triphenyltin chloride solution in benzene, into vials and evaporating in the airbath followed by the treatment described above for the sample. In addition, it is necessary initially to compare the fluorescence intensities of a series of standards prepared as described with a series taken through the complete procedure in order to assess the efficiency of the extraction step.

Results and discussion

The results are expressed in terms of the weight of tin present as triphenyltin and, with the highest instrumental sensitivity, a calibration curve was constructed over the range 0–0.77 μg of tin. Slight curvature in the working range was found with a limit of detection of 0.16 μg of tin (Fig. 1). Recovery work was carried out with standard triphenyltin solutions containing 1.0 μg of tin; thirteen determinations were made, the standards being taken through the complete

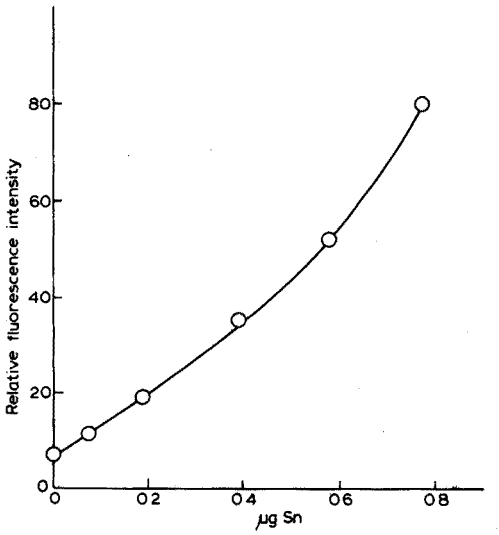

Fig. 1. Calibration curve.

procedure, and a standard deviation of ± 5.7% was obtained. Accordingly, the more convenient calibration technique described above was adopted, as the extraction step proved to be efficient. However, it was found that at the solvent removal stage, if the solvent was completely evaporated and any "baking" of the residue occurred, very low recoveries were obtained.

Interference studies. The possible effects of the presence of inorganic tin, monophenyltin and diphenyltin compounds were examined. The excitation and emission maxima of each species with the reagent, and of the reagent alone, were determined in addition to their fluorescence properties at the triphenyltin–3-hydroxyflavone emission and excitation maxima. No fluorescence from the reagent or from diphenyltin was detected at these wavelengths; inorganic tin and monophenyltin gave a slight fluorescence but the relative intensities, on a weight for weight basis, were low (Table I). These low values, considered in conjunction with the extraction procedure which would tend to eliminate inorganic tin and any monophenyltin species which would probably hydrolyse to phenylstannonic acid, indicate that no interference by other tin compounds should be observed in the triphenyltin determination.

TABLE I

FLUORESCENCE PROPERTIES OF ORGANOTIN–3-HYDROXYFLAVONE COMPLEXES

Species	λ_{ex}	λ_{em}	*Relative intensity at triphenyltin wavelengths*
Triphenyltin	415	497	100
Diphenyltin	465	495	0
Monophenyltin	470	496	1.4
Tin(IV)	470	496	3.1
3-Hydroxyflavone	382	525	0

Nature of the complex. In the initial stage of the work, triphenyltin chloride solutions were reacted with various ligands and the fluorimetric properties of the resulting complexes were examined. The complex formed between triphenyltin chloride and 3-hydroxy-flavone exhibited a blue fluorescence (λ_{ex} 412 nm and λ_{em} 450 nm). However, when solutions of the reagent and triphenyltin acetate in benzene were allowed to interact, a green fluorescent species (λ_{ex} 415 nm and λ_{em} 497 nm) of twice the intensity was observed. A plot of mole fraction against fluorescence intensity showed the formation of a 1:1 complex. If the complex contains pentacoordinated tin as expected, the existence of two different fluorescent species dependent on the nature of the anion, cannot be explained. The more highly fluorescent green complex was chosen for this work with incorporation of the sodium acetate equilibration step, but further investigation into the natures of these complexes is obviously desirable.

Application to potatoes. Two potato samples were treated by injecting known volumes of acetone solution containing 1 μg of tin present as triphenyltin. After three weeks, the samples were taken through the extraction procedure and triphenyltin recoveries were determined. Values of 87% and 93.5% were obtained, demonstrating the efficiency of the method and also the fact that breakdown

of organotin material to harmless inorganic tin compounds either does not occur or is a relatively slow process.

Samples of two varieties of potato which had been sprayed with three times the recommended dosage of a formulated triphenyltin fungicide during growth were analysed by the described method and gave the following results, expressed as p.p.m. of tin present as triphenyltin:

Type 1. 0.0023, 0.0032, 0.0035

Type 2. 0.0009, 0.0014, 0.0012.

Conclusions

The very high sensitivity and selectivity of this method together with the fact that the toxic triphenyltin moiety is determined directly, suggests that it will prove to be a most useful technique in triphenyltin residue analysis. Stoner's suggested figure for a maximum daily intake of triphenyltin can be interpreted as 0.07 mg per day for a person weighing 70 kg. If the maximum daily diet were to include 1 kg of potato, the tin present as triphenyltin should not therefore be greater than 0.027 p.p.m. Of the six samples analysed, three were approximately one tenth of this maximum but these samples had been treated with three times the recommended dosage. It appears likely therefore, that triphenyltin formulations can be used safely in the control of potato blight. Extensive trials will be required but it is suggested that this method will allow the determination of triphenyltin residues at the required level.

The author is indebted to the Plant Pathology Laboratory of the Ministry of Agriculture, Fisheries and Food, for treated potato samples.

REFERENCES

1 H. B. Stoner, *Brit. J. Ind. Med.*, 23 (1966) 222.
2 H. B. Stoner, private communication.
3 C. F. Coyle and C. E. White, *Anal. Chem.*, 29 (1957) 1486.
4 B. Thomas and H. L. Tann, *Pestic.*, 2 (1971) 45.
5 G. E. Coates, M. L. H. Green, P. Powell and K. Wade, *Principles of Organometallic Chemistry*, Methuen, London, 1968.

Analytica Chimica Acta, 71 (1974) 196–201

SHORT COMMUNICATION

3-Hydroxy-1,3-diphenyltriazene and its substituted derivatives as spectrophotometric reagents for vanadium(V)

D. CHAKRABORTI

Department of Chemistry, Jadavpur University, Calcutta-700032 (India)

(Received 2nd January 1974)

If a sulfonic acid group (Na-salt) is introduced, in addition to the chelating groups, a water-insoluble organic reagent can often be made water-soluble without substantial alteration in its other properties; yet sometimes the sulfonic acid group may cause anomalous behavior[1, 2]. Work of this type has been reported from this laboratory for colorometric analyses[3, 4].

This communication describes the effects of the introduction of a sulfonic acid group (Na-salt), and a sulfonic acid group along with a methyl group, on the parent organic reagent 3-hydroxy-1,3-diphenyltriazene[5]. A comparative study of all these reagents for the spectrophotometric determination of vanadium(V) is also described.

The reagents examined are:

I. 3-Hydroxy-1,3-diphenyltriazene (ref. 5)
II. 3-Hydroxy-(1-*p*-sulfonatophenyl, sodium salt)-3-phenyltriazene (ref. 6)
III. 3-Hydroxy-(1-*o*-sulfonatophenyl, sodium salt)-3-phenyltriazene (ref. 7)
IV. 3-Hydroxy-(1-*m*-sulfonatophenyl, sodium salt)-3-phenyltriazene
V. 1-(4-Sulfonato, sodium salt-6-methylphenyl)-3-hydroxy-3-phenyltriazene
VI. 1-(4-Sulfonato, sodium salt-5-methylphenyl)-3-hydroxy-3-phenyltriazene

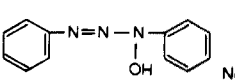

I

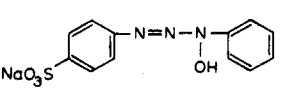

II

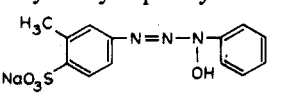

VI

Several workers have already investigated reagents I and II and a comprehensive review is available[8]. Reagents IV, V and VI are new reagents.

Introduction of a sulfonic acid group into the parent reagent (I) makes it water soluble. When the reagent contains a methyl group and a sulfonic acid group (sodium salt), it becomes highly water-soluble. The order of water solubility of the reagents can be represented as: V = VI > IV = II > III.

Studies of the color reaction of these reagents with vanadium(V) showed that reagents I, II, IV and VI are sensitive to vanadium and their reactions are very similar, but reagents III and V are not very sensitive and are therefore unsuitable for spectrophotometry; reagent V is the least sensitive. Clearly the positioning of substituents next to the triazene group seriously affects sensitivity.

TABLE I

SPECTROPHOTOMETRIC DETERMINATION OF VANADIUM(V) WITH 3-HYDROXY-1,3-DIPHENYLTRIAZENE AND ITS DERIVATIVES

Reagent	*Solvent*	*(a) Color (b) λ_{max}(nm) (c) Working wavelength (nm)*	*(a) Beer's Law range (b) Optimal range (p.p.m.)*	*Sensitivity ($\mu g\ cm^{-2}$)*	*ε*	*pH range*	*(a) Composition (b) Dissociation constant*	*Reagent required[a] (ml)*
I	Water + ethanol (1 + 1)	(a) Yellow (b) 410 (c) 410	(a) 0.25–10 (b) 0.5–10	0.0085	5875	3.1–4.2	(a) 1:1 (b) $6.0 \cdot 10^{-5}$	4.0
II	Water	(a) Yellow green (b) 400 (c) 410	(a) 0.25–10 (b) 0.5–10	0.0085	5875	3.3–4.3	(a) 1:1 (b) $6.5 \cdot 10^{-5}$	5.0
III	Water	(a) Yellow green (b) 400 (c) 410	–	0.026	—	—	—	—
IV	Water	(a) Yellow green (b) 400 (c) 410	(a) 0.25–12 (b) 0.5–10	0.0095	5250	3.6–4.6	(a) 1:1 (b) $5.0 \cdot 10^{-5}$	6.0
V	Water	(a) Yellow green (b) 410 (c) 410	—	0.05	—	—	—	—
VI	Water	(a) Yellow green (b) 400 (c) 410	(a) 0.1–8 (b) 0.5–8	0.0075	6625	3.0–4.4	(a) 1:1 (b) $7.5 \cdot 10^{-5}$	4.0

[a] A 0.1% (w/v) solution was used.

Of these six reagents, reagent VI is most suitable for the spectrophotometric determination of vanadium(V); it provides the highest sensitivity with the widest permissible pH range, and has the lowest absorbance itself. Reagent VI is therefore described in detail here, whereas data for the other reagents are simply tabulated (Table I). An interesting observation is that reagent I, in acetone at about pH 2–3, gives, in the presence of vanadium(V), a green precipitate which can be extracted into chloroform, λ_{max} at 640 nm; unfortunately this color complex decomposes rapidly and a turbidity appears. Other reagents did not exhibit this behavior.

Experimental

Preparation of reagents. Reagents I and II were prepared as suggested by Sogani and Bhattacharyya[9]. Reagents III, IV, V and VI were also prepared by this method; the starting materials were orthanilic acid, metanilic acid, 2-amino-5-sulfotoluene and 3-amino-toluene-6-sulfonic acid, respectively. Reagent III is a yellowish white compound (m.p. 168°C, decomp.). Reagents IV, V and VI are light yellow, pale yellow and yellowish white (m.p. 164°C, 157°C and 159°C decomp.), respectively.

Apparatus and solutions. Apparatus and solutions of ammonium vanadate and other ions were the same as reported previously[4]. Doubly distilled water was used in all preparations. All the chemicals used were of A.R. quality.

The reagent was used as a 0.1% (w/v) solution in water.

Absorbance curve for Vanadium(V). To an aliquot of the standard solution containing 100 μg of vanadium in a 50-ml beaker, add 4 ml of the reagent (VI) solution. Add dilute hydrochloric acid to adjust the pH to 3–4. Then dilute with water

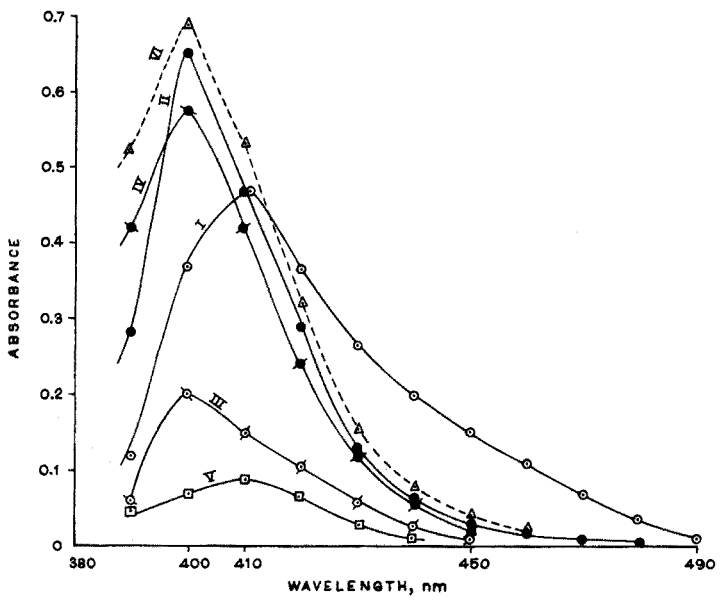

Fig. 1. Absorption spectra of vanadium(V) complexes (4 p.p.m. vanadium). The Roman numerals on the curves correspond to the reagent numbers.

to 25 ml in a volumetric flask and measure the absorbance against the reagent solution as blank. The yellowish green color of the system, corresponding to 4.0 p.p.m. of vanadium, shows maximum absorbance at 400 nm (curve VI, Fig. 1).

All measurements for vanadium(V) are made at 410 nm because, at this wavelength, the absorption of the reagent itself is much less.

Effect of pH, reagent and time

The absorbance of the system remains unchanged in the pH range 3.0–4.4, but decreases outside these limits.

For complete color development, 4 p.p.m. of vanadium requires 3 ml of 0.1% (w/v) reagent solution.

The absorbances of the system so produced remain constant for more than 24 h.

Beer's law, optimal range, photometric errors, sensitivity and molar absorptivity

The system follows Beer's law over the range 0.125–8.0 p.p.m. The optimal concentration range evaluated by Ringbom's method[10] is 0.5–8.0. The percentage relative error per 1% absolute photometric error[11] for the system is 2.74. The sensitivity when log I_0/I is 0.001, calculated as described by Sandell[12], is 0.0075 μg cm^{-2}, and the molar absorptivity is 6625.

Composition and stability of the complex

The composition of the vanadium complex was determined by the modified Job's method of continuous variations[13] and the mole ratio method[14]. Figure 2 indicates that vanadium combines with the reagent in the ratio 1:1.

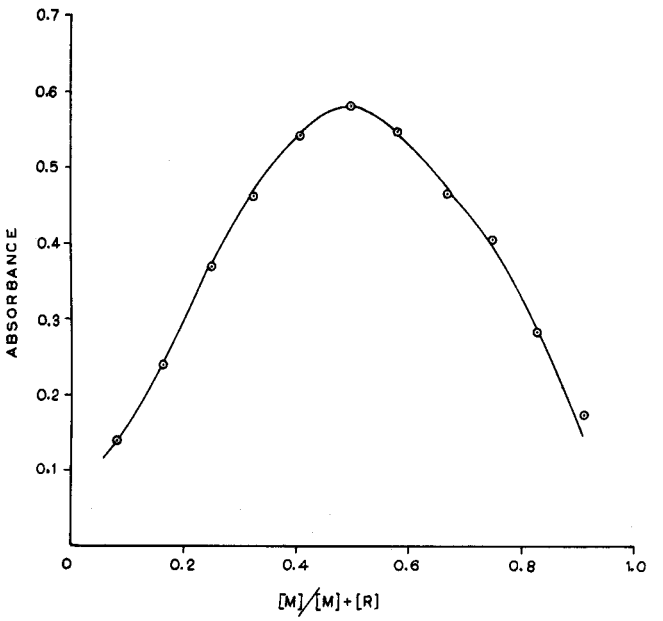

Fig. 2. Job curves; vanadium(V) = reagent VI = $5.0 \cdot 10^{-4}$ *M*.

The degree of dissociation, α, was calculated from Harvey and Manning's equation[15]. The instability constant evaluated from the equation $K=(m\alpha c)^m(n\alpha c)^n/c(1-\alpha)$ where $m=n=1$ for vanadium(V) was found to be $7.5\cdot10^{-5}$ ($E_m=0.56$; $E_s=0.38$; $c=5\cdot10^{-4}$; $\alpha=0.32$).

The dissociation constant of the complex was also evaluated from a study of the absorbance of complementary mixtures of non-equimolar solutions of metal ions and reagent (Fig. 3). The color of the solution was developed as described previously. The value calculated from the conventional equation[16] was found to be $7.5\cdot10^{-5}$ ($m=n=1$; $p=3$; $x=0.33$).

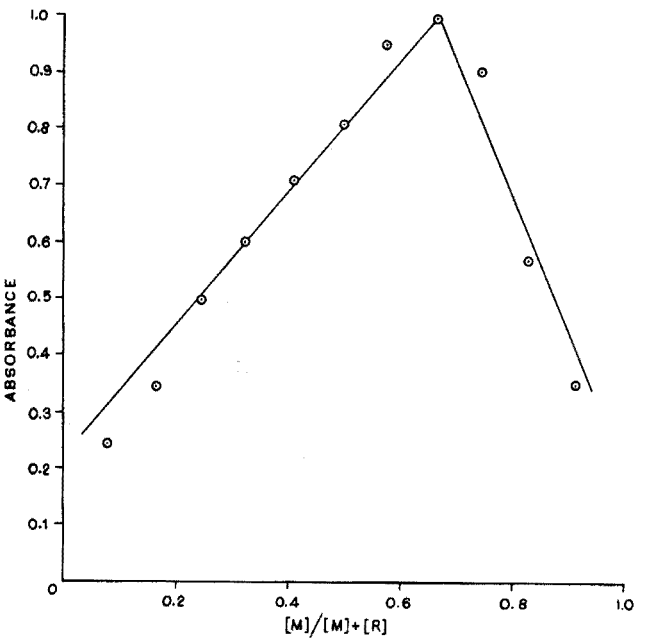

Fig. 3. Job's method for the dissociation constant; vanadium(V) $=0.5\cdot10^{-3}$ *M*, reagent VI $=1.5\cdot10^{-3}$ *M*.

Effect of diverse ions

In the vanadium(V)–reagent VI system, EDTA, oxalate, fluoride, Fe^{3+}, Pd^{2+}, Mo^{6+}, Cr^{3+} and Ti^{4+} interfered. The system, however, tolerates the presence of the following ions, the tolerance limits of which in p.p.m. are given in parentheses: Ni^{2+}(50), Co^{2+}(10), Mn^{2+}(10), WO_4^{2-}(20), UO_2^{2+}(10), La^{3+}(30), Ce^{3+}(20), Zn^{2+}(100), Cd^{2+}(200), Hg^{2+}(100), As^{3+}(100) and Th^{4+}(40). Cu^{2+} interfered but in the presence of sodium thiosulfate (5 ml of 1% solution), it could be tolerated up to 50 p.p.m. Li^+, Na^+, K^+, Br^-, I^-, Cl^-, PO_4^{3-}, boric acid, citrate and tartrate did not interfere.

REFERENCES

1 H. C. Wingfield and J. H. Yoe, *Anal. Chim. Acta*, 14 (1956) 446.
2 E. L. Stelle and J. H. Yoe, *Anal. Chem.*, 29 (1957) 1622; *Anal. Chim. Acta*, 20 (1959) 205.

3 D. Chakraborti, *Anal. Chim. Acta*, 00 (1974) 000.
4 A. K. Majumdar and D. Chakraborti, *Anal. Chim. Acta*, 53 (1971) 127, 393.
5 N. C. Sogani and S. C. Bhattacharyya, *Anal. Chem.*, 28 (1956) 81.
6 N. C. Sogani and S. C. Bhattacharyya, *Anal. Chem.*, 35 (1958) 542.
7 B. C. Roy, *Ph.D. Thesis*, Jadavpur University, India.
8 D. N. Purohit, *Talanta*, 14 (1967) 353.
9 N. C. Sogani and B. C. Bhattacharyya, *J. Indian Chem. Soc.*, 36 (1959) 563.
10 A. Ringbom, *Z. Anal. Chem.*, 115 (1938) 332.
11 G. H. Ayres, *Anal. Chem.*, 21 (1949) 652.
12 E. B. Sandell, *Colorometric Determination of Trace Metals*, Interscience, New York, 3rd Edn., 1959, p. 84.
13 P. Job, *Compt. Rend.*, 180 (1925) 928; *Ann. Chim. (Paris)*, 9 (1928) 113.
14 J. H. Yoe and A. K. Jones, *Ind. Eng. Chem., Anal. Ed.*, 16 (1944) 111.
15 A. E. Harvey Jr. and D. L. Manning, *J. Amer. Chem. Soc.*, 72 (1950) 4488.
16 A. K. Majumdar and B. Sen, *Anal. Chim. Acta*, 8 (1953) 369.

Analytica Chimica Acta, 71 (1974) 202–204

SHORT COMMUNICATION

A spot test for the detection of some aromatic hydrazides

P. S. MURTI, G. BALA BHASKARA RAO and P. V. KRISHNA RAO
Department of Chemistry, Andhra University, Waltair (India)
(Received 4th January 1974)

Because of the extensive use of aromatic hydrazides in chemotherapy, in fungicides and in pesticides, their detection and determination is of considerable importance. While many spot tests[1–7] have been reported for the detection of isonicotinic acid hydrazide, very few tests are available for other aromatic hydrazides. Larue[1] proposed trinitrobenzenesulphonic acid for the detection of benzoic acid hydrazide, its *m*- and *p*-nitro derivatives, salicylic acid hydrazide and phenylacetic acid hydrazide. In a recent communication[8], 2,3,5-triphenyltetrazolium chloride has been proposed for the detection of some aromatic hydrazides in the presence of compounds of similar composition and anions such as chloride, bromide, sulphate, nitrate, acetate, oxalate and citrate. In this communication, potassium hexacyanoferrate(III) or potassium hexacyanoferrate(II) is proposed for the detection of some aromatic hydrazides. The test is very simple and the reagents are inexpensive.

Experimental

Light source. A Philips 125 Watts "Repro" lamp was used for irradiating the reaction mixture. Alternatively, bright sunlight can be used with prolonged exposure times.

Reagents. All the hydrazides were obtained from Fluka AG. Aqueous 0.1% (w/v) solutions of nicotinic, isonicotinic and benzoic acid hydrazides were prepared in double-distilled water; aqueous 0.01% solutions of the *m*- and *p*-nitro derivatives of benzoic acid hydrazide, and salicylic and phenylacetic acid hydrazides were used because of their limited solubility in water.

Aqueous 0.1% solutions of potassium hexacyanoferrate(II) or aqueous 0.01% solutions of potassium hexacyanoferrate(III) (p.a. Merck) were prepared in double-distilled water and stored in amber coloured bottles.

Recommended procedure. Place one drop of the nearly neutral test solution in the cavity of a spot plate, add 0.2 ml of either hexacyanoferrate reagent, and stir with a glass rod. Expose the spot plate for about 1 min to light from a Philips "Repro" lamp. A pink colour indicates the presence of an aromatic hydrazide except for salicylic acid hydrazide, which gives a bluish violet colour.

Interferences. HPO_4^{2-} (130-fold), $C_2O_4^{2-}$ (330-fold), SO_3^{2-} (320-fold), NO_3^- (360-fold), tartrate (260-fold), *p*-aminosalicylic acid (500-fold), I^- (760-fold), Cl^- (520-fold), Br^- (320-fold), SO_4^{2-} (500-fold), NO_2^- (320-fold), acetate (1200-fold), gum acacia (500-fold), glucose (500-fold), ClO_4^- (1000-fold), all in weight amounts, did not interfere.

Results

The aromatic hydrazides listed in Table I all gave a positive test by the recommended procedure. It is interesting to note that while these aromatic acid hydrazides responded to the test even at very low concentrations (5 μg) almost within a minute after exposure to the light, the aliphatic hydrazides (oxalic and malonyl) gave brownish red and greenish red colours, respectively, only at concentrations above 500 μg, and after prolonged exposure (above 20 min) to light. The bluish violet colour observed in the case of salicylic acid hydrazide is a specific test for the compound.

The most suitable range of pH for the detection of these hydrazides was found to be 5.0–8.0. Below pH 5.0 a blue colour (which ultimately settled as a precipitate) was observed, while above pH 9.0 none of these hydrazides responded to the test.

The pink colour developed on exposure of the reaction mixture to light was stable up to about 6 h, even after removal from the light source. Thereafter, the colour changed to blue and ultimately settled as a precipitate presumably because of the formation of Prussian blue.

The limits of identification of various hydrazides were determined, the results being shown in Table I.

TABLE I

LIMITS OF IDENTIFICATION OF HYDRAZIDES

Hydrazide	*Smallest amount detected (μg)*	*Colour obtained*	*Limiting proportion*
Salicylic acid hydrazide	2.5	Bluish violet	$1:10^5$
Benzoic acid hydrazide	5.0	Pink	$1:0.5\cdot10^5$
m-Nitrobenzoic acid hydrazide	5.0	Pink	$1:0.5\cdot10^5$
p-Nitrobenzoic acid hydrazide	5.0	Pink	$1:0.5\cdot10^5$
Nicotinic acid hydrazide	5.0	Pink	$1:0.5\cdot10^5$
Isonicotinic acid hydrazide	5.0	Pink	$1:0.5\cdot10^5$
Phenylacetic acid hydrazide	5.0	Pink	$1:0.5\cdot10^5$

Discussion

Moggie *et al.*[9] considered that $Fe(CN)_6^{3-}$ and $Fe(CN)_6^{4-}$ undergo a photoaquation reaction while Balzani and Carasitti[10] reported a photochemical substitution of the cyanide by bipyridine or phenanthroline under 365-nm radiation. Since the aromatic hydrazides have comparable ligand properties with bipyridine or phenanthroline by virtue of having a lone pair of electrons on the terminal nitrogen atom, ($RCONHNH_2$), the colour is most probably due to complexation of $Fe(CN)_6^{4-}$ with the hydrazide by a photosubstitution mechanism. However, a detailed mechanistic study of the reaction is in progress to elucidate the nature of the pink coloured product.

Two of us (P.S.M. & G.B.B.R.) thank the Council of Scientific and Industrial Research, India, for the award of Research Fellowships.

REFERENCES

1 T. A. Larue, *Talanta*, 14 (1967) 1344.
2 T. Watanabe, *Eisei Shikenjo Hokoku*, 74 (1956) 111.
3 P. Castil, H. Orzalezi and A. Dubois, *Trav. Soc. Pharm. Montpellier*, 12 (1952) 73.
4 H. L. Avanza, *Jornada Med. (Buenos Aires)*, 9 (1955) 673.
5 P. G. W. Scott, *J. Pharm. Pharmacol.*, 4 (1952) 681.
6 E. Paunescu, *Stud. Cercet. Biochim.*, 4 (1961) 117.
7 F. Leuschner, *Naturwissenschaften*, 40 (1954) 554.
8 P. V. Krishna Rao and R. Sambasiva Rao, *Mikrochim. Acta*, in press.
9 L. Moggie, F. Bolletta, V. Balzani and F. Scandola, *J. Inorg. Nucl. Chem.*, 28 (1966) 2589.
10 V. Balzani and V. Carasitti, *Ann. Chim. (Paris)*, 54 (1964) 103, 251.

Analytica Chimica Acta, 71 (1974) 205–209

SHORT COMMUNICATION

Complex formation of indium(III) or thallium(III) with 8-hydroxy-7-iodoquinoline-5-sulphonic acid (ferron)

A. MASSOUMI*, P. OVERVOLL and F. J. LANGMYHR
Department of Chemistry, University of Oslo, Oslo 3 (Norway)
(Received 15th January 1974)

A previous paper[1] described an investigation by potentiometric titration of the complex formation in aqueous solution of gallium(III) with ferron, and a redetermination of the dissociation constants of the ligand. A new computer program made it possible to make allowance for a considerable number of equilibria.

The present communication describes the use of the above technique for the study of the complexes formed between ferron and indium(III) or thallium(III).

Experimental

Apparatus. The equipment employed has already been described[1]. The determination of the activity coefficient of the hydrogen ion, and the recalculation of hydrogen ion activities to concentrations were also given in this earlier paper.

Reagents. The ferron (AnalaR, Hopkin and Williams) was checked by alkalimetric titration and was found to be satisfactory.

The standard solutions of the two metals were prepared from indium shot and thallium wire (Koch-Light, purity 99.999%), the latter metal was delivered and kept in an oily liquid.

The acids were of high purity (Suprapur, Merck); all other chemicals were of reagent-grade quality.

Standard solutions. A $5 \cdot 10^{-3}$ *M* ferron solution, 0.1 *M* in potassium nitrate, was prepared by dissolving 1.756 g of ferron and 10.11 g of potassium nitrate in boiled distilled water and diluting the solution to 1 l.

A $5 \cdot 10^{-2}$ *M* indium solution was prepared by dissolving 5.741 g of metal in a small excess of nitric acid and diluting the solution to 1 l with boiled distilled water. More dilute ($5 \cdot 10^{-3}$ *M*) solutions, 0.1 *M* in potassium nitrate, were prepared.

Thallium wire was washed with acetone and water; after drying with filter paper, about 11 g were dissolved in a small excess of nitric acid. Oxidation to thallium(III) was accomplished by passing chlorine gas through the solution[2], until thallium(I) could no longer be detected by spot tests; the solution was finally made up to 1 l with boiled distilled water. The solution was standardized by

* On leave from Department of Chemistry, Pahlavi University, Shiraz, Iran.

titration with EDTA standard solution[3]; $5 \cdot 10^{-3}$ *M* thallium solutions, 0.1 *M* in potassium nitrate, were prepared by dilution.

Standard solutions of sodium hydroxide (about 0.05 *M*) were prepared by diluting the proper volumes of a 50% solution with freshly boiled distilled water; the solutions were standardized with potassium hydrogeniodate.

A 1 *M* solution of potassium nitrate was prepared.

For the adjustment of pH, 0.05 *M* and 0.01 *M* solutions of potassium hydrogenphthalate (pH 4.008 at 25°) and borax (pH 9.180 at 25°), respectively, were prepared.

Titrations. Indium or thallium solutions (25 ml of $5 \cdot 10^{-3}$ *M*) were mixed with 25, 50 or 75 ml of $5 \cdot 10^{-3}$ *M* ferron solution and titrated with standard alkali, and the titration curves were recorded.

The excess of nitric acid in the two metal standard solutions was determined by titrating 1:1 mixtures of metal and EDTA standard solution with standard alkali; the excess of acid was found from the difference between the amount of alkali added and the amount required to neutralize the two hydrogen ions released by the complex formation.

Definitions and calculations

The equilibria considered and the procedure followed in the present calculations have been described previously[1]. The dissociation constants of ferron were taken from this earlier paper.

The hydrolysis constants of indium used in the present calculations were those reported by Alimarin *et al.*[4], and the hydrolysis constants for thallium were taken from a paper by Biederman[5]. All data were converted from stepwise to overall hydrolysis constants.

The computer program also took into account the amount of free acid present in the metal solutions.

Results

In Fig. 1 the titration curves of the three mixtures of indium or thallium with ferron are reproduced; for comparison the titration curve of ferron alone is also included (the latter curve is reproduced from a previous paper[1]).

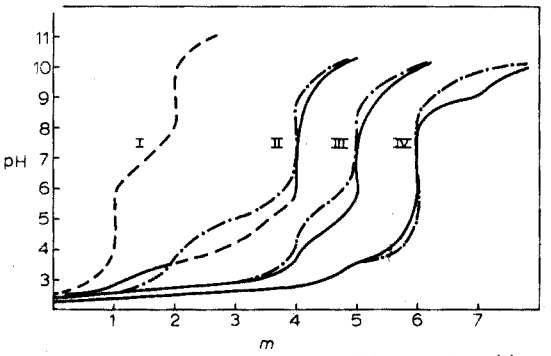

Fig. 1. Alkalimetric titration curves of ferron alone (I) and of 1:1(II), 1:2(III) and 1:3(IV) mixtures of indium (——) or thallium (–·–·–) with ferron; m = mole of sodium hydroxide added per mole of metal.

For indium, the 1:1 curve exhibits inflections corresponding to the addition of about 1.5 and 4 equivalents of base per mole of metal. The dashed part of the curve indicates the range in which a precipitate was observed. The precipitate (probably the neutral slightly soluble compound InOHL, where L is the ligand) appeared after the addition of two equivalents of alkali; on further addition of base it dissolved, and after the addition of four equivalents the precipitate was completely redissolved.

In Fig. 2, the mole fractions of the various species appearing in the 1:1 mixtures of indium and ferron are shown as a function of pH, the dashed parts of the solid lines representing the range in which the precipitate appeared. It can be seen that in the pH range examined the indium-containing species were: InL, InOHL, $In(OH)_2L$, InL_2, $InOHL_2$ and InL_3. In addition, small amounts of the hydrogen complex InHL are likely to be formed at low pH values; the presence of this species is indicated by the inflection on the 1:1 curve at m-values around 1.5. From the calculations by the computer, no definite conclusions could be drawn as to the absence or presence of the hydrogen complex.

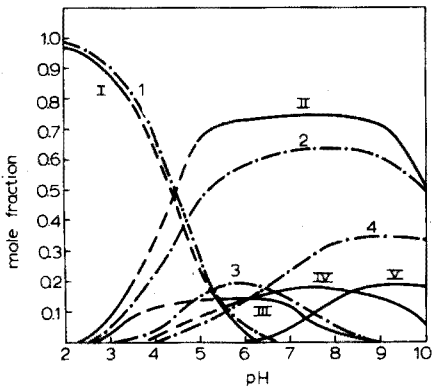

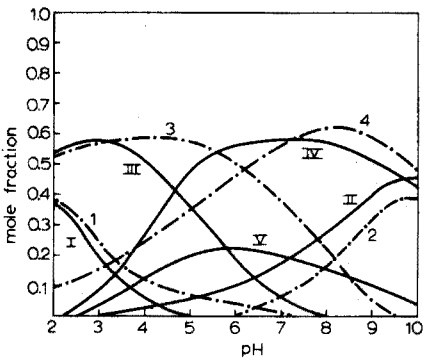

Fig. 2. The mole fractions in 1:1 mixtures of InL (I), $In(OH)_2L$ (II), InL_2 (III), $InOHL_2$ (IV) and InL_3 (V); and of TlL (1), $Tl(OH)_2L$ (2), TlL_2 (3) and TlL_3 (4) plotted as a function of pH.

Fig. 3. The mole fractions in 1:2 mixtures of InL (I), $In(OH)_2L$ (II), InL_2 (III), $InOHL_2$ (IV) and InL_3 (V); and of TlL (1), $Tl(OH)_2L$ (2), TlL_2 (3) and TlL_3 (4) plotted as a function of pH.

The 1:1 thallium curve differs from the corresponding indium curve by exhibiting an inflection after the addition of two equivalents of alkali; both curves have an inflection at $m=4$. No precipitate was observed during the titration of the 1:1 thallium–ferron mixtures. Figure 2 again shows the mole fractions of the species detected in the 1:1 mixtures of thallium and ferron as a function of pH. In the pH range examined the compounds detected were: TlL, $Tl(OH)_2L$, TlL_2 and TlL_3.

As is apparent from Fig. 1, both titration curves of the 1:2 mixtures have inflections at $m=4$ and $m=5$. No precipitates were observed during the titrations. Figure 3 shows the mole fractions of the various species found in the 1:2 mixtures. For indium, these were: InL, $In(OH)_2L$, InL_2, $InOHL_2$ and InL_3. For thallium, they were: TlL, $Tl(OH)_2L$, TlL_2 and TlL_3.

Both titration curves of the 1:3 mixtures showed inflections at m-values about 4.8 and at 6; in addition, the indium and thallium curves exhibited in-

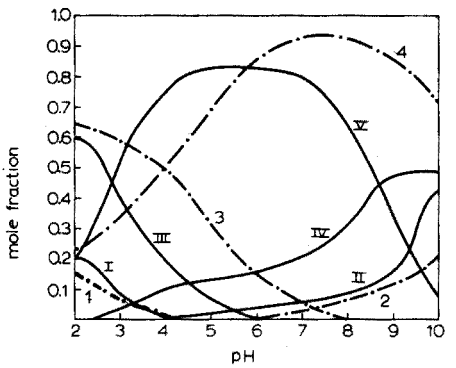

Fig. 4. The mole fractions in 1:3 mixtures of InL (I), $In(OH)_2L$ (II), InL_2 (III), $InOHL_2$ (IV) and InL_3 (V); and of TlL (1), $Tl(OH)_2L$ (2), TlL_2 (3) and TlL_3 (4) plotted as a fraction of pH.

TABLE 1

ABSOLUTE STABILITY CONSTANTS OF THE INDIUM–FERRON AND THALLIUM-FERRON COMPLEXES

(Ionic strength, 0.1 *M*; 25±0.1°C)

Complex	*Constant*[a]	*Log stability const.*	
		Indium–ferron	*Thallium–ferron*
MHL	K_2	~12[b]	—
ML	K_3	15.1	18.9
$M(OH)_2L$	K_5	34.3	33.0
ML_2	K_7	24.2	27.7
$MOHL_2$	K_8	32.7	—
ML_3	K_9	30.7	35.4

[a] As defined in an earlier paper[1]
[b] Estimated value.

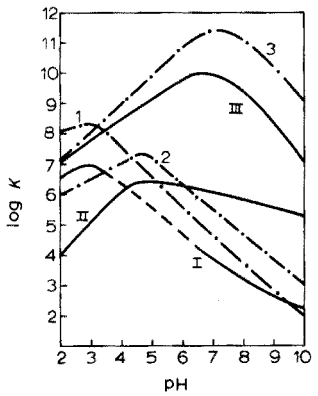

Fig. 5. The logarithm of the conditional constants (log K') of InL (I), InL_2 (II), InL_3 (III), TlL (1), TlL_2 (2) and TlL_3 (3) plotted as a function of pH.

flections at *m*-values of about 7.2 and about 6.3, respectively. No precipitates were formed. Figure 4 shows the species detected in the 1:3 mixtures. The indium complexes were: InL, $In(OH)_2L$, InL_2, $InOHL_2$ and InL_3; the thallium-containing compounds were: TlL, $Tl(OH)_2L$, TlL_2 and TlL_3. The inflections appearing on both curves at *m*-values above 6 are believed to be caused by the formation of more complicated hydroxy compounds.

Table I gives the absolute stability constants of the complexes detected in the two systems. The root mean square error sums were calculated from the absolute stability constants (the constant for InHL was not included) of the indium–ferron and thallium–ferron complexes, and were found to be 0.050 and 0.061, respectively.

The logarithm of the conditional constants of the species ML, ML_2 and ML_3 as a function of pH is plotted in Fig. 5.

Conclusions

This study of the complex formation in aqueous solution of 8-hydroxy-7-iodoquinoline-5-sulphonic acid (ferron) with indium(III) or thallium(III), by potentiometry and a new computer program has proved the existence of various equilibria. In the pH range 2–10, the main species are as follows: InHL, InL, $In(OH)_2L$, InL_2, $InOHL_2$, InL_3, TlL, $Tl(OH)_2L$, TlL_2, and TlL_3. The stability constants and the mole fractions of the various complexes as a function of pH have been calculated and the effect of pH on the conditional constants of the species ML, ML_2 and ML_3 established.

REFERENCES

1 A. Massoumi, P. Overvoll and F. J. Langmyhr, *Anal. Chim. Acta*, 68 (1974) 103.
2 J. F. Spencer and M. Lepla, *J. Chem. Soc.*, 93 (1908) 859.
3 G. Schwarzenbach, H. Flaschka and H. M. N. H. Irving, *Complexometric Titrations*, Methuen, London, 1969, p. 277.
4 S. A. Hamid, J. P. Alimarin and J. V. Puzdrenkova, *Vestn. Mosk. Univ., Ser. II, Khim.*, 20 (1965) 71.
5 G. Biederman, *Arkiv. Kemi*, 5 (1953) 441; *Rec. Trav. Chim.*, 75 (1956) 716.

Analytica Chimica Acta, 71 (1974) 210–214

SHORT COMMUNICATION

Some observations on the determination of copper with thiocyanate

W. P. HAYES, A. H. SASA, V. SHIEK FAREED and D. THORBURN BURNS

Department of Chemistry, Loughborough University of Technology, Loughborough, Leics. LE11 3TU (England)

(Received 20th January 1974)

The precipitation of copper as thiocyanate for analytical purposes was first proposed by Rivot[1] in 1854. The method involves a change in oxidation state from copper(II) to copper(I) before precipitation. Rivot used sodium sulphite as reducing agent, but other reagents have since been proposed. The precipitated copper(I) thiocyanate may be weighed or titrated[2–6]. The conditions for complete precipitation of the copper as thiocyanate have been summarized by Erdey[7]. It is necessary to have sufficient reducing agent, and to avoid excessive acidity and oxidizing agents[8]. The danger of excess thiocyanate has also been noted[9]. Some authors[10] maintain that copper(II) should be reduced to copper(I) before the addition of thiocyanate, and that this is best achieved by boiling the solution with the reducing agent[11]. Taylor[12] indicated that thiocyanate may itself act as a reductant. The precipitation of copper(I) thiocyanate from homogeneous solution, by slow reduction, achieved with glucose formed on hydrolysis of sucrose, by slow liberation of copper(II) on liberation of ammonia, and by temperature-controlled reduction with hydroxylammonium chloride, has been reported by Newman[13].

Pavlikova and Zyka[14] have described a potentiometric titration, for up to 50 mg of copper, with excess of ammonium thiocyanate and hydroquinone as reductant; ammonium chloride and sodium acetate were added to raise the redox potential. An earlier paper by Erdey and Siposs[15] describes a similar procedure with ascorbic acid as reductant which has been confirmed here to be simpler and directly applicable to certain copper alloys.

The first part of the present study was concerned with investigating the relative merits of various reducing agents in gravimetric procedures, the interferences caused by diverse ions, and the conditions under which thiocyanate acts as reductant. The second part describes studies of the titration of copper in the presence of thiocyanate.

Experimental

Standard copper solution. Pure (99.9%) copper foil (2.5000 g) was dissolved in a mixture of concentrated nitric acid (3 ml) and water (3 ml). Concentrated sulphuric acid (5 ml) was added and the solution evaporated to fumes. Water (20 ml) was added and the evaporation repeated. This process was carried out three times. The final solution was diluted to 1 l.

Ammonium thiocyanate solution. A 10% (w/v) solution was prepared daily.

Wash solution. Sodium sulphite (3 g; AnalaR) and ammonium thiocyanate (1 g; AnalaR) were dissolved in water and diluted to 1 l.

Ascorbic acid solution. A 0.025 *M* solution was prepared daily (1 ml ≡ 3.177 mg of copper).

2,6-Dichlorophenol. One tablet (Hopkin and Williams Ltd.), equivalent to 1 mg of ascorbic acid, was dissolved in 5 ml of water.

AnalaR reagents were used where available.

Precipitation of copper(I) thiocyanate

Determination with the addition of various reducing agents. Standard copper solution (50 ml) was taken, and water (150 ml), the reducing agent solution and, where necessary, appropriate amounts of acid or alkali were added. The solution was boiled on a hot plate and sufficient ammonium thiocyanate solution added to give a 0.03 *M* excess. The mixture was left overnight and filtered on a No. 5 sintered glass crucible. The precipitate was washed with the wash solution (300 ml), followed by aqueous 20% ethanol and ether, and finally dried at 120°C to constant weight.

The following reducing agents were used: sulphurous acid (20 ml of water saturated with sulphur dioxide), sodium sulphite (10 ml of aqueous 10% solution), sodium hydrogensulphite (10 ml of aqueous 10% solution), ammonium iron(II) sulphate (65 ml of 0.1 *M*), hydroxylammonium chloride (15 ml of aqueous 3% solution), and ascorbic acid (8.5 ml of aqueous 3% solution). With ascorbic acid it was unnecessary to heat the solution since precipitation proceeded readily at room temperature.

The average recoveries, with each reductant used, were in the range 99.9–100.1%, and coefficients of variation were of the order of 0.2%. No reductant gave significantly better results than any other under the standard conditions examined.

Determination without the addition of a reducing agent. Reddy *et al.*[16] maintain that quantitative reduction of copper(II) and precipitation as copper(I) thiocyanate occurs in acetic acid at 85°C if ammonium thiocyanate is used as reducing agent and precipitant. Their findings were confirmed in the present work and the parameters examined in more detail.

To establish the optimal pH range, a series of solutions were prepared with pH values adjusted in the range 1.35–5.70 by addition of universal buffer and acetic acid or sodium hydroxide solution before addition of ammonium thiocyanate. The solutions were heated on a water bath for 30 min at 85°C. The recovery of copper was quantitative (100 ± 0.1%) in the pH range 2.2–2.8; recoveries were 3% low at pH 1.4, and very low above pH 3.5; no precipitate was formed above pH 5.

To check the effect of varying thiocyanate concentrations, the experiment was repeated on solutions containing 45 ml of 6 *M* acetic acid (resultant pH 2.30). A quantitative yield of copper (100 ± 0.1%) was obtained with 2.5–3.5 g of ammonium thiocyanate. Outside these limits recoveries were low.

Sulphate ions are produced as a result of the reduction reaction. The yield of sulphate ion determined by precipitation as barium sulphate was consistent with the following half-reactions:

$$6\,Cu^{2+} + 6\,e^- \rightarrow 6\,Cu^+;\ SCN^- + 4\,H_2O - 6\,e^- \rightarrow SO_4^{2-} + HCN + 7\,H^+$$

to give an overall reaction:

$$6\,Cu^{2+} + SCN^- + 4\,H_2O \rightarrow SO_4^{2-} + HCN + 7\,H^+ + 6\,Cu^+$$

In checking the effects of diverse ions, no interference was found from As(V), Mo(VI), Co(II), Ni(II), Zn(II), Cr(III), Na, K, sulphate, or phosphate, when added in amounts equal to the copper. Low results were obtained in the presence of equal amounts of cadmium (1.5%), manganese(II) (1.1%) and nitrate (0.6%). High results were found in the presence of silver (10%), mercury(II) (0.5%), and bismuth (4%), present at levels one-fifth that of copper.

Potentiometric titration of copper(II) in the presence of thiocyanate

Potentiometric titrations were carried out by Erdey and Siposs' procedure[15] with solutions containing 20–120 mg of copper diluted to 100 ml with water, 2.5 g of hydrated sodium acetate, 3 g of ammonium chloride and 10 ml of ammonium thiocyanate solution. A bright platinum–saturated calomel electrode pair was used.

The pH of the above solution before titration was 6.2. The titration was repeated but the initial pH was varied with dilute solutions of acetic acid or sodium hydroxide. The workable range was found to be pH 5.7–7.2, low results being obtained outside these limits. The low values for the copper, obtained above pH 7.2, were probably due to the fact that in alkaline solutions the dehydroascorbic acid produced by the reaction tends to be more readily oxidized[17]. The low values obtained below pH 5.7 may well be because, at low pH, ammonium thiocyanate itself acts as a reducing agent.

The ascorbic acid solution was stable for only one day. Formic acid (1.2 ml 90%/l) and disodium–EDTA (0.04 g l^{-1}) were added separately[18] and together, in an attempt to stabilize the ascorbic acid. This aim was achieved, solutions being stable for up to one week, but the additives interfered slightly in the reaction. A stabilized solution was found to be satisfactory, if standardized against a known copper(II) solution or potassium iodate.

Many reducing agents have been suggested for reducing copper(II) to copper(I) before its precipitation as copper(I) thiocyanate. Some of these were used as titrants in the above method instead of ascorbic acid. Compounds examined included hydroxylammonium chloride, sodium thiosulphate, sodium sulphite, hydrazinium sulphate, sodium arsenite, sodium nitrite and manganese(II) sulphate. These all proved unsatisfactory. Ammonium iron(II) sulphate appeared promising but the variance of results was too large.

Visual titration of copper(II) in the presence of thiocyanate

Erdey and Siposs[15] found that, with 2,6-dichlorophenol as indicator, sharp end-points, from blue to colourless, with the precipitate white, were obtained under similar conditions as in the potentiometric titration. These findings were confirmed, the working pH range being 5.7–7.2 and blanks 0.04 ml. Indicators giving colour changes in the appropriate redox potential region that might replace the indophenol include indigo, methylene blue, phenosafranine and variamine blue. None of these was satisfactory; methylene blue gave a response but the blanks were unacceptably large.

Interferences had previously[15] been checked at the 1:10 level. The present

results indicated slightly greater effects in some cases, based on concentration ratios, to give relative errors of 0.25%. Silver, mercury(II) and bismuth, in concentrations equal to that of the copper, had no effect on the end-point. Cd, Mn(II), Zn, Mo(VI), W(VI), Pb and NO_3^-, in amounts up to five times the concentration of copper, did not affect the titration. Similar quantities of cobalt and nickel could be tolerated, but owing to the colour of the solution more indicator was required; this could be allowed for in a blank titration. Aluminium concentrations up to one quarter that of the copper had no effect on the titration, but greater amounts interfered. Solutions containing chromium(III) were too highly coloured for the end-point to be visible, whereas chromium(VI) reacted with the ascorbic acid. Iron(III), even in trace amounts and when complexed with fluoride, could not be tolerated because of the coloration of the solution. Tin(II) and tin(IV), in a soluble form, affected the titration, but if the tin was rendered insoluble as the hydrated oxide by prior treatment, it no longer affected the end-point.

Application of the titrimetric method

Both the potentiometric and indicator methods were tested against pure (99.99%) copper and AnalaR copper sulphate. Quantitative recoveries (99.9–100.1%) were obtained, with a coefficient of variation of 0.2% for the potentiometric method and 0.3% for the indicator method, with solutions containing between 50 and 120 mg of copper. Larger amounts of copper can be determined if the amounts of reagents are increased and the solution diluted to the previous concentration conditions.

A sample of bronze containing 85.0% Cu, 5.03% Sn, 5.16% Zn and 3.35% Pb, and small amounts of Ni, Sb and As, was degreased and warmed with 50% nitric acid, care being taken to avoid loss by effervescence. The solution was then evaporated to low bulk. The operation was repeated after addition of a further quantity of 50% nitric acid. Water (10 ml) was added and concentrated sulphuric acid (5 ml). The solution was heated until fuming and cooled; water (10 ml) was again added, and the solution was evaporated again to fumes. The final mixture was diluted with water so that a 50-ml aliquot contained *ca.* 20 mg of copper. The hydrated tin(II) oxide and the lead sulphate settled sufficiently quickly to allow the clear supernate to be pipetted off for analysis. The volume of the settled solids did not affect the concentration of the supernate within the overall error of the determination. Titration with ascorbic acid to the indicator end-point gave a copper content of 84.7% with a coefficient of variation of 0.3%.

A high tensile brass with 57.2% Cu, 35.5% Zn, 2.2% Mn, 2.5% Al and small amounts of other metals, gave 57.0% copper by the same method, also with a coefficient of variation of 0.3%.

Potentiometric titration gave the same result in both cases but with a slightly smaller coefficient of variation (0.15%).

Discussion and conclusions

Determination of copper in solution by reduction from copper(II) to copper(I) and precipitating as copper(I) thiocyanate can be achieved by using a variety of reducing agents. Thiocyanate itself can act as the reducing agent in the pH range 2.0–2.8, but above pH 5.1 no precipitate is produced, probably because a soluble copper(II) thiocyanate complex is formed. Below pH 2.0 mineral acids cause low recoveries.

In the autoreduction, as in other thiocyanate procedures, it is necessary to have prior knowledge of the approximate amount of copper present in order to achieve precise results. The choice of reductant may be influenced by factors other than efficiency of reduction and overall recovery. When iron(II) is used[19], the large amount of thiocyanate, in excess of that required to react with copper(I), is bound in a complex with iron(III). The indicator properties of the iron(III)–thiocyanate complex provide a convenient means of estimating the correct amount of thiocyanate to add. Ascorbic acid[20] reduces silver salts to the metal, which can be filtered off before the addition of thiocyanate.

The titration of copper(II) by the ascorbic acid procedure[15] is preferred to the hydroquinone procedure[14]. In potentiometric titrations the potential change with ascorbic acid was much greater than found with hydroquinone, making the end-point determination simpler and more precise. No suitable visual indicator was found to use with hydroquinone, but 2,6-dichlorophenol was confirmed to be satisfactory with ascorbic acid. In view of the precision and simplicity of the volumetric procedures their neglect for the routine determination of high levels of copper is hard to explain.

The authors wish to thank Professor R. Belcher, University of Birmingham, for suggesting this study, and Dr. W. T. Elwell, Imperial Metal Industries Ltd., for supplying the analysed samples of brass and bronze and for helpful discussions. One of us (A.H.S.) thanks the Natural Resources Authority, Amman, and the British Council for financial support.

REFERENCES

1 L. E. Rivot, *Compt. Rend.*, 38 (1854) 868.
2 G. S. Jamieson, L. H. Levy and H. L. Wells, *J. Amer. Chem. Soc.*, 30 (1908) 760.
3 A. H. SaSa, *M.Sc. Dissertation*, Loughborough University of Technology, 1971.
4 E. A. Henriques, *J. Chem. Soc., London*, 64 (1893) 345.
5 W. E. Garrigues, *J. Amer. Chem. Soc.*, 19 (1897) 940.
6 S. W. Parr, *J. Amer. Chem Soc.*, 22 (1900) 685.
7 L. Erdey, *Gravimetric Analysis*, Part II, Pergamon, London, 1965.
8 R. Belcher and A. J. Nutten, *Quantitative Inorganic Analysis*, Butterworths, London, 3rd. edn., 1970.
9 I. A. Korshunov and N. I. Malyugina, *Zh. Obshch. Khim.*, 20 (1950) 1399.
10 W. T. Elwell and D. Price in C. L. Wilson and D. W. Wilson (Eds.), *Comprehensive Analytical Chemistry*, Vol. 1c, Elsevier, Amsterdam, 1962, p. 368.
11 I. M. Kolthoff and G. H. P. Van der Meene, *Z. Anal. Chem.*, 72 (1927) 337.
12 F. S. Taylor, *Inorganic and Theoretical Chemistry*, Heinemann, London, 9th. edn., 1952.
13 E. J. Newman, *Analyst (London)*, 88 (1963) 500.
14 M. Pavlikova and J. Zyka, *Z. Anal. Chem.*, 172 (1960) 321.
15 L. Erdey and J. Siposs, *Z. Anal. Chem.*, 157 (1957) 166.
16 D. V. Reddy, S. B. Rao and N. A. Rayu, *Curr. Sci.*, 36 (1967) 149.
17 I. M. Kolthoff and R. Belcher, *Volumetric Analysis*, Vol. III, Interscience, New York, 1957.
18 L. Erdey and E. Bodor, *Anal. Chem.*, 24 (1952) 418.
19 R. Belcher and T. S. West, *Anal. Chim. Acta*, 6 (1952) 337.
20 E. C. Stathis, *Anal. Chim. Acta*, 16 (1957) 21.

Analytica Chimica Acta, 71 (1974) 215–217

SHORT COMMUNICATION

Gravimetric and turbidimetric determination of silver with thione reagent

M. EDRISSI
Department of Chemistry and Chemical Engineering, Tehran Polytechnique, Tehran (Iran)
A. MASSOUMI and M. REZAZADEH
Department of Chemistry, Pahlavi University, Shiraz (Iran)
(Received 21st December 1973)

The sodium salt of 2-mercaptopyridine-N-oxide (thione) which has been used for the gravimetric determination of iron(III)[1] and for spectrophotometric determinations of iron(III)[2] and palladium(II)[3] can be used for the gravimetric or turbidimetric determination of silver(I). The white insoluble complex of silver is formed over a wide range of pH (2–12), is not light-sensitive, and is suitable for the determination of 5–110 mg of silver. Smaller quantities (0.6–6.5 p.p.m.) of silver can be measured turbidimetrically with the same reagent. In acidic media the reagent reacts with about twenty cations giving insoluble chelates, but in alkaline solutions of pH 9–12 and in the presence of tartrate as a masking agent, the cations which form precipitates with the reagent are Ag(I), Hg(II), Cu(II), Pd(II), Co(II), Ni(II), Sn(II) and Au(III).

Experimental

Reagents. The sodium salt of 2-mercaptopyridine-N-oxide (Aldrich) was recrystallized from chloroform–ethanol mixture (m.p. 251–252°C). Standard silver ion was prepared by dissolving metal shot (B.D.H.; 99.9999% purity) in nitric acid. All other reagents were prepared from analytical-grade chemicals.

Apparatus. A Klett and Summerson photoelectric colorimeter was used for turbidimetric determinations with 1-cm diameter tubes. A Corning pH meter model 5 with a glass–calomel electrode was used for checking pH.

Gravimetric procedure. Place an aliquot of silver(I) solution containing 5–110 mg of silver in a 400-ml beaker. Dilute to 100 ml with distilled water and add 10 ml of 10% potassium sodium tartrate. Adjust the pH to about 9–10 by addition of 1 *M* sodium hydroxide or ammonia solution using universal indicator paper. Add 20 ml of borax–sodium hydroxide buffer pH 10 (50 ml of 0.025 *M* borax and 18.3 ml of 0.1 *M* sodium hydroxide followed by about a 20% excess of 0.02 *M* sodium thione, with constant stirring. Heat for 20 min on a hot water bath, filter through a medium-porosity sintered glass crucible, wash 5–6 times with 10-ml portions of water and dry at 120°C for 30 min. Weigh the precipitate as AgC_5H_4NOS which contains 46.10% silver.

Turbidimetric procedure. Place an aliquot of silver(I) solution containing

0.03–0.43 mg of silver in a 50-ml volumetric flask, add 5 ml of 10% tartrate and make slightly alkaline with 1 *M* sodium hydroxide. Add 10 ml of borax buffer solution (see above) and 2 ml of 0.02 *M* sodium thione solution and make up to the mark with distilled water. Invert the flask three times, place in a water bath about 60°C for 5 min, cool to room temperature and mix well. Measure the turbidity at 420 nm using a blue filter and light filter No. 3788G. Run a blank determination in the same way. Prepare a calibration curve over the specified range.

Results and discussion

The optimal pH for the precipitation of the silver–thione complex in an alkaline solution was established by determining 20.8-mg amounts of silver by the above procedure with borate–sodium hydroxide buffer solutions. Within the pH range 9.6–10.8, results were reproducible within 1.6%, therefore pH 10.0 was chosen as the optimum. In acidic media (pH 3.0±1) the precipitation of silver is also

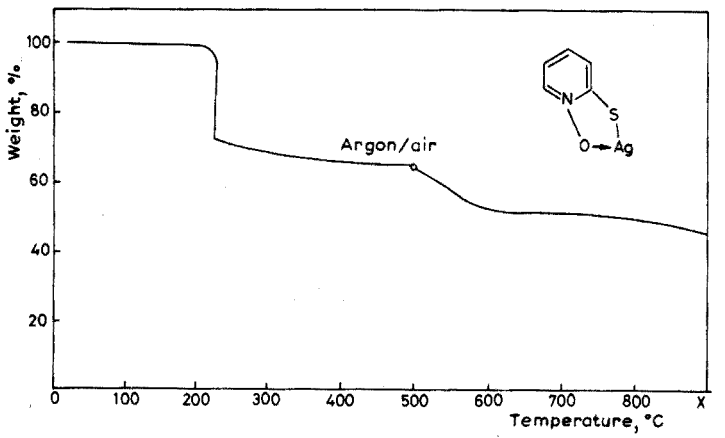

Fig. 1. Thermogravimetric curve of silver–thione chelate.

TABLE I

GRAVIMETRIC DETERMINATION OF SILVER

Ag taken (mg)	*pH ±0.3*	*Ag found (mg)*	*Relative error (%)*
5.2	10.0	5.1	−1.9
		5.2	0
20.8	10.0	20.6	−0.9
		20.9	+0.5
43.2	3.0	43.1	−0.2
		43.3	+0.2
53.6	10.0	53.7[a]	+0.25[a]
75.5	10.0	75.2	−0.4
		75.1	−0.5
109.6	3.0	109.9	+0.3
		109.7	+0.1

[a] Average of 6 determinations: standard deviation, 0.14; coefficient of variation, 0.26%.

quantitative; in this case tartrate and buffer are not added. Precipitation from an acidic solution is only suitable for the standardization of pure solutions of silver(I). Typical results for standard solutions of silver are given in Table I. Application of the Student t-test to the 6 results obtained for 53.6 mg of silver, showed that the difference between mean and true value is not significant at the 95% confidence level ($t = 0.21$); the deviations found are therefore due to random errors.

From the gravimetric results and from elemental microanalysis of the precipitate (calc.: 26.65% C, 1.7% H, 5.95% N, 13.7% S; found: 25.61% C, 1.70% H, 5.92% N, 13.61% S), can be seen that the silver–ligand ratio in the complex is 1:1. A five-membered ring is formed by chelation of silver ion to oxygen and sulphur of the reagent (coordination number 2). The thermogravimetric curve of the precipitate (Fig. 1) shows that the weight of the complex is constant up to about 190°C and therefore it can be easily dried at 120°C.

The advantages of the proposed method over silver chloride precipitation are its lack of light sensitivity and its much more favorable gravimetric factor (0.4610 compared to 0.7526); the gravimetric factor for a commonly used organic reagent of moderate selectivity for silver—1,2,3-benzotriazole[5]—is 0.4774.

In the turbidimetric method for silver with thione as reagent, the calibration graph is linear over the range 0.6–6.5 p.p.m. of Ag^+.

Five determinations on 50 ml of standard silver solution containing 3.2 p.p.m. silver showed a coefficient of variation of 0.96%, which is better than the reproducibility of 2% reported for 8–400 μg silver in 10.0 ml of solution[4] determined by the silver chloride turbidimetric method.

In the gravimetric and turbidimetric determination of silver in alkaline solutions, Cu(II), Pd(II), Ni(II), Au(III), I^- and Br^- seriously interfere. Cobalt(II) was masked by oxidation to cobalt(III) and addition of appropriate amounts of ammonia. Interference of tin(II) was prevented by oxidation to tin(IV) with a suitable amount of iron(III). Thiocyanate and cyanide mask silver ion and must be absent; 1 g of chloride, EDTA, thiosulphate, citrate, sulphate, oxalate, fluoride, carbonate, nitrite, acetate, orthophosphate and chromate did not interfere in the determination of 50 mg (gravimetrically) or 3.0 p.p.m. (turbidimetrically) of silver.

Conclusion

In the pH range 2–12, the white insoluble silver–2-mercaptopyridine-N-oxide complex is not light-sensitive and can be used to determine as little as 5 mg of silver gravimetrically. Smaller quantities (0.6–6.5 p.p.m.) of silver can be measured turbidimetrically. In acidic media the method is not selective but at pH 10 in the presence of tartrate, only Hg(II), Cu(II), Pd(II), Co(II), Ni(II), and Au(III) interfere.

REFERENCES

1 J. A. W. Dalziel and M. Thompson, *Analyst*, 89 (1964) 707.
2 J. A. W. Dalziel and M. Thompson, *Analyst*, 91 (1966) 98.
3 M. Edrissi and A. Massoumi, *Microchem. J.*, 16 (1971) 177.
4 A. Massoumi and A. H. Cornfield, *Analyst*, 88 (1963) 321.
5 M. Kolthoff, P. G. Elving and E. B. Sandell, *Treatise on Analytical Chemistry, Part II*, Vol. 4, Interscience, New York, 1966, p. 38–40.

Analytica Chimica Acta, 71 (1974) 218–221

SHORT COMMUNICATION

A simple microtitrimetric method for alkaline earth metals

V. FANO, F. LICCI and L. ZANOTTI
Laboratorio Maspec del C.N.R., Parma (Italy)
(Received 22nd December 1973)

Recently, several methods have been suggested to improve the sensitivity of determinations of certain alkaline earth elements[1–3]. This communication reports a very sensitive titration, which is applicable to the alkaline earth elements (magnesium, calcium, strontium and barium) either separately or in the presence of calcium. The method is relatively simple, and the analysis time is about 30 min. The method is particularly useful in the analysis of small hexagonal ferrite monocrystals which may show site-dependent concentration for each constituent.

The method involves a microtitration with an extractive end-point. The trace amounts of alkaline earth metals are titrated with EDTA (disodium salt) in the presence of a very small amount of a suitable foreign cation and of dithizone in chloroform. The end-point is obtained by plotting the metal dithizonate concentration in the organic phase, against the EDTA volume added. Calcium can be titrated in the presence of other alkaline earth metals by working at a definite pH value.

Experimental

Apparatus. Extractions were performed in pear-shaped 100-ml separatory funnels with teflon stopcocks. A Beckman model DU2 spectrophotometer was used with glass microcells having a capacity of 1 ml and a path length of 10 mm. A Sargent–Welch NX pH meter was also employed.

Reagents. The aqueous cation solutions used ($0.2 \cdot 10^{-3}$ *M*) were prepared from the respective analytical-grade chlorides.

Buffer solution, pH 10.5, was obtained by dissolving 14 g of ammonium chloride in 114 ml of concentrated ammonia solution and diluting to 200 ml. This solution was purified by shaking with dithizone, the excess of dithizone dissolved in the aqueous solution being back-extracted with chloroform.

The alkaline solution for copper extraction was obtained by adding sufficient ammonia to a 10% ammonium citrate solution to obtain pH 9.5. This solution was purified with dithizone as described above.

Aqueous disodium EDTA solution ($0.2 \cdot 10^{-3}$ *M*) was prepared from the purified salt[4].

The distilled water used was shaken with dithizone and stored in quartz vessels over dithizone solution.

Determination of magnesium, calcium, strontium or barium

Transfer the alkaline earth sample to a 100-ml separatory funnel. Add 5 ml of buffer solution pH 10.5, 0.5–1 ml of aqueous $0.2 \cdot 10^{-4}$ *M* cadmium chloride solution, an appropriate volume of EDTA solution and 2 or 3 ml of $5 \cdot 10^{-5}$ *M* dithizone solution in chloroform. Extract by shaking for a few seconds. Measure the absorbances of the organic phase at 520 and 605 nm, relative to chloroform. Add a new aliquot of EDTA and repeat the operating steps. Repeat this procedure until the equivalence point is reached. This is obtained by plotting the absorbance values of cadmium dithizonate or the derivative value, $\Delta A/\Delta V$, against the added EDTA volume.

Simultaneous determination of calcium and magnesium, strontium or barium. Transfer the solution of the alkaline earth metal mixture to a separatory funnel. Add 5 ml of ammoniacal citrate solution, 0.5–1 ml of aqueous $0.2 \cdot 10^{-4}$ *M* copper chloride solution and a suitable volume of EDTA (enough to complex all of the calcium present, plus an excess). Adjust the pH to 9.5 exactly with ammonia. Shake with 1 or 2 ml of dithizone solution for 5 min. Measure the absorbance of the organic phase at 550 and 605 nm, relative to chloroform. Add a known amount of standard $0.2 \cdot 10^{-3}$ *M* calcium solution, and repeat the extraction and the spectrophotometric measurement. Plot the absorbance values or the derivative value, $\Delta A/\Delta V$, against the added calcium solution volumes, and calculate the equivalence point of the titration. Extract all the copper from the aqueous solution with dithizone. Discard the organic phase. Add concentrated ammonia to the aqueous solution to give pH 10.5. Then proceed as described above.

Results

The described method was verified with alkaline earth metal solutions of known content ranging from 0.1 to 1 μmole. Typical titration curves are reported in Figs. 1 and 2, and some results are summarized in Tables I and II. The absorbances of the cadmium and copper dithizonates were calculated from measurements of the organic phase at two suitable wavelengths (520 and 605 nm for cadmium, and 550 and 650 nm for copper) and from the molar absorptivities of dithizone and the metal dithizonates at the same wavelengths[5].

Discussion

Alkaline earth metals do not react with dithizone[5] but react completely with

TABLE I

DETERMINATION OF ALKALINE EARTH METALS AT pH 10.5

Added (μmole)	*Found (μmole; av. of 3 detns.)*			
	Mg	*Ca*	*Sr*	*Ba*
0.100	0.096	0.102	0.098	0.099
0.200	0.200	0.190	0.206	0.194
0.500	0.490	0.505	0.510	0.500
1.000	1.040	1.000	0.985	1.050

TABLE II

DETERMINATION OF BINARY MIXTURES OF ALKALINE EARTHS

Ca (μmole)		*Mg (μmole)*		*Sr (μmole)*		*Ba (μmole)*	
Added	*Found*	*Added*	*Found*	*Added*	*Found*	*Added*	*Found*
0.500	0.498	0.500	0.506				
0.500	0.499	1.000	1.030				
0.500	0.503			0.500	0.497		
0.500	0.496			1.000	1.020		
0.500	0.495					0.500	0.505
0.500	0.501					1.000	0.990

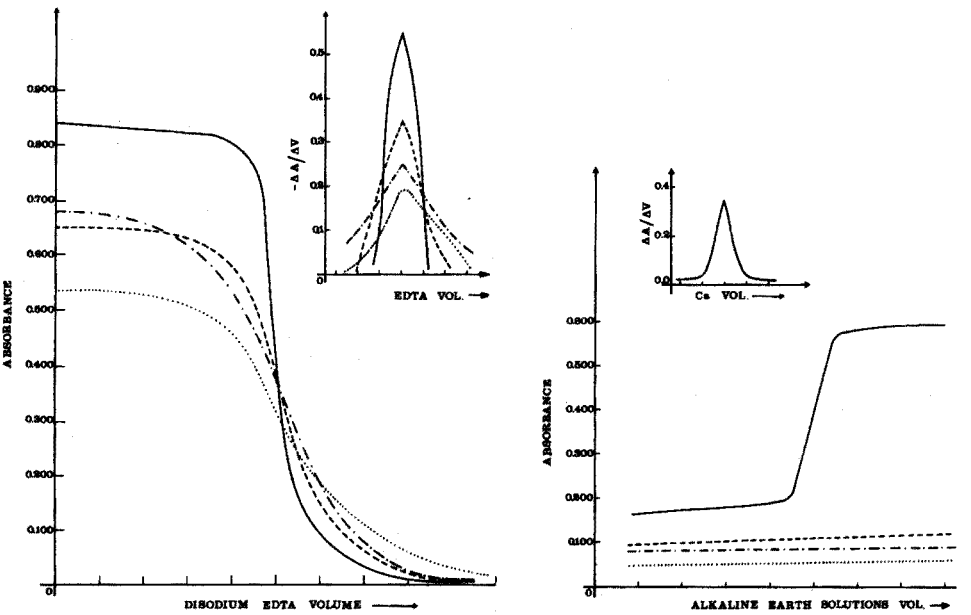

Fig. 1. Titration curves of 0.5 μmole of magnesium (–·–·), calcium (——), strontium (– – – –) and barium (· · · ·) at pH 10.5 with $0.2 \cdot 10^{-3}$ *M* EDTA solution.

Fig. 2. Titration curve of 0.5 μmole of calcium (——) at pH 9.5. Excess of standard $0.2 \cdot 10^{-3}$ *M* disodium EDTA solution was added and back-titrated with standard $0.2 \cdot 10^{-3}$ *M* calcium solution. Magnesium (–·–·), strontium (– – – –) and barium (· · · ·) cannot be titrated.

EDTA at appropriate pH values[4], whereas cadmium and copper form complexes with both reagents. If a sufficient excess of EDTA is present, cadmium—and copper—EDTA complexes are unaffected by dithizone[6]. However, if the concentrations of EDTA and dithizone are of the same order of magnitude, then dithizone and EDTA compete for the cadmium or copper under appropriate pH conditions, as has been proved theoretically[5]. Accordingly, although alkaline earth metals may form weaker complexes with EDTA, they can displace cadmium and copper from their EDTA complexes in the presence of dithizone.

While an excess of alkaline earth metals with respect to EDTA is present in the solution at pH 10.5, all the cadmium is complexed by dithizone in the organic phase. As soon as an amount of EDTA equivalent to alkaline earth ions has been added, the cadmium dithizonate concentration decreases abruptly and consequently there is a sudden decrease in the absorbance of the organic phase. The end-point can therefore be detected by plotting either the absorbance (A) or the derivative value (dA/dV) against the EDTA added. If this titration is used at pH 10.5, the total alkaline earth metal content is obtained.

Calcium can be titrated separately from other alkaline earths because the stability constant of the calcium–EDTA complex ($10^{10.59}$) is higher than those of the magnesium–, strontium– and barium–EDTA complexes ($10^{8.69}$, $10^{8.63}$ and $10^{7.76}$, respectively)[4]. Thus, at lower pH values, only calcium forms a strong enough complex with EDTA to be used analytically. It was shown that 9.5 was the best pH value for determining calcium in the presence of other alkaline earth metals. However, at pH 9.5 cadmium cannot be used as the indicator ion because cadmium dithizonate cannot be extracted into chloroform in a reasonable time, for any ratio of calcium/EDTA present in the aqueous phase. Therefore, copper was preferred as the indicator because it forms a sufficiently strong dithizonate[5]. At pH 9.5, calcium can displace copper from its EDTA complex whereas under the conditions used, magnesium, strontium and barium cannot (Fig. 2). However, calcium cannot be titrated directly, because copper dithizonate, once formed, is unaffected by EDTA. A back-titration is therefore necessary: an excess of standard EDTA solution is added and back-titrated with standard calcium solution. (Citrate medium is employed to prevent precipitation of copper at pH 9.5; see ref. 7). However, whenever possible, cadmium is preferred to copper as the indicator for various reasons: (1) direct titration can be applied; (2) cadmium dithizonate can be extracted more rapidly; and (3) the molar absorptivity is much higher so that the equivalence point is sharper (Fig. 1) and can even be detected visually. Cadmium is preferred to zinc or lead because cadmium dithizonate can also be extracted from strongly alkaline solutions[5].

Conclusions

The proposed analytical procedure can be applied to hexagonal ferrite samples and to a large variety of other substances. As little as 2 μmole l^{-1} of magnesium, calcium, strontium and barium can be titrated with an error less than 5–6%. The determination of calcium in the presence of other alkaline earths may be achieved by a very simple procedure. Up to a ratio of alkaline earth to calcium of 2:1, the simultaneous determination is satisfactory.

REFERENCES

1 V. Mikhailova and P. Ilkova, *Anal. Chim. Acta*, 53 (1971) 194.
2 H. Berge and A. Drescher, *Fresenius Z. Anal. Chem.*, 231 (1967) 11.
3 K. Hagiwara, *Rev. Polarog.*, 13 (1965) 78, 84.
4 F. J. Welcher, *The Analytical Uses of Ethylenediaminetetraacetic Acid*, Van Nostrand, New Jersey, 1958.
5 J. Starý, *The Solvent Extraction of Metal Chelates*, Pergamon, Oxford, 1964.
6 H. Friedeberg, *Anal. Chem.*, 27 (1955) 305.
7 G. H. Morrison and H. Freiser, *Solvent Extraction in Analytical Chemistry*, Wiley, New York, 1957.

Analytica Chimica Acta, 71 (1974) 222–224

SHORT COMMUNICATION

A universal ion-selective electrode based on graphite paste*

JOSEPH P. SAPIO, J. F. COLARUOTOLO and J. M. BOBBITT
Department of Chemistry, University of Connecticut, Storrs, Conn. 06268 (U.S.A.)
(Received 9th February 1973)

Růžička and his co-workers have recently described[1–4] a design for a universal electrode which can be used as an ion-selective electrode for a number of anions and cations. The functioning portion of the electrode (called a Selectrode) is porous Teflon-treated graphite powder compressed into a semi-solid rod. One end of this graphite rod holds the material responsible for the ion selectivity. This material may be either a solid or a liquid and may be easily replaced by another material containing the ion of interest. In this communication, a design is proposed for a universal ion-selective electrode with many of the advantages of the Selectrode and a much simplified construction (Fig. 1). It is based on the Adams graphite paste electrode[5] and represents a continuation of our work on these electrodes[6].

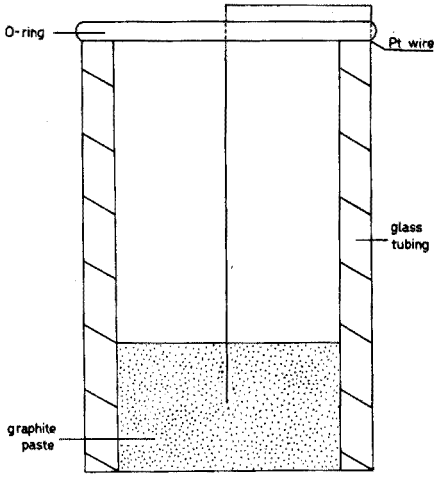

Fig. 1. An ion-selective graphite paste electrode.

Construction of electrodes

The electrode consists of a graphite paste prepared from a liquid ion exchanger containing the ion of interest (a cation or an anion) and commercial

* This Short Communication was previously published with the reference *Anal. Chim. Acta*, 67 (1973) 240–242. Unfortunately, the printer introduced a number of serious errors which render parts of the paper unintelligible. For this reason it is repeated here, after correction, in its entirety.

graphite powder (technical grade, cat. no. G-64, Fisher Scientific Co., Fairlawn, N.J.; washed with 6 *M* hydrochloric acid, water, and methanol; and dried at 110° for 3 h). A chloride ion-selective paste was prepared from 5 g of graphite and 3 ml of Aliquat 336, a liquid quaternary ammonium chloride (General Mills Chemicals Inc., Minneapolis)*. A nitrate ion-selective paste was prepared similarly, with Aliquat 336 in the nitrate form. The exchanger was converted to the nitrate form by shaking 25 ml of the exchanger (in the chloride form) in 100 ml of hexane with six 100-ml portions of 1.5 *M* sodium nitrate. A calcium ion-selective paste was prepared by mixing the same proportions of graphite powder and the liquid ion-exchanger solution, 0.1 *M* calcium didecylphosphate in di-n-octylphenylphosphonate (Orion Research. Inc., Cambridge, Mass.). A 10-mm thick layer of the graphite paste was packed into one end of a length of 6 mm to 11 mm o.d. glass tubing around a platinum wire which was secured at the other end of the tubing with a rubber O-ring. No other conditioning of these electrodes was necessary.

Potential measurements were made at 25° with a Leeds-Northrup pH meter (model 7401) with a saturated calomel reference electrode. With the chloride electrode, a double-junction reference electrode was used, with saturated potassium nitrate solution separating the SCE from the chloride solutions.

Results and discussion

The chloride and nitrate ion-selective electrodes were found to give linear plots of *E vs.* $-\log a$ over the activity range of 0.003–0.85 *M*, with a slope of 54 mV/decade activity change (curve A, Fig. 2). Although this slope is not Nernstian (59.5 mV/decade at 25°), the potential measurements were reproducible (within a few hours) over the activity range of 0.0001–0.85 *M*. With regard to selectivity, it was found that, at an activity level of 0.001 *M* chloride, interference-free measurements were obtained with the chloride electrode in the presence of 0.0001 *M* Br^-, I^-, NO_3^-, and ClO_4^-. Similarly, at an activity level of 0.001 *M* nitrate, interference-free measurements were obtained with the nitrate electrode in the

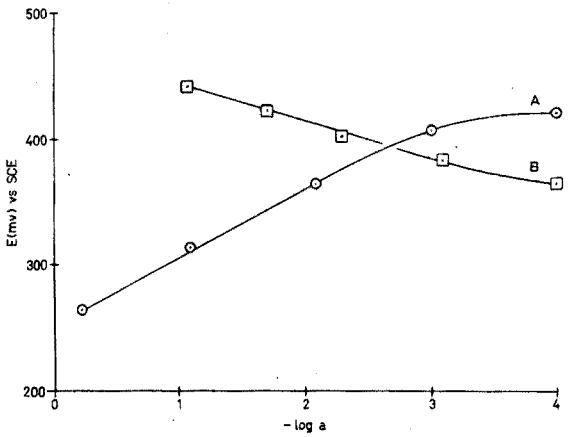

Fig. 2. Response of the paste electrode to the activity of chloride or nitrate ion (A) and calcium ion (B).

* For applications of Aliquat 336 involving other ions, see ref. 7.

presence of 0.0001 M Cl^-, Br^-, I^-, and ClO_4^-. For both electrodes, measurements at pH greater than 9 should be avoided because of interference from the hydroxide ion.

The calcium ion-selective electrode was found to give a linear plot of E *vs.* $-\log a$ over the activity range of 0.001–0.1 M with a slope of 30 mV/decade activity change (curve B, Fig. 2). However, the potential measurements were reproducible (within a few hours) over the activity range of 0.0001–0.1 M. The calcium electrode displayed a somewhat better selectivity over interferences than the chloride and nitrate electrodes. At an activity level of 0.0001 M calcium(II), interference-free measurements were obtained in the presence of 0.001 M Mg^{2+} and Ba^{2+}, and 0.01 M Na^+.

Measurements at pH less than 6 should be avoided because of interference by the hydrogen ion.

The drawbacks to these electrodes are their sensitivity to stirring and their need for periodic restandardization. The measurements were carried out in unstirred solutions, but it was found that moderately rapid magnetic stirring caused fluctuations in potential measurements of ± 3 mV. The value of E^0, which was obtained for each of these electrodes by extrapolating the plot of E *vs.* $-\log a$ to $-\log a = 0$, changed with daily use.

A number of new electrodes could result from further investigation of paste systems. Many ions, both anions and cations, can be exchanged into such liquids as Aliquat 336 (for anions) and the liquid phosphonates (for cations), and these can easily be converted to selective pastes[7].

We wish to thank Professor J. T. Stock of this Department for his many helpful suggestions.

REFERENCES

1 J. Růžička and K. Rald, *Anal. Chim. Acta*, 53 (1971) 1.
2 J. Růžička and C. G. Lamm, *Anal. Chim. Acta*, 53 (1971) 206.
3 J. Růžička and C. G. Lamm, *Anal. Chim. Acta*, 54 (1971) 1.
4 J. Růžička, C. G. Lamm and J. C. Tjell, *Anal. Chim. Acta*, 62 (1972) 15.
5 R. N. Adams, *Electrochemistry at Solid Electrodes*, Marcel Dekker, New York, 1969, pp. 280–283.
6 J. M. Bobbitt, J. F. Colaruotolo and S. J. Huang, *J. Electrochem. Soc.*, 120 (1973) 773.
7 C. J. Coetzee and H. Freiser, *Anal. Chem.*, 40 (1968) 2071.

Analytica Chimica Acta, 71 (1974) 225–227

SHORT COMMUNICATION

Determination of the hydrogensulphite content in wine by means of the air-gap electrode

ELO HARALD HANSEN, HENRIQUE BERGAMIN FILHO* and JAROMIR RŮŽIČKA
Chemistry Department A, The Technical University of Denmark, Building 207, Lyngby (Denmark)
(Received 28th January 1974)

The recently introduced ammonia[1] and sulphur dioxide[2] gas-sensing electrodes facilitate and speed up a number of determinations. Thus, the Orion sulphur dioxide electrode is said[2] to be useful for measurement of sulphur dioxide in flue gases, industrial atmospheres, and sulphite pulping liquors, and for determination of the sulphur content in fuel oil. Moreover, the determination of sulphur dioxide in wine[3], cider[4] and soft drinks[5], which normally requires a time-consuming distillation (in a nitrogen atmosphere[3] or at a reduced pressure[4]) followed either by titration (alkalimetry[4] or iodimetry[3]) or by spectrophotometry[5], might be simplified by application of SO_2-sensing electrodes.

Similarly to the ammonia electrode, the sulphur dioxide electrode employs, as a pH-sensing element, a glass electrode covered by a thin layer of an electrolyte that at the same time covers a reference electrode. The gas from the sample diffuses through a hydrophobic, gas-permeable membrane and changes the pH of the electrode layer. According to the reaction:

$$SO_2 + H_2O \rightleftharpoons HSO_3^- + H^+ \quad (1)$$

the pH_e sensed by the electrode should decrease with increasing partial pressure of SO_2, established within the hydrophobic membrane, if the inner electrolyte contains a suitable concentration of hydrogensulphite. Provided that the equilibrium has been reached, and that the HSO_3^- concentration of the electrode surface remains constant, a tenfold change in $p\,SO_2$ would correspond to a change of one pH_e unit. For measurements of sulphite or hydrogensulphite in aqueous samples, these have to be acidified to below pH 1.7 in order to achieve quantitative conversion to SO_2. At the same time oxidizing conditions (which would cause a negative error by converting SO_2 to HSO_4^-) should be avoided. Owing to few interferences ($3 \cdot 10^{-3}$ *M* hydrofluoric acid, $5 \cdot 10^{-3}$ *M* acetic acid and .1 *M* hydrochloric acid would give the same response as $1 \cdot 10^{-4}$ *M* HSO_3^-)[2] and to the fast response of gas sensors, a rapid method for food and beverage analysis can be envisaged. However, shortcomings like clogging of the gas-permeable membrane and leakage of the inner electrolyte around the gas membrane, as recently reported to occur with the Orion ammonia

* Present address: CENA, Escola Superior de Agricultura "Luiz de Queiroz", Caixa Postal 96, 13.400-Piracicaba, Estado de Sao Paulo (Brazil).

electrode[6], might also impair the use of the sulphur dioxide sensor. It was therefore decided to test the recently developed air-gap electrode[7, 8], which is free of such shortcomings, as a sulphur dioxide sensor, and apply it for determination of the hydrogensulphite content in wines of various origin.

Experimental

The apparatus and electrodes were the same as described previously[7]. The larger electrode chamber, having a total volume of 8.0 ml, was used in all experiments. The electrolyte solution ($1 \cdot 10^{-3}$ *M* $NaHSO_3$ in aqueous 20% ethanol) was saturated with a wetting agent (Victawet 12, Stauffer Chemical Co., U.S.A.) and its pH was adjusted to 5.0 with sodium hydroxide. This solution as well as the standard solutions of sodium hydrogensulphite were prepared fresh each day. The electrolyte layer on the surface of the glass electrode was renewed after each measurement by letting the air-gap electrode rest in a perspex holder containing a sponge soaked with the electrolyte solution[7]. When not in use, the electrode was similarly stored in the electrode holder.

Calibration curve. This was obtained by pipetting 1.00 ml of the standard solution of sodium hydrogensulphite into a polyethylene reaction beaker, which fitted snugly into the electrode chamber. A Teflon-covered magnetic stirring bar was placed into the beaker, followed by 1.00 ml of acid solution (20% v/v phosphoric acid in aqueous 20% ethanol). The chamber was then immediately closed by the body of the air-gap electrode and the magnetic stirrer was started. When the pH_e reached a steady-state value, it was read to 0.001 pH_e. For each standard hydrogensulphite solution ($1.00 \cdot 10^{-2}$ *M*, $1.00 \cdot 10^{-3}$ *M*, $1.00 \cdot 10^{-4}$ *M* and $3.00 \cdot 10^{-5}$ *M*), three measurements of pH_e were taken and used for construction of the calibration curve.

The calibration curve was computed on a Wang 700B Programmable Electronic Calculator provided with a Wang 702 Plotting Output Writer by means of a linear regression analysis programme. The calibration curve was then used in

TABLE I

DETERMINATION OF THE HYDROGENSULPHITE CONTENT IN WINES

Sample	*Type of wine*	*Hydrogensulphite content (mol l^{-1})*	*pH*[a]	*Taste*[b]
Cordier, Saint-Julien-Medoc, Château Grand-Larose, Cru Classé, 1960	Red	$(3.7 \cdot 10^{-7})$[c]	3.54	E
Côtes du Rhône, App. Contr. A. Bichot & Cie., 1971	Red	$\sim 5.8 \cdot 10^{-7}$	3.61	G
Chatelet (France)	Red	$3.1 \cdot 10^{-6}$	3.52	F
Home made, 1973	Red	$1.8 \cdot 10^{-4}$	3.35	F
Chablis (France)	White	$2.1 \cdot 10^{-4}$	3.50	G
Home made I, 1973	White	$\sim 6.7 \cdot 10^{-7}$	3.15	G
Home made II, 1973	White	$1.0 \cdot 10^{-4}$	3.17	F

[a] Natural pH of the wine.
[b] E, excellent; G, good; F, fair.
[c] Limit of the method.

the subsequent evaluations of the wine samples. With the standard solutions, a straight line was obtained with a slope of 0.50 pH_e per decade of hydrogensulphite concentration, the standard deviation being 0.04 pH_e (regression coefficient 0.9990).

When the wine samples were analysed, the same procedure was used, but a parallel blank was run for each sample in order to make sure that the reading was related to the hydrogensulphite content and not to any volatile acid present. This was done by adding 0.05 ml of saturated potassium dichromate to the wine sample before analysis. None of the samples of wine, in which the hydrogensulphite was thus oxidized, gave a reading which was higher than $4 \cdot 10^{-7}$ *M* $NaHSO_3$—corresponding to the actual limit of the electrode response.

Results and discussion

The results of the analyses are summarized in Table I, where the pH of the wines before analysis, the origin of the wines, and a subjective taste evaluation are also given.

The white wines generally had a higher hydrogensulphite content than red wines, and the most expensive wine had a content lower than the detection limit of the method. None of the wines were found to have a hydrogensulphite content higher than that permissible for human consumption[9] (350 p.p.m. SO_2 corresponding to $5.5 \cdot 10^{-3}$ *M* $NaHSO_3$).

It takes only a few minutes to make an analysis which is selective, although not very accurate (0.04 pH_e corresponds to a standard deviation of about 16%). Thus the present results must be considered as preliminary, and further improvements of the experimental technique are necessary. The discrepancy between the predicted slope of the calibration curve, which according to eqn. (1) should amount to 1.0 pH_e per decade of hydrogensulphite concentration, and the value found in the present investigation, which was exactly half that value, also remains to be explained. As the reason was certainly not an error in electrode function (as confirmed by calibration in buffer solutions), another chemical reaction seems to take place at the electrode surface. Further research is planned to establish the relation between the free SO_2 content, the hydrogensulphite content and the acetaldehyde-bound hydrogensulphite[4,5], and to confirm the utility of the method on a larger number of wine samples of different origin.

REFERENCES

1 *Orion Research Specifications List for Ammonia Electrode Model 95-10*, Form DS 95-10/1711, Massachusetts, U.S.A.; Electronic Instruments Limited, Leaflet No. 8002-2/3.
2 *Orion Research Specifications List for Sulfurdioxide Electrode Model 95-64*, Form DS 95-64/373, (1973) Massachusetts, U.S.A.; Electronic Instruments Limited, Advanced Information 8010-2/1, 1973.
3 L. Deibner and N. Heredia, *Chim. Anal. (Paris)*, 48 (1966) 66.
4 L. F. Burroughs and A. H. Sparks, *Analyst*, 89 (1964) 55.
5 W. J. Lloyd and B. C. Cowle, *Analyst*, 88 (1963) 394.
6 H. F. Proelss and B. W. Wright, *Clin. Chem.*, 19 (1973) 1162.
7 J. Růžička and E. H. Hansen, *Anal. Chim. Acta*, 69 (1974) 129.
8 E. H. Hansen and J. Růžička, *Anal. Chem.*, (submitted for publication).
9 *List of Approved Food Additives and Their Use*, The National Food Institute of Denmark, 1973.

Analytica Chimica Acta, 71 (1974) 228–231

BOOK REVIEWS

G. Guiochon and C. Pommier, *Gas Chromatography in Inorganics and Organometallics*, Ann Arbor Publishers, Ann Arbor, Michigan—J. Wiley, New York, 1973; vii + 332 pp., price $ 20.00 (£ 10.00).

The practice of gas chromatography as a major analytical technique has encouraged the publication of numerous general and specialized texts. In recent years the latter have concentrated more on instrumentation and techniques than on specific areas of chemical application; review texts in the latter areas are particularly welcome.

This monograph by Guiochon and Pommier is a competent and readable translation of their French text *La Chromatographie en Phase Gazeuze en Chemie Inorganique* published in 1971, the authors having updated much of the text with references through early 1973; it is unfortunate however that a better English title was not devised. The authors have provided a critical review of an important and expanding area which should remain definitive for a considerable time. The work has many strong points, not least among which is the consistency of style and subject coverage frequently absent from the now ubiquitous multi-author texts. The authors also frequently comment on and expand specific reviewed subject matter thus generally enhancing the value to the reader.

Included first is a section on general theoretical concepts and instrumentation aimed expressly at the reader with no previous background in gas chromatography. It is arguable whether this could not be better gained in a general rather than a specialized text. However, the major chapters on inorganic gases, halogens and non-metallic halides, metals and metal halides, hydrides, organo-metallic compounds, metal chelates and isotopes are of a high standard and will supply ample background for analytical problem solving in any of these areas. General analytical and non-analytical applications are also well reviewed and comprehensive compound indices included.

There is no question that this text will be essential for any chemist involved in the study of volatile inorganic compounds and, despite its high price, it can be strongly recommended.

P. C. Uden (Amherst)

Modern Practice of Liquid Chromatography, edited by J. J. Kirkland, Wiley–Interscience, New York, 1971, xix + 454 pp., price £7.00.

This book is the printed version of a series of lectures presented at a course on column liquid chromatography in April 1970. The following subjects are discussed in the twelve chapters: relationship of theory to practice (51 p.), apparatus for separation (40 p.), detectors (30 p.), role of the mobile phase (33 p.), practice of liquid–liquid chromatography (44 p.), practice of liquid–solid chromatography

(32 p.), practice of gel permeation chromatography (49 p.), practice of ion-exchange chromatography (37 p.), overview of liquid chromatography (16 p.), comparison of separation mechanism (32 p.), applications using controlled surface porosity support (41 p.) and analysis of nucleic acids constituents (23 p.). A preface, a list of symbols and a subject index is included. A bibliography is given at the end of each chapter comprising a total of 268 references covering the period up to 1970.

The names of the authors of the various chapters guarantee a competent treatment of the subjects. Most of them have made significant contributions to the development of modern column liquid chromatography. The book was written at a rather early state of development of the method. Consequently, significant progress has been made in the meantime. Nevertheless, it contains a large amount of information which is still very relevant. The presentation of a subject in the form of a compilation of articles written by different authors has inherent advantages and disadvantages. The reader has the benefit of being confronted with different approaches and views, but this results in a certain heterogeneity in the presentation. The editor has succeeded to a high degree in his task of homogenizing the presentation.

The book can be recommended to anybody who works or intends to work in the field of chromatography. It tries to give the necessary understanding of the theoretical background in order to give help in the practical application. The printing is good and the price reasonable.

J. F. K. Huber (Amsterdam)

Analytical Chemistry–4, edited by Mitsugi Senda, Butterworths, London, 1973 vi + 170 pp., price £5.00.

This book contains the eleven plenary lectures presented at the International Congress on Analytical Chemistry, Kyoto, 1972. It covers widely differing aspects of the subject, from kinetics of complex formation (Alimarin) and the application of chelate compounds (Belcher) to radiochemical methods (Meinke), non-dispersive atomic absorption systems (Walsh), and precipitate-based ion selective electrodes (Pungor and Toth). Electrochemistry in non-aqueous solvents (Charlot) is described, as are developments in quantitative organic ultramicro elementary analysis (Kirsten) and mathematical concepts relating to trace analysis (Kaiser). Analytical studies of the environment (West) are topical, and the discussion of the development of chromatographic detectors (Martin) is a delightful exercise in unconditioned thinking. Finally, the account of the development of analytical chemistry in Japan (Somiya) throws light on a subject little exposed outside that country. All the papers are in English, apart from that by Charlot which is in French.

Many of the articles are of the length that one could normally expect to be delivered in about an hour's lecture. Those of Kaiser, and especially of Pungor and Toth, however, appear to be expanded versions with much additional information. All the articles are well produced, and the Editor is to be congratulated in uniting them into a single volume without too marked a contrast between styles.

A. Townshend (Birmingham)

I. I. Nazarenko and A. N. Ermakov, *Analytical Chemistry of Selenium and Tellurium*, Israel Program for Scientific Translations, Jerusalem–J. Wiley, London, 1972, x+281 pp., price £9.35.

This monograph, a translation of the 1971 Russian edition, follows the usual format of this series. General information on the two elements is followed by an account of physical and chemical properties of the elements and their compounds, especially their complexes. There is a brief discussion of qualitative analysis. Gravimetric and titrimetric methods are dealt with first, followed by an extensive account of spectrophotometric and fluorimetric methods. Other instrumental methods described include various electrochemical and flame spectroscopic techniques, emission, spectrography, X-ray fluorescence and radioactivation methods. The next chapter discusses solvent extraction, chromatographic methods, precipitation and distillation as means of separating selenium and tellurium from other elements, and the final chapter is concerned with methods for the determination of selenium and tellurium in a wide range of samples. The bibliography (1185 references) occupies 44 pages and is followed by a subject index.

Like previous volumes in this series, the treatment is comprehensive rather than critical, although the treatment of some of the instrumental techniques is rather brief in relation to their current importance. Also, work published after 1968 is not included. Nevertheless, since nearly half of the papers (479) quoted are from the Russian literature, the text provides a valuable summary of the Russian contribution to the analytical chemistry of selenium and tellurium, as well as giving an overall account of the subject. The material is clearly presented, and appears to be free of significant errors.

A. Townshend (Birmingham)

M. Spiteller and G. Spiteller, *Massenspektrensammlung von Lösungsmitteln, Verunreinigungen, Säulenbelegmaterialien und einfachen aliphatischen Verbindungen*, Springer-Verlag, Wien, 1973, xvi+232 pp., price DM 58,—.

After a brief discussion of mass spectrometry, the authors outline the most important considerations in dealing with the spectra of solvents, impurities and simple aliphatic compounds. The detailed spectra of 170 compounds of these types are then given. For ease of comparison, all the spectra were obtained on a Varian MAT CH4 mass spectrometer. The compilation should facilitate the interpretation of mass spectra, particularly in g.c.–m.s. work.

Bibliography of Column Chromatography 1967–1970, Edited by Z. Deyl, J. Rosmus, M. Juricova and J. Kopecky (*J. Chromatogr.*, Supplementary Vol. 3, 1973), Elsevier, Amsterdam, 1973, xix+1067 pp., price Dfl. 180.000 (paperback).

This large bibliography is divided into two parts. The first general part lists reviews, books, theory and general information, techniques, elution, comparisons with other techniques, and quantitative analysis. The second part treats organic compounds by class; generally the references are listed as reviews, techniques

and applications, though sometimes the compound classes themselves are subdivided. The first part contains 800 references, whereas the special part contains 9382, only about 450 of which deal with inorganic materials. Altogether, over 10,000 references are listed—a rather daunting total for only 4 years of published work. The energy which has gone into this compilation should be greatly appreciated by everyone who uses chromatography.

Gas and Liquid Chromatography Abstracts, 1972, Edited by C. E. H. Knapman and R. J. Maggs, Applied Science Publishers, Barking, England, 1973, xviii+251 pp., price £8.00.

This compilation, sponsored by the Institute of Petroleum, requires no introduction to gas chromatographers. The collection for 1972 maintains the usual high standard of the series, containing 853 abstracts for gas chromatography and 69 abstracts for liquid chromatography. This is the last volume of the series, which will now appear as a journal on a quarterly basis.

J. G. Gibson and J. L. Sudworth, *Specific Energies of Galvanic Reactions and Related Thermodynamic Data*, Chapman and Hall, London, 1973, xvi+820 pp., price £10.00.

In a search for suitable galvanic reactions for high-energy battery systems, the authors started to calculate the specific energies of various reactions, and ended up calculating cell voltages and temperature coefficients also, for an enormous number of reactions involving metal oxides, sulphides and halides. This book contains the photostated computer outputs, which are estimated to correspond to 6 man-years of calculation, and would be useful to anyone concerned with energy conversion.

F. Seel, *Atombau und Chemisch Bindung. Eine Einfuhrung in die moderne Theorie der chemischen Bindung auf anschaulicher Grundlage*, 8. Auflage, F. Enke, Stuttgart, 1974, viii+117 S., PVC-katoniert: DM 16.80.

M. H. Jones and J. T. Woodcock, *Ultraviolet spectrometry of flotation reagents with special reference to the determination of xanthate in flotation liquors*, Institution of Mining and Metallurgy, London W1N 4BR, 1973, 25 pp., price £2.50.

Analytica Chimica Acta, 71 (1974) 232

ANNOUNCEMENTS

9th International Congress on Clinical Chemistry

The 9th International Congress on Clinical Chemistry will be held in Toronto during the week July 13th–18th, 1975, at the new Four Seasons Sheraton Hotel.

The Congress will offer exceptional opportunities for contact with new scientific and technical advances in this field, as well as the chance of exciting vacation travel in Canada and the United States of America. A full social programme for members and associate-members is also being planned.

An advance brochure will be distributed to National Societies early in 1974, but others who are interested may obtain a brochure on application to Dr. F. H. Sims, Chairman of the Publicity Committee, Women's College Hospital, Toronto, Ontario, Canada.

7th Materials Research Symposium

The 7th Materials Research Symposium will be held on October 7th–11th, 1974, at the National Bureau of Standards, Gaithersburg, Maryland, U.S.A.

The object of the Symposium is to define the present status of accuracy, and the means of obtaining accuracy, in trace analytical chemistry. Over the past several years there has been an explosion in the number of chemical analyses performed, especially in the areas of environmental quality (both air and water), plant and animal tissues, biological fluids, high purity materials, and geological samples. Because the results of these analyses are used in making important projections and decisions, both short and long term, it is essential that they be reliable. The various factors which contribute to obtaining accurate analytical results will be explored in the Symposium. Particular emphasis will be placed on the whole analysis, from taking the sample through interpretation of the results, rather than upon the measurement only.

The Symposium will consist of a series of invited lectures by experts as well as the presentation of particularly appropriate contributed papers. Because of time limitations, some manuscripts may be accepted for inclusion in the written proceedings which were not presented orally at the Symposium. A break-down of the topics to be covered is presented:

1. Sampling: Techniques; Contamination; How Representative
2. Sample Handling: Storage Problems; Dissolution; Reagent Purity; Laboratory Environment
3. Analysis: Control of the Analytical Blank; Choosing the Most Appropriate Technique; Reporting and Interpreting Results

Further details can be obtained from: Dr. Philip D. LaFleur, B108 Reactor Building, National Bureau of Standards, Washington D.C. 20234. Telephone: (301) 921-2613.

Analytica Chimica Acta, 71 (1974) 233–253

THE USE OF FLAME PROCEDURES IN METALLURGICAL ANALYSIS

PART I. DETERMINATION OF SILICON IN SULPHIDE AND SILICATE MINERALS

R. J. GUEST and D. R. MACPHERSON

Chemical Analysis Section, Extraction Metallurgy Division, Department of Energy, Mines and Resources, Ottawa, Ontario K1A 0G1 (Canada)

(Received 12th December 1973)

The need for rapid analytical methods for process control has led to the more extensive use of flame procedures in this laboratory. As part of a continuing study on the development of such methods, the atomic absorption analysis of silicon was investigated with a view to its application to complex sample materials from hydrometallurgical and pyrometallurgical process work.

The first and, in many ways, the most important requirement is to obtain complete dissolution of the silica in a stable solution which is compatible with the method and apparatus used. Two dissolution procedures were chosen for investigation: (a) a Teflon bomb procedure based on the procedure of Ito[1], as modified by Langmyhr and Sveen[2], Langmyhr and Paus[3], and Bernas[4], and (b) a sodium peroxide fusion in a zirconium crucible as described by Petretic[5], and later by Dinnin[6]. Although the Teflon bomb procedure is known to be suitable for application before atomic absorption analysis of silicon[3,4], the use of sodium peroxide fusion for this purpose has received little attention. It was chosen for use here, as an alternative to the Teflon bomb procedure, because of its simplicity and its known effectiveness on difficultly soluble sample material. The stability of the silicon in the sample solution and the effect of contaminants on results in the media used were tested because information found in the literature is sometimes conflicting, probably because of the different conditions and equipment used by investigators.

The procedures were used on fourteen hand-picked minerals, chosen as typical of those encountered in common silicate and sulphide gangue material. Also, from the individual minerals, six mixtures were made up, similar in composition to typical ores and products from process work. It was felt that the use of pure minerals, alone and in combination, would enable analysts who are familiar with the mineralogy of their sample materials to extrapolate the data of this report to the analysis of specific materials. In addition, the use of pure minerals permitted the simulation of a number of different ores by using a comparatively small number of samples. Also, it simplified the establishment of the silicon content of the complex mixtures because they were put together from simpler, more easily analysed components.

The procedures were also used on some typical sample materials, including

high iron–titanium and high iron–manganese samples from pyrometallurgical process work, types of sample material for which atomic absorption analysis for silicon has been sparsely reported. Analysed Standard samples of similar composition to the samples were not available; therefore, it was necessary to simulate them by combining Standard Reference Materials in a series of combinations, then analysing these samples by the recommended procedures.

EXPERIMENTAL

Apparatus

Teflon bombs, model 4745 (Parr Instrument Company, Moline, Illinois, U.S.A.), and zirconium crucibles (45 ml) were used.

A Jarrell–Ash atomic absorption spectrophotometer, model 82–300 dual double-beam fully compensated unit, was used with a Hetco total consumption burner, with a Jarrel–Ash Tri-flame laminar-flow head. The burner height was 19 cm from the burner top to the bottom of the burner holder.

A Techtron atomic absorption spectrophotometer, model AA-3, was used with a model AA-5 burner–atomizer with plain-slot and grooved burner heads.

Reagents

The acids used were of analytical-reagent grade, where available. The sodium peroxide was reagent grade. Sodium solutions prepared from the peroxide, chloride or nitrate were 5% (w/v) and were stored in plastic.

Standard silicon solution

Weigh out fused silica powder and take it into solution with either a Teflon bomb or a sodium peroxide fusion procedure. Treat the standard in the same manner as the samples and as described later under Dissolution procedures. This solution should contain between 200 and 500 p.p.m. of silicon.

Take an aliquot of the main silicon solution, add enough hydrochloric acid to ensure that the final solution will be acidic, add enough sodium solution to bring the sodium content to about 6000 p.p.m., and dilute the solution to volume.

If solutions of silicon plus contaminants are required, add the contaminant to the diluted silicon standard just before making up the standard to the mark in the volumetric flask.

The final solution should contain between 10 and 200 p.p.m. silicon.

Dissolution procedures

Teflon bomb procedure. Weigh 0.2–0.5 g of sample into the sample container of the Teflon bomb. Add 2–3 ml of aqua regia as a wetting agent, then 3 ml of concentrated hydrofluoric acid. Cover the Teflon cup, enclose it in the metal shell, and close the bomb hand-tight. Place the bomb in a drying oven at 140°C for about 45 min, and then cool it to room temperature in a cold-water bath before loosening its screw-top. Transfer the sample to a plastic beaker; rinse the Teflon cup with 20 ml of warm 14% boric acid solution, transfer the sample solution to a 100-ml volumetric flask, and dilute to the mark with water. Mix, and transfer the solution to a plastic bottle for further dilution, for direct atomization, or for storing.

Sodium peroxide fusion. Weigh 0.5–2 g of sample into a zirconium crucible, add sodium peroxide from a 5-g weighed portion and mix intimately, finally covering with the remaining sodium peroxide. Cover the crucible with a zirconium cover and place it in a muffle furnace at 640°C for 30 min. Cool.

Place the crucible and contents in a plastic beaker and add water gradually to keep the reaction moderate, until the melt is leached from the crucible. Add concentrated hydrochloric acid to the beaker containing the crucible until the solution becomes acid and clears. The entire amount of acid should be added at once, otherwise silicon may come out of solution. Add enough acid to bring the solution to between 3 and 5% hydrochloric acid, remove the crucible, and rinse it with distilled water. Transfer the solution to an appropriate volumetric flask and dilute to the mark.

Atomic absorption procedure

Take an aliquot of the main sample solution and place it in an appropriate volumetric flask. Add enough of a sodium solution (see Reagents) so that the final dilution for atomization will be about 6000 p.p.m. in sodium, making sure that the sample solution remains well on the acid side by adding hydrochloric acid. Dilute to the mark with water. This solution should contain between 10 and 200 p.p.m. of silicon.

Atomize the sample directly, and, on the Jarrell–Ash atomic absorption spectrophotometer, compare readings with pure silicon standards which are close to the amount of silicon expected in the sample and which, preferably, span the sample content.

Atomic absorption parameters

	Jarrell–Ash Model 82-300	*Techtron Model AA-3*
Wavelength	251.6 nm	251.6 nm
Lamp current	10 mA	12 mA
Range	variable	
Slit	100 and 150 μm (bandpass 0.16 nm)	50 μm (bandpass 0.17 nm)

In both cases, nitrous oxide–acetylene flames were used, the flames being just luminous.

APPLICATION OF ATOMIC ABSORPTION PROCEDURES TO SYNTHETIC SOLUTIONS

Stability and sensitivity shown by standard silicon solutions

Opinions are known to differ concerning the stability of silicon solutions in various media[4,7–11]. Although the hydrofluoric–boric acid system is generally acknowledged to be satisfactory, a greater difference of opinion is found concerning silicon stability in mineral acid solution in the absence of hydrofluoric acid.

In an attempt to clarify this point, tests were carried out to establish the effect of ageing and dilution on the sensitivity and/or linearity found for pure silicon solutions in (a) hydrochloric acid, (b) hydrochloric–hydrofluoric–boric acid, and (c) hydrofluoric–boric acid media. In (a) and (b), a sodium peroxide fusion was used to solubilize pure silica powder, whereas in (c), a Teflon bomb procedure

was used. In all tests, the sodium content was normalized at between 3000 and 6000 p.p.m.

It was found that, following a sodium peroxide fusion and the addition of a 3–5% excess of hydrochloric acid to its water leach, the stability of a 400-p.p.m. silicon solution was good for at least 4 weeks, with or without further dilution. The 400-p.p.m. silicon solution, following the Teflon bomb procedure, was also stable for at least four weeks but, after fourfold dilution, it had deteriorated in strength, by the fourth week, by about 8%.

The sensitivity obtained for atomic absorption readings after dissolution by bomb and fusion varied with the instrumental parameters and, especially, with the type of flame used. It was found that a barely luminous flame gave the best combination of sensitivity and low flame background. A comparison of the sensitivity for silicon in hydrochloric acid and hydrofluoric–boric acid media, run at approximately the same time and with the same flame type and instrumental parameters, showed little difference in sensitivity.

Satisfactory linearity was found for silicon absorption in hydrofluoric–boric acid medium after a bomb procedure at the normal 3% (w/v) level and after dilutions of this solution. However, if the 3% solution was concentrated (*i.e.* more $HF–H_3BO_3$ added), results became erratic and linearity was very poor in the 10–100-p.p.m. working range. In any event, as a matter of routine practice, it was more convenient to dilute the 3% hydrofluoric–boric solution when preparing samples and their matching silicon standards.

Silicon standards in either hydrochloric acid or in hydrochloric–hydrofluoric–boric acid solution after a sodium peroxide fusion, showed satisfactory linearity. However, erratic results and loss of linearity ensued after hydrofluoric and boric acids had been added to a silicon solution, in hydrochloric acid after a fusion, that had been allowed to stand for a few weeks.

Effects of contaminants on silicon results

The extent of elemental interference in the atomic absorption determination of silicon has been reported by a number of workers[8,12–15]. Some of the variations in their findings presumably reflect the effects of the different solution media used, as well as the different instrumental types and parameters used. Several investigators[10,13,16–18] have compensated for interfering effects by running analysed standard samples with regular samples, for comparison purposes. This technique, though possible in some cases, is not always practical in this laboratory because of the wide variety of materials to be analysed. It was considered important, therefore, that the procedure permit comparison against pure silicon standards. Accordingly, synthetic solutions were tested to ascertain better the points at which common contaminants interfered with results.

Measured amounts of solutions of iron, titanium, potassium, copper, lead, aluminum, magnesium, calcium, and manganese were added alone and, at times, together, to standard silicon solutions. The contaminants, in most instances, were put into solution with both Teflon bomb and sodium peroxide fusion procedures. Aliquots of these solutions in hydrochloric acid medium and/or hydrofluoric–boric acid medium were then combined with aliquots of a standard silicon solution. Sodium was present in all tests. The amounts of contaminant added represented the

TABLE I

EFFECT OF CONTAMINANTS ON SILICON RESULTS BY ATOMIC ABSORPTION AFTER TEFLON BOMB DISSOLUTION

($HF–H_3BO_3$ medium)

Silicon present (p.p.m.)	*Contaminant[a] and amount present (p.p.m.)*	*Ratio of silicon to contaminant*	*Silicon found (p.p.m.)*	*Deviation (%)*
100	3000 Fe	1:30	99.1	− 0.9
50	3000 Fe	1:60	50.0	0.0
100	1500 Ti	1:15	100.3	+ 0.3
50	1500 Ti	1:30	49.6	− 0.8
100	700 Al	1:7	96.8	− 3.2
50	700 Al	1:14	52.0	+ 4.0
100	430 Mg	1:4	100.3	+ 0.3
50	430 Mg	1:9	50.8	+ 1.6
100	285 Ca	1:3	99.4	− 0.6
50	285 Ca	1:6	51.1	+ 2.2
50	200 Mn	1:4	97.8	− 2.2
100	200 Mn	1:2	97.8	− 2.2
20	5800 Pb	1:290	33.5	+67.5
20	12000 Pb	1:600	31.4	+57.0
100	200 K	1:2	93.5	− 6.5
50	200 K	1:4	48.4	− 3.2
48	4400 Cu[b]	1:90	60.6	+26.3
24	2400 Fe+2200 Cu	1:100 Fe: 90 Cu	27.7	+15.4
100	50 Al+20 Ca	1:0.5 Al: 0.2 Ca	100.0	0.0
100	430 Fe+215 Ti +100 Al+ 60 Mg + 40 Ca+ 30 Mn + 30 K		99.8	− 0.2

[a] From 3000 to 5000 p.p.m. sodium present except where noted.
[b] No sodium added.

highest ratio of each contaminant to silicon found in the types of sample material encountered during this study.

Teflon bomb dissolution: $HF–H_3BO_3$ medium. Results, as shown in Table I, indicated that in the hydrofluoric–boric acid system following a Teflon bomb dissolution, most of the contaminants added did not cause recoveries to vary beyond experimental limits of ±5%. However, large amounts of copper and lead caused high results, which would necessitate addition of comparable amounts of the respective contaminants to the silicon comparison standards. None of the other elements, except iron, was present in this sample material in quantities comparable to copper and lead, therefore similarly high contaminant:silicon ratios for the other elements were not tested.

Fusion dissolution: HCl medium. After the silicon and the contaminant had been fused in sodium peroxide and the melt dissolved in hydrochloric acid, it was found that most of the elements added did not affect results beyond experimental limits. However, large amounts of iron, copper, and lead caused very high results

TABLE II

EFFECT OF CONTAMINANTS ON SILICON RESULTS BY ATOMIC ABSORPTION AFTER SODIUM PEROXIDE FUSION

(HCl medium)

Silicon present (p.p.m.)	*Contaminant[a] and amount present (p.p.m.)*	*Ratio of silicon to contaminant*	*Silicon found (p.p.m.)*	*Deviation (%)*
100	3000 Fe	1:30	100.00	0.0
50	3000 Fe	1:60	53.0	+ 6.0
50	6500 Fe	1:130	60.3	+20.1
100	1500 Ti	1:15	100.2	+ 0.2
50	2000 Ti	1:40	51.9	+ 3.8
100	700 Al	1:7	101.0	+ 1.0
50	1000 Al	1:20	49.6	− 0.8
100	430 Mg	1:4	100.8	+ 0.8
50	600 Mg	1:12	49.0	− 2.0
100	285 Ca	1:3	99.8	− 0.2
50	430 Ca	1:9	50.5	+ 1.0
100	200 Mn	1:2	100.2	+ 0.2
20	12000 Pb	1:600	30.4	+52.0
100	200 K	1:2	100.0	0.0
50	300 K	1:6	50.0	0.0
100	50 Al+20 Ca	1:0.5 Al: 0.2 Ca	100.5	+ 0.5
48	4400 Cu	1:90	61.5	+28.1
24	2200 Cu+2400 Fe	1:90 Cu: 100 Fe	28.2	+17.5
100	430 Fe+215 Ti +100 Al+60 Mg + 40 Ca+30 Mn + 30 K	—	99.6	− 0.4

[a] From 3000 to 6000 p.p.m. sodium present.

(Table II). It was clearly indicated that, when samples containing preponderant amounts of these elements are analysed, the addition of the main contaminant to the standard silicon solutions would be essential.

Fusion dissolution: HCl–HF–H_3BO_3 medium. With the hydrofluoric–boric acid system after fusion dissolution, most of the contaminants added tended to cause high (apparent) silicon recoveries at lower levels of sodium content. This could be compensated for, to a major extent, by increasing the sodium content. These tests, which were carried out with the Techtron atomic absorption spectrophotometer, encountered burner problems at these sodium levels, and especially beyond 12,000 p.p.m. sodium, because of clogging of the burner slot, which necessitated frequent washing of the burner. This technique then, while useable when necessary, was not pursued further as it was not considered to be especially suitable for routine work.

APPLICATION OF THE PROCEDURES TO SULPHIDE AND SILICATE MINERALS AND THEIR MIXTURES

In the literature on atomic absorption procedures, relatively little has been

reported on pure minerals, especially on mineral mixtures. Dissolution techniques for minerals with hydrofluoric acid, with and without a Teflon bomb, have been reported[1,2,19], while other dissolution procedures with lithium compounds have also been used[11,20].

Individual minerals

Decomposition of the minerals. Teflon bomb and sodium peroxide fusion procedures were applied to the fourteen hand-picked minerals selected. The minerals chosen were considered to be the most common constituents of the type of silicate and sulphide gangue minerals in the rock-types commonly encountered here. The composition of these minerals may be seen in Table III.

It was found that all of the minerals could be dissolved by a sodium peroxide fusion. However, with a Teflon bomb dissolution, some residue remained from the pyrite sample, although each of the other minerals was completely soluble. Smaller amounts of pyrite, if mixed with other minerals, went completely into solution in the bomb procedure (see *Mineral mixtures*). In the case of galena, a white precipitate, probably lead sulphate, came down in the solution left standing after both dissolution procedures.

In the peroxide fusion in zirconium crucibles, it was found important to prevent the fusion temperature from going much higher than the 640°C normally used. Otherwise, some fine white precipitate, which could contain some silicon, appeared in the acid solution after fusion of some of the minerals. This precipitate was probably zirconia, formed by attack of the sodium peroxide on the zirconium crucible.

Comparison of atomic absorption results with chemical results. All of the samples were analysed for silicon by atomic absorption procedures after both Teflon bomb and fusion dissolutions. The silicon results obtained gravimetrically and by atomic absorption were compared and the deviation was calculated. It was difficult to obtain consistent gravimetric results on several of the samples, and this made comparison of results more difficult than had been expected.

As shown in Table IV, gravimetric and atomic absorption results showed an average deviation of less than 5% for all samples, including those at both extremes of the procedural range. On the two samples which were low in silicon (galena and chalcopyrite), the ratio of major contaminant to silicon was as high as 600:1. In these cases, the results obtained were corrected by adding the major contaminant to the standard, otherwise the silica values would have been high. Following this procedural step, agreement with gravimetric results was considered to be satisfactory at this low silicon level.

Discrepancies were found, however, between atomic absorption and gravimetric results on the feldspar (labradorite) and amphibole samples. As the contaminant present in these samples was well below the amount previously found to cause interference in the atomic absorption procedure, this lack of agreement was surprising. In an attempt to resolve the greater of these discrepancies, a synthetic sample was prepared to simulate the composition of the feldspar (labradorite). Also, as will be shown in Table VI, a mixture of minerals was made up to approximate the chemical composition of the same feldspar. In both cases, no difficulties were found with the atomic absorption procedures on these prepared

TABLE III

COMPOSITION OF THE MINERALS ANALYSED FOR SILICON

Mineral type	*Source of mineral*	*Mineral composition (approximate %)*								
		Si	*Al*	*Ca*	*Mg*	*Fe*	*Na*	*K*	*S*	*Other*
Amphibole (hornblende): metasilicate of Na, Ca, Mg, Al, Fe	Faraday Mine, Bancroft, Ont.	20	5	7	9	12	—		—	—
Biotite: silicate of Fe, Mg, K, Al	Douglas, Ont.	18	6	—	10	15	—			—
Chalcopyrite: sulphide of Cu, Fe	Temagami, P.Q.	0.4	<0.1	—	—	33	—	—	31	30
Pyroxene: metasilicate of Ca, Mg, Fe	Sandy Creek, New Otter Lake, P.Q.	25	<0.1	18	11	3	—	—	—	—
Feldspar (labradorite)	Tabor Island, Coast of Labrador	25	14	7	—	—	—	—	—	—
Oligoclase: feldspar, albite and anorthite blend	Kragero, Norway	30	12	2	—	—	—	—	—	—
Feldspar (albite): disilicate	Villeneuve, P.Q.	30	12	—	—	—	—	—	—	—
Feldspar (microcline)	Black Mine, Buckingham Area, P.Q.	30	12	—	—	—	—	—	—	
Muscovite: hydrous silicate	Purdy Mine, Eau Claire, Ont.	20	15	—	—	—	—	—	—	—
Serpentine: hydrous silicate	Portland Township, P.Q.	20	<0.1	—	25	—	—	—	—	—
Talc	Madoc, Ont.	28	<0.1	—	17	—	—	—	—	—
Galena	Keno Hill, Yukon	0.1	—	—	—	—	—	—	13	87 Pb
Pyrite: sulphide of Fe	Ambasaguas, Spain	0.9	<0.1	—	—	46	—	—	53	—
Quartz	Lyndhurst, Ont.	46	<0.1	—	—	1	—	—	—	<0.1

TABLE IV

COMPARISON OF ATOMIC ABSORPTION RESULTS WITH CHEMICAL RESULTS ON COMMON MINERALS

Mineral type	*Silicon found gravimetrically (%)*	*Silicon found by a.a.s. (%)*		*Deviation of a.a.s. and chemical results (%)*	
		Teflon bomb dissolution	*Fusion dissolution*	*Bomb*	*Fusion*
Amphibole (hornblende)	19.6[a]	21.7	21.0	+10.7	+ 7.1
Biotite	18.1[b]	18.3	18.55	+ 1.1	+ 2.5
Chalcopyrite	0.31[b]	0.34[g]	0.35[g]	+10.	+13.
Pyroxene	24.5[c]	24.0	25.15	− 2.0	+ 2.7
Feldspar (labradorite)	25.2[a]	28.9	29.1	+14.7	+15.5
Oligoclase	28.8[a]	29.2	29.5	+ 1.5	+ 2.4
Feldspar (albite)	29.9[a]	30.95	30.3	+ 3.5	+ 1.4
Feldspar (microcline)	29.95[a]	30.6	30.55	+ 2.2	+ 2.0
Muscovite	20.8[a]	20.55	21.9	+ 1.2	+ 5.1
Serpentine	19.3[b]	19.05	19.35	− 1.2	+ 0.4
Talc	28.15[c]	28.3	28.7	+ 0.5	+ 1.95
Galena	0.10[d]	0.11[h]	0.116[h]	+10.	+16.
Pyrite	0.94[b]	0.935	0.935	− 0.5	− 0.5
Quartz	45.5[b,e]	47.4	47.3	+ 4.1	+ 3.9
	46.0 (by diff.)[f]	47.4	47.3	+ 2.8	+ 2.5

[a] Multi-acid attack to perchloric fumes, followed by Na_2CO_3 fusion of the insoluble residue, then a single dehydration with perchloric acid.

[b] Multi-acid attack, single perchloric dehydration. This method was unsatisfactory on amphibole, pyroxene, the feldspars, muscovite, talc and galena—yielded low and/or erratic results.

[c] Multi-acid attack to sulphuric fumes, then Na_2CO_3 fusion of the insoluble residue, followed by a double dehydration with hydrochloric acid. This method was unsatisfactory for amphibole, the feldspars and muscovite—yielded low and/or erratic results.

[d] Multi-acid attack to perchloric fumes, then digestion of the insoluble residue with ammonium acetate solution (range of results was 0.12–0.09% Si).

[e] Multi-acid attack to perchloric fumes, Na_2CO_3 fusion of the insoluble residue, then double dehydration with $HClO_4$.

[f] Value obtained by subtracting impurities found in the mineral.

[g] Corrected value to compensate for Cu and Fe present (0.40% without correction).

[h] Corrected value to compensate for Pb present (0.17% without correction).

samples.

The amphibole and feldspar samples were submitted for fluorine analysis by neutron activation; 1.46% fluorine was found in the amphibole sample but less than 0.05% in the feldspar. This could account for the lower gravimetric result on the amphibole, because no precautions were taken in the chemical procedure to prevent premature loss of silicon tetrafluoride. However, the cause of the disagreement between the atomic absorption and gravimetric results on the feldspar (labradorite) sample has not been established.

TABLE V

PRECISION OF ATOMIC ABSORPTION RESULTS FOR SILICON ON SOME COMMON MINERALS

Sample type	*Sample treatment*	*Average result*[a] *(% Si)*	*Standard deviation*	*Coefficient of variation (%)*	*95% Confidence limits for average result*
Feldspar	Teflon bomb	28.3	±0.30	±1.06	±0.37
Feldspar	Fusion	28.5	±0.26	±0.90	±0.32
Muscovite	Teflon bomb	20.55	±0.43	±2.09	±0.53
Muscovite	Fusion	21.9	±0.56	±2.56	±0.69
Quartz	Teflon bomb	47.4	±0.17	±0.36	±0.21
Quartz	Fusion	47.3	±0.495	±1.05	±0.60

[a] Average of 5 determinations.

Precision found for the atomic absorption procedures

The precision of the two atomic absorption procedures was calculated by the methods of Dean and Dixon[21], and of Bauer[22]. In each case, a single sample weighing, each of feldspar, muscovite and quartz was taken, with five individual sets of atomic absorption measurements being made, representing two readings in each case. It was intended that, as the sample was carefully mixed and completely in solution, the precision found would be a measure of the reproducibility of the instrumental and flame conditions. The latter variable, in particular, was difficult to reproduce without elaborate gas control equipment, and it was considered to be the largest single factor affecting the precision found. The coefficient of variation obtained for the Teflon bomb procedure averaged 1.2%, compared with 1.5% obtained for the fusion procedure (Table V).

Mineral mixtures

Decomposition of mineral mixtures. Six mineral mixtures of the composition shown in Table VI were prepared and were put into complete solution by both the Teflon bomb and the fusion dissolution procedures. The solutions of the mixtures remained clear during the analyses. After 10 days, however, a precipitate, which appeared to be siliceous, became apparent in the hydrochloric acid solution of the fused Mixtures 1 and 4 and in the solution from Teflon bomb dissolution of Mixture 4.

Comparison of atomic absorption with chemical results. Silicon results found on the sample mixtures were compared with calculated silicon values for the mixtures, as determined both by atomic absorption and by gravimetric analyses on the individual minerals making up the sample. The deviation found, calculated for atomic absorption results *versus* both atomic absorption and gravimetric results on the individual minerals, was considered acceptable in that it was within 2%. The satisfactory agreement, between the atomic absorption results on the mineral mixtures and on individual minerals, indicated that interaction of minerals did not affect results (Table VII).

Application of the procedures to certified standard samples and their mixtures

A number of Certified Standard samples were chosen, and mixtures of them

TABLE VI

COMPOSITION OF THE MINERAL MIXTURES PREPARED FOR SILICON DETERMINATION

Mineral mixture	*Element present (%)*						
	Si	*Al*	*Ca*	*Mg*	*Fe*	*Cu*	*Pb*
1[a]	40.4	2	<1	<1	3–4	—	—
2[b]	27.4	6	<1	2–3	7–8	3	—
3[c]	24.4	3	1	1–2	15–20	1–2	—
4[d]	9.56	3	<1	<1	23–27	6	9
5[e]	3.43	1	<1	<1	20–25	12	26
6[f]	25.9	10	0.5–1	0.2–0.5	1–2	—	—

[a] Elliot Lake uranium ore (80% quartz, 13% muscovite, 5% pyrite, 1% oligoclase and 1% biotite).
[b] High-copper ore (50% feldspar(albite), 20% quartz, 10% chalcopyrite, 5% pyrite, 5% amphibole, 5% biotite and 5% serpentine).
[c] Low-copper ore (20% feldspar(microcline), 30% quartz, 30% pyrite, 5% talc, 5% chalcopyrite, 5% pyroxene and 5% oligoclase).
[d] Flotation concentrate (40% pyrite, 20% chalcopyrite, 10% galena and 30% feldspar(microcline)).
[e] Flotation concentrate (20% pyrite, 40% chalcopyrite, 30% galena and 10% feldspar(microcline)).
[f] Feldspar(labradorite) (25% pyroxene, 50% oligoclase and 5% muscovite).

TABLE VII

COMPARISON OF ATOMIC ABSORPTION AND CHEMICAL RESULTS ON PREPARED MINERAL MIXTURES

Mineral[a] mixture	*Silicon present[b]*		*Silicon found by a.a.s.[c]*		*Deviation— a.a.s. vs. calculated results*		
	A.a.s. average (%)	*Gravimetric average (%)*	*Bomb (%)*	*Fusion (%)*	*Previous result for comparison*	*Bomb (%)*	*Fusion (%)*
1	41.2	40.0	40.45	40.05	A.a.s.	−1.7	−2.7
					Grav.	+1.0	+0.05
2	27.8	27.2	27.6	27.3	A.a.s.	−0.79	−1.9
					Grav.	+1.4	+0.29
3	24.7	24.2	24.4	24.25	A.a.s.	−1.4	−2.0
					Grav.	+0.99	+0.37
4	9.65	9.43	9.65	9.97	A.a.s.	0.0	+3.3
					Grav.	+2.3	+5.7
5	3.46	3.34	3.40	3.55	A.a.s.	−1.7	+2.6
					Grav.	+1.8	+6.3
6	26.1	25.7	25.8	26.1	A.a.s.	−1.3	0.0
					Grav.	+0.27	+1.4

[a] For sample composition see Table VI.
[b] Calculated silicon content based on (a) the average of atomic absorption results, and (b) gravimetric results, found on the individual minerals making up the sample.
[c] Based on two sets of readings from one sample weighing.

TABLE VIII

COMPOSITION OF CERTIFIED STANDARD REFERENCE SAMPLES ANALYSED FOR SILICON

Sample type		*SiO_2 (%)*[a]	*Al (%)*	*CaO (%)*	*MgO (%)*	*TiO_2 (%)*	*Fe (%)*
BCS 27C, Mesabi ore		2.08	—	—	—	—	65
NBS 116a, ferrotitanium		6.68	3	—	—	25	65
BCS 301, Lincolnshire iron ore		7.20	2	22	2	0.1 (Ti)	25
BCS 302, iron ore		20.0	4	3	1	0.4	36
BCS 303, iron ore sinter		16.5	4	20	2	0.2 (Ti)	36
Mixture of 208/1 (ferromanganese) and BCS305(ferrosilicon)	Ratio 6:1	25.0	0.2	0.1	—	0.1	16
Mixture of NBS 27C	1:2	0.69	—	—	—	66	22
(Mesabi ore) and NBS	2:1	1.39	—	—	—	33	43
154a(titanium dioxide)							
Mixture of BCS 301	1:2	2.40	1	7	0.6	66	8
(iron ore) and NBS 154a	1:1	3.60	1	11	1	50	12
(titanium dioxide)							
Mixture of BCS 303	1:2	5.50	1	7	1	66	12
(iron ore) and NBS 154a	1:1	8.25	2	10	1	50	18
(titanium dioxide)							

[a] Certified.

prepared, to approximate in content the type of sample material encountered in high-temperature furnace work. The compositions of these sample mixtures (Table VIII) leaned heavily toward high-titanium sample material, as methods to obtain gravimetric silicon results on slags from smelting of ilmenite ore were especially time-consuming and not always reliable. All samples analysed were found to be readily dissolved by the Teflon bomb and sodium peroxide fusion procedures.

Comparison of silicon results with both pure and contaminant-added standards

Hydrofluoric–boric acid medium. Two mixtures of certified iron ore and titanium dioxide, a 1:1 mixture of BCS 301 and NBS 154a, and a 1:2 mixture of BCS 303 and NBS 154a (see Table VIII), were analysed for silicon by the Teflon bomb and peroxide fusion procedures. In all cases, hydrofluoric and boric acids, and sodium were present or added, and atomic absorption measurements were compared with both pure and contaminant-added silicon standards. The samples were analysed in two sets, which were done at different times, but are disparate primarily because of the varying atomizer efficiency encountered during their analyses. For these tests, with the Techtron spectrophotometer, the atomic absorption results obtained by comparison with pure silicon standards were inconsistent and showed poor agreement with certified results, the deviation varying over a range of 8.9–23.6%. When standards similar in composition to the samples were used for comparison, the deviation from the certified results was much better, varying over a range of 0.3–6.4%. Also, the consistency of results was good, a coefficient of variation of 2% being found. During this test the Techtron atomizer system showed a gradual deterioration in efficiency over a period of time and cleaning was necessary at frequent intervals.

Hydrochloric acid medium. The same two mixtures of certified iron ore and titanium dioxide used in the previous test, were fused with sodium peroxide and solubilized in hydrochloric medium. Atomic absorption measurements were then made by comparison with pure silicon standards and with contaminant-added standards, with the Techtron atomizer–burner.

It was found that comparison standards containing either single- or multi-contaminants gave results that were much more consistent than those found when pure silicon comparison standards were used, as the latter results fluctuated widely. With contaminant-added standards for comparison, however, an average deviation of 0.35% from the certified results was found, with the average coefficient of variation being about 1.2% (Table IX).

From this test and the previous one, it was concluded that hydrofluoric–boric acid, and hydrochloric acid media were each suitable for use, and that when the Techtron atomizer was used, a major contaminant should be added to the comparison standards.

Comparison of atomic absorption results with the certified chemical results

Five Certified Standard samples, and seven mixtures made from Certified Standard samples, were put into solution by the Teflon bomb procedure. Also, six of these samples were fused with sodium peroxide and dissolved in hydrochloric acid medium. Atomic absorption results found with the Jarrell–Ash spectrophotometer for pure silicon standards, and with the Techtron spectrophotometer for con-

TABLE IX

ATOMIC ABSORPTION RESULTS FOR SILICON ON MIXTURES OF CERTIFIED STANDARD SAMPLES

(Pure and contaminant-added standards for comparison, HCl medium)

Sample	*Sodium[a] present (p.p.m.)*	*Ratio silica: contaminant in comparison standard*	*Silica found (% SiO_2)*
Mixture of certified iron ore and titanium dioxide 1:1 BCS 301 and NBS 154a	12,000	SiO_2:No contaminant	3.67[b], 2.96[b]
	6,000	SiO_2:No contaminant	2.55[b], 3.89[b]
	6,000 and 12,000	1 SiO_2:10 Fe	3.60
	6,000	1 SiO_2: 4 Fe	3.66
	6,000 and 12,000	1 SiO_2:10 TiO_2	3.67
	6,000	1 SiO_2: 4 TiO_2	3.61
Ratio 1 SiO_2:	6,000 and 12,000	1 SiO_2:10 Al_2O_3	3.60
3 CaO	6,000	1 SiO_2: 4 Al_2O_3	3.59
14 TiO_2	6,000 and 12,000	1 SiO_2:10 MgO	3.56
4 Fe	6,000	1 SiO_2: 4 MgO	3.59
0.3 Al_2O_3	6,000 and 12,000	1 SiO_2:10 CaO	3.57
0.3 MgO	6,000	1 SiO_2: 4 CaO	3.59
(3.60% SiO_2)	12,000	1 SiO_2:Multi-contaminant[c]	3.70
Mixture of certified iron ore and titanium dioxide	6,000	SiO_2:No contaminant	4.05
	6,000 and 12,000	1 SiO_2:10 Fe	5.69
	6,000	1 SiO_2: 4 Fe	5.42
1:2 BCS 303 and NBS 154a	6,000 and 12,000	1 SiO_2:10 TiO_2	5.63
	6,000	1 SiO_2: 4 TiO_2	5.42
Ratio 1 SiO_2:	6,000 and 12,000	1 SiO_2:10 Al_2O_3	5.55
1 CaO	6,000	1 SiO_2: 4 Al_2O_3	5.48
11 TiO_2	6,000 and 12,000	1 SiO_2:10 MgO	5.55
2 Fe	6,000	1 SiO_2: 4 MgO	5.47
0.2 Al_2O_3	6,000 and 12,000	1 SiO_2:10 CaO	5.55
0.2 MgO	6,000	1 SiO_2: 4 CaO	5.44
(5.50% SiO_2)			

[a] 100 p.p.m. SiO_2 present per 12,000 p.p.m. Na; 50 p.p.m. SiO_2 present per 6,000 p.p.m. Na.
[b] Results obtained on different sets using different atomizer–burner combinations.
[c] Ratio 1 SiO_2:15 Fe, 5 TiO_2, 3 MgO, and 5 Al_2O_3.

taminant-added standards, were then compared with the certified results.

As can be seen from Table X, results were in good agreement with the certified values, and the average deviation found between certified values and atomic absorption results was within 2%. This indicated that either of the dissolution procedures was satisfactory for application to these types of sample material, with ease of sample dissolution and handling being the determining factor.

APPLICATION OF THE ATOMIC ABSORPTION PROCEDURES TO SLAGS AND ASSOCIATED MATERIALS

Comparison of atomic absorption and gravimetric results on typical sample material

A number of typical samples of slag and associated materials from high-

TABLE X

COMPARISON OF ATOMIC ABSORPTION WITH CHEMICAL RESULTS FOR SILICON ON CERTIFIED STANDARD SAMPLES AND THEIR MIXTURES

Sample[a] *type*	*Silica value given* (% SiO_2)	*Silica found by a.a.s.*[b]		*% Deviation from chemical results*	
		Teflon bomb dissolution (% SiO_2)	*Fusion dissolution* (% SiO_2)	*Bomb*	*Fusion*
BCS 27C iron ore	2.08	2.04	—	−1.9	—
BCS 301 iron ore	7.20	7.21	—	+0.14	—
BCS 302 iron ore	20.0	19.85	19.3	−0.75	−3.5
BCS 303 iron ore sinter	16.5	16.5	—	0.0	—
NBS 116a ferrotitanium	6.68	6.50	6.79	−2.7	+1.65
6:1 Mixture of BCS 208/1 and BCS 305	25.0	24.25	24.2	−3.0	−3.2
1:2 Mixture of BCS 27C and NBS 154a	0.69	0.71	—	+2.9	—
2:1 Mixture of BCS 27C and NBS 154a	1.39	1.46	—	+5.0	—
1:2 Mixture of BCS 301 and NBS 154a	2.40	2.37	—	−1.25	—
1:1 Mixture of BCS 301 and NBS 154a	3.60	3.60 3.65[c]	3.46[c] 3.61[d]	0.0 +1.4	−3.9 +0.28
1:2 Mixture of BCS 303 and NBS 154a	5.50	5.48 5.54[c]	5.43[c] 5.52[d]	−0.36 +0.73	−1.3 +0.36
1:1 Mixture of BCS 303 and NBS 154a	8.20	8.22	8.30	+0.24	+1.2

[a] For chemical composition, see Table I
[b] Sodium content, 5000–6000 p.p.m. Na.
[c] Techtron *vs.* contaminated standards in HF–H_3BO_3 medium.
[d] Techtron *vs.* contaminated standards in HCl medium.

temperature furnace work were analysed for silicon by the Teflon bomb procedure. The composition of these samples is shown in Table XI. In all cases the Jarrell–Ash spectrophotometer was used and comparison of the sample with pure silicon standards was done.

Several of the samples were put into solution with a sodium peroxide fusion–hydrochloric acid treatment, and comparisons were made similar to those above. All samples contained about 6000 p.p.m. sodium.

TABLE XI

COMPOSITION OF TYPICAL SLAG SAMPLES ANALYSED FOR SILICON BY ATOMIC ABSORPTION PROCEDURES

Sample type	SiO_2 (%)	Al_2O_3 (%)	*CaO (%)*	*MgO (%)*	TiO_2 (%)	*Fe (%)*	*MnO (%*
EMP 1552 slag from iron ore smelting	27	15	38	8	—	6	—
EMP 2958 slag from ilmenite smelting	5	6	0.5	4	67	13	—
EMP 2715 ilmenite head sample	1.5	2	0.1	2	38	42	—
Slag B manganese ore smelting	24	21	6	3	—	0.7	43
Slag H manganese ore smelting	24	19	3	1	—	0.6	49

The comparison of results obtained on these samples by atomic absorption and gravimetric procedures is shown in Table XII. Most of the samples analysed were ferromanganese slags, on which gravimetric results were assumed to have reasonably good credibility because results were from two different laboratories. With high-titanium material, however, gravimetric results on the high-titanium slags and ilmenite head samples were considered to be less reliable, because of the difficulty in analysing for silicon on this type of sample material. It has been found in this laboratory, for example, that results will be erratic and often low unless special precautions are taken when analysing this type of sample gravimetrically.

Agreement between gravimetric and atomic absorption procedures was found to be generally satisfactory, although, on one sample of titanium-bearing slag (EMP 2958), apparently high results were obtained from the fusion procedure. The reason for this was not clear because the ratio of silicon to contaminants in this sample was less than would be expected to cause trouble (see Table XI). Also, the amount of contaminant present was less than in the ilmenite head sample (EMP 2715) for which good agreement was found. Moreover, agreement was good between chemical and atomic absorption procedures on Certified sample material similar to EMP 2958 (see Tables VIII, X and XI). As a precaution, atomic absorption was applied to standards made up to simulate this slag sample, but there was no difference in results.

Precision found for the atomic absorption procedures

The precision found was calculated for a number of slag samples and one mixture of Certified Standard samples, by the methods of Dean and Dixon[21], and of Bauer[22]. The results of these tests (Table XIII) showed satisfactory precision for either material; the average coefficient of variation was 1.3%.

TABLE XII

COMPARISON OF ATOMIC ABSORPTION RESULTS WITH CHEMICAL RESULTS FOR SILICON ON TYPICAL SLAG SAMPLES

Sample type	*Silica value (gravimetric) (% SiO_2)*	*Silica found by a.a.s.*		*Deviation of a.a.s. results from chemical results (%)*	
		Teflon bomb dissolution (% SiO_2)	*Fusion dissolution (% SiO_2)*	*Bomb*	*Fusion*
EMP-1552, slag from iron ore smelting	27.3[b]	26.9	27.3	−1.5	0.0
EMP-2846, slag from ilmenite smelting	4.27[b]	—	4.14[c]	—	−3.0
EMP-2958, slag from ilmenite smelting	4.81[b]	5.03	5.51	+4.6	+14.6
EMP-2715, ilmenite head sample	1.53[b]	1.535	1.54	+0.33	+ 0.65
Ferromanganese slag A	23.9[a,b]	23.6	—	−1.25	—
Ferromanganese slag B	24.45[a,b]	24.3	—	−0.6	—
Ferromanganese slag C	23.45[a,b]	24.8	—	+5.8	—
Ferromanganese slag D	23.9[a,b]	25.1	—	+4.8	—
Ferromanganese slag E	24.7[a,b]	24.4	—	−1.2	—
Ferromanganese slag F	22.0[a]	22.7	—	+3.2	—
Ferromanganese slag G	23.0[a]	24.2	—	+5.2	—
Ferromanganese slag H	23.7[a]	24.5	—	+3.4	—
Ferromanganese slag I	22.9[a]	22.4	—	−2.2	—
Ferromanganese slag J	25.4[a]	24.8	—	−2.4	—
EMP-2711 ferromanganese slag	24.4[b]	25.0	—	+2.4	—

[a] Results provided by George Ascroft, Chief Chemist, Union Carbide Canada Ltd., Welland Ontario.
[b] Gravimetrically by Extraction Metallurgy Division.
[c] Techtron *vs.* contaminated standards.

DISCUSSION

Dissolution

Neither of the recommended dissolution procedures showed a clear superiority over the other, because each had certain advantages. Between them, they offered an effective method of attack for any of the mineral and mineral mixtures, and for the ores, slags, and other sample material.

The Teflon bomb procedure showed a slight superiority in accuracy and precision over the fusion procedure. The behaviour of its solution in the flame was

TABLE XIII

PRECISION OBTAINED FOR SILICON ANALYSES AFTER SAMPLE DISSOLUTION BY TEFLON BOMB AND SODIUM PEROXIDE FUSION

Sample type	*Sample treatment*	*Average result*[a] *(% SiO_2)*	*Standard deviation*	*Coefficient of variation (%)*	*95% Confidence limits for average results*
Slag from iron ore smelting	Teflon bomb	26.51	0.39	1.46	0.47
	Fusion—HCl	27.31	0.39	1.42	0.47
Slag from menite smelting	Teflon bomb	5.01	0.047	0.94	0.059
Slag from manganese ore smelting	Teflon bomb	24.55	0.39	1.58	0.47
Mixture of Certified ferromanganese and ferrosilicon	Fusion—HCl	24.10	0.24	0.98	0.29

[a] Average of 5 determinations.

at least as good as the solution following the fusion procedure. The effects of contaminants on results after either dissolution procedure were similar. An advantage of the bomb dissolution procedure over most others would be its suitability for silicon determination in samples containing fluorine.

Among advantages found for the fusion procedure were its greater flexibility in allowing a choice of sample size, and its effectiveness on certain sample material which was difficult to dissolve by other procedures. With the Teflon bomb procedure, samples weighing more than 0.5 g were difficult to dissolve, and certain refractory samples were harder to dissolve than by the fusion procedure.

Solution stability

It was observed that the stability of the silicon standard solutions and of the sample solutions could be affected by a number of factors. Among these, acid strength, ageing time, the amount of silicon and other elements present, and the manner of handling during the procedure were of paramount importance. Also, after long standing, samples and pure silicon samples sometimes behaved differently. It was our experience, however, that if the procedures described here were followed, pure silicon solutions normally remained stable for several weeks and that, generally, samples behaved in a similar manner.

Effect of interfering elements

The Jarrell–Ash atomizer–burner system behaved better than the Techtron system with the type of highly salted sample solutions used. The Techtron atomizer would at times block up during operation and changes in air pressure could be observed when partial blockage of the atomizer began; this seriously

affected absorption readings. With the Techtron atomizer–burner system, a major contaminant was usually added to the comparison standard in analyses of difficult sample material.

The Techtron grooved burner head was prone to formation of solids on the edge of the burner slot, as has been reported by Goguel[23] who recommended the use of the flat-top burner head. Although the latter type of burner head can be used with either atomizer–burner system, less carbon formation was found with the Jarrell–Ash burner system.

With the Jarrell–Ash burner–atomizer system, the use of comparison solutions of contaminants plus standards was not normally required. In some cases, however, in which the ratio of contaminant to silicon was unusually high, the addition of one or more major contaminants to the silicon standards served to correct for any effect from this source. This latter technique could be considered to be a good general compensatory measure, because the effect of contaminants varied with flame changes and these changes should be reflected as accurately as possible. It would be expected, therefore, that the closer the matching of standard and sample, the greater the improvement in accuracy and precision. For most work, however, the procedural addition of the major contaminant to the standard could be eliminated. In such cases, the saving in time realized from measuring against pure standards, particularly if the composition of the sample were unknown, would be very advantageous.

The presence of sodium has been reported to cause an enhancement of the absorption of silicon, and this can be beneficial, if controlled, because its effect levels off at higher sodium content levels. Its function has been explained in terms of suppression of silicon ionization[12]. A working level of about 6000 p.p.m. sodium in the final solution for atomization was found to be beneficial for use after both dissolution procedures, as this amount was both effective and convenient. The use of much higher amounts of sodium than this caused burner clogging that necessitated frequent washing of the burner. With the recommended procedure, the Jarrell–Ash burner required scraping 3–4 times an hour, but washing of the burner was not required for at least 2 h.

General comments

A major advantage of the recommended atomic absorption procedures over gravimetric methods lies in the saving of analysis time. When silicon is determined gravimetrically, especially in difficult sample material (feldspars, amphibole, muscovite, galena, chalcopyrite and pyroxene), the analysis time is several times longer than that needed for atomic absorption procedures. Also, on the series of minerals analysed, a number of different analytical approaches had to be made in applying gravimetric methods, in order to obtain acceptable accuracy and precision. By comparison, the same atomic absorption procedures were used on all the minerals and their mixtures, except galena and chalcopyrite for which simple modifications of major-contaminant addition to the comparison standard were made.

The usable range of the atomic absorption procedure was wide, with samples containing between 0.1 and 45% silicon being analysed. It was found that 0.1% is close to the lower limit of the described atomic absorption procedure and that special techniques such as solvent extraction would be necessary to extend its range to lower levels.

CONCLUSIONS

The two dissolution procedures described are satisfactory for use preceding the atomic absorption determination of silicon, and give solutions that have excellent long-term stability with respect to silicon and which are suitable for the determination of other constituents of the samples. The applicability of the given operating parameters for the atomic absorption procedure is confirmed for comparable highly-salted solutions that contain contaminants. Adequate results will normally be obtained by using comparison standards prepared from pure silicon, but a significant gain in accuracy can be realized, even in moderately complex materials, by using comparison standards adjusted to contain comparable amounts of the predominant contaminant.

The method is generally applicable to mineral specimens or mixtures typical of sulphide ores and tailings, and to ores, slags and associated materials. It is especially well-suited to operational control as it is fast, accurate and precise. Silicon contents between 0.1 and 45% can be determined at between one-fifth and one-third of the cost of gravimetric procedures and with comparable, or better, accuracy. The precision, expressed as the relative standard deviation, is about 1.4%. The average deviation from certified results is less than 2%, considerably lower than the average deviation of some 3–4% from gravimetric results on minerals and slag samples, much of which can be attributed to inaccuracies in the gravimetric method.

The authors wish to thank H. R. Steacy, Curator of the Geological Survey of Canada, for supplying the mineral samples, G. A. Hunt for his assistance in resolving instrumental problems, and J. C. Ingles for his helpful advice during this investigation.

SUMMARY

Rapid atomic absorption procedures are described for determining silicon in typical sulphide and silicate minerals and their mixtures, in ores, and in slags. Two sample decomposition procedures are shown to give solutions which have good long-term stability for silicon and are suitable for use in the atomic absorption finish. The applicability of the given operating parameters for the atomic absorption procedure is confirmed for comparable highly-salted solutions that contain contaminants. Although satisfactory results are obtainable when pure silicon standards are used for comparison, the addition of a predominant sample contaminant to the comparison standard can improve the accuracy and precision of the procedure.

REFERENCES

1 J. Ito, *Bull. Chem. Soc. Jap.*, 35 (1962) 225.
2 F. J. Langmyhr and S. Sveen, *Anal. Chim.-Acta*, 32 (1965) 1.
3 F. J. Langmyhr and P. E. Paus, *Anal. Chim. Acta*, 43 (1968) 397.
4 B. Bernas, *Anal. Chem.*, 40 (1968) 1682.
5 G. J. Petretic, *Anal. Chem.*, 23 (1951) 1183.

6 J. I. Dinnin, *U.S. Geol. Surv., Bull., 1084B*, 1959.
7 J. C. Van Loon and C. Parissis, *Anal. Letters.*, 1, No. 8 (1968) 519.
8 S. H. Omang, *Anal. Chim. Acta*, 46 (1969) 225.
9 N. R. Suhr and C. O. Ingamells, *Anal. Chem.*, 38 (1966) 730.
10 J. M. Galloway and J. Reid, *Spectrovision (Pye Unicam)*, 11 (1970).
11 J. H. Medlin, N. R. Suhr and J. B. Bodkin, *At. Absorption Newslett.*, 8 (1969) 25.
12 W. J. Price and J. H. T. Roos, *Analyst (London)*, 93 (1968) 709.
13 J. A. Bowman and J. B. Willis, *Anal. Chem.*, 39 (1967) 1210.
14 P. L. Boar and L. K. Ingram, *Analyst (London)*, 95 (1970) 124.
15 A. Katz, *Amer. Mineral.*, 53 (1968) 283.
16 D. E. Campbell, *Anal. Chim. Acta*, 46 (1969) 31.
17 J. C. Van Loon and C. Parissis, *Analyst (London)*, 94 (1969) 1057.
18 S. Abbey, *Paper 70-23*, Geol. Surv. Can., Dept. of Energy, Mines and Resources, Ottawa, Canada, 1970.
19 F. J. Langmyhr and P. E. Paus, *Anal. Chim. Acta*, 50 (1970) 515.
20 V. S. Biskupsky, *Anal. Chim. Acta*, 33 (1965) 333.
21 R. B. Dean and W. J. Dixon, *Anal. Chem.*, 23 (1951) 636.
22 E. L. Bauer, *A Statistical Manual for Chemists*, Academic Press, New York, 1960, pp. 16, 137.
23 R. Goguel, *Spectrochim. Acta, Part B*, 26 (1971) 313.

Analytica Chimica Acta, 71 (1974) 255–262

MOLECULAR EMISSION CAVITY ANALYSIS (MECA)—A NEW FLAME ANALYTICAL TECHNIQUE

PART III. THE DETERMINATION OF BORON

R. BELCHER, S. A. GHONAIM and A. TOWNSHEND

Chemistry Department, Birmingham University, PO Box 363, Birmingham B15 2TT (England)

(Received 3rd January 1974)

Several methods for the flame photometric determination of boron have been established by measuring the green emission of the BO_2 radical. Dean and Thompson[1], for example, measured the intensity of the BO_2 band emission at 518 nm from an oxyacetylene flame; the optimal range of applicability was 50–200 p.p.m. in a 1:1 water–methanol mixture. Such determinations were first discussed by Stahl[2], who prepared methyl borate by reacting boric acid with a mixture of methanol and sulphuric acid, and introduced the volatile product into a bunsen flame. The colour intensity was estimated visually with the aid of a colorimetric scale; down to 5 μg of boric acid could be detected. Stahl also studied the effects of the ratio of boric acid to alcohol, the temperature of the solution and the amount of water present, on the production of the green flame colouration.

Weber and Jacobson[3] simplified Stahl's apparatus and introduced the gas into a fish-tail burner. Boron, in the range 20–100 μg, was determined by measuring the duration of the green colour in the flame. Maeck *et al.*[4] determined sub-mg quantities of boron, after extraction from aqueous solution into methyl isobutyl ketone (MIBK), as tetrabutylammonium tetrafluoroborate, and aspirated the organic phase into an oxyhydrogen flame. Yoshizaki[5], who established a flame photometric method for the determination of boron in organoboron compounds, observed that the emission intensity depended not only on the boron content but also on the molecular structure of the boron compound. This necessitated the complete decomposition of various boron compounds to boric acid before the boron emission was measured. Many other flame photometric methods for the determination of boron by measuring the emission intensity of the BO_2 radical have been described. They are usually based on the use of oxyhydrogen or oxyacetylene flames or, occasionally, air–hydrogen flames.

DETERMINATION OF BORON BY MECA

The present work is concerned with the application of molecular emission cavity analysis[6] (MECA) to the determination of boron. In the simplest form of this technique, the sample is deposited in a cavity at the end of a rod, which is placed into a hydrogen–nitrogen flame in such a way that the flame gases flow

almost vertically past the entrance to the cavity. The apparatus and the technique of measurement have been described previously[6].

In this study, it was found that injecting an aqueous solution of boric acid into a stainless steel cavity gives a green emission, mainly in that part of the flame above the cavity, probably because there is insufficient oxygen inside the cavity to form many excited BO_2 radicals, the emitting species. When a slow flow of oxygen is introduced through a hole in the side wall of the cavity (Fig. 1), the emission is restricted within the cavity. Under such conditions, after injection of an aqueous solution of boric acid into the cavity, the BO_2 emission begins within 5 s after contact with the flame, and continues to increase until it becomes swamped by the incandescent emission from the cavity (Fig. 2). BO_2 emission from sodium borate could not be observed satisfactorily, because the cavity incandesces appreciably before any boron emission occurs (Fig. 2); sodium borate requires a high temperature to achieve decomposition. In order to avoid this problem, it is necessary to introduce the boron sample into the cavity as a more volatile product so that the emission intensity can be measured within 10 s of introducing the cavity into the flame. A solvent extraction procedure, in which boron is chelated with 2-ethylhexane-1,3-diol and extracted into methyl isobutylketone (MIBK) from acidic solution[7], gives a suitably volatile species.

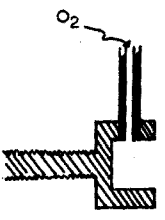

Fig. 1. Device for introducing oxygen into the cavity.

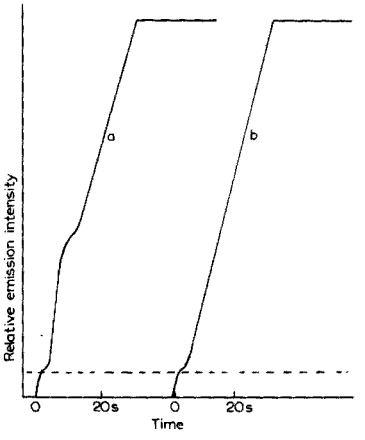

Fig. 2. Emission-time response from (a) boric acid, (b) sodium borate, or (--) an empty cavity, under the conditions recommended for boron determination after extraction.

As an alternative approach, the BO_2 emission from methyl borate can be measured. Methyl borate, produced by reaction of boric acid or a metal borate with a mixture of sulphuric acid and methanol, can be introduced into the cavity *via* a rear opening as shown in Fig. 3. The methyl borate is carried by a stream of nitrogen to the cavity. This system also gives emission outside the cavity, unless it is restricted to within the cavity by supplying a small flow of oxygen directly into the cavity through the rear entrance as shown in Fig. 3. This system was also found to be very suitable for scanning the spectrum of the BO_2

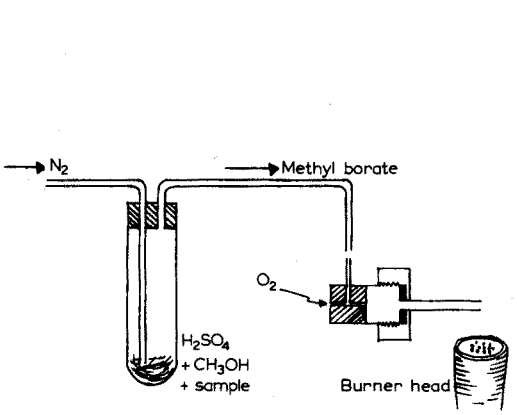

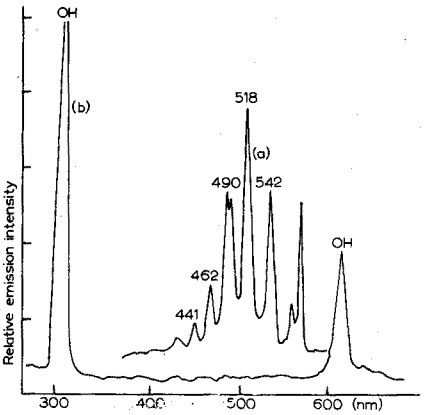

Fig. 3. System for generating methyl borate and conveying it to the cavity. The reaction vessel is a small test tube (6 cm high).

Fig. 4. Spectrum obtained (a) from methyl borate, (b) in the absence of boron, using the volatilization system. Flow rates (l min^{-1}): $H_2 = 3.4$, $N_2 = 5.5$, $O_2 = 0.090$. Slit, 0.39 mm.

emission arising from methyl borate, by reacting mg-amounts of boric acid in the reaction tube. The rate of transfer of methyl borate to the cavity under these conditions is constant for at least 3 min, so that the emission intensity remains constant over this period. The BO_2 spectrum obtained in this way is shown in Fig. 4. In all subsequent experiments, boron emission was measured at 518 nm, the most intense peak.

USE OF MECA FOR THE DETERMINATION OF BORON AFTER SOLVENT EXTRACTION

The extraction conditions established by earlier workers[7] were used. Preliminary experiments showed that μl volumes of the blank extract, containing no boron, give a blue emission in the cavity. To avoid significant interference from this effect, the solvent must be allowed to evaporate before the cavity is placed

TABLE I

THE EFFECT OF EVAPORATION TIME ON BACKGROUND EMISSION

(25 ml of water + 5 ml of 6*M* HCl extracted with 10 ml of 20% 2-ethylhexane-1,3-diol in MIBK; extract diluted to 50 ml with MIBK; 5 μl of extract used for each experiment)

Cavity heating time (s)	*Cooling time (s)*	*Evaporation time (s)*	*Background intensity (mV)*
0	0	0	16.0
30	45	30	6.5
30	60	60	6.0
30	60	120	5.0
30	60	150	3.2
30	60	300	3.0

in the flame. This can be achieved by injecting the sample into a cavity that is still warm from a previous determination. The effect of evaporating the solvent is shown in Table I. An evaporation time of 2.5 min from a cavity previously heated for 30 s under the optimal conditions for boron determination and then allowed to cool for 60 s gives a relatively low background from the solvent.

The effect of the position of the cavity in the flame was investigated. Positioning the cavity opening 14 mm into the flame from the outside edge gives the maximal emission intensity, in the presence of oxygen, in the cavity (Fig. .5). The height of the cavity above the burner is not very critical measured at the optimal flame-gas flow rates with oxygen introduced into the cavity; the centre of the cavity was positioned 31 mm above the burner in all further studies.

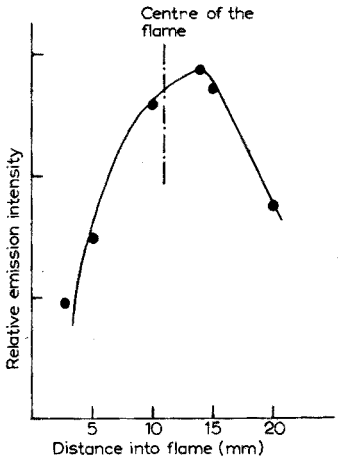

Fig. 5. Effect of horizontal displacement of cavity in flame on boron emission intensity (flow rates as in Fig. 4).

The addition of air into the flame reduces the boron emission intensity. However, the addition of oxygen into the cavity enhances the boron emission intensity but the more oxygen is added, the more the background increases; an oxygen flow rate of 90 ml min^{-1} is optimal. The optimal flow rate for hydrogen is 3.3–3.5 l min^{-1} at a nitrogen flow of 5.5 l min^{-1}.

On the basis of these results, it was possible to devise a procedure for the determination of boron by the extraction of its chelate with 2-ethylhexane-1,3-diol into MIBK, and measurement of the emission intensity at 518 nm, by injecting a microlitre sample of the extract into the cavity. Two methods for obtaining calibration graphs can be used; either (a) extraction of one standard solution of boron and injection of different volumes (say 1–5 μl) of the extract, or (b) extraction of a set of standard solutions and the injection of fixed volumes (5 μl) of each extract. Linear calibration graphs for the amount of boron *versus* emission intensity are obtained in the range 5–80 ng of boron by both methods. Emission–time responses for different volumes of extract having the same boron concentration are shown in Fig. 6. The emission from similar volumes of blank extract is also shown. The calibration graph obtained therefrom is shown in Fig. 7. Where

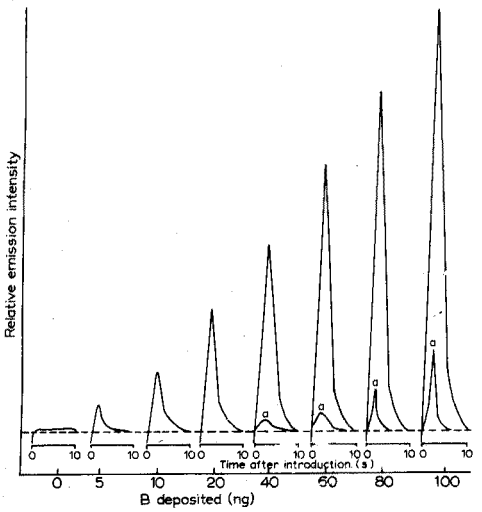

Fig. 6. Emission–time responses of various volumes of an extract containing 20 μg B ml^{-1}. The smaller peaks (a) are for the same volume of blank extract.

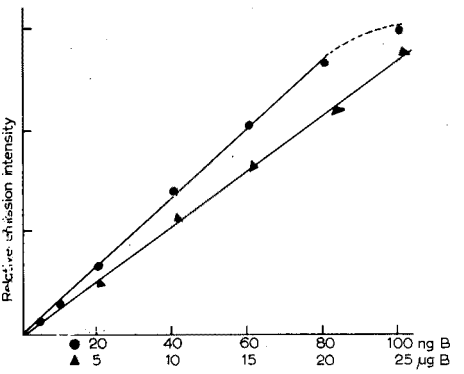

Fig. 7. Calibration graphs for boron by the extraction method (●) and the volatilization method (▲).

different volumes of extract are run, the blank value for that particular volume must be subtracted; it is only significant for greater than 2 μl of extract. The standard deviation in the range 5–80 ng was found to be about 4%.

The effect of different cations and anions on the determination of 200 μg of boron in 20 ml of aqueous solution was studied; 1 mg of As(III), Sb(III), Co^{2+}, Ni^{2+}, Mn^{2+}, Ba^{2+}, Na^{+}, Ca^{2+}, Cl^{-}, NO_3^{-} and PO_4^{3-} did not interfere. The only interference arose from 100 μg of fluoride which suppressed the extraction by about 10%; 50 μg of fluoride had no effect.

USE OF THE VOLATILIZATION SYSTEM

The optimal conditions for the production of methyl borate were established by Stahl[2]. He recommended the use of a (5+1) mixture of methanol and concentrated sulphuric acid, at a temperature below the boiling point of methanol (60°C). In the present work, 40°C was used. Stahl also found that all water in aqueous samples should first be evaporated, as even a small amount of water decreases the amount of methyl borate evolved. The effect of the flame gases and the position of the cavity in the flame on the emission intensity of BO_2 from methyl borate, were similar to those obtained for the solvent extraction procedure. Thus, the conditions used in that procedure were again employed. The emission intensities of the same amounts of boron as boric acid and sodium borate were found to be the same when this procedure was used (Table II).

As maximal emission intensity is not reached for 2 min, this necessitates leaving the cavity in the flame for at least this period of time. For this reason a brass cavity was used. Since brass has a greater thermal conductivity than

TABLE II

THE EMISSION INTENSITY (mV) OF BORON FROM BORIC ACID AND SODIUM BORATE AFTER CONVERSION TO METHYL BORATE

10 μg of B as		*20 μg of B as*	
Acid	*Borate*	*Acid*	*Borate*
4.0	4.2	8.1	8.0
4.1	4.4	8.0	7.9
4.0	4.1	8.3	8.2

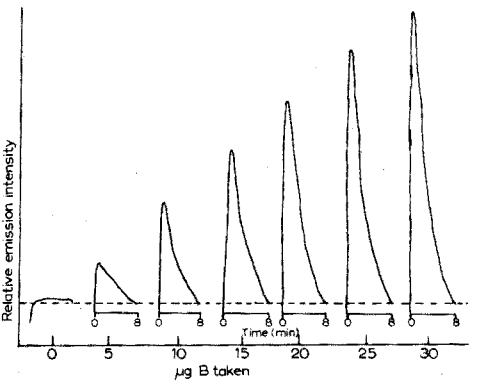

Fig. 8. Emission–time responses of various amounts of boron for the volatilization procedure. The time axis represents the time, from starting, to warm the reaction tube. The stated amounts of boron are those added initially to the volatilization system.

stainless steel, the cavity does not reach such high temperatures and there is no incandescence to interfere with the measurement of the boron emission. There is, however, a continuous background emission owing to the presence of methanol. The nitrogen-flow through the cavity is adjusted to allow a reasonably rapid sweep-through of methyl borate, without excessive carryover of methanol. With the volatilization procedure, a linear calibration graph (Fig. 7) is obtained in the range 2–30 μg of boron, with a standard deviation of about 3%. Typical response–time curves are shown in Fig. 8.

The effect of different cations and anions on the determination of 10 μg of boron was investigated; 100 μg of Ga^{3+}, Ge(IV), As(III), Sb(III), Co^{2+}, Ni^{2+}, Zn^{2+}, Mn^{2+}, Ba^{2+}, Na^{+}, Ca^{2+}, Cl^{-}, NO_3^{-}, PO_4^{3-} and F^{-} do not interfere.

EXPERIMENTAL

Apparatus

The spectroscopic equipment used was the same as described previously[6].

Determination of boron by solvent extraction

Reagents. For the boron stock solution (1000 p.p.m.) dissolve 2.86 g of A.R. boric acid in 500 ml of distilled water.

Flame conditions. Nitrogen flow rate. 5.5 l min^{-1}; hydrogen flow rate, 3.4 l min^{-1}; oxygen flow rate, 90 ml min^{-1}.

Procedure. To a separating funnel, add an appropriate volume of the test solution (10–100 ml) containing not less than 10 μg of boron, followed by 5 ml of 6 *M* hydrochloric acid for each 25 ml of the aqueous test solution. Extract twice with 5 ml of a 10% solution of 2-ethylhexane-1,3-diol in MIBK, and combine the extracts in a 10-ml volumetric flask. When necessary, add a few drops of MIBK to make up to volume. Determine boron as described below.

Calibration with one standard solution. Mix 25 ml of an aqueous solution containing 200 μg of boron as boric acid and 5 ml of 6 *M* hydrochloric acid. Extract as described above. Prepare a blank extract under the same conditions. Ignite the cavity in the flame for 30 s and turn off the flame gases except for the nitrogen, to allow the cavity to cool in the nitrogen stream for 60 s, before injecting an aliquot of the extract (0.25–5 μl). Allow the solvent to evaporate by waiting for about 2.5 min. Reignite the flame and record the maximal or integrated emission intensity at 518 nm. Extinguish the flame as before after 30 s, allow to cool as before, and inject another aliquot of standard extract. Repeat the procedure for each aliquot of standard extract. Repeat the experiments by injecting the same volumes of the blank extract and subtract the measured emission intensities from those obtained from the borate extracts. Plot a graph of amount of boron *versus* corrected emission intensity.

Calibration with a set of standard solutions. Prepare standard solutions containing 0, 10, 20, 40, 60, 80 and 100 μg of boron as boric acid in 25 ml of aqueous solution. Add 5 ml of 6 *M* hydrochloric acid to each solution. Follow the same extraction procedure as above. Inject in turn, using the heating and cooling sequence described above, 5 μl of each extract, and measure the peak or integrated emission intensity at 518 nm. Subtract the blank emission before constructing the calibration graph.

Determination of boron by conversion to methyl borate

The flame conditions are the same as for the solvent extraction procedure. The nitrogen flow rate in the volatilization system is adjusted to give a background of 4.5 mV for methanol and oxygen. This compares with a peak of 2.4 mV given by 10 μg of boron (10 mV f.s.d.).

To the reaction vessel, add an appropriate volume (*e.g.* 1.5 ml) of the test solution containing 2–30 μg of boron. Evaporate to dryness in an oven at less than 150°C, and add 2.5 ml of the methylating mixture (freshly prepared 5 + 1 methanol–concentrated sulphuric acid). Connect the tube to the nitrogen flow system. Ignite the flame and warm the reaction vessel in a water bath at 40°C until the boron emission reaches its maximal intensity and begins to decrease (about 2 min). The time required for complete evolution of methyl borate under these conditions is about 8 min (Fig. 8).

CONCLUSION

MECA is a simple, versatile and very effective way for carrying out cool-flame emission analyses. The incorporation of the reaction–volatilization system

produces an additional source of selectivity. The methods described here for the determination of boron are simple and sensitive and could readily be made more sensitive by applying the concentration techniques (solvent extraction or evaporation of water) to larger sample volumes.

The volatilization technique might be applied successfully to the analysis of other elements which give volatile compounds by simple reactions. Arsenic and antimony, for example, can be converted to their volatile hydrides by reaction with sodium borohydride[8], and arsenic, boron and silicon can be converted to their volatile fluorides. Detailed descriptions of the determination of these elements and of fluoride by the volatilization technique will be the subject of further papers.

The authors thank Dr. S. L. Bogdanski for his help and advice and the University of King Abdulaziz, Saudi Arabia, for financial support for S.G.

SUMMARY

Two highly selective methods are described for the determination of boron by molecular emission cavity analysis. In one, boron (>0.1 p.p.m.) is extracted as its 2-ethylhexane-1,3-diol chelate into methyl isobutylketone; 5–80 ng of boron in 5 μl of the extract is determined by injection into the MECA cavity. In the other, boron (2–30 μg) is converted into volatile methyl borate, and carried into the rear of the cavity by a stream of nitrogen. In both methods, the emission intensity at 518 nm, stimulated by a hydrogen–nitrogen–oxygen flame, is measured. Of the other ions tested, none interfered in the volatilization procedure, and only fluoride ($\geq$100 μg) interfered in the extraction method. The precision is $\pm$4%.

REFERENCES

1 J. A. Dean and C. Thompson, *Anal. Chem.*, 27 (1955) 42.
2 W. Stahl, *Z. Anal. Chem.*, 83 (1930) 268; 101 (1935) 342, 348.
3 H. C. Weber and R. D. Jacobson, *Ind. Eng. Chem., Anal. Ed.*, 10 (1938) 273.
4 W. J. Maeck, M. E. Kussy, B. E. Ginther, G. V. Wheeler and J. E. Rein, *Anal. Chem.*, 35 (1963) 62.
5 T. Yoshizaki, *Anal. Chem.*, 35 (1963) 2177.
6 R. Belcher, S. L. Bogdanski and A. Townshend, *Anal. Chim. Acta*, 67 (1973) 1.
7 J. C-M. Pau, E. E. Pickett and S. R. Koirtyohann, *Analyst (London)*, 97 (1972) 860.
8 S. A. Ghonaim, Lecture, *4th Atomic Absorption Conference, Toronto, Nov. 1973.*

Analytica Chimica Acta, 71 (1974) 263–275

ACTIVATION ANALYSIS OF BIOLOGICAL MATERIAL WITH RUTHENIUM AS A MULTI-ISOTOPIC COMPARATOR

R. VAN DER LINDEN, F. DE CORTE* and J. HOSTE
Institute for Nuclear Sciences, Rijksuniversiteit Gent, Proeftuinstraat 86 (Belgium)
(Received 30th November 1973)

Nowadays the analysis of biological materials, extended to the p.p.m. range, has found a wide application in studies of biological processes. The classical neutron activation technique offers in principle the possibility of determining a large number of elements. However, every element has to be related to a standard which has been treated identically. Difficulties arise when the irradiation facility is limited, when a multi-element analysis is performed or when analysing for unexpected elements.

To overcome these inconveniences, a practical method was developed[1,2] to replace the standards, based on the use of two or more comparator isotopes. In earlier work[3], the method was checked by analysing geological material of known composition. This paper describes activation analysis, by the relative multiple comparator method, of lyophilized bovine liver distributed by the U.S. National Bureau of Standards as a Standard Reference Material (SRM 1577) for use in analysis for trace metals in animal tissue. The concentrations determined for Fe, Zn, Rb, Se and Co are compared with the values of the NBS analysis certificate and with the results of a recent activation analysis of a multi-element serum standard[4].

The relative multiple comparator method and its error

In the relative multiple comparator method, a k factor for each standard is defined as:

$$k_{\mathrm{ref}} = \left(\frac{A_{\mathrm{sp,st}}}{A_{\mathrm{sp,comp}}} \right)_{\mathrm{ref}} \tag{1}$$

where $A_{\mathrm{sp,st}}$ and $A_{\mathrm{sp.comp}}$ denote the specific activity of standard and comparator isotopes, respectively, and where the subscript ref denotes a reference irradiation position. The experimentally determined k_{ref} factors can be converted to k_{anal} factors, valid for the analysis reactor position, by the relation:

$$k_{\mathrm{anal}} = k_{\mathrm{ref}} \frac{(f_{\mathrm{anal}} + D_{\mathrm{st}})(f_{\mathrm{ref}} + D_{\mathrm{comp}})}{(f_{\mathrm{anal}} + D_{\mathrm{comp}})(f_{\mathrm{ref}} + D_{\mathrm{st}})} \tag{2}$$

where

* Research associate of the NFWO.

$$D = \frac{I_0}{\sigma_{th}} = \frac{\text{activation resonance integral at infinite dilution}}{\text{thermal neutron activation cross section}}$$

$$f = \frac{\phi_{th}}{\phi_{epi}} = \text{thermal-to-epithermal neutron flux ratio}$$

The specific standard activities in the analysis reactor position can be computed from the calculated k_{anal} factors if the comparator is co-irradiated with the samples:

$$(A_{sp.st})_{anal} = k_{anal} \cdot (A_{sp.comp})_{anal} \tag{3}$$

From eqn. (2), it is apparent that the values of f_{ref} and f_{anal} are needed for the conversion of the k factors. The flux ratio f_{ref} can be determined from cadmium ratio measurements of isotopes with a known I_0/σ_{th} value. The value of f_{anal} can be calculated from:

$$f_{anal} = \frac{R(f_{ref}D_1 + D_1D_2) - (f_{ref}D_2 + D_1D_2)}{(f_{ref} + D_1) - R(f_{ref} + D_2)} \tag{4}$$

where R is an experimental ratio obtained by irradiation of two comparator isotopes (denoted as 1 and 2) in the reference reactor position and, together with the samples, in the analysis reactor position. It is defined as:

$$R = \left(\frac{A_{sp.1}}{A_{sp.2}}\right)_{ref} \Big/ \left(\frac{A_{sp.1}}{A_{sp.2}}\right)_{anal} \tag{5}$$

Obviously, one of the comparator isotopes from eqn. (4) may be the same as the comparator isotope used to define the k factor (eqn. (1)).

As discussed in the previous papers[1,2], the following equations hold for the error factors:

$$Z_f = \left|\frac{df_{anal}}{f_{anal}}\right| \Big/ \left|\frac{dR}{R}\right| = \left|\frac{(f_{anal} + D_1)(f_{anal} + D_2)}{f_{anal}(D_2 - D_1)}\right| \geqslant 1 \tag{6}$$

Optimal conditions: large spreading between D_1 and D_2; D_1D_2 close to f_{anal}.

$$Z_k = \left|\frac{dk_{anal}}{k_{anal}}\right| \Big/ \left|\frac{df_{anal}}{f_{anal}}\right| = \left|\frac{f_{anal}(D_{st} - D_{comp})}{(f_{anal} + D_{comp})(f_{anal} + D_{st})}\right| \leqslant 1 \tag{7}$$

Optimal conditions: D_{st} close to D_{comp}; large spreading between $(D_{st}D_{comp})^{\frac{1}{2}}$ and f_{anal}.

$$Z = Z_f \cdot Z_k = \left|\frac{dk_{anal}}{k_{anal}}\right| \Big/ \left|\frac{dR}{R}\right| = \left|\frac{(f_{anal} + D_1)(f_{anal} + D_2)(D_{st} - D_{comp})}{(f_{anal} + D_{comp})(f_{anal} + D_{st})(D_2 - D_1)}\right| \tag{8}$$

Optimal conditions: same as for Z_f and Z_k.

Ruthenium as a multi-isotopic comparator element

From eqns. (2) and (4) it is obvious that one of the most important parameters of a comparator isotope is the ratio of epithermal to thermal neutron cross-section. From the compilation of I_0/σ_{th} values for all isotopes useful in γ-ray spectrometry[5,6], it appeared that a number of isotope combinations can be used as a comparator set.

The element gold ($^{197}Au(n,\gamma)^{198}Au$ with $I_0/\sigma_{th} = 15.7$), which is internationally accepted as an absolute flux monitor, can be used in combination with cobalt ($^{59}Co(n,\gamma)^{60}Co$ with $I_0/\sigma_{th} = 2.03$) as a comparator pair. However, if two elements are used, the weight of the irradiated target nuclides needs to be known, in order to derive the flux ratio from the relative photopeak intensities. Thus, two samples must be prepared and treated separately. Another disadvantage of the gold monitor is its high cross-section, not only for the $^{197}Au(n,\gamma)^{198}Au$ reaction ($\sigma_{th} = 98.8$ *b*, $I_0 = 1550$ *b*), thus causing shielding effects if not sufficiently diluted, but also for the burn-up reaction $^{198}Au(n,\gamma)^{199}Au$ ($\sigma_{th} = 2.4 \cdot 10^4$ *b*).

To avoid these difficulties, the element ruthenium is proposed as a triple comparator set. By (n,γ) reactions the following isotopes are formed: ^{97}Ru ($I_0/\sigma_{th} = 23.1$), ^{103}Ru ($-I_0/\sigma_{th} = 3.3$) and ^{105}Ru ($I_0/\sigma_{th} = 13.0$). The nuclear data for these ruthenium isotopes are summarized in Table I. As the isotopic abundances are known and constant, the flux ratio f_{anal} (eqn. 4) can be calculated without knowledge of the comparator weight, thus excluding weighing errors. From the spreading of the I_0/σ_{th} values and from the optimal conditions mentioned above, it follows that the most convenient comparator pair, causing the smallest Z_f multiplication factor, is ^{97}Ru–^{103}Ru. The other pairs ^{103}Ru–^{105}Ru and especially ^{97}Ru–^{105}Ru, can be used if $(D_1 D_2)^{\frac{1}{2}}$ is close to f_{anal} and if the D values of the standard isotopes are not far different from the D value of one of the comparator isotopes used to define the k factors. In the latter case, the Z_k, and thus also the Z factor is reduced markedly. In any case the pairs ^{97}Ru–^{105}Ru and ^{103}Ru–^{105}Ru can be used as a check for the determination of f_{anal} or to obtain a weighted average of the flux ratio, taking the $1/Z_f$ factors as the respective weighted factors.

The shortest-lived isotope ^{105}Ru ($t_{\frac{1}{2}} = 4.44$ h) decays to a γ-emitting daughter ^{105}Rh with a half-life of 35.5 h, so that it is unnecessary to measure immediately after irradiation. Self-shielding and γ-attenuation as well as burn-up effects are negligible with samples not exceeding 10 mg. In Fig. 1, a γ-ray spectrum of ruthenium is shown. As can be seen, the 497-keV line of ^{103}Ru is disturbed by

TABLE I

NUCLEAR DATA FOR THE RUTHENIUM ISOTOPES

	Target nuclide			*Ref.*
	^{96}Ru	^{102}Ru	^{104}Ru	
Reaction	$^{96}Ru(n,\gamma)^{97}Ru$	$^{102}Ru(n,\gamma)^{103}Ru$	$^{104}Ru(n,\gamma)^{105}Ru$ $^{105}Ru \xrightarrow{\beta^-} {}^{105}Rh$	
Half-life	2.89 d	39.8 d	4.44 h ^{105}Rh: 35.5 h	11
Abundance %	5.51	31.61	18.58	11
σ_{th}	0.21	1.3	0.5	11
I_0	4.8	4.3	6.5	5
I_0/σ_{th}	23.1	3.3	13.0	5
Main γ-energies (keV)	216	497	724, 130 ^{105}Rh: 319	9

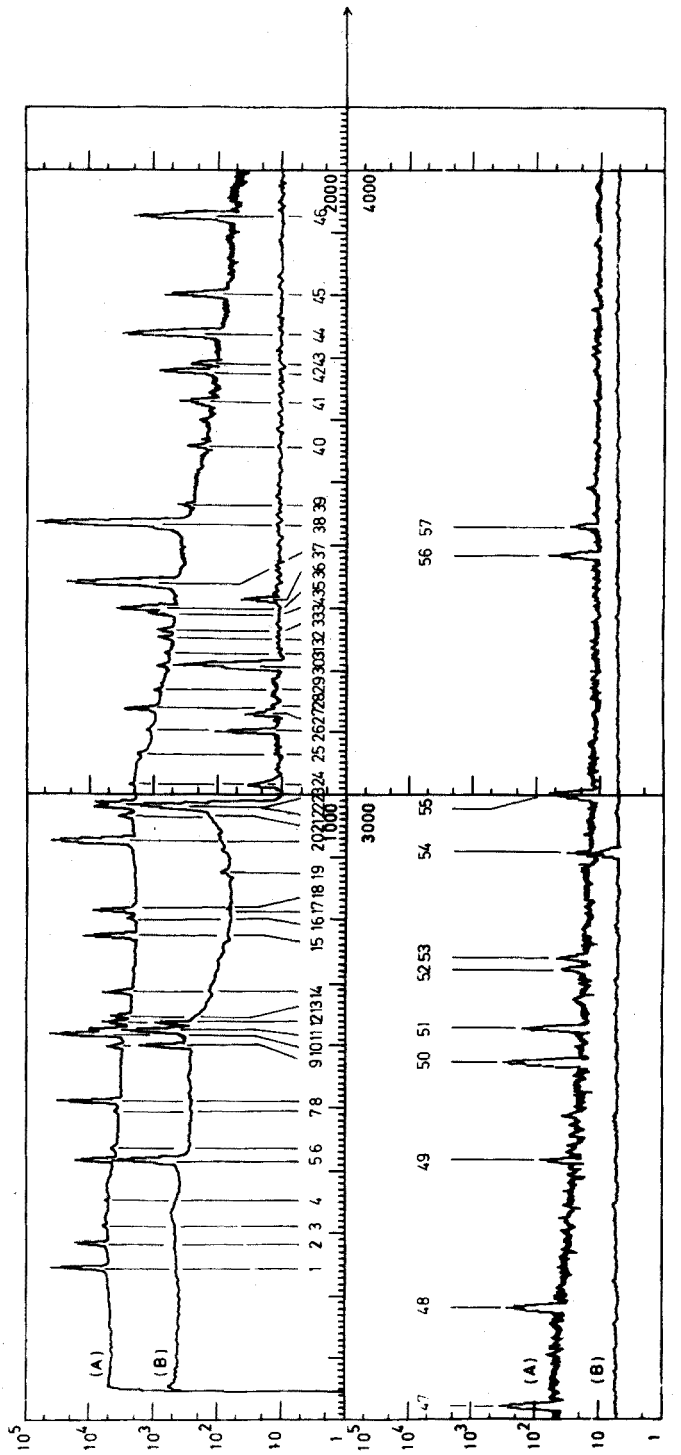

Fig. 1. γ-Ray spectrum of elemental ruthenium measured A: 4 h after irradiation and B: 3 days after irradiation.

Peak-number	*Energy (keV) + reference*	*Isotope*	*Peak-number*	*Energy (keV) + reference*	*Isotope*
1	129.7(8)	^{105}Ru	30	610.406(8)	^{103}Ru
2	149.2(8)	^{105}Ru	31	621.0(8)	^{105}Ru
3	163.6(8)	^{105}Ru	32	625.0	
4	183.6(8)	^{105}Ru	33	632.3(8)	^{105}Ru
5	215.71(8)	^{97}Ru	34	652.6(8)	^{105}Ru
6	225.0(8)	^{105}Ru	35	656.1(8)	^{105}Ru
7	255.1(8)	^{105}Ru	36	663(7)	^{137}Cs
8	262.9(8)	^{105}Ru	37	676.4(8)	^{105}Ru
9	306.1(8)	^{105}Rh	38	724.5(8)	^{105}Ru

10	316.5(8)	^{105}Ru	39	738.3(8)	^{105}Ru
11	318.9(8)	^{105}Rh	40	785	
12	324.48(8); 326.1(8)	^{97}Ru; ^{105}Ru	41	818.8(7); 822.1(8)	^{116m}In;
13	330.9(8)	^{105}Ru			^{105}Ru
14	350.2(8)	^{105}Ru	42	845.9(8)	^{105}Ru
15	393.4(8)	^{105}Ru	43	852.0(8)	^{105}Ru
16	407.5(8)	^{105}Ru	44	875.8(8)	^{105}Ru
17	413.5(8)	^{105}Ru	45	907.7(8)	^{105}Ru
18	417.0(7)	^{116m}In	46	969.4(8)	^{105}Ru
19	443.77(8)	^{103}Ru	47	1017.2(8)	^{105}Ru
20	469.4(8)	^{105}Ru	48	1097(7)	^{116m}In
21	489.6(8)	^{105}Ru	49	1215.2(8)	^{105}Ru
22	497.08(8)	^{103}Ru	50	1292(7)	^{116m}In
23	499.2(8)	^{105}Ru	51	1321.3(8)	^{105}Ru
24	513.7(8)	^{105}Ru	52	1368.4(7)	^{24}Na
25	539.2(8)	^{105}Ru	53	1376.8(8)	^{105}Ru
26	557.11(8)	^{103}Ru	54	1460.0(7)	^{40}K
27	569.33(8)	^{97}Ru	55	1507.7(7)	^{116m}In
28	575.3(8)	^{105}Ru	56	1697.4(8)	^{105}Ru
29	591.3(8)	^{105}Ru	57	1720.2(8)	^{105}Ru

the 499-keV γ-line of ^{105}Ru. The 499-keV γ-line of ^{105}Ru is mentioned in some references[7,8] but not elsewhere[9,10].

When the water-soluble compound, $(NH_4)_2Ru(H_2O)Cl_5$, is irradiated, it is possible to perform γ-ray counting of ruthenium as a liquid source.

ACTIVATION ANALYSIS OF N.B.S. BOVINE LIVER (SRM 1577)

The reference and analysis reactor position

All irradiations were carried out in reactor Thetis of the Rijksuniversiteit Gent. In each of the 16 irradiation facilities the flux ratio at the bottom of the irradiation containers was determined by means of the cadmium ratio method with gold and cobalt flux monitors. Values from 20 to 200 were found, in going from the irradiation position nearest to the core to the most thermalized one. If the mathematical operations and conclusions of the error propagation are correct (eqns. 6–8), the error change factors should be independent of the spreading between the flux ratios in the reference and in the analysis reactor positions. To check this statement, the analyses were performed with one reference reactor position and two analysis reactor positions, the spreading on the respective flux ratios being as large as possible. As the samples needed to be irradiated at a rather high neutron flux, channels 3 ($\phi_{th} = 1.6 \cdot 10^{12}$; $\phi_{th}/\phi_{epi} = 23.8$) and 13 ($\phi_{th} = 1.1 \cdot 10^{12}$; $\phi_{th}/\phi_{epi} = 42.7$) were selected as analysis reactor positions. Even then, irradiation periods of 32 h were needed to produce reasonable activities. Channel 8 ($\phi_{th} = 1.7 \cdot 10^{11}$; $\phi_{th}/\phi_{epi} = 191$) was chosen as the reference reactor position. The low fluxes in this channel were sufficient because the weight of the standards, used to determine the k_{ref} factors, could be increased so as to reach acceptable counting statistics.

Sampling, irradiation and measurements

Before irradiation, the bovine liver was treated as recommended in the NBS analysis certificate. After lyophilization for 48 h at -45°C at a pressure of 10^{-2} mm Hg, the dry liver material was divided into samples of 500 mg, weighed and encapsulated in cylindrical polyethylene boxes (16 mm diam. $\times$ 8 mm height). The ruthenium comparators to be co-irradiated were carefully weighed on a microbalance as 1-mg samples and encapsulated in small cylindrical polyethylene boxes (8 mm diam. $\times$ 9 mm height).

In channel 3 as well as in channel 13, 3 samples and 4 comparator sets were irradiated for a 32-h period. The packing of each irradiation container is shown in Fig. 2.

The measurements were performed on a Philips Ge(Li) detector (efficiency 14.2%; FWHM for the 1332-keV γ-ray of ^{60}Co: 2.1 keV) coupled to a 4000-channel analyser (Didac Intertechnique).

After irradiation, the bovine liver had to be cooled for one month, because the phosphorus content produced too much β-activity, which interfered with the γ-ray measurements by Bremsstrahlung. After one month, the ^{32}P activity had decreased to about 25% of its initial intensity, so that it was possible to detect the γ-rays of the isotopes ^{75}Se, ^{86}Rb, ^{65}Zn, ^{59}Fe and ^{60}Co by measuring for 12 h in a standardized geometry at a distance of 3.5 cm from the detector (Fig. 3). Two

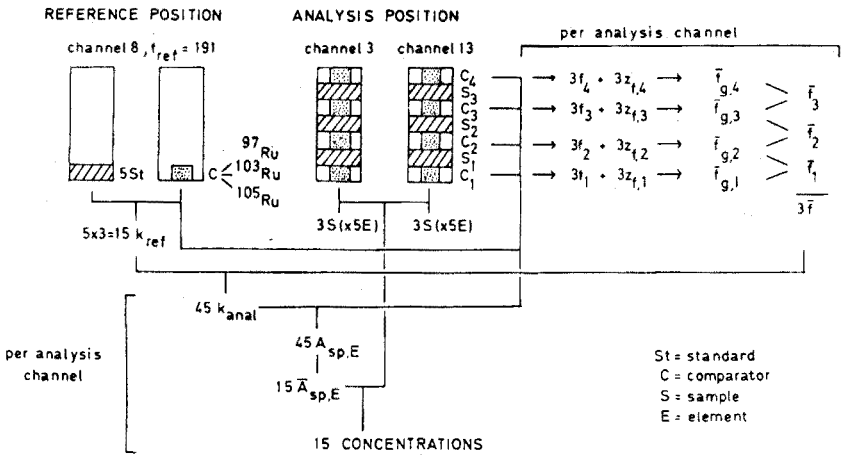

Fig. 2. Scheme of analysis for the NBS bovine liver.

months after irradiation, all the samples were remeasured, thus avoiding systematic errors of the measurements. The ruthenium samples had to be cooled for 5 days to decrease the total activity, so that the measurements could be made with low dead-time corrections. After 5 days, the 4.44-h ^{105}Ru isotope had completely decayed to its 35.5-h ^{105}Rh daughter, so that the three isotopes ^{97}Ru, ^{103}Ru and ^{105}Rh could be measured simultaneously in a standardized geometry at a distance of 11.5 cm from the detector. A second measurement was performed after a cooling period of 14 days, so that only the ^{97}Ru and ^{103}Ru isotopes were counted. All γ-ray spectra were transferred to a PDP-9 computer for calculation of the photopeak areas.

After the bovine liver spectra had been analysed, standards were prepared for the five detected isotopes. Selenium, zinc and rubidium solutions were spotted on ultrapure alumina, which is an inert matrix for shielding effects. The polyethylene boxes were filled with the dried mixtures up to the same volume as the bovine liver samples. After being shaken, the homogeneous and diluted standards were irradiated in channel 8. As ^{58}Fe has a low response to (n,γ) activation, the capsules for the iron standards were filled with 1 g of carbonyl iron, which gives no detectable shielding ($\sigma_a = 2.55$) and yields reasonable counting statistics without excessive irradiation or measuring times. The ^{60}Co standard was obtained by irradiation of a cobalt and aluminium wire ($2.00 \pm 0.02\%$ Co), delivered and certified by CBNM (Geel) and commonly used for absolute flux calibration; this wire was coiled and placed in the middle of the capsule. The specific activities of the ruthenium comparator were determined by irradiating in channel 8, four 10-mg samples of ruthenium powder.

For all standards and comparators irradiated in channel 8, the γ-spectra were transferred to the PDP-computer and the photopeak areas were evaluated with the same data reduction program.

Calculation of the results

Combination of the three specific activities of each comparator set in the

analysis reactor positions with the specific activities of the comparator isotopes in the reference reactor position, yields three R values and thus three flux ratios (f_{anal}) for each comparator set. This means 24 flux ratios in total. The three flux ratios for each comparator set were weight-averaged. As was stated earlier, for each flux ratio a Z_f factor can be calculated. As can be seen in Table II, the Z_f factor was the highest for the combination ^{97}Ru–^{105}Rh with D values of 23.1 and 13.0, and it was the lowest for the combination ^{97}Ru–^{103}Ru with D values of 23.1 and 3.3, which is in agreement with the former conclusions. It is obvious that $1/Z_f$ is a good criterion to be used as a weighing factor. After averaging, four flux ratios remain per analysis channel. As outlined in Fig. 2, the flux ratios calculated from the comparators surrounding a sample were averaged.

TABLE II

RESULTS FOR THE FLUX RATIO DETERMINATION BY THE RMCM

^{97}Ru–^{103}Ru		^{97}Ru–^{105}Ru		^{103}Ru–^{105}Ru	
f	Z_f	f	Z_f	f	Z_f
Channel 3 (f_{Rcd}: 23.8)					
22.8	2.6	22.6	7.1	22.8	4.2
21.7	2.5	24.5	7.1	20.3	4.0
20.1	2.5	21.8	7.1	19.3	3.8
23.9	2.7	28.7	7.5	21.5	4.2
Channel 13 (f_{Rcd}: 42.7)					
45.1	3.7	42.3	8.7	47.3	6.5
41.8	3.5	42.6	8.5	41.2	6.0
44.2	3.6	39.7	8.3	48.0	6.7
43.6	3.5	41.4	8.4	45.4	6.3

The flux ratio thus obtained was believed to occur at this particular sample position. From the specific activities of the five standards and the three comparator isotopes irradiated in channel 8, fifteen k_{ref} values could be obtained. For each sample position it was possible, with the aid of f_{anal}, to convert the fifteen k_{ref} values to fifteen k_{anal} values. In Table III, the k_{ref} values with the corresponding $(D_{st}D_{comp})^{\frac{1}{2}}$ values as well as the k_{anal} values, computed for two f_{anal} determinations, with the respective Z_k factors are given. From Table III the following conclusions can be made: the closer the f_{ref} and f_{anal}, the closer the k_{ref} and k_{anal} values; the more $(D_{st}D_{comp})^{\frac{1}{2}}$ and f_{anal} differ, the lower the Z_f value; the closer D_{st} and D_{comp}, the lower the Z_f value.

These conclusions are in complete agreement with the optimal conditions for the application of the relative multiple comparator method.

Thus, for the three samples, forty five k_{anal} values per analysis channel can be computed. Combining these k_{anal} values with the corresponding specific activities of

TABLE III

CONVERSION FROM k_{ref} TO k_{anal}

Standard isotope	*D value*	k_{ref} (f_{ref}: 191)					
		Reference comparator					
		^{97}Ru	$(D_{st}D_{comp})^{\frac{1}{2}}$	^{103}Ru	$(D_{st}D_{comp})^{\frac{1}{2}}$	^{105}Ru	$(D_{st}D_{comp})^{\frac{1}{2}}$
^{86}Rb	7.93	3.719	13.5	0.2887	5.1	3.284	10.1
^{59}Fe	1.4	0.4729	5.7	0.03670	2.1	0.4177	5.3
^{65}Zn	2.2	22.40	7.1	1.739	2.7	19.79	6.7
^{75}Se	8.2	216.9	13.8	16.83	5.2	191.6	10.3
^{60}Co	2.03	8889	6.8	689.8	2.6	7851	5.1

Standard isotope	*D value*	f_{anal}: 22.2						f_{anal}: 43.5					
		Reference comparator						*Reference comparator*					
		^{97}Ru		^{103}Ru		^{105}Ru		^{97}Ru		^{103}Ru		^{105}Ru	
		k_{anal}	Z_k	k_{anal}	Z_k	k_{anal}	Z_k	k_{anal}	Z_k	k_{anal}	Z_k	k_{anal}	Z_k
^{86}Rb	7.93	2.660	0.247	0.3329	0.134	2.881	0.106	3.090	0.193	0.3097	0.084	3.065	0.076
^{59}Fe	1.4	0.2741	0.451	0.03430	0.070	0.2969	0.310	0.3548	0.316	0.03556	0.039	0.3520	0.199
^{65}Zn	2.2	13.37	0.420	1.680	0.039	14.48	0.279	17.03	0.299	1.708	0.022	16.90	0.182
^{75}Se	8.2	156.4	0.240	19.57	0.140	169.4	0.100	181.0	0.188	18.13	0.088	179.50	0.071
^{60}Co	2.03	5273	0.426	659.7	0.046	5711	0.285	6740	0.302	675.5	0.026	6686	0.185

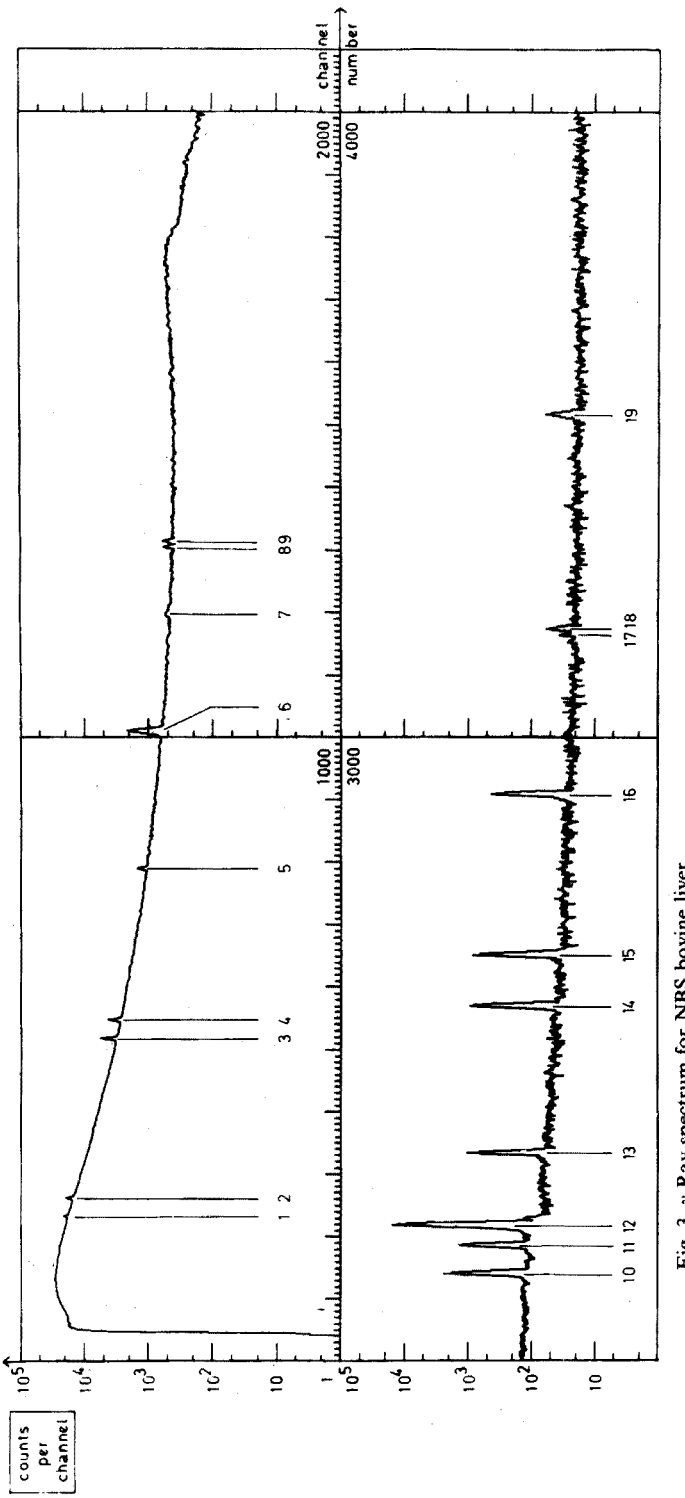

Fig. 3. γ-Ray spectrum for NBS bovine liver.

Peak number	*Energy (keV) (ref. 7)*	*Isotope*	*Peak number*	*Energy (keV) (ref. 7)*	*Isotope*
1	121.1	^{75}Se	11	1099.3	^{59}Fe
2	136.0	^{75}Se	12	1115.5	^{65}Zn
3	264.7	^{75}Se	13	1173.2	^{60}Co
4	279.5	^{75}Se	14	1291.5	^{59}Fe
5	400.8	^{75}Se	15	1332.5	^{60}Co
6	511	β^+	16	1460.0	^{40}K
7	605.0	^{134}Cs	17	1588	^{228}Ac
8	657.7	^{110m}Ag	18	1592	^{203}Tl
9	661	^{137}Cs	19	1765	^{214}Bi
10	1078.8	^{86}Rb			

TABLE IV

RESULTS FOR THE NBS/SRM 1577

Element	*Concentration (p.p.m.)*								
	RMCM							*NBS Analysis certificate*	*Multi-element serum-standard (ref. 4)*
	Channel 3			*Channel 13*			*Average*		
	S_1	S_2	S_3	S_1	S_2	S_3			
Rb	19.60	18.96	18.49	18.04	17.79	17.71	18.5 ± 0.4	18.3 ± 1.0	18.7 ± 1.0
Fe	272.8	273.2	278.5	281.9	283.3	270.0	277 ± 2	270 ± 20	270 ± 12
Zn	133.5	135.3	135.6	139.5	135.4	133.4	135 ± 1	130 ± 10	131.8 ± 6.5
Se	1.10	1.06	1.07	1.14	1.08	1.05	1.08 ± 0.01	1.1 ± 0.1	1.13 ± 0.09
Co	0.257	0.254	0.259	0.265	0.252	0.258	0.257 ± 0.002	0.18	0.24 ± 0.01

the comparators in the analysis reactor position, forty five specific standard activities are obtained.

For each element in each sample, one obtains three $A_{sp.E}$ values, resulting from the relation of a standard to each of the three comparators. As only one $A_{sp.E}$ per element per sample is needed, those three connected $A_{sp.E}$ values are averaged. This results in fifteen $A_{sp.E}$ values. If now each activity of each element in each sample is related to its specific activity, fifteen concentrations for each analysis channel are obtained.

RESULTS AND DISCUSSION

Table IV summarizes the analytical results for channel 3 and 13. The standard deviations are given on the mean at the 95% confidence limit. The results are compared with the values of the NBS analysis certificate and with those of an analysis based on a multi-element serum standard. No systematic deviations seem to occur, indicating that there is no significant difference between the results of the applied techniques. The advantages of the RMCM are clear. No difficulties arise in the preparation of complex standards, because each element can be treated separately in a sufficiently diluted form to determine the k_{ref} values. The composition of the sample need not to be known before irradiation, because k_{ref} values can be determined afterwards. The method is only restricted to the number of isotopes, for which the photopeaks can be undoubtedly calculated from the γ-ray spectrum of the sample, and not to the number of standards that can be co-irradiated in the same irradiation container without introducing shielding or flux gradient errors. Finally, for serial analysis, the k_{ref} values can be repeatedly used so that only one spectrum of ruthenium is necessary to give all the information about the irradiation parameters.

The authors wish to thank the Nationaal Fonds voor Wetenschappelijk Onderzoek for financial support.

SUMMARY

The elements Fe, Zn, Se, Rb and Co were determined in NBS bovine liver (SRM 1577) by non-destructive activation analysis; ruthenium was used as triple comparator element. The results were compared with the values of the analysis certificate and with those of an analysis based on a multi-element serum standard; the agreement was excellent. The conclusions of the error theory of the comparator method were experimentally confirmed.

REFERENCES

1 R. Van der Linden, F. De Corte and J. Hoste, *J. Radioanal. Chem.*, 13 (1973) 169.
2 R. Van der Linden, F. De Corte and J. Hoste, *Symposium on Applications of Nuclear Data in Science and Technology, IAEA/SM-170/32*, Paris, 12–16 March 1973.
3 R. Van der Linden, F. De Corte and J. Hoste, *J. Radioanal. Chem.*, in press.
4 R. Cornelis, A. Speecke and J. Hoste, *Anal. Chim. Acta*, 68 (1974) 1.

5 R. Van der Linden, F. De Corte, P. Van den Winkel and J. Hoste, *J. Radioanal. Chem.*, 11 (1972) 3.
6 R. Van der Linden, F. De Corte and J. Hoste, *J. Radioanal. Chem.*, in press.
7 R. H. Filby, A. I. Davis, K. R. Shah, G. G. Wainscott, W. A. Haller and W. A. Cassat, *Gamma-Ray Energy Tables for Neutron Activation Analysis, WSUNRC*, 97 (2) 1970.
8 S. O. Schriber and M. W. Johns, *Nucl. Phys, A*, 96 (1967) 337.
9 F. Adams and R. Dams, *J. Radioanal. Chem.*, 3 (1969) 99.
10 I. M. H. Pagden, G. J. Pearson and J. M. Bewers, *J. Radioanal. Chem.*, 8 (1971) 127.
11 N. E. Holden and F. W. Walker, *Chart of the Nuclides*, Gen. Electric Co., Schenectady, N.Y., 1968.

Analytica Chimica Acta, 71 (1974) 277–288

REMOTE SENSING OF AIR POLLUTANTS BY LASER-INDUCED INFRARED FLUORESCENCE—A REVIEW

J. W. ROBINSON and J. D. DAKE

Department of Chemistry, Louisiana State University, Baton Rouge, Louisiana 70803 (U.S.A.)

(Received 24th January 1974)

At the present time federal, state, and local agencies are monitoring a wide variety of atmospheric pollutants[1,2]. Usually the monitoring techniques require sample collection at selected points[1,2]. All methods for collecting trace pollutants are subject to variations in collection efficiencies and to contamination from the scrubbing agents used. In addition, the method is subject to interferences from other constituents collected[3,4]. Usually, the scrubbing methods require an extended period of time to obtain a single sample, and in all cases only one location may be investigated at a given time by a single sample collection station[2–4].

There is a need for sensitive and instantaneous detection methods which can monitor selected atmospheric pollutants at extended ranges. Such detection methods would offer several advantages over the methods presently used for air pollution analysis. First of all, an instrument with sufficient analytical sensitivity would eliminate the need for sample collection. This would provide the analyst with instantaneous or "real time" results rather than time-averaged results presented at some time after the sample collection of time-averaged period. Secondly, inaccessible areas could be monitored remotely for air pollution. Air quality could be readily determined at various altitudes, and suspected air pollution sources could be monitored. Finally, a single remote air pollution monitoring device could be the basis for the air pollution control of an entire city. By continuously monitoring pollution levels at a variety of locations over a city, and by maintaining surveillance of potential pollution sources, early warning of dangerous pollutant levels could be provided, and action could be taken to restrict the activities of the offending sources.

Several techniques which employ lasers have been proposed for use in the remote sensing of air pollutants. The techniques depend either on the absorption of the laser beam by the pollutant species or on laser-induced backscatter from the pollutant.

Laser-beam absorption experiments are relatively simple to conduct and offer high sensitivities for a number of compounds[5,6]. An infrared laser beam absorption experiment has been constructed which can determine molecular atmospheric pollutants over a path length of 3.2 km[7]. A typical laser absorption experiment is shown in Fig. 1. Although the absorption techniques are simple and operational at this time, they suffer from two disadvantages. First of all, absorption methods require fixed reflectors to return the laser beam to the detector. This permits analysis of the air only along the path between the laser and the reflector. Of

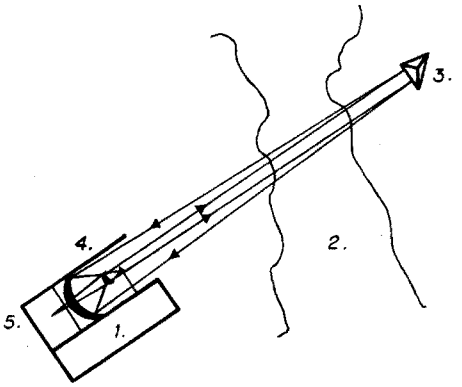

Fig. 1. Absorption remote sensing apparatus. (1) Tuneable laser, (2) polluted region, (3) remote retroreflector, (4) telescope, (5) detector.

course, many reflectors could be installed around a single laser-detector location, but still only a very limited fraction of the atmosphere could be monitored by one apparatus. Secondly, absorption methods can determine only the total amount of a given pollutant along the laser path. Absorption methods do not have the capability to determine the distribution of the pollutant along the laser path.

The backscatter techniques proposed for the remote sensing of air pollutants are Mie scattering, the Raman effect, electronic fluorescence, and vibrational fluorescence[5,8–20]. These scattering or fluorescence methods require no fixed reflectors; therefore, the atmosphere may be monitored in any direction from the sensing apparatus. More importantly, by using a modulated laser beam and a time-gated backscatter detection system, the range of a scattering or fluorescing atmospheric species may be determined. The term "Lidar" meaning laser radar, has been applied to these backscatter techniques[9,21]. A typical Lidar apparatus is shown in Fig. 2. The apparatus employs three principal parts: (1) a laser which is used to induce fluorescence or scattering by the pollutant species in the atmosphere at ranges up to several kilometers from the apparatus; (2) a telescope

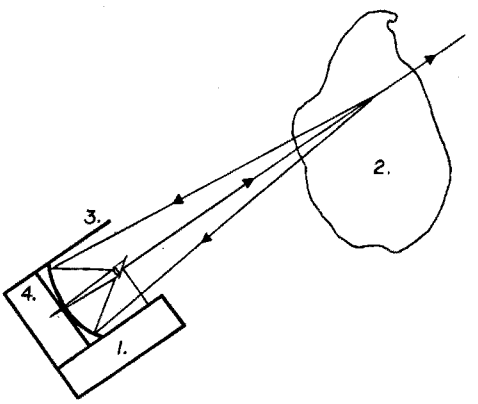

Fig. 2. Backscatter remote sensing apparatus. (1) Laser, (2) polluted region, (3) telescope, (4) spectrometer and detector.

which is aligned coaxially with the path of the laser beam and which collects part of the radiation from the laser-stimulated molecules or particles; and (3) a spectrometer and detector system which analyzes the radiation collected by the telescope.

In 1964, Collis and Ligda[8] reported the observation of Mie scattering of a laser beam by particulates in the atmosphere. In subsequent work, the technique was developed to the point that particulate mapping of a large volume of the atmosphere by a single instrument was possible[9]. A typical Mie scattering remote-sensing device uses a single wavelength, pulsed, visible laser and a visible light detection system. No spectral analysis is required for this method. Mie scattering remote sensing instruments are commercially available[10].

The Raman effect scheme for the remote sensing of molecular pollutants has been described in detail[5,11]. The Raman lines of a molecule are shifted from the laser frequency by the characteristic vibrational frequencies of the molecule. As in the Mie scattering technique, a fixed-wavelength, pulsed laser is used. A high-resolution spectrometer is required to separate the Raman lines from the more intense Mie and Rayleigh scattering of the laser beam. The construction of Raman-effect backscatter remote-sensing devices has been reported[12,13]. The instruments are capable of determining molecular species which are present in concentrations of a few hundred parts per million at ranges from 1 to 10 km. This sensitivity is insufficient to monitor most pollutants in the atmosphere. The sensitivity is sufficient, however, to sense many species in industrial stack gas effluents.

The theoretical usefulness of laser-induced electronic fluorescence for the remote monitoring of air pollutants has been investigated[5,14,15]. Both atomic and molecular species may be monitored by this technique. A tunable, visible-wavelength laser has been used to excite electronic fluorescence in sodium atoms in the upper atmosphere[16]. The laser-induced sodium fluorescence could be detected at ranges over 100 km[16].

The theoretical potential of laser-induced infrared fluorescence for the remote sensing of molecular air pollutants has been described[5,17–20]. No operational remote-sensing devices based on infrared fluorescence have been reported. The hypothetical remote monitor would employ a tunable infrared laser and an infrared spectrometer.

As stated above, the use of laser-induced Mie scattering for the remote sensing of particulates is well developed. Kildal and Byer[5] have recently evaluated the comparative remote-sensing potentials of the Raman effect, electronic fluorescence, infrared fluorescence, and infrared absorption. Infrared absorption is a simple and sensitive technique; but, as stated above, absorption is inferior to backscatter methods for remote sensing. The Raman effect is general and very reproducible for molecules. However, the Raman effect is very weak and, therefore, offers less sensitivity for remote sensing than do electronic and infrared fluorescence. Because of their large backscatter cross-sections, laser-induced electronic and infrared fluorescence have the greatest potential for the remote sensing of molecular air pollutants[5]. The development of the electronic and infrared fluorescence techniques has been limited by the lack of laser-induced fluorescence data for pollutant molecules in air at atmospheric pressure, and by the lack of high-

powered tunable lasers.

In this paper, a review of infrared fluorescence is presented with emphasis on experiments which are applicable to the evaluation of laser-induced infrared fluorescence as a method for the remote sensing of molecular air pollutants. Previously published experimental results and calculations presented in this paper indicate that the construction of an infrared fluorescence remote-sensing device is feasible.

HISTORICAL REVIEW OF INFRARED FLUORESCENCE

Before the advent of the infrared laser, several workers attempted to observe vibrational fluorescence in molecules. In 1957, Benson and Porter[22] reported the exposing gases such as carbon monoxide, carbon dioxide, hydrogen cyanide, and hydrogen chloride, to intense polychromatic infrared radiation. Using the best infrared detectors available at the time, they were unable to detect infrared fluorescence in any of the gases investigated. In 1962, Millikan[23] reported observing vibrational fluorescence from carbon monoxide which had been excited by infrared radiation from flame-heated bricks of ZrO_2. In a following paper, Millikan[24] reported enhanced vibrational excitation of carbon monoxide which was exposed to the thermal radiation of carbon monoxide in rich methane–oxygen flames.

In 1966, Hocker *et al.*[25] reported the observation of vibrational fluorescence from carbon dioxide which was excited by laser radiation inside the cavity of a CO_2 gas laser. Following this paper, Yardley and Moore[26,27] reported the usefulness of laser-induced infrared fluorescence for investigating vibrational energy transfer in carbon dioxide. As in Hocker's original experiment, carbon dioxide was excited by radiation inside the cavity of a CO_2 gas laser.

The first experiments in which molecules were excited by laser radiation outside the laser cavity were reported in 1966 by Yardley and Moore[28] and by Borde *et al.*[29,30]. Since 1966, infrared lasers have been used to excite vibrational fluorescence in a wide variety of molecules[31–46].

In 1968, Robinson *et al.*[47] reported the analytical usefulness of laser-induced infrared emission. In subsequent papers, they presented infrared fluorescence spectra, detection limits and other analytical data for several compounds[48,49]. Robinson *et al.*[17] also proposed laser-induced infrared fluorescence as a useful technique for the remote analysis of molecular air pollutants. Later, infrared fluorescence spectra for 36 compounds[50] and quantitative analytical data for nine compounds[51,52] were presented. Robinson and Guagliardo[53] reported the use of a tunable CO_2 gas laser for the selective excitation of ozone infrared fluorescence[53].

A series of papers which describe analytical parameters which would be important in the remote-sensing of air pollutants by laser-induced infrared fluorescence[54–57] has been published. A lifetime for vibrationally excited ethylene in air at atmospheric pressure has been given[54]; it has been shown that laser-induced infrared fluorescence is isotropic[55], and that considerable selectivity can be introduced into laser-induced infrared fluorescence experiments by tuning the excitation source over a narrow wavelength range[56]. Robinson and Dake[57] also presented data which demonstrated the effects of laser power, sample concentration, collisional deactivation, and pressure broadening on the intensity of laser-induced

ethylene fluorescence. The published results indicate that, among other things, the shorter wavelength fluorescence, which is frequently observed in laboratory experiments, probably will not be useful in remote-sensing procedures. Dake has presented an evaluation of various analytical parameters which will be important in the remote sensing of air pollutants by laser induced infrared fluorescence[58].

SHORTER WAVELENGTH FLUORESCENCE

In many experiments, infrared fluorescence has been observed at wavelengths shorter than the wavelength of the stimulating laser radiation[17,26–30,37,38,42,43,47–53]. In the case of carbon dioxide, the shorter wavelength fluorescence was satisfactorily explained by demonstrating the occurrence of absorption by a thermally populated excited vibrational state[26,27]. For other molecules, similar mechanisms have been proposed, but in no case other than carbon dioxide is there clear evidence that thermally assisted fluorescence is the only mechanism operating[42,46,52].

Other mechanisms have been proposed for the shorter wavelength fluorescence. Bailey *et al.*[37,38] have proposed that vibrational–rotational energy transfer may be responsible for the higher energy fluorescence. There is considerable evidence that a combination of intermolecular and intramolecular vibrational–vibrational energy transfer and excited state absorption is responsible for the shorter wavelength fluorescence[42,43,46].

Robinson and Dake[7] have demonstrated that infrared fluorescence at wavelengths shorter than the excitation wavelengths are frequently an order of magnitude weaker than fluorescence at the resonance wavelength. In addition, short wavelength fluorescence is much more subject to collision deactivation, suggesting a time-dependent activation process. Each of these characteristics militates against their use as analytical lines.

IMPORTANT FACTORS IN LASER-INDUCED INFRARED FLUORESCENCE

Methods of excitation

Several interesting phenomena have been observed in laser-induced infrared fluorescence experiments: (1) the occurrence of infrared fluorescence at wavelengths shorter than the exciting laser wavelength; (2) the exponential increases in fluorescence intensity with increasing laser power[50,57]; and (3) the exponential increases in fluorescence intensity with increasing partial pressure of ethylene[57]. These observations indicate that mechanisms other than resonance absorption and fluorescence occur.

It is proposed that the following methods of excitation may be important in laser-induced infrared fluorescence: (1) ground state absorption, (2) intramolecular energy transfer, (3) excited state absorption, (4) intermolecular energy transfer, and (5) thermal excitation.

Ground-state absorption. In the case of ethylene fluorescence, ground-state absorption is undoubtedly the principal method of excitation. Ethylene is a strong absorber of laser radiation at 10.6 μm and is observed to fluoresce strongly at 10.6 μm. The fluorescence intensity of the 10.6 μm band is linear with laser

power and is approximately linear with the partial pressure of ethylene[57].

In the case of carbon dioxide infrared fluorescence, ground-state absorption is apparently not an important method of excitation. Carbon dioxide excited by laser radiation at 10.6 μm fluoresces at 4.3 μm (ref. 26). It is not a strong absorber of laser radiation at 10.6 μm and does not fluoresce strongly at 10.6 μm.

Intramolecular energy transfer. Intramolecular redistribution of vibrational energy is a common phenomenon for molecules excited by infrared laser radiation. In all cases, when one rotational line in a vibrational band is excited, fluorescence is observed from many other rotational lines within the vibrational band. This redistribution of energy throughout the vibrational band is thought to occur within a few nanoseconds[5].

Intramolecular redistribution of vibrational energy to other vibrational modes has been demonstrated for a number of molecules[27,31,44]. It is thought that this intramolecular energy transfer is stimulated by molecular collisions[27]. Intramolecular vibrational energy transfer is undoubtedly an important mechanism in the excitation of the wide variety of vibrational modes which are observed to fluoresce in ethylene and other molecules.

Excited state absorption. It has been demonstrated that excited state absorption is the dominant mechanism in laser-induced carbon dioxide fluorescence[26]. An excited vibrational level of carbon dioxide at 0.1721 eV (1388 cm^{-1} or 7.2 μm) is slightly populated at room temperature. The thermally excited carbon dioxide molecules absorb 10.6-μm laser radiation and are further excited to an energy level 0.2913 eV (2350 cm^{-1} or 4.3 μm) above the ground state. The excited molecules then may return to the ground state with the emission of 4.3 μm photons.

It has been shown that the vibrational energy levels of monofluoromethane[42], ethylene[43], and acetone[59] are spaced such that excited-state absorption may be occurring during laser-induced fluorescence experiments. Although excited-state absorption has not been clearly demonstrated for ethylene and other organic molecules, it is quite probable that excited-state absorption is an important mechanism in the laser excitation of higher energy vibrational bands[42,43,59].

Intermolecular vibrational energy transfer. It has been demonstrated that intermolecular vibrational energy transfer occurs in laser-induced fluorescence experiments[58]. It is possible that two vibrationally excited molecules may collide and that one of the molecules transfers some of its vibrational energy to the second molecule[43]. This would be a possible explanation for the shorter wavelength fluorescence which is observed.

Experimental results showed that the intensities of the shorter wavelength fluorescence bands of ethylene vary exponentially with the partial pressure of ethylene[57]. These results demonstrate a concentration dependence for the shorter wavelength fluorescence, which indicates that intermolecular vibrational energy transfer is at least partially responsible for the shorter wavelength fluorescence of ethylene.

In the case of carbon dioxide, which absorbs laser energy at a thermally excited vibrational state, the fluorescence intensity has been observed to vary in a linear manner with laser power[42]. The fact that the fluorescence intensities of the shorter wavelength bands of ethylene vary exponentially with laser power

indicates that mechanisms other than room temperature excited state absorption are operating.

It is proposed that intramolecular and intermolecular vibrational energy redistribution significantly increase the populations of the excited vibrational states of ethylene, and this in turn leads to enhanced excited state absorption by ethylene.

Thermal excitation. It is well known that infrared emission can be produced by simply heating a gas sample. Experimental results have indicated that thermal excitation may occur in laser-induced infrared fluorescence experiments[52]. Thermally excited molecular species would be expected to emit radiation at all vibrational modes of the species.

It is thought that, by modulating the exciting laser beam and detecting only emission with the same frequency as the modulation frequency, most of the thermal emission would not be recorded. Particulates do not cause thermal excitation of ethylene to any measurable extent[58]. Ethylene fluorescence at 7 and 10.6 μm can be observed without the use of a walled cell[55,58]. These results indicate that thermal excitation is not the principal mechanism operating in laser-induced ethylene fluorescence.

Fluorescence lifetimes

Fluorescence lifetimes are important in the investigation of the excitation mechanisms discussed above. In the evaluation of a remote-sensing apparatus which employs laser-induced infrared fluorescence, the fluorescence lifetime will undoubtedly be the limiting factor in the range resolution of the apparatus[5].

Previously published work has shown that two decay processes occur in laser-induced infrared fluorescence experiments[48]. One process has a lifetime of a few microseconds and is thought to be the infrared fluorescence lifetime. The other process has a lifetime of several milliseconds and is attributed to vibrational–translational energy transfer in the molecule followed by fluorescence.

A lifetime has been calculated for the shorter decay process of vibrationally excited ethylene[54]. The calculated lifetime restricts the range resolution of a remote ethylene sensing experiment to 100 m. Considerable variations in fluorescence lifetimes of other vibrationally excited species are expected[5], and fluorescence lifetimes for some molecules are expected to be much longer than the lifetime of ethylene. The data processing will be very complicated in a remote-sensing experiment in which fluorescence is collected from several different molecular species. And in the remote sensing of molecules with fluorescence lifetimes longer than 1 μs, the range resolution will be greater than 200 m.

Analytical interferences in laser-induced infrared fluorescence

Normal atmospheric constituents. The efficiencies of collisional deactivation of ethylene fluorescence by nitrogen, oxygen, or water-vapor are quite low[54]. Considerable variations in oxygen and water-vapor concentrations do not greatly affect ethylene fluorescence intensities[54].

Other molecular interferences. Robinson and Katayama[60] have investigated other possible molecular interferences in laser-induced ethylene fluorescence. The molecules used in the interference studies were propylene, benzene, methane,

propane, 1-butene, chloroform, carbon tetrachloride, acetone and sulfur dioxide. None of the molecules was a severe interference in the observation of laser-induced ethylene fluorescence. All of the molecules studied quenched ethylene fluorescence only slightly even at concentrations up to several percent. It is suspected that molecular species present in a few parts per million will not interfere in the observation of fluorescence from ethylene in p.p.m. concentrations in the air. It is unknown whether severe molecular interferences will be found for other fluorescing species.

Particulate interferences. It has been shown that particulates do not interfere in the fluorescence process of ethylene. Particulate matter strongly scatters the laser radiation, and this scattering must be separated from the molecular fluorescence in a remote-sensing experiment. Since the laser radiation is quickly distributed over a large number of rotational lines of an absorbing molecule, and since the laser line is very narrow compared to the spectral width of the vibrational band, it will be possible to separate the molecular fluorescence from the scattered laser radiation.

EVALUATION OF A HYPOTHETICAL REMOTE-SENSING APPARATUS

Laser parameters

Relatively low-powered, continuous CO_2 gas lasers have been used in most of the laser-induced infrared fluorescence work[47–60]. The total fluorescence intensity of ethylene increases in a linear manner with laser power[57]. Thus, greater sensitivities in the remote monitoring of ethylene should be realized by using more powerful lasers as excitation sources.

If ranges of the fluorescing species are to be determined, a pulsed laser will be required to induce fluorescence. Pulsed CO_2 gas lasers are available and can produce power levels of several megawatts in pulses which are a fraction of a microsecond long. Several publications have reported the use of pulsed carbon dioxide gas lasers for inducing infrared fluorescence[39,42,43]. The results obtained with pulsed lasers are very similar to those obtained with continuous lasers[42,43] It is not known how fluorescence intensities will vary with laser power from the low-power continuous lasers to the high-peak power-pulsed lasers.

A potential problem in the use of high-powered pulsed lasers is that a laser beam with sufficient power density will ionize the air[61]. This effect does not occur until power densities of approximately 10^8 W cm^{-2} are reached. A possible solution to this problem in the design of a remote-sensing apparatus would be to expand the beam diameter and thus reduce the power density of the laser beam. Results obtained in the course of this work indicate that ethylene fluorescence intensities do not vary significantly with laser power density so long as the total power applied to the ethylene remains constant.

By increasing the diameter of the laser beam, another potential problem may be avoided. It has been found that infrared laser beams are distorted by air of varying densities, and by wind currents[62]. By increasing the diameter of the laser beam, these distortions relative to the size of the laser beam may be greatly reduced[7].

Perhaps the most severe limitation of laser-induced infrared fluorescence

as a remote-sensing method is the lack of high-powered lasers with wavelengths appropriate for all potential pollutant molecules. The CO_2 laser can be used to excite fluorescence in a wide variety of compounds including unsaturated hydrocarbons, aromatics, aldehydes, ketones, sulfur dioxide, and ozone. The CO_2 laser is not particularly useful for inducing fluorescence in many saturated hydrocarbons, nitric oxide, and nitrogen dioxide. It should be possible to induce fluorescence in these nitrogen oxides with a carbon-monoxide infrared laser beam[18]. Solid-state infrared lasers have also been proposed for inducing fluorescence in a variety of pollutant molecules[5]

Published results have indicated that considerable selectivity may be added to a remote-sensing experiment by tuning the infrared laser over a narrow wavelength range. All molecules which have been investigated exhibit unique absorption and fluorescence patterns with variation of the laser wavelength. The variation of the laser wavelength from a wavelength which produces strong fluorescence to a wavelength which produces weak fluorescence will be useful in resolving possible laser beam-scattering interferences. Optical scanners may be used to produce a rapid sequence of laser pulses with each pulse having a different wavelength[7,63].

Spectral analysis

A remote-sensing apparatus would require an efficient spectrometer for the qualitative analysis of the fluorescing species. It is possible that a non-dispersive detection system could be used, but it is more likely that a scanning interferometer will be required for the spectral analysis. Spectral analysis techniques for infrared absorption by pollutant molecules are well developed[64]. These same techniques could be extended for the analysis of infrared fluorescence signals.

Detectors

The sensitivity of a remote-monitoring apparatus will vary directly with the detector. Although there are considerable maintenance problems inherent in the use of cryogenic detectors, the increased analytical sensitivity available with these detectors outweighs the maintenance problems.

Calculated ethylene detection limits with a hypothetical remote sensing apparatus

Data and assumptions used in calculations. Ethylene detection limits were calculated for various ranges from a hypothetical remote-sensing apparatus. The order of magnitude detection limits were extrapolated from data obtained in experiments in which a tunable laser, 20-cm gas cell, and pyroelectric detector were used[58].

The data used in the calculations were as follows:

Laboratory experiment	*Hypothetical remote sensing experiment*
Laser power = 5 W	Laser power = 1000 W
Sample thickness = 0.5 cm	Sample thickness = 1 m
Distance of sample to detector = 8 cm	Area of telescope mirror = 1 m^2
Area of detector element = $4 \cdot 10^{-2}$ cm^2	Detectivity of detector = 10^{13}
Detectivity of detector = 10^8	Efficiency of spectrometer = 0.1
Detection limit of ethylene in air = 1000 p.p.m.	

As noted above, infrared lasers with output power of 1000 W or more are commercially available. Infrared detectors with detectivities of 10^{13} are also available.

The laboratory data were obtained with an amplifier time constant of 0.3 s. If a scanning interferometer were used in the hypothetical experiment, the detection limits could be lowered by collecting spectral data for a longer period of time. And conversely, data could be analyzed more rapidly than every 0.3 s by sacrificing some analytical sensitivity.

In the calculations, ethylene fluorescence intensity was assumed to increase linearly with laser power and sample concentration. The total ethylene fluorescence intensity has been found to vary with the 1.2 power of the sample concentration for concentrations between 0.2 and 4% (ref. 57). For ethylene concentrations around 0.1%, the total fluorescence intensity was approximately linear with sample concentration. For the purposes of these calculations, the fluorescence intensity of ethylene was assumed to be linear with sample concentration, for concentrations less than 1000 p.p.m. ethylene in air.

It was further assumed that absorption of the laser beam by the atmosphere was negligible and that self-absorption by the ethylene in the 1-m thick sample was also negligible. Lower detection limits would, of course, be obtained with samples thicker than 1 m. In order to calculate the detection limits for the thick sample case, corrections would have to be made for laser beam "pump" depletion and self-absorption by the sample molecules.

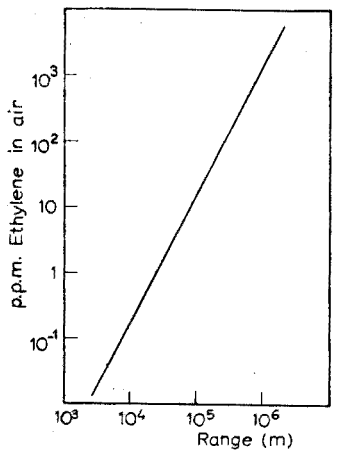

Fig. 3. Detection limits for ethylene using a hypothetical remote sensing apparatus.

Results of calculations. The results of the calculations are shown in Fig. 3. Ethylene at 0.1 p.p.m. may be detected at a range of 10 km. This sensitivity is certainly sufficient to monitor concentrations of ethylene which are of interest in an urban environment. Figure 3 also shows that it may be possible to detect 100 p.p.m. ethylene at ranges of 1000 km. At this range, an earth satellite could possibly be used as a monitoring station for industrial stack effluents which contained relatively high concentrations of ethylene.

SUMMARY

A review of infrared fluorescence is presented. Emphasis is placed on the experimental evaluation of laser-induced infrared fluorescence as a method for the remote sensing of molecular air pollutants. Methods of fluorescence excitation, fluorescence lifetimes, and possible interferences are discussed. The performance of a hypothetical remote sensing apparatus is evaluated. Experimental results and theoretical calculations indicate that the construction of an infrared fluorescence remote sensing device is feasible.

REFERENCES

1 G. B. Morgan, E. C. Tabor and R. L. Thompson in G. Mamantov and W. D. Shults (Eds.), *Determination of Air Quality*, Plenum Press, New York, 1972, p. 1.
2 G. B. Morgan, *Science*, 170 (1970) 289.
3 W. Leithe, *The Analysis of Air Pollutants*, Ann Arbor Humphrey Science Publishers, Ann Arbor, 1970, p. 226.
4 W. E. Ruch, *Quantitative Analysis of Gaseous Pollutants*, Ann Arbor Humphrey Science Publishers, Ann Arbor, 1970, p. 1.
5 H. Kildal and R. L. Byer, *Proc. IEEE*, 59 (1971) 1644.
6 P. L. Hanst, *Appl. Spectrosc.*, 24 (1970) 161.
7 L. R. Snowman and R. J. Gillmeister, *AIAA Paper No. 71-1059*, 1971.
8 R. T. H. Collis and M. G. H. Ligda, *Nature (London)*, 203 (1964) 508.
9 R. T. H. Collis, *Appl. Opt.*, 9 (1970) 1782.
10 Laser Associates Ltd., Rugby, England, 1972.
11 H. Inaba and T. Kobayasi, *Nature (London)*, 224 (1969) 170.
12 T. Kobayasi and H. Inaba, *Appl. Phys. Lett.*, 17 (1970) 139.
13 E. R. Schildkraut, *American Laboratory*, December 1972, p. 23.
14 R. M. Measures, *UTIAS Report No. 174*, 1971.
15 S. A. Ahmed, *Appl. Opt.*, 12 (1973) 901.
16 M. R. Bowman, A. J. Gibson and M. C. W. Sanford, *Nature (London)*, 221 (1969) 456.
17 J. W. Robinson, H. M. Barnes, D. Truitt, D. M. Hailey, H. P. Loftin, C. Woodward and J. D. Rosamond, *Research on New Techniques in Absorption and Emission Spectroscopy, Final Comprehensive Report*, Department of the Army, Contract DA-18-035-AMC-378(A), 1969.
18 R. T. Menzies, *Appl. Opt.*, 10 (1971) 1532.
19 I. Melngailis, *Trans. IEEE, GE-10*, (1972) 7.
20 R. T. Menzies, *Appl. Phys. Lett.*, 22 (1973) 592.
21 G. G. Goyer and R. Watson, *Bull. Amer. Meteorol. Soc.*, 44 (1963) 564.
22 S. W. Benson and G. B. Porter, *J. Chem. Phys.*, 26 (1957) 714.
23 R. C. Millikan, *Phys. Rev. Lett.*, 8 (1962) 253.
24 R. C. Millikan, *J. Chem. Phys.*, 38 (1963) 2855.
25 L. O. Hocker, M. A. Kovacs, C. K. Rhodes, G. W. Flynn and A. Javan, *Phys. Rev. Lett.*, 17 (1966) 223.
26 C. B. Moore, R. E. Wood, B. Hu and J. T. Yardley, *J. Chem. Phys.*, 46 (1967) 4222.
27 J. T. Yardley and C. B. Moore, *J. Chem. Phys.*, 46 (1967) 4491.
28 J. T. Yardley and C. B. Moore, *J. Chem. Phys.*, 45 (1966) 1066.
29 C. Borde, A. Henry and L. Henry, *C.R. Acad. Sci., Ser. B*, 262 (1966) 1386.
30 C. Borde, A. Henry and L. Henry, *C.R. Acad. Sci., Ser. B*, 263 (1966) 619.
31 J. T. Yardley and C. B. Moore, *J. Chem. Phys.*, 49 (1968) 1111.
32 J. T. Yardley, M. Fertig and C. B. Moore, *J. Chem. Phys.*, 52 (1970) 1450.
33 J. C. Stephenson, R. E. Wood and C. B. Moore, *J. Chem. Phys.*, 54 (1971) 3097.
34 H. Chen and C. B. Moore, *J. Chem. Phys.*, 54 (1971) 4080.
35 A. M. Ronn, *J. Chem. Phys.*, 48 (1968) 511.
36 R. D. Bates, G. W. Flynn and A. M. Ronn, *J. Chem. Phys.*, 49

37 R. T. Bailey, F. R. Cruickshank and T. R. Jones, *Carbon Dioxide Laser Excited Infrared Fluorescence*, presented at the Swansea Symposium on Gas Kinetics, 1971.
38 R. T. Bailey, F. R. Cruickshank and T. R. Jones, *Nature (London)*, 234 (1971) 92.
39 Z. Karny, A. M. Ronn, E. Weitz and G. W. Flynn, *Chem. Phys. Lett.*, 17 (1972) 347.
40 D. F. Heller and C. B. Moore, *J. Chem. Phys.*, 52 (1970) 1005.
41 Y. V. Chalapati Rao, V. Subba Rao and D. Ramachandra Rao, *Chem. Phys. Lett.*, 17 (1972) 531.
42 E. Weitz, G. W. Flynn and A. M. Ronn, *J. Chem. Phys.*, 56 (1972) 6060.
43 R. C. L. Yuan and G. W. Flynn, *J. Chem. Phys.*, 57 (1972) 1316.
44 R. D. Bates, J. T. Knudtson, G. W. Flynn and A. M. Ronn, *Chem. Phys. Lett.*, 8 (1971) 103.
45 J. K. Hancock and W. H. Green, *J. Chem. Phys.*, 57 (1972) 4515.
46 R. C. L. Yuan and G. W. Flynn, *J. Chem. Phys.*, 58 (1973) 649.
47 J. W. Robinson, H. M. Barnes and C. Woodward, *Spectrosc. Lett.*, 1 (1968) 109.
48 J. W. Robinson, C. Woodward and H. M. Barnes, *Anal. Chim. Acta*, 43 (1968) 119.
49 J. W. Robinson, D. M. Hailey and H. M. Barnes, *Talanta*, 16 (1969) 1109.
50 D. M. Hailey, H. M. Barnes, C. W. Woodward and J. W. Robinson, *Anal. Chim. Acta*, 56 (1971) 161.
51 D. M. Hailey, H. M. Barnes and J. W. Robinson, *Anal. Chim. Acta*, 56 (1971) 175.
52 C. M. Christian and J. W. Robinson, *Spectrosc. Lett.*, 4 (1971) 255.
53 J. W. Robinson and J. L. Guagliardo, *Spectrosc. Lett.*, 6, (1973) 271.
54 J. W. Robinson and J. D. Dake, *Spectrosc. Lett.*, 6 (1973) 377.
55 J. W. Robinson and J. D. Dake, *Spectrosc. Lett.*, 6 (1973) 499.
56 J. W. Robinson and J. D. Dake, *Spectrosc. Lett.*, 6 (1973) 569.
57 J. W. Robinson and J. D. Dake, *Spectrosc. Lett.*, 6 (1973) 685.
58 J. D. Dake, *Analytical Parameters in the Remote Sensing of Air Pollutants Using Laser Induced Infrared Fluorescence*, Dissertation, Louisiana State University, 1973.
59 C. M. Christian, *Direct Determination of Selected Atmospheric Pollutants*, Dissertation, Louisiana State University, 1971.
60 J. W. Robinson and N. Katayama, unpublished results.
61 R. T. Brown and C. Smith, *Appl. Phys. Lett.*, 22 (1973) 245.
62 F. G. Gebhardt and D. C. Smith, *Appl. Phys. Lett.*, 14 (1969) 52.
63 R. A. Lucht and O. Jarrett, *Appl. Opt.*, 11 (1972) 1568.
64 P. L. Hanst, A. S. Lefohn and B. W. Gay, *Appl. Spectrosc.*, 27 (1973) 188.

Analytica Chimica Acta, 71 (1974) 289–294

THE USE OF A NON-DISPERSIVE ATOMIC FLUORESCENCE SPECTROMETER FOR THE DETERMINATION OF ZINC IN SOILS AND NON-FERROUS METAL ALLOYS

J. D. NORRIS and T. S. WEST

Chemistry Department, Imperial College of Science and Technology, London SW7 2AY (England)

(Received 2nd January 1974)

The advantages to be found in the use of non-dispersive detection systems for atomic fluorescence flame spectrometry have been discussed elsewhere[1–5] Larkins and Willis[2, 3] have employed a simple non-dispersive atomic fluorescence spectrometer for the determination of about thirty elements, in every case obtaining superior detection limits to those attainable with similar instrumentation incorporating a monochromator. Detection limits reported for zinc were respectively 0.0003 p.p.m. and 0.003 p.p.m., in an air–acetylene flame with a high-intensity hollow-cathode lamp as the spectral source[2]. However, no applications of non-dispersive atomic fluorescence spectrometry to the analysis of technical materials have yet been reported.

This paper describes the construction of a non-dispersive atomic fluorescence spectrometer and its application to the determination of zinc in soil extracts and non-ferrous metal alloys.

EXPERIMENTAL

Instrumentation

The general arrangement of the instrumentation employed for non-dispersive atomic fluorescence determinations is shown in Fig. 1. The spectral source was a zinc electrodeless discharge lamp, operated at 2450 ± 25 MHz in a $\frac{3}{4}$-wave (Broida type) resonant cavity, powered from a Microtron 200 microwave generator. The optimal incident power for the operation of this lamp was 60 W. An asbestos screen, with a slit 30×15 mm, was placed in front of the resonant cavity. This screen was arranged to move backwards and forwards to act as a shutter, so that the flame could, when required, be illuminated by the spectral source. The zinc electrodeless discharge lamp was placed as near as possible to the flame (*ca.* 35 mm from the centre of the flame). A slightly fuel-lean, argon-separated air–acetylene flame was supported on a Unicam SP900 burner, which had been adapted for use with a separated flame[6]. A slit of 12-mm diameter was positioned 35 mm from the centre of the flame. The light path from this slit to the photomultiplier was enclosed in a metal tube to prevent stray radiation from falling onto the photomultiplier. Two lenses of focal length 70 mm and diameter 35 mm were held in this tube. The EMI 9616B end-window, solar-blind photomultiplier was powered from a Brandenburg model 472R photomultiplier power supply. The output signal

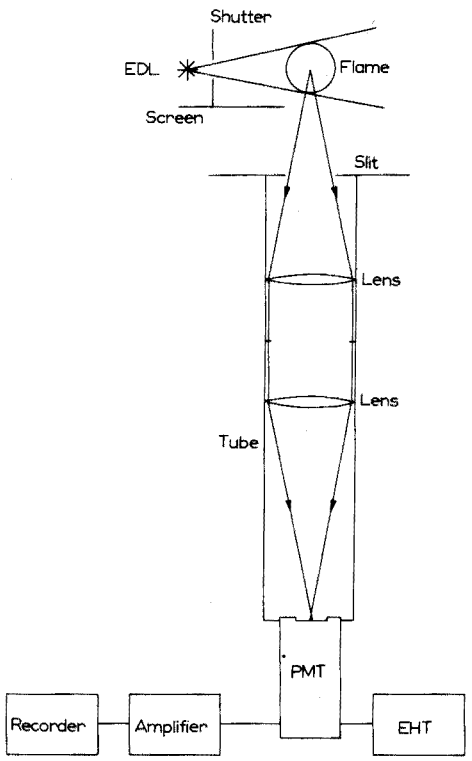

Fig. 1. Instrumentation for non-dispersive atomic fluorescence spectrometry.

from the photomultiplier was fed through an operational amplifier curcuit, similar to one described previously[7], to a Servoscribe potentiometric chart recorder.

Comparative conventional atomic fluorescence measurements were made with a Southern Analytical A1740 grating flame spectrometer[8]. The flame and the spectral source employed were the same as those used for the non-dispersive atomic fluorescence measurements.

Atomic absorption measurements were made with a Techtron AA4 atomic absorption spectrometer, with a 100-mm path air–acetylene flame. The spectral source was a zinc hollow-cathode lamp. A monochromator slit-width equivalent to a spectral bandpass of 0.1 nm was employed at a wavelength of 213.9 nm.

Reagents

Zinc stock solution (1,000 p.p.m.). Dissolve 1.0000 g of A.R. grade zinc metal in the minimum volume of hydrochloric acid, and dilute to 1 dm^3 with water.

Strontium chloride solution. Dissolve 30.43 g of A.R. grade strontium chloride and dilute to 100 cm^3 with water.

All acids used were of A.R. grade. Deionized water was used throughout.

Procedure for the analysis of soils

The acetic acid extraction technique[9] was used. Weigh 2 g of the air-dried soil into a 250-cm^3 stoppered conical flask, and add 80 cm^3 of the 2.5% (v/v) acetic acid solution. Shake the flask overnight (*ca.* 16 h) with a mechanical agitator.

Filter and wash with water into a 100-cm^3 volumetric flask. Add 1.5 cm^3 of the strontium chloride solution, and dilute to volume with water. The above procedure was carried out in duplicate for each soil sample.

Prepare a 5-p.p.m. zinc solution from the zinc stock solution. Prepare standard solutions (0.05–0.5 p.p.m. zinc) by transferring 1, 2, 5 and 10-cm^3 aliquots of this solution to 100-cm^3 volumetric flasks, adding 80 cm^3 of the acetic acid solution and 1.5 cm^3 of the strontium solution, and diluting to volume with water. Prepare a reagent blank solution similarly.

Nebulize the blank solution into the argon-separated air–acetylene flame. Back off the flame emission signal produced, using the input offset facility of the operational amplifier, with the radiation from the electrodeless discharge lamp blocked off by means of the shutter. Then illuminate the flame with the zinc radiation from the source to check that no signal due to scatter has been produced. Nebulize the strongest standard solution; with the radiation from the source blocked off, only a slight increase in the signal is noted. Then illuminate the flame and note the signal. The atomic fluorescence signal is the difference between these two readings. Repeat this procedure with the other standard and sample solutions. In the normal manner for atomic fluorescence determinations, measure a standard solution after each unknown solution. Prepare an analytical curve between 0.05 p.p.m. and 0.5 p.p.m. with the standard solutions, and read off the concentrations of the sample solutions.

Comparative atomic absorption measurements were made with these solutions in the usual manner.

Procedure for the analysis of non-ferrous metal alloys

For alloys of zinc containing *ca.* 0.5% zinc, weigh 0.1–0.2 g of the alloy into a 100-cm^3 beaker. Add 5 cm^3 of concentrated hydrochloric acid and 2.5 cm^3 of concentrated nitric acid. Cover the beaker and warm on a hot-plate to dissolve the alloy in the usual manner. When all of the alloy has dissolved, dilute the solution to *ca.* 50 cm^3 with water and filter, collecting the filtrate and washings in a 100-cm^3 volumetric flask. Dilute to volume, transfer a 10-cm^3 aliquot to a 100-cm^3 volumetric flask, and dilute to volume again. For alloys of different zinc contents, take proportionate weights of sample, or dilute appropriately so that the final solution contains 0.1–1 p.p.m. of zinc. For the aluminium alloy (BCS 300), 2.5 cm^3 of hydrochloric acid, 2.5 cm^3 of nitric acid and 2.5 cm^3 of sulphuric acid were necessary to achieve complete dissolution. The above procedure was carried out in duplicate for each alloy analysed.

Prepare standard solutions containing 0.1–1 p.p.m. of zinc by diluting aliquots of the zinc stock solution with water.

Nebulize the standard and sample solutions alternately into the argon-separated air–acetylene flame, as described for the analysis of soil extracts, and measure the atomic fluorescence signals. Prepare an analytical curve, and read off the concentrations of the sample solutions.

RESULTS

Detection limits and calibration data

A detection limit for the non-dispersive atomic fluorescence determination

of zinc in aqueous solution of 0.0005 p.p.m. was obtained. The detection limit was defined as the concentration of zinc in aqueous solution which produced a signal equivalent to twice the noise, near the lower limit of the analytical curve. This compared with a detection limit of 0.001 p.p.m., under similar conditions, with the Southern Analytical A1740 spectrometer. The analytical curve was linear up to *ca.* 5 p.p.m., above which it curved towards the concentration axis.

Analysis of soil extracts

Results for the determination of zinc in the range 0.5–20 p.p.m. in eight soils by non-dispersive atomic fluorescence are compared, in Table I, with those obtained by atomic absorption. The concentration range used for these determinations was considerably greater than the detection limit attainable for aqueous

TABLE I

NON-DISPERSIVE ATOMIC FLUORESCENCE DETERMINATION OF ZINC IN SOILS

Soil sample	*Zinc concentration (p.p.m.)*	
	Atomic absorption	*Non-dispersive atomic fluorescence*
1	0.7	0.5
2	1.5	1.4
3	19.0	19.3
4	2.6	2.5
5	1.5	1.4
6	4.2	4.2
7	4.8	4.9
8	13.2	13.5

TABLE II

NON-DISPERSIVE ATOMIC FLUORESCENCE DETERMINATION OF ZINC IN NON-FERROUS METAL ALLOYS

Sample	*Standard analysis*[a] *(%)*	*Non-dispersive atomic fluorescence (%)*
B.C.S. 179/1 High tensile brass	35.5	36.0
B.C.S. 180/1 Cupro-nickel	0.05	0.049
Copper-base alloy	0.049	0.047
Nimonic 90 Nickel-base alloy	0.002	0.003
B.C.S. 307 Ce–Zn–Zr–Mg alloy	2.08	2.02
B.C.S. 304 Aluminium bronze	0.60	0.59
B.C.S. 207/1 Bronze	1.81	1.75
B.C.S. 183/3 Leaded gunmetal	3.25	3.22
B.C.S. 364 Leaded bronze	0.13	0.14
B.C.S. 300 Aluminium alloy	5.98	6.05

[a] Certificate values for B.C.S. samples. Nimonic 90 standard analysis by Firth Brown Research Laboratories, and copper-based alloy standard analysis by Imperial Metal Industries Ltd.

solutions. The lowest concentration of zinc determined in a soil was 0.5 p.p.m., equivalent to 0.01 p.p.m. in the final solution. This represented the limit of determination for zinc in soils by the method used, since the acetic acid and the strontium chloride added gave an appreciable background signal, which had to be backed off. This greatly increased the noise, so that the maximum instrumental gain could not be used with advantage, and the sensitivity and detection limit were lowered.

Analysis of non-ferrous metal alloys

Results for the determination of zinc in the range 0.002–35% in a variety of aluminium-, copper- and nickel-base alloys (mainly from the BCS range), by non-dispersive atomic fluorescence, are compared, in Table II, with the standard values. In this case also, the concentration range used for the final determination was significantly greater than the detection limit for aqueous solutions, owing to the noise produced by other species present in the samples.

DISCUSSION

The results obtained for the determination of zinc in soil extracts and in non-ferrous metal alloys compare favourably with the standard analyses of these materials, and illustrate the application of non-dispersive atomic fluorescence spectrometry to the analysis of actual substances.

The superiority of the detection limit in aqueous solution by non-dispersive atomic fluorescence over that obtained for conventional atomic fluorescence indicates the advantages to be found in the use of this method of analysis. This is attributable to the higher value of the solid angle which can be used to observe the atomic fluorescence radiation. However, the need to use a working range which fails to take advantage of this superior detection limit for the analysis of technical materials, because of the accompanying increase in the flame background emission noise, illustrates the limitations of d.c. detection systems in atomic fluorescence, particularly non-dispersive, spectrometry.

Despite the above limitation, the results obtained indicate that with an a.c. detection system, non-dispersive atomic fluorescence should be a valuable tool for the determination of trace elements in technical materials.

We are grateful to the Science Research Council for the award of a studentship to J.D.N., to the Macaulay Institute for Soil Research, Aberdeen, for the provision of the soil samples, and to Mr. B. Bagshawe, Firth Brown Research Laboratories, Sheffield, and Dr. W. T. Elwell, Imperial Metal Industries Ltd., Birmingham, for supplying the non-ferrous metal alloy samples.

SUMMARY

The instrumentation for a simple non-dispersive atomic fluorescence spectrometer is described. A detection limit of 0.0005 p.p.m. was obtained for the determination of zinc in aqueous solution with this spectrometer and an argon-separated air–acetylene flame; a detection limit of 0.001 p.p.m. was obtained with

similar instrumentation incorporating a monochromator. Procedures for the determination of zinc in soils and non-ferrous metal alloys are described. Results are given for the analysis of eight soils containing 0.5–20 p.p.m. of zinc and ten non-ferrous metal alloys containing 0.002–35% of zinc. Since the detection system employed was d.c., maximum sensitivity could not be used for the analysis of these materials because of the significant emission noise of the flame. However, the results indicate the potential of non-dispersive atomic fluorescence spectrometry for the analysis of technical materials.

REFERENCES

1 P. L. Larkins, R. M. Lowe, J. V. Sullivan and A. Walsh, *Spectrochim. Acta, Part B*, 24 (1969) 187.
2 P. L. Larkins, *Spectrochim. Acta, Part B*, 26 (1971) 477.
3 P. L. Larkins and J. B. Willis, *Spectrochim. Acta, Part B*, 26 (1971) 491.
4 T. J. Vickers and R. M. Vaught, *Anal. Chem.*, 41 (1969) 1476.
5 T. J. Vickers, P. J. Slevin, V. I. Muscat and L. T. Farias, *Anal. Chem.*, 44 (1972) 930.
6 R. S. Hobbs, G. F. Kirkbright and T. S. West, *Talanta*, 15 (1968) 997.
7 D. Alger, R. G. Anderson, I. S. Maines and T. S. West, *Anal. Chim. Acta*, 57 (1971) 271.
8 J. D. Norris and T. S. West, *Anal. Chim. Acta*, 55 (1971) 359.
9 R. M. Dagnall, G. F. Kirkbright, T. S. West and R. Wood, *Anal. Chem.*, 43 (1971) 1765.

Analytica Chimica Acta, 71 (1974) 295–302

AN ION EXCHANGER–EPOXY RESIN PELLETIZATION METHOD FOR SAMPLE PREPARATION IN X-RAY FLUORESCENCE ANALYSIS

MICROANALYSIS OF METAL IONS IN INDUSTRIAL WASTE WATER

MICHIHIRO MURATA and MAKOTO NOGUCHI

Murata Mfg. Co. Ltd., Nishijin-cho, Nagaokakyo-shi (Japan)

(Received 24th December 1973)

An ion-exchange resin is often used as a matrix for elemental analysis by x-ray fluorescence spectrometry. Collin[1] has separated strontium from calcium by using a column of an ion-exchange resin. The resin, which is washed with acetone and air-dried, is mixed with boric acid and pressed into a pellet for x-ray spectrometry. Kashuba and Hines[2] have developed an x-ray fluorescence ion-exchange method for the determination of rare earths in carbon steels. This method involves the use of a small column and the preparation of pellets with cellulose powder. Blount *et al.*[3] have proposed a technique for the preparation of pellets for x-ray fluorescence analysis; paraffin is used as the binder. The disadvantages of these techniques of pelletization are the dilution of the sample by the addition of a binder and the friable nature of the pellets.

Recently, the authors have found a technique to produce pellets of excellent quality with epoxy resin binder. This technique results in the production of hard pellets which show good stability against swelling, water absorbance and crumbling. The pellets are easily handled and no detrimental effect is observed in evacuation or radiation during analysis. The dilution of the sample can be also minimized by using epoxy resin.

This new technique combined with x-ray fluorescence spectrometry is applied to the microanalysis of manganese, iron, nickel, copper, zinc, strontium, barium, lead and bismuth ions in industrial waste water. In the determination, a cation-exchange resin is equilibrated with solutions containing the metal ions, because this process is considerably faster than column-equilibration for the separation of ions from solution; homogeneous distribution of the element on the resin is also achieved.

EXPERIMENTAL

Reagents

Solutions (1000 μg ml^{-1}) of manganese, iron, cobalt, nickel, copper, zinc, strontium, barium, lead and bismuth were prepared from analytical reagent-grade salts of the elements. These were diluted to prepare solutions for use as calibration standards and experimental samples.

The cation-exchange resin used was DAIYA-ION SK-1B (30 mesh, H form).

The epoxy resin and the hardener used were the Mitsubishi Petrochemical Co. Ltd. No. 815, and the Fuji Chemical Industry Co. Ltd. Tohmide No. 255, respectively. A mixture of epoxy resin and the hardener in the ratio of 2:1 (weight) was used as a binder in making pellets.

Apparatus

The x-ray fluorescence spectrometer used was of the type described in Table I.

TABLE I

X-RAY SPECTROGRAPHIC CONDITIONS

Instrument	*Rigaku-denki x-ray spectrometer KG-X*
Target	Tungsten
Voltage	45 kV
Current	30 mA
Crystal	LiF
Detector	SC
Slit	0.45 mm
Internal standard	Cobalt
Analytical lines	Kα for Mn, Fe, Co, Ni, Cu, Zn and Sr Lα for Ba, Pb and Bi
Counting time	80 s

Procedure

In a 1-1 beaker, take an aliquot of a sample solution and add 5 ml of concentrated nitric acid. Add 5 ml of a standard solution of cobalt (200 μg ml^{-1}) as an internal standard. With pure water, bring the solution volume to 500 ml. Adjust the temperature of the solution to within 40$\pm$1°C. Add 6 g of the cation-exchange resin and stir for 10 min. Filter off the resin, and wash the resin with pure water. Dry the resin at 100°C for 1–2 h. Add 1.5 g of epoxy resin binder and mix well. Place an aluminum ring (5 mm high and 40 mm in diameter) on an iron plate coated with Teflon. Transfer the mixture into the ring. Spread the mixture evenly and allow to stand at room temperature in order to harden.

Remove the pellet from the iron plate. Prepare a pellet for a blank test with the same procedure but without the addition of the sample solution. Measure the x-ray fluorescence intensities of the elements analyzed. Subtract the background from the peak counts, and calculate the intensity ratio of the element determined against the cobalt intensity. Determine the concentration of the element from calibration curves which are previously prepared in the case of zinc, strontium, nickel, copper, bismuth, lead, iron and manganese in the range of 0–5 p.p.m., and in the case of barium in the range of 0–20 p.p.m.

RESULTS AND DISCUSSION

The cation-exchange separation

A nitric acid medium was chosen for the cation-exchange separation because

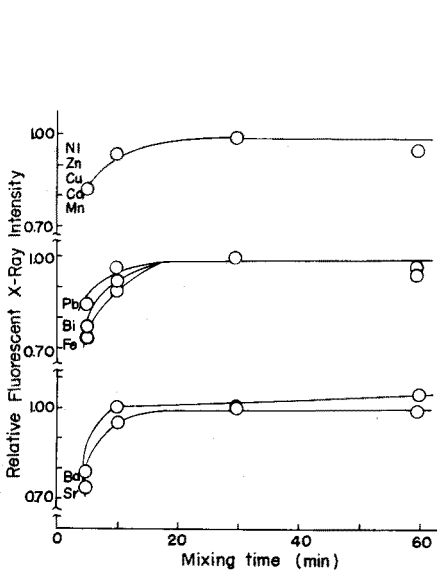

Fig. 1. Effect of mixing time on the cation-exchange separation. Concentration of metal ion: Ba 20 p.p.m., other ions 4 p.p.m.

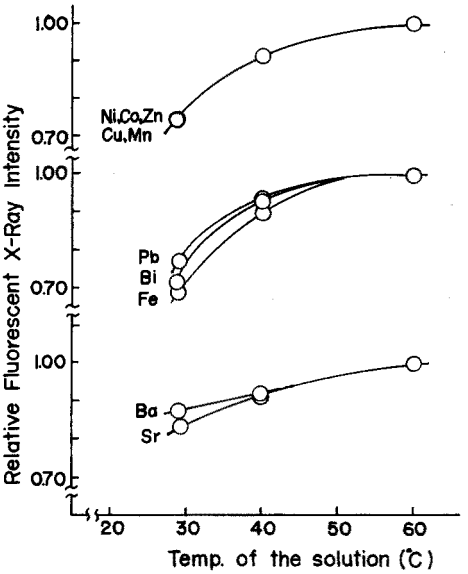

Fig. 2. Effect of temperature on the cation-exchange separation. Concentration of metal ion: Ba 20 p.p.m., other ions 4 p.p.m.

of the high distribution coefficients of the ions in question[4].

Figure 1 shows the effect of the mixing time on the cation-exchange separation. The ion-exchange reaction requires more than 10 min to attain the equilibrium state.

Figure 2 shows the effect of solution temperature on the cation-exchange separation. The amount of ion adsorbed by the resin increases as the temperature of the solution is increased. Although this effect is almost eliminated by the use of an internal standard, the temperature of the solution was kept within 40 ± 1°C in this work, to enhance the sensitivity and reproducibility of the x-ray analysis.

Figure 3 shows the effect of the nitric acid concentration on the cation-exchange separation. No significant change of the analytical value can be recognized for zinc, nickel, copper, manganese and barium determinations with variation of the nitric acid concentration. However, analytical results for strontium, bismuth, lead and iron vary with the nitric acid concentration. Therefore, the concentration of nitric acid was fixed at 0.13 *M* throughout this work.

Table II shows the effect of particle size of the cation-exchange resin on the analytical results. The effect of particle size on precision is not significant for manganese, nickel and copper determinations. However, the finer resin gives more precise results for zinc and iron determinations; the reason for this is not clear yet. It was found that the fluorescence x-ray intensities increased when the resin of finer particle size was used, as shown in Table II. In this work, the cation-exchange resin of 30 mesh was used, because this resin is easily separated

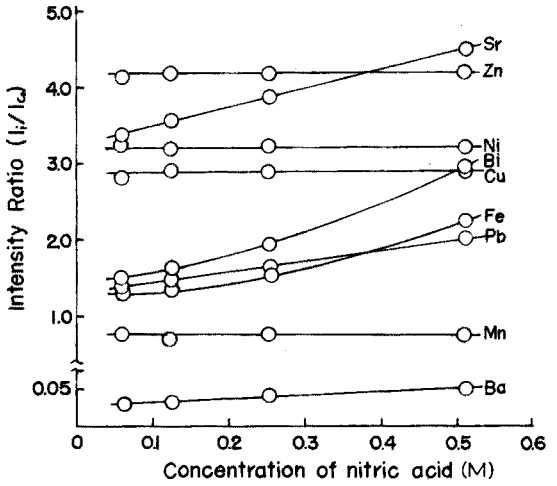

Fig. 3. Effect of the concentration of nitric acid on the cation-exchange separation. Concentration of metal ion: 4 p.p.m.

TABLE II

EFFECT OF PARTICLE SIZE OF CATION EXCHANGE RESIN ON RELATIVE STANDARD DEVIATIONS AND FLUORESCENCE X-RAY INTENSITIES

(Solutions contained 4 p.p.m. for each of the five elements. The relative standard deviation is calculated for five separate runs)

Element	*Relative standard deviation (%)*		*Intensity ratio* I_{100}/I_{30}
	30 mesh	*100 mesh*	
Fe	1.27	0.53	1.096
Ni	0.29	0.35	1.044
Mn	0.51	0.51	1.161
Zn	0.76	0.24	1.038
Cu	0.36	0.30	1.067

from the solution and because the increase of the x-ray fluorescence intensity is only about 10%.

Effects of diverse ions

The effects of sodium, magnesium and calcium ions on the determination of the metal ions were investigated. Sodium ions at concentrations of 10, 200 and 1000 p.p.m. have no effect on any of the determinations. Magnesium at concentrations of 10 and 200 p.p.m. and calcium at 10 and 100 p.p.m. likewise do not interfere; their interferences at higher levels are summarized in Table III. An ion is considered to interfere with the analysis when it produces a variation in x-ray intensity ratio of greater than twice the relative standard. The interference of the calcium ion is more serious than that of the magnesium ion, because the

TABLE III

EFFECT OF DIVERSE IONS ON THE DETERMINATION OF THE NINE ANALYTE ELEMENTS

(Solutions contained 10 p.p.m. of barium and 2 p.p.m. for each of the other elements)

Diverse ion	*Concentration (p.p.m.)*	*Effect of element (%)*								
		Mn	*Fe*	*Ni*	*Cu*	*Zn*	*Sr*	*Ba*	*Pb*	*Bi*
Mg	1000	—	+57	—	—	—	+41	—	+31	−35
Ca	200	—	—	—	—	—	—	−15	−13	−15
	1000	−14	+32	—	−24	−10	+20	−48	−79	

distribution coefficient of the calcium ion in the cation-exchange separation is greater than that of the magnesium ion[4].

Industrial waste water often contains cyanide. In order to examine the application of the proposed method to the analysis of cyanide wastes, direct analyses of nickel, copper and zinc cyanides were carried out. The results indicate a 4% negative error as shown in Table IV. If the cyanide is decomposed in a phosphoric acid medium by steam distillation, an accurate analysis can be achieved.

TABLE IV

EFFECT OF THE PRESENCE OF CYANIDE

Element	*Compound added*	*Directly determined (p.p.m.)*	*After decomposing cyanide (p.p.m.)*	*Relative error (%)*
Cu	CuCN	1.90	1.99	−4.5
Ni	$Ni(CN)_2$	2.22	2.30	−3.4
Zn	$Zn(CN)_2$	1.87	1.95	−4.1

The influence of some chelating agents on the cation-exchange separation can be summarized as follows: sodium acetate, sodium citrate and EDTA at concentrations of 1 *M* do not interfere with the determinations of manganese, iron, nickel, copper, zinc, strontium, lead and bismuth in the concentration range 0–5 p.p.m., or with the determination of barium in the concentration range 0–20 p.p.m. However, the presence of EDTA causes a serious negative error for the determination of bismuth because of the formation of the bismuth–EDTA complex.

In order to establish the effect of secondary excitation, the effect of the nickel ion on the determination of iron was examined as an example. No significant error in the determination of 0.5 p.p.m. iron was caused by the presence of 5 p.p.m. nickel.

Stability of pellets

Figure 4 presents observations pertaining to the aging effect on x-ray fluorescence intensities. It is clear from Fig. 4 that the pellets are very stable;

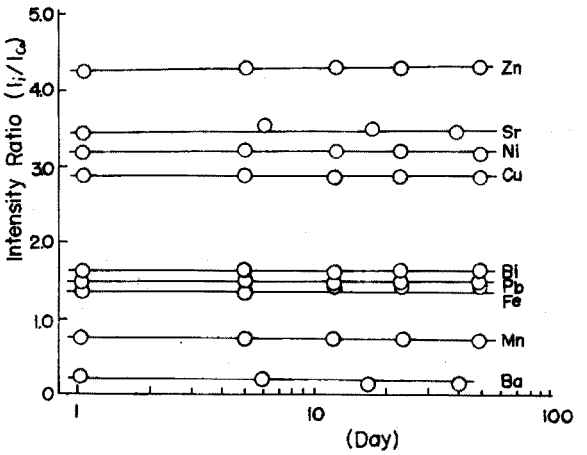

Fig. 4. Ageing effect on fluorescent x-ray intensities.

and successive analyses give essentially identical results. The greatest advantage of the proposed pelletization procedure is its ability to produce harder and more stable pellets than the other procedures mentioned.

Sensitivity and precision

Calibration curves of excellent linearity were obtained. When 500 ml of sample solution is taken, detection limits calculated from the value of the blank intensity ratio plus 3σ are 0.015, 0.012, 0.005, 0.008, 0.004, 0.009, 0.29, 0.017 and 0.020 p.p.m., related to the original volume of the sample solution, for manganese, iron, nickel, copper, zinc, strontium, barium, lead and bismuth, respectively.

The content of binder in the pellets produced by earlier procedures[1,2] is 50–60%. The procedure proposed can produce pellets with a binder content of less than 20%. This fact helps to enhance the sensitivity of the proposed x-ray analysis.

TABLE V

PRECISION DATA OBTAINED AT THE 1 P.P.M. LEVEL FOR EACH ELEMENT

Element	*Experimentally determined*[a] *(p.p.m.)*	*Relative standard deviation (%)*
Mn	1.02	2.2
Fe	1.04	4.9
Ni	1.02	0.8
Cu	1.00	3.2
Zn	1.04	2.8
Sr	1.01	2.0
Ba	1.02	5.1
Pb	1.00	6.5
Bi	1.02	9.5

[a] Average of five determinations.

Table V shows the precision data, obtained at the 1 p.p.m. level, for each element investigated. The relative standard deviation obtained from five successive measurements is presented. The apparently lower precision for lead, bismuth and barium can be attributed to the weak x-ray fluorescence intensities of these elements, so that the correction by the internal standard is not sufficient. However, better precision on the barium determination is obtained by the proposed procedure than by the others[3].

The results of the analysis of synthetic samples for the elements investigated are shown in Table VI; they are in good agreement with the other values listed. The proposed method can save time when many samples are to be analyzed and requires less operating skill.

TABLE VI

RESULTS OF ANALYSIS OF SYNTHETIC SAMPLES

Element	*Experimentally determined (p.p.m.)*		
	Proposed method	*Atomic absorption*	*Emission spectroscopy*
Mn	2.16	2.20	
Fe	2.62	2.86	
Ni	3.58	3.72	
	0.08[a]		0.09[a]
Cu	0.91	0.92	
	0.02[a]		0.02[a]
Zn	2.72	2.80	
Pb	1.32	1.30	
	0.10[a]		0.09[a]
Sr	2.20	1.90	

[a] Another sample.

The author wishes to thank the Director of Research at Murata Mfg. Co. Ltd. for his encouragement, and permission to publish this paper.

SUMMARY

A pelletization procedure with epoxy resin as a binder for ion-exchange resin has been developed for sample preparation in x-ray fluorescence analysis. This new technique is applied to microanalysis of manganese, iron, nickel, copper, zinc, strontium, barium, lead and bismuth in industrial waste water. The pellets prepared by the proposed procedure are very stable, and high sensitivity and good reproducibility can be achieved. Detection limits of manganese, iron, nickel, copper, zinc, strontium, barium, lead and bismuth based on a 500-ml sample solution are 0.015, 0.012, 0.005, 0.008, 0.004, 0.009, 0.29, 0.017 and 0.020 p.p.m., respectively.

REFERENCES

1 R. L. Collin, *Anal. Chem.*, 33 (1961) 605.

2 A. T. Kashuba and C. R. Hines, *Anal. Chem.*, 43 (1971) 1758.
3 C. W. Blount, W. R. Morgan and D. E. Leyden, *Anal. Chim. Acta*, 53 (1971) 463.
4 F. W. E. Strelow, R. Rethemeyer and C. J. C. Bothma, *Anal. Chem.*, 37 (1965) 106.

Analytica Chimica Acta, 71 (1974) 303–310

THE USE OF ION-INDUCED X-RAYS FOR SPECTROCHEMICAL ANALYSIS

H. KAMADA
Department of Industrial Chemistry, University of Tokyo, Tokyo (Japan)
M. TERASAWA
Toshiba R & D Center, Tokyo Shibaura Electric Co., Ltd., Kawasaki (Japan)
(Received 27th November 1973)

The excitation of characteristic x-rays by proton or other heavy ion bombardment can be favorably applied for x-ray spectrochemical analysis because backgrounds are low, so that high peak-to-background ratios are possible, and because of small matrix effects. The disadvantage is that the bombarding energy must be much higher than that in electron excitation to obtain the same x-ray intensity. However, recent work has shown that high excitation efficiencies are obtained for soft x-rays of long wavelength, such as K x-rays of light elements, even below a bombarding energy of a few 100 keV. Moreover, efficiencies in heavy ion bombardment are often higher than in proton bombardment.

Ion-induced x-ray generation as an analytical probe has been investigated by several workers[1–4]. Their results suggest that this method is promising for more extensive applications to x-ray analysis. In this study, the intensity of characteristic x-rays excited by protons and heavy ions of 200 keV was measured for K, L and M x-rays of long wavelength in the crystal dispersion mode, and the application of this excitation method to x-ray spectrochemical analysis is discussed below.

EXPERIMENTAL

The apparatus used consisted of an ion accelerator, deflecting magnet, target chamber and x-ray spectrometer, as shown in Fig. 1. The ions were accelerated by a Toshiba 200-kV accelerator with a PIG-type ion source and passed to the target specimen through the deflecting magnet. The target was set so that the ions bombarded its surface vertically. The take-off angle of emitted x-rays was assumed to be 45°. Dispersion of x-rays was accomplished with a flat crystal of rubidium hydrogenphthalate, lead stearate or lead lignocerate, and with Soller slits, whose dispersion angles were 2.0° and 0.86°. The detector was a gas-flow proportional counter with a 1.3-μm thick stretched polypropylene film window, supported by 85% transmission nickel mesh. A gas mixture of 25% argon and 75% methane was used. X-Ray counts were normalized by the total number of incident ions on the target by means of a current integrator.

RESULTS

Yields of ion-induced x-rays

Figure 2 shows the yields of characteristic x-rays generated by the bom-

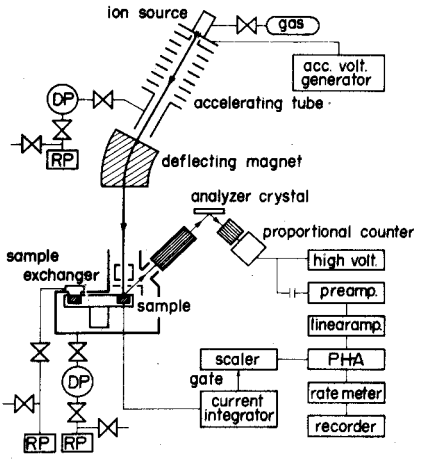

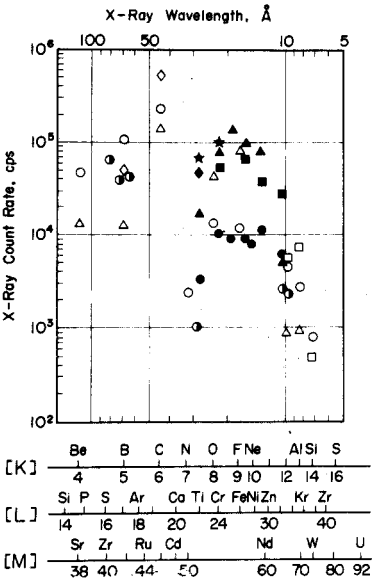

Fig. 1. Diagram of experimental arrangement, showing the 200-kV ion accelerator, beam deflecting magnet, sample (target) chamber, x-ray spectrometer and x-ray counting electronics system. Samples are exchanged without breaking vacuum in the sample chamber.

Fig. 2. Yields of characteristic x-rays generated by bombardment of protons and other heavy ions at 200 keV as a function of x-ray wavelength. The x-ray count rates are normalized by an incident ion current of 100 μA. K: (○) H^+, (◇) N^+, (☆) O^+, (△) Ne^+, (□) Kr^+, L: (●) H^+, (◆) N^+, (★) O^+, (▲) Ne^+, (■) Kr^+. M: (◑) H^+.

bardment with protons and other ions, of nitrogen, oxygen, neon and krypton at 200 keV. The x-ray count rate data are the peak intensities of x-ray spectra diffracted by the lead stearate analyzing crystal, except for the beryllium K x-ray data, which were obtained with the lead lignocerate analyzing crystal. These data are normalized by an ion beam current of 100 μA. No correction was made for background, counter window transmission and analyzing crystal reflection efficiency. As the excitation functions show a monotonic increase with the bombarding energy (though this is not discussed here) the higher energy excitation is preferable. However, as shown in Fig. 2, high intensities are obtained for soft x-rays even at 200 keV. From proton data, it was found that excitation efficiencies are almost independent of the atomic shell with which the x-rays are associated, and are dependent on wavelength only. The efficiencies are higher for longer wavelength x-rays, suggesting that quantitative analysis for light elements can be achieved with high sensitivity. The proton bombardment method is also applicable to the determination of heavy elements by measuring their L- or M-shell x-rays of long wavelength.

Heavy ion bombardment sometimes shows very high excitation for a special combination of projectile ions and target elements. For x-rays ranging from 30 Å to 10 Å, for example, neon ion bombardment shows efficiencies greater by about one order of magnitude than proton bombardment. For shorter wavelength

x-rays down to about 8 Å, krypton ions are more efficient. For L x-rays of chromium and titanium, oxygen ions are preferable. Nitrogen ions are more efficient for carbon K x-ray excitation than proton, neon or oxygen ions. These heavy ion results can be understood within the framework of the Fano–Lichten and Lichten–Barat model in ion–atom collisions[5,6], higher inner-shell excitations being expected when the energy levels of projectile and target atoms match or come close to each other. It is clear from Fig. 2 that higher x-ray intensities are obtained in close connection with the L-shell level of krypton and the K-shell levels of neon, oxygen and nitrogen. The selective x-ray excitation attained by choosing an appropriate projectile ion makes more extensive application possible.

One would expect to determine amounts of the order of p.p.m. for the elements which show an x-ray count rate of 100,000 c.p.s., if there are no interfering lines in the x-ray spectra.

It is important to know how the violent collisions, caused by heavy ion bombardment, bring about changes of the emitted x-ray spectra, before the heavy ion-induced x-rays can be applied to spectrochemical analysis. The spectra of heavy ion-induced x-rays generally show a shift of the peak to higher energies and a broadening in width at half the peak height. These observations have been discussed elsewhere[7–9], and it is not the purpose of this paper to go into further detail.

Determination of light elements

X-Ray excitation by ion bombardment was applied to the determination of some light elements: fluorine, oxygen, nitrogen, carbon, boron and beryllium. The results for carbon and boron have been presented in an earlier paper[1].

Fluorine. The determination of fluorine was investigated with proton and neon ions. Samples of soda-lime glasses were used; they were powdered to a grain size smaller than 1 μm and pressed into pellets at a pressure of 10 tons/cm^2, together with 10 wt.% graphite, which was added to make the sample electrically conductive. The beam current was 11 μA for protons or 8 μA for neon ions. The K x-rays of fluorine were analyzed with a rubidium hydrogenphthalate crystal, and counted with a proportional counter for an integrated current of 1100 μC for protons or 800 μC for neon ions, which corresponds to a measurement of about 100 s. Figure 3 shows calibration curves for the determination of fluorine in soda-lime glasses, illustrating how neon ions are superior to protons for FK x-ray excitation and fluorine determinations. Detection limits of 42 p.p.m. for 200-keV neon ions and 83 p.p.m. for 200-keV protons were obtained by calculation from the formula, detection limit $= 2(2B)^{\frac{1}{2}}/P$, where P is the gradient of the calibration curve and B is the background.

Oxygen. Figure 4 shows an example of oxygen determination. Mild steel which contains 2230 p.p.m. oxygen was examined. The emission spectra of O Kα and Fe L x-rays show up when the lead stearate analyzing crystal is used. Neon ions are more efficient for excitation of O Kα x-rays, as well as Fe L x-rays, than hydrogen ions. In Ne^+ bombardment, since there are too many Fe L x-rays, the O K line cannot readily be resolved from the former. As a result, the neon is not always superior to the hydrogen ion. From the data for peak intensity and background, the detection limits in the oxygen determination are estimated to be 48 p.p.m. with neon ions and 51 p.p.m. with hydrogen ions for 100-s measurements.

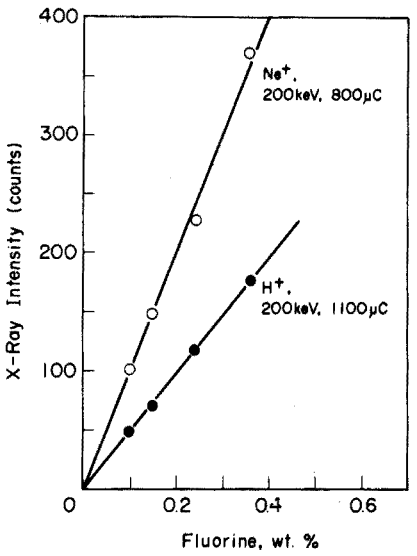

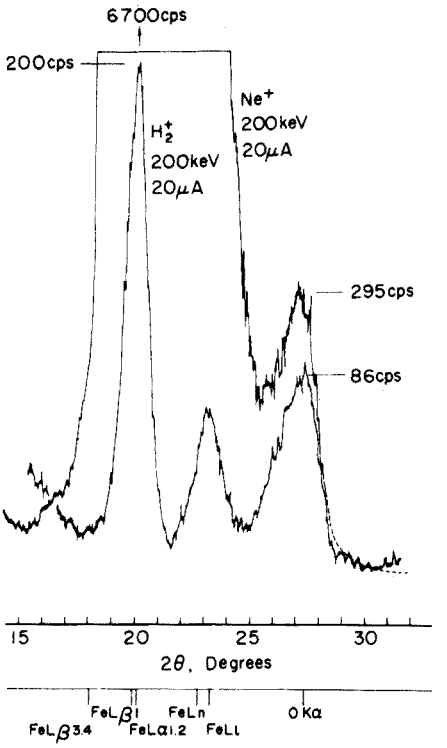

Fig. 3. Calibration curves for fluorine in soda-lime glasses obtained by proton and Ne^+ bombardment. A rubidium hydrogenphthalate analyzing crystal was used.

Fig. 4. O Kα and Fe L emission spectra from mild steel sample bombarded by Ne^+ and H^+. A lead stearate analyzing crystal was used. The oxygen concentration of the sample is 0.223 wt.%.

The O K x-ray excitation by neon ion bombardment was favorably applied to determining oxygen in zircaloy-2 for nuclear fuel cladding tubes. Samples of zircaloy-2 contain about 0.1% oxygen, together with 1.4% Sn, 0.2% Fe, 0.1% Cr and less than 0.01% of impurities, such as N, C, Si, Mn, Ni, Cu and Hf. Figure 5 shows an O Kα emission spectrum observed in Ne^+ bombardment of a zircaloy-2 sample which contains 0.14% O. Figure 6 shows the calibration curve for oxygen determinations in zircaloy-2; Ne^+ beams of 200 keV and 10 μA were used. The O Kα x-rays were measured at the peak of the emission spectra analyzed by lead stearate for the incident ions of 1000 μC. It took about 100 s for each measurement. A good linear relationship between x-ray counts and oxygen concentrations was obtained. The detection limit of oxygen was calculated to be 36 p.p.m.

Nitrogen. Neon ions can excite N Kα x-rays with higher efficiency than protons, so that bombardment with neon ions is promising for the determination of small amounts of nitrogen. Figure 7 shows the N Kα emission spectrum observed in Ne^+ bombardment,of zircaloy-2, which contains 69 p.p.m. N. The N Kα line appears above a rather high background, which is presumed to be due to the low-angle specular reflection of the long wavelength x-rays, especially the Zr M and

C K x-rays. Figure 8 shows the calibration curve for the determination of nitrogen in zircaloy-2. Neon ions of 200 keV and 15 μA were used. The N Kα x-rays were analyzed by lead stearate and counted for the incident ions of 2000 μC. The detection limit of nitrogen was 26 p.p.m.

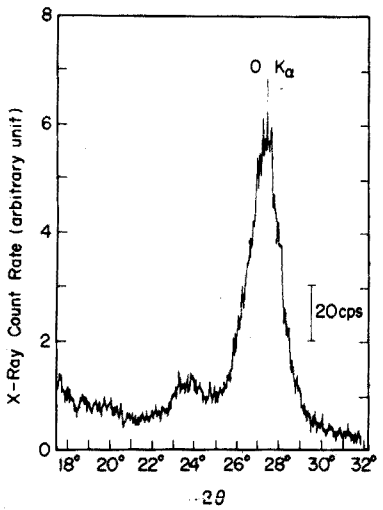

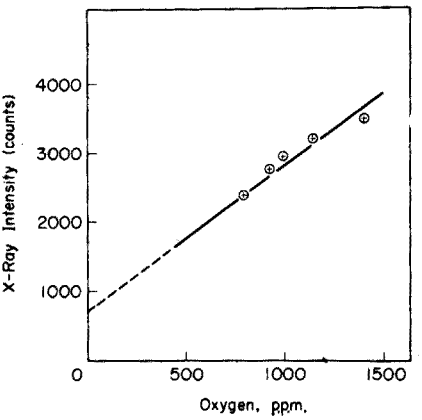

Fig. 5. O Kα emission spectrum observed in 200-keV Ne^+ bombardment (20 μA) on zircaloy-2 which contains 0.14 wt.% O. A lead stearate analyzing crystal was used.

Fig. 6. Calibration curve for oxygen in zircaloy-2 obtained by 200-keV Ne^+ bombardment of 1000 μC.

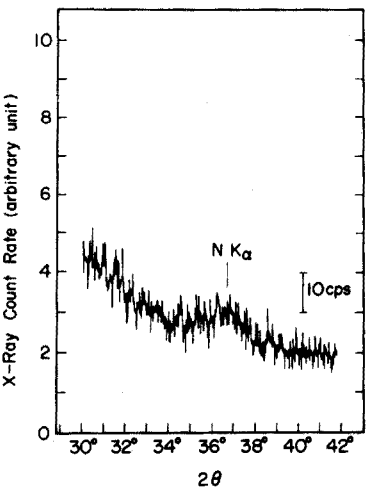

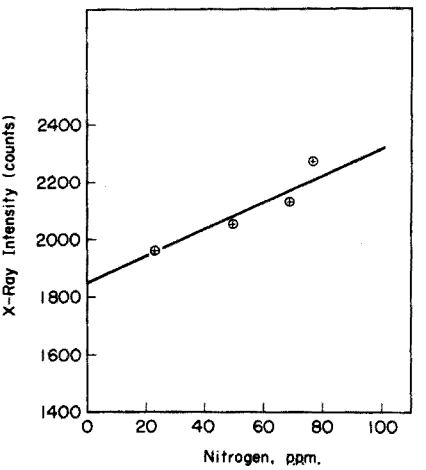

Fig. 7. N Kα emission spectrum observed in 200-keV Ne^+ bombardment (20 μA) on zircaloy-2 which contains 69 p.p.m. N. A lead stearate analyzing crystal was used.

Fig. 8. Calibration curve for nitrogen in zircaloy-2 obtained by 200-keV Ne^+ bombardment of 2000 μC.

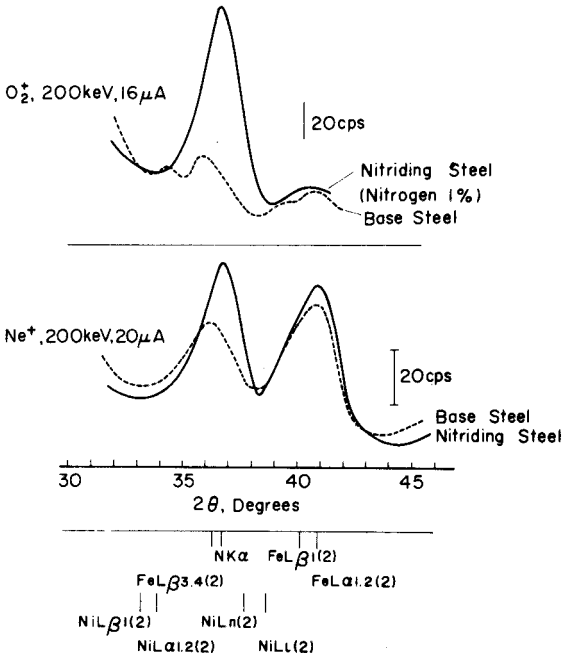

Fig. 9. N Kα emission spectra from stainless steels, with and without nitriding surface treatment, showing how oxygen ions are useful for analysis of steels for nitrogen. A lead stearate analyzing crystal was used.

Figure 9 is another example of a nitrogen determination. The N Kα emission spectra shown are from a sample of stainless steel which had undergone surface nitriding treatment to give about 1% of nitrogen at the surface. For comparison, the x-ray spectra of the untreated base steel are also shown in the Figure. With Ne^+ bombardment, since many L lines of base metals, *i.e.* Fe and Ni, are excited with high intensity and give a rise in the background level at the N Kα line, the determination of nitrogen seems quite difficult. On the other hand, in O^+ bombardment, a prominent N Kα peak appears above the background from the base stainless steel. It is concluded that oxygen ions are more useful for determining nitrogen in stainless steels or other steels, than neon ions.

Beryllium. 200-keV protons were used to determine beryllium in Cu–Be alloys. Protons are more efficient than any other ions for Be K x-ray excitation[10]. The excitation efficiency of Cu L x-rays is 10^2 times less than that of Be K x-rays, and there is little contribution of Cu L x-rays to any background. Figure 10 shows the calibration curve obtained by Be K X-ray counting for protons of 2000 μC. The detection limit was calculated to be 0.03%.

DISCUSSION

Because of the good quality of ion-induced x-rays with low background, it should be possible to employ the non-dispersion method for high sensitivity x-ray analysis. However, neither proportional counters nor solid-state detectors are ap-

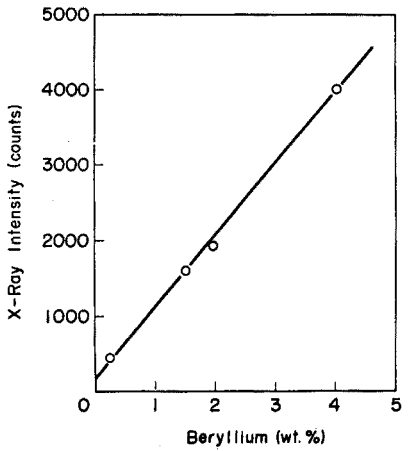

Fig. 10. Calibration curve for beryllium in Cu–Be alloys. The x-rays were excited by 200-keV protons (2000 μC) and analyzed with lead lignocerate.

plicable to the complete resolution of long wavelength soft x-rays at present. In this paper, the application of ion-induced x-rays to spectrochemical analysis was achieved by means of the dispersion method with flat crystals. For x-rays of longer wavelength than 10 Å, x-ray count rates of the order of 10^4 to 10^5 c.p.s. were obtained. The use of heavy ions such as Kr^+, Ne^+, O^+, was shown to be quite effective for x-rays shorter than about 30 Å, whereas protons were superior for longer wavelengths.

The x-ray excitation method by proton and heavy ion bombardment was successfully applied to quantitative analysis. The detection limits for the light elements, F, O, N, C and B, were found to be about 10 p.p.m., though these results are not thought to be optimal, and it may be possible to lower the detection limits to the order of 1 p.p.m. by improving the x-ray diffraction and detection systems.

Because of the short penetration depth of heavy ions, x-ray intensities depend strongly on the surface state of the specimen and it was therefore feared that precise quantitative analysis would be difficult. However, the effect was found not to be serious. With regard to 200-keV neon ion bombardment of steels, in which the range of the ions is about 0.1 μm, the detection limit of 10 p.p.m. is estimated to correspond to about 1 ng of impurities. This high sensitivity suggests the usefulness of the ion excitation method in the quantitative microanalysis of surface and thin films as well as analysis of whole samples.

One of the authors (M.T.) would like to thank Dr. I. Fujii for his encouragement, Dr. H. Kamei for his helpful discussions and suggestions, and Mr. M. Iimura for his general technical assistance.

SUMMARY

The application of ion-induced x-rays to spectrochemical analysis was examined by means of a dispersive method with a flat crystal and a 200-kV ion

accelerator. For x-rays of longer wavelength than 10 Å, x-ray count rates of the order of 10^4–10^5 c.p.s. were obtained; the use of heavy ions such as Kr^+, Ne^+ and O^+ was shown to be effective for x-rays shorter than about 30 Å, while protons were more efficient for longer wavelengths. X-Ray excitation efficiencies are almost independent of the atomic shell with which the x-rays are associated and are dependent on wavelength only, indicating that almost all elements can yield K, L or M x-rays of considerable intensity. The x-ray excitation method by proton and heavy ion bombardment was applied to the determination of some light elements, F, O, N and Be. Detection limits of 10 p.p.m. could be readily achieved for these elements.

REFERENCES

1 H. Kamada, R. Inoue, M. Terasawa, Y. Gohshi, H. Kamei and I. Fujii, *Anal. Chim. Acta*, 46 (1969) 107.
2 D. M. Poole and J. L. Shaw, *Proceedings of the 5th International Congress on X-Ray Optics and Microanalysis*, Springer-Verlag, New York, 1969, p. 319.
3 J. A. Cairns, D. F. Holloway and R. S. Nelson, AERE-R6490, 1970; *Radiat. Eff.*, 7 (1971) 167.
4 J. A. Cairns, *AERE-R6988*, 1972.
5 W. Lichten, *Phys. Rev.*, 164 (1967) 131.
6 M. Barat and W. Lichten, *Phys. Rev., A*, 6 (1972) 211.
7 A. Knudson, D. Nagel, P. Burkhalter and K. L. Dunning, *Phys. Rev. Lett.*, 26 (1971) 1149.
8 D. Burch, P. Richard and R. L. Blake, *Phys. Rev. Lett.*, 26 (1971) 1355.
9 H. Kamada, T. Tamura and M. Terasawa, *Proceedings of the 6th International Congress on X-ray Optics and Microanalysis*, University of Tokyo Press. Tokyo, 1971, p. 541.
10 M. Terasawa, T. Tamura and H. Kamada, *Abstracts of Papers of the VIIth International Conference on the Physics of Electronic and Atomic Collisions*, North-Holland Publishing Co., Amsterdam, 1971, p. 416; *J. Phys. Soc. Japan*, 33 (1972) 1420.

Analytica Chimica Acta, 71 (1974) 311–320

ANALYTICAL APPLICATIONS OF AN AUTOMATIC MATERIALS ANALYZER*

D. G. ROHRBAUGH and J. RAMÍREZ-MUÑOZ
Beckman Instruments, Inc., Irvine, California 92664 (U.S.A.)
(Received 6th October 1973)

During recent years there has been an increasing need for improved automatic systems for chemical analyses. Several factors have contributed to this need: (a) purely economic factors (analytical costs are steadily increasing in terms of labor, materials, and equipment), (b) the increasing demand for accuracy and repeatability, and (c) the trend towards content assaying of materials. For instance, content assay of pharmaceutical tablets and/or capsules has multiplied the load on pharmaceutical quality control laboratories. The content uniformity tests of U.S. Pharmacopeia XVIII require individual assays on a sampling of 30 dosage units, and the statistical lot acceptance criteria based upon those 30 assays are outlined. Basically, the lot quality requirements are met if not less than 28 are within 85–115%, and none outside the 75–125% limits of the specified potency.

These factors have led to the development of an entire new automatic analyzer system for materials of different nature, the Beckman AMA 40 (Automatic Materials Analyzer). In pharmaceutical analyses the AMA 40 is capable of analyzing a group of 30 tablets. In addition, 10 more working positions are included for replicas, standards and blanks, which can provide calibration experimental points and can help to verify the system accuracy.

The purpose of this paper is to describe some of the objectives and restraints that have affected its design, to describe the system itself, and to discuss some analytical results obtained.

DESCRIPTION OF THE SYSTEM

The most important design objective was to provide a versatile, accurate system which would be totally automatic in its operation (from initial sample preparation to the recording of the results), and which would reliably provide the results required for lot quality control. Secondary objectives were speed and ease of operation, and minimum set-up time. The major restraint was the requirement to provide a system which could duplicate established analytical procedures, so that the new data could be related directly to the existing data obtained by manual procedures.

* This paper was read in part at the Pittsburgh Conference of Analytical Chemistry and Spectroscopy, Cleveland, Ohio, March, 1972, and the Eastern Analytical Symposium, Atlantic City, New Jersey, November, 1972.

The automatic analyzer system, developed on this basis, consists of a central chemistry table with individual sample containers inserted into a large revolving round platform. These containers are used for sample treatment and the chemical operations of the analysis. Above the table are reagent and diluent supply reservoirs, plus the positive displacement pump assemblies for drawing samples and delivering liquids to the chemistry table. To the left is the disruption station, where the sample is first homogenized and dissolved. To the right is the analytical station, which is usually a spectrophotometer and a recorder. A colorimeter, a fluorimeter (with the corresponding flow cell), a flame photometer, an atomic-absorption spectrometer, *etc.* can replace the u.v.–visible spectrophotometer without change in the basic system.

The instrument includes the control electronics that govern the automatic operation of the system and the wet incubator assembly.

If permanent recording of data is desired, a digital recorder, a printer with sequencer, a teletype or other computer interface can be used. The system can be mounted on a cart, or used on an ordinary bench.

The modular design of the unit is emphasized in Fig. 1, which shows the flow from the original samples to the chemical table, the chemical operations, and the delivery of the prepared solution to the readout systems. The rotating platform of the table moves counterclockwise and has a total of 40 sample containers. Over the round platform are various probes, each of which has a particular function in the procedure. The probes are mounted on a central pedestal that lowers and raises the probes twice during the time that each sample is resident in a particular position on the table. The two actions allow, for example, (a) the drawing of a measured sample from the outer container and the transfer of this sample, plus the diluent, to one of the inner tubes, or (b) the drawing of a measured volume of treated sub-sample from an inner tube and the transfer of this aliquot, plus the diluent, to one of the external tubes. The sample is drawn during the first lowering of the pedestal, and the transfer is made during the second.

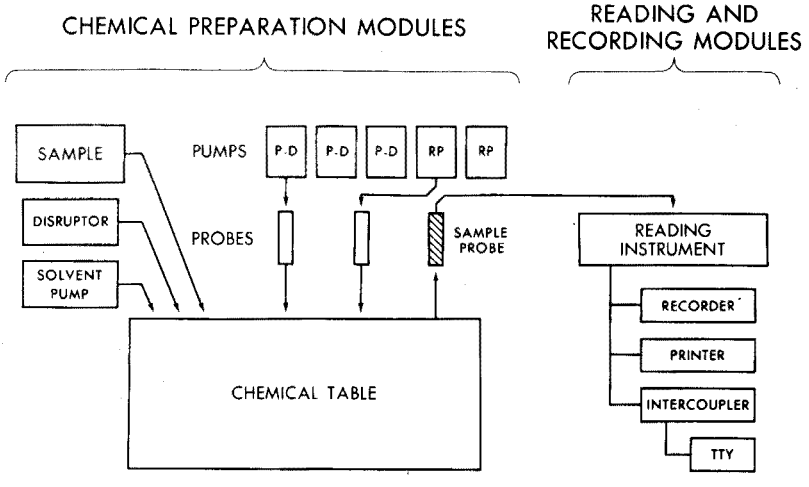

Fig. 1. Modular design of the System AMA 40.

The samples move around the table at stepped intervals. The interval at each station can be varied from a minimum of 1 min to a maximum of 2.5 min. The probe positions can therefore be used to determine the interval between procedural events. For instance, if the table is moving at the 1 min-per-position-rate and 5 min are to elapse between two procedural events, the two probes are simply placed five positions apart.

The variety of probes available for filtering, pipetting, diluting, adding reagent, mixing and drawing samples, plus the time positioning of the probes, gives the system a high degree of flexibility, which readily permits the duplication of manual procedures. Because of the automatic control from one processing station to the next, repeatability is easily achieved.

OPERATION OF THE SYSTEM

In the application of a particular procedure the first step is the selection and positioning of suitable probes. The probes are attached to the pedestal by a single knurled bolt with a corresponding electrical connector. With the probes in place, the proper diluent and reagent reservoirs are positioned in front of the pumps and the pumps are adjusted to the proper setting. More detailed information on preliminary adjustment and setting has been given elsewhere[1].

The next step is to insert the sample containers (T-cups) into the revolving platform, plus the set of five test tubes (T-tubes), for each one of the 40 positions of the table. The T-cup is a disposable plastic unit which goes far toward solving the problems of solid sample disruption and sample handling without cross-contamination. Each sample is contained within its own vessels from initial disruption through to the final analysis.

If filtering is required, a filter tube is inserted in the sample container. These parts, plus the T-tube, are cheap disposable items, molded of polypropylene. Thus, samples and chemicals are only exposed to inert materials which are compatible with most chemicals utilized in industrial analyses.

The final preparation step is to drop a sample into each sample container (outside the filter tube, if this is used). With up to 40 positions per run, several blanks and calibration samples can be included without significantly increasing the length or cost of the analysis. The total elapsed time for setting up the system is in the order of 30 min. Results are then recorded automatically within about an hour.

During the travel of the sample around the table for a typical analytical assay, the first step is the disruption and dissolution of the sample; this is the function of the disruptor module. Earlier research on automatic analysis indicated that the disruption stage is the principal limitation on the throughput of a system. Once a sample is in the system, any reasonable amount of time can elapse between procedural events. But the throughput—the number of samples that can be processed per hour—is a direct function of how fast it is possible to start successive samples into the system, *i.e.* how fast an individual solid sample can be disrupted and dissolved. It was, therefore, important to reduce the disruption time, as well as to avoid any change of cross-contamination during the disruption stage, and to eliminate any problems created by particulate matter.

It was decided to disrupt each solid sample within its own container. The container (T-cup) is of a special design, with a hemispherical projection at the bottom which serves to collect and redirect the particles back into the teeth of the disruptor itself. Initially, a measured amount of solvent is injected into the T-cup by a syringe pump that can be adjusted to add up to 100 ml. The disruptor is then automatically inserted and within 30 s to 2 min, depending on the setting of the timer, the sample is disrupted and dissolved. During this process, a positive air pressure is applied to the filter tube to prevent seepage of the solvent through the filter before the sample has fully dissolved. The disruptor station is activated by a magnetic rod at position No. 1 of the 40 positions around the revolving platform. As the magnet rotates around with the table, it activates each probe in turn. Then on its second trip around, it deactivates each probe, allowing the operator to leave the system completely unattended.

The sample disruption is achieved by the rotating head of the disruptor, which dips into the T-cup. The disruptor head consists of a stator with a series of metallic teeth; inside the head, there is a rotor which carries another series of teeth placed very near the stator (Fig. 2). The rotation of the rotor directs the liquid against the teeth of the stator, and produces a negative pressure under the disruptor head. A continuous flow is produced, and liquid and original sample (or its particles) are directed towards the central cone of the rotor. The flow is deflected from there against the rotating teeth.

The disruptor follows a series of movements electronically programmed. These movements are schematized in a sequence of phases, some of which are represented in Fig. 3. In phase 1, from its "home position" (1), the disruptor begins a rotation of 90° until it stops over the T-cup. In phase 2 (position 2), the disruptor descends into the T-cup. After the disruption has been accomplished, the disruptor ascends (phase 3) and then swings back to its "home position" (phase 4). In phase 5, the disruptor is in position (1), and then descends to dip

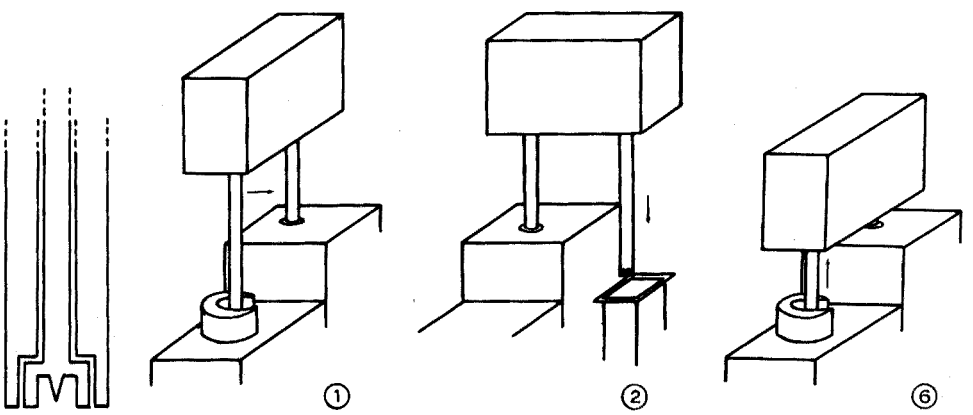

Fig. 2. Schematic section of the lower part of the disruptor shaft showing the location of the stationary teeth of the external stator and the teeth of the inner rotor.

Fig. 3. Some of the positions in the programmed automatic operation of the disruptor. See explanation in text.

the head and shaft into the decontaminating washing solution (phase 6); this is essential to avoid cross-contamination. The disruptor ascends again, after having rotated for some seconds in the wash solution. Finally, in phase 7, the disruptor remains in the "home position" (1) for a few seconds more, before starting a new cycle. Here the head receives a strong current of compressed air to blow out residual droplets of wash solution.

If the sample, once disrupted and dissolved, has to be filtered, a vacuum filter probe is installed on the pedestal.

In Fig. 4 is shown a schematic section of a T-cup containing a filter tube with filter paper at the bottom. The filter probe descends in each working cycle over the filter tube and presses the vacuum head over its upper end. The filter head carries an adjusting flat rubber ring. The vacuum forces the liquid through the filter paper until vacuum and hydrostatic head are equilibrated. Enough liquid remains inside the filter tube for subsequent transfer and dilution operations. Suction tips of transfer probes later enter the filter tube to aspirate aliquots of filtered liquid. The filter tube leaves enough space to allow the disruptor shaft to enter the T-cup in the disruption stage. The vacuum can be regulated. Filter tubes are available with different qualities of paper according to the analytical system.

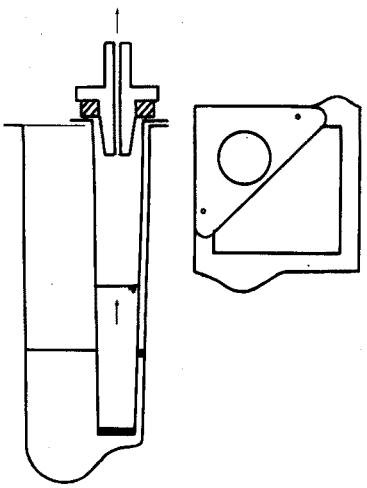

Fig. 4. Schematic section of a T-cup containing a filter tube and receiving the vacuum head of the filter probe. The filter tube is located in a corner of the cup, and is maintained in position by means of two small plastic pins.

When samples require extraction processes, the extraction is performed by means of a mixing probe, and aliquots of the extract are pipetted and transferred by a pipetter-diluter probe.

If the chemical reaction involves incubation, the solution is transferred to the inside tube of the T-tube, which is submerged in a liquid bath, adjustable from 30 to 90°C.

Solutions already processed come to the sampling probe which operates by drawing solution out of the T-tube and through the flow cell of the readout

system. Between cycles, while the chemical table is revolving from one position to the next, a vacuum pump draws air through the sampling line to clear it of the last sample. Then, during the first lowering of the pedestal, slugs of solution are drawn into the flow cell for a preset length of time, so as to rinse the line and

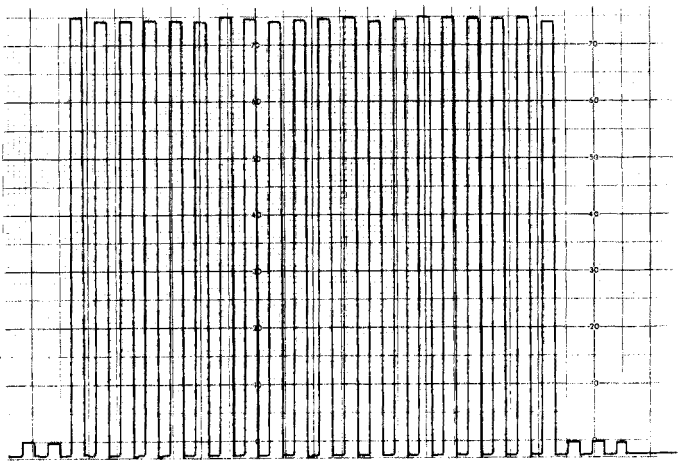

Fig. 5. Repeatability test. Three blanks at the beginning, repeated readings on separated aliquots of the same sample, and two blanks at the end. Final blanks show lack of contamination (carry-over effects) after readings of about 0.75 A.U.

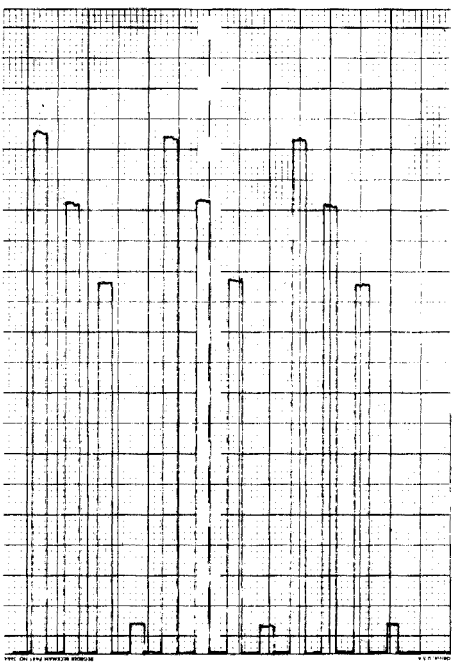

Fig. 6. Three repeated readings of a blank and three standards prepared to cover the range of variability in content uniformity tests.

flow cell. Since differing viscosities require different flow times, a time adjustment is provided.

As a final step, the response of the analyte in the solution is read and the answer is recorded.

ANALYTICAL RESULTS

Special attention has been devoted to studies of repeatability. As a typical example, Fig. 5 shows a repeatability test in a chemical operation in which a pipetter-diluter, a reagent pump, a mixer and the sampling system were used in order to check uniformity of volume delivery and sample pick-up. The significance of repeated readings of different standards can be judged from Fig. 6. The record is consistent both in repeatability and in minimal cross-contamination.

When single tablets are examined, variations from tablet to tablet may be expected. Figure 7 shows several samples compared with readings of a blank and two standards.

In order to facilitate the interpretation and presentation of data, simple computer programs have been prepared to convert the final analytical data into

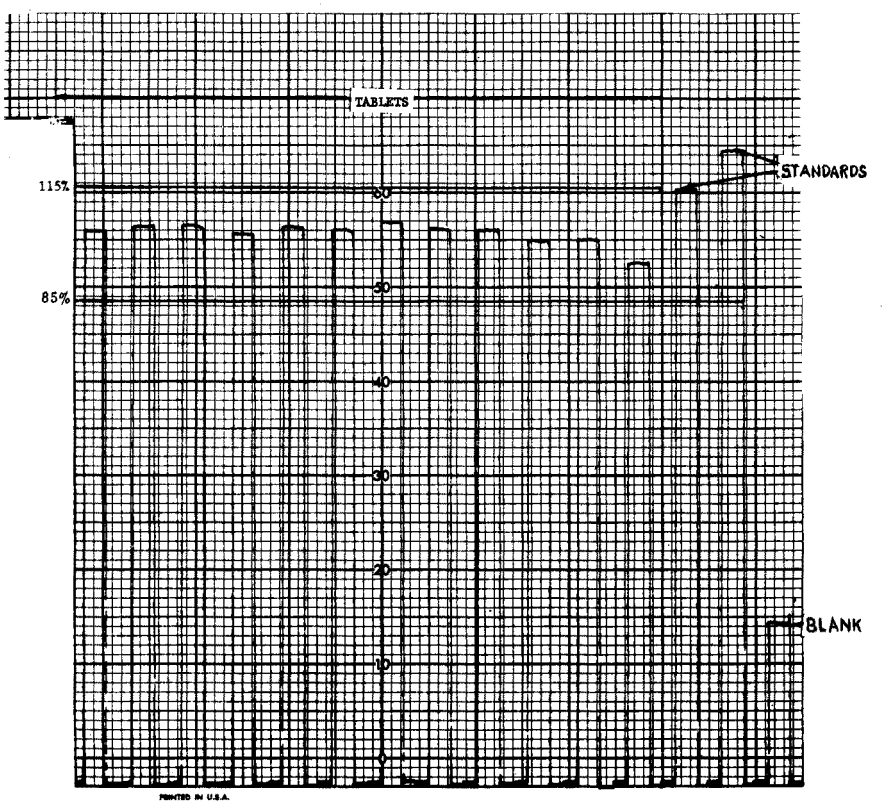

Fig. 7. Variability of samples recorded in a normal run, where samples are measured under the same operating conditions used for the blank solution and standards.

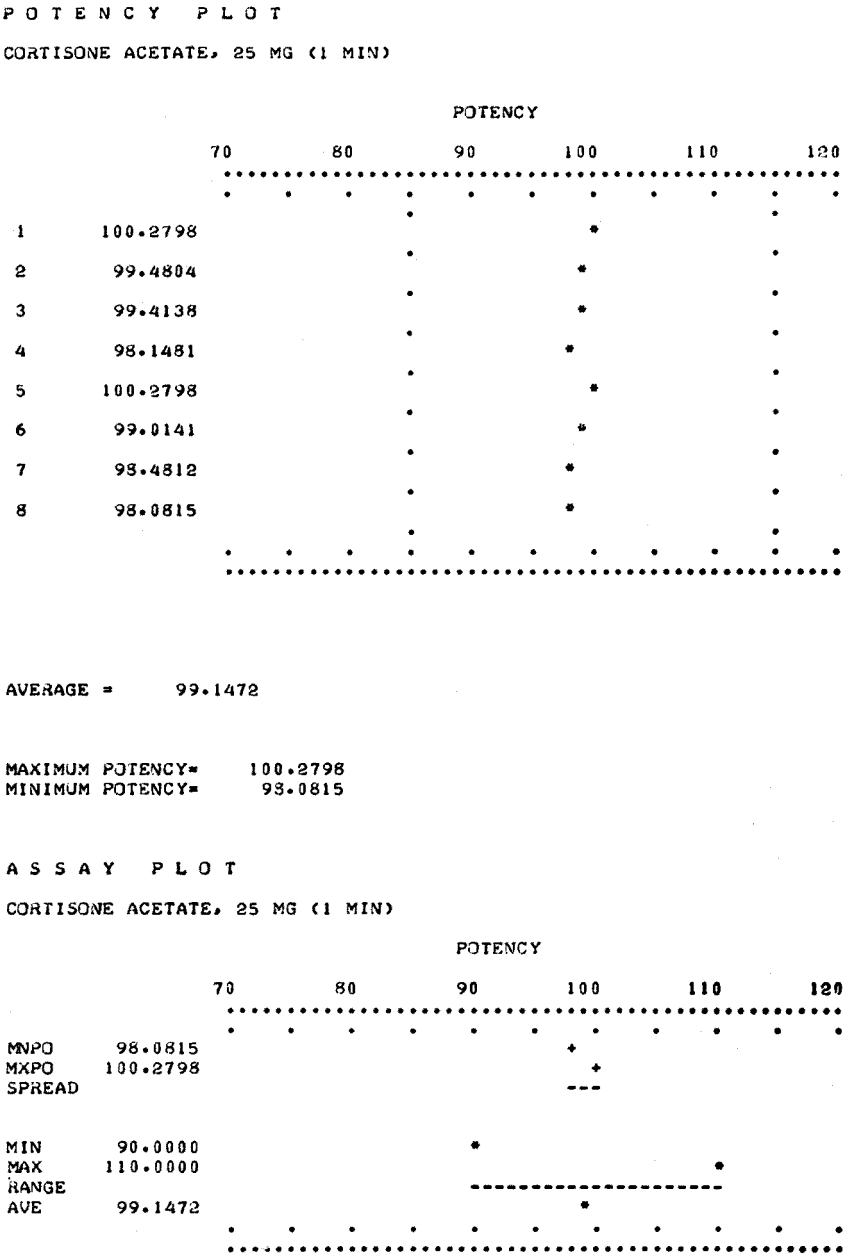

Fig. 8. Potency and assay plots. Photographic reproduction of a computer-prepared plot in a test for content uniformity and assay.

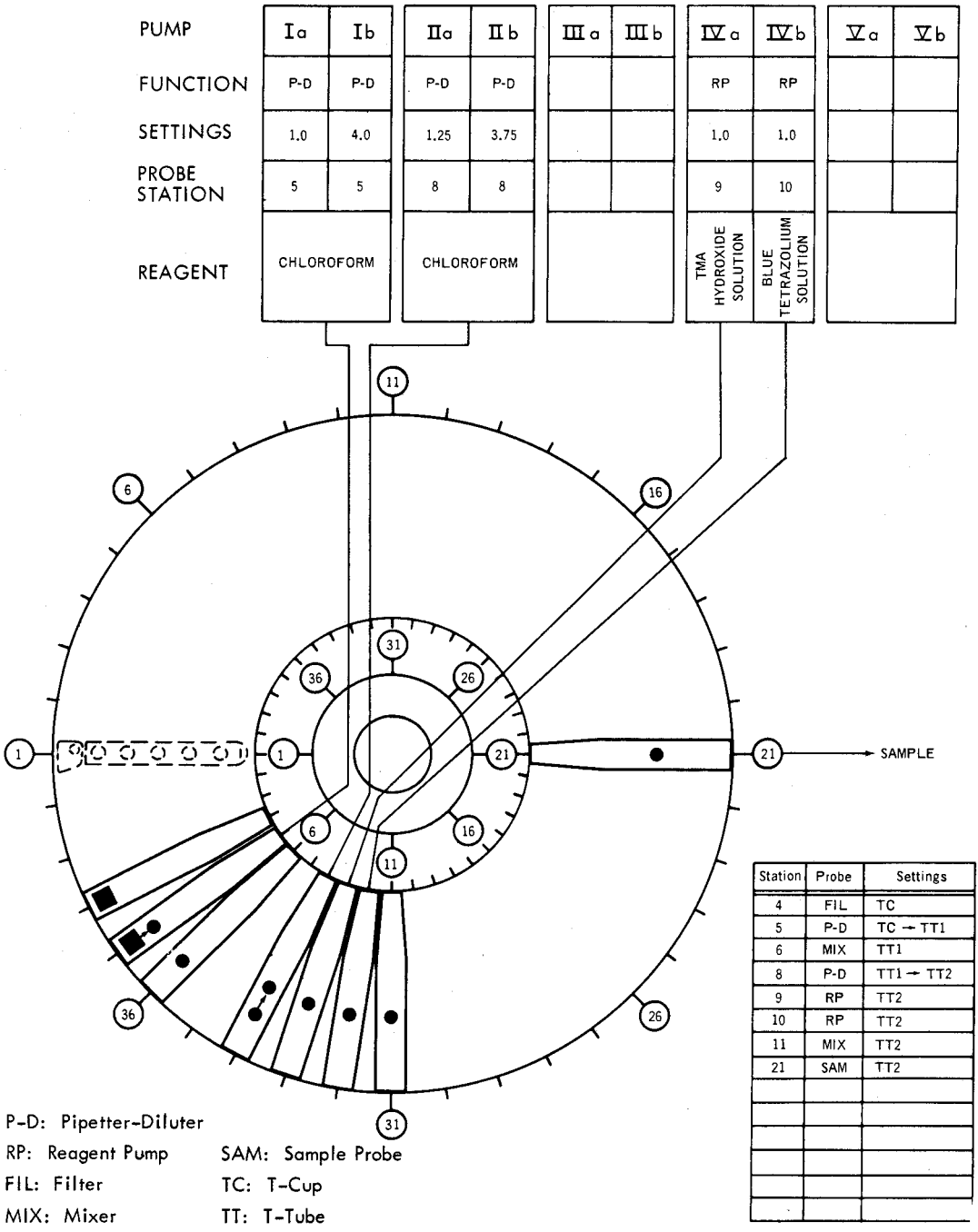

Station	Probe	Settings
4	FIL	TC
5	P-D	TC → TT1
6	MIX	TT1
8	P-D	TT1 → TT2
9	RP	TT2
10	RP	TT2
11	MIX	TT2
21	SAM	TT2

Fig. 9. Experimental arrangement of pumps and probes in the chemical table for the test summarized in Fig. 7.

easily readable formats. Figure 8 shows a computer-made format in which potency plots for content uniformity and assay are included. Cortisone acetate analysis corresponding to the data shown in Fig. 8 was done by the experimental procedure summarized in the instrument set up shown in Fig. 9.

In pharmaceutical analysis, the instrument has been applied successfully to tablets of sodium saccharin (at different potencies), pipazetate, norethindrone acetate, pyridoxine hydrochloride, triamcinolone, fluorocortisone acetate, fluphenazine hydrochloride, prednisone, prednisolone, tolbutamide, diazepam, imipramine and other oral dosages.

CONCLUSIONS

The AMA 40 system is a highly versatile instrument which can be adapted to a wide variety of chemical procedures needed in pharmaceutical analysis, with minimal changeover time between successive chemical determinations.

Repeatability is good. The relative standard deviation is sometimes less than 1%, but 1–2% is normal in average procedures. For very complex cases, a 2–4% relative standard deviation has been realized. Accuracy within 1–3% is usual.

The discrete sample handling methods provide minimal carry-over effects. Carry-over effects tested with aqueous, water–alcohol, ethanol, and chloroform systems, have usually produced effects under 1%.

The instrument typically operates at a rate of 40–60 samples per hour. Lower rates (25–40 samples per hour) are produced when prolonged disruption times are necessary (over 1 min). Consumption of reagent is minimal since all operations are performed on a semi-micro scale (under 12 ml volume). Human attention is reduced to analysis planning, changes of probes and reaction recipients, settings and interpretation of results.

The instrument is appropriate for single and multi-channel operation required in pharmaceutical analyses for the determination of one or more active components in tablets, capsules and other pharmaceutical dosage forms.

The authors are very grateful to the scientific personnel of E. R. Squibb & Sons, Inc., New Brunswick, New Jersey, FDA, St. Louis, and the Department of National Health and Welfare, Toronto, for their opinions, suggestions and comments during the first stages of the development and evaluation of the instrument described.

SUMMARY

The design, instrumental functioning and chemical operation of a new automatic system developed for pharmaceutical analysis is briefly described. Graphical and numerical results are included as typical examples of the analytical data obtained. The system is suitable for application to content uniformity and assay tests in discrete-sample analysis as required for quality-control pharmaceutical work.

REFERENCES

1 J. Ramírez-Muñoz, *AMA 40 Chemical Operations Manual*, Beckman Instruments, Inc., Industrial Technical Report TR-581, 1973 (reprinted 1974).

Analytica Chimica Acta, 71 (1974) 321–331

DETERMINATION OF NIACIN AND NIACINAMIDE IN PHARMACEUTICAL PRODUCTS BY AUTOMATIC DISCRETE-SAMPLE ANALYSIS

J. RAMÍREZ-MUÑOZ

Beckman Instruments, Inc., Irvine, California 92664 (U.S.A.)

(Received 6th October 1973)

The analysis of niacin in pharmaceutical products is described in full in the *U.S. Pharmacopeia XVIII*[1], and *National Formulary XIII*[2]. The determination of niacinamide has been described by Pelletier and Campbell[3] and by Pelletier[4]. These products are very frequently determined by manual analysis in pharmaceutical quality-control laboratories. Particularly niacinamide is determined not only in single pharmaceutical dosages, but also in polyvitamin tablets and capsules.

Owing to recent regulations for the analytical control of pharmaceutical products, a large number of single tablets have to be analyzed, instead of analyzing aliquots of groups of tablets reduced to powder form as a homogeneous average sample. Automatic discrete-sample analysis is the most appropriate answer to the problem of analyzing large numbers of pharmaceutical samples, in order to provide quantitative results quickly, accurately, and with enough precision.

An attempt has been made to adopt for automatic determinations the classical procedures used for many years in pharmaceutical laboratories.

In this paper, the analysis of both compounds has been studied, and niacin has been considered under two different experimental approaches, with and without the use of sulfanilic acid. Reagents, operating conditions, procedures, and results are summarized in the following paragraphs.

EXPERIMENTAL

Instrumentation

The instrument used has been the Beckman Automatic Materials Analyzer (AMA 40) mounted with a Beckman DB-GT spectrophotometer as readout module and also with a Beckman 10-in. potentiometric recorder and a teletype as printer and tape puncher. The instrument was installed in a well-ventilated laboratory, in order to avoid problems from any fumes that might be generated when priming or emptying reagent pumps or during operation. The AMA 40 system has already been described[5].

Other readout modules, such as Beckman models 24 or 25 spectrophotometers, can be used for the same purposes.

Determination of niacin. Method A. Cyanogen bromide without sulfanilic acid

This procedure is based on very old experimentation by König[6], who described

the yellowish color produced by cyanogen bromide on niacin in ammoniacal medium. This method has not been much used because of the preferred formation of color compounds with sulfanilic acid, as described later. However, the use of cyanogen bromide alone has the advantage of avoiding the use of a solution of sulfanilic acid, with a general reduction in time, cost, and equipment.

Reagents. Deionized-distilled water was used as solvent for niacin tablets. The pumped reagents were as follows.

Cyanogen bromide (10% solution) was prepared as recommended by the *U.S. Pharmacopeia XVIII*[1] and *National Formulary XIII*[2], under a hood, to avoid any fumes in the laboratory. The well-known precautions advised for the handling of cyanogen bromide were taken.

Ammonium hydroxide (2%) was prepared by the dilution of concentrated ammonia liquor with deionized-demineralized water.

Deionized-demineralized water was used as the diluent solution.

Operating conditions. Operating conditions are summarized in Table I.

TABLE I

OPERATING CONDITIONS FOR NIACIN (CNBr)

Disruption:	YES
Disruption speed:	Position 30
Disruption time:	60 s
Incubation:	NO
Filter tubes:	YES
Filter vacuum:	15 in. Hg
Operation:	AUTO
Analysis rate:	*ca.* 40 h^{-1}
Spectrophotometer operation:	
Mode:	Double beam
Analytical wavelength:	405 nm
Reference cell:	Deionized-distilled water
Lamp:	Tungsten
Range setting:	2*A*
Slit program:	Normal
Sample volume:	6.0 ml (Position 12)
Recorder chart speed:	5 in min^{-1}
Recorder span setting:	100 mV
Solvent pump:	50 ml deionized-distilled water
Sample vacuum:	15 in. Hg
Sequence:	3 blanks, 4 standards, 30 samples, 3 blanks. Standards in reference tubes.

Procedure. The procedure for the AMA 40 system was the same as that shown in Fig. 1, which is actually the set-up diagram for the method with sulfanilic acid, except for the following points: (a) pump Va is left empty; (b) ammonia solution is introduced at position 24 on the chemical table (instead of position 23); (c) the action required on Station 23 is omitted.

Determination of niacin. Method B. Cyanogen bromide with sulfanilic acid

Reagents. In this case also, deionized-distilled water was used as solvent.

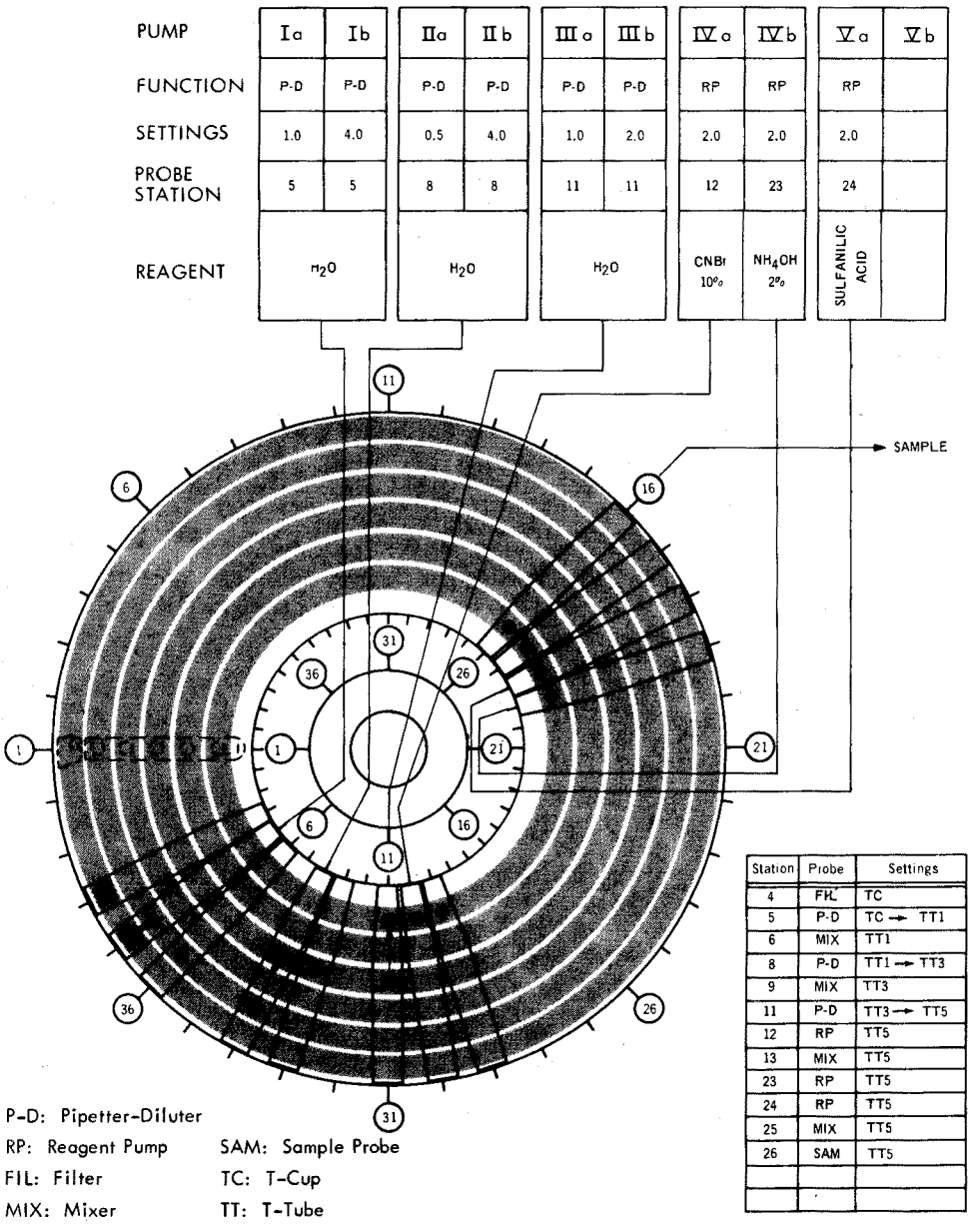

Station	Probe	Settings
4	FIL	TC
5	P-D	TC → TT1
6	MIX	TT1
8	P-D	TT1 → TT3
9	MIX	TT3
11	P-D	TT3 → TT5
12	RP	TT5
13	MIX	TT5
23	RP	TT5
24	RP	TT5
25	MIX	TT5
26	SAM	TT5

Fig. 1. Setup diagram for the procedure for niacin (CNBr + sulfanilic acid).

The reagents used in the pumps were 10% cyanogen bromide, 2% ammonium hydroxide and diluent solution as described above. In addition, sulfanilic acid solution was prepared according to the recommendation of the U.S. *Pharmacopeia XVIII*[1].

Operating conditions. Operating conditions were exactly the same as those

given in Table I, except that the analytical wavelength was 465 nm.

Procedure. The procedure is summarized in Fig. 1.

Determination of niacinamide

Reagents. As the solvent, a solution of 0.3% (w/v) dipotassium hydrogenphosphate was used.

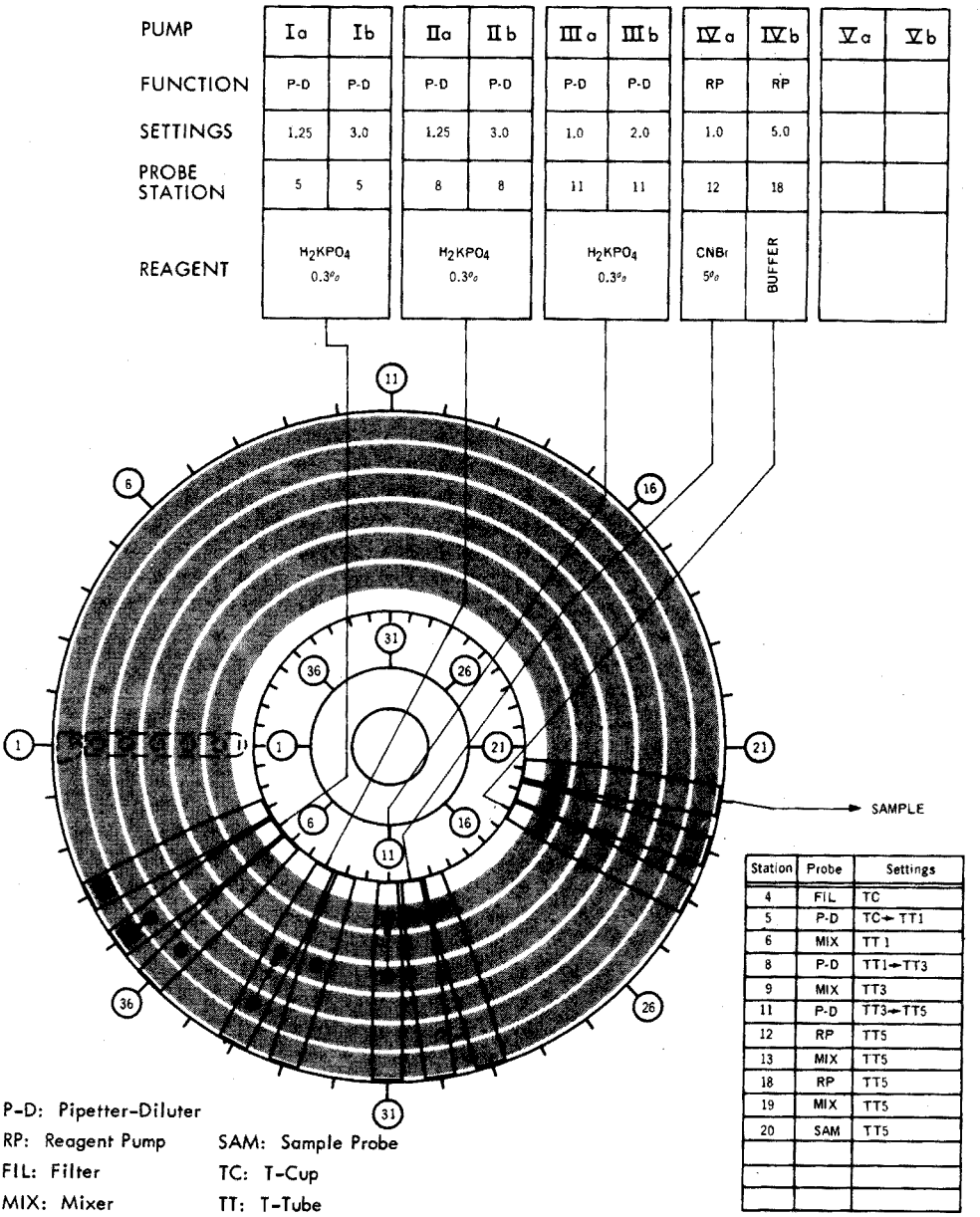

Station	Probe	Settings
4	FIL	TC
5	P-D	TC→TT1
6	MIX	TT1
8	P-D	TT1→TT3
9	MIX	TT3
11	P-D	TT3→TT5
12	RP	TT5
13	MIX	TT5
18	RP	TT5
19	MIX	TT5
20	SAM	TT5

Fig. 2. Setup diagram for the procedure for niacinamide.

The pumped reagents were as follows.

Cyanogen bromide (5%) was prepared under the same conditions as described above. A solution of dipotassium hydrogenphosphate (0.3% w/v) was used as diluent in the pumps.

For the barbituric acid reagent, 10 g of barbituric acid was added to 500 ml of 3% dipotassium hydrogen phosphate solution; this was heated and stirred, and left to stand overnight, before being filtered. A mixture was prepared with 300 ml of filtrate, 100 ml of ethanol and 100 ml of deionized-distilled water.

Operating conditions. The operating conditions were the same as those given in Table I except for the following points: (a) analytical wavelength, 555 nm; (b) range setting, 1*A*; (c) sample volume 7 ml (position 14); (d) solvent pump, 50 ml 0.3% K_2HPO_4.

Procedure. The procedure is summarized in Fig. 2.

RESULTS

Most of the results given here were prepared with the use of a computer, by processing the experimental data obtained in punched tape through a time-shared terminal (IBM 360 system).

Niacin by the cyanogen bromide method (Method A)

Repeatability, linearity and tablet analysis were tested. Repeatability was acceptable and some examples are given in Table II.

TABLE II

REPEATABILITY FOR NIACIN BY THE CYANOGEN BROMIDE METHOD

Solutions tested	*No. of readings*	*Average absorbance*	*Standard deviation*	*Relative standard deviation (%)*
Standards	5	0.968	0.0214	2.21
Aliquots of mixed solutions from disrupted tablets	4	1.022	0.0082	0.80

Linearity of response was accomplished over the range 0–0.5 mg/100 ml. The first part of the computer output, consisting of data for linear and quadratic fits, is shown in Fig. 3. The second part (not shown) gave a plot of concentration of niacin over the above range against absorbance at 0.01 A.U. intervals. The total computer time required was 4 s.

Tablet analysis. Several series of tablets of niacin, with a potency of 100 mg per tablet, were analyzed. Figure 4 shows some final results as prepared by the computer.

LINEAR FIT. SLOPE = 0.012090

PAIR	X VALUES	Y VALUES	Y CALCD.	DIFFERENCE	% ERROR
1	11.8000	0.1420	0.1427	0.0007	0.4702
2	22.0000	0.2690	0.2660	-0.0030	-1.1187
3	31.6000	0.3820	0.3821	0.0001	0.0156
4	40.0000	0.4790	0.4836	0.0046	0.9644
5	47.5000	0.5770	0.5743	-0.0027	-0.4683

QUADRATIC FIT. COEFFICIENTS:

T1 = 0.012090

T2 = 0.000001

PAIR	VALUES	Y VALUES	Y CALCD.	DIFFERENCE	% ERROR
1	11.8000	0.1420	0.1427	0.0007	0.5192
2	22.0000	0.2690	0.2662	-0.0028	-1.0271
3	31.6000	0.3820	0.3826	0.0006	0.1494
4	40.0000	0.4790	0.4844	0.0054	1.1359
5	47.5000	0.5770	0.5755	-0.0015	-0.2672

Fig. 3. Computer linearity plot for niacin by the cyanogen bromide method. The plot shows perfect linearity. See values of slope and T1, and the small value of T2.

TABLE III

REPEATABILITY FOR NIACIN BY THE CYANOGEN BROMIDE–SULFANILIC ACID METHOD

Solutions tested	*No. of readings*	*Average absorbance*	*Standard deviation*	*Relative standard deviation (%)*
Standards	5	0.872	0.0092	0.94
Aliquots of mixed solutions from disrupted tablets	3	0.924	0.0064	0.69

Niacin by the cyanogen bromide–sulfanilic acid method (Method B)

Repeatability is illustrated by results given in Table III. Linearity was again achieved over the range 0–0.5 mg/100 ml. The first part of the computer output is shown in Fig. 5.

Tablet analysis. Several series of tablets were also examined by this procedure. The computer output was prepared analogously to that shown in Fig. 4. The potency values obtained by the two methods, with and without sulfanilic acid, are shown in Table IV. With the exception of sample nos. 5 and 6, all values agree within $\pm 1.5\%$.

NIACIN (CNBR)

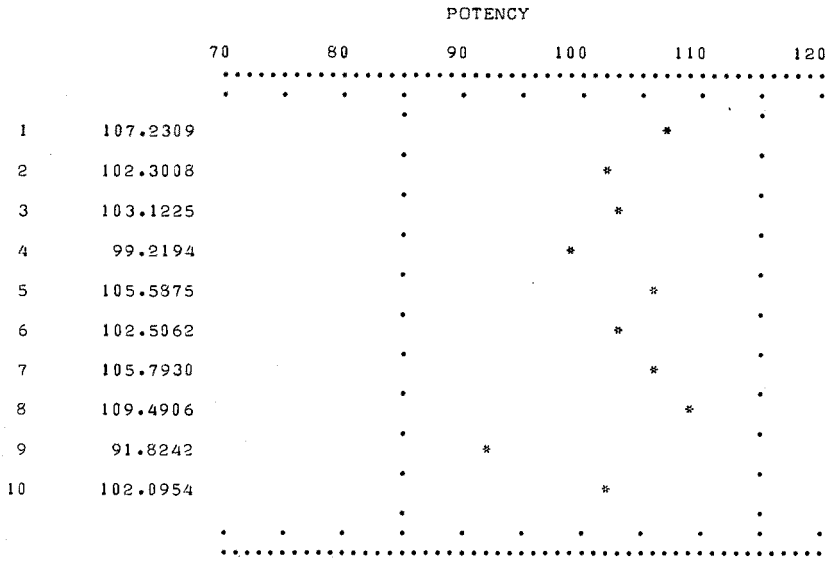

AVERAGE? (ANSWER Y OR N)
?Y

AVERAGE = 102.9169

ASSAY PLOT?, (ANSWER Y OR N)
?Y

MAXIMUM POTENCY= 109.4906
MINIMUM POTENCY= 91.8242

WHICH ARE ASSAY LIMITS?, (TYPE MIN,MAX IN FIGURES AS REAL NUMBERS)
?95.,115.

A S S A Y P L O T

NIACIN (CNBR)

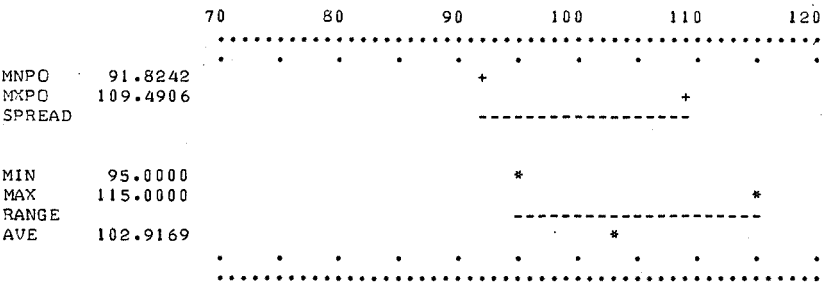

Fig. 4. Computer-prepared potency and assay plots for niacin by the cyanogen bromide method.

LINEAR FIT. SLOPE = 0.010112

PAIR	X VALUES	Y VALUES	Y CALCD.	DIFFERENCE	% ERROR
1	11.8000	0.1190	0.1193	0.0003	0.2687
2	22.0000	0.2260	0.2225	-0.0035	-1.5661
3	31.6000	0.3200	0.3195	-0.0005	-0.1455
4	40.0000	0.4050	0.4045	-0.0005	-0.1299
5	47.5000	0.4780	0.4803	0.0023	0.4838

QUADRATIC FIT. COEFFICIENTS:

T1 = 0.010303

T2 = -0.000004

PAIR	VALUES	Y VALUES	Y CALCD.	DIFFERENCE	% ERROR
1	11.8000	0.1190	0.1210	0.0020	1.6544
2	22.0000	0.2260	0.2246	-0.0014	-0.6384
3	31.6000	0.3200	0.3212	0.0012	0.3825
4	40.0000	0.4050	0.4051	0.0001	0.0367
5	47.5000	0.4780	0.4796	0.0016	0.3267

Fig. 5. Computer linearity plot for niacin by the cyanogen bromide–sulfanilic acid method. Linear fit shows less error than the quadratic fit. Slope and T1 differ only by about 2%. T2 is a very small value.

TABLE IV

CORRELATION BETWEEN POTENCY VALUES FOR NIACIN TABLETS BY THE TWO METHODS

(Data for potencies and correlations have been rounded to one and two decimal figures, respectively.)

Sample	*Potency values by Method A*	*Potency values by Method B*	*Correlation (%)*
1	107.2	105.7	1.45
2	102.3	103.3	−0.97
3	103.1	104.4	−1.21
4	99.2	99.8	−0.61
5	105.6	100.8	4.71
6	102.5	105.4	−2.74
7	105.8	107.0	−1.14
8	109.5	110.4	−0.83
9	91.8	92.9	−1.14
10	102.1	103.5	−1.32

Niacinamide by the barbituric acid method

Repeatability, linearity, and tablet analysis were also tested for this procedure.

Repeatability was found to be acceptable. For a series of five standards, a standard deviation of 0.0114 was found on an average absorbance reading of 0.630 (r.s.d. 1.81%).

LINEAR FIT. SLOPE = 0.010417

PAIR	X VALUES	Y VALUES	Y CALCD.	DIFFERENCE	ERROR
1	15.4000	0.1690	0.1604	-0.0086	-5.0766
2	28.6000	0.3070	0.2979	-0.0091	-2.9563
3	40.0000	0.4270	0.4167	-0.0103	-2.4175
4	50.0000	0.5230	0.5208	-0.0022	-0.4118
5	58.8000	0.5970	0.6125	0.0155	2.5989

QUADRATIC FIT. COEFFICIENTS:

T1 = 0.011430

T2 = -0.000020

PAIR	X VALUES	Y VALUES	Y CALCD.	DIFFERENCE	% ERROR
1	15.4000	0.1690	0.1712	0.0022	1.3070
2	28.6000	0.3070	0.3103	0.0033	1.0736
3	40.0000	0.4270	0.4247	-0.0023	-0.5330
4	50.0000	0.5230	0.5208	-0.0022	-0.4292
5	58.8000	0.5970	0.6019	0.0049	0.8215

Fig. 6. Computer linearity plot for niacinamide. A slight curvature is shown by the smaller errors found in the quadratic fit. Observe differences between slope and Tl, and the significant value of T2.

Linearity was achieved in the concentration range 0–1 mg ml^{-1}. The first part of the computer output is shown in Fig. 6.

Tablet analysis. An example of the runs done in the instrument with niacinamide tablets containing 100 mg of niacinamide is shown in Fig. 7.

DISCUSSION

When the results obtained in the determination of niacin and niacinamide by the procedures described are considered, attention should be given to the aspects of repeatability and linearity, because repeatability brings a full picture of the precision that may be expected for a single determination of a single tablet. Linearity is also of interest because, if it is satisfactory, a single standard can be used in order to interpolate or extrapolate close readings of samples in a single curve calculated between the blank and the standard used. Of course, it is more reliable to use several repeated readings of the standard, either at the beginning of a run, or distributed along the series of working positions of the chemical table of the instrument. The instrument has 40 working positions, so that the table will hold up to 30 tablets and several standards and blanks, distributed as required.

The tablet analysis seems to be within the acceptance limits recommended by official regulations; the averages of samples shown in the Figures are within the limits of assay recommended for each particular tablet.

The analytical method studied and tested with tablets containing only niacinamide were also tested with polyvitamin preparations. In most cases good

```
NIACINAMIDE, 100 MG

                                    POTENCY
                    70        80        90        100       110       120
                    .....................................................
                    .   .   .   .   .   .   .   .   .   .   .   .   .
                                .                           .
 1       101.4724               .                   *       .
                                .                           .
 2       106.1284               .                       *   .
                                .                           .
 3       100.4193               .                   *       .
                                .                           .
 4       108.2902               .                       *   .
                                .                           .
 5       106.9599               .                       *   .
                                .                           .
 6       111.5051               .                           * .
                                .                           .
 7       108.8445               .                       *   .
                                .                           .
 8       106.0176               .                       *   .
                                .                           .
 9        86.7283               .   *                       .
                                .                           .
10       105.5741               .                       *   .
                                .                           .
                    .   .   .   .   .   .   .   .   .   .   .   .   .
                    .....................................................


AVERAGE? (ANSWER Y OR N)
?YES

AVERAGE =     104.1939


ASSAY PLOT?, (ANSWER Y OR N)
?YES

MAXIMUM POTENCY=     111.5051
MINIMUM POTENCY=      86.7283

WHICH ARE ASSAY LIMITS?, (TYPE MIN,MAX IN FIGURES AS REAL NUMBERS)
?95.,115.

A S S A Y   P L O T

NIACINAMIDE, 100 MG

                    70        80        90        100       110       120
                    .....................................................
                    .   .   .   .   .   .   .   .   .   .   .   .   .
MNPO      86.7283                       +
MXPO     111.5051                                           +
SPREAD                                 ---------------------


MIN       95.0000                           *
MAX      115.0000                                           *
RANGE                                      ---------------------
AVE      104.1939                                  *
                    .   .   .   .   .   .   .   .   .   .   .   .   .
                    .....................................................
```

Fig. 7. Computer-prepared potency and assay plots for niacinamide.

agreement with standards was found. In a few cases, the signals showed some distortion. Excessive signals can be studied by running placebos under the same conditions and at the same time as standards and samples. Decreased signals may require the use of an addition method in cases where the concomitants produce a chemical interference in the cyanogen bromide reaction and/or in the development of the color after the addition of barbituric acid buffered solution.

Another effect found in these tests was the difficulty of filtering some solutions from polyvitamin compounds (solutions obtained by disruption). For this purpose, a higher angle was allowed on the chemical table between the disruption station and the station in which the filtering probe is located. This gives time to achieve some diffusion of the liquid into the filtering tube, and the negative pressure applied is enough to force a sufficient amount of filtrate into the filtering tube so that it can be pipetted from there by the first pipetter diluter pump.

Conclusions

The operating conditions described offer very rapid analyses for niacin and niacinamide in tablets; only about 1 min is required to obtain a final result for each single tablet, which gives an analysis rate of about 60 results per hour.

The repeatability values found give a good degree of confidence in the application of the methods, and the results obtained with tablets supposed to be within the recommended limits in the potency scale, show a good agreement with the ranges established by the standards. Accuracy was tested by repeated determination of solutions prepared in the same conditions used to prepare the standards.

All the operating conditions described are advantageous in reducing the cost per unit analyzed. All the characteristics described offer a rapid and reliable approach to the analysis of pharmaceutical oral dosages.

SUMMARY

Automatic analytical procedures for the determination of niacin and niacinamide in pharmaceutical dosages by means of an automatic discrete-sample analyzer are described. Two procedures are given for niacin based on cyanogen bromide without and with the use of sulfanilic acid. Niacinamide is determined by the cyanogen bromide—barbituric acid method. Data on repeatability, linearity, potency determination (for content uniformity) and assay are included.

REFERENCES

1 *U.S. Pharmacopeia XVIII*, U.S. Pharmacopeia Convention, Inc., Bethesda, Maryland, 1970.
2 *National Formulary XIII*, American Pharmaceutical Association, Washington, D.C., 1970.
3 O. Pelletier and J. A. Campbell, *J. Pharm. Sci.*, 50 (1961) 926.
4 O. Pelletier, *J. Offic. Assoc. Anal. Chem.*, 51 (1968) 828.
5 D. G. Rohrbaugh and J. Ramírez-Muñoz, *Anal. Chim. Acta*, 71 (1974) 311.
6 W. König, *J. Prakt. Chem.*, 69 (1904) 105; 70 (1904) 19.

Analytica Chimica Acta, 71 (1974) 333–342

PHOTOMETRIC INVESTIGATION OF SYSTEMS OF TWO COMPLEXES WITH POLYDENTATE LIGANDS

B. W. BUDESINSKY

Analytical Laboratory, Phelps Dodge Corporation, Morenci, Arizona 85540 (U.S.A.)

(Received 9th October 1973)

The theory for investigation of systems of several complexes with monodentate ligands is well developed[1,2], but this is not true about the complexes of polydentate ligands. There have been several[3,4] more or less successful attempts to solve this problem, but a systematic theory of investigation, taking into the account the real situation in the solution, is not available.

It should be stated that a general approach to solve this problem without a knowledge of the composition and stability of the main complex is extremely difficult. That approach is avoided in this paper. Recently[5,6], it was shown that the combination of complexes with metals:ligand molar ratios of 1:1 and 1:2 can occur in two different situations, and each of these requires a special approach. A convenient generalization of those theories for the combination of any two complexes of the same metal and ligand is discussed here. The practical application is demonstrated on complexes of uranium(VI) with xylenol orange, and lanthanum with 8-quinolinol.

EXPERIMENTAL

Apparatus

All photometric measurements were made with a Gilford Spectrophotometer, Model 2400 (Oberlin, Ohio) and 1-cm quartz cells. An Orion Model 801 pH Meter (A. H. Thomas Co., Philadelphia, Pa.). with a glass and calomel electrode pair, was used for pH measurements.

Reagents

Xylenol orange and uranyl perchlorate were used as 0.01 *M* stock solutions, and 8-quinolinol and lanthanum perchlorate were used as 0.05 *M* stock solutions. The solution of 8-quinolinol was in ethanol; all other solutions were in water. The concentrations of uranyl and lanthanum were checked by titration with EDTA. Xylenol orange was of the same quality as described earlier[5]. The purity of 8-quinolinol was checked by paper chromatography, in the system of n-butanol–acetic acid–water, 4:1:5, with the paper Chrom AR 500 (Mallinckrodt Chemical Works, St. Louis, Missouri) (R_F=0.83), and by melting point (75°C, required 75–76°C). The product used was chromatographically pure. The pH was adjusted by means of perchloric acid and hexamine. Uranyl and lanthanum perchlorate were products of G. F. Smith Co., Columbus, Ohio. All other chemicals were "Bakers Analyzed Reagents".

Procedure

Metals and reagents, in constant ratio, were prepared as stock solutions to ensure exactly the same metals:ligand ratio in all diluted solutions. The sequence of metal, reagent and buffer was adhered to during the preparation of solutions. Dilutions were made with solutions containing the same concentration of the buffer as the solution diluted. The ionic strength was kept at 0.10 *M* (sodium perchlorate), and the temperature at $25 \pm 1°C$. The absorbance of solutions was measured against a buffer blank after 10 min. The absorbance of reagent was determined in the same way.

THEORETICAL

Limits of the reagent (or metal) concentration and pH

These limits can be determined from the composition and stability of the main complex. They are important for the proper investigation of the side complex.

Knowing the composition $M_mH_jL_n$ and the overall stability constant of the main complex,

$$\beta_{mjn} = c[M]^{-m}[H]^{-j}[L]^{-n} \tag{1}$$

(where c, [M], [H] and [L] are the actual concentrations of the complex, metal ion, hydrogen ion and ligand, respectively), then in order to obtain 99% complexation of the metal, we must use the lowest acceptable total ligand concentration

$$c_{L(lim)} = \alpha_{L(H)}(100^m \beta_{mjn}^{-1}[H]^{-j} m^{-1} c_M^{1-m})^{1/n} \tag{2}$$

providing that we have $c_L \gg c_M$ to get

$$c_L = [L]\alpha_{L(H)} \tag{3}$$

where $\alpha_{L(H)}$ is the coefficient of side reactions of the ligand with hydrogen ions; and c_M and c_L are the total concentrations of the metal and ligand.

Another important factor is the highest pH that can still be used with negligible metal hydrolysis. Since every metal hydrolysis is initiated by the formation of the complex of M(OH) with the stability constant

$$\beta^* = [M(OH)][H][M]^{-1} \tag{4}$$

and since the values of β^* are well known, the limiting pH can be defined as 1% formation of the complex M(OH) of the total metal concentration, so that

$$100[M(OH)] = c_M = 100\beta^*[M][H]_{lim}^{-1} \tag{5}$$

Combining this equation with eqns. (1), (3) and (4), we obtain

$$pH_{lim} = \frac{1}{m+j} \log \frac{m\beta_{mjn}}{c_M} \left(\frac{c_M}{100\beta^*}\right)^m \left(\frac{c_L}{\alpha_{L(H)}}\right)^n \tag{6}$$

In the case of $c_M \gg c_L$, from eqn. (1), we can write for 99% complexation of the ligand

$$c_{M(lim)} = (100^n \beta_{mjn}^{-1}[H]^{-j} n^{-1} c_L^{1-n})^{1/m} \tag{7}$$

and for the limiting pH from eqns. (1), (5) and (7)

$$pH_{lim} = \frac{1}{m+j} \log \frac{n\beta_{mjn}}{c_L} \left(\frac{c_M}{100\beta^*}\right)^m \left(\frac{c_L}{100\alpha_{L(H)}}\right)^n \quad (8)$$

In practice, the limiting values cannot be sometimes reached because of the low solubility or strong absorption of the reagent. The latter drawback can be eliminated by the use of cells with shorter pathlength.

Investigation of the side complex

To determine the composition and stability of the side complex $M_pH_hL_q$, it is necessary to differentiate two cases.

(a) The number of ligands (metals) in the side complex increases with increasing ligand (metal) concentration. This case requires: $p(n-1) \neq m(q-1)$ [or $q(m-1) \neq n(p-1)$]. Systems with monodentate ligands (containing only two complexes) and similar systems with polydentate ligands represent this case. Examples are the metal complexes of glycine, xylenol orange, tiron, 4-(2-pyridylazo)resorcinol, *etc.* An excess of ligand is most typical for this case. According to the experimental approach it can be called the "dilution method".

(b) The number of ligands (metals) in the complex decreases with increasing metal (ligand) concentration. The basic requirement is: $n \neq q$ [or $m \neq p$]. Examples are the metal complexes of 8-quinolinol, dithizone, cupferron, acetylacetone, *etc.* An excess of metal is most typical for this case. According to the experimental approach, it can be called the "constant concentration method", since the concentration of the component used in excess remains constant.

In both cases the expressions in brackets indicate the second (less usual) alternative. Only the first alternative will be discussed below. The second is obtained by interchange: $c_L \longleftrightarrow c_M$, $m \longleftrightarrow n$ and $p \longleftrightarrow q$.

(a) Dilution method, $p(n-1) \neq m(q-1)$. The effective stability constants of the main and side complex are given by

$$K_{mn} = c(c_M - mc - p\bar{c})^{-m}(c_L - nc - q\bar{c})^{-n} \quad (9)$$

$$K_{pq} = \bar{c}(c_M - mc - p\bar{c})^{-p}(c_L - nc - q\bar{c})^{-q} \quad (10)$$

respectively, where $\bar{c} = [M_pH_hL_q]$, is the actual concentration of the side complex. Assuming the validity of eqns. (2) and (6) (*i.e.* quantitative complexation and $c_L \gg c_M$) and introducing

$$x = c_M c_L, \quad y = c/c_L, \quad z = \bar{c}/c_L \quad (11abc)$$

$$K_{mn}^{-1} c_L^{1-m-n} = R_{mn}, \quad K_{pq}^{-1} c_L^{1-p-q} = R_{pq} \quad (12ab)$$

we obtain from eqns. (9) and (10) the normalized equations

$$R_{mn} y = (x - my - pz)^m \quad (13)$$

$$R_{pq} z = (x - my - pz)^p \quad (14)$$

Combining eqns. (13) and (14) to eliminate the expressions in parentheses, we get

$$R y^p = z^m \quad (15)$$

where

$$R = R_{mn}^p / R_{pq}^m = c_L^{p(1-n)-m(1-q)} K_{pq}^m / K_{mn}^p \quad (16)$$

If the solution is diluted twice, with the concentration of the buffer kept constant, we have, instead of eqns. (11abc) and (13), (14),

$$x = c_M/c_L,\ y' = 2c'/c_L,\ z' = 2\bar{c}'/c_L \tag{17abc}$$

$$R_{mn}2^{m+n-1}y' = (x - my' - pz')^m \tag{18}$$

$$R_{pq}2^{p+q-1}z' = (x - my' - pz')^p \tag{19}$$

so that

$$aRy'^p = z'^m \tag{20}$$

where

$$a = 2^{p(n-1)-m(q-1)} \tag{21}$$

Because the complexation is quantitative, we can write

$$x = my + pz, \quad x = my' + pz' \tag{22ab}$$

If the absorbance is measured against a reagent–buffer blank, we have

$$\Delta A = \Delta\varepsilon c + \Delta\bar{\varepsilon}\bar{c}, \quad \Delta A' = \Delta\varepsilon c' + \Delta\bar{\varepsilon}\bar{c},$$

and after substitution from eqns (11bc) and (17bc)

$$P = y + kz, \quad P' = y' + kz' \tag{24ab}$$

where

$$P = \Delta A/(c_L\Delta\varepsilon), \quad P' = 2\Delta A'/(c_L\Delta\varepsilon) \tag{25ab}$$

and

$$k = \Delta\bar{\varepsilon}/\Delta\varepsilon \tag{26}$$

$\Delta\varepsilon$ and $\Delta\bar{\varepsilon}$ are the effective molar absorptivities of the individual complexes (the value of $\Delta\varepsilon$ is known). Combining eqns. (24ab) by elimination of k, and substituting for y, y' from eqns. (22ab), we get

$$(mP - x)/(mP' - x) = (m\Delta A - xc_L\Delta\varepsilon)/(2m\Delta A' - xc_L\Delta\varepsilon) = z/z' = t \tag{27}$$

Introducing eqns. (22b) and (27) into eqn. (20), we obtain

$$R = \frac{1}{a}(x/p)^m(m/x)^p[(1-T)/(t-T)]^m[(t-T)/(t-1)]^p \tag{28}$$

where $T = (at^m)^{1/p}$. The combination of eqns. (16) and (28) results in

$$K_{pq} = \left[\frac{1}{a}K_{mn}^p c_L^{m(1-q)-p(1-n)}(x/p)^m(m/x)^p\left(\frac{1-T}{t-T}\right)^m\left(\frac{t-T}{t-1}\right)^p\right]^{1/m} \tag{29}$$

This equation can be used for the determination of the values of K_{pq}, p and q. The values of m, n, x, t and T are either known or can be estimated experimentally. The value of K_{pq} is calculated by varying the values p and q; K_{pq} is a constant for true values of p and q. The relationship between R and t is useful if an adequate computer is not available. It is given graphically in Fig. 1. The value of t is between 1 (lowest limit) and $2^{-m[p(n-1)-m(q-1)]}$ or $2^{[p(n-1)-m(q-1)]/(p-m)}$ (highest limit). The smaller value comes from the latter two values. The optimal

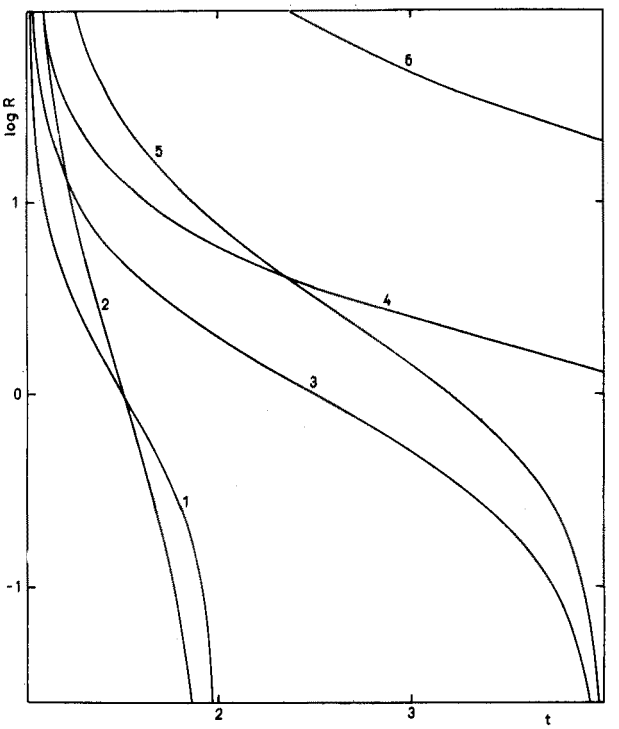

Fig. 1. Dependence between log R and t. The values of m, n, p, q for individual curves: (1) 1,1,1,2 or 1,2,1,3 or 1,3,1,4; (2) 2,2,2,3 or 2,1,2,2; (3) 1,1,1,3; (4) 1,1,1,4; (5) 1,1,2,3; (6) 1,1,3,4; μ=0.1 for all curves.

value of t is approximately midway between the two limits, where the determination of K_{pq} or R is most accurate.

The combination of eqns. (15), (22a) and (24a) results in

$$R(kx-pP)^p(mk-p)^{m-p}=(mP-x)^m \tag{30}$$

This equation can be used for the determination of k and $\Delta\bar{\varepsilon}$ (in combination with eqn. (26).

(b) Constant concentration method, $n \neq q$. Considering again the equations of the effective stability constants (9) and (10), assuming $c_M \gg c_L$ and quantitative complexation, and introducing

$$u=c_L/c_M, \quad v=c/c_M, \quad w=\bar{c}/c_M \tag{31abc}$$

$$K_{mn}^{-1}\,c_M^{1-m-n}=S_{mn}, \quad K_{pq}^{-1}\,c_M^{1-p-q}=S_{pq} \tag{32ab}$$

we obtain

$$S_{mn}v=(u-nv-qw)^n, \quad S_{pq}w=(u-nv-qw)^q \tag{33ab}$$

The combination of these equations results in

$$Sv^q=w^n \tag{34}$$

where

$$S=S_{mn}^q/S_{pq}^n=c_M^{q(1-m)-n(1-p)}K_{pq}^n/K_{mn}^q \tag{35}$$

If the concentration $c_L/2$ is used instead of c_L, we have

$$u' = c_L/(2c_M) = u/2, \quad v' = c'/c_M, \quad w' = \bar{c}'/c_M \tag{36abc}$$

and again

$$Sv'^q = w'^n \tag{37}$$

In the same way as for eqns. (22ab) and (24ab), we can write

$$u = nv + qw, \quad u = 2nv' + 2qw' \tag{38ab}$$

$$Q = v + kw, \quad Q' = v' + kw' \tag{39ab}$$

The elimination of k from eqn. (39ab) and substitution from eqn. (38ab) leads to

$$\frac{2(nQ-v)}{2nQ'-v} = \frac{2(n\Delta A - uc_M\Delta\varepsilon)}{2n\Delta A' - uc_M\Delta\varepsilon} = \frac{w}{w'} = f \tag{40}$$

Combining eqns. (35), (37), (38b) and (40), we get finally

$$S = \left(\frac{u}{2q}\right)^n \left(\frac{2n}{u}\right)^q \left(\frac{2-f^{n/q}}{f-f^{n/q}}\right)^n \left(\frac{f-f^{n/q}}{f-2}\right)^q \tag{41}$$

and

$$K_{pq} = \left[K_{mn}^q c_M^{n(1-p)-q(1-m)} \left(\frac{u}{2q}\right)^n \left(\frac{2n}{u}\right)^q \left(\frac{2-f^{n/q}}{f-f^{n/q}}\right)^n \left(\frac{f-f^{n/q}}{f-2}\right)^q\right]^{1/n} \tag{42}$$

The latter equation is used for calculation of K_{pq}. The values of n, q, u and f are known or can be estimated. By varying n and q the value of K_{pq}, which is a constant for true n and q, can be calculated. The relationship of eqn. (41) is given graphically in Fig. 2. It can be used if no convenient computer is available. The value of f is between $2^{q/n}$ (lowest limit) and 2 (highest limit). The optimal value of f (most accurate determination of K_{pq}) is approximately midway between these two limits.

Combining eqns. (34), (38a) and (39a), we get

$$S(ku - qQ)^q(nk - q)^{n-q} = (nQ - u)^n \tag{43}$$

which can be used for the determination of k and $\Delta\bar{\varepsilon}$ (in combination with eqn. 26).

Determination of h and overall stability constant β_{phq}

These data for the complex $M_pH_hL_q$ are determined by means of the well known relationship between the overall and effective constant[7],

$$\log \beta_{phq} = \log K_{pq}\alpha_{L(H)}^q + j\,\mathrm{pH} \tag{44}$$

The values of K_{pq} must be known for several different pH values; β_{phq} is a constant only for true j. The determination can also be extended if a masking reagent is present[7].

RESULTS AND DISCUSSION

The application of the dilution method was demonstrated for the complexation between uranyl ions and xylenol orange. The results are collected in Table I. They indicate that the formation of the complexes MH_2L and MH_4L_2 is probably the

TABLE I

COMPLEXATION OF URANYL ION WITH XYLENOL ORANGE

($x = 0.042$)[a]

pH	$10^4 c_L$	λ *(nm)*	*500*	*510*	*520*	*530*	*540*	*550*	*log* K_{11} *or log* K_{12}*	*log* β_{121} *or log* β_{142}**
4.50	2.58	ΔA	0.687	0.644	0.562	0.500	0.433	0.353		
		$\Delta A'$	0.316	0.296	0.258	0.230	0.199	0.163	4.97	29.77 ± 0.02
		$\Delta\varepsilon$	3261	3062	2680	2373	2060	1660		
	8.00	ΔA	—	—	—	0.094	0.150	—		
		$\Delta A'$	—	—	—	0.052	0.073	—		
	4.00	ΔA	—	—	—	0.052	0.073	—		
		$\Delta A'$	—	—	—	0.029	0.036	—	7.29*	56.87 ± 0.09**
5.01	2.58	ΔA	0.925	0.951	0.917	0.829	0.717	0.586		
		$\Delta A'$	0.448	0.457	0.439	0.397	0.342	0.281	5.59	29.87 ± 0.10
		$\Delta\varepsilon$	3872	4057	3948	3566	3115	2513		
	16.00	ΔA	—	—	—	—	0.139	0.125		
		$\Delta A'$	—	—	—	—	0.073	0.065		
	8.00	ΔA	—	—	—	0.079	0.073	0.065		
		$\Delta A'$	—	—	—	0.048	0.042	0.037	7.93*	56.49 ± 0.16**
5.33	2.58	ΔA	—	1.199	1.133	1.007	0.848	0.672		
		$\Delta A'$	—	0.581	0.548	0.486	0.411	0.325	5.79	29.76 ± 0.04
		$\Delta\varepsilon$	—	5013	4758	4252	3544	2823		
	8.00	ΔA	—	—	—	0.066	0.103	0.081		
		$\Delta A'$	—	—	—	0.034	0.054	0.042		
	4.00	ΔA	—	—	—	—	0.054	0.042		
		$\Delta A'$	—	—	—	—	0.028	0.022	8.50*	56.44 ± 0.03**

[a] Logarithmic overall stability constants of hydrogen complexes of xylenol orange: 12.23 (HL), 22.58 (H_2L), 29.28 (H_3L), 32.13 (H_4L), 34.45 (H_5L), 35.85 (H_6L), 34.81 (H_7L), 32.98 (H_8L), 29.66 (H_9L)[5].

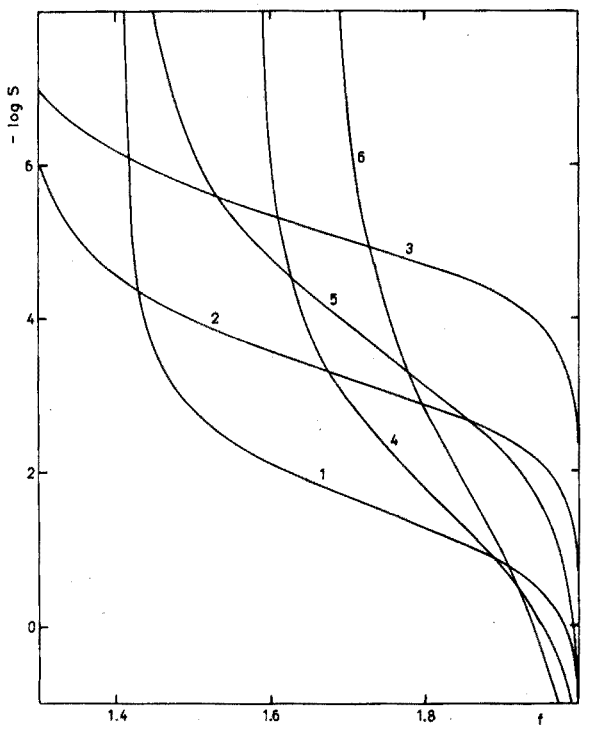

Fig. 2. Dependence between $-\log S$ and f. The values of n, q for individual curves: (1) 2,1; (2) 3,1; (3) 4,1; (4) 3,2; (5) 4,2; (6) 4,3; $\mu=0.1$ for all curves.

most general mode of xylenol orange complexation (for the probable structure of those complexes, see ref. 5).

The constant concentration method was used for the complexation between lanthanum and 8-quinolinol. The results are given in Table II.

In both cases the data for the main complex were determined by the stoichiometric dilution method[7]. The same method also makes it possible to decide whether a 1:1 or 2:2 complex is formed between uranyl ion and xylenol orange. Only the first ratio was found.

For the dilution or constant concentration method, the mathematics (minimum standard deviation) alone is insufficient to decide which particular side complex is formed. The same standard deviation can be found for several different complexes; for example, the side complexes 2:2 and 1:2 for lanthanum and 8-quinolinol. For this reason, the coordinative properties of the metal ion, and donating as well as stereochemical properties of the ligand, should also be taken into the account.

There is no need to develop the final eqns. (29) and (42) by means of the normalized eqns. (13), (14) and (33ab), since this can be done directly, from eqns. (9) and (10). The normalized equations were only used to obtain the relationship between R and t, or S and f, which is convenient for the presentation in form of a table or graph. Figure 1 shows that the same values of $p(1-n)-m(1-q)$, m and q correspond to the same curves.

TABLE II

COMPLEXATION OF LANTHANUM WITH 8-QUINOLINOL

(pH 5.83)[a]

u	$10^4 c_M$	λ (nm)	370	380	390	400	log K_{13} or log K_{12}*	log β_{103} or log β_{102}**
1/3	4.00	ΔA	0.083	0.069	0.054	0.035		
		$\Delta A'$	0.027	0.022	0.017	0.012	10.10	21.89±0.10
		$\Delta\varepsilon$	455	380	300	186		
0.08	200	ΔA	1.677	1.446	1.089	0.713		
		$\Delta A'$	0.889	0.763	0.573	0.373		
0.04		ΔA	0.889	0.763	0.573	0.373		
		$\Delta A'$	0.459	0.395	0.296	0.194		
0.02		ΔA	0.459	0.395	0.296	0.194		
		$\Delta A'$	0.237	0.204	0.152	0.099	6.76*	14.62±0.02**

[a] All measurements were made in aqueous 50% ethanol; logarithmic overall stability constants of hydrogen complexes of 8-quinolinol: 9.71 (HL), 14.63 (H_2L).

The condition $p(n-1) \neq m(q-1)$ (for the dilution method) or $n \neq q$ (for the constant concentration method) are given by the final eqns. (29) and (42). If they are disobeyed, all significant changes of measured data disappear, and the value of K_{pq} becomes indefinite. Also the method of stoichiometric dilution has a similar limitation[8] which can obviously be expected in all methods of this type.

Another failure of the dilution and constant concentration methods occurs if the measurement of absorbance is performed in the area of the isosbestic point of both complexes. For this reason it is desirable to perform the absorbance measurement in a wider range of the spectrum.

The author is grateful to Mrs. Jane Svec, Chemistry Department, University of Waterloo, Waterloo, Ontario, Canada, where part of this work was performed. The calculations were made by means of Monroe 1860 machine (Monroe Co., Orange, New Jersey). The programs are available upon request.

SUMMARY

A general approach to the determination of the composition and stability of a side complex $M_pH_hL_q$, if the data for the main complex $M_mH_jL_n$ are known, is developed. Two cases and two experimental methods should be differentiated: (a) $p(n-1) \neq m(q-1)$, dilution method; (b) $n \neq q$, constant concentration method. The case (a) was demonstrated on the uranyl–xylenol orange system (log β_{121} = 29.80±0.05, log β_{142} = 56.60±0.10), and case (b) on the lanthanum–8-quinolinol system (log β_{103} = 21.89±0.10, log β_{102} = 14.62±0.02 in aqueous 50% ethanol); β_{mjn} and β_{phq} are the overall stability constants of the corresponding complexes measured at the ionic strength 0.1 M and 25±1°C.

REFERENCES

1 F. J. C. Rossotti and H. Rossotti, *The Determination of Stability Constants*, McGraw–Hill, New York,

1961.
2 H. L. Schläfer, *Komplexbildung in Lösung*, Springer, Berlin, 1961.
3 L. P. Varga and F. C. Veatch, *Anal. Chem.*, 39 (1967) 1101.
4 T. Kaden and A. Zuberbühler, *Talanta*, 18 (1971) 61.
5 B. W. Budesinsky and J. Svec, *Anal. Chim. Acta*, 61 (1972) 465.
6 B. W. Budesinsky and M. Sagat, *Talanta*, 20 (1973) 228.
7 B. W. Budesinsky, *Z. Anal. Chem.*, 258 (1972) 186.
8 B. W. Budesinsky, *Z. Phys. Chem., N.F.*, 76 (1971) 310.

Analytica Chimica Acta, 71 (1974) 343–347

PHOTOMETRIC DETERMINATION OF CALCIUM WITH ANTIPYRYLAZO III

B. W. BUDESINSKY

Analytical Laboratory, Phelps Dodge Corporation, Morenci, Arizona 85540 (U.S.A.)

(Received 22nd October 1973)

Since 1960 the bisazo derivatives of chromotropic acid have attracted attention because of their chromogenic properties, stability in aqueous solution and ease of preparation[1]. The 3,6-bis(4-antipyrylazo)-4,5-dihydroxy-2,7-naphthalenedisulfonic acid (antipyrylazo III or diantipyrylazo) was the first compound of that group prepared from a heterocyclic amine[2]. It has been used for the photometric determination of lanthanides[3] and the equilibria of its complexation with protons, lanthanum, samarium, gadolinium and copper have been investigated[4].

Analytically, the most important reaction of antipyrylazo III is that with calcium ions. Its description and application to the photometric determination of calcium are the subject of this paper.

EXPERIMENTAL

Apparatus

All photometric measurements were made with a Gildford Spectrophotometer Model 2400 (Oberlin, Ohio), with 1-cm silica cells. An Orion Model 801 pH-meter (A. H. Thomas Co., Philadelphia, Pa.), with a glass and calomel electrode pair, was used for pH measurements.

*Preparation of antipyrylazo III**

Dissolve 4-aminoantipyrine (6.1 g) in 60 ml of 2 *M* hydrochloric acid, and cool to −3°C; add a solution of 2.1 g of sodium nitrite in 10 ml of water, dropwise with mechanical stirring, maintaining the temperature between −3 and 5°C. Dissolve 3.4 g of the anhydrous disodium salt of chromotropic acid and 5 g of calcium chloride (hexahydrate) in 50 ml of water. Cool to −3°C, and add 20 ml of 10 *M* sodium hydroxide and then the above solution of the diazonium salt, dropwise with stirring, maintaining the temperature at −3–5°C. Stir and cool for 30 min, then add 8 ml of glacial acetic acid, and refrigerate the solution overnight. Filter under suction and remove the mother liquor from the precipitate as much as possible. Dissolve the precipitate, in small portions, in a hot solution of 6 g of sodium hydrogencarbonate in 50 ml of water. Boil for 2–5 min, filter hot, using filter paper, and allow to crystallize at room temperature for 12–24 h. Filter the crystal-

* This procedure is different from that described in the patent[2]. Antipyrylazo III is also available from Aldrich Chemical Co., Milwaukee, Wisconsin.

line product under suction, wash with 20 ml of absolute ethanol and finally with 50 ml of ethyl ether. Dry at room temperature for 6 h (Yield, 3.5–4.5 g). Redissolve in a hot solution of 4 g of sodium hydrogencarbonate in 40 ml of water and crystallize at room temperature for 12–24 h; filter under suction and wash with 10 ml of absolute ethanol and 20 ml of ethyl ether. (Yield, 2.5–3.5 g).

The product, grayish-green lustered crystals, was chromatographically pure. The R_F is 0.95 (bluish-violet spot) on Whatman No 1 paper at 25°C in aqueous 1 *M* ammonia saturated with n-butanol. It was analyzed with the following results: 14.0% N, 5.9% Na, 8.1% S; required for $C_{32}H_{26}N_8Na_2O_{10}S_2$: 14.1% N, 5.8% Na, 8.1% S.

It is possible to obtain an additional 1.5–2.0 g of the product from the mother liquor. The aqueous solution of antipyrylazo III, stored in brown bottles at room temperature, is stable for 3–4 months.

Reagents

Antipyrylazo III and metal chlorides or perchlorates were used as aqueous 10^{-2}, 10^{-3} and 10^{-4} *M* solutions. The concentrations of the stock 10^{-2} *M* metal solutions were checked by titration with EDTA. The combined buffer and masking solution contained 20 g of sodium hydroxide, 5 g of sodium cyanide and 0.5 g of citric acid per liter. The buffers used in the study of equilibria were described earlier[5]. All chemicals were "Baker Analyzed" reagents.

Equilibria measurements

The sequence of metal ion, buffer and reagent was adhered to during the preparation of all solutions. The ionic strength was kept at 0.1 *M* (sodium perchlorate), and the temperature at 25 ± 1°C. The absorbances of solutions were measured against a buffer blank.

Determination of calcium

Adjust the pH of the sample solution to 3.0 ± 0.2 (or 6.0 ± 0.2 if some trivalent lanthanons are present). If the solution contains some tri- or tetravalent metal ions, pipet a 20-ml aliquot containing 10–140 μg of calcium into a 60-ml separatory funnel. Add 100–120 mg of cupferron (ammonium salt) and 20 ml of chloroform. Shake well for 3 min, remove the chloroform layer, add another 20 ml of chloroform, and repeat the extraction and separation again. Then pipet 10 ml of the aqueous phase into a 25 ml-volumetric flask. (If the basic solution contains no tri- or tetravalent metal ions, the procedure can be started at this point.) Add 5 ml of combined buffer and masking solution and mix well. Add 5 ml of 10^{-3} *M* antipyrylazo III solution, dilute with water to the mark and mix well. After 10 min measure the absorbance at 605 nm against a reagent–buffer blank. Construct the calibration curve for the given range of calcium under the same conditions.

RESULTS AND DISCUSSION

Characteristics of complexation

The absorbance spectra of antipyrylazo III and its calcium complex is presented in Fig. 1. The effect of pH is given by the competitive protonation of

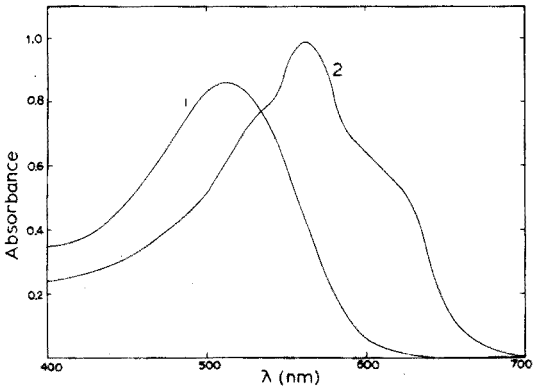

Fig. 1. Absorbance spectra of antipyrylazo III (1) and its calcium complex (2): $c_{Ca}=c_L=4.00\cdot10^{-5}$ *M*, pH 12.70.

antipyrylazo III connected with a strong chromogenic effect[4]. The maximal effective absorbance of the calcium complex is reached at pH 12.7 and ±0.2 deviations in pH are tolerable. For the concentration of antipyrylazo III given in the above procedure, the Beer law is obeyed over the whole range of absorbance of modern instruments, 0.0–2.0. There is no change in the absorbance of solutions during the first 6 h. The reason for the 10-min waiting period in the procedure is just to allow other ions to form complexes with the masking reagents.

The sensitivity of determination is indicated by the value of 21,500±100 l mole^{-1} cm^{-1} for the effective molar absorptivity, and 23,000±150 l mole^{-1} cm^{-1} for the absolute molar absorptivity under the above conditions. Multiple analyses of series of solutions containing 40 μg of calcium gave a precision of ±1.5% (relative standard deviation) corresponding to 0.6 μg of calcium.

Effect of foreign ions

The effects of 30 cations and 15 anions on the calcium determination were investigated. The limiting value of the concentration of a foreign ion was taken as that which caused an error of less than ±5% in the determination of 40 μg (1 μmole) of calcium. The results obtained are summarized in Table I. The interfering ions (in μmole) are: EDTA (0.1), oxalate (2.0), citrate (15.0), tartrate (20.0), phosphate (30.0), sulfate (60.0), acetate (60.0), strontium (0.5), barium (20.0) and magnesium (20.0). The limit of interference, for most tri- or tetravalent ions and divalent transition ions, can be regulated by the amount of cupferron and sodium cyanide, respectively. Thus, for the amounts given in the procedure, the limits are 200 μmole for tri- and tetravalent ions and 150 μmole for divalent transition ions.

Composition and stability of the complex

The molar ratio of metal to ligand of the calcium complex was determined by the continuous variations method for $(c_{Ca}+c_L)=8.00\cdot10^{-5}$ *M* (the sum of total concentrations), pH 12.7 and the wavelengths 510 nm and 605 nm. The ratio 2:1 was found.

The composition and stability constant of the complex were determined by the method of stoichiometric dilution[6]. The calculation was performed by means of a

TABLE I

DETERMINATION OF CALCIUM IN THE PRESENCE OF FOREIGN IONS

Foreign ion	*Absorbance*			*Foreign ion*	*Absorbance*		
	a	*b*	*c*		*a*	*b*	*c*
	0.430	0.430	0.430	Ta(V)	0.428	0.432	0.434
Al	0.432	0.428	0.430	Tl(III)	0.430	0.427	0.425
Ba	0.431	0.433	0.435	Th	0.428	0.425	0.431
Be	0.428	0.434	0.435	Sm	0.427	0.430	0.434
Cd	0.431	0.432	0.432	Sn(IV)	0.428	0.431	0.432
Ce(III)	0.428	0.431	0.434	U(VI)	0.431	0.432	0.433
Cr(III)	0.429	0.432	0.425	V(V)	0.432	0.428	0.435
Co(II)	0.430	0.427	0.429	Zn	0.430	0.431	0.432
Cu(II)	0.429	0.430	0.431	F^-	0.428	0.423	0.415
Ga	0.430	0.428	0.427	Cl^-	0.430	0.431	0.430
Fe(III)	0.428	0.432	0.433	Br^-	0.429	0.430	0.430
Hf	0.430	0.432	0.435	I^-	0.430	0.428	0.427
La	0.427	0.425	0.421	NO_3^-	0.431	0.430	0.431
Pb(II)	0.426	0.428	0.425	SO_4^{2-}	0.432	0.432	0.425
Mg	0.430	0.429	0.425	PO_4^{3-}	0.430	0.425	0.418
Mn(II)	0.430	0.427	0.426	AcO^-	0.431	0.430	0.429
Mg(II)	0.430	0.428	0.429	Oxalate	0.430	0.425	0.416
Mo(VI)	0.428	0.430	0.433	Tartrate	0.431	0.427	0.420
Ni(II)	0.430	0.431	0.430	Citrate	0.430	0.424	0.412
Pd(II)	0.429	0.428	0.430	Malonate	0.428	0.426	0.420
Sc	0.428	0.430	0.435	Benzoate	0.429	0.430	0.425
Ag(I)	0.430	0.428	0.433	Glycinate	0.431	0.428	0.421
Sr	0.431	0.617	1.723	EDTA	0.387	0.022	0.002

[a] 0.1 μmole of foreign ion present.
[b] 1.0 μmole of foreign ion present.
[c] 10.0 μmole of foreign ion present.

general program for that method with the minicomputer Monroe 1860 (Monroe Co., Orange, New Jersey). The results are given in Table II.

Given the composition of the complex and the structure of the reagent, the following structure of the complex seems probable

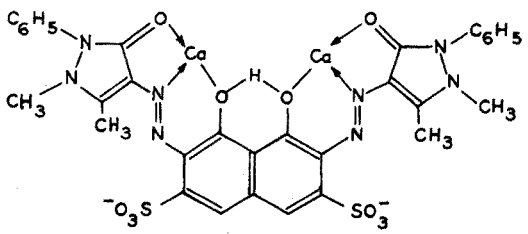

According to this structure, the selectivity of the determination is achieved by the chelate cage effect of the reagent. This effect is well known in this group of reagents. The selectivity of sulfonazo III, phosphonazo III and arsenazo III for barium and thorium, respectively, is of a similar type, although the composition of complexes is different[1]. The formation of a binuclear complex with antipyrylazo III is

TABLE II

COMPOSITION AND OVERALL STABILITY CONSTANT OF CALCIUM COMPLEX[a]

pH	*ΔA*	*ΔA'*	*log* β_{210}	
12.56	0.483	0.165	23.97	
12.23	0.457	0.159	24.04	23.99 ± 0.03
11.91	0.411	0.135	23.98	for Ca_2HL

[a] ΔA and $\Delta A'$ are the effective absorbances at 605 nm for c_{Ca} and $c_{Ca}/2$, respectively; $c_{Ca} = 2c_L = 5.33 \cdot 10^{-5}$ M; log $\beta_1 = 14.60$, log $\beta_2 = 25.60$, log $\beta_3 = 32.70$ (see ref. 4) where $\beta_n = [H_nL][H]^{-n}[L]^{-1}$.

facilitated by the relatively longer distance between the carbonyl oxygens of both pyrazolone rings[1]. From the viewpoint of obeying Beer's law, the formation of a binuclear complex is a drawback of the method. The reasons for this were first discussed by Asmus[7]. Therefore only a relatively high concentration of the reagent must be used. However, this drawback is compensated by a good selectivity and sensitivity of the reagent, which are considerably better than those of calcichrome or calcion[8]. These reagents have been considered as the most selective available for calcium. The obtained value of molar absorptivity is in a good agreement with binuclear complex formation.

The author is grateful to Mrs. Jane Svec of Chemistry Department, University of Waterloo, Waterloo, Ontario, Canada, for technical assistance.

SUMMARY

Antipyrylazo III or diantipyrylazo (3,6-bis(4-antipyrylazo)-4,5-dihydroxy-2,7-napthalenedisulfonic acid) forms at pH 12.7 a complex Ca_2HL with calcium. The logarithmic overall stability constant, log β_{211}, is 23.99 ± 0.03 (0.1 M $NaClO_4$, 25°C). The effective molar absorptivity is $21{,}500 \pm 100$ l mole^{-1} cm^{-1} at 605 nm. The complex can be used for a selective photometric determination of calcium (0.25–3.50 μmole) if tri- and tetravalent ions are removed by extraction with cupferron (into chloroform) and transition divalent ions are masked with sodium cyanide. Only strontium (0.5 μmole) and EDTA (0.1 μmole) interfere seriously.

REFERENCES

1 B. W. Budesinsky in H. A. Flaschka and A. J. Barnard, Jr. (Eds.), *Chelates in Analytical Chemistry*, Vol. 2, Dekker, New York, 1969.
2 B. W. Budesinsky and D. Vrzalova, *French Patent 1, 514, 643*, 1968; *Chem. Abstr.*, 70 (1969) 7796Or.
3 B. W. Budesinsky and D. Vrzalova, *Anal. Chim. Acta*, 36 (1966) 246.
4 A. Bezdekova and B. W. Budesinsky, *Collect. Czech. Chem. Commun.*, 33 (1968) 4178.
5 B. W. Budesinsky and T. S. West, *Anal. Chim. Acta*, 42 (1968) 455.
6 B. W. Budesinsky, *Z. Anal. Chem.*, 258 (1972) 186.
7 E. Asmus, *Z. Anal. Chem.*, 183 (1961) 321.
8 A. Bezdekova and B. W. Budesinsky, *Collect. Czech. Chem. Commun.*, 30 (1965) 811.

Analytica Chimica Acta, 71 (1974) 349–354

ACID DISSOCIATION REACTION OF PALLADIUM–4-(2-PYRIDYLAZO)-RESORCINOL COMPLEXES

TAKAO YOTSUYANAGI, HITOSHI HOSHINO and KAZUO AOMURA

Laboratory of Analytical Chemistry, Faculty of Engineering, Hokkaido University, Sapporo-shi 060 (Japan)

(Received 12th November 1973)

Several authors have studied the palladium-chelates with 4-(2-pyridylazo)-resorcinol(PAR)and their application to the photometric determination of palladium. Busev and Ivanov[1] found that two kinds of complex were formed: a red-purple PAR complex at pH 5.7–6.1 and a green complex in 0.35–5 *M* sulfuric acid solution, the latter complex being extractable into ethyl acetate. Based on these findings, they proposed an extraction–photometric method for palladium. However, Flaschka and Hicks[2] demonstrated that the green complex was extracted only in the presence of suitable amounts of chloride ion. Flaschka and Hicks[2] also developed a highly selective and sensitive spectrophotometric method for palladium with PAR by using EDTA and citrate as masking agents at pH 7. Saxena *et al.*[3] claimed that PAR formed at least three complexes with palladium(II) ion at different pH values: at pH 2.0 a very unstable green complex, and at pH 4.0 and pH 10.5 stable red complexes with the composition (metal–PAR ratio) 1:1 and 3:2, respectively. These authors pointed out that palladium–PAR complexes change their color and/or their composition as a function of hydrogen ion concentration, but no quantitative study was made on the acid properties of the complexes.

In the course of an investigation about the possibility of extracting transition metal–PAR chelates with quarternary ammonium ion[4–7], it was found that a red palladium–PAR (1:1) chelate can be extracted into chloroform under slightly acidic to alkaline conditions. This result indicates the presence of an anionic complex, which can only be produced by dissociation of the two phenolic protons on the PAR ligand in the palladium(II)–PAR (1:1) complex. In order to understand these properties of palladium–PAR chelates, the acid dissociation reactions of the complex were studied.

EXPERIMENTAL

Materials

PAR (Dojindo Co., Kumamoto, Japan) was purified by recrystallization from aqueous dimethylformamide. The purity was checked by potentiometric and photometric titrations. Palladium(II) perchlorate solution was prepared as follows: 0.17 g of palladium chloride was heated in a glass dish with about 20 ml of 60% perchloric acid and evaporated almost to dryness three times.

The residue was dissolved in 100 ml of 1 *M* perchloric acid solution, and the resulting solution was standardized by titration with EDTA. All chemicals used were of reagent-grade quality.

Apparatus

Absorption spectra and absorbance were measured with a Hitachi-124 model double beam recording spectrophotometer equipped with 10-mm and 5-mm quartz cells. Measurements of pH value were made with a Horiba M-5 model pH-meter which was standardized with Horiba standard buffer solutions of pH 4.00 ± 0.02, pH 6.88 ± 0.02 and pH 9.22 ± 0.02, respectively, at 25 ± 0.1°C.

Titration

Titrations were carried out by essentially the same procedure as described elsewhere[8]. The standard sodium hydroxide solution was added to the aqueous 50% (v/v) dioxane solution, $\mu = 0.10$ ($NaClO_4$), at 25 ± 0.1°C, under a nitrogen atmosphere. The relationship between the readings of the pH-meter and hydrogen ion concentrations in aqueous 50% dioxane was established by Irving and Rossotti's procedure[9], based on the titration curve of standard sodium hydroxide solution with standard perchloric acid solution.

Color development and extraction

Pipette an aliquot of sample solution (not exceeding 35 ml), containing up to 20 μg of palladium, into a beaker, add 5 ml of 0.05 *M* EDTA solution and adjust the pH to 2.5. After 2 min, add 2 ml of 0.1% PAR solution and allow to stand for 15 min (formation of the green complex). Adjust the pH to 9.3 with 5 ml of 0.05 *M* borax solution and with 2 ml of 0.1 *M* sodium hydroxide solution (formation of the red complex); then add 7 ml of 0.05 *M* tetradecyldimethylbenzylammonium chloride ($TDBA^+Cl^-$), dilute to about 50 ml with distilled water and transfer to a 100-ml separatory funnel. Extract the aqueous solution with 10.0 ml of chloroform by shaking for 15 min. Allow to stand for 30 min, separate the chloroform layer, and measure the absorbance at 540 nm, against the reagent blank as reference.

RESULTS AND DISCUSSION

The results shown in Fig. 1 seem to indicate the formation of at least three kinds of complexes, *i.e.*, a green complex below pH 4 ($\lambda_{max} = 420$ nm and 590 nm), a red complex at pH 4–7 ($\lambda_{max} = 525$ nm) and a red complex above pH 8 ($\lambda_{max} = 520$ nm), respectively. The compositions of those complexes, determined by the continuous variations method, showed the same metal to ligand ratio of 1:1 in aqueous 50% dioxane solutions at pH values of 2.65, 6.75 and 9.40, respectively. Therefore, the observed spectral change should be attributed to the dissociation of the acidic protons in the complexes, and not to the formation of complexes other than that containing a PAR: Pd ratio of 1:1.

The red palladium–PAR chelates were extracted with $TDBA^+$ (at $c_{TDBA^+} \geqslant 5 \cdot 10^{-3}$ *M*) into chloroform, to give a red ion-association complex, which had maximal absorbance at 540 nm; its molar absorptivity was $3.29 \cdot 10^4$ (see Fig. 1)

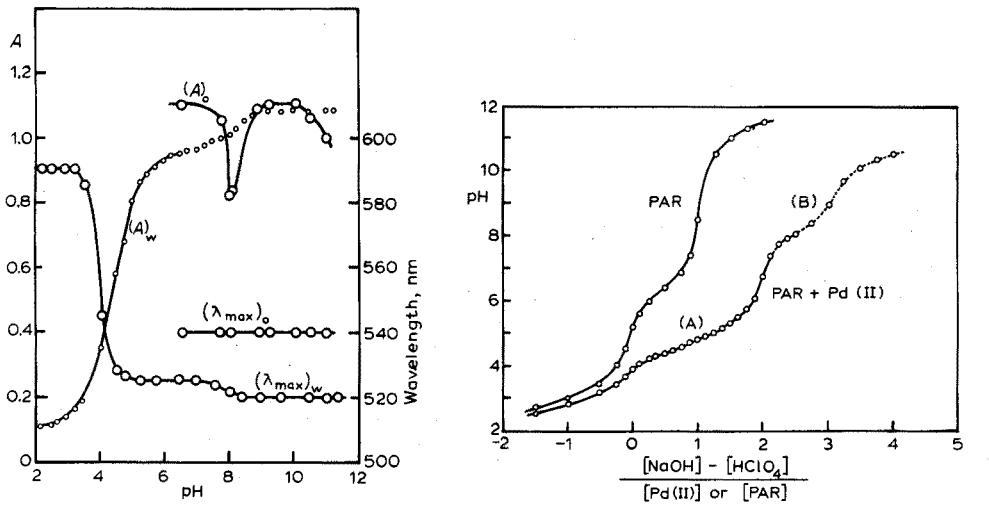

Fig. 1. Absorbance–pH curve and λ_{max}–pH curve. For A_w and $(\lambda_{max})_w$, $c_{Pd}=c_{PAR}=6.78\cdot10^{-5}$ M in aqueous 50% dioxane, $\mu=0.10$ ($NaClO_4$), at 25°C. In A_w–pH curve, circles are experimental points measured at 515 nm with 5.0-mm cells, and the solid curve is calculated from eqn. (4). For A_0 and $(\lambda_{max})_0$, $c_{Pd}=3.39\cdot10^{-5}$ M in chloroform. A_0 was measured at 540 nm with 10-mm cells at 25°C.

Fig. 2. Titration curves. PAR: $c_{PAR}=4.76\cdot10^{-4}$ M. PAR+Pd(II):$c_{PAR}=c_{Pd}=4.76\cdot10^{-4}$ M, $\mu=0.10$ ($NaClO_4$) in aqueous 50% dioxane solution at 25.0±0.1°C.

throughout the pH range 6–11. This result indicates that the same species was formed in the organic phase on extraction, even though the species in the aqueous phase were changed by altering the pH. This is most likely due to the effect of the $TDBA^+$ micelle on the acid dissociation of the complex, described recently by Kohara *et al.*[10,11]. It is also noteworthy that the extraction curve passed through a minimum at about pH 8. Curves of very similar form have also been found in the extraction of the 8-hydroxyquinoline–tungsten(IV) system, *etc.*[12,13], and this unusual behavior has been attributed to the hydrolytic polymerization of metal ions or metal complexes.

The titration curve (Fig. 2) shows that dissociation of protons took place in two different stages, at the buffer region A (two protons) and at the region B (one proton), respectively. By comparing with the spectral data (Fig. 1) and the pH titration curve (Fig. 2), it can indeed be concluded that the first remarkable spectral change, found in pH range 3–6, is due to the dissociation of two protons, and the second one found at about pH 9 is due to dissociation of one proton. In the case of aqueous solutions (no dioxane), the palladium–PAR complex formed a precipitate at pH 5–7. This fact suggests the presence of a neutral complex $(Pd(R))^0$ under these conditions.

Making use of the above information, the forms of the complexes at various pH conditions can be estimated as: a red anionic complex in alkaline solutions, which was extractable with $TDBA^+$, $(Pd(R)(OH))^-$, and a red neutral complex $(Pd(R))^0$, a red cationic complex $(Pd(HR))^+$ and a green complex in acidic solutions $(Pd(H_2R))^{2+}$. If K_{a_1} and K_{a_2} are the acid dissociation constants of the complexes

$(Pd(H_2R))^{2+}$ and $(Pd(HR))^{+}$, respectively, it can be shown that the relationship between hydrogen ion concentration and the acid dissociation constants at the buffer region A in Fig. 2 is:

$$-\left\{1-\frac{2c_{Pd}}{H}\right\}[H^+]^2 = K_{a_1}K_{a_2} + \left\{1-\frac{c_{Pd}}{H}\right\}[H^+]K_{a_1} \tag{1}$$

where c_{Pd} is the total concentration of palladium–PAR complex, and $H=[HClO_4]-[NaOH]+2c_{Pd}-[H^+]+[OH^-]$. The acid dissociation constants were obtained from a plot of $-[1-(2c_{Pd}/H)][H^+]^2$ against $[1-(c_{Pd}/H)][H^+]$, the slope of the straight line being K_{a_1}, and the intercept $K_{a_1}\cdot K_{a_2}$ (see Fig. 3).

$$K_{a_1} = \frac{[Pd(HR)^+][H^+]}{[Pd(H_2R)^{2+}]} = 10^{-4.35\pm0.05} \tag{2}$$

$$K_{a_2} = \frac{[Pd(R)][H^+]}{[Pd(HR)^-]} = 10^{-5.38\pm0.05} \tag{3}$$

at 25.0 ± 0.1°C, $\mu=0.10\,(NaClO_4)$ in aqueous 50% dioxane.

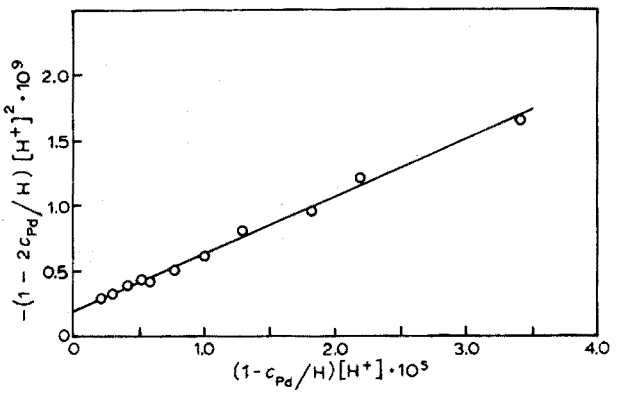

Fig. 3. Plots of $-\{1-(2c_{Pd}/H)\}[H^+]^2$ *vs.* $\{1-(c_{Pd}/H)\}[H^+]$

These results were checked by the absorbance–pH curve shown in Fig. 1 (curve A_w). It can be shown that absorbance is

$$A = \left\{\frac{\varepsilon_3+\varepsilon_2\dfrac{[H^+]}{K_{a_2}}+\varepsilon_1\dfrac{[H^+]^2}{K_{a_1}K_{a_2}}}{1+\dfrac{[H^+]}{K_{a_2}}+\dfrac{[H^+]^2}{K_{a_1}K_{a_2}}}\right\}c_{Pd} \tag{4}$$

where ε_1, ε_2 and ε_3 are the molar absorptivities of the complexes $(Pd(H_2R))^{2+}$, $(Pd(HR))^{+}$ and $(Pd(R))^{0}$, respectively. At 515 nm, ε_1 was determined as $2.98\cdot10^3$ from the constant absorbance value below pH 2. ε_2 and ε_3 were estimated as $2.68\cdot10^4$ and $2.86\cdot10^4$, respectively, based on eqn. (4) and the values of ε_1, K_{a_1} and K_{a_2}. Thus, the theoretical curve for pH–absorbance relationship can be drawn from eqn. (4), and this is shown in Fig. 1 as a solid curve. Excellent agreement is obtained between the calculated curve and the experimental points.

The third acid dissociation step at buffer region B is assigned to the protolysis of the water molecule bound to the fourth coordination site of the planar palladium(II) complex, since the neutral complex, $(Pd(R))^0$, has no dissociable proton other than that in the aquo ligand. This assignment is also supported by the fact that an anomalous minimum was observed in the extraction curve (Fig. 1) at the pH range of buffer region B. This is most likely due to hydrolytic polymerization of the complex, which is caused by the bridge-forming property of the hydroxo ligand in the complex. Even though the direct analysis of buffer region B was impossible, owing to the complexities discussed above, an approximate value of the acid dissociation constant of $(Pd(R))^0$, K_{a_3}, can be estimated as about 8.5 from the location of buffer region B.

Freiser *et al.*[14] demonstrated that the order of the acid dissociation constants of the *p*-hydroxy group in the PAR complexes of divalent metal ions was in accordance with the stability constants of the PAR complexes of these metal ions. According to them[14], the pK_a value of the *p*-hydroxy group of the palladium(II)–PAR chelate should be somewhat smaller than that of the copper(II) complex, $pK_a = 5.5$. Therefore, it seems to be reasonable to assign the acid dissociation constant, $pK_{a_2} = 5.38$, to the dissociation of the *p*-hydroxy group.

Consequently, the first dissociation constant, $pK_{a_1} = 4.35$, should be that of the *o*-hydroxy group. This assignment is quite acceptable, since this proton dissociation was accompanied by a drastic change in the spectrum—a color change from green to red with a remarkable increase in the molar absorptivity (see Fig. 1); this type of spectral change is usually attributed to the formation of a new coordination bond, that is, in this case, the bond between the dissociated *o*-hydroxy (phenolate) group and the palladium(II) ion.

Thus, the green complex in acidic solution, $(Pd(H_2R))^{2+}$, should have a PAR ligand with two undissociated hydroxy groups. Further work is necessary to clarify the nature of the ligand coordination in the green complex, *i.e.*, whether PAR coordinates as a bidentate ligand with two nitrogen atoms on the pyridyl

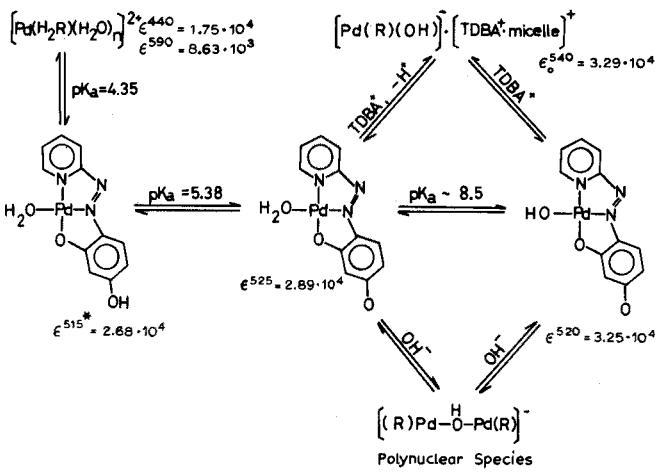

Fig. 4. Acid dissociation scheme of palladium–PAR complexes. ε_0^{540}: measured in chloroform. ε^{515*}: molar absorptivity at 515 nm. The λ_{max} of $[Pd(HR)(H_2O)]^+$ could not be determined.

and azo groups, or as a tridentate ligand with the two nitrogen atoms and the undissociated *o*-hydroxy group.

The scheme of the acid dissociation reaction can be summarized as shown in Fig. 4.

Based on these results, a new extraction–spectrophotometric method for palladium can be developed; this will be published at a later date.

SUMMARY

Palladium(II) formed four kinds of stable 1:1 chelates with 4-(2-pyridylazo)-resorcinol (PAR or H_2R): below pH 4, a green chelate $[Pd(H_2R)H_2O]^{2+}$ ($\varepsilon = 1.75 \cdot 10^4$ at 440 nm and $\varepsilon = 8.63 \cdot 10^3$ at 580 nm); at pH 4–7 two kinds of red chelate $[Pd(HR)H_2O]^+$ ($\varepsilon = 2.68 \cdot 10^4$ at 515 nm) and $[Pd(R)H_2O]^0$ ($\varepsilon = 2.89 \cdot 10^4$ at 525 nm); and at pH 8–11 a red chelate $[Pd(R)OH]^-$ ($\varepsilon = 3.25 \cdot 10^4$ at 520 nm). The acid dissociation constants of the chelates were estimated as $K_{a_1} = [Pd(HR)H_2O^+][H^+]/[Pd(H_2R)H_2O^{2+}] = 10^{-4.35 \pm 0.05}$ and $K_{a_2} = [Pd(R)H_2O] \cdot [H^+]/[Pd(HR)H_2O^+] = 10^{-5.38 \pm 0.05}$ in aqueous 50% dioxane solution at 25°C, $\mu = 0.1$ ($NaClO_4$). At pH 6–11, the red palladium(II)–PAR chelates react with tetradecyldimethylbenzylammonium chloride to form an ion-association complex which is easily extracted into chloroform and has maximal absorbance at 540 nm with a molar absorptivity of $3.29 \cdot 10^4$.

REFERENCES

1 A. I. Busev and I. M. Ivanov, *Zh. Anal. Khim.*, 19 (1964) 232.
2 H. Flaschka and J. Hicks, *Microchem. J.*, 1 (1966) 517.
3 K. K. Saxena, B. V. Agarwala and A. K. Dey, *Mikrochim. Ichnoanal. Acta*, (1969) 694.
4 T. Yotsuyanagi, R. Yamashita and K. Aomura, *Jap. Anal.*, 19 (1969) 981.
5 T. Yotsuyanagi, R. Yamashita and K. Aomura, *Anal. Chem.*, 44 (1972) 1091.
6 T. Yotsuyanagi, Y. Takeda, R. Yamashita and K. Aomura, *Anal. Chim. Acta*, 67 (1973) 297.
7 R. Yamashita, T. Yotsuyanagi and K. Aomura, *Jap. Anal.*, 20 (1971) 1282.
8 H. Freiser, R. G. Charles and W. D. Johnston, *J. Amer. Chem. Soc.*, 74 (1952) 1383.
9 H. M. Irving and H. S. Rossoti, *J. Chem. Soc., London*, (1954) 2904.
10 H. Kohara, *Jap. Anal.*, 17 (1968) 1147.
11 H. Kohara, N. Ishibashi and T. Masuzaki, *Jap. Anal.*, 19 (1970) 467.
12 I. P. Alimarin and Yu. A. Zolotov, *Talanta*, 9 (1962) 891.
13 F. Umland and W. Hoffmann, *Z. Anal. Chem.*, 168 (1959) 268.
14 A. Corsini, Q. Fernando and H. Freiser, *Inorg. Chem.*, 2 (1963) 224.

Analytica Chimica Acta, 71 (1974) 355–366

AN IMPROVED METHOD FOR DETERMINATION OF TRACE QUANTITIES OF PHENOLS IN NATURAL WATERS

B. K. AFGHAN, P. E. BELLIVEAU*, R. H. LAROSE and J. F. RYAN

Canada Centre for Inland Waters, Department of the Environment, Burlington, Ontario (Canada)

(Received 5th December 1974)

The toxic nature of phenolic compounds has made it necessary to detect accurately very low concentrations of these compounds in natural waters and industrial effluents. There are several methods for the determination of phenols[1–5]. All these methods utilize a distillation step to separate phenols from interfering substances, followed by the formation of a coloured product with various reagents. For determining low levels of phenols, large volumes of a sample, after the colour development, are extracted into a non-miscible organic solvent before the determination.

In this laboratory, the above methods were critically evaluated. The studies showed that it is very difficult to determine accurately the phenol content of a sample below 5 $\mu g\ l^{-1}$. The experimental work indicated that the inaccuracy was mainly due to atmospheric contamination during the distillation of the samples, but precautions to minimize possibe contamination did not improve the reproducibility. Therefore, attempts were made to devise a simpler or faster procedure which could be used to concentrate and separate phenols as an alternative to the conventional distillation procedure.

This paper describes a new extraction procedure in which n-butyl acetate or isoamyl acetate is used for the separation and concentration of low levels of phenols, and the subsequent determination by various absorptiometric or fluorescence methods.

The sensitivities of these procedures together with the ability of the individual methods to measure different types of phenolic compounds such as phenol, cresols and chlorinated phenols are also discussed. A new method of preservation of natural waters is described which could preserve the samples for a period of 2–3 weeks without any noticeable loss from biodegradation, chemical transformation and/or adsorption.

EXPERIMENTAL

Reagents

All solutions used were made from reagent-grade chemicals. The magnesium nitrate (10%) solution was equilibrated with chloroform before use. The bismuth solution (10^{-3} *M*) was prepared from bismuth nitrate in concentrated hydrochloric acid.

* Atlantic Region Water Quality Laboratory, Department of the Environment, Moncton, New Brunswick, Canada.

Apparatus

The equipment used consisted of standard Technicon AutoAnalyzer modules. Polyethylene tubing with acidflex sleeving was built into the manifold for the transport of chloroform by the displacement technique. The displacement bottles were glass winchesters with polypropylene caps. The cap of the chloroform displacement bottle was drilled to accept, with a tight fit, two lengths of 0.066-in. i.d. polyethylene tubing, to deliver magnesium nitrate solution and as an air vent, respectively. The ends of the tubing were flared with a hot spatula and pulled flush with the inside cap. A third hole was also drilled in the cap to accept 0.015-in. i.d. polyethylene tubing whose end touched the bottom of the bottle, to deliver chloroform. The cap was sealed on the outside around the polyethylene tubing with silicone sealant.

The waste displacement bottle was essentially the same as the chloroform displacement bottle except that only two lengths of polyethylene were required. One was inserted flush with the inside of the cap to draw water from the bottle, and the other, through which chloroform from the flow cell entered, extended to the bottom of the bottle.

The solvent separator was built as described for automated solvent extraction with the Technicon AutoAnalyzer, by Carter and Nickless[6].

A Hitachi MPF-2A fluorescence spectrophotometer was used for fluorescence measurements. Absorptiometric measurements were made in 10-cm quartz cells (5-ml capacity) with a Baush and Lamb Spectronic 600 spectrophotometer.

Preservation

All samples were preserved by adding 5 ml of 10^{-3} *M* bismuth solution to 1 litre of sample stored in glass bottles. Bismuth precipitates sulfides and mercaptans from the samples.

Extraction procedure

Acidified aliquots (500 ml) of phenol standards or samples were adjusted to pH 2 ± 0.1 with dilute sodium hydroxide solution. Samples which did not contain bismuth solution as preservative were spiked with the recommended amount of bismuth stock solution before the pH adjustment. The aqueous phase was extracted with 60 ml of n-butyl acetate for 3 min. The separated organic phase was back-extracted with 8 ml of 1.6 *M* sodium hydroxide solution. The resultant alkaline solution was diluted to 10 ml and analyzed by the adsorptiometric or spectrofluorimetric methods discussed below.

RESULTS AND DISCUSSION

Concentration and separation of phenols from natural waters

Considerable work has been reported on the recovery and/or removal of phenolic compounds from industrial wastes before they are discharged into natural waters. Adsorption[7–9], ion exchange[10,11], and solvent extraction[12], have been utilized extensively; but no study has been carried out to check their concentration efficiency at low levels so that these approaches could be used for analytical purposes. Therefore, work was initiated to develop the above techniques for the concentration of phenols, so that they might replace the time-consuming distillation step.

Initial studies indicated that solvent extraction was the most convenient and accurate method for the concentration of phenols, cresols and chlorinated phenols. Therefore, this approach was chosen and optimized.

In the preliminary experiments, various phenolic compounds such as phenol, cresols and chlorinated phenols were extracted, as described above, for 15 min. The accumulated organic phase was back-extracted twice with 4 ml of 5 *M* sodium hydroxide solution to ensure complete extraction of the phenols. The combined sodium hydroxide extract was adjusted to pH 10 ± 0.2 and analyzed by the standard 4-aminoantipyrine (4-AAP) method. For phenols which could not be analyzed by this method, such as *p*-cresol and polychlorinated phenols, the u.v. spectrophotometric method[13] was used.

Petroleum ether, benzene and chloroform were found to extract quantitatively highly substituted phenols such as pentachlorophenol and trimethylphenol. These solvents did not extract phenol, *o*-, *m*- and *p*-cresols. n-Butyl acetate and iso-amyl acetate quantitatively extracted phenol, cresols and chlorinated phenols.

By the use of the above procedure, various pertinent extraction variables such as time and number of extractions, pH, and the volume of organic solvent necessary to extract phenols were studied. Up to 90% of phenol could be extracted with a 50-ml volume of the organic solvent over a period of 2–3 min, and this recovery did not improve when the solvent volume was increased to 100 ml. Similar recoveries were also obtained for various ratios of organic: aqueous phase up to 1:25. The effect of various concentrations of alkaline solutions, such as sodium hydroxide and ammonium hydroxide, to back-extract phenol from the organic phase indicated that up to 85% recovery was obtained with 1.5 *M* sodium hydroxide; only 15–20% recovery was achieved with similar concentrations of ammonia solution.

The overall extraction efficiency with sodium hydroxide was also verified with radioactive ^{14}C-phenol in lake waters, in the range 1–10 $\mu g\ l^{-1}$. The resultant

TABLE I

EXTRACTABILITY OF PHENOL FROM LAKE WATER

Sample	*Amount spiked*	*% Recovery in n-butyl acetate*[a]	*% Recovery in alkali from n-butyl acetate*[a]	*Total extraction efficiency (%)*[a]
Distilled water	1	89.6	83.4	74.8
	5	90.2	81.9	73.9
	10	89.5	83.9	75.1
Synthetic lakewater	1	89.9	84.6	76.1
	5	91.6	78.7	72.1
	10	89.2	81.9	73.1
Lake water 1	1	91.7	81.7	75.0
	5	89.6	84.5	75.8
	10	90.3	85.4	77.2
Lake water 2	1	90.4	82.7	74.8
	5	90.2	84.4	76.2
	10	90.9	82.6	75.1

[a] The above results are the average of four determinations.

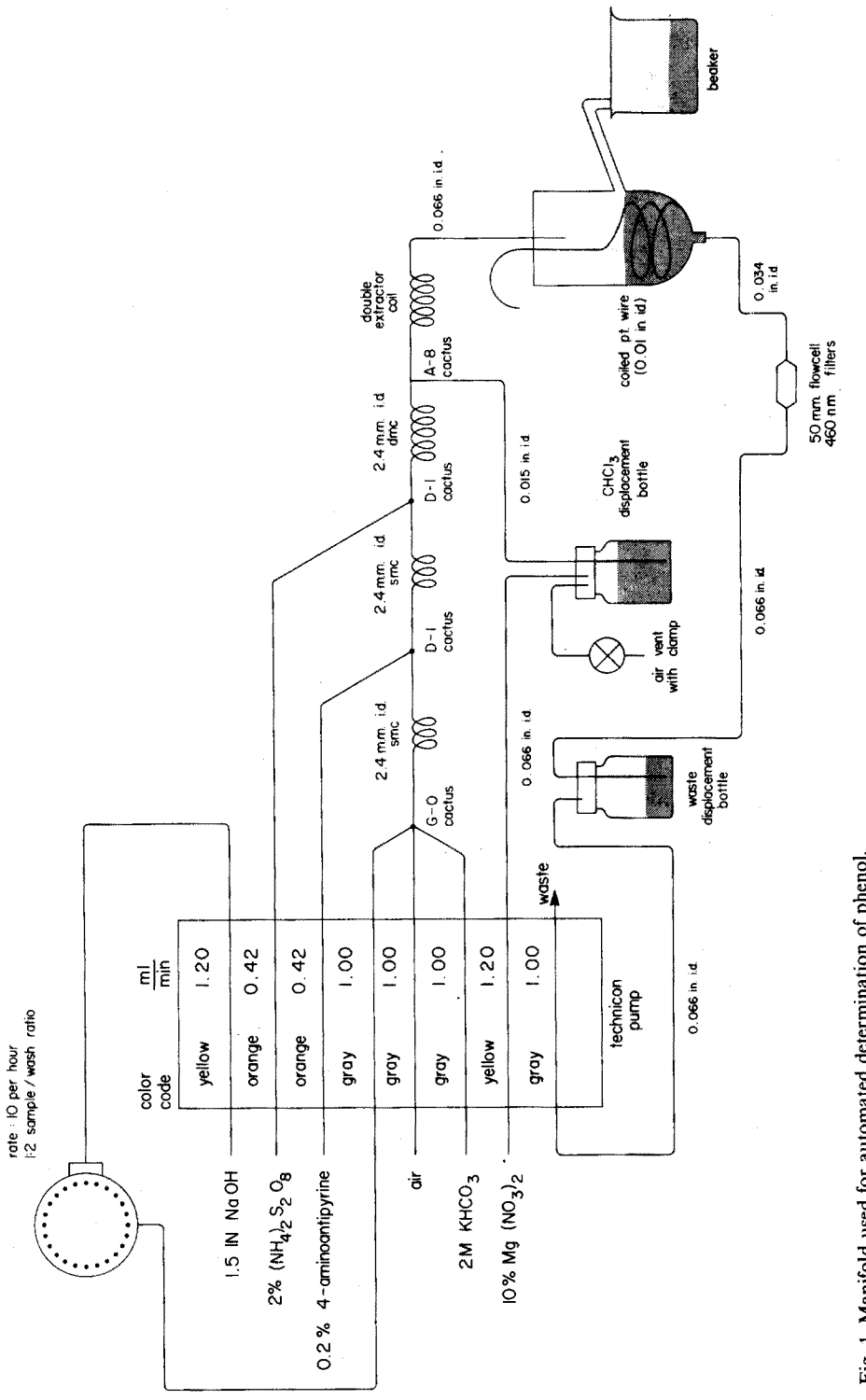

Fig. 1. Manifold used for automated determination of phenol.

aqueous phase, after n-butyl acetate extraction, and the final alkaline extract were analyzed for the radioactive phenol content. It can be seen from the results in Table I that the overall efficiency was about 75% and that of the initial n-butyl acetate extraction about 90%. These results agree with the previous results obtained with the 4-aminoantipyrine method.

Interferences

The effect of different contaminants, normally present in natural water, on the overall extraction procedure for phenols was investigated for synthetic lake water. The final extract was analyzed by the standard 4-aminoantipyrine method. The various contaminants included 10–100-fold amounts of heavy metals, amino-acids, sulfide, and fulvic acid, together with the major ions normally present in natural waters. None of these ions interfered, except sulfide when it was present above 10 $\mu g\ l^{-1}$. This interference was eliminated by precipitating sulfide with bismuth under acidic conditions before the extraction of phenols.

Methods for the determination of phenols

Spectrophotometric method. Phenols are usually routinely determined by the method based on the condensation of phenol with 4-aminoantipyrine at pH 10 ± 0.2. This method was automated and the resultant alkaline extract was directly analyzed for phenol. The automated method was identical to the manual procedure, except for the buffer, where equal volumes of 1.5 *M* sodium hydroxide and 2 *M* potassium hydrogen carbonate were used.

During the analysis of actual samples, it was found that considerably lower absorbances were obtained for equivalent concentrations when analyzed by the automated method with the sodium hydroxide–potassium hydrogencarbonate buffer compared to the manual method which utilizes ammonia–ammonium chloride buffer. Furthermore, a very noisy baseline was obtained which made it difficult to determine low levels of phenols. Therefore, an extraction step was incorporated in the automated method to isolate the condensation product of 4-aminoantipyrine–phenol, and the absorbance of the organic phase was measured. It was expected that this would improve the sensitivity as well as remove the baseline noise. The extraction procedure used in manifold, for the isolation of the coloured product, was essentially the same as that described by Carter and Nickless[6] except that a short length of platinum wire was coiled and placed inside the separator to enhance the coalescing of the chloroform drops entering the separator. In addition, the overflow of the separator was immersed in deionized water to minimize the fluctuation of the level of the liquid in the separator. This in turn smoothed the baseline considerably. The final manifold used for the automated method is shown in Fig. 1.

Figure 2 shows typical results obtained for the various levels of phenol in synthetic lake water by the above method. It was possible to attain a minimum detection limit of 0.5 $\mu g\ l^{-1}$. A straight-line calibration curve was obtained for the 1–10 $\mu g\ l^{-1}$ range.

U.v. spectrophotometric method. Direct and differential u.v. spectrophotometric procedures for the determination of phenols are well known[13,14]. These methods are known to determine all phenolic compounds which react with 4-aminoantipyrine, as well as cresols which cannot be determined accurately by the 4-aminoantipyrine

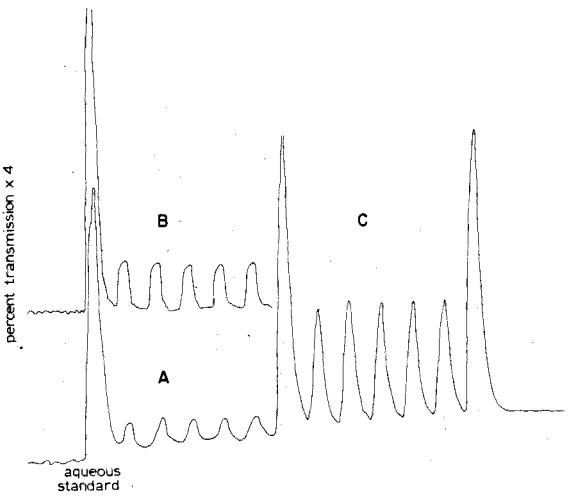

Fig. 2. Analytical reproducibility of the determination of various levels of phenols in synthetic water: (A) 1 $\mu g\ l^{-1}$; (B) 2 $\mu g\ l^{-1}$; (C) 5 $\mu g\ l^{-1}$.

TABLE II

ULTRAVIOLET AND FLUORESCENCE CHARACTERISTICS OF SOME PHENOLS

	Ultraviolet				*Fluorescence*[a]		
	pH 2		*1 M Sodium hydroxide*		*λ ex (nm)*	*λ em (nm)*	*Relative fluorescence intensity*
	λ_{max} *(nm)*	*Molar absorptivity (ε)*	λ_{max} *(nm)*	*Molar absorptivity (ε)*			
Phenol	270	1,550	285	2,640	275	300	55
o-Cresol	270	1,515	290	2,920	275	300	48
m-Cresol	270	1,350	290	2,595	275	300	56
p-Cresol	275	1,570	295	2,490	280	300	52
p-Chlorophenol	280	1,555	300	2,950	[b]	[b]	[b]
2, 4, 6-trichloro-phenol	290	2,875	310	4,650	[b]	[b]	[b]
Pentachlorophenol	300	2,530	320	5,335	[b]	[b]	[b]

[a] 100 $\mu g\ l^{-1}$ stock solutions were used, and spectra were recorded with ex slit 5 nm, em slit 10 nm and sensitivity 4.0.

[b] No fluorescence obtained.

method. However, this method is not used routinely for determination of total phenols because the majority of phenols have low molar absorptivities.

However, with the development of the extraction procedure to concentrate phenols, it became possible to use this approach for the determination of phenols, cresols and chlorinated phenols. Table II shows the optical characteristics of some phenols and indicates that the molar absorptivities (ε) of phenols increase in basic

solutions. Furthermore, some of the phenols and cresols absorb in a narrow range 285–295 nm. Therefore, it is possible to analyze these compounds by measuring the absorbance at an intermediate wavelength of 292 nm. It is also possible to determine other phenols, in particular, trichlorophenol and pentachlorophenol, by this approach. The latter application does not seem to have been previously reported.

The minimum detection limit for individual phenols was 5 $\mu g\ l^{-1}$ for a 10-cm path length. A straight-line calibration curve was obtained in the range 10–100 $\mu g l^{-1}$ for the phenols discussed. The relative standard deviation was found to be 6–10%.

Spectrofluorimetric method. The use of fluorescence spectrometry for the determination of phenol has been reported[15,16]. The method is based on the measurement of the fluorescence intensity of an acidified sample at 305 nm when excited at 275 nm. Although the method is inherently capable of detecting as low as 0.1 $\mu g\ l^{-1}$ of phenol, its ability to detect these low concentrations is limited by the fact that water also exhibits a Raman emission at 305 nm when excited at a wavelength of 275 nm. This strong Raman emission varies with the solute content of the sample[4], and therefore it is very difficult to determine low concentrations of phenols in samples with varying dissolved solid content. The solvent extraction procedure made it possible to eliminate this variation of Raman scatter, by separating the phenols before their determination. Therefore, this solvent extraction–fluorimetric approach was used, towards improving the accuracy and limit of detection for phenols.

In preliminary investigations, several phenols were carried through the above extraction procedure. The excitation and emission spectra were then recorded after the alkaline extract had been acidified to pH 2 with sulfuric acid. Table II shows the fluorescence characteristics of some phenolic compounds which might be present in natural waters. The data indicate that phenols and cresols have similar characteristics and can be determined by this technique. Although some variation in excitation wavelength and relative fluorescence intensities is obtained for individual compounds, it is possible to determine these by selecting an intermediate wavelength of excitation. During actual analysis, the analytical wavelengths of 278 and 305 nm were chosen as the most suitable for excitation and emission, respectively. Figure 3 shows a typical emission spectra obtained for a blank and synthetic lake water containing phenol (2.5 $\mu g\ l^{-1}$) analyzed by this approach. Blank indicates the magnitude of Raman emission obtained with excitation at 278 nm. It is possible to detect as little as 0.1 $\mu g\ l^{-1}$ for phenol and all cresols. The relative standard deviation for replicate analysis of spiked samples in the range 1–10 $\mu g\ l^{-1}$ was established at 3–10%.

During the analysis of natural water samples, it was observed that the alkaline extract from some samples produced an emulsion which was very difficult to remove, and this increased the fluorescence intensity owing to scatter. This emulsion was removed by bubbling nitrogen through the extract at 80–85°C for 15 min before acidification.

Preservation

Samples containing low levels of phenols are generally preserved to inhibit any biodegradation or chemical oxidation during storage. The various preservation techniques include the addition of copper sulfate and phosphoric acid[1], and sodium

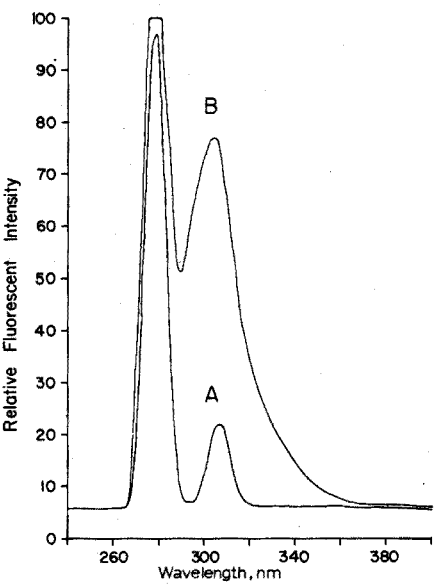

Fig. 3. Emission spectra: (A) blank, (B) sample containing 2.5 $\mu g\ l^{-1}$ phenol. Excitation λ 278 nm; ex. slits 1 nm, em. slits 10.0 nm.

TABLE III

EFFECT OF THE VARIOUS PRESERVATIVES ON BACTERIAL ACTIVITY

Preservative	*Suspension conc. per ml*	*Contact time (min)*		
		1	*10*	*60*
0.1% $CuSO_4$ adjusted to	7,900	+[a]	+	−[b]
pH 4 with phosphoric acid	1,500,000	+	+	−
0.5% NaOH	7,900	−	−	−
	1,500,000	−	−	−
0.1 *M* HCl	7,900	−	−	−
	1,500,000	−	−	−
10^{-4} *M* Bi^{3+} in 0.1 *M* HCl	7,900	−	−	−
	1,500,000	−	−	−

[a] Indicates growth of organism after stated contact time.
[b] Indicates no growth of organism after stated contact time.

hydroxide[15]. It is also recommended that samples be stored in the dark below 10°C and analyzed as soon as possible.

This practice of preservation makes routine analysis of phenol very difficult; furthermore, no detailed study has been carried out to confirm whether the loss is due to biodegradation, chemical transformation or adsorption.

In this laboratory, the effectiveness of various preservatives was tested for inhibiting the activity of bacteria known to degrade phenols, and the effect of temperature on the degradation was studied. Initial tests were carried out to determine

the efficiency of various preservatives against two concentrations of Pseudomonas aeruginoso containing 7,900 and 1,500,000 bacteria per ml. The initial time of contact varied between 1 and 60 min. From the data in Table III, it is clear that all Pseudomonas organisms were killed by all preservatives; however, hydrochloric acid and sodium hydroxide were effective even when the contact time was only 1 min. Furthermore, there was no significant difference when preserved samples were kept at different temperatures ranging from 5 to 35°C, or whether these samples were stored in the dark or under normal laboratory conditions. Preservation of phenol with hydrochloric acid was chosen since most water quality laboratories use this routinely to preserve samples for trace metals.

Loss of phenols during storage

Many workers have reported high losses of trace contaminants by adsorption[16,17], and earlier workers have also reported that some loss of phenol occurred during storage. This may be attributed to the adsorption of phenol on the walls of container. Therefore this effect was investigated in detail.

During this study, ^{14}C-labelled phenol was spiked at 1, 5 and 10 $\mu g\ l^{-1}$ levels in deionized water, filtered, and unfiltered lake water. Spiked samples were stored in plastic and glass bottles and the radioactivities of these samples were measured at 1-, 2-, 4-, 8- and 16-day intervals. Unfiltered samples were filtered through 0.45-μm filter paper before the measurement of radioactivity. The results (Table IV) indicate that the samples stored in glass suffered no apparent loss during a 16-day period. However, there was a marked decrease in radioactivity of the samples stored in plastic bottles during the first two days; a plateau was reached after four days.

TABLE IV

LOSS OF PHENOL DURING STORAGE

Sample	*Conc. ^{14}C phenol ($\mu g\ l^{-1}$)*	*Storage container*	*% Loss of phenol (days)*				
			1	*2*	*4*	*8*	*16*
Deionized	1	glass	2.6	3.8	4.6	3.9	4.5
water	1	plastic	22	28	30	31	34
	5	glass	nil	1.5	3.7	2.9	5.1
	5	plastic	9.7	21	24	24	27
	10	glass	nil	nil	nil	2.0	3.6
	10	plastic	6.1	9.2	9.5	9.1	9.7
Filtered	1	glass	1.8	3.8	4.6	5.9	4.8
lakewater	1	plastic	16	34	32	35	36
	5	glass	3.9	3.8	5.1	4.6	4.4
	5	plastic	6.7	12.9	13.7	13.9	18.0
	10	glass	nil	nil	1.2	1.2	nil
	10	plastic	7.9	21	23	26	24
Unfiltered	1	glass	6.4	5.8	5.2	6.9	7.2
lakewater	1	plastic	36	45	52	56	53
	5	glass	nil	2.0	1.8	2.7	3.2
	5	plastic	18	29	31	34	33
	10	glass	nil	nil	nil	nil	nil
	10	plastic	10	21	18	20	27

TABLE V

COMPARATIVE DETERMINATIONS MADE ON SYNTHETIC SOLUTIONS

Phenols in synthetic lakewater ($\mu g\ l^{-1}$)	*4-Aminoantipyrine*			*Ultraviolet*			*Fluorescence*		
	% Recovery	*Ratio 4-AAP: u.v.*	*Ratio 4-AAP: fluorescence*	*% Recovery*	*Ratio u.v.: 4-AAP*	*Ratio u.v.: fluorescence*	*% Recovery*	*Ratio fluorescence: 4-AAP*	*Ratio fluorescence: u.v.*
Phenol (10)	97	1.17	1.07	83	0.85	0.91	91	0.94	1.09
(25)	98	1.00	1.01	98	1.00	1.01	97	0.99	0.99
p-Cresol (10)	[c]	—	—	93	—	0.99	94	—	1.01
(25)	[c]	—	—	91	—	0.89	103	—	1.13
p-Chlorophenol (10)	38	0.42	—	89	2.34	—	[c]	—	—
(25)	46	0.47	—	97	2.11	—	[c]	—	—
2,4,6-Trichlorophenol (10)	11	0.14	—	86	7.82	—	[c]	—	—
(25)	16	0.17	—	93	5.82	—	[c]	—	—
Phenol (10) + *p*-cresol (10) + *p*-chlorophenol (10) + 2,4,6 trichlorophenol (10)	134	—	0.65	285; 98[a]	—	—	204[b]	1.52	—

[a] First figure corresponds to the combined recovery of phenol, *p*-cresol, and *p*-chlorophenol when absorbances were measured at 292 nm. The second figure indicates the recovery of 2,4,6-trichlorophenol at a wavelength of 310 nm.

[b] This indicates that only phenol and cresol can be determined by this method.

[c] Not detected.

Therefore, it is recommended that the samples be collected and stored in glass bottles.

Analysis of waters

Table V shows the comparative determinations made on known solutions of phenols in synthetic lake water by the automated 4-aminoantipyrine, u.v., and spectrofluorimetric methods. These results indicate that 4-aminoantipyrine is only capable of determining phenol; considerable error can be introduced if other phenolic compounds are present in sample. However, it is possible to determine phenol and *o*-, *m*- and *p*-cresols accurately even at levels as low as 0.5 $\mu g\ l^{-1}$ by measuring the fluorescence of the sample. An additional advantage of the fluorescence method is that it does not require many reagents, and hence the possibility of contamination is minimized. The main disadvantage of this procedure is that it is not capable of determining chlorophenols. The u.v.–spectrophotometric method can determine phenols, cresols and polychlorinated phenols, but the limit of detection is only 5 $\mu g\ l^{-1}$ for individual phenols.

TABLE VI

COMPARISON OF VARIOUS METHODS FOR DETERMINATION OF PHENOLIC COMPOUNDS IN NATURAL WATERS

Sample composition	*Automated 4-aminoantipyrine ($\mu g\ l^{-1}$)*	*Ultraviolet ($\mu g\ l^{-1}$)*	*Fluorescence ($\mu g\ l^{-1}$)*
LW_1 (lake water)	1.2	[a]	1.6
LW_2 (lake water)	2.0	[a]	2.8
LW_3 (lake water)	4.6	[a]	7.2
LW_3 + phenol (10 p.p.b.)	14.2	10	16.8
LW_3 + *p*-cresol (10 p.p.b.)	5.0	10	17.2
LW_3 + *p*-chlorophenol (25 p.p.b.)	6.2	25	9.6
LW_3 + 2,4,6-trichlorophenol (25 p.p.b.)	4.2	30	6.8

[a] Not detected.

Table VI compares the values obtained for the analysis of lake water by the three methods. The data indicate that the fluorescence approach, for determining phenols and cresols, gives the most precise and accurate results. The ultraviolet method offers considerable promise for determining polychlorinated phenols.

The authors thank Dr. R. W. Durham and Mr. B. J. Dutka of this department for carrying out some of the experimental work and providing the necessary facilities for the tracer and microbiological investigations.

SUMMARY

A solvent extraction procedure for the separation and concentration of low levels of phenols is described. Phenols are extracted with n-butyl acetate or iso-amyl acetate from natural waters and then back-extracted with sodium hydroxide solution.

The final extract can be analyzed by the 4-aminoantipyrine, u.v. spectrophotometric and/or fluorimetric methods. These methods have been evaluated in terms of sensitivity, selectivity, precision, accuracy and ability to determine different phenolic compounds. The solvent extraction–fluorimetric method was found to be the most sensitive and accurate for the determination of phenol and cresols; the detection limit is 0.1 $\mu g\ l^{-1}$ for individual phenols. Samples were preserved by addition of hydrochloric acid and storage in glass bottles. The use of acid effectively kills bacteria which biodegrade phenols. There is no significant loss of phenols by adsorption if the samples are collected and stored in glass bottles.

REFERENCES

1 American Public Health Association, American Water Works Association and American Pollution Control Federation. *Standard methods for the Examination of Water and Wastewater*, American Public Health Association, New York, 13th edn. 1971, p. 501.
2 E. I. Mohler Jr. and L. N. Jacob, *Anal. Chem.*, 29 (1957) 1369.
3 H. O. Friestad, D. E. Ott and F. A. Gunther, *Advances in Automated Analysis, Technicon International Congress 1969*, Mediad, New York, 1970, p. 21.
4 Z. Regnier and A. E. P. Watson, *Water Quality Division Research Report*, Department of the Environment, Ottawa, 1971.
5 M. J. Murray, *Anal. Chem.*, 21 (1949) 941.
6 J. M. Carter and G. Nickless, *Analyst (London)*, 95 (1970) 148.
7 R. Fox, R. Keller, C. Pinamont and J. Severson, *Ind. Water Eng.*, 3 (1970) 36.
8 N. Myrick, A. W. Busch and D. S. Dawkins, *Province of Ontario Ind. Waste Conf.*, 10 (1963) 193.
9 M. Massin and B. Lindenberg, *Bull. Soc. Chim. Fr.*, 1 (1964) 33.
10 F. X. Pollio and R. Kunin, *Environ. Sci. Technol.*, 1 (1967) 160.
11 J. Sherma and Wm. Rieman III, *Anal. Chim. Acta*, 18 (1958) 214.
12 M. V. Ramanayao, U. S. Telkikar and A. Hussain, *Indian J. Technol.*, 5 (1967) 343.
13 L. J. Schmauch and H. M. Grubb, *Anal. Chem.*, 26 (1954) 308.
14 M. J. Murray, *Anal. Chem.*, 21 (1949) 941.
15 V. T. Kaplin and N. G. Frenko, *Gig. Sanit.*, 26 (1961) 68.
16 F. K. West and P. W. West, *Anal. Chem.*, 38 (1966) 1566.
17 G. G. Fichnolz, A. E. Nagel and R. H. Hughes, *Anal. Chem.*, 37 (1965) 863.

Analytica Chimica Acta, 71 (1974) 367–374

THE DETERMINATION OF MICRO AMOUNTS OF POLYTHIONATES

PART VIII.* CYANOLYSIS OF TRITHIONATE BY CATALYSIS WITH LANTHANUM(III) AND PHOTOMETRIC DETERMINATION OF TRITHIONATE

TOMOZO KOH, AKIRA WAGAI and YASUYUKI MIURA
Department of Chemistry, Faculty of Science, Tokai University, Hiratsuka, Kanagawa (Japan)
(Received 9th October 1973)

Rapid and accurate determinations of polythionates are desirable for studies of sulfur chemistry. In previous papers[1–3] of this series, the reaction of polythionates (tetra-, penta- and hexathionate) with cyanide has been described in detail, and methods for the determination of the polythionate when tetra-, penta- or hexathionate alone is present, have been presented. It has been possible to increase the sensitivity by approximately sixty-fold for the determination of polythionates, by extracting an ion-pair between the cation of methylene blue and the anion of thiocyanate formed from the polythionates with an organic solvent[4]. However, no similar consideration has been given to the determination of trithionate because the cyanolysis of trithionate is a much slower reaction, as has been pointed out by Kurtenacker[5].

Urban[6] and Kelly *et al.*[7] have presented photometric methods for determining trithionate. Urban's method has the disadvantage of requiring 16 h for cyanolysis of trithionate; even then, cyanolysis is not quantitative. Under the conditions employed by Kelly *et al.*, only some 87% of the trithionate was converted to thiocyanate and the rest to thiosulfate. Accordingly, their methods are laborious and time-consuming, and cannot be accurate. Therefore, a catalyst for the cyanolysis of trithionate was sought for a rapid and accurate determination of trithionate; lanthanum(III) has been found to have a catalytic effect on the conversion of trithionate to thiocyanate. The present paper is concerned with the determination of trithionate; the method is based on the formation of thiocyanate from trithionate in the presence of lanthanum(III) by the following reaction

$$S_3O_6^{2-} + 3\ CN^- + H_2O = SO_3^{2-} + SO_4^{2-} + 2\ HCN + SCN^- \qquad (1)$$

and on the photometric measurement of the thiocyanate thus formed with iron(III). The proposed method appears to be much more rapid and accurate than any previous method for trithionate.

---

* Part VII: T. Koh and K. Taniguchi, *Anal. Chem.*, 45 (1973) 2018.

EXPERIMENTAL

Apparatus

Photometric measurements were made with a Hirama Model II-B photometer with a 460-nm filter (maximum transmission at 460 nm) and 10.0-mm glass cells. pH measurements were made with a Hitachi–Horiba Model M-5 pH meter. Temperatures below room temperature were controlled by a Tajiri Model ECW-6WE electronic thermostat, and those above room temperature, by a Taiyo Model M-1 thermostat. Volumetric flasks of 25.0-ml were coated with black paint, except for small vertical areas on opposite sides near the top graduation.

Potassium trithionate

Potassium trithionate was prepared as described by Stamm *et al.*[8]. The trithionate so obtained was recrystallized with redistilled water at a temperature below 35 °C, and then dried in a desiccator containing, concentrated sulfuric acid at room temperature, before storage at -10 ± 2°C. The water physically adsorbed on the trithionate was estimated to be 0.14% by the Karl Fischer method.

Purity of potassium trithionate. The purity of this salt was estimated by determining its total potassium and sulfur contents as follows[9]. The trithionate was decomposed to potassium sulfate by heating it to about 800°C; $K_2S_3O_6 \rightarrow K_2SO_4$. The potassium was determined by weighing the potassium sulfate thus formed. To determine sulfur, the trithionate was oxidized to sulfate by bromine in an alkaline medium on heating. The total sulfur was determined by the usual gravimetric method for sulfate. The results listed in Table I confirm that the potassium trithionate was pure enough for the present purpose.

TABLE I

DETERMINATION OF POTASSIUM AND SULFUR FOR THE POTASSIUM TRITHIONATE[a] USED IN THE PRESENT STUDY

Taken (mg)	*As $K_2S_3O_6$ (mg)*	*Found as K_2SO_4 or $BaSO_4$ (mg)*	*Element found for $K_2S_3O_6$ (%)*	*Element calcd. for $K_2S_3O_6$ (%)*
Potassium				
265.3	264.9	170.2	28.84	28.92
232.8	232.5	149.3	28.82	
Sulfur				
139.3	139.1	358.4	35.39	35.57
108.7	108.6	279.9	35.41	

[a] Water content was estimated to be 0.14%.

Chemicals

All other chemicals were of analytical grade and were used without further purification. All solutions were prepared with redistilled water.

Standard trithionate solution, $1.0\cdot10^{-3}$ M. Dissolve 135.4 mg of the potassium trithionate (water content 0.14%) in water, and dilute to 500 ml. This solution proved to be stable; when it was stored at 5 ± 2°C, no measurable change was

found by the present method even after 6 weeks. Prepare working solutions by appropriate dilution.

Standard thiocyanate solution. Standardize a thiocyanate solution by Volhard's method. Prepare working solutions by suitable dilution. These standards were used to ascertain whether or not the reaction of trithionate with cyanide went to completion and was stoichiometric.

Perchloric acid solution of iron(III) nitrate. Dissolve 303.0 g of iron(III) nitrate nonahydrate in a small volume of water containing 217.4 ml of 60% perchloric acid, and dilute to 500 ml to give a 1.5 *M* iron(III) nitrate solution in 4 *M* perchloric acid.

Recommended procedure

Add 0.5 ml of 3 *M* lanthanum nitrate, 1.0 ml of 1 *M* acetic acid, and then 10.0 ml of sample solution containing trithionate, to a 25.0-ml volumetric flask. Place the flask in a thermostat at 10°C. To this mixture, add 3.0 ml of 3 *M* sodium cyanide solution previously maintained at 10°C. The pH of the solution is thereby brought to 9.1. Keep the flask at 10 °C for 20 min, to convert the trithionate quantitatively to thiocyanate. Then, add 2.0 ml of 60% perchloric acid and 3.0 ml of 1.5 *M* iron(III) nitrate in 4 *M* perchloric acid, and fill the flask to the mark with redistilled water. Mix the contents well, and measure the absorbance of the clear solution of the iron–thiocyanate complex, thus formed, against distilled water at 460 nm.

RESULTS AND DISCUSSION

Calibration plots

A series of standard solutions containing various amounts of thiocyanate and trithionate were treated as described in the procedure. The resulting graphs (reagent blank subtracted) showed that Beer's law was obeyed for both thiocyanate and trithionate over the range $0.1–6 \cdot 10^{-4}$ *M*. According to eqn. (1), when one mole of trithionate undergoes cyanolysis, one mole of thiocyanate is formed. Therefore, if the trithionate is pure enough and converted to thiocyanate stoichiometrically and completely, the calibration graph of trithionate should coincide with that of thiocyanate when plotted as molar concentrations. In fact, the calibration graph for trithionate coincided exactly with that for thiocyanate, demonstrating that the cyanolysis of trithionate went to stoichiometric completion.

Effect of temperature

Before the effect of temperature on the cyanolysis was investigated, the stability of trithionate solution against temperature was studied. The trithionate solution was allowed to stand for 30 min at a temperature in the range from room temperature to 40°C, and then treated as in *Recommended procedure*. The results are given in Table II; it was confirmed that trithionate does not undergo thermal decomposition on standing for 30 min at temperatures below 35°C.

In order to study the effect of temperature on the cyanolysis of trithionate in the presence of lanthanum(III) ions, the reaction was carried out for 20 min at various temperatures ranging from 5 to 40°C. The results listed in Table III

TABLE II

THE STABILITY OF TRITHIONATE SOLUTION[a] AT DIFFERENT TEMPERATURES

Sample	*Temp. (°C)*	*Absorbance*[b]	
		$4.0 \cdot 10^{-4}$ *M*	$6.0 \cdot 10^{-4}$ *M*
SCN^-	5–40	0.727	1.091
$S_3O_6^{2-}$	Room temp.	0.728	1.091
$S_3O_6^{2-}$	30	0.729	1.090
$S_3O_6^{2-}$	35	0.721	1.080
$S_3O_6^{2-}$	40	0.632	0.971

[a] Trithionate solution was allowed to stand for 30 min.
[b] Reagent blank was subtracted.

TABLE III

EFFECT OF TEMPERATURE ON THE CYANOLYSIS OF TRITHIONATE IN THE PRESENCE OF LANTHANUM(III) IONS

Sample	*Temp. (°C)*	*Absorbance*[a]	
		$4.0 \cdot 10^{-4}$ *M*	$6.0 \cdot 10^{-4}$ *M*
SCN^-	5–40	0.727	1.091
$S_3O_6^{2-}$	5	0.727	1.090
$S_3O_6^{2-}$	10	0.728	1.091
$S_3O_6^{2-}$	15	0.722	1.082
$S_3O_6^{2-}$	20	0.720	1.077
$S_3O_6^{2-}$	30	0.712	1.076
$S_3O_6^{2-}$	40	0.700	1.065

[a] Reagent blank was subtracted.

show that cyanolysis above 20°C gave lower absorbances than those of thiocyanate. However, trithionate below 15°C gave the same absorbances as those of thiocyanate, the cyanolysis being quantitative. The lower absorbances above 20°C were thought to be caused by the fact that the reaction is exothermic. Therefore, it was concluded that the reaction must be carried out below 15°C; the temperature was fixed at 10°C in the present work.

Effect of pH

Figure 1 shows the rate of cyanolysis of trithionate at 10°C for various pH values. The maximal absorbance corresponding to complete and stoichiometric reaction of trithionate was attained in 15 h at pH 8.1, 1 h at pH 8.5, 15 min at pH 9.0, and 5 min at pH 9.1 respectively. The reaction was then carried out for 20 min at 10°C for various pH values. The results summarized in Fig. 2 show that complete and stoichiometric cyanolysis occurred over the pH range 9.0–9.3. The decrease in absorbance at the lower pH values could be attributed to

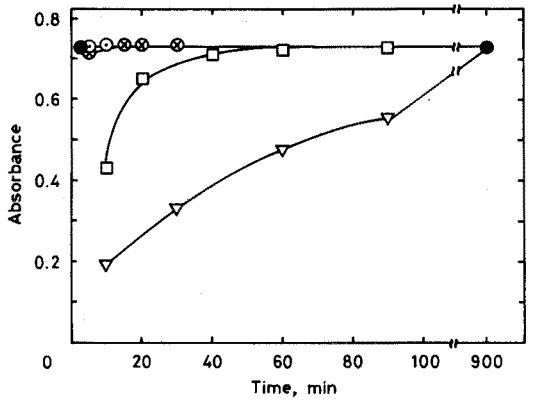

Fig. 1. Rate of cyanolysis of trithionate at 10°C (reagent blank subtracted). Concentration of trithionate was $4.0 \cdot 10^{-4}$ *M*. (●) $4.0 \cdot 10^{-4}$ *M* SCN^-; (⊙) pH 9.1; (⊗) pH 9.0; (□) pH 8.5; (▽) pH 8.1.

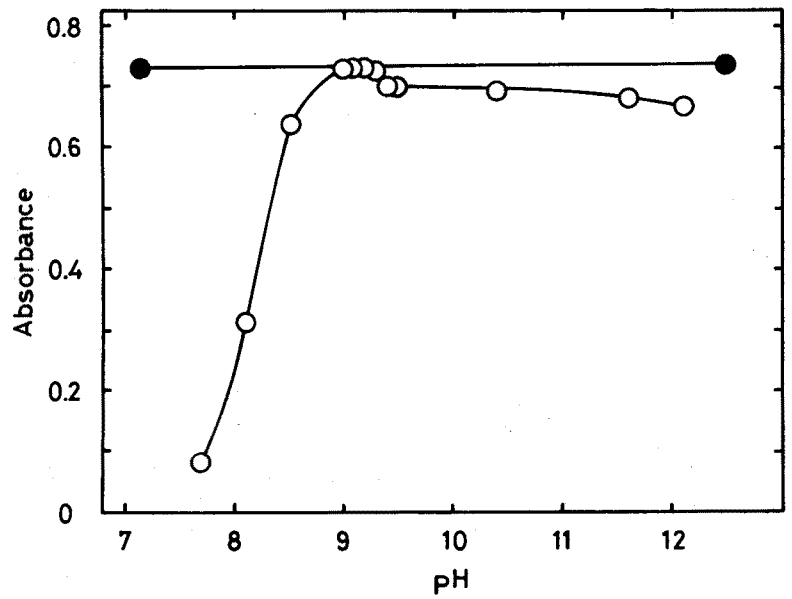

Fig. 2. Effect of pH on the cyanolysis of trithionate (reagent blank subtracted). (●) $4.0 \cdot 10^{-4}$ *M* SCN^-; (○) $4.0 \cdot 10^{-4}$ *M* $S_3O_6^{2-}$.

a decrease in the rate of cyanolysis because of a decrease in the concentration of cyanide ion by lowering the pH. Consequently, the optimal pH range can be extended from 9.0 to a lower pH by making the cyanolysis time longer. In order to investigate the decrease in absorbance at the higher pH values, trithionate solution was allowed to stand for 10 min at 10°C and pH 11.6, and then treated as described in the procedure, where the reaction solution was buffered to the optimal pH range, 9.0–9.3. The experiment showed that trithionate does not undergo any alkaline decomposition on standing at pH 11.6. Accordingly, the incomplete cyanolysis at the higher pH levels appears to be caused by a decrease in the catalytic action of lanthanum(III).

Effect of amount of sodium cyanide

In measuring the effect of the amount of sodium cyanide on the conversion of trithionate to thiocyanate, various amounts of sodium cyanide were employed; in all cases the solutions were buffered to pH 9.0–9.3. The effects are shown in Fig. 3. Cyanolysis of the trithionate was not stoichiometric with 3.0 ml of 0.1, 1, or

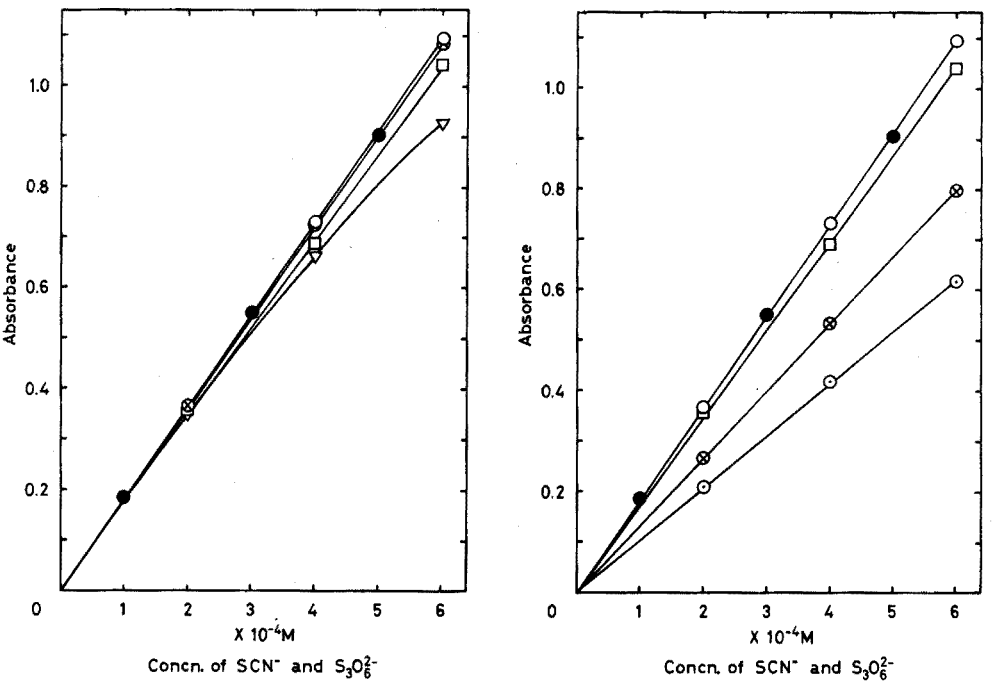

Fig. 3. Effect of amount of sodium cyanide on the cyanolysis of trithionate (reagent blank subtracted). All other conditions are as in the procedure. (●) SCN^-; (○) $S_3O_6^{2-}$ with 2.0, 3.0 and 4.0 ml of 3 *M* NaCN; (⊗) $S_3O_6^{2-}$ with 3.0 ml of 2 *M* NaCN; (□) $S_3O_6^{2-}$ with 3.0 ml of 1 *M* NaCN; (▽) $S_3O_6^{2-}$ with 3.0 ml of 0.1 *M* NaCN.

Fig. 4. Effect of amount of lanthanum nitrate on the cyanolysis of trithionate (reagent blank subtracted). All other conditions are as in the procedure. (●) SCN^-; (○) $S_3O_6^{2-}$ with 0.5, 1.0 and 1.5 ml of 3 *M* La(III); (□) $S_3O_6^{2-}$ with 0.5 ml of 2 *M* La(III); (⊗) $S_3O_6^{2-}$ with 0.5 ml of 1 *M* La(III); (⊙) $S_3O_6^{2-}$ with 0.5 ml of 0.1 *M* La(III).

2 *M* cyanide solutions; but when 2.0, 3.0, and 4.0 ml of 3 *M* cyanide were used, the calibration graph of trithionate coincided exactly with that of standard thiocyanate. When 4.5 ml of 2 *M* cyanide and 6.0 ml of 1.5 *M* cyanide were employed, although the absolute amount of the cyanide was equal to 3.0 ml of 3 *M* cyanide, that is, 9.0 mmol, the absorbance obtained for trithionate did not accord with that of standard thiocyanate. From these results, it was concluded that the concentration of cyanide solution added has to be higher than 3 *M* for stoichiometric cyanolysis of the trithionate. On employing 3 *M* cyanide, 2.0 ml was sufficient for the complete cyanolysis. Therefore, 3.0 ml of 3 *M* sodium cyanide was employed in the recommended procedure.

Effect of amount of lanthanum nitrate

It is obvious that the cyanolysis of trithionate may be affected by the amount of lanthanum(III) used as a catalyst. In order to establish the optimal quantity, different amounts of lanthanum nitrate were employed; in all cases the solutions were buffered to pH 9.0–9.3. Figure 4 shows that the cyanolysis of trithionate with 0.5 ml of 0.1, 1, and 2 *M* lanthanum was incomplete, because of an insufficient amount of lanthanum, but 0.5 ml of 3 *M* lanthanum nitrate was sufficient for complete cyanolysis. When 3.0 ml of 0.5 *M*, 1.5 ml of 1 *M*, and 0.75 ml of 2 *M* lanthanum were used, the results were the same as those obtained with 0.5 ml of

TABLE IV

EFFECT OF FOREIGN IONS

Ion	*Added as*	*Concn. (p.p.m.)*	*Absorbance*	
			Reagent blank	$4.0 \cdot 10^{-4}$ *M* $S_3O_6^{2-}$
None			0.016	0.742
NH_4^+	$(NH_4)_2SO_4$	1000	0.018	0.747
K^+	K_2SO_4	1000	0.018	0.747
Na^+	Na_2SO_4	1000	0.018	0.747
Mg^{2+}	$MgSO_4 \cdot 7\ H_2O$	1000	0.019	0.747
Al^{3+}	$Al_2(SO_4)_3 \cdot 18\ H_2O$	1000	0.018	0.747
Ca^{2+}	$CaCO_3$	500	0.018	0.740
Zn^{2+}	$ZnSO_4 \cdot 7\ H_2O$	100	0.016	0.740
Mn^{2+}	$MnSO_4 \cdot H_2O$	50	0.019	0.697
Pb^{2+}	$Pb(CH_3COO)_2 \cdot 3\ H_2O$	100	0.018	0.733
NO_3^-	KNO_3	1000	0.017	0.740
F^-	NaF	100	0.017	0.740
		1000	0.016	0.717
Cl^-	NaCl	100	0.018	0.742
		1000	0.024	0.733
Br^-	KBr	100	0.028	0.755
		1000	0.147	0.854
I^-	KI	100	0.018	0.745
		1000	0.076	0.745
Borate ion	H_3BO_3	1000	0.018	0.738
Silicate ion	(as SiO_2)	1000	0.021	0.757
SO_4^{2-}	Na_2SO_4	1000	0.018	0.747
SO_3^{2-}	$Na_2SO_3 \cdot 7\ H_2O$	100	0.019	0.740
$S_2O_3^{2-}$	$Na_2S_2O_3 \cdot 5\ H_2O$	1	0.024	0.752
		10	0.102	0.830
S^{2-}	$Na_2S \cdot 9\ H_2O$	1	0.017	0.755
		10	0.021	0.785
		100	0.091	0.872
$S_4O_6^{2-}$	$K_2S_4O_6$	1	0.032	0.760
$S_5O_6^{2-}$	$K_2S_5O_6$	1	0.038	0.762
$S_6O_6^{2-}$	$K_2S_6O_6$	1	0.043	0.767

3 *M* lanthanum. This experiment indicates that the cyanolysis of trithionate goes readily to completion, as long as the absolute amount of lanthanum is sufficient, regardless of the initial concentration of the lanthanum(III) solution. In the present procedure, 0.5 ml of 3 *M* lanthanum nitrate was used.

Effect of foreign ions

Solutions containing various amounts of the ions in question, both in the presence of $4.0 \cdot 10^{-4}$ *M* trithionate and in its absence, were treated exactly as in the recommended procedure. The results are given in Table IV. Thiosulfate interferes seriously, even when present in amount of 10 p.p.m., because of its conversion to thiocyanate. The interference of sulfide seems to be caused by the formation of both thiocyanate and thiosulfate, as a result of its reaction with cyanide and trithionate. Polythionates interfere even when present in amount of 1 p.p.m., for they are converted to thiocyanate by cyanolysis.

SUMMARY

Lanthanum(III) has been found to catalyze the reaction of trithionate with cyanide. A rapid and accurate determination of trithionate is proposed. The method is based on the formation of thiocyanate equivalent to trithionate, and on the photometric determination of the thiocyanate with iron(III). The factors affecting cyanolysis of trithionate in the presence of lanthanum(III), such as amounts of cyanide and lanthanum, pH, and reaction time and temperature, were examined in order to establish the conditions under which trithionate is converted stoichiometrically to thiocyanate. Beer's law is obeyed in the range $0.1\text{–}6 \cdot 10^{-4}$ *M* trithionate. Complete cyanolysis is obtained in 20 min at 10°C over the pH range 9.0–9.3. The only serious interferences are thiosulfate, sulfide and other polythionates.

REFERENCES

1 T. Koh, *Bull. Chem. Soc. Japan*, 38 (1965) 1510.
2 T. Koh and I. Iwasaki, *Bull. Chem. Soc. Japan*, 38 (1965) 2135.
3 T. Koh and I. Iwasaki, *Bull. Chem. Soc. Japan*, 39 (1966) 352.
4 T. Koh, N. Saito and I. Iwasaki, *Anal. Chim. Acta*, 61 (1972) 449.
5 A. Kurtenacker, *Analytische Chemie der Sauerstoffsäuren des Schwefels*, Ferdinand Enke Verlag, Stuttgart, 1938.
6 P. J. Urban, *Z. Anal. Chem.*, 179 (1961) 422.
7 D. P. Kelly, L. A. Chambers and P. A. Trudinger, *Anal. Chem.*, 41 (1969) 898.
8 H. Stamm, M. Goehring and U. Feldmann, *Z. Anorg. Allgem. Chem.*, 250 (1942) 226.
9 F. Martin and L. Metz, *Z. Anorg. Allgem. Chem.*, 127 (1923) 83.

Analytica Chimica Acta, 71 (1974) 375–381

ION-EXCHANGE SEPARATION AND SPECTROPHOTOMETRIC DETERMINATION OF ZIRCONIUM, THORIUM AND URANIUM IN SILICATE ROCKS WITH ARSENAZO III

TETSUYA KIRIYAMA

Laboratory for Chemistry, Faculty of Education, Kagoshima University, Kagoshima (Japan)

ROKURO KURODA

Laboratory for Analytical Chemistry, Faculty of Engineering, University of Chiba, Yayoi-cho, Chiba (Japan)

(Received 28th November 1973)

Arsenazo III (2,2′-[1,8-dihydroxy-3,6-disulpho-2,7-naphthylenebis(azo)]dibenzenearsonic acid) is an extremely sensitive colorimetric reagent for zirconium, thorium and uranium[1]. Onishi and Sekine[2] have developed a method for the spectrophotometric determination of microamounts of zirconium, uranium(VI), thorium and the rare earths with arsenazo III, after consecutive extractive separation, with thenoyltrifluoroacetone and tri-n-octylamine. The method described is generally useful, but further investigation is necessary, if the method is applied to the simultaneous determination of zirconium, uranium and thorium in complicated matrices such as silicate rocks.

The adsorption behavior of a number of metals on Dowex 1 in acidic sulfate media has been studied, and an anion-exchange chromatographic method has been developed for the consecutive separation of the rare earths, scandium, thorium, zirconium and uranium[3]. The method was used successfully for the determination of scandium in standard rocks (G-1 and W-1), ores and stony meteorites by neutron activation analysis with radiochemical separations[4]. Shimizu and Momo[5,6] also developed a combined ion-exchange–photometric method for the determination of scandium in silicate rocks using this chromatographic method for the isolation and purification of scandium.

The present investigation concerns the development of a highly sensitive spectrophotometric method with arsenazo III for the determination of zirconium, thorium and uranium in silicate rocks, coupled with the anion-exchange chromatographic separation in sulfate media. Spectrophotometric determinations of thorium[7–9] and uranium[10] with arsenazo III in silicate rocks and materials of geochemical interest, have already been reported individually. The present method allows the three metals in silicate rocks to be determined simultaneously on only 1 g of sample.

EXPERIMENTAL

Reagent and apparatus

Stock solutions. For zirconium and thorium solutions. dissolve an appropriate

amount of $Zr(SO_4)_2 \cdot 4\ H_2O$ or $Th(SO_4)_2 \cdot 9\ H_2O$ in 1.5 or 0.1 *M* sulfuric acid, respectively, to yield *ca.* 10 mg metal per ml. The zirconium solution was standardized by backtitration with bismuth(III) in excess of EDTA, with xylenol orange as indicator. The thorium solution was standardized by titration with EDTA, with xylenol orange indicator.

For the uranium(VI) solution, evaporate an appropriate amount of $UO_2(NO_3)_2 \cdot 6\,H_2O$ with sulfuric acid to fumes, and then dilute with distilled water to yield *ca.* 10 mg U(VI) per ml of 0.15 *M* sulfuric acid. This solution was standardized by back-titration with thorium in excess of EDTA, with xylenol orange indicator.

Ion-exchange columns

Column A. Dowex 1–X8, in the sulfate form (100–200 mesh) was used. Dried resin (air-dried and stored in a desiccator over saturated potassium bromide solution) weighing 10.0 g was slurried with water and poured into a conventional glass column (i.d. 1.0 cm) drawn to a tip and plugged with glass wool at the outlet. The resulting bed was 25 cm long. Before use the column should be conditioned with a sufficient volume of 0.025 *M* sulfuric acid–0.1 *M* ammonium sulfate solution.

Column B. Dowex 1–X8, in the chloride form (100–200 mesh) was used. Air-dried resin (1.0 g) was slurried with distilled water and poured in a conventional column (i.d. 1.0 cm, 10 cm long). Before use, the column was conditioned with 20 ml of 6 *M* hydrochloric acid. The bed was 2.5 cm long.

The other reagents and chemicals used were of analytical grade unless otherwise mentioned.

Spectrophotometric measurements were made with a Hitachi 101 Spectrophotometer in 1-cm glass cells.

Dissolution and chromatographic separation

Place a powdered rock sample, weighing about 1 g, into a platinum dish and moisten with 5 ml of distilled water. Add 2 ml of perchloric acid and 5 ml of hydrofluoric acid, heat gently and evaporate. Complete the decomposition by addition of 1-ml portions of hydrofluoric acid. Finally, expel perchloric acid. Moisten the residue with 1 ml of perchloric acid and again evaporate to dryness. Dissolve the residue in 10 ml of 6 *M* hydrochloric acid, and dilute to 100 ml with distilled water. Heat gently and add (1+1) ammonia in a slight excess to precipitate hydroxides. Digest for a short time on a steam bath. Filter the precipitate through a coarse filter paper and wash with 2% ammonium chloride solution. Dissolve the precipitate in 30 ml of 6 *M* hydrochloric acid and evaporate to dryness, after the addition of 5 ml of 6 *M* sulfuric acid. Dissolve this residue in a mixture of 0.5 ml of 5 *M* sulfuric acid and 10 ml of distilled water, by gentle heating. If any residue remains, filter and fuse with 200 mg of sodium carbonate. Reserve the filtrate. Dissolve the melt with 2 ml of 6 *M* sulfuric acid and evaporate to dryness along with 2 ml of hydrofluoric acid. Take up the residue in 10 ml of distilled water containing 0.5 ml of 5 *M* sulfuric acid, heat and maintain the solution just under boiling for about 30 min. Add 100 ml of distilled water and warm to get a clear solution. Cool. Add 10 ml of 30-vol% hydrogen peroxide. Combine with the filtrate above and dilute to 200 ml with distilled water. Pass the solution down column A. Wash the column with 100 ml of 0.025 *M* sulfuric acid–0.1 *M* ammonium sulfate, which contains 5 ml of

hydrogen peroxide. Discard all the effluents. Remove thorium by elution with 100 ml of 0.025 *M* sulfuric acid–1.0 *M* ammonium sulfate. Strip the zirconium by elution with *ca.* 50 ml of 4 *M* hydrochloric acid. Finally elute uranium with 30 ml of 1 *M* perchloric acid.

Photometric determinations with arsenazo III

Thorium. Add 1.0 ml of an iron(III) chloride solution (*ca.* 6 mg Fe(III) ml^{-1} in 0.1 *M* HCl) to the sulfate effluent, heat and precipitate iron(III) hydroxide with (1 + 1) ammonia. Filter the precipitate and wash with 2% ammonium chloride solution. Dissolve the precipitate in a small volume of 6 *M* hydrochloric acid and evaporate to dryness. Take up the residue in 5 ml of 6 *M* hydrochloric acid and pass through the column B. Wash the column with the same acid. Collect all the effluents and evaporate to dryness. Transfer the residue to a 25-ml volumetric flask with the aid of 18.5 ml of hydrochloric acid. Add 1 ml of freshly prepared 1% (w/v) gelatin solution and 1.0 ml of aqueous 0.1% (w/v) arsenazo III solution, and dilute to the mark with distilled water. Measure the absorbance at 665 nm with a reference of distilled water.

Zirconium. Place an aliquot of the effluent into a 25-ml volumetric flask. Add 18.5 ml of hydrochloric acid, 1 ml of the above gelatin solution and 1.0 ml of the above arsenazo III solution. Dilute to the mark with distilled water. Measure the absorbance at 665 nm against distilled water as reference.

Uranium. Evaporate the effluent to dryness. Add to the residue 1 ml of perchloric acid and a few ml of nitric acid, and evaporate to dryness. Take up the residue with 5 ml of 8 *M* hydrochloric acid, add 0.7 g of metallic zinc and let stand for 15 min. Transfer to a 25-ml volumetric flask with the aid of 14 ml of an oxalic acid solution (7 *M* hydrochloric acid saturated with oxalic acid). Add 1.0 ml of the arsenazo III solution and dilute to the mark. Measure the absorbance at 665 nm against distilled water.

RESULTS AND DISCUSSION

Comparatively few metal ions can be adsorbed on a strongly basic anion-exchange resin from sulfuric acid media[3,11,12]. The metals most strongly adsorbed are the transition metals of the 4th, 5th and 6th groups of the periodic table. Uranium(VI) is also adsorbed very strongly, but the distribution coefficient of thorium is much smaller. At first, an attempt was made to collect zirconium, thorium and uranium directly on a resin column from the dilute sulfuric acid solutions which resulted from the decomposition of rock samples. However, the recovery of thorium was low, ranging from 10 to 50%. It was therefore necessary to separate the three metals from the majority of the major components of rocks, which inevitably increases the sulfate concentration, thus causing the incomplete recovery of thorium. Zirconium, thorium and uranium were therefore concentrated as hydroxides by precipitation with ammonia, and the hydroxides were dissolved in sulfuric acid to yield a 0.025 *M* acid solution. In this medium, the distribution coefficients for zirconium, thorium and uranium(VI) on Bio-Rad AG1–X8 are $>10^3$, 60 and 800 (interpolated values), respectively, decreasing rapidly with increasing concentration of sulfuric acid[12]. Most other metals present in rocks, including beryllium, the

alkaline earths, the rare earths, titanium(IV), vanadium(IV), manganese(II), iron(III), cobalt(II), nickel(II), copper(II), zinc, cadmium, aluminum, gallium, germanium(IV), *etc.*, do not adsorb on strongly basic resin from sulfate media[1,2].

Thorium, zirconium and uranium(VI), thus retained, can be chromatographed effectively by elution with 0.025 *M* sulfuric acid–1 *M* ammonium sulfate, 4 *M* hydrochloric acid and 1 *M* perchloric acid, respectively[3]. This chromatographic separation provides sufficiently pure fractions of thorium, zirconium and uranium(VI) to allow direct determinations with arsenazo III, which reacts with all three metals in concentrated hydrochloric acid, providing highly sensitive determinations.

Because of the inconveniently large volume of the thorium fraction, thorium must be recovered initially from the sulfate effluent by coprecipitation with iron(III) hydroxide. The separation of thorium and iron(III) can easily be accomplished by column B; iron(III) is adsorbed, while thorium comes through, being concentrated in a moderate volume of 6 *M* hydrochloric acid.

In order to establish the effectiveness of the separation of thorium, zirconium and uranium(VI) from each other, as well as from common rock matrices, a mock solution containing sodium, potassium, magnesium, calcium, aluminum, titanium(IV) and iron(III) was prepared, to which known amounts of thorium, zirconium and uranium(VI) were added; this was analyzed by the above procedure. The composition of the mock solution was made up to resemble that of the Japanese geochemical standard basalt[13]. Results obtained are quoted in Table I, where the results for simple mixtures of the three metals are also given. The amounts of matrix metals listed are those equivalent to 1 g of the standard basalt, and were contained in 100 ml of 6 *M* hydrochloric acid solution. The mock solutions were processed by the above procedure, starting from the ammonia precipitation. As can be judged from the standard deviations given, thorium, zirconium and

TABLE I

ANION-EXCHANGE SEPARATION OF THORIUM, ZIRCONIUM AND URANIUM(VI)

Run	*Added (μg)*			*Found (μg)*		
	Th	*Zr*	*U(VI)*	*Th*	*Zr*	*U(VI)*
1	61.5	101	108	61.1	98.5	109
2	61.5	101	108	60.3	92.9	101
3	61.5	101	108	60.0	100	100
4	6.15	101	108	6.45	101	108
5	61.5	101	10.8	60.0	99.8	10.7
6[a]	61.5	101	108	60.9	94.4	106
7[a]	61.5	101	108	58.4	94.9	109
8[a]	61.5	101	108	59.0	94.7	105
9[a]	61.5	101	108	63.3	97.3	112
				Av. 60.4[b] ±1.5	Av. 97.1 ±2.9	Av. 106[c] ±4

[a] To these mixtures were added 22.7 mg Na, 20.0 mg K, 54.2 mg Ca, 45.3 mg Mg, 68.7 mg Al, 72.2 mg Fe(III) and 8.3 mg Ti(IV).

[b] Calculated with omission of run 4.

[c] Calculated with omission of run 5.

uranium(VI) were effectively separated from one another, as well as from the matrix metals. Among the latter, calcium, titanium(IV) and iron(III) interfere in the determination with arsenazo III.

The results of repeated determinations of thorium, zirconium and uranium in three representative types of igneous rocks are shown in Table II. Known amounts of thorium, zirconium and uranium(VI) were added to each analyzed sample and overall recoveries were obtained. The averages and errors (standard deviation) are based on all determinations, including the addition tests. In general, overall precisions are satisfactory, the relative error being 6.9–8.0% for thorium, 1.6–4.4% for zirconium, and 5.4–10.1% for uranium.

TABLE II

DETERMINATION OF THORIUM, ZIRCONIUM AND URANIUM IN TYPICAL IGNEOUS ROCKS

Rock (location)	*Added (μg)*			*Found (μg)*			*Content in original rock (p.p.m.)*		
	Th	*Zr*	*U*	*Th*	*Zr*	*U*	*Th*	*Zr*	*U*
Basalt (Tanega-shima)				21.5	288	1.97	21.2	284	1.94
				19.7	282	1.73	19.7	282	1.73
				18.5	302	1.94	18.5	302	1.94
	12.3	202	2.12	29.4	488	4.32	17.1	286	2.16
	24.6	404	4.32	43.7	680	5.99	19.1	276	1.67
							Av. 19.1	286	1.89
							±1.5	±10	±0.19
Andesite (Sakura-jima)				11.3	127	1.73	11.3	127	1.73
				12.6	131	1.89	12.6	131	1.89
				11.1	131	1.89	11.1	131	1.89
	12.3	101	2.16	22.8	227	4.10	10.5	126	1.94
	24.6	202	4.32	35.1	330	6.05	10.5	128	1.73
							Av. 11.2	129	1.84
							±0.9	±2	±0.10
Granite (Yaku-shima)				12.0	133	7.02	11.9	132	6.97
				11.8	142	7.13	11.8	142	7.13
				12.3	141	8.21	12.3	141	8.20
	12.3	101	6.48	22.6	238	15.1	10.3	137	8.59
	24.6	202	13.0	36.3	330	20.1	11.7	128	7.09
							Av. 11.6	136	7.60
							±0.8	±6	±0.74

To obtain some idea about the accuracy of the present method, standard rocks of the U.S. Geological Survey and the Geological Survey of Japan were analyzed; the results are quoted in Table III. For comparison, recommended values for W-1 by Fleischer[14], averages for the new series of standard rocks, given by Flanagan[15,16], and some compiled values[13] for JG-1 and JB-1, are also listed. The present results are generally in satisfactory agreement. However, the zirconium values for JG-1 and JB-1 are too few for comparison, and there is considerable disagreement within each rock.

TABLE III

DETERMINATION OF THORIUM, ZIRCONIUM AND URANIUM IN STANDARD ROCKS

(All results as p.p.m.)

	W-1	*G-2*	*GSP-1*	*AGV-1*	*BCR-1*	*JG-1*	*JB-1*
Th	2.81	28.0	105	6.77	5.29	12.6	9.04
	2.58	27.7	95.3	6.40	5.54	13.6	9.4[d]
	2.71	24.6	92.2	7.38	4.98	13.4[d]	
	Av. 2.70	Av. 26.8	Av. 97.5	Av. 6.85	Av. 5.27		
	2.4[a]	25.2[b]	110.6[b]	6.96[b]	6.81[b]		
	2.42[c]	24.2[c]	104[c]	6.41[c]	6.0[c]		
Zr	100	312	539	263	196	103	151
	95.7	313	560	262	185	92.6	140–360[d]
	98.2	301	546	262	195	74–160[d]	
	Av. 98.0	Av. 309	Av. 548	Av. 262	Av. 192		
	100[a]	316[b]	544[b]	227[b]	185[b]		
	105[c]	300[c]	500[c]	225[c]	190[c]		
U	0.50	2.05	2.86	2.00	1.94	4.00	1.84
	0.81	2.21	2.32	2.21	2.05	4.43	1.8[d]
	1.03	1.94	2.00	1.94	1.84	3.3[d]	
	Av. 0.78	Av. 2.07	Av. 2.39	Av. 2.05	Av. 1.94		
	0.5[a]	1.99[b]	1.98[b]	1.94[b]	1.73[b]		
	0.58[c]	2.0[c]	1.96[c]	1.88[c]	1.74[c]		

[a] Recommended value[14].
[b] Average value[15].
[c] Recommended value[16].
[d] Average value or range[13].

SUMMARY

A combined chromatographic–spectrophotometric method has been developed for the simultaneous determination of thorium, zirconium and uranium in silicate rocks. After sample decomposition with a mixture of perchloric and hydrofluoric acids, the three metals are precipitated with iron(III) and aluminum hydroxides, and adsorbed by anion-exchange on a Dowex 1-column from dilute sulfuric acid containing hydrogen peroxide. The adsorbed thorium, zirconium and uranium are separated by elution with acid ammonium sulfate solution, hydrochloric acid and perchloric acid, respectively. The sorption from sulfate media and subsequent elution provide selective separation of thorium, zirconium and uranium, allowing their direct spectrophotometric determination with arsenazo III. Results on the determination of thorium, zirconium and uranium in standard rocks of the U. S. and Japan Geological Survey are quoted.

REFERENCES

1 S. B. Savvin, *Talanta*, 8 (1961) 673; 11 (1964) 1, 7.
2 H. Onishi and K. Sekine, *Talanta*, 19 (1972) 473.

3 H. Hamaguchi, A. Ohuchi, T. Shimizu, N. Onuma and R. Kuroda, *Anal. Chem.*, 36 (1964) 2304.
4 H. Hamaguchi, T. Watanabe, N. Onuma, K. Tomura and R. Kuroda, *Anal. Chim. Acta*, 33 (1965) 13.
5 T. Shimizu, *Talanta*, 14 (1967) 473.
6 T. Shimizu and E. Momo, *Anal. Chim. Acta*, 52 (1967) 146.
7 S. Abbey, *Anal. Chim. Acta*, 30 (1964) 176.
8 J. G. Sen Gupta, *Anal. Chem.*, 39 (1967) 18.
9 P. Pakalns, *Anal. Chim. Acta*, 58 (1972) 463.
10 A. A. Nemodruk and L. P. Glukhova, *Zh. Anal. Khim.*, 21 (1966) 688.
11 L. Danielsson, *Acta Chem. Scand.*, 19 (1965) 670.
12 F. W. E. Strelow and C. J. C. Bothma, *Anal. Chem.*, 39 (1967) 595.
13 A. Ando, *Geochem. J.*, 1 (1967) 155; A. Ando, H. Kurasawa, T. Ohmori and E. Takeda, *Geochim. J.*, 5 (1971) 151.
14 M. Fleischer, *Geochim. Cosmochim. Acta*, 33 (1969) 65.
15 F. Flanagan, *Geochim. Cosmochim. Acta*, 33 (1969) 81.
16 F. Flanagan, *Geochim. Cosmochim. Acta*, 37 (1973) 1189.

Analytica Chimica Acta, 71 (1974) 383–391

THE EXTRACTION OF TRACE AMOUNTS OF TUNGSTEN(VI) FROM DIFFERENT MINERAL ACID SOLUTIONS BY AMINE OXIDES

M. EJAZ

Pakistan Institute of Nuclear Science and Technology, Nilore, Rawalpindi (Pakistan)

(Received 2nd January 1974)

For the extraction of metal ions from mineral acid solutions, aliphatic and heterocyclic amine oxides have been shown as potentially good solvent extraction reagents. Kennedy and Perkins[1] studied the extraction of uranium(VI) and plutonium(IV) in alamine oxide–dibutyl carbitol systems. Torgov *et al.*[2–5] investigated the extraction of uranium(VI) with 2-alkylpyridine oxides and trioctylamine oxide. Torgov *et al.*[6] reported studies on the extraction of uranium(VI), and some other elements, from nitric acid solutions with 2-nonylpyridine oxide in benzene. Chernyak *et al.*[7,8] made observations on the extraction of niobium(V) and tantalum(V) from hydrofluoric and sulphuric acid solutions with 2-nonylpyridine oxide and oxidized mixture of tertiary amines, and Maksimović and Puzić[9] have carried out the extraction of some actinides by trilaurylamine oxide. However, data on the extraction of tungsten(VI) are few. The present study was therefore undertaken to obtain information on the extraction of trace amounts of tungsten(VI) from different mineral acid solutions by 4-(5-nonyl)pyridine oxide and trioctylamine oxide.

EXPERIMENTAL

Reagents

4-(5-Nonyl)pyridine oxide(NPyOx). This was prepared by the *N*-oxidation of 4-(5-nonyl)pyridine (K & K Labs Inc., Plainview, N.Y.) which was purified by vacuum distillation before use. Oxidation was done by the procedure of Kotlyarevskii *et al.*[10] as described below.

A drop of sulphuric acid (98%) was added to 8.45 ml of acetic anhydride and the solution thus obtained was mixed with 8.45 ml of 30% hydrogen peroxide with proper stirring and cooling so that the temperature did not exceed 18–20°C; 11.385 g of 4-(5-nonyl)pyridine were then added to the prepared solution of peracetic acid. The mixture was stirred at 70–72°C for 5 h, and acetic acid and water were then distilled out under vacuum. The residue was diluted with ether, washed with 10% sodium hydroxide until near neutralization and then equilibrated repeatedly with water. The organic layer was dried with anhydrous magnesium sulphate and subjected to vacuum distillation.

4-(5-Nonyl)pyridine N-oxide, a thick oily liquid, distils at 159°C (0.8 mm Hg) and has a density d^{20} of 0.9655 g cm^{-3} and a refractive index n_D^{20} of 1.53. Elemental analysis gave the following results: 76.1%C, 10.4%H, 6.3%N; required for $C_{14}H_{23}NO$, 76.0%C, 10.4%H, 6.3%N. Analyses were done by the University of

New South Wales. A further confirmation was obtained from the i.r. absorption band at 1240 cm^{-1} assigned to the N→O stretching vibration, characteristic of heterocyclic amine oxides[11].

Trioctylamine oxide (TOAO). This was synthesized by the N-oxidation of trioctylamine (Aldrich Chemical Co. Inc., Milwaukee) which had been purified by vacuum distillation. Oxidation was done with hydrogen peroxide[5,12] as given below.

Hydrogen peroxide (6.8 g of 50%) was added slowly to a solution of 17.6 g of trioctylamine in 150 ml of ethanol, over a period of 10–20 h. The mixture was stirred at 25°C for about 100 h. Ice-cold water (1 l) was then added and the upper layer was separated, diluted with ether and washed repeatedly with cold water. The organic layer was dried with anhydrous magnesium sulphate and TOAO was freed of unoxidized amine impurities by chromatography on an alumina column.

The absence of traces of trioctylamine in the final product was checked by thin-layer chromatography; the R_F values for TOA and TOAO in a 1:1 acetone–heptane mixture were 0.995 and 0.045, respectively. The melting point of the purified product, 48–49°C, corresponds to the literature value[5]. The infrared spectra gave an absorption band centred at 930 cm^{-1}, typical of the absorption of aliphatic amine oxides[11]. Elemental analysis gave the following results: 77.9%C, 13.9%H, 3.7%N; required for $(C_8H_{17})_3NO$, 78.0%C, 13.9%H, 3.7%N. Pure TOAO was stored in a desiccator over silica gel, and in a refrigerator when not in use.

The other chemicals used were of analytical-reagent grade.

Tracers and equipment

^{185}W and ^{187}W were used as tracers in this work. ^{185}W was obtained (Radiochemical Centre, Amersham) as a solution of sodium tungstate in sodium hydroxide; ^{187}W was obtained by neutron activation of reagent-grade tungsten trioxide in the research reactor of this Institute. A stock solution of ^{187}W-labelled

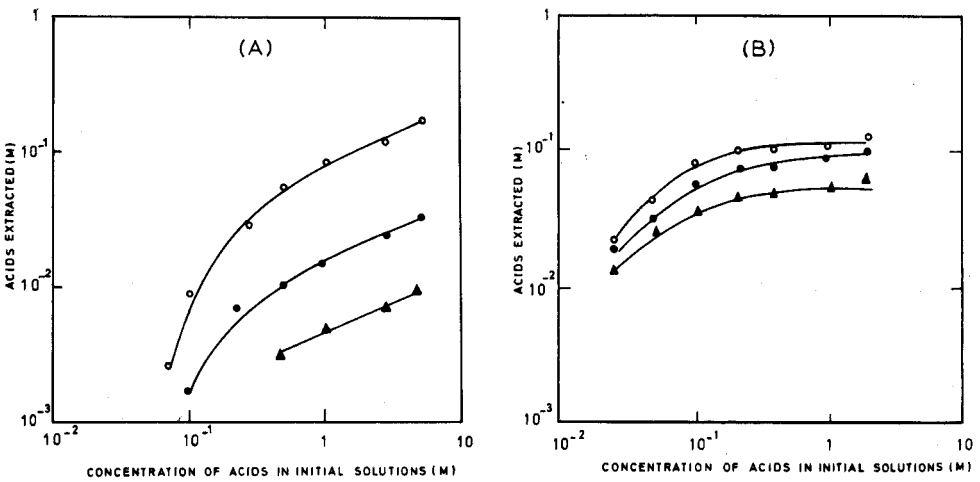

Fig. 1. Extraction of nitric (○), hydrochloric (●) and sulphuric (▲) acids by 0.1 *M* solutions of 4-(5-nonyl)pyridine oxide (A) and trioctylamine oxide (B) in xylene *vs.* acid molarity in the initial aqueous solution. Phase ratio, 1:1. Stirring time, 3 min.

tungsten(VI) was prepared by dissolving the irradiated sample in dilute ammonia solution. The tracers were taken up in different acid solutions by repeated evaporation with the corresponding acids. (The concentration of tungsten in the initial aqueous phases was less than 10^{-7} mole l^{-1}).

Solid β-emitting samples were assayed with the aid of an end-window Geiger assembly equipped with a G.E.C. tube type EGM 2/S; γ-ray count rates were determined with a Labgear type D-410S, thallium-doped sodium iodide well-type scintillation counter.

Procedure

Equal volumes of the aqueous solution containing the tracer, and the organic phase (equilibrated previously with a solution of the same composition as the aqueous phase) were stirred in a 15-ml graduated centrifuge tube with an electric stirrer for 3 min at 25°C. After equilibration, the phases were separated by centrifugation. Aliquots of equal volume were pipetted with a micropipette from the organic and aqueous phases onto stainless steel or glass planchets for β-counting. For γ-counting, the liquid samples were placed in small 5-ml bottles and counted directly in the scintillation counter.

RESULTS AND DISCUSSION

Extraction of acids

Preliminary experiments were carried out to establish the affinity of the amine oxides for mineral acids. The dependence of the extraction of nitric, hydrochloric or sulphuric acid, by 0.1 *M* solutions of 4-(5-nonyl)pyridine oxide and trioctylamine oxide in xylene, on the initial acidity of the aqueous phase, is shown in Fig. 1. The results are consistent with those reported by Torgov *et al.*[3,5]. The extraction of acids by aliphatic amine oxides has been reported by Bezinger *et al.*[13] to occur as follows:

$$2\,R_3N{\rightarrow}O + HA \rightleftharpoons \{R_3N{-}O \ldots H \ldots O{-}NR_3\}^+ A^-$$

$$\{R_3N{\rightarrow}O \ldots H \ldots O{\leftarrow}NR_3\}^+ A^- + HA \rightleftharpoons 2(R_3NOH)^+ A^-$$

The formation of such salts has also been reported[11] in the case of heterocyclic amine oxides.

Extraction of tungsten(VI) by 0.1 M 4-(5-nonyl)pyridine oxide in xylene at different acidities

The extraction of tungsten(VI) from aqueous solutions of nitric, hydrochloric and sulphuric acids with 4-(5-nonyl) pyridine oxide in xylene was examined. Figure 2 shows that tungsten(VI) is readily extracted from dilute solutions of mineral acids. From the strongly acidic solutions, tungsten(VI) is quantitatively extracted from chloride media but to a lesser extent from the nitric and sulphuric acid solutions. Paper electrophoresis experiments[14] and other techniques[15–17] have shown that tungsten(VI), in trace amounts (below $5 \cdot 10^{-5}$ *M*), exists as monomeric oxyanions in dilute acid solutions. Therefore, it can be assumed that tungsten(VI) is extracted from dilute acid solutions as the protonated oxyanion. This assumption is confirmed by the fact that other elements which form oxyanions in their highest oxidation state

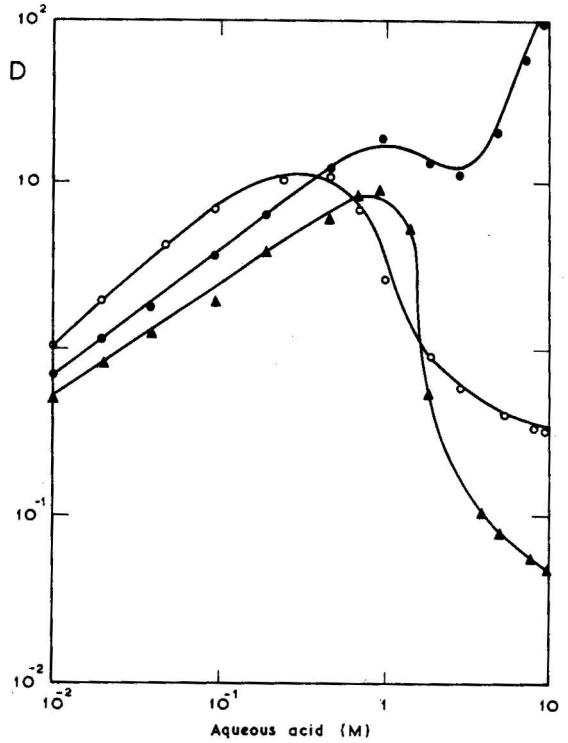

Fig. 2. Variation of distribution coefficient of tungsten(VI) with concentration of aqueous acids for extraction by 0.1 *M* 4-(5-nonyl)pyridine oxide in xylene; (○) HNO_3, (●) HCl, (▲) H_2SO_4.

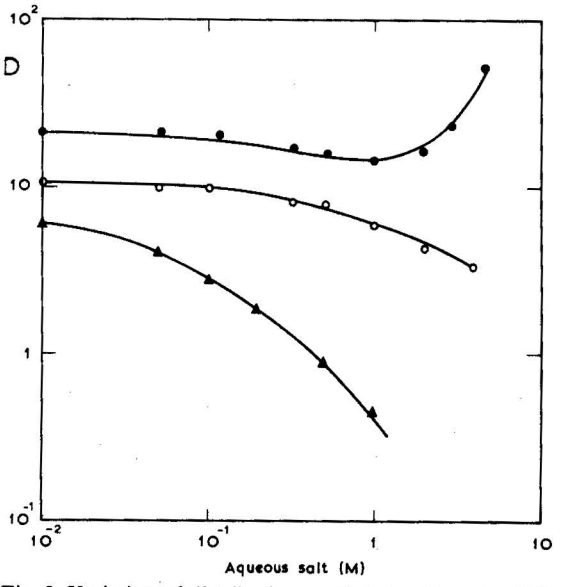

Fig. 3. Variation of distribution coefficient of tungsten(VI) with concentration of salting-out agents at constant acidity for extraction by 0.1 *M* 4-(5-nonyl)pyridine oxide in xylene; (●) NaCl in 1 *M* HCl, (○) $NaNO_3$ in 0.5 *M* HNO_3, (▲) Na_2SO_4 in 1 *M* H_2SO_4.

are extracted by oxygen-donor extractants as protonated oxyanions, *e.g.* chromium(VI) (refs. 18–22), tungsten(VI) and molybdenum(VI) (ref. 18) and rhenium(VII) and technetium(VII) (refs. 23–28). The decrease in extraction at high concentrations of nitric or sulphuric acid is probably due to the competition of the acids for the available extractant. In the case of hydrochloric acid, the extraction shows that after the first maximum at 1 *M* hydrochloric acid, the partition coefficient decreases, but then starts increasing again from 3 *M* hydrochloric acid. The fact that tungsten(VI) is extracted from concentrated solutions of hydrochloric acid but not from the other two acids suggests that tungsten(VI) is extracted as chloro complexes. The extracted complex, like the analogous tri-n-butyl phosphate system[18], may be WO_2Cl_2.

Results in Fig. 3 show that in the nitrate and sulphate media no enhancement in extraction is realized when neutral salts are added to the aqueous nitric and sulphuric acid solutions of 0.5 *M* and 1 *M*, respectively. Indeed, the degree of extraction decreases in both systems. This may be due to a shift in the equilibrium of the species, favouring the formation of unextractable complexes. The addition of chloride ions to a constant strength solution of hydrochloric acid (1 *M*) leads to a slight decrease in the distribution coefficient, up to about 1.5 *M* sodium chloride solutions. A further increase in the concentration of the added sodium chloride leads to a continuous increase in the distribution coefficient. This could be due to the formation of neutral chloro complexes of tungsten at high chloride ion concentrations.

Dependence on concentration of 4-(5-nonyl)pyridine oxide

The distribution of tungsten in relation to the concentration of NPyOx in xylene was studied at constant aqueous phase concentrations of nitric, hydrochloric and sulphuric acids. In the nitric acid system, slope analysis of the distribution data indicates that the solvation number depends on the concentration of the acid. At low acid concentration, the slope of the plot of logarithm of the distribution coefficient against the logarithm of the amine oxide concentration in the organic phase shows that the solvation number is close to 3 (Fig. 4). As the concentration in the aqueous phase is increased, the stoichiometric ratio of the components approaches unity (Fig. 5); but before this ratio is reached, the formation of a bis-solvate, as a possible intermediate of considerable stability, is possible. This indicates that when the amine oxide is reaching saturation by nitric acid, mono-solvates are formed. The formation of the lower solvates when the extractant becomes saturated with the metal oxyacid or the supporting acid or by both, has been reported by many authors[24–26]. Kertes and Beck[24] suggested that the competition between the metal oxyacid and the mineral acid, for solvation with the extractant, should be regarded as a step-by-step degradation process. The extraction of tungsten(VI) by 4-(5-nonyl)pyridine oxide can thus be represented as

$$H_2WO_4 \cdot 3(NPyOx) + HNO_3 \rightleftharpoons H_2WO_4 \cdot 2(NPyOx) + HNO_3 \cdot (NPyOx)$$

$$H_2WO_4 \cdot 2(NPyOx) + HNO_3 \rightleftharpoons H_2WO_4 \cdot (NPyOx) + HNO_3 \cdot (NPyOx)$$

$$H_2WO_4 \cdot (NPyOx) + HNO_3 \rightleftharpoons 2\,H^+ + WO_4^{2-} + HNO_3 \cdot (NPyOx)$$

The solvation number from 0.01 *M* hydrochloric and sulphuric acid solutions, as is evident from the slope of the lines relating the distribution coefficient with the amine

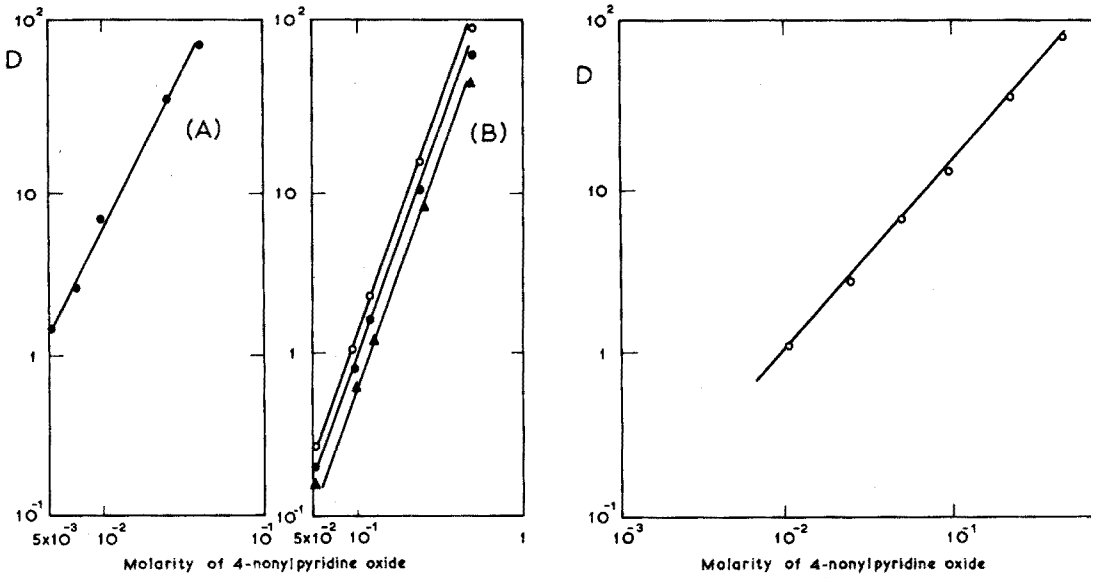

Fig. 4. Variation of distribution coefficient of tungsten(VI) with concentration of 4-(5-nonyl)pyridine oxide from constant acidity solutions; (A) (●) 10 *M* HCl, (B) (○) 0.01 *M* HNO_3, (●) 0.01 *M* HCl, (▲) 0.01 *M* H_2SO_4.

Fig. 5. Variation of distribution coefficient of tungsten(VI) with concentration of 4-(5-nonyl)pyridine oxide from 0.5 *M* nitric acid.

oxide concentration (Fig. 4), is also close to 3. The slope of the line from hydrochloric acid concentration of 10 *M* is about 2 (Fig. 4), indicating the formation of a bis-solvate. The extracted tungsten complex is presumably the neutral dioxodichloride.

Extraction by 0.1 M trioctylamine oxide in xylene at different acidities

As Fig. 6 shows, tungsten is quantitatively extracted by TOAO from nitric and sulphuric acid solutions only in narrow acid ranges: 10^{-2}–$5 \cdot 10^{-1}$ *M* nitric acid ($D_w = 65$), and 10^{-2}–10^{-1} *M* sulphuric acid ($D_w = 46$). The curve giving the dependence of the distribution coefficient on hydrochloric acid concentration shows two maxima, corresponding to 0.05 *M* and 8 *M* hydrochloric acid. Clearly at low acid concentrations, protonated oxyanions like the NPyOx system are extracted; these, with increase in hydrochloric acid concentration, are displaced from the organic phase. The subsequent increase in the distribution coefficient could be associated with the extraction of chloro complexes of the type $WO_2Cl_n^{(n+2)-}$ (where $n = 2,3,4$), which have been suggested by Kraus and Nelson[29] to be formed in the concentrated acid solutions.

The results presented in Fig. 7 show that the addition of neutral sulphate ions to an aqueous phase containing a constant sulphuric acid concentration (0.1 *M*) has no appreciable effect on the distribution coefficient. This indicates that the addition of the sulphate ions does not lead to the formation of unextractable complexes. In nitrate media, the extraction coefficient gradually decreases with the

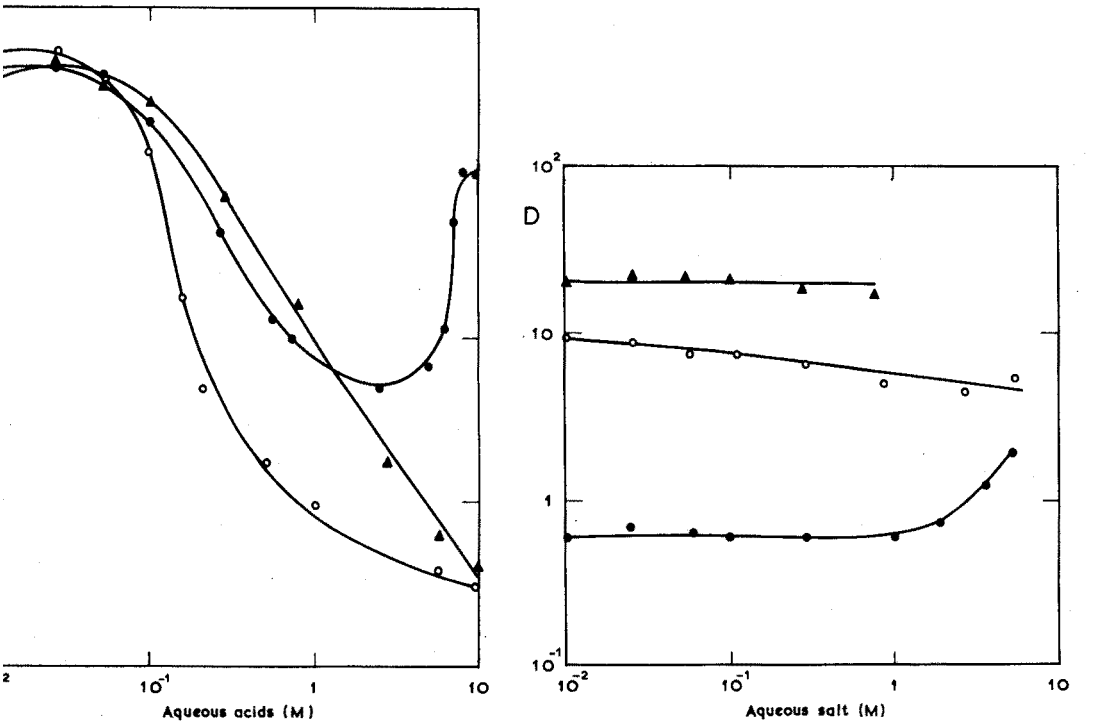

Fig. 6. Variation of distribution coefficient of tungsten(VI) with concentration of aqueous acids for extraction by 0.1 *M* trioctylamine oxide in xylene; (○) HNO_3, (●) HCl, (▲) H_2SO_4.

Fig. 7. Variation of distribution coefficient of tungsten(VI) with concentration of salting-out agents from constant acidity solutions for extraction by 0.1 *M* trioctylamine oxide in xylene; (●) NaCl in 2.5 *M* HCl, (○) $NaNO_3$ in 0.1 *M* HNO_3, (▲) Na_2SO_4 in 0.1 *M* H_2SO_4.

addition of nitrate ions (as sodium nitrate) to 0.1 *M* nitric acid. This may be due to a shift in the equilibrium between the two coexisting species to favour the unextractable species. The addition of the chloride ions to 2.5 *M* hydrochloric acid solution gives rise to increased extraction at high salt concentrations. This could be due to the extraction of chlorocomplexes of tungsten(VI) formed at high chloride concentrations.

Dependence on concentration of trioctylamine oxide

The dependence of the distribution ratio on the amine oxide concentration from aqueous nitric, hydrochloric and sulphuric solutions (0.1 *M*) shows a slope of about unity (Fig. 8). This indicates that the extraction mechanism in all the cases is similar, and that approximately one molecule of the amine oxide is utilized for the extraction of tungsten species, *i.e.* tungstic acid. The slope of the straight line from 10 *M* hydrochloric acid is equal to 1.5 (Fig. 8). This indicates that extraction of a mixture of compounds, which contain one or two molecules of the extractant, takes place.

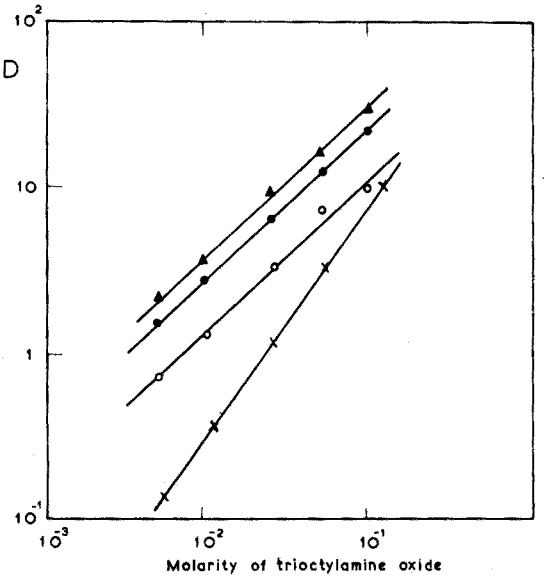

Fig. 8. Variation of distribution coefficient of tungsten(VI) with concentration of trioctylamine oxide from solutions of constant acidity; (×) 10 *M* HCl, (○) 0.1 *M* HNO_3, (●) 0.1 *M* HCl (▲) 0.1 *M* H_2SO_4.

SUMMARY

The solvent extraction of tungsten(VI) from nitric, hydrochloric and sulphuric acid solution by 4-(5-nonyl)pyridine oxide and trioctylamine oxide in xylene has been studied. The influence of the concentration of the solvents and salting-out agents is described. From the results of partition experiments, attempts have been made to deduce the nature of the extraction process.

REFERENCES

1 J. Kennedy and R. Perkins, *J. Inorg. Nucl. Chem.*, 26 (1964) 1601.
2 V. G. Torgov, A. V. Nikolaev, V. A. Mihailov and I. L. Kotlyarevskii., *Dok. Akad. Nauk SSSR*, 156 (1964) 616.
3 V. G. Torgov, V. A. Mihailov and A. V. Nikolaev, *Izv. Sib. Otd. Akad. Nauk SSSR, Ser. Khim. Nauk*, 3 (1964) 95.
4 V. G. Torgov and V. A. Mihailov, *Zh. Neorg. Khim.*, 10 (1965) 2780.
5 V. G. Torgov, V. A. Mihailov and E. A. Starceva, *Dok. Akad. Nauk SSSR*, 168 (1966) 836.
6 E. N. Gilbert, V. G. Torgov, V. A. Mihailov, P. I. Arthyukhim and A. V. Nikolaev, *Dok. Akad. Nauk SSSR*, 174 (1967) 1329.
7 A. S. Chernyak, V. G. Torgov, G. Y. Druzina, E. N. Gilbert and V. A. Mihanilov, *Izv. Sib. Otd. Akad. Nauk SSSR, Ser. Khim. Nauk*, 5 (1967) 118.
8 A. S. Chernyak, V. G. Torgov, V. A. Mihailov and G. Drugena, *Izule Chenee Zolota Almazov, Chaetnye Metalov Iz Rud*, Nenchnnye Trudy Vyp 20 Moskva Uzd Nedra, 1970, p. 331.
9 Z. B. Maksimović and R. G. Puzić, *J. Inorg. Nucl. Chem.*, 34 (1972) 1031.
10 I. L. Kotlyarevskii, V. G. Torgov, A. V. Nikolaev, V. A. Mihailov, L. N. Rovolenko and L. G. Stadnikova, *Izv. Sib. Otd. Akad. Nauk SSSR, Ser. Khim. Nauk*, 3 (1964) 95.
11 E. Ochiai, *Aromatic Amine Oxides*, Elsevier, Amsterdam, 1967, pp. 117, 322.
12 M. M. Davais and H. B. Hetzer, *J. Amer. Chem. Soc.*, 76 (1954) 4247.

13 N. N. Bezinger, G. D. Galpern, N. G. Ivanova and G. A. Semeskhina, *Zh. Anal. Khim.*, 23 (1968) 1538.
14 E. Blasius and A. Czekay, *Z. Anal. Chem.*, 157 (1957) 268.
15 G. Jander, and U. Kruerke, *Z. Anorg. Allgem. Chem.*, 265 (1951) 244.
16 Y. Saski, *Acta Chem. Scand.*, 15 (1961) 175.
17 G. Schwarzenhach and J. Meier, *J. Inorg. Nucl. Chem.*, 8 (1958) 302.
18 K. H. Arend and H. Specker, *Z. Anorg. Allgem. Chem.*, 333 (1964) 18.
19 H. Specker, *Z. Anal. Chem.*, 197 (1963) 109.
20 H. Specker and K. A. Arend, *Naturwissenschaften*, 48 (1961) 524.
21 D. G. Tuck and R. M. Walters, *J. Chem. Soc., London*, (1963) 1111.
22 W. C. White and W. J. Ross, *USAEC Rept. NAS-NS 3102*, 1961.
23 T. J. Conocchioli, M. I. Tocher and R. M. Diamond, *USAEC Rept. UCRL – 10913*, 1963; *J. Phys. Chem.*, 69 (1965) 1106.
24 A. S. Kertes and A. Beck, *J. Chem. Soc., London*, (1961) 1922; *Proc. 7th Intern. Conf. Coord. Chem., Stockholm, 1962*, 352.
25 A. V. Petrov, A. V. Karyakin and K. V. Marunova, *Zh. Neorg. Khim.*, 10 (1965) 986.
26 D. C. Whitney and R. M. Diamond, *J. Phys. Chem.*, 67 (1963) 209.
27 G. E. Boyed and Q. V. Larsen, *J. Phys. Chem.*, 64 (1960) 988.
28 J. J. Butcher and R. M. Diamond, *J. Phys. Chem.*, 73 (1969) 675.
29 K. A. Kraus and F. Nelson, *J. Chem. Soc., London*, (1955) 3972.

Analytica Chimica Acta, 71 (1974) 393–403

EXTRACTION OF REDUCED MOLYBDOPHOSPHORIC AND MOLYBDOANTIMONYLPHOSPHORIC ACIDS WITH OXYGENATED SOLVENTS

S. J. EISENREICH and J. E. GOING*

Department of Chemistry, University of Wisconsin–Milwaukee, Milwaukee, Wisconsin 53201 (U.S.A.)

(Received 26th November 1973)

Molybdophosphoric acid has been used in a variety of ways for the determination of phosphate from trace to macro levels. The usual procedure for trace analysis is photometric, based on the reduced heteropoly acid. It is generally agreed that the preferred reductant is either ascorbic acid, or ascorbic acid with potassium antimony tartrate, as in the Murphy and Riley procedure[1]. The latter procedure is preferred since reduction is complete in 5–10 min at room temperature and does not require heating. The product is reduced molybdoantimonylphosphoric acid[2].

Analysis approaching the part per billion level requires either extraordinarily long cells or an increase in concentration by solvent extraction, or a combination of both. Many extraction schemes have been proposed for oxidized molybdophosphoric acid with few intercomparisons[3–10]. No systematic study of the solvent extraction of reduced molybdoantimonylphosphoric acid, encompassing a comparison of solvents, a study of acidity, or an explanation of the solvent effects, if any, has been reported. Alimarin *et al.*[6] have reported a limited study of the extraction of reduced molybdophosphoric acid. Such information is needed for the proper choice of an extraction solvent and in the development of extraction conditions.

Thus, the present study of the extraction of the two heteropoly acids was undertaken, with the aim of surveying a wide variety of solvent types and structures, of developing an explanation of the role of the solvent, and of providing the chemical background for the development of optimum extraction systems.

EXPERIMENTAL

Apparatus

Spectrophotometric masurements were made with a Cary 14, Cary 16, or Beckman DU spectrophotometer. Radioactivity measurements of ^{32}P-labeled heteropoly acids were made with a halogen-quenched Geiger–Mueller tube with a Picker Nuclear Spectroscaler III.

Specific gravity measurements, used to determine pH values at high sulfuric acid concentrations, were obtained with a Fisher Specific Gravity Hydrometer, Type 11-542A.

* To whom correspondence should be addressed.

Acidity measurements

The hydrogen ion activity of the sulfuric acid solution used in the extraction studies was calculated based on activity coefficient data, acid titration data, and specific gravity measurements. Solutions ranging in sulfuric acid from 0.0003 to 2.465 *M* identical to those used in extraction, were prepared and analyzed by titration. The molalities of the acid solutions were calculated from specific gravity measurements and related to activity coefficient data compiled by Harned and Hamer[11]. The activity was then calculated from measured molarity and activity coefficient data. Calculated pH values could then be related to sulfuric acid concentrations which were easily reproduced with standard sulfuric acid and sodium hydroxide. The relationship between pH and molarity can be seen in the extraction figures.

Extraction studies

Stock solution of reduced molybdophosphoric acid and molybdoantimonylphosphoric acid were prepared at 42.4 μM phosphate, 90.0 μM antimony, 1.40 m*M* molybdenum, and 0.06 *M* sulfuric acid. The solutions were spiked with ^{32}P-phosphate. Ascorbic acid was added and the solution of molybdophosphoric acid was heated to 75°C for 30 min. Reduction of molybdoantimonylphosphoric acid with ascorbic acid did not require heating. The final volume after dilution was 250 ml.

Extractions were performed in 50-ml standard taper centrifuge tubes by taking 5.00 ml of the reduced heteropoly acid, appropriate quantities of sulfuric acid or sodium hydroxide to produce the desired acidity, and water to give a volume of 10.0 ml; 10 ml of the extractant were added and the tubes were shaken for 10 min and centrifuged for 3 min. Absorbance measurements of the organic phase were made.

Distribution coefficients were measured with labeled solutions by pipetting 1.00 ml of the organic and aqueous phases into planchettes, evaporating to dryness, and counting the activity for 10.00 or 20.00 min. Background was automatically subtracted. The precision of the extraction–counting techniques was determined to be ± 0.05 log *D* units.

Spectral measurements

Solutions for near i.r. spectral measurements were prepared by extracting at the pH of maximum extraction for the solvent of interest. The initial heteropoly acid concentrations were $2.120 \cdot 10^{-5}$ *M*.

Reagents

The stock solutions were prepared from reagent grade KH_2PO_4, $(NH_4)_6Mo_7O_{24} \cdot 4\ H_2O$, and $K(SbO)C_4H_4O_6 \cdot \frac{1}{2}H_2O$. All solutions were prepared from doubly distilled water. The organic solvents were either analytical grade or purified by distillation. Purity was checked by refractive index measurements.

Acetophenone solvation number

Solutions of labeled molybdophosphoric acid were prepared $2.12 \cdot 10^{-5}$ *M* in phosphate at pH 1.590 (0.0315 *M*). Solutions of acetophenone in pentyl acetate

and dichloroethylene were prepared at various mole fractions. Equal volumes of mixed solvent and reduced molybdophosphoric acid solution were equilibrated for 15 min, centrifuged, separated, and counted for ^{32}P activity.

RESULTS AND DISCUSSION

The two factors that have appeared to affect most strongly the extraction of heteropoly acids have been the nature of the solvent and the solution acidity. Recently, it has been suggested that a solvation process is involved in the extraction mechanism. Keggins initially reported that extraction is favored if the solvent contains oxygen atoms. Murata and Kiba[7] have stated that the solvent forms an adduct with the heteropoly acid, and produces the extractable species. Alimarin *et al.*[6] refer to a donor–acceptor interaction between the solvent and the acid. The distinction has been made that solvation occurs with the heteropoly anion[6,12,13].

The large shifts in the near i.r. and u.v. spectra have been cited as the principal evidence of solvation[14,15]. Chalmers and Sinclair[14] concluded that polar organic solvents such as acetone can displace water molecules from the surface of the anion. Recent i.r. data of Ptushkina and Lebedeva[12] also support a solvation mechanism. The carbonyl frequencies of methyl ethyl ketone, cyclohexanone and acetophenone solvates with molybdophosphoric acid were shifted 50–80 cm^{-1} to lower frequency. The same negative shift has been observed for the P–O band of tributylphosphate solvates of molybdophosphoric acid[16].

Very little has been reported on the specific effect of solvent type or structure upon extraction or solvation. Alimarin *et al.*,[6] have reported that the extracting power of aliphatic alcohols decreases with increasing carbon number. Similar results were reported by Heslop and Pearson[4]. The type of solvent will determine its basicity, which can be expected to follow the order, alcohols > ketones > esters. The structure can influence the basicity by means of the C:O ratio, the polarity, and by steric hindrance[17].

The nature of the effect of solution acidity is not immediately clear in some cases. As many studies have shown, extraction frequently increases with increasing acidity. This has been attributed both to the attainment of proper formation conditions and to providing sufficient hydronium ion to extract with the anion. Under certain conditions, the latter may be dominant. Murata and Kiba[7], for example, have shown by slope analysis that the molybdophosphate anion requires three protons for extraction. Souchay *et al.*[18] have reported an overall dissociation constant of 0.75 for molybdovanadophosphoric acid by extraction into isopentanol. Tsigdinos and Hallada[19], however, have questioned the results, in reporting that the heteropoly acid is a strong electrolyte in 20% dioxane–water. As shown in this study, the acidity effect is not necessarily related to the formation conditions or suppression of dissociation. As yet unexplained is why a greater acidity is required for extraction with longer chain alcohols and acetate esters as reported by Heslop and Pearson[4], and for acetate esters as reported herein.

If solvation by means of replacement of surface water molecules[14] is necessary to form an extractable species, then the factors which influence the solvating ability or basicity of a solvent become critical. A solvent such as pentyl acetate may not be

TABLE I

SPECTRAL AND EXTRACTION DATA

Solvent	*Reduced molybdophosphoric acid*				*Reduced molybdoantimonylphosphoric acid*			
	λ_{nm}	$\varepsilon \cdot 10^{-4}$	$\log D_{max}$	*Acidity (M)*	λ_{nm}	$\varepsilon \cdot 10^{-4}$	$\log D_{max}$	*Acidity (M)*
Water	840	2.64	—	—	882, 710	2.24, 1.69	—	—
Butanol	792	2.89	2.0	0.04–1.25	802, 690	1.64, 1.64	1.6	0.01–2.45
Isobutanol	793	2.07	1.9	0.02–1.25	805, 690	1.66, 1.61	1.3	0.02–2.45
Pentanol	793	2.87	2.0	0.1–1.25	802, 691	1.64, 1.64	1.6	0.01–2.45
Isopentanol	792	2.54	1.9	0.1–1.25	805, 695	1.75, 1.70	1.3	0.01–2.45
Ethyl acetate	778	3.52	1.7	0.35–2.45	720, 660	1.70, 1.65	1.6	0.2–2.45
Propyl acetate	780	3.43	1.5	1.5–2.45	720, 660	1.64, 1.69	1.4	0.25–2.45
Isobutyl acetate	782	3.17	1.5	1.5–2.45	721, 640	1.98, 2.03	1.5	0.01–2.45
Butyl acetate	782	2.71	1.5	2.5	720, 640	1.20, 1.25	1.2	1.25–2.45
Pentyl acetate	780	2.90	0.94	2.5	723, 640	1.44, 1.49	1.4	1.25–2.25
Isopentyl acetate	778	2.90	1.4	2.5	723, 640	1.58, 1.62	1.2	1.25–2.25
Benzaldehyde	785	3.55	1.5	0.003–1.3	— —	— —	—	—
Acetophenone	783	3.60	1.5	0.003–1.3	805, 687	1.97, 1.97	2.0	0.0003–2.45
Acetylacetone	798	4.20	2.1	0.0003–2.45	840, 694	2.55, 2.28	1.3	0.0003–2.45
MIBK	787	2.51	1.6	0.035–2.45	800, 687	— —	—	—

sufficiently basic to solvate the heteropoly acid by displacement of the water molecules at a given acidity. The cause may be the high C:O ratio or steric hindrance. At a higher acidity, however, the water activity will be noticeably lower. This may assist in weakening the hydration sphere and allow the solvent to compete favorably for solvation sites on the anion surface. Consequently, at the appropriate acidity, poorly solvating extractants may be able to extract the heteropoly acid.

In a study of the extraction of MoO_2X_2 from hydrohalic acid solution, Nelidow and Diamond[20] reported that the dehydrating effect of increasing acid concentration tended to drive the molybdenum species into the organic phase, where it coordinated with the oxygenated solvent. It was further shown that the effect was, in fact, related to dehydration and not solely to the increase in hydronium ion concentration. A similar salting-out effect was very recently reported for the extraction of tungsten from HCl–LiCl solution[21].

The criteria of solvation and hydronium ion concentration as a counter ion can be used to develop an extraction equation, neglecting the dehydration factor.

$$[MPA^{n-}]_{aq} + n[H^+] + s[S] \rightleftharpoons [H_nMPA\text{-}S_s]_{org}$$

$$K_{extn} = \frac{[H_nMPA\text{-}S_s]_{org}}{[MPA^{n-}][H^+]^n[S]^s}$$

D is defined as $\dfrac{[H_nMPA\text{-}S_s]_{org}}{[MPA^{n-}]}$

$$D = K_{extn}[H^+]^n[S]^s$$

$$\log D = \log K_{extn} - n\,pH + s \log [S] \qquad (1)$$

As the equation shows, a study of log D *vs.* pH should yield a curve of slope $(-n)$ while a study of log D *vs.* log [S] should yield the solvation number.

Initially solutions of reduced heteropolyacids were prepared according to the results of Going and Eisenreich[2]. Once formed, the acidity could be varied from 0.0003 to 2.45 M sulfuric acid with no effect on the absorbance. Thus, hydronium ion in these studies is not related to any formation equilibria or to stability. Extractions were performed with alcohols, esters and carbonyl-containing solvents and are discussed in terms of the above.

Alcohols

The near i.r. spectra of the heteropoly acids extracted by the normal- and iso-butanols, and pentanols, are shown in Fig. 1. A summary of all extraction data is given in Table I. All four alcohols caused hypsochromic shifts, 48 nm for molybdophosphoric acid, and 77 and 28 nm for the long and short wavelength bands of molybdoantimonylphosphoric acid, respectively. The shifts in spectra indicate that solvation of the heteropoly anion has occurred, although no significant effect of structure was evident in the spectra.

The extraction curves as a function of solution acidity are shown in Fig. 2. It is immediately apparent that the two heteropoly acids behave quite differently. While not surprising, this has not been previously pointed out. The structural effects are minimal The log D values for molybdophosphoric acid extracted with

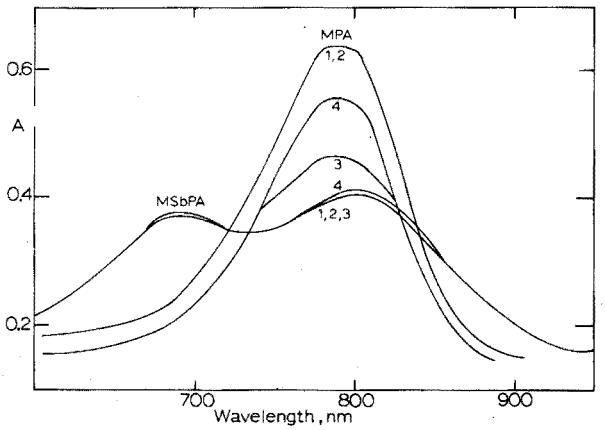

Fig. 1. Spectra of reduced heteropoly acid in alcohols. (1) Butanol, (2) pentanol, (3) isobutanol, (4) isopentanol; $[PO_4^{3-}] = 21.2\ \mu M$.

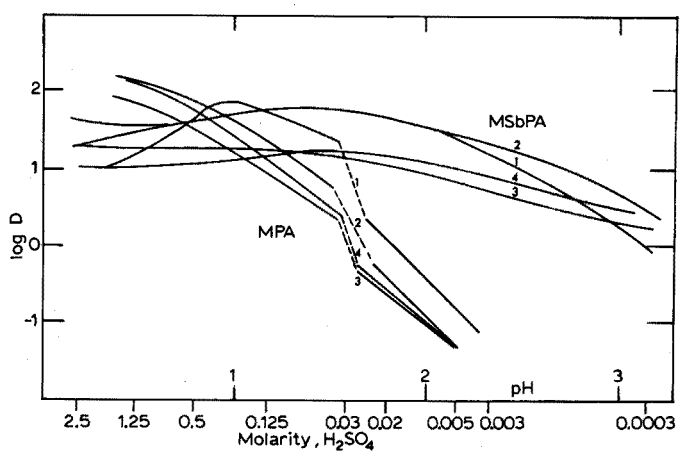

Fig. 2. Extraction curves with alcohols. (1) Butanol, (2) pentanol, (3) isobutanol, (4) isopentanol.

the isoalcohols are slightly lower than for the normal isomers. The difference is less apparent for molybdoantimonylphosphoric acid. The discontinuities in the extraction curves of molybdophosphoric acid cannot be explained, although stepwise protonation is a possibility. The results for molybdoantimonylphosphoric acid preclude any attempt to determine the number of protons required for extraction. The extraction is, in fact, relatively independent of pH suggesting that the heteropoly acid is readily solvated by the alcohols. While molybdophosphoric acid requires a more acidic solution for extraction, the acidity is not such that any noticeable change in the water activity would occur. The difference would seem to be due to fundamental differences in the behavior of the two heteropoly acids.

Esters

The spectra of the heteropolyacids extracted into a series of acetate esters are shown in Fig. 3. The spectra of molybdophosophoric acid are shifted 58 nm. The

absorbance appears to decrease with increasing chain length. The greater aqueous solubility of lower esters changing the volume partially account for this. The spectra of molybdoantimonylphosphoric acid have two maxima, at 720 and 660 nm, for ethyl and propyl acetate, respectively, and 720 and 640 nm for the remainder. The hypsochromic shifts are quite large, 160 and 50–70 nm, respectively. The decrease in absorbance is partially accounted for by the decrease in percentage extraction for the iso-esters. The very large spectral shifts again indicate that solvation occurs on extraction.

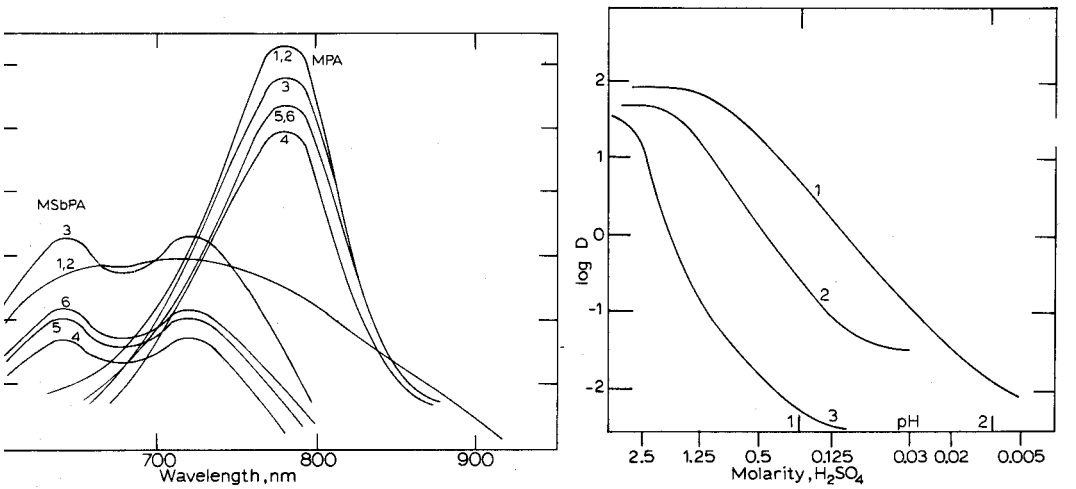

Fig. 3. Spectra of reduced heteropoly acids in esters. (1) Ethyl acetate, (2) propyl acetate, (3) butyl acetate, (4) isobutyl acetate, (5) pentyl acetate, (6) isopentyl acetate; $[PO_4^{3-}] = 21.2\ \mu M$.

Fig. 4. Extraction curves for molybdophosphoric acid with esters. (1) Ethyl acetate, (2) propyl acetate, butyl acetate, (3) isobutyl acetate, pentyl acetate, isopentyl acetate.

A marked structural effect is observed in the extraction curves of molybdophosphoric acid shown in Fig. 4. As the ester chain increases in carbon number, a significantly higher acidity is required for maximum extraction to be reached. The maximum log D values decrease from 1.7 for ethyl acetate to 0.94 for pentyl acetate. Chalmers and Sinclair[14] reported the same effect for the extraction of oxidized molybdophosphoric acid. Within the ester series, a decrease in basicity is predictable due to both a lowering of the active functional group concentration and for steric reasons. In fact, the order of heats of reaction of the acetate esters with titanium(IV) chloride is ethyl > propyl > butyl > pentyl[22]. At a given acidity, the shorter esters solvate to a greater extent than the longer esters and the percentage extraction is accordingly larger. Butyl and pentyl acetates only extract at very high acidities, which may be due to a lowering of the water activity, allowing the ester to compete more favorably for solvation sites.

To test this proposal, reduced molybdophosphoric acid was extracted with pentyl acetate from solutions of increasing ionic strength (LiCl and $NaClO_4$). The results, shown in Fig. 5, demonstrate that dehydration at high ionic strength does increase the extent of extraction. The fact that extraction occurs at the same concentrations of lithium chloride and sodium perchlorate indicates that it is a

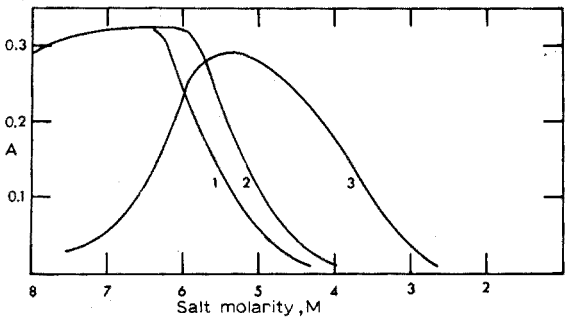

Fig. 5. Salt effect on extraction of molybdophosphoric acid into pentyl acetate. (1) $NaClO_4$ at 0.03 *M* H_2SO_4, (2) LiCl at 0.03 *M* H_2SO_4, (3) LiCl at 0.30 *M* H_2SO_4; $[PO_4^{3-}] = 12.7\ \mu M$.

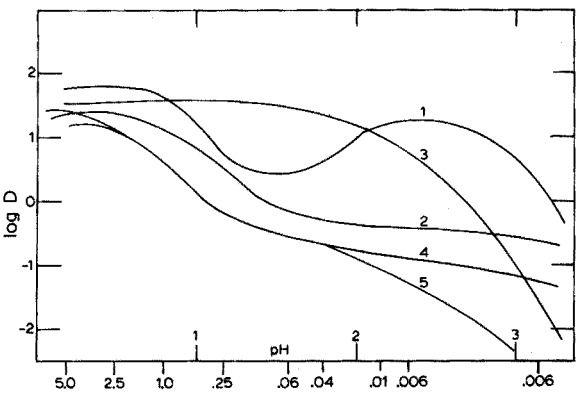

Fig. 6. Extraction curves for molybdoantimonylphosphoric acid with esters. (1) Ethyl acetate, (2) propyl acetate, (3) Butyl acetate, (4) isobutyl acetate, pentyl acetate, isopentyl acetate.

salting-out effect. The shift of the extraction curve to lower lithium chloride concentrations at higher acidity, indicates that the hydronium ion concentration is also a factor.

The extraction curves for molybdoantimonylphosphoric acid in Fig. 6 show a similar but less distinctive structural effect. Again, since the two heteropoly acids are different species, close agreement in behavior is not necessarily expected. Ethyl, propyl and butyl acetate extract molybdoantimonylphosphoric acid at lower acidities than molybdophosphoric acid. This again suggests that molybdoantimonylphosphoric acid is more easily solvated. The dip observed with ethyl acetate was confirmed by absorbance measurements and repeated experiments. A similar but less dramatic dip has been reported by Umland and Wunsch[9] for the extraction of oxidized molybdophosphoric acid. Propyl, isobutyl, pentyl, and isopentyl acetates show the expected behavior of requiring a higher acidity for maximal extraction. Butyl acetate is anomalous, extracting efficiently over a fairly wide acidity range. The argument, with respect to solution acidity affecting the extent of solvation, can be applied to the molybdoantimonylphosphoric acid extractions.

Carbonyls

The spectra from the extractions with carbonyl solvents are shown in Fig. 7.

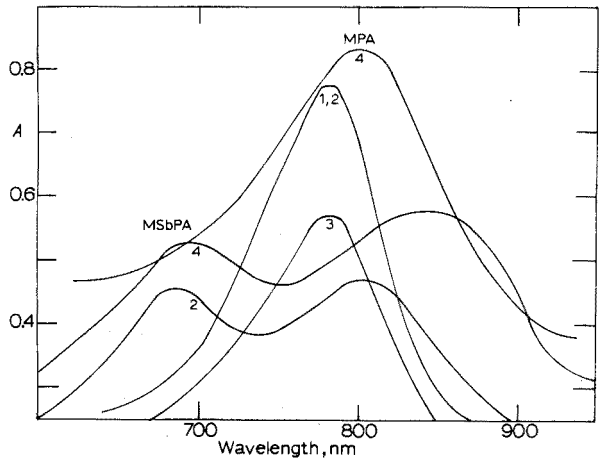

Fig. 7. Spectra of reduced heteropoly acid in carbonyl solvents. (1) Benzaldehyde, (2) acetophenone, (3) methyl isobutyl ketone, (4) acetylacetone; $[PO_4^{3-}] = 21.2\ \mu M$.

The hypsochromic shifts are again evident. The absorbance maxima for molybdophosphoric acid are shifted to 783 nm with acetophenone, benzaldehyde, and MIBK, and to 798 nm with acetylacetone. The shifts were also hypsochromic with molybdoantimonylphosphoric acid in acetophenone, MIBK, and acetylacetone. The benzaldehyde extract was not stable. The most intriguing aspect is the dramatic change in molar absorptivities. For molybdophosphoric acid, ε increases from 25,400 to 36,000, and to 35,500 when extracted with acetophenone and benzaldehyde, but decreases to 25,100 with MIBK. For molybdoantimonylphosphoric acid, ε decreases from 22,400 to 19,700 with acetophenone, and increases to 25,500 with acetylacetone. Since acetophenone is virtually water-immiscible, no volume change is possible. The volume change that occurs with acetylacetone largely explains the changes in ε for molybdophosphoric acid that occur with that solvent. The common factor in the ε enhancement is the presence of an aromatic ring conjugated to the carbonyl group. Conjugation would be expected to increase electron density at the carbonyl bond which in turn increases solvation ability. No steric hindrance should exist for the aldehyde and methyl ketone groups. Propiophenone gave an unstable extract which appeared to show the enhancement effect. Phenylacetone gave very unstable extracts.

The extraction curves shown in Fig. 8 are equally unusual. The heteropoly acids are quantitatively extracted by acetophenone, benzaldehyde, and acetylacetone from 0.0003 to 2.45 M sulfuric acid. Solvation evidently is very strong with these solvents regardless of acidity. The greatest extraction of molybdophosphoric acid was obtained with acetylacetone, followed by acetophenone and benzaldehyde, although the acetylacetone values are inflated owing to volume changes. No volume changes occurred with acetophenone and benzaldehyde. MIBK extracts molybdophosphoric acid at pH 1.6 or lower. Acetophenone was a better extractant of molybdoantimonylphosphoric acid than acetylacetone. Propiophenone likewise extracted over a wide acidity range but was unstable. The necessary conditions appear to be conjugation to an aromatic ring and minimal steric interference.

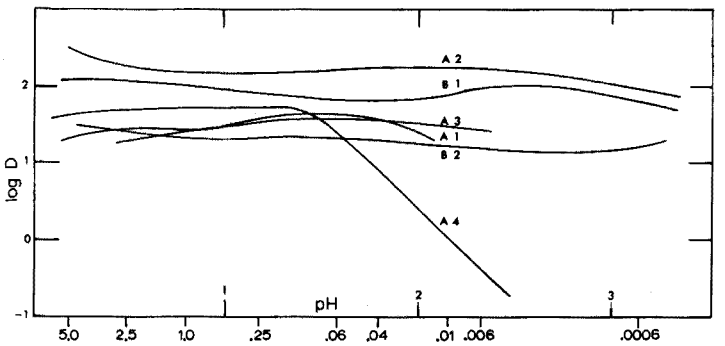

Fig. 8. Extraction curves with carbonyl solvents. (A) Molybdophosphoric acid, (B) molybdoantimonylphosphoric acid, (1) acetophenone, (2) acetylacetone, (3) benzaldehyde, (4) methyl isobutyl ketone.

It was initially surprising that acetylacetone extracted like the aromatic carbonyl solvents. Acetylacetone, however, has the ability to solvate at two sites which could be expected to alter its basicity, and is also a well known extractant for molybdenum. The slopes of all the extraction curves defied interpretation.

Acetophenone solvation number

As eqn. (1) indicates, a study of log D *vs.* log [S] should yield a curve of slope s, the solvation number. Murata and Kiba[7] reported a value of 6 for the extraction of oxidized molybdophosphoric acid by n-butanol in kerosine. Ptushkina and Lebedeva[16] reported values of 7–10 from i.r. data for the solvation of molybdophosphoric acid by tributyl phosphate. In this work, a solvation number of 7 was observed for molybdophosphoric acid with acetophenone in pentyl acetate, and 7–10 for acetophenone in dichloroethylene.

Significance

If it is intended to use an extraction step in a phosphate determination, ideally the acidity of the heteropoly acid formation should correspond to the acidity of optimal extraction. This is slightly complicated, because of the interrelationship of solution acidity and molybdate concentration, and its effect upon formation. The recent results of Going and Eisenreich should be consulted[2]. In a practical sense, acidities of greater than 0.5 M are seldom used in formation. A summary[23] of the formation conditions for the Murphy and Riley procedure[1] shows a range in suggested acidity from 0.055 to 0.5 M. By this criterion, any of the alcohols would be suitable for the extraction of molybdoantimonylphosphoric acid although the log D values are not large and the phase volume change can be a nuisance. Extractions of molybdophosphoric acid would require an acidity higher than 0.5 M.

None of the esters would be practical for the extraction of molybdophosphoric acid unless the solution was made very acidic after formation. For the extraction of molybdoantimonylphosphoric acid, butyl acetate would be a very good choice, since the acidity range is wide and the volume change is small.

Acetophenone appears to be a potentially useful solvent for either heteropoly acid. The acidity is essentially not critical. Since the solvent and water are

virtually immiscible, there is no volume change upon equilibration. Consequently, it is not necessary to collect the solvent and dilute to a known volume. Actually, it is not even necessary to recover all of the solvent quantitatively for colorimetric measurements. The possibility of using very large aqueous:organic volume ratios likewise exists. Studies are under way in this area.

SUMMARY

The extractability of reduced molybdophosphoric acid and molybdoantimonylphosphoric acid depends principally on the solution acidity and the solvent. The effect of acidity is not related to the formation equilibria or stability of the heteropoly acids in the ranges studied (0.0003–2.5 *M*). A number of solvents extract independently of acidity, which suggests that suppression of dissociation is not a major factor. In certain instances, extraction is related to the ionic strength and acidity rather than just the acidity. The solvent influence can be related to its basicity or ability to solvate the heteropoly anion. Generally, the less basic the solvent, the greater the acidity or ionic strength must be to reach maximal extraction. The effect is probably one of dehydration or salting-out. Butyl acetate and acetophenone appear to be the best choices as extractants for reduced molybdoantimonylphosphoric acid based on minimal mutual solubility, acidity dependency, and extraction efficiency.

REFERENCES

1 J. Murphy and J. P. Riley, *Anal. Chim. Acta*, 27 (1962) 31.
2 J. Going and S. Eisenreich, *Anal. Chim. Acta*, 70 (1974) 95.
3 M. A. DeSesa and L. B. Rogers, *Anal. Chem.*, 26 (1954) 1381.
4 R. B. Heslop and E. F. Pearson, *Anal. Chim. Acta*, 39 (1967) 209.
5 R. B. Heslop and A. C. Ramsey, *Anal. Chim. Acta*, 47 (1969) 305.
6 V. I. Klitina, F. P. Sudakov and I. P. Alimarin, *Russ. J. Anal. Chem.*, 20 (1965) 1197.
7 K. Murata and T. Kiba, *J. Inorg. Nucl. Chem.*, 32 (1970) 1667.
8 J. Paul, *Mikrochim. Acta*, (1965) 830.
9 F. Umland and G. Wunsch, *Z. Anal. Chem.*, 225 (1966) 362.
10 C. Wandelin and M. G. Mellon, *Anal. Chem.*, 25 (1953) 1668.
11 H. S. Harned and W. J. Hamer, *J. Phys. Chem.*, 57 (1925) 27.
12 M. N. Ptushkina and L. I. Lebedeva, *Russ. J. Inorg. Chem.*, 13 (1968) 1579.
13 V. I. Klitina, F. P. Sudakov and I. P. Alimarin, *J. Anal. Chem. USSR*, 21 (1966) 297.
14 R. A. Chalmers and A. G. Sinclair, *Anal. Chim. Acta*, 33 (1965) 384.
15 T. Fujinaga, M. Koyama and T. Hori, *Talanta*, 18 (1971) 960.
16 M. N. Ptushkina and L. I. Lebedeva, *J. Anal. Chem. USSR*, 25 (1970) 707.
17 Y. Marcus and A. S. Kertes, *Ion Exchange and Solvent Extraction of Metal Complexes*, Wiley–Interscience, New York, 1969, Ch. 9.
18 P. Souchay, F. Chauveau and P. Courtin, *Bull. Soc. Chem. Fr.*, 6 (1968) 2384.
19 G. A. Tsigdinos and C. J. Hallada, *Inorg. Chem.*, 9 (1970) 2488.
20 I. Nelidow and R. M. Diamond, *J. Phys. Chem.*, 59 (1955) 710.
21 S. P. Patil and V. M. Shinde, *Anal. Lett.*, 6 (1973) 709.
22 J. Lindquist, *Inorganic Adduct Molecules of Oxo-Compounds*, Academic Press, New York, 1963, p. 61.
23 S. Olsen, *Contribution 254*, College of Fisheries, University of Washington, 1966.

Analytica Chimica Acta, 71 (1974) 405–410

THE DIRECT SPECTROPOLARIMETRIC TITRATION OF PALLADIUM(II) ION WITH D-(–)-1,2-PROPYLENEDIAMINETETRAACETIC ACID

K. W. STREET, Jr. and K. H. PEARSON *

Department of Chemistry, Cleveland State University, Cleveland, Ohio 44115 (U.S.A.)

(Received 9th October 1973)

Spectropolarimetric titrimetry is a relatively new analytical technique first described by Kirschner *et al.*[1,2]. Continued interest in this technique and its potentialities was enhanced by the introduction of readily available commercial photoelectric polarimeters and by improvements in design and versatility[3,4]. The optical rotation of the system is constantly monitored with the modified photoelectric polarimeter while the titration proceeds. The conditions must be chosen so that an inflection in the optical rotation occurs at the titration end-point. This technique has been successfully applied to many different acid–base type systems, and its scope has been broadened by the introduction of two stereospecific ligands, D-(–)-1,2-propylenediaminetetraacetic acid (D(–)PDTA) and D-(–)-*trans*-1,2-cyclohexanediaminetetraacetic acid (D(–)CDTA). The successful analyses of many different metals[5–10] indicate its wide range.

For the direct spectropolarimetric titrations of palladium(II) ion, the stereospecific ligand D(–)PDTA was selected as the titrant, because of its chelating strength and its intrinsic optical activity[5]. The characteristics and advantages of this chelating agent and its metal chelates have been discussed previously[6]. The spectropolarimetric method of analysis offers several advantages over other chelometric methods: the pH range is not limited by the need to insure a sharp indicator color transition; a pH where the kinetics of the titration are rapid can be selected; and the optically active ligand and the stereospecifically formed palladium(II) complex serve as self-indicators. Since the observed rotation is essentially linear over the concentration ranges studied, the end-points are determined by graphical extrapolation. The spectropolarimetric methods suggested here for palladium(II) are performed at 40°C and are rapid and simple.

EXPERIMENTAL

Apparatus

A modified Perkin–Elmer Model 141 photoelectric polarimeter was used to monitor the optical rotation of the solution during the titrations and to run the optical rotatory dispersion (ORD) spectrum of the palladium–D(–)PDTA complex at pH 3.0. The modifications consisted essentially of: (1) attaching a Bausch and Lomb double-grating monochromator and high-intensity xenon light source to the Perkin–Elmer polarimeter; and (2) adding a Perkin–Elmer potentiometer and Coleman Model 165 multi-speed, multi-millivolt recorder. The modified instrument

* To whom all correspondence should be addressed.

has a wavelength range of 650–240 nm and because of the high intensity of the xenon lamp, can handle samples of high absorbance throughout the entire spectrum.

A 5-ml, 10-cm quartz flow-through polarimeter cell with optically inactive end plates was used in all titrations. The polarimeter cell was connected to a jacketed titration vessel for constant temperature work. An unjacketed titration vessel and the titrimetric apparatus have been described previously[6]. A Haake Model KT41 Kryokool constant-temperature circulator was used to maintain a constant temperature of 40°C for the titrations. The control accuracy of the Haake KT41 Kryokool is ±0.01°C.

A Corning Model 104 digital pH meter with a Sargent combination glass electrode was used for all pH measurements.

Reagents

All solutions were prepared from analytical reagent-grade chemicals with demineralized water, and were stored in polyethylene bottles.

D-(−)-1,2-propylenediaminetetraacetic acid monohydrate was prepared by a modification of the method of Dwyer and Garvan[11]. An aqueous 0.5% solution of the D-(−)-1,2-propylenediaminetetraacetic acid monohydrate gave $[\alpha]_{589}^{22} = -47.2°$. All D(−)PDTA solutions were prepared by dissolving the appropriate amounts of the free acid monohydrate in enough sodium hydroxide solution to form the disodium species. Any cloudy solutions were filtered through a fine sintered glass funnel and then diluted to 100 ml. The solutions were standardized against standard lead nitrate solutions at pH 5, with 10% hexamethylenetetramine solution to adjust the pH, and xylenol orange as the indicator[12].

Standard solutions of EDTA were prepared from dry primary standard disodium ethylenediaminetetraacetate dihydrate (G. F. Smith Chemical Co.).

The aqueous *ca.* 0.1 *M* lead nitrate solutions were standardized against the primary standard EDTA solution by the procedure for standardization of the D(−)PDTA solutions.

Two stock solutions of palladium(II) chloride were prepared by dissolving 1.7692 and 1.6685 g of palladium(II) chloride (Alfa Inorganics) in a small volume of concentrated hydrochloric acid, adjusting to pH 3.0 with sodium hydroxide and diluting to 1 l. The molarities of the respective solutions were calculated to be $9.978 \cdot 10^{-3}$ and $9.410 \cdot 10^{-3}$ *M*, assuming the palladium chloride was of primary standard quality. The first solution was standardized gravimetrically by the 4-methylnioxime method[13]. A triplicate analysis yielded 100.1% palladium(II) chloride.

Acetic acid–sodium acetate buffer pH 3.0 was prepared by dissolving 50 g of sodium acetate in water, adjusting to the proper pH with glacial acetic acid, and diluting to 1 l. The 10% HMTA buffer was prepared from reagent-grade hexamethylenetetramine (Eastman Organics).

Spectropolarimetric titrimetric procedures

The general technique was similar to that described previously; volume corrections were applied as before[6]. Place an aliquot of the palladium(II) solution in the titration vessel, and add 25 ml of pH 3.0 buffer solution and sufficient deionized water to bring the total volume to a known volume between 100 and

125 ml; this is done to simplify dilution corrections. A large volume of buffer is required to insure that the D(−)PDTA complexes or the excess D(−)PDTA do not change coordination states or ionic species during the titration. Insert the flow-through quartz polarimeter cell into the cell compartment, and zero the polarimeter after thermal equilibrium has been obtained; this is necessary because the change in temperature produces differential strain on the cell end-plates, causing spurious readings.

Titrate the palladium(II) solutions with a relatively concentrated solution of $Na_2D(-)PDTA$, from a 5-ml microburet readable to ± 0.001 ml. The molar concentration ratio of the $Na_2D(-)PDTA$ titrant to metal ion solution is approximately 60:1. After each incremental addition of titrant, allow the digital readout to stabilize; this requires no more than 1 min for titrations at 40°C.

RESULTS

The molecular rotations of the palladium–D(−)PDTA complex were obtained by preparing a $1.00 \cdot 10^{-4}$ *M* solution adjusted to the desired pH value with the acetate buffer. The ORD spectrum was run at ambient temperatures in a 10-cm quartz polarimeter cell (Fig. 1). The palladium–D(−)PDTA complex exhibits a much greater rotational dependence on wavelength than does D(−)PDTA. The ORD spectrum of the palladium complex shows positive "Cotton Effects" both in the visible and ultraviolet, whereas D(−)PDTA itself exhibits a plain negative ORD curve from 600 to 250 nm (ref. 9). The differences in molecular rotations between the positive rotations for the Pd–D(−)PDTA and the negative molecular rotations for D(−)PDTA are sufficiently large that, for the most concentrated solution determined here, wavelengths up to 550 nm gave extremely sharp end-points. However, with the most dilute solution, a wavelength of around

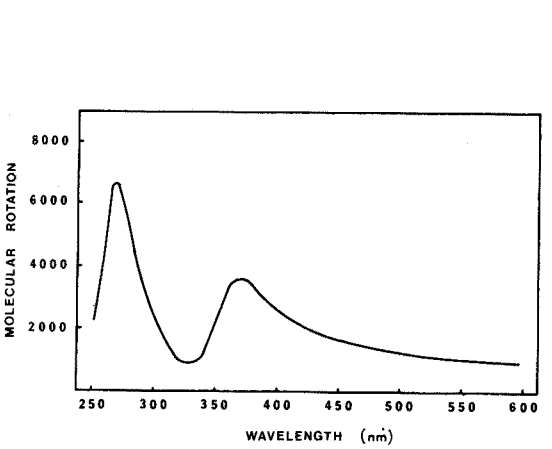

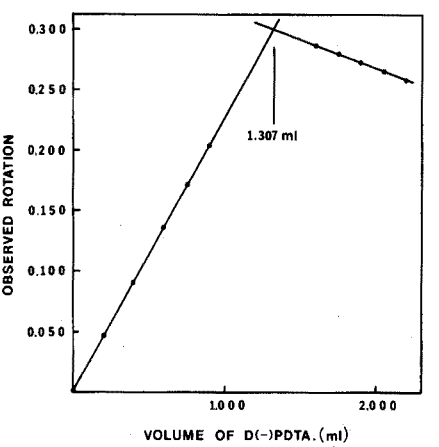

Fig. 1. Optical rotatory dispersion spectrum of palladium–D(−)-1,2-propylenediaminetetraacetic acid complex at pH 3.0

Fig. 2. Spectropolarimeter titration of 53.08 mg of palladium with standard D(−)PDTA at 550 nm and at pH 3.0.

450 nm was used since there was then a greater rotational difference between the Pd–D(−)PDTA complex and the D(−)PDTA. Both the Pd–D(−)PDTA complex and the palladium(II) ion absorb light too strongly in the ultraviolet region of the spectrum for spectropolarimetric titrations. The ORD spectrum indicates that there are two strongly absorbing optically active transitions in the ultraviolet region.

The protonation–deprotonation of D(−)PDTA changes its structure and charge in solution, resulting in an optical rotational dependence on pH. However, the molecular rotation of D(−)PDTA is essentially constant over the pH range 3.0–5.5, hence the acetate buffer is suitable for spectropolarimetric titrimetry[6].

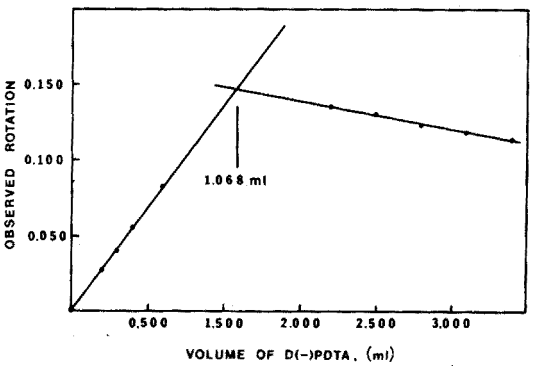

Fig. 3. Spectropolarimetric titration of 10.01 mg of palladium with standard D(−)PDTA at 450 nm and at pH 3.0.

Figure 2 shows a titration plot which is typical for the case where the metal complex has a large positive molecular rotation and the optically active titrant has a negative molecular rotation. Figure 3 shows the plot for a more dilute palladium(II) solution, which was titrated at 450 nm. It can be seen that, for dilute solutions, a wavelength of around 450 nm gives a much sharper titration end-point than at 525–550 nm, although the latter is perfectly satisfactory for concentrated solutions.

Table I gives the results of the palladium(II) ion titrations.

TABLE I

RESULTS OF SPECTROPOLARIMETRIC TITRATIONS

Pd(II) (mg)		*Deviation*		*Wavelength*
Taken	*Found*[a]	*(mg)*	*(%)*	*(nm)*
53.08	53.06±0.13	−0.02	−0.04	550
53.08	53.04±0.04	−0.04	−0.08	525
10.01	10.02±0.02	+0.01	+0.10	450

[a] Average of three titrations.

DISCUSSION

In visual chelometry a quantitative end-point depends on a sharp color transition at the equivalence point where the kinetics of the reaction will be the slowest. Likewise, in visual titrimetry the pH has to be in the range of complete formation of the metal complex.

In the back-titration of palladium(II) proposed by Harris and Sweet[14], in the concentration range above about 30 mg of palladium, the yellow color of the palladium–EDTA complex tends to mask the color transition of the indicator. Even at lower concentrations of palladium, a large amount of indicator is required. MacNevin and Kreige[15] have reported results of analytical significance by the above-mentioned method in the range of 0.6–30 mg of palladium, but it was found that the longer the indicator was left in the sample solution, the more indistinct the end-point became; addition of indicator during the titration unfortunately gave different results.

The spectropolarimetric determinations of palladium(II) at 40°C, are simple and rapid, and give sharp end-points. This is the first practical direct titration reported for palladium(II) by chelometric techniques, due to the extremely slow kinetics at room temperature throughout the titration and especially near the end point, and because of problems arising from the use of visual indicators. The spectropolarimetric titration is only limited by the amount of light absorbed by the sample.

The results described here confirm the general advantages of the spectropolarimetric titration method. Particular benefits are gained by its application to the determination of palladium(II); direct titrations with good end-points are possible because at pH 3.0 and at 40°C the kinetics of the overall reaction are sufficiently rapid.

This study was supported by a C.S.U. research grant, and was presented at the 165th National Meeting of the American Chemical Society on April 13, 1973, at Dallas, Texas.

SUMMARY

A direct spectropolarimetric titration of palladium(II) at 40°C with the optically active ligand D-(−)-1,2-propylenediaminetetraacetic acid (D(−)PDTA) is described. The optical rotation is monitored with a modified photoelectric polarimeter, and both the palladium-D(−)PDTA complex and the titrant serve as optically active indicators. End-points are obtained by extrapolations. The proposed titration is compared with the visual back-titration method.

REFERENCES

1 S. Kirschner and D. C. Bhatnager, *Anal. Chem.*, 35 (1963) 1069.
2 K. H. Pearson and S. Kirschner, *Anal. Chim. Acta*, 48 (1969) 339.
3 P. E. Reinbold and K. H. Pearson, *Anal. Chem.*, 43 (1971) 293.
4 S. J. Simon and K. H. Pearson, *Anal. Chem.*, 45 (1973) 620.
5 R. J. Palma, P. E. Reinbold and K. H. Pearson, *Anal. Chim. Acta*, 51 (1970) 329; *Anal. Chem.*, 42 (1970) 47; *Anal. Lett.*, 2 (1969) 553; *Chem. Commun.*, 6 (1969) 254.

6 R. J. Palma and K. H. Pearson, *Anal. Chim. Acta*, 49 (1970) 497.
7 D. L. Caldwell, P. E. Reinbold and K. H. Pearson, *Anal. Chem.*, 42 (1970) 416; *Anal. Chim. Acta*, 49 (1970) 505; *Anal. Lett.*, 3 (1970) 93.
8 K. H. Pearson, J. R. Baker and P. E. Reinbold, *Anal. Chem.*, 44 (1972) 2090.
9 K. W. Street, Jr. and K. H. Pearson, *Anal. Chim. Acta*, 63 (1973) 107.
10 J. R. Baker and K. H. Pearson, *Anal. Chim. Acta*, 50 (1970) 255.
11 F. P. Dwyer and F. L. Garvan, *J. Amer. Chem. Soc.*, 81 (1959) 2955.
12 G. Schwarzenbach, *Die Komplexometrische Titration*, Fredinand Enke Verlag, Stuttgart, 1955.
13 A. I. Vogel, *A Text-Book of Quantitative Inorganic Analysis*, Wiley, London, 3rd edn., 1961.
14 W. F. Harris and T. R. Sweet, *Anal. Chem.*, 26 (1954) 1649.
15 W. M. MacNevin and O. H. Kriege, *Anal. Chem.*, 27 (1955) 535.

Analytica Chimica Acta, 71 (1974) 411–417

THE IDENTIFICATION OF NON-PRESCRIPTION INTERNAL ANALGESICS BY THERMAL ANALYSIS

W. W. WENDLANDT and L. W. COLLINS*

Department of Chemistry, University of Houston, Houston, TX77004 (U.S.A.)

(Received 28th November 1973)

There are numerous non-prescription preparations that possess analgesic properties[1]. These preparations, which relieve pain arising from organic disorders or of psychosomatic origin, contain various analgesic agents, the most common of which are the following:

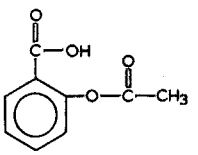

I
Acetylsalicylic acid (aspirin)

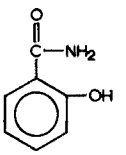

II
Salicylamide

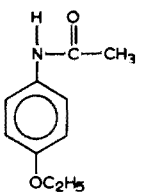

III
Phenacetin

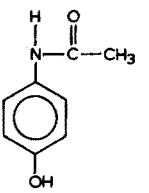

IV
N-Acetyl-*p*-aminophenol
(acetaminophen)

Aspirin (I) is effective in musculoskeletal pain and headache but less effective for such pain as toothache and sore throat. N-Acetyl-*p*-aminophenol (IV) has a reasonable antipyretic effect and may be used as a substitute for aspirin in cases where fever reduction is important; it is second only to aspirin for use as a non-prescription analgesic. Acetanilide and phenacetin (III) are also effective as analgesic and antipyretic agents. Most of the acetanilide is metabolized to (IV), which is thought to be the active agent. However, compounds (III) and (IV) are less toxic than acetanilide so that the latter is no longer widely used. Salicylamide (II) is used for its analgesic as well as its slight sedative properties.

There have been few studies of the application of thermal analysis to pharmaceutical compounds or research. Ferrari[2,3] described the application of d.t.a. to

* Present address: The Johnson Space Center, Houston, Texas.

TABLE I

COMMERCIAL SOURCES OF ANALGESIC COMPOUNDS

Brand name	*Manufacturer*	*Reported composition (mg per tablet)*				
		Aspirin	*Salicylamide*	*Acetaminophen*	*Caffeine*	*Other*
Aspirin, Bayer	Sterling Drug Co., New York, N.Y.	325	—	—	—	—
Aspirin, St. Joseph	Plough, Inc., Memphis, Tenn.	325	—	—	—	—
Aspirin, Squibb	Squibb & Sons, New York, N.Y.	325	—	—	—	—
Anacin	Whitehall Labs., New York, N.Y.	400	—	—	33	—
BC	Block Drug Co., Memphis, Tenn.	[a]	[a]	—	[a]	—
Bufferin	Bristol–Myers Co., New York, N.Y.	325	—	—	—	Aluminum dihydroxy-aminoacetate, 49
Empirin	Burroughs Wellcome Co., Research Triangle Park, N.C.	163	163	—	33	Phenacetin, 163
Excedrin	Bristol–Myers Co., New York, N.Y.	190	130	98	60	
Stanback	Stanback Co., Salisbury, N.C.	325	98	—	16	
Tylenol	McNeil Lab., Inc., Fort Washington, Pa.	—	—	325	—	
Vanquish	Sterling Drug Co., New York, N.Y.	227	—	194	33	Aluminum hydroxide, 25 Magnesium hydroxide, 50

[a] Indicates compound present but concentration unknown.

organic compounds of interest in pharmaceutical research. He showed that d.t.a. could be very useful in the determination of polymorphic transitions in these compounds, as well as assist in their purity determination. Our interest here is to use the thermal analysis techniques of d.t.a. (d.s.c.) and t.g. to aid in the characterization and identification of commercial non-prescription analgesics, the most popular of which is aspirin. These data may be of interest also for criminalistic applications of these compounds. It has recently been demonstrated by DeHaan and Rynearson[4] that d.t.a. and other thermal analysis techniques have important uses for the criminalistic identification of various materials.

EXPERIMENTAL

Equipment

Thermobalance. A DuPont Model 950 thermobalance was used to record the t.g. curves. Sample sizes ranged in mass from 5 to 20 mg and were run under a dynamic nitrogen atmosphere at a heating rate of 10°C min^{-1}.

D.t.a. (d.s.c.) apparatus. The DuPont DSC cell was used in conjunction with the Model 900 d.t.a. console. Samples ranged in mass from 5 to 10 mg and were contained in small aluminum cups. All samples were heated in a dynamic nitrogen atmosphere at a heating rate of 10°C min^{-1}.

Analgesic compounds

The sources of the non-prescription analgesic compounds and their reported compositions are given in Table I. The tablets of the above compounds were ground to a fine powder (usually *ca.* 60 mesh) in a mortar and pestle just before use.

The acetylsalicylic acid was obtained from Matheson Coleman and Bell Division, The Matheson Co., Norwood, Ohio.

RESULTS AND DISCUSSION

The most common analgesic agent, which is present in all of the preparations but one, is acetylsalicylic acid (2-hydroxybenzoic acetate, aspirin). It is generally prepared in 5-grain (325 mg) tablets which contain a small amount of binder, such as starch or other substances. The thermal analysis curves of aspirin preparations, are, essentially, those of pure acetylsalicylic acid. A small residue is obtained (if heated in a nitrogen atmosphere) of the binding agent, which is in the form of a black, charred residue at 500°C.

The d.t.a. and t.g. curves of acetylsalicylic acid have previously been reported by Wendlandt and Hoiberg[5]. The large endothermic peak, at a ΔT_{min} of 140°C, was due to the fusion of the compound, as the reported m.p. is 135°C (ref. 6). This was followed by a broad endothermic peak, caused by sublimation and/or dissociation phenomena. The t.g. curve reported indicated a continuous loss in mass, starting at an initial temperature (T_i) of 150°C. No horizontal mass plateaus were observed although a region of decreased rate of dissociation (or sublimation) was found at higher temperatures.

The d.t.a. (d.s.c.) and t.g. curves of the analgesics found in this study are given in Figs. 1–4.

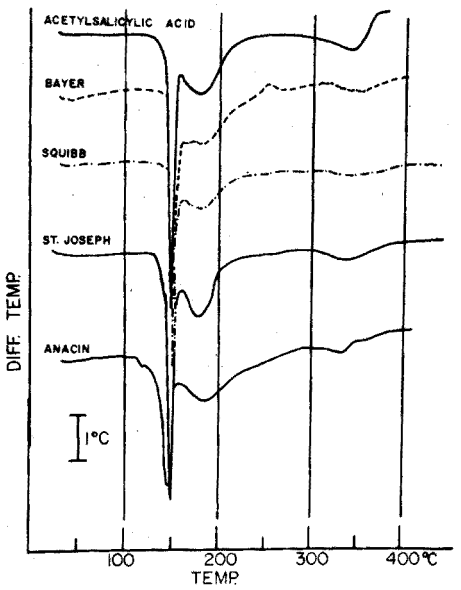

Fig. 1. D.t.a. curves of analgesics.

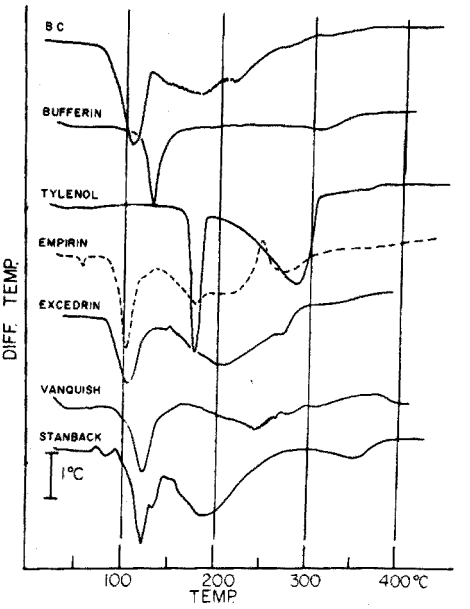

Fig. 2. D.t.a. curves of analgesics.

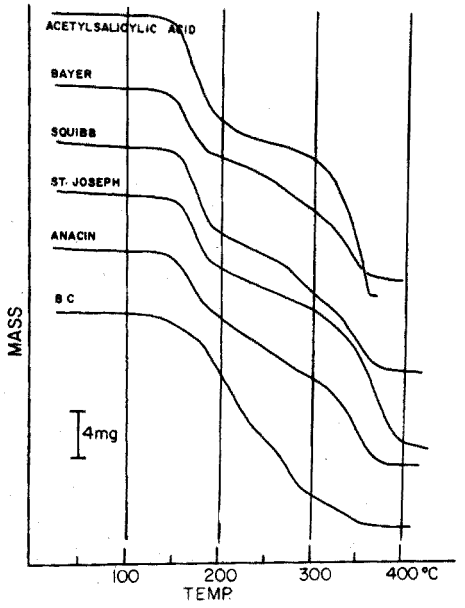

Fig. 3. T.g. curves of analgesics.

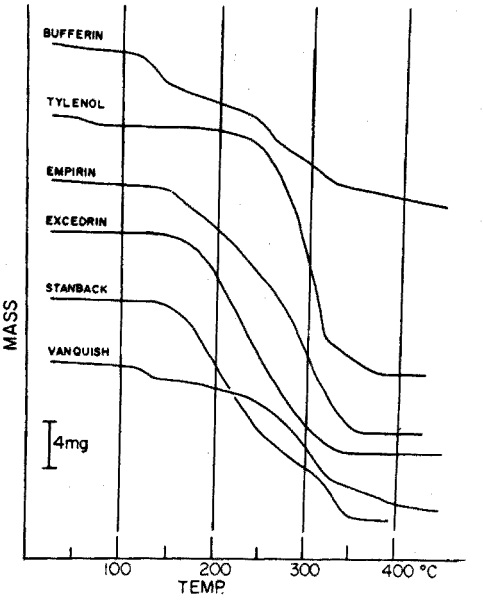

Fig. 4. T. g. curves of analgesics.

Differential thermal analysis curves

For identification purposes, the d.t.a. (d.s.c.) curves are perhaps the most useful. Prominent endothermic peaks, which are due to fusion and sublimation or vaporization phenomena, are present in each of the curves. All of the preparations contain aspirin except Tylenol, hence, a completely different curve is expected for this preparation. Pure aspirin (acetylsalicylic acid) has a d.t.a. curve with a rather sharp endothermic peak at a ΔT_{min} of 147°C although the peak begins at an initial ΔT temperature (ΔT_i) of 120°C. This fusion peak is followed by a sublimation endothermic peak ($\Delta T_{min} = 180$°C) and then a broad vaporization peak at a ΔT_{min} of 340°C.

The d.t.a. curves for Bayer, Squibb and St. Joseph aspirin are all similar to that of acetylsalicylic acid. There are small differences in the curves above 200°C which may be due either to the presence of a binder or the packing density of the sample in the d.t.a. sample container.

The d.t.a. curves for preparations containing aspirin and, among other compounds, caffeine and salicylamide, contain a broad endothermic peak in the temperature range 150–250°C. Also, the fusion peak of the aspirin is shifted to lower temperatures—in Empirin, ΔT_{min} was 102°C, a decrease of 45°C. Empirin, Excedrin and Vanquish all exhibited similar d.t.a. curves, although the ΔT_{min} temperatures were different.

Tylenol, which contains acetaminophen only, has a d.t.a. curve which contains a fusion peak with a ΔT_{min} of 180°C, and a broad vaporization and/or sublimation peak at a ΔT_{min} of 290°C.

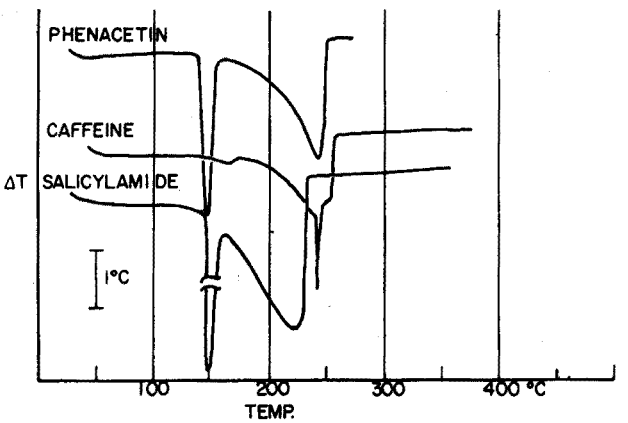

Fig. 5. D.t.a. curves of some analgesic compounds.

Since six of the analgesics contain caffeine and four contain salicylamide, the d.t.a. curves of these compounds, as well as phenacetin, are illustrated in Fig. 5. Phenacetin and salicylamide contain endothermic fusion peaks at ΔT_{min} values of 140°C and 145°C, respectively. Thus, these compounds would interfere with the determination of aspirin (m.p. 135°C) in the analgesic preparations. This interference appears in the d.t.a. curves of Bufferin, Empirin, Excedrin, Stanback and BC. Caffeine

exhibits a broad endothermic peak in the temperature range 175–260°C with a narrow peak superimposed on it at a ΔT_{min} of about 242°C.

Thermogravimetric curves

The same generalizations that were applied to the d.t.a. curves can be used in discussing the t.g. curves. In the case of acetylsalicylic acid, the first mass-loss began at an initial temperature (T_i) of 125°C. The rate of mass-loss increased greatly above 150°C but then decreased in the 225–300°C temperature range. This was followed by another region of rapid mass-loss, which terminated at 360°C. The sample container was empty at the latter temperature, indicating complete loss of the sample. As in the case of the d.t.a. curves, the Bayer, Squibb and St. Joseph aspirin preparations all gave similar t.g. curves. A residue of the charred binder was present in each of the preparations.

The preparations, Empirin, Excedrin, and Stanback, yielded similar t.g. curves. Bufferin and Vanquish also gave similar t.g. curves, perhaps because of the presence of aluminum and magnesium hydroxy compounds. Tylenol, since it has a composition which does not contain acetylsalicylic acid, gave an entirely different type of t.g. curve. Hence it is probably the simplest to identify of all the analgesics studied here.

CONCLUSIONS

By means of the d.t.a. and t.g. curves presented here, it should be possible to identify qualitatively the various commercial analgesic preparations, with perhaps the exception of the pure aspirin preparations. All of the latter preparations gave similar d.t.a. and t.g. curves. However, it is possible to distinguish between these preparations and those containing other compounds such as caffeine, salicylamide and others. The thermal analysis curves are simple to obtain and the instrumentation is relatively inexpensive and widely available. It should be noted, however, that the curves are dependent on the instrumental variables of heating rate, sample container geometry, furnace atmosphere, and so on. These parameters are discussed in detail by Wendlandt[7].

SUMMARY

The techniques of differential thermal analysis (differential scanning calorimetry) and thermogravimetry were used to aid in the identification of 12 non-prescription internal analgesics. Analgesic preparations studied included pure acetylsalicylic acid, Bayer, Squibb and St. Joseph's aspirin, Anacin, BC tablets, Bufferin, Tylenol, Empirin, Excedrin, Stanback, and Vanquish. A potential use of these curves is for criminalistic investigations.

REFERENCES

1 W. H. Barr and R. P. Penna, *Handbook of Non-Prescription Drugs*, Amer. Pharm. Assoc., Washington, 1969, p. 26.
2 H. Ferrari, in R. F. Schwenker and P. D. Garn (Eds.), *Thermal Analysis*, Vol. 2, Academic Press, New York, 1969, p. 41.

3 L. M. Brancone and H. J. Ferrari, *Microchemical J.*, (1966) 10.
4 J. D. DeHaan and J. M. Rynearson, *MPI Application Notes*, VII, No. 3 (1972) 17.
5 W. W. Wendlandt and J. A. Hoiberg, *Anal. Chim. Acta*, 29 (1963) 539.
6 R. C. Weast, *Handbook of Chemistry and Physics*, CRC Press, Cleveland, Ohio, 54th edn., 1973, c-185.
7 W. W. Wendlandt, *Thermal Methods of Analysis*, 2nd edn., Wiley–Interscience, New York, in press.

Analytica Chimica Acta, 71 (1974) 419–424

A NEW DESIGN AND COATINGS FOR PIEZOELECTRIC CRYSTALS IN MEASUREMENT OF TRACE AMOUNTS OF SULFUR DIOXIDE

K. H. KARMARKAR and G. G. GUILBAULT

Department of Chemistry, Louisiana State University in New Orleans, New Orleans, Louisiana 70122, (U.S.A.)

(Received 17th January 1974)

There have been several research reports describing the use of coated piezoelectric quartz crystals as highly sensitive detectors for gas chromatography. King[1] and Karasek and Gibbins[2] have successfully used coated crystals as highly sensitive gas-chromatographic detectors operable at room temperatures. Guilbault[3] and Scheide and Guilbault[4] have used coated crystals also in static systems for the detection of organophosphorus compounds. Janghorbani and Freund[5] have evaluated coated piezoelectric quartz crystals as digital sensors in completely digital detection systems. In recent years there has been a growing interest in developing coated piezoelectric crystals for selective detection of various air pollutants. Piezoelectric crystal detectors for sulfur dioxide have been described by Lopez-Roman and Guilbault[6] and by Frechette *et al.*[7,8].

This paper describes a new cell design for the piezoelectric crystal detector in a flowing system. Various amines are used as coating materials which enable the detection of sulfur dioxide even at p.p.b. levels, with the new cell design. This is a thousand times more sensitive than other published piezoelectric crystal detectors for sulfur dioxide[6–8]

EXPERIMENTAL

Apparatus

A new design for an all-glass detector cell is shown in Fig. 1. The important feature of this design is that the column effluent is split into two equal streams which directly and simultaneously fall on the opposite faces of a coated crystal. This arrangement is expected to improve the sensitivity since the amount of the sample gas reacting with the coating at any moment is appreciably increased. The two streams of the column effluent are brought very close to the crystal is situated in the flattened position of the cell, the parallel walls of which possible at the center of the coated crystal, the center being the most weight-sensitive position. This reduces the possibility of an undetected escape of the sample gas. The cell is made from a flattened pyrex tube (1.6-cm o.d.). A pyrex 14/20 ground joint is connected to the flattened tube which facilitates the change or removal of the crystal from the detector cell if so required. The crystal is situated in the flattened position of the cell, the parallel walls of which are separated by a distance of 0.6 cm. The parallel cell walls 2 cm long and

1.2 cm wide, making the effective cell volume about 1.5 ml ($2 \times 1.2 \times 0.6$ ml). The column effluent is equally divided by two 0.5-cm (o.d.) pyrex tubes. These tubes are connected through the two parallel walls in such a way that their tapered ends (0.2-cm o.d.) reach as close to the center of the opposite faces of the crystal as possible. The gas escapes through an exit tube (0.7-cm o.d.) connected at the bottom of the cell (Fig. 1).

A block diagram for the experimental set up is shown in Fig. 2. Dry nitrogen at a rate of 20 ml min^{-1} is used as carrier gas which passes through an empty (30 cm long and 0.7-cm o.d.) pyrex column.

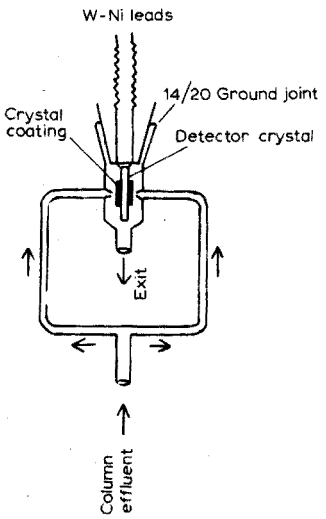

Fig. 1. New design for the piezoelectric crystal detector cell.

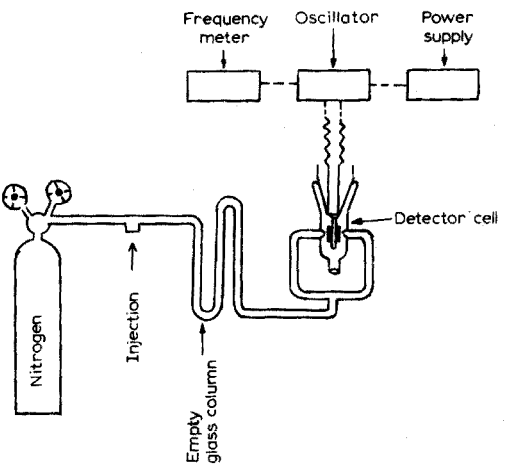

Fig. 2. Experimental setup with a piezoelectric crystal detector.

The crystals used in these studies are 9 MHz AT cut quartz crystals with silver-plated metal electrodes on both sides (International Crystal Co., Oklahoma). A low-frequency OX transistor oscillator was built from an oscillator kit (International Crystal Co., Oklahoma) to use in this study. The crystal is connected to the oscillator via two wolfram–nickel (W–Ni) leads. The oscillator is connected to a Heath 1–30 V d.c. solid-state regulator power supply model 1P-28. The applied voltage to the oscillator is 9 V though it was found that, under these conditions, applied voltage has no effect on the sensitivity of the crystal. The frequency meter used is a Systron–Donner model 8050 which has a range of 0–30 MHz with a resolution of 0.1 Hz and an accuracy of ± 1 count.

Reagents

p-Toluidine (Matheson, Coleman and Bell); Amine 220, triethanolamine, quadrol and Armeen 2S (Applied Science Lab., Inc.) were used as coatings. SO_2, NO_2, NO, CO, CO_2, NH_3, air and oxygen were obtained from Matheson Co., Inc., in lecture bottles.

Method of application of coatings

The amine coating compounds are dissolved in suitable solvents, and the solutions thus obtained are applied over the entire surface of the electrode, on both sides, with a tiny brush. Care must be taken to apply the coating as uniformly as possible; but the uniformity of coating was not checked. This method of application was found to be a fast and satisfactory one. The organic solvent evaporates quickly leaving the amine coating on the crystal. The amount of coating in each case roughly corresponds to a decrease of 5000 Hz in the basic frequency (9 MHz) of the crystal.

Syringe dilution method

A syringe dilution method is used to obtain very high dilutions of sample gases with nitrogen. Pure test gas (1 ml) is sucked into a 10-ml syringe. Nitrogen is then sucked from a nitrogen stream so that the total volume becomes 10 ml. The tip of the syringe needle is closed, either by piercing it into the body of a serum rubber or by finger, depending on the toxicity of the sample gas. In about one minute the mixture in the syringe becomes homogeneous by diffusion. Thus sulfur dioxide, for example, is 10 times diluted. In the second operation, 1 ml of this diluted mixture is again diluted to 10 ml, giving a mixture of 100 times dilution. By repeating this procedure, a mixture of any p.p.m. or p.p.b. level can be obtained. From 1 ml to 10 ml of this mixture of required dilution can be injected into the flowing system to note the response. This method of dilution is very fast, reliable and avoids the use of big dilution flasks. Unless otherwise mentioned, a 5-ml mixture is always injected in these studies.

RESULTS AND DISCUSSION

That the new design with two inlets and one outlet is more sensitive than the earlier design with one inlet and an opposite outlet[6] is demonstrated by comparing the responses using the triethanolamine-coated crystal. A 10 p.p.m. sulfur dioxide mixture gave a 42-Hz response with the earlier design and a 122-Hz response with the new design. With 6 p.p.m. sulfur dioxide, the responses were 26 Hz and 82 Hz, respectively.

Out of the coatings studied, only *p*-toluidine evaporated very rapidly from the crystal, even though it gave a good response with sulfur dioxide. In Figs. 3 and 4, the response for sulfur dioxide at varying p.p.m. levels is plotted for various coatings. Sulfur dioxide showed good response with Armeen 2S and Amine 220 coatings, but showed bending or a kind of saturation in the curves at high concentrations. Similar bending in the response curve has been reported[5] for Amine 220. Amines are known to form 1:1 charge transfer complexes with sulfur dioxide. The bending occurs after uptake of a characteristic amount of sulfur dioxide. This is evident from Fig. 3 in which the accurate positions of bending are obtained by extrapolating the sides of the curves (shown by dotted lines). Thus the 10-ml sample injection curve bends at 2.5 p.p.m., the 5-ml curve bends at 5 p.p.m., and the 2-ml curve bends at 12.5 p.p.m. The effective amount at the bending of each curve, as calculated from the observed values of p.p.m. and the corresponding sample volume, comes out to about $1 \cdot 10^{-9}$ moles of pure sulfur

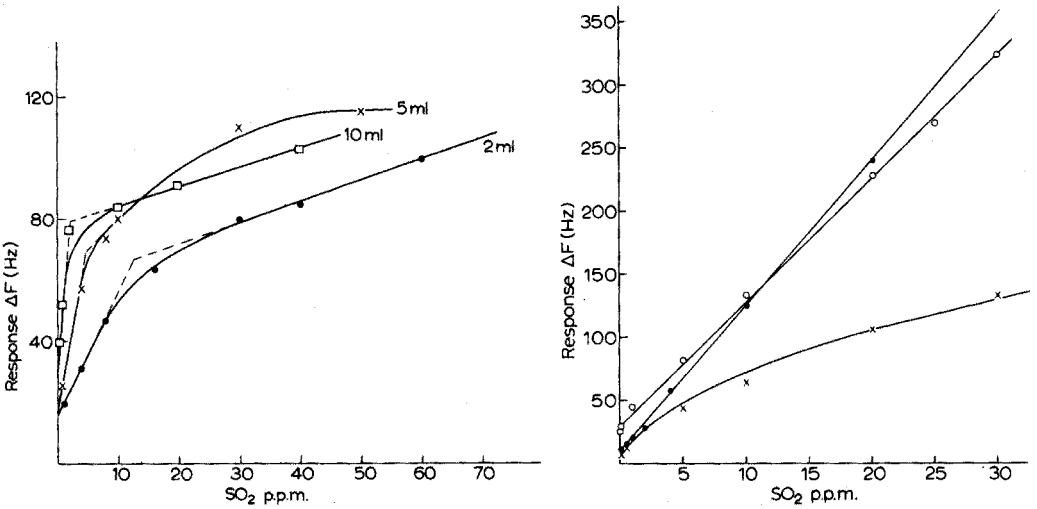

Fig. 3. Response to sulfur dioxide with Amine 220 coating.

Fig. 4. Response to sulfur dioxide with Triethanolamine (●), Quadrol (○) and Armeen 2S (×) coatings.

dioxide. A 5-ml sample injection was used for convenience and uniformity in the data.

Both triethanolamine and quadrol proved to be very satisfactory coatings for sulfur dioxide detection. Both gave fairly linear responses from 10 p.p.b. to 30 p.p.m. concentrations of sulfur dioxide. Linear response for 10 p.p.b. to 30,000 p.p.b. sulfur dioxide with triethanolamine is shown in Fig. 5. The response time is a few seconds and especially with quadrol, a complete reversibility of response

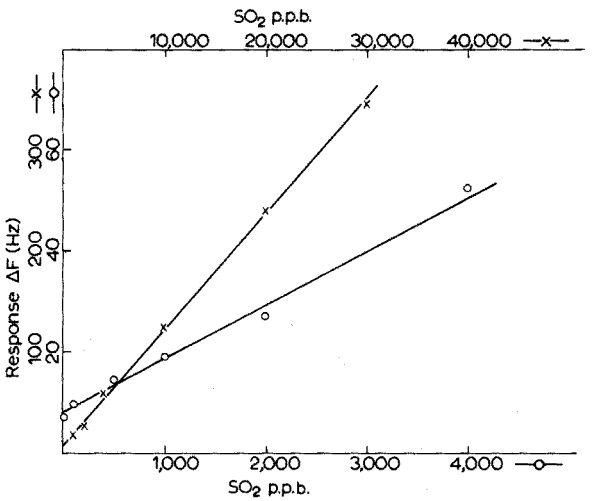

Fig. 5. Linearity of response in the range 10 p.p.b.–30 p.p.m. sulfur dioxide with triethanolamine coating.

is observed in about 5 min. With these coatings and the new design, linearity of response can be achieved from 1 p.p.b. to concentrations far above 30 p.p.m. In some experiments even 1 p.p.b. sulfur dioxide was detected but with less reproducibility. Dilution at this concentration level also becomes difficult to reproduce.

Interferences from other gases in the detection of sulfur dioxide are listed in Table I. The interfering concentrations are those which produce a response roughly equivalent to that for 1 p.p.b. sulphur dioxide.

TABLE I

INTERFERENCE STUDY

Coating	*Gas and interfering concentration (p.p.m.)*						
	CO	CO_2	NH_3	*NO*	NO_2	O_2	*Dry air*
Amine 220	10,000	10,000	10,000	1,000	100	No interference	No interference
Armeen 2S	10,000	10,000	10,000	1,000	10	No interference	No interference
Triethanolamine	10,000	No interference	1,000	1,000	1	No interference	No interference
Quadrol	100,000	100,000	1,000	1,000	1	No interference	No interference

Moisture physically condenses on the crystal surface thereby giving a strong response. Nitrogen dioxide and moisture are the major interferences. For upper atmospheric clean air studies, these interferences will not have any effect on the detection of sulfur dioxide. The use of a g.c. column or drier to separate sulfur dioxide, nitrogen dioxide or moisture, followed by separate detection, will solve this problem.

The authors gratefully acknowledge the financial assistance of the Public Health Service (Grant No. 2 RO1 OH 00345-04) and the Army Research Office (Grant No. D-31-124-70-G69).

SUMMARY

A new design for the coated piezoelectric crystal detector cell is described; this provides very high sensitivity. Triethanolamine and quadrol are the new substrates used for the detection of sulfur dioxide. The new design and the new coatings together make possible the selective detection of sulfur dioxide in nitrogen even at p.p.b. levels.

REFERENCES

1 W. H. King, *Anal. Chem.*, 36 (1964) 1735.

2 F. W. Karasek and K. R. Gibbins, *J. Chromatogr. Sci.*, 9 (1971) 535.
3 G. G. Guilbault, *Anal. Chim. Acta*, 39 (1967) 260.
4 E. P. Scheide and G. G. Guilbault, *Anal. Chem.*, 44 (1972) 1764.
5 M. Janghorbani and H. Freund, *Anal. Chem.*, 45 (1973) 325.
6 A. Lopez-Roman and G. G. Guilbault, *Anal. Lett.*, 5 (1972) 225.
7 M. W. Frechette, J. L. Fasching and D. M. Rosie, *Anal. Chem.*, 45 (1973) 1765.
8 M. W. Frechette and J. L. Fasching, *Environ. Sci. Technol.*, 7 (1973) 1135.

Analytica Chimica Acta, 71 (1974) 425–432

THE APPLICATION OF HYDRODYNAMIC VOLTAMMETRY IN CHEMICAL ANALYSIS

ZS. FEHÉR*
EGYT Pharmacochemical Works, Budapest (Hungary)
E. PUNGOR
Institute for General and Analytical Chemistry, Technical University, Budapest (Hungary)
(Received 2nd January 1974)

In a previous paper[1], a measuring techniqe used for the rapid serial analysis of various samples in small volumes was reported. The technique is an injection one, *i.e.* small volumes of the test solution are injected into a supporting electrolyte streaming continuously at a constant flow rate. After suitable mixing, the test solution enters the flow-through cell containing the working and reference electrodes. The change in current is recorded at a constant voltage, which has been selected in the limiting current range of the component to be measured.

Owing to the "impulse" of the electroactive test solution, the current increases suddenly and then decreases to the base-line, so that the signal appears as a peak.

For a working electrode placed parallel to the flowing stream, it was found—in correlation with our theoretical considerations—that the area under the peak depends on the amount of the electroactive material injected and the flow rate, according to the following equation:

$$T = \frac{KM}{V}(a + V^{\frac{1}{2}})$$

where T is the area under the peak, M the amount of material injected, V the flow rate, K the proportional factor ($K = knFD^{\frac{2}{3}}v^{-\frac{1}{6}}bl^{\frac{1}{2}}$), and a a constant.

With a proper selection of the streaming solution or the solution injected, this technique offers many possibilities for the determination of different compounds or samples.

The aim of this paper is to demonstrate some of the possible applications.

GENERAL CONSIDERATIONS

The types of application of the injection technique are as follows:

1. Analysis of electroactive samples[1].

(a) The solution injected is the test solution; the streaming solution is the supporting electrolyte.

2. Analysis of electroinactive samples.

---

* Present address: Institute for General and Analytical Chemistry, Technical University, Budapest, Hungary.

(a) The solution injected is an electrochemically inactive test solution; the streaming solution is a supporting electrolyte containing the electroactive material which reacts with the test solution.

(b) The solution injected is an electroinactive test solution; the streaming solution is the supporting electrolyte containing an electrochemically inactive material which reacts with the test solution resulting in an electroactive reaction product.

3. Analysis of streaming electroinactive solutions.

(a) The streaming solution is the test solution containing the supporting electrolyte; the solution injected is an electroactive reagent which reacts with the test solution.

(b) The streaming solution is the test solution containing the supporting electrolyte; the solution injected is an electroinactive reagent which reacts with the electroinactive test solution resulting in an electroactive reaction product.

In all these techniques, the signal measured appears as a peak, and the area under the peak is related to concentration.

Except for procedure 3(a), the area under the peak is proportional to the concentration of the test solution, while in the case of 3(a) the decrease in the signal of the electroactive reagent is proportional to the concentration of the streaming test solution.

Another way of dividing the possible applications of the injection technique is based on the character of the chemical reaction taking place between the test solution and the reagent. Accordingly, the determinations can be related to complex formation, oxidation–reduction reactions, precipitation, *etc.*

In the determination of the concentration of electroactive samples, a silicone rubber-based graphite electrode has been used as a working electrode[1]. This type of electrode is especially good in the anodic potential range[2]. Naturally other types of working electrodes can also be used, and not only amperometric, but biamperometric detection techniques can be applied.

The selection of parameters used for the determinations

The potential applied. The constant potential is chosen on the basis of the voltammetric curve of the electroactive component, and lies in the limiting current range. The proper selection of the potential is especially important for those cases in which the product of the chemical reaction taking place between the electroinactive test solution and the electroactive reagent is also electroactive.

The flow rate. The effect of the flow rate can be predicted on the basis of eqn. (1) for determinations which do not involve a chemical reaction, or if the connecting chemical reaction is extremely rapid. However, if the chemical reaction is relatively slow, then the flow rate also determines the reaction time and therefore a suitable selection of the flow rate is very important.

The concentration of the reagent. In the selection of the appropriate concentration of the reagent, it must be considered that the electroactive reagent or the reaction product of the chemical reaction should give a signal which changes linearly with concentration throughout the possible range.

Another important point is that the reagent must always be in excess compared to the test solution. Naturally the dilutions must be considered.

The medium used. This parameter can play an important role in the electrochemical reaction, *e.g.* it influences the half-wave or half-peak potential of the electroactive component; and the medium can affect the rate of the chemical reaction.

As examples, two methods are discussed in detail. These are the determination of calcium and magnesium by sample injection, and the determination of phenol in flow streams.

DETERMINATION OF CALCIUM AND MAGNESIUM

EDTA (ethylenediaminetetraacetic acid) gives a well defined anodic wave on a dropping mercury electrode, as has been reported by Fleet *et al.*[3] and others[4]. At pH 10 the electrochemical reaction is as follows:

$$HY^{3-} + Hg^0 \rightarrow HgY^{3-} + H^+ + 2e^-$$

According to this reaction, the amount of calcium and magnesium can be determined on the basis of the decrease in the anodic wave of the EDTA if the measuring conditions are chosen properly.

Procedure

The determinations were carried out in the measuring set-up shown in Fig. 1. Solution transport was ensured with a peristaltic pump (Type S 33, Unipan, Poland). The sample was injected into the system with a Hamilton syringe (type 710N). For the deaeration of the EDTA solution nitrogen gas was bubbled continuously into the solution container. The volume of the mixing chamber was about 5 ml. The measuring cell was a simple flow-through one, incorporating a dropping mercury electrode and a mercury pool reference electrode (Fig. 2). The level of the mercury was adjusted to the same value after about 5 recordings, so that the conditions of the measurements were almost the same for each recording.

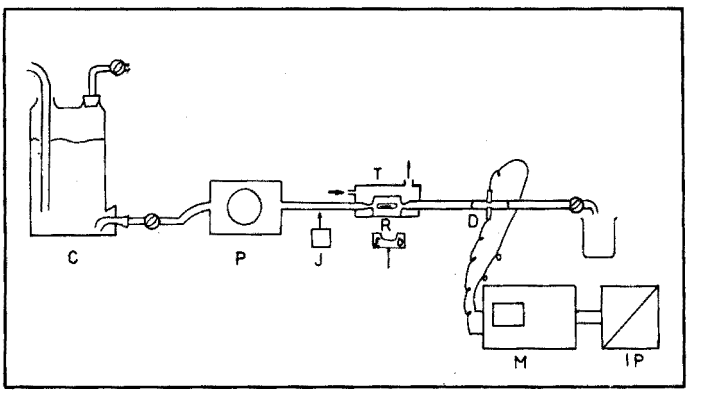

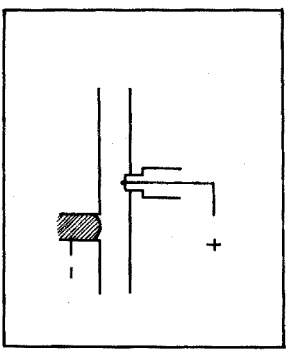

Fig. 1. Measuring set-up used for continuous analysis: C, container; P, peristaltic pump; I, injection unit; R, magnetic stirrer; T, thermostat; D, detector cell; M, measuring unit; IP, integrating unit.

Fig. 2. Detector cell incorporating a dropping mercury measuring electrode and a mercury pool reference electrode.

Since the volume of samples injected was only 1–2% of the volume of the mixing unit, calcium and magnesium solutions prepared with distilled water or

other solvent could be injected without altering the final pH of the streaming solution.

A polarograph (type OH 102, Radelkis, Hungary) was used for the measurements.

The areas under the peaks were determined also by weight.

Results

The potential of the dropping mercury electrode was selected to be −0.05 V compared to the mercury pool electrode, on the basis of the voltammetric curve recorded in stationary solution.

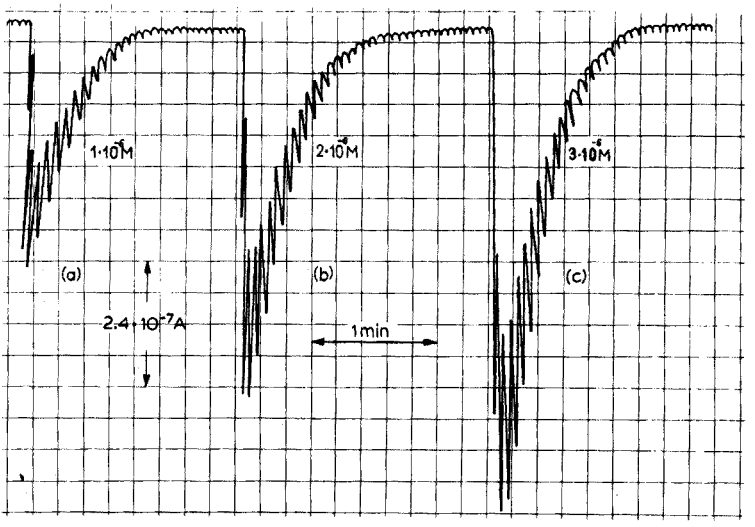

Fig. 3. Signals obtained by injection of calcium solutions into an EDTA stream; potential, −0.05 V; flow rate, 7 ml min^{-1}; EDTA solution, $1 \cdot 10^{-3}$ *M*; calcium solutions, 100 µl of (a) $1 \cdot 10^{-2}$ *M*, (b) $2 \cdot 10^{-2}$ *M* and (c) $3 \cdot 10^{-2}$ *M*.

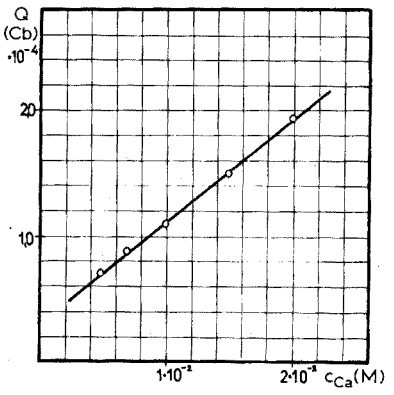

Fig. 4. Calibration curve for calcium determinations: potential, −0.05 V; flow rate, 7 ml min^{-1}; EDTA solution, $1 \cdot 10^{-3}$ *M*.

A study of the buffer composition and concentration of the streaming solution showed that the most suitable buffer was 0.06 *M* ammonium nitrate–0.18 *M* ammonia solution, as was stated by Fleet *et al.*[3]. In this buffer, the determination could be carried out successfully in the concentration range $1 \cdot 10^{-3}$–$5 \cdot 10^{-4}$ *M* EDTA. Accordingly $1 \cdot 10^{-3}$–$1 \cdot 10^{-1}$ *M* calcium and magnesium solutions could be analysed by this method. The minimal volume of the sample was 10 μl. In Fig. 3 the voltammetric signals of various concentrations of calcium solutions are shown, while Fig. 4 shows a calibration curve.

A flow rate of 5–8 ml min^{-1} was found to be optimal; this corresponds to a linear flow rate of 0.43–0.68 cm s^{-1}, if the diameter of the cell is 0.5 cm.

The relative standard deviation of the determinatons was about 3%, including errors in the evaluation of the results. The latter does not exceed 1.5%. The precision of the determination can be improved if the dropping of the mercury is controlled, *e.g.* with a Tast-Rapid adapter (type OH-991, Radelkis, Hungary).

DETERMINATION OF PHENOL IN STREAMING SOLUTIONS

For the determination of phenol, various amperometric and biamperometric methods have been reported[5,6]. With an applied voltage of 50–300 mV between two identical or different electrodes, the phenol solution is titrated with a mixture of potassium bromate and bromide or with bromine generated coulometrically. By measuring the amount of bromine present in phenol solutions, it is possible to determine the concentration of phenol.

Procedure

The measuring set-up was the same as that shown in Fig. 1. The solutions were streamed with a peristaltic pump (Type 304, Unipan, Poland). The measuring cell contained two platinum electrodes made of platinum wire of 1-mm diameter, protruding 1.5 mm into the cell.

A d.c. polarograph (Type OH-102, Radelkis, Hungary) served as the source of the constant voltage between the two platinum electrodes (100 mV), and for recording the current–time curves.

A given amount of potassium bromate–bromide mixture was injected first into the acidic supporting electrolyte, and then into acidic phenol solutions of various concentrations. After the area under the peaks had been determined (Fig. 5), a calibration curve for phenol was prepared on the basis of the decrease in the signal of the bromine injected into the phenol solutions. Phenol solutions of unknown concentration were also passed through the system after acidification. By injecting the same amount of bromate–bromide solution, their concentrations could be determined from the calibration curve.

Results

Determination of bromine. In the investigation of the bromine determination, the effect of the constant voltage applied between the two electrodes, as well as the effects of the ratio and the concentration of the bromate–bromide mixture, were studied.

The correlation obtained on changing the applied voltage between 50 and

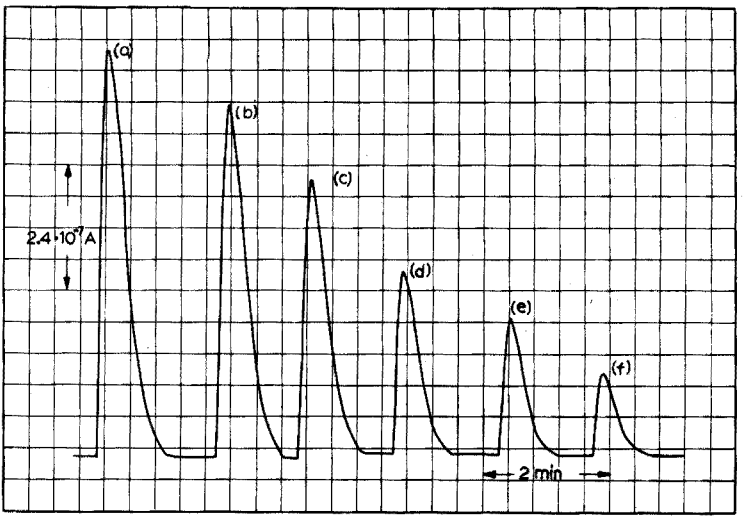

Fig. 5. Current–time curves obtained for the injection of bromate–bromide mixture into streaming phenol solutions: potential, 100 mV; solution injected, 100 μl of 10^{-1} *M* KBr–10^{-1} *M* $KBrO_3$; streaming solutions, 10^{-1} *M* KCl–10^{-1} *M* HCl containing (a) no phenol, (b) 10^{-5} *M* phenol, (c) $2 \cdot 10^{-5}$ *M* phenol, (d) $3 \cdot 10^{-5}$ *M* phenol, (e) $4 \cdot 10^{-5}$ *M* phenol, (f) $5 \cdot 10^{-5}$ *M* phenol; flow rate, 5 ml min^{-1}.

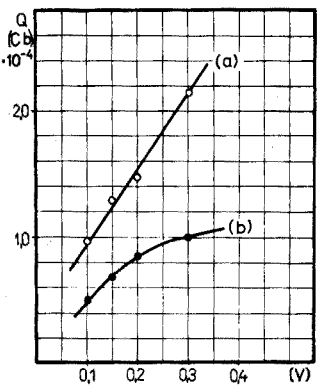

Fig. 6. Variation of the bromine signal with the applied potential: flow rate, 4 ml min^{-1}; solution injected, 100 μl of 10^{-2} *M* KBr–10^{-2} *M* $KBrO_3$; streaming solution, (a) 10^{-1} *M* KCl–10^{-1} *M* HCl, (b) $5 \cdot 10^{-5}$ *M* phenol in 10^{-1} *M* KCl–10^{-1} *M* HCl.

300 mV is shown in Fig. 6; on this basis, 100 mV was selected for the determinations so as to avoid possible side reactions.

When the amount of the bromate–bromide solution injected was altered, the signal increased linearly with increasing amount (Fig. 7). This linear dependence was found for various bromate–bromide ratios; but any change in the bromate–bromide ratio from the 1 : 1 ratio caused an increase in the signal.

When the same amount of bromate–bromide solution was injected into 10^{-1} *M* HCl and $5 \cdot 10^{-2}$ *M* H_2SO_4 solutions, the signals obtained in hydrochloric acid solution were greater than those in sulphuric acid solution.

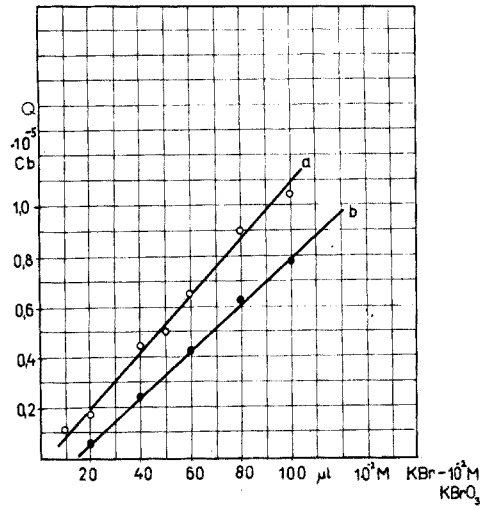

Fig. 7. Variation of the bromine signal with increasing amount of bromine injected; streaming solution, (a) 10^{-1} *M* KCl–10^{-1} *M* HCl, (b) $5 \cdot 10^{-6}$ *M* phenol; solution injected, 10^{-2} *M* KBr–10^{-2} *M* $KBrO_3$.

These findings were used to select the optimal parameters for the phenol determination.

When a phenol solution was titrated in stirred solution with bromate–bromide mixture at two platinum wire electrodes, the current did not change during the titration until bromine was in excess; the titration of 1 mole of phenol required 4 equivalents of bromine. However, it must be mentioned that the conditions of the titration are not the same as in streaming solutions, because in streaming solutions the bromine is in excess. The titration curve showed that the signals obtained on injection of bromate–bromide mixture into phenol solutions are due only to the excess of bromine, and the product of the chemical reaction shows no electroactivity under these measuring conditions.

Phenol determination. At a given ratio and concentration of the bromate–bromide mixture—an excess of bromine over phenol being ensured—the signal increased linearly with increase in the amount of electroactive material injected (Fig. 7). This means that with a proper excess of bromine, the rate of the reaction between the phenol and bromine is not influenced by the amount of bromine.

The effect of the bromate–bromide ratio was the same as in the case of the determination of bromine. In serial phenol determinations, the molar ratio of bromate to bromide was 1 : 1 and their concentrations were 10^{-1} *M*.

To obtain a linear calibration curve in a given concentration range, the rate of the chemical reaction had to be changed by altering the flow rate and the acidity of the solution. Linear calibration curves were obtained in the range of 10^{-6}–10^{-5} *M* in $5 \cdot 10^{-1}$ *M* sulphuric acid solution. In every case 100 µl of 10^{-1} *M* bromate–10^{-1} *M* bromide solution was injected into the phenol solutions, and the flow rate was 4 ml min^{-1} (Fig. 8a). In the concentration range 10^{-5}–10^{-4} *M* a linear calibration curve was obtained in 10^{-1} *M* hydrochloric acid under the same conditions (Fig. 8b). The limit of the detection was found to be 10^{-7} *M*. In the lower concentration range, the relative standard deviation of the bromine determination was

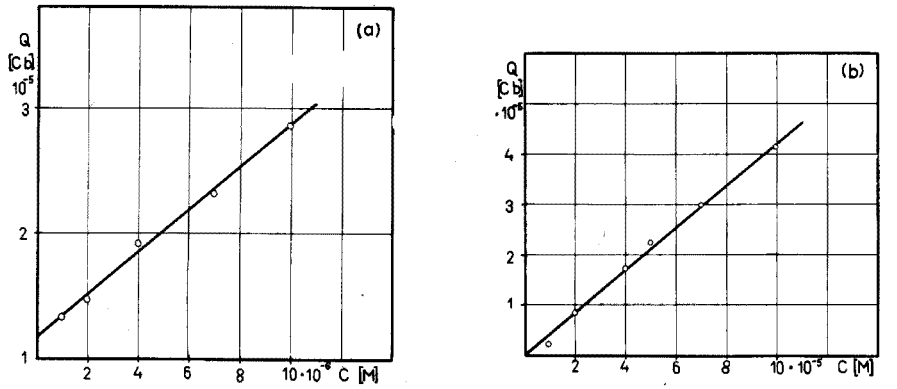

Fig. 8. Calibration curves for phenol: potential, 100 mV; solution injected, 100 μl of 10^{-1} *M* KBr–10^{-1} *M* $KBrO_3$; flow rate, 4 ml min^{-1}. Supporting electrolyte: (a) 10^{-1} *M* KCl–$5 \cdot 10^{-2}$ *M* H_2SO_4; (b) 10^{-1} *M* KCl–10^{-1} *M* HCl.

3% in blank solution, and 5% when the solution contained phenol.

In this method phenol has been used as a model, but naturally the technique can be used for the determination of any component which reacts with bromine.

CONCLUSIONS

Many amperometric and biamperometric titrations can serve as a basis for the injection technique. The injection technique has many advantages over titration techniques; it is less time-consuming, automation of the technique is easier, *etc.* In addition to practical applications the technique can be used for studying the kinetics of chemical reactions.

SUMMARY

A special application of hydrodynamic voltammetry, *i.e.* the injection technique, is described in detail. General considerations concerning the selection of the measuring conditions are discussed. The determinations of calcium and magnesium as well as that of the phenol are discussed.

REFERENCES

1 G. Nagy, Zs. Fehér and E. Pungor, *Anal. Chim. Acta*, 52 (1970) 47.
2 E. Pungor and É Szepesváry, *Anal. Chim. Acta*, 43 (1968) 289.
3 B. Fleet, S. Win and T. S. West, *Analyst*, 94 (1969) 269.
4 J. T. Stock, *Amperometric Türations*, Interscience, New York, 1965, p. 370.
5 W. Bielenberg and K. Kühn, *Z. Anal. Chem.*, 126 (1943) 88.
6 F. Cuta and Z. Kucera, *Chem. Listy*, 52 (1958) 595.

Analytica Chimica Acta, 71 (1974) 433–441

ELECTROANALYTICAL STUDY OF ISOMERIC TRIFLUOROMETHYLNITROSOBENZENE INTERMEDIATES

R. L. DICKERSON and J. W. ROGERS*

Department of Chemistry, Midwestern University, Wichita Falls, Texas 76308 (U.S.A.)

(Received 17th January 1974)

The nitro group of various nitroaromatic compounds is electrochemically reduced, in one polarographic step, to the corresponding phenylhydroxylamine in basic aqueous media, and to the corresponding amine in acidic media[1,2]. In purified nonaqueous solvents such as acetonitrile, dimethylsulfoxide and N,N-dimethylformamide (DMF) most nitroaromatics are reduced, to hydroxylamines and other products, only at the higher potential step of two polarographic steps[3]. In general, the lower potential step represents the production of a long-lived anion π-radical[4,5]. If intermolecular coupling reactions are ignored, the reduction of the nitro function in an aprotic medium at the second polarographic step may be conveniently represented by the following scheme:

$$RNO_2^{\cdot-} \xrightarrow[+2H^+]{+e^-} RNO \xrightarrow[+2H^+]{+2e^-} RNHOH$$

Kemula and Sioda[6], who used rapid-sweep cyclic voltammetry with oscilloscopic recording, found evidence of a very transient nitrosobenzene anion radical in the electrochemical reduction of nitrobenzene. However, the nitroso group is known to couple readily with hydroxylamines as well as dimerize to form azoxy compounds[7–9]. Also, under the influence of sufficiently negative potentials, electron transfer to the nitroso intermediate may compete effectively with intermolecular coupling reactions to produce hydroxylamine and amino compounds[10]. Consequently, the nitrosobenzene intermediate is not commonly detected in the reduction of nitroaromatics. A notable exception to this is found in the electrochemical reduction of *o*- and *m*-trifluoromethylnitrobenzene in DMF[11]. These compounds are reduced to abnormally long-lived trifluoromethylnitrosobenzene anion π-radicals at the more cathodic of two polarographic steps via a mechanism in which a chemical reaction is coupled between two reversible electron transfers (e.c.e. mechanism). The *ortho* isomer exhibits the greatest stability, both being stable enough to be detected in cyclic voltammetric experiments conducted at the lower limits of potential sweep rate.

Synthesis of *p*-trifluoromethylnitrobenzene has made it possible to investigate the relative stabilities of the nitroso radical reduction intermediates of all three isomers in aprotic media. A very significant and interesting trend in stability of the *o*-, *m*- and *p*-trifluoromethylnitrosobenzene radical is observed. Potential step

* To whom correspondence and requests for reprints should be directed.

experiments with concomitant cyclic sweep voltammetry measurements at a planar platinum disc electrode (p.p.d.e.) were employed to compare the lifetimes of the three species. Auxiliary techniques employed were chronoamperometry, and mass electrolysis with spectrophotometric identification of products.

EXPERIMENTAL

Apparatus

The p.p.d.e. employed in the cyclic voltammetric experiments was a Beckmann platinum button electrode with an area of 80 mm^2. The reference electrode employed in all experiments, saturated calomel (s.c.e.), made contact with the solution through an agar plug behind a Pyrex frit. Water leakage through this tip was found to be negligible. The cyclic voltammetric and chromoamperometric data were recorded on a Bolt–Barnak–Newman X–Y plotter with a PAR Model 173 potentiostat and Exact wave form source for potential variation and control. The mass electrolytic experiments were performed with a Wenking Potentiostat in a nitrogen-stirred solution at a platinum gauze electrode. The platinum foil anode and s.c.e. reference were isolated from the cathode compartment with fine porosity glass frits. The u.v. spectra of the electrolysis products were recorded on a Perkin–Elmer Model 202 scanning spectrophotometer in quartz cells with pure DMF solvent as reference.

Chemicals

All solutions were 1 m*M* in electroactive compound and 0.1 *M* in the supporting electrolyte, tetra-N-propylammonium perchlorate. Spectroquality DMF containing *ca.* 0.03% water was obtained from Eastman Organic Chemicals. The solvent was vacuum-distilled from anhydrous copper(II) sulphate before use. The preparation and purification of TPAP has been described previously[16]. *o*- and *m*-Trifluoromethylnitrobenzene were purchased from K and K Chemicals. The *para* isomer was prepared by diazotization of α,α,α-trifluoro-*p*-toluidine after the method of Starkey[17].

RESULTS

Cyclic voltammetry.

For purposes of comparison, typical multi-sweep cyclic voltammograms of *o*-, *m*- and *p*-trifluoromethylnitrobenzene are shown in Fig. 1. Pertinent electrochemical data from cyclic voltammetric experiments conducted on the three isomers at a p.p.d.e. in dry DMF are given in Table I. These criteria include variations of the cathodic peak potential, $(E_p)_c$, the ratio of anodic to cathodic current for a single peak, $(i_p)_a/(i_p)_c$, and the current function, $(i_p)_c/v^{\frac{1}{2}}$, where v denotes the potential sweep rate[12,13]. Data presented previously[11] from similar experiments on the *ortho* and *meta* isomers were taken at a hanging mercury drop electrode. Owing to peak potential differences at the two electrodes and for completeness, some data are represented herein.

Each of the three parent compounds exhibits an initial voltammetric current peak at which it is reduced to a radical anion via a one-electron reversible

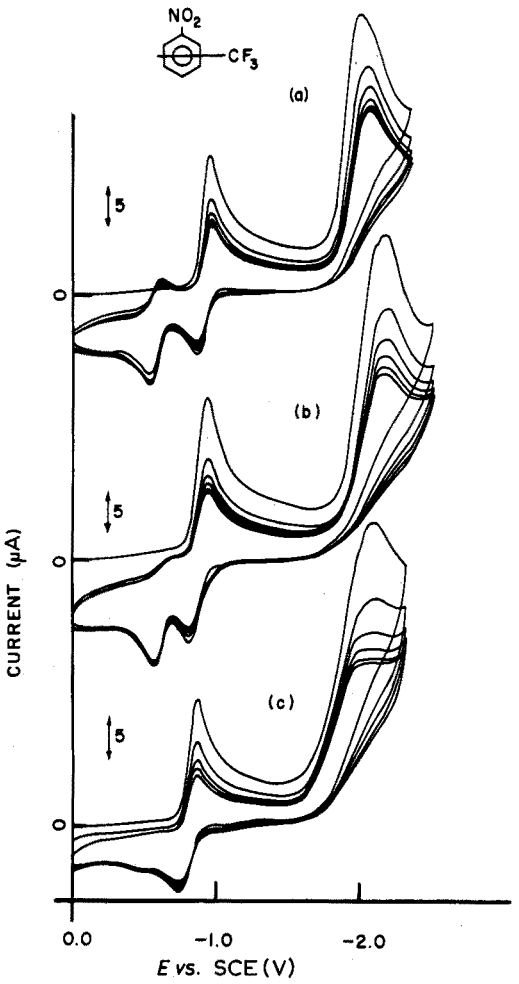

Fig. 1. Multi-sweep cyclic voltammograms at a p.p.d.e. at 3.0 V min^{-1} of 1 m*M* DMF solutions of (a) *o*- (b) *m*- and (c) *p*-trifluoromethylnitrobenzene.

transfer[12]. The lifetime of these species is long relative to the potential sweep rate as evidenced by data in Table 1 and Fig. 1. Each isomer exhibits a second cathodic current response at higher potentials on the initial voltage excursion (Fig. 1). As previously discussed, application of the Nicholson and Shain diagnostic criteria[13] to data for the *ortho* and *meta* isomers suggests that each is primarily reduced via a chemical reaction coupled between two reversible electron transfers. The anion radical of the corresponding nitroso compound is a product of the electrochemical step.

$$RNO_2^{\cdot -} + e^- \rightleftarrows RNO_2^{2-}$$

$$RNO_2^{2-} + 2\,H^+ \rightarrow RNO + H_2O$$

$$RNO + e^- \rightleftarrows RNO^-$$

TABLE I

CYCLIC VOLTAMMETRIC DATA FOR TRIFLUOROMETHYLNITROBENZENES IN DMF SOLVENT AT A PLANAR PLATINUM DISC ELECTRODE[a]

v ($V\ min^{-1}$)	First wave				Second wave	
	$-(E_p)_c$ (V)	$(E_p)_c-(E_p)_a$ (mV)	$(i_p)_a/(i_p)_c^b$	$(i_p)_c/v^{\frac{1}{2}}$ ($\mu A\ V^{-\frac{1}{2}}\ min^{-\frac{1}{2}}$)	$-(E_p)_c$ (V)	$(i_p)_c/v^{\frac{1}{2}c}$ ($\mu A\ V^{-\frac{1}{2}}\ min^{-\frac{1}{2}}$)
p-Trifluoromethylnitrobenzene						
16.06	0.88	60	1.0	33.54	1.95	78.55
10.71	0.88	60	1.0	33.64	1.95	81.04
5.35	0.88	60	1.0	33.55	1.94	88.31
2.14	0.87	60	1.0	33.60	1.93	94.24
1.61	0.87	60	1.0	35.43	1.90	98.43
m-Trifluoromethylnitrobenzene						
17.71	0.99	65	1.0	42.16	2.21	77.20
11.81	0.98	65	1.0	42.88	2.20	80.67
5.90	0.97	60	1.0	44.24	2.15	88.48
2.36	0.97	60	1.0	44.45	2.09	89.29
1.77	0.97	60	1.0	41.35	2.07	92.11
o-Trifluoromethylnitrobenzene						
16.99	1.02	70	1.0	26.70	2.10	49.15
11.33	1.02	70	1.0	26.71	2.10	49.70
5.66	1.00	70	1.0	27.36	2.09	52.52
2.27	1.00	60	1.0	26.49	2.04	53.00
1.70	1.00	60	1.0	26.92	2.02	54.85

[a] All solutions 0.1 M in tetra-N-propylammonium perchlorate.
[b] Scan reversal 120 mV past $(E_p)_c$.
[c] (i_p) measured by extrapolating current from first wave.

This assertion is substantiated by the appearance of a reversible one-electron couple at potentials less cathodic than that representing the reduction of the parent compound (Fig. 1). This couple is only present after voltage excursion past the second wave and is consistent with the production of the nitroso group, known to be more reducible than the parent nitro compound[6,10]. Data recorded for *p*-trifluoromethylnitrobenzene demonstrate similar electrochemical activity, with a weak nitroso couple apparent (Fig. 1, Table I). Chronoamperometric data taken under duplicate conditions at a p.p.d.e. confirms an n (apparent) value of 1.8, 1.9 and 2.1 for the second reduction wave of *o*-, *m*- and *p*-trifluoromethylnitrobenzene, respectively.

Mass electrolysis

In order to determine the nature of reactions occurring in bulk solution and not totally evident from the rapid voltammetric experiments, the compounds *o*- and *p*-trifluoromethylnitrobenzene were mass electrolyzed at a platinum gauze cathode, at a constant potential above the second voltammetric wave of each. The progress of the electrolysis was monitored by current decay. The relative decay rates at an applied potential of -2.0 V for electrolysis of 1 mM solutions of the *ortho* and *para* isomers are given in Fig. 2. The cell current for electrolysis of the

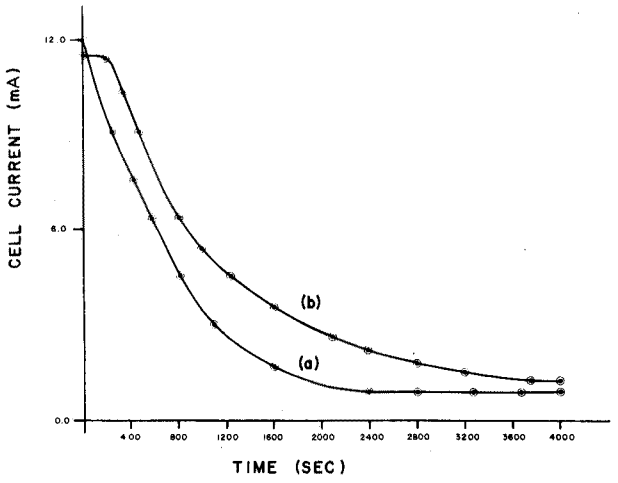

Fig. 2. Decay of cell current in mass electrolysis of 150 ml of 1m*M* solutions of (a) *o*- and (b) *p*-trifluoromethylnitrobenzene at a platinum gauze electrode.

ortho isomer decayed exponentially to a residual current. Current decay for electrolysis of the *para* isomer was approximately exponential and decayed to a residual current slightly above that of the *ortho* isomer (Fig. 2).

Aliquots of the catholyte were removed periodically and diluted with an appropriate amount of dry DMF, and the u.v.–visible spectrum recorded. The *para* isomer exhibits a u.v. absorption peak with a λ_{max} near 270 nm in DMF solvent (Fig. 3). A broad peak at 320 nm is observed after 15 min of electrolysis. It intensifies with continued electrolysis and predominates when a limiting cell current is established (Fig. 3). This broad absorption band is consistent with the azoxy coupling product. The broad visible absorption band near 425 nm is consistent with an azo coupling product. These results are analogous to those from electrolysis of *o*-trifluoromethylnitrobenzene[11].

In summary, results of the voltammetric experiments demonstrate that each

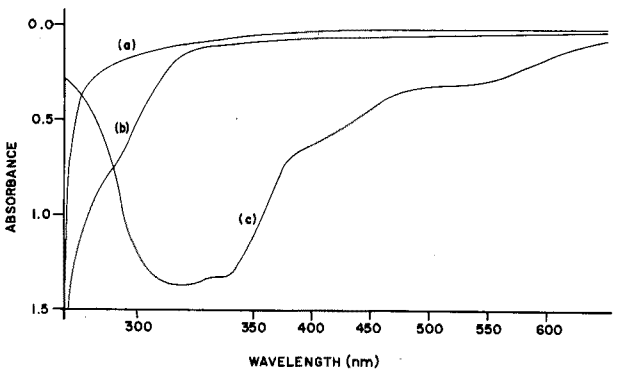

Fig. 3. U.v.–visible spectra of (a) DMF solvent (b) *p*-trifluoromethylnitrobenzene in DMF and (c) catholyte solution after electrolysis of *p*-trifluoromethylnitrobenzene to a residual cell current.

nitro isomer is initially reduced to the nitroso anion radical at its second current plateau by a common mechanism. Some competing reactions are suggested. Long-term experiments show that the products of exhaustive mass electrolyses of each nitro compound are primarily azoxy and azo compounds.

Potential step

Comparison of the cyclic voltammograms shown in Fig. 1 reveals that the follow-up wave, identified as the nitroso couple, produced by voltage excursion past the second wave of each parent nitro compound, is much less pronounced in the *para* isomer than in either the *ortho* or *meta*. In general, under the same conditions of concentration, electrode size, potential sweep rate, and reversing potential, the order of peak current intensity of the nitroso couple is *ortho* > *meta* > *para*.

The relative intensities of these couples produced from each nitro isomer, *i.e.* the quantity of nitroso compound present after electrolysis at the second wave for a fixed time, was further investigated with potential step and hold experiments at a p.p.d.e. coupled with cyclic voltammetry following a predetermined holding time. Specifically, five experiments were conducted on each parent compound. In each experiment the potentiostat potential was stepped to a fixed potential on the diffusion plateau of the second wave and held for 15 s. The potential was then stepped to 0.0 V and triangularly swept at a predetermined sweep rate to a switching potential 100 mV cathodic of the nitroso-couple current maximum. Only the sweep rate of the cycle was varied in each experiment. Experiments conducted in such a manner, with following multi-cycles, demonstrated that diffusion of the nitroso product away

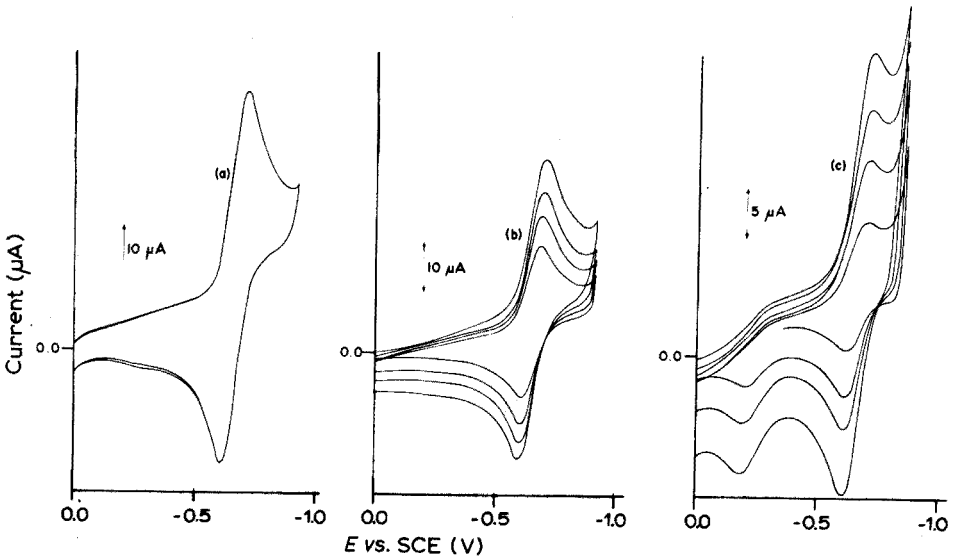

Fig. 4. Cyclic voltammograms of trifluoromethylnitrosobenzene intermediates produced at a p.p.d.e. electrode by stepping potential of electrode to second reduction wave of the parent nitro compound. (a) Two separate voltammograms of *o*-trifluoromethylnitrosobenzene produced by potential step and hold to demonstrate reproducibility of technique, (b) *o*-Trifluoromethylnitrosobenzene recorded at varying potential sweep rates. (c) *m*-Trifluoromethylnitrosobenzene recorded at varying potential sweep rates.

from the stationary electrode is slow relative to the time of the experiment, and the voltammetric data proved to be reproducible, (Fig. 4). Such experiments not only signified the quantity of nitroso compound available at the electrode but allowed investigation of the electrochemistry of the intermediate at its lowest reduction potential.

Potential step and hold produced a nitroso couple from *o*-trifluoromethylnitrobenzene with a cathodic peak current approximately twice that for the *meta* isomer (Fig. 4). Experiments on *p*-trifluoromethylnitrobenzene, conducted under identical conditions, produced only a very weak nitroso couple.

TABLE II

CYCLIC VOLTAMMETRIC DATA FOR REDUCTION OF TRIFLUOROMETHYLNITROSOBENZENE INTERMEDIATES PRODUCED BY POTENTIAL JUMP[a]

Sweep rate ($V\ min^{-1}$)	*First wave*			
	$-(E_p)_c$ (V)	$(E_p)_c-(E_p)_a$ (mV)	$(i_p)_a/(i_p)_c$	$(i_p)_c/v^{\frac{1}{2}}$ ($\mu A\ V^{-\frac{1}{2}}\ min^{-\frac{1}{2}}$)
o-Trifluoromethylnitrosobenzene				
10.80	0.68	59	1.0	9.12
8.64	0.68	59	1.0	9.18
6.48	0.68	59	1.0	9.24
4.32	0.68	58	1.0	9.00
2.16	0.68	57	1.0	4.76[b]
m-Trifluoromethylnitrosobenzene				
10.56	0.72	70	—[c]	3.90
8.45	0.72	70	—[c]	4.12
6.34	0.72	67	—[c]	3.77
4.22	0.72	67	—[c]	3.76
2.11	0.71	65	—[c]	2.76[b]

[a] Potential jumped to value 200 mV cathodic of second wave current peak of parent nitro compound.

[b] Diffusion of intermediate away from working electrode becomes significant at extremely slow sweep rates.

[c] Reliable measurement of anodic current no possible due to close proximity of couple to least negative couple of parent nitro compound.

The diagnostic criteria[12] taken from the cyclic voltammograms of the nitroso couple derived from the *ortho* and *meta* isomers are given in Table II. The anodic to cathodic peak current ratio of 1.0 and the constant current function at all sweep rates is clearly consistent with the reversible production of a long-lived nitroso anion radical. Unsubstituted nitrosobenzene does not exhibit parallel behavior under similar conditions[6].

DISCUSSION

The data presented herein suggest that the isomeric trifluoromethylnitrobenzenes are reduced by the same mechanism to the corresponding trifluoro-

methylnitrosobenzene anion radical. However, cyclic voltammetric data demonstrate a significant difference in lifetimes of these radical species. The lifetime of the nitroso intermediate is determined by following reactions of a chemical and/or electrochemical nature[10]. The azoxy and azo products, found to predominate in bulk solution after electrolysis, are the result of coupling reactions between two nitroso groups, two hydroxylamine groups or nitroso with hydroxylamine[7–9]. The abundance and stability of the *o*-trifluoromethylnitrosobenzene intermediate near the electrode surface suggests that the product found in long-term mass electrolysis of this isomer is largely a result of coupling between two of the nitroso intermediates. The lack of *p*-trifluoromethylnitrobenzene near the electrode after voltage excursion suggests that the electrochemical formation of reduced products, such as the hydroxylamine, competes favorably with coupling reactions at potentials of the second wave, or conversely that the coupling rate of *p*-trifluoromethylnitrosobenzene radicals is very rapid. The difference in the current–time curves in the long-term constant potential electrolysis experiments suggests that the route to the azoxy product of the *para* isomer is via intermediates other than nitrosobenzene, and is consequently consistent with the former suggestion. The slightly larger chronoamperometric *n* (apparent) value of the second wave of the *para* isomer is also consistent with these observations.

Holtz[14] has presented a discussion of the unique Hammett behavior of the trifluoromethyl substituent. An inductive model, called the π-inductive effect[15], was employed to rationalize the greater than normal negative charge delocalization by the trifluoromethyl group on an aromatic ring. In this model, the strong electron-withdrawing effect of the trifluoromethyl group is explained by the existence of a dipole external to the benzene ring polarizing the π-system and enhancing negative charge delocalization as shown in structure I. A model of this type appears to be consistent with the reactivity of the isomeric trifluoromethylnitrosobenzene radical intermediates as evidenced by the present data. The overall enhanced stability of these radical species is probably due to inductive charge delocalization from the nitroso group. The *p*-substituted intermediate would be more susceptible to further electron addition by structure I, and visualization of a contributing structure such as II for the *ortho* isomer explains its great stability relative to further reduction and coupling reactions. Stability of the *meta* isomer should be intermediate between the *ortho* and *para* by this model.

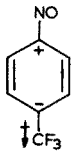

I

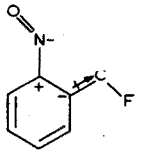

II

The authors gratefully acknowledge the financial support of the Robert A. Welch Foundation (Grant No. AO-337). The authors are indebted to Dr. E. H. Sund for the synthesis and purification of *p*-trifluoromethylnitrobenzene.

SUMMARY

The relative lifetimes of the *o*-, *m*- and *p*-trifluoromethylnitrosobenzene anion radicals produced in the electroreduction of the corresponding nitro compounds in N,N-dimethylformamide are compared. Potential step experiments coupled with cyclic voltammetry facilitate the comparison. The fate of the nitroso species is discussed in relation to the results of experiments in which *o*-, *m*- and *p*-trifluoromethylnitrobenzene were mass electrolyzed and the products spectrophotometrically identified.

REFERENCES

1 J. Pearson, *Trans. Faraday Soc.*, 44 (1948) 683.
2 I. M. Kolthoff and J. J. Lingane, *Polarography*, Vol. 2, Interscience, New York, 2nd edn., 1952.
3 O. Paez, E. T. Seo and H. P. Silverman, *Technical Report ECOM-02464-1*, U.S. Army Electronic Command.
4 A. H. Maki and D. H. Geske, *J. Amer. Chem. Soc.*, 83 (1961) 1852.
5 P. H. Rieger and G. K. Fraenkel, *J. Chem. Phys.*, 39 (1963) 609.
6 W. Kemula and R. Sioda, *Bull. Acad. Pol. Sci., Ser. Sci. Chim.*, 10 (1962) 507.
7 C. R. Noller, *Chemistry of Organic Compounds*, Saunders, Philadelphia, 3rd edn. 1965.
8 E. J. Geels, R. Konaka and G. A. Russell, *Proc. Chem. Soc. London*, (1965) 13.
9 G. A. Russell and E. J. Geels, *J. Amer. Chem. Soc.*, 87 (1965) 122.
10 R. D. Allendoerfer and D. H. Rieger, *J. Amer. Chem. Soc.*, 88 (1966) 3711.
11 W. N. Greig and J. W. Rogers, *J. Amer. Chem. Soc.*, 91 (1969) 5495.
12 R. S. Nicholson and I. Shain, *Anal. Chem.*, 36 (1964) 706.
13 R. S. Nicholson and I. Shain, *Anal. Chem.*, 37 (1965) 178.
14 D. Holtz, *Chem. Rev.*, 71 (1971) 139.
15 M. J. S. Dewar, *Hyperconjugation*, Ronald Press, New York, 1962, pp. 155, 156.
16 J. W. Rogers and W. H. Watson, *J. Phys. Chem.*, 72 (1968) 68.
17 E. B. Starkey, *J. Amer. Chem. Soc.*, 59 (1937) 1479.

Analytica Chimica Acta, 71 (1974) 443–450

SOME CONSIDERATIONS ON REACTION RATE METHODS—THE ANALYTICAL USE OF MODIFYING EFFECTS OF LIGANDS IN SOME ELECTRON-TRANSFER REACTIONS

HORACIO A. MOTTOLA

Department of Chemistry, Oklahoma State University, Stillwater, Oklahoma 74074 (U.S.A.)

(Received 26th November 1973)

The increased concern with health-related problems and the desire to examine (or re-examine) the sources of environmental change have generated renewed interest in the analytical chemistry of materials in solution, particularly at low concentrations. As a logical consequence of this emphasis, solution chemistry—and its analytical chemistry in particular—has evolved with new projections which create a demand for manpower with the expertise to solve contemporary, as well as future, analytical problems[1]. Trace metals, for instance, are of great importance in all branches of chemistry and allied sciences. The list of elements considered essential, in trace amounts, to animal nutrition and health continues to grow. There is need for improved methods for detection and estimation of these elements, as well as of organic species at trace levels, in particular those capable of coordinating metal ions: the need is mostly for (a) highly sensitive methods which can detect and determine traces and ultratraces of these materials, (b) more selective and accurate methods, and (c) easily automated procedures permitting fast acquisition of information.

Time, cost, better sampling, safety, and accuracy are, among others, strong reasons for the move of applied analytical chemistry toward automated analysis. Commercially available automatic analyzers are generally based on optical-absorption measurements, easily adapted to continuous as well as repetitive automatic analysis in solution.

Although all chemical systems at equilibrium have arrived there by a kinetic background rich in analytically useful information, the practice of analytical chemistry has been dominated by a methodology based on measurements made at equilibrium. Analytical methods utilizing reaction-rate measurements have, however, received increased attention since the early 1960's. This interest has been stimulated by research in academic circles which has, in recent years, been largely responsible for the instrumentation necessary to make kinetic methods competitive with the dominant thermodynamically based determinations. Kinetic methods offer an attractive alternative for trace analysis in solution compared to most equilibrium-based methods. Their sensitivity is considered comparable to that obtained in activation analysis and by luminescence methods[2], and reaction-rate measurements are easily automated. Only recently, however, have these methods found a place in undergraduate textbooks[3], and two monographs devoted to them have been published since 1966[2,4]. Several recent reviews have updated the use of rate measurements in analytical chemistry[5–9].

The kinetic approach to analysis has been successfully applied to the detection and determination of traces of metals which act as catalysts, and is probably the most sensitive technique presently available for the direct or indirect determination of anions and some organic species in solution. Its application to the latter area, however, is rather recent. Broadly speaking, kinetic methods of analysis are based on monitoring the rate of change in a reactant (or product) concentration. In catalytically based methods, the main reaction in which the monitored species participates, written as a stoichiometric and over-all reaction, is termed the indicator reaction. Tabulation of some indicator reactions can be found in the literature[2,9,10]. With only a few exceptions, these tabulations list reactions used for the determination of metal ions or inorganic anions that act as catalysts of the indicator reaction. The catalyzed reactions (particularly redox) are the most widely applicable of the kinetic methods and the proven chemical systems for the direct or indirect determination of low concentrations of organic species in solution[11–19]. These applications are mainly based on the modifying effect of complexing agents (chelating agents in particular) on the catalytic action of metal ion species for the oxidation of selected dyes exhibiting high molar absorptivities.

MODIFICATION OF CATALYTIC REACTION RATES BY ORGANIC SPECIES IN SOLUTION

The potential use of some of such modifying effects was recognized by Yatsimirskii in his monograph[2], but he did not describe chemical applications for the determination of organic species in solution. The use of metal ion catalysis in detection and determination of complexing agents has, however, been reported, and a method has been developed for the determination of ethylenediamino-N,N,N′,N′-tetraacetic acid (EDTA) at the 10^{-6} *M* level[12]. Previous to that, Olson and Margerum[20] pointed out the use of "coordination chain" reactions for the determination of metal ions in low concentrations, and complexing ligands of the EDTA family. Recently, Janjič and Milovanovič[11] reported the use of a new "indicator reaction" for the determination of amino acids at low concentrations. Their method makes use of the copper-catalyzed pyrocatechol violet–hydrogen peroxide indicator reaction. The modifying effect of nitrogen-containing ligands, aminopolycarboxylic acids, and some other ligands on a copper(II)-catalyzed reaction had previously been employed[13], with the ascorbic acid–oxygen indicator reaction.

The work initiated in 1966 (ref. 12) on the modifying effect of ligands on redox reactions involving organic species (many of them dyes) of high molar absorptivity, has been continued, and a few analytical methods exploiting such modifying effects have been developed. At this stage of development it is possible to distinguish, from an analytical viewpoint, three general types of effects, which can be classified[21] as (a) inhibition, (b) true metal-complex catalysis, and (c) promotion (Table I). This classification results from adopting, as the definition of a catalyst, a chemical species which remains unaltered at the end of each reaction cycle. Any of these modifying effects can be used for the determination of the modifying species or, in some cases, for increasing further the sensitivity in the determination of the metal catalyst itself[22,23]. The choice of kinetic approach to be used in the determination, however, depends to a large extent on the role played by the ligand (inhibition, true catalysis, or promotion).

TABLE I

RATE MODIFICATIONS OF CATALYTIC REACTIONS BY ORGANIC LIGANDS

Ligand effect	*Kinetic approach recommended*	*Observations*	*Ref.*
Inhibition	Initial rate or catalytic end-point indication	The catalytic end-point indication offers a more extended concn. range amenable to determination—the initial rate should offer, however, a lower limit of detection	15, 24, 25
True metal-complex catalysis	Variable time or initial rate	Besides being of theoretical and practical consideration, the variable time offers greater flexibility by choice of reference signals	17, 26, 27
Promotion	Initial rate or variable time	If the transient effect characterizing promotion is very short, implementation of the variable time is difficult—the initial rate approach seems to offer the best alternative	19

Inhibition

Experience accumulated at present indicates that the titrimetric approach with catalytic end-point indication[24, 25] offers a very convenient analytical means for the determination of inhibitors. An advantage of this approach is the increase in concentration range in which the inhibitor can be determined. Although some sacrifice in the limit of detection may be expected (not necessarily in all cases) depending on the instrumental approach used to carry out the titrations, in general the time required for analysis is also greatly reduced.

True metal-complex catalysis

If the modifying effect results in true metal-complex catalysis and the determination of either component, modifying species or metal catalyst, is contemplated, the variable-time procedure[26] appears superior from both a theoretical[27] as well as a practical viewpoint[17, 27]. In a review on the applications of kinetics to automated analysis, Pardue[28] has pointed to some advantages of the variable-time procedure. One is the fact that time can be measured with great accuracy and precision, and modern instrumentation[17, 29] allows synchronous measurements at different pre-selected compositions of the reacting systems, even with very simple devices easily adapted to common instrumental systems[17]. Judicious selection of signal levels permits determinations even after induction periods of variable length. Table II shows changes in the length of the induction period preceding the decolorization of malachite green in the determination of NTA[17] and the corresponding Δt values for the variable-time determination[30]. The Table also shows that selection of reference signals sufficiently beyond the induction period will allow reliable determinations by the variable-time procedure despite uncertainties in the length of this period. The uncertainties are assigned, in the particular case under consideration, to scattered effects arising from the order of reagent mixing and time elapsed for initiation of the reaction (injection of periodate to the system).

TABLE II

LENGTH OF INDUCTION PERIOD AND Δt VALUES IN THE DETERMINATION OF NITRILOTRIACETIC ACID[17]

([Mn(II)] = $5.0 \cdot 10^{-6}$ *M*. Other experimental and instrumental parameters were as reported previously[17])

NTA concn · 10^6 *(M)*	*Length of induction period (s)*	*Δt (s)*
0.00	153	30.5
2.00	153	21.1
4.00	189	15.2
4.00	159	15.2

Promotion

In the particular case of promotion, the metal complex provides a path requiring a lower activation energy than the uncatalyzed or even the metal-catalyzed reaction, but in doing so, the ligand is destroyed or converted to an inactive form. If the modifying effect is to be used for the determination of the ligand, this species must be the limiting factor for complexation (*i.e.*, $c_{metal} > c_{ligand}$, where c denotes the analytical concentration), and as soon as the ligand is destroyed (or inactivated) the overall rate tends toward the rate of the indicator reaction in the absence of a rate modifier. This is shown in Fig. 1 curve B, in a computer-simulated situation[31]. The result of this may be a rather brief, almost transient, modifying effect, and also a small effect at low ligand concentrations, but with adequate rapid mixing and signal monitoring devices—and application of the initial reaction rate (slope) kinetic method of determination (or the variable time in some cases)—a simple and fast determination of the modifying species can be accomplished.

ANALYTICAL APPLICATIONS OF INHIBITION, TRUE METAL-COMPLEX CATALYSIS, AND LIGAND PROMOTION

Recent reviews by Bontchev[23, 32] provide useful information for the development of analytical procedures for the determination of organic species, and include references to the application of ligand-modifying effects to increase the sensitivity for metal-catalyst determinations. Also recently, a selective determination of nitrilotriacetic acid (NTA)[17] has been reported using the variable-time approach, in which the modifying effect of NTA on the manganese(II)-catalyzed oxidation of malachite green cation appears as a true metal-complex catalysis both from equilibrium considerations[17] and from independent studies with ^{14}C-labeled NTA[33]. The experiments with ^{14}C-labeled NTA were performed in order to rule out promotion, since manganese(III) has been observed to induce decarboxylation in some redox reactions in which it is complexed by carboxyl oxygen[34, 35]. These studies were performed following modified procedures reported in the literature[36, 37] Some pertinent observations are discussed below.

(a) Some degree of decarboxylation was detected in samples containing labeled NTA. Decarboxylation after 30-min runs was found to be around 10% and constant over a wide range of concentrations ($1.0 \cdot 10^{-6}$–$1.0 \cdot 10^{-2}$ *M*) of

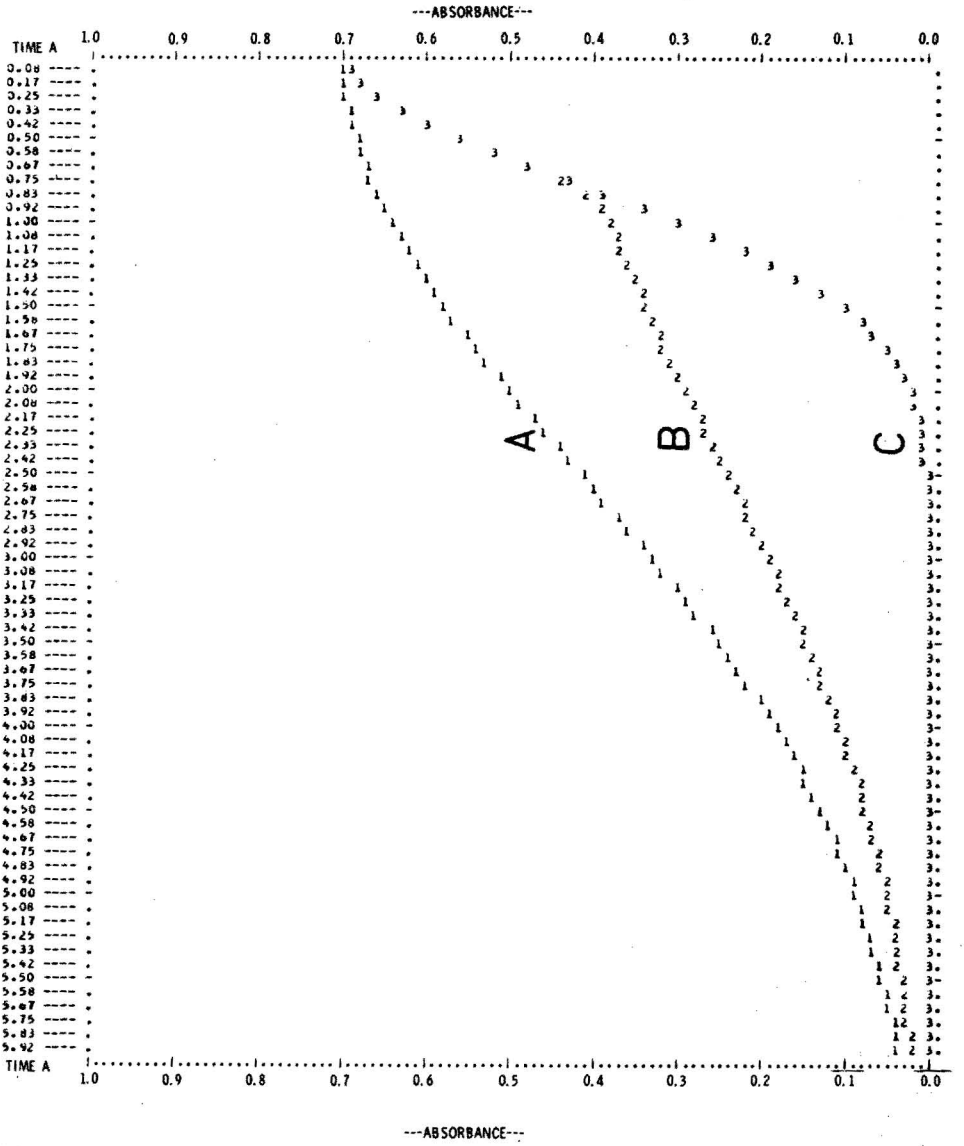

Fig. 1. Computer-simulated curves assuming ligand promotion and the following mechanism: $M^{n+} + Ox \rightleftarrows M^{(n+1)+} + Red$, $K_{eq} = 2.5 \cdot 10^6$; $M^{(n+1)+} + L \rightleftarrows ML$, $K_f = 3.2 \cdot 10^{19}$; $ML + Red' \overset{k'}{\rightarrow} Red\text{–}M\text{–}L$ (rate-determining) $k' = 10^6$ min^{-1}; Red′–M–L $\rightarrow M^{n+} + P + P'$. K_{eq}, conditional equilibrium constant; K_f, conditional formation constant; M^{n+} and $M^{(n+1)+}$, lower and higher oxidation state of the metal catalyst, respectively; L, modifying ligand; Ox and Red stand for oxidizing and reducing species respectively; P, products of oxidation of Red′; P′, products of decomposition of L. The normal catalytic path was assumed as $M^{(n+1)+} + Red' \overset{k}{\rightarrow} P + M^{n+}$, $k = 10^5\ M^{-1}$ min^{-1}. Curve A, no L added, $c_{M^{n+}} = 1.00 \cdot 10^{-5}$ M; curve B, $c_L = 5.00 \cdot 10^{-6}$ M, $c_{M^{n+}} = 1.00 \cdot 10^{-5}$ M; curve C, $c_L = 5.00 \cdot 10^{-5}$ M, $c_{M^{n+}} = 1.00 \cdot 10^{-5}$ M. Monitored species Red′; reaction pseudo-zero order with respect to Ox.

unlabeled NTA. Interestingly enough, runs with only 10^{-10} *M* labeled NTA show faster decolorization of malachite green than runs carried out in absence of NTA. The effect, however, is preceded by long induction periods.

(b) Runs performed in absence of malachite green gave the same trends and yields as those in presence of the triphenylmethane dye. This leads to the conclusion that the NTA decarboxylation is not due to the reaction of the Mn–NTA complex in the rate-limiting step, but to the normal rate of decarboxylation of the complex. Decarboxylation is first order with an approximate half-life of 7 h (Fig. 2). These results reinforce belief in a true metal-complex catalytic effect, probably involving a manganese(III)–NTA complex as the rate-limiting species.

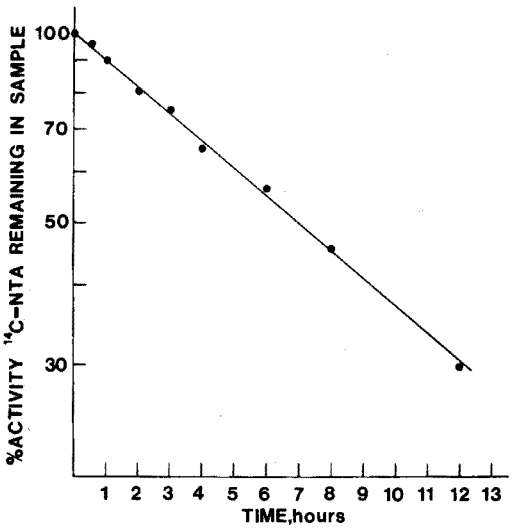

Fig. 2. Decay in ^{14}C-NTA activity (by $^{14}CO_2$ evolution) in the oxidation of malachite green cation (acetate–phosphate buffer of pH 3.5) by periodate and manganese(II) in the presence of nitrilotriacetic acid (NTA).

(c) Experiments using buffers (phosphate–acetate pH 3.5) containing labeled acetic acid yielded only 1–2% activity in the form of $^{14}CO_2$ in 30 min. Acetate ion is known to complex manganese(III) but the formation constant is much smaller than that for the manganese(III)–NTA complex. The low yield in decarboxylation may be due to the smaller amount of complex present, as well as a lower rate of spontaneous decarboxylation.

With the knowledge that NTA forms a series of mixed ligand complexes with transition metal ions and a variety of oxygen- and nitrogen-containing ligands, a few experiments were performed in the presence of pyridine, 1,10-phenanthroline, and 8-quinolinol. The data obtained confirmed the observed trend that if the complexing agent reacts quickly and forms a strong complex with manganese(II) (refs. 15, 17), inhibition is observed. 8-Quinolinol completely quenched the reaction if present in larger concentrations than NTA. At a pH of 4, the ratio of free manganese to complexed (by 8-quinolinol) manganese is only $7.0 \cdot 10^{-19}$. This suggests the use of catalytic end-point indication for the determination of extremely low concentrations of 8-quinolinol. Pyridine addition resulted in only a slight increase

(18–22%) of decarboxylation in 30-min periods and thus appears of very little analytical interest. However, the 1,10-phenanthroline experiments produced several points of interest.

(1) Increasing amounts of 1,10-phenanthroline dramatically reduced the rate of carbon dioxide evolution. This was observed even at NTA: 1,10-phenanthroline ratios of 1:1. Hence, mixed ligand complex formation cannot be completely ruled out because of the pK_a value of 1,10-phenanthroline. The manganese(II) complex of 1,10-phenanthroline has a formation constant for the 3:1 complex of about the same magnitude as that of the 1:1 manganese(II)–NTA complex.

(2) 1,10-Phenanthroline, on an equimolar basis, accelerates the rate of oxidation of malachite green by periodate in the presence of substoichiometric amounts of manganese(II) 10 times as much as NTA does. This observation is of analytical significance.

The procedure reported by Janjič and Milovanovič[11] is based on the formation of 1:1 copper–amino acid complexes possessing lower catalytic activity than the solvated copper ion. As such, the effect could either be termed a partial inhibition or be classified as a true metal-complex catalytic effect. Application of catalytic end-point indication or the variable time procedure would be difficult because very little difference in rate in the absence and in the presence of ligand is reported[11]. From an analytical viewpoint, inhibition or the formation of a complex exercising a markedly different catalytic rate constitutes a modifying effect with greater analytical promise.

No analytical applications of a recognized case of promotion to the determination of organic species in solution, have as yet been published. However, microgram amounts of oxalic acid remarkably enhance the initial rate of oxidation of the tris(1,10-phenanthroline)iron(II) complex, ferroin, by chromium(VI) in relatively low concentrations of sulfuric acid[19]. The modifying effect of oxalic acid has been successfully applied to the determination of the oxalic acid content of human blood serum and urine[19]. Citric acid behaves like oxalic acid but its effect is less pronounced. All observations accumulated up to the present point to partial destruction of the oxalic acid and citric acid during their action on the main reaction. Formation of a reactive complex involving the carboxylic acid and chromium(VI), (V) or (IV) seems to account for the promoting effect. Conversion of the ratemodifying species to an inactive form by destruction or, mainly, by complexation with chromium(III)—one of the products of the indicator reaction—is probably responsible for the lack of a catalytic cycle.

This work was supported by the National Science Foundation (Grant GP-38822X) and by the College of Arts and Sciences, Oklahoma State University.

SUMMARY

The utilization of modifications of the rate of metal-catalyzed reactions (mainly redox reactions involving organic dyes of relatively high molar absorptivities) by other organic species (ligands) is outlined. This extension of catalytic reaction-rate methods in solution is of recent development and suggests the possibility of further analytical procedures. Three main types of modifications, (a) inhibition,

(b) true metal complex catalysis, and (c) promotion, are distinguished, and their applications to analytical determinations are discussed.

REFERENCES

1 See for instance: (a) *Annual Report of the Division of Chemistry and Chemical Technology*, National Research Council–National Academy of Sciences, Washington, D.C., 1972; (b) *Chem. Eng. News*, 20th Nov. 1972, p. 13.
2 K. B. Yatsimirskii, *Kinetic Methods of Analysis*, Pergamon, Oxford, 1966.
3 (a) H. A. Laitinen, *Chemical Analysis*, McGraw-Hill, New York, 1960, Ch. 24; (b) J. Fritz and G. Schenk, *Quantitative Analytical Chemistry*, Allyn and Bacon, Boston, 1966, Ch. 13; (c) R. L. Pecsok and L. D. Shields, *Modern Methods of Chemical Analysis*, Wiley, New York, 1968, Ch. 18; (d) W. F. Pickering, *Modern Analytical Chemistry*, Dekker, New York, 1972.
4 H. B. Mark, Jr. and G. A. Rechnitz, *Kinetics in Analytical Chemistry*, Interscience, New York, 1968.
5 R. A. Greinke and H. B. Mark, Jr., *Anal. Chem.*, 44 (1972) 295R.
6 H. B. Mark, Jr., *Talanta*, 19 (1972) 717.
7 H. V. Malmstadt, *Critical Reviews in Analytical Chemistry*, 2 (1972) 559.
8 H. V. Malmstadt, E. A. Cordos and C. J. Delaney, *Anal. Chem.*, 44 (1972) 26A, 79A.
9 A. M. Gary and J. P. Schwing, *Bull. Soc. Chim. Fr.*, (1972) 3657.
10 Z. Gregorowicz and T. Suwinska, *Chem. Anal. (Warsaw)*, 11 (1966) 3.
11 T. J. Janjič and G. A. Milovanovič, *Anal. Chem.*, 45 (1973) 390.
12 H. A. Mottola and H. Freiser, *Anal. Chem.*, 39 (1967) 1294.
13 H. A. Mottola, M. S. Haro and H. Freiser, *Anal. Chem.*, 40 (1968) 1263.
14 H. A. Mottola and H. Freiser, *Anal. Chem.*, 40 (1968) 1266.
15 H. A. Mottola, *Anal. Chem.*, 42 (1970) 630.
16 G. L. Ellis and H. A. Mottola, *Anal. Chem.*, 44 (1972) 2037.
17 H. A. Mottola and G. L. Heath, *Anal. Chem.*, 44 (1972) 2322.
18 D. W. Margerum and D. K. Steinhaus, *Anal. Chem.*, 37 (1965) 225.
19 V. V. S. Eswara Dutt and H. A. Mottola, *Biochem. Med.*, 9 (1974) 148.
20 D. C. Olson and D. W. Margerum, *J. Amer. Chem. Soc.*, 85 (1963) 297.
21 A. E. Martell, *Pure Appl. Chem.*, 17 (1968) 129.
22 H. A. Mottola and C. R. Harrison, *Talanta*, 18 (1971) 683.
23 P. R. Bontchev, *Talanta*, 19 (1972) 675.
24 H. Weisz and S. Pantel, *Anal. Chim. Acta*, 62 (1972) 361.
25 H. A. Mottola, *Talanta*, 16 (1969) 1267.
26 W. J. Blaedel and G. P. Hicks in C. N. Reilley (Ed.), *Advances in Analytical Chemistry and Instrumentation*, Vol. 3, Interscience, New York, 1964, pp. 130–133.
27 J. D. Ingle, Jr. and S. R. Crouch, *Anal. Chem.*, 43 (1971) 697.
28 H. L. Pardue in C. N. Reilley and F. W. McLafferty (Eds.), *Advances in Analytical Chemistry and Instrumentation*, Vol. 7, Wiley, New York, 1969, pp. 154–155.
29 R. A. Parker, H. L. Pardue and B. G. Willis, *Anal. Chem.*, 42 (1970) 56.
30 G. L. Heath, *M. S. Thesis*, Oklahoma State University, 1972.
31 B. E. Simpson and H. A. Mottola, unpublished results, 1972.
32 P. R. Bonchev, *Talanta*, 17 (1970) 499.
33 R. J. Everett and H. A. Mottola, unpublished results, 1972.
34 H. Taube, *J. Amer. Chem. Soc.*, 69 (1948) 1216.
35 K. A. Schroeder and R. E. Hamm, *Inorg. Chem.*, 3 (1964) 391.
36 J. M. Passman, N. S. Radin and J. A. D. Cooper, *Anal. Chem.*, 28 (1956) 484.
37 J. R. Herberg, *Anal. Chem.*, 32 (1960) 42.

Analytica Chimica Acta, 71 (1974) 451–457

POTENTIOMETRIC DETERMINATION OF BORON IN BOROSILICATE GLASSES

ROBERT L. KOCHEN

The Dow Chemical Company, Rocky Flats Division, Golden, Colorado 80401 (U.S.A.)

(Received 22nd December 1973)

Borosilicate glass Raschig rings are used as a nuclear poison to prevent any critical incident in the processing of solutions containing fissionable material. The Raschig rings are randomly packed into containers[1] before the fissile solutions are added. A critical reaction is prevented by the boron-10 present in the rings. Boron-10 absorbs thermal neutrons as shown in the following reaction[2],

$$^{10}B_5 + {}^1n_0 \rightarrow {}^7Li_3 + {}^4He_2 + 2.5 \text{ MeV}$$

and is the key isotope for the absorption of thermal neutrons. Natural boron contains an isotopic average of 19.78 wt% ^{10}B and 88.22 wt% ^{11}B.

Boric oxide is the boron compound used in the manufacture of Raschig rings. Specifications call for a composition of 11.8 wt% minimum and 13.8 wt% maximum B_2O_3 (ref. 3). If the quantity of boric oxide in a Raschig ring is known, the amount of ^{10}B present can be calculated from the isotopic composition. Mechanical abrasion and chemical corrosion can cause weight losses of Raschig rings[4] resulting in boron-depleted rings. In addition, boron may be chemically leached from the Raschig rings, which also decreases their effectiveness. It is therefore necessary that the rings be sampled and checked periodically for their boron content.

To determine rapidly the boron content of borosilicate glasses, a new quantitative method has been developed. It involves an ion-exchange separation and a direct electrode potentiometric determination of boron as the tetrafluoroborate ion. The potentiometric determination is a modification of a published method[5].

EXPERIMENTAL

Equipment

Anion-exchange columns were prepared by placing a small cotton plug into a plastic 25-ml burette followed by 2 ml of Amberlite XE-243 (20–80-mesh) boron-specific resin. Distilled water was passed through the burette to settle the resin. Cation-exchange columns were prepared in a similar manner, except that 5 ml of Dowex 50W-X8 (50–100-mesh) resin in the hydrogen form was used. Before each use, the Dowex 50W-X8 resin was regenerated by first adding 16 ml of 3 *M* hydrochloric acid followed by 32 ml of distilled water. However, after each use, the Amberlite XE-243 resin in each anion-exchange column was replaced

with new resin. Efforts to regenerate the Amberlite XE-243 resin completely for repeated use were unsuccessful.

An Ionalyzer Model 801 digital pH meter was used with a Model 92-05 Ionalyzer fluoroborate ion electrode and a Model 90-01 Ionalyzer single-junction reference electrode. The single-junction reference electrode was filled with a saturated solution of potassium chloride saturated with silver ions.

Reagent-grade chemicals were used throughout all procedures and Nalgene plastic laboratory ware was generally used for concentrated hydrofluoric acid solutions.

Sample preparation

National Bureau of Standards Borosilicate Glasses Nos. 92 and 93 were used to prepare 15 glass standards. The NBS samples Nos. 92 and 93 (in powder form) contained 0.70 and 12.76 wt% B_2O_3, respectively. The standards were first dried at 105°C for 24 h, placed inside a desiccator, and allowed to reach ambient temperature. Five samples containing 5 wt% B_2O_3 and five samples containing 10 wt% B_2O_3 were then prepared by weighing and combining the appropriate amounts of the standards. Five samples containing 12.76 wt% B_2O_3 were weighed directly from the NBS No. 93 standard. Each of the 15 prepared glass standards had a weight of 1.6099 g.

In addition to these fifteen glass standards, three borosilicate Raschig rings (Corning Glass Works) were used as samples. Each of these rings was divided into three rings to give a total of nine rings. Each ring and two 25-mm diameter steel ball bearings were placed into a 3-mm thick steel container (5-cm i.d. × 13-cm). This assembly was mounted in a commercial paint shaker and shaken for 15 min to pulverize the glass to a fine powder. Three 1.6099-g aliquots were then taken from each of the nine pulverized rings, resulting in a total of 27 samples.

Sample analysis

Place each weighed sample in a 250-ml plastic Erlenmeyer flask. Add 2 ml of distilled water to each flask to form a slurry, followed by 10 ml of concentrated (48 wt%) hydrofluoric acid. Cover each flask with a plastic stopper and swirl under a stream of cold tap water to dissipate the heat of reaction. Complete dissolution of the borosilicate glass and formation of the tetrafluoroborate ion should be achieved in 10 min at room temperature. Add about 100 ml of distilled water to each sample flask, and quantitatively transfer the contents of each flask to a 1-l volumetric flask, partially filled with distilled water. Add distilled water to bring the volume to 1 l. This results in a 0.2 *M* HF solution. Pipette 25 ml of this solution onto a wet anion-exchange column. Allow the solution to set for 2 min before releasing it through the column. After passing through the column at a flow rate of about 2 ml min^{-1}, discard the solution. Elute the tetrafluoroborate, adsorbed by the anion-exchange resin, by passing 20 ml of 0.3 *M* sodium hydroxide through the column. Collect the eluate in a 250-ml beaker and then pour into a wet cation-exchange column. Collect the resulting effluent, a mixture of tetrafluoroboric acid in dilute hydrofluoric acid, in a 25-ml volumetric flask and dilute to 25 ml with 0.5 *M* ammonia solution. This produces a pH value in the range 6–7.

Transfer the 25 ml of solution to a 250-ml beaker and stir magnetically. Place a 6-mm thick sheet of cork between the stirrer and the beaker to act as a thermal insulator. As each sample is stirred, obtain the potential measurements, representing tetrafluoroborate ion concentrations, with the ion electrode. The measurements should be conducted within 30 min of sample preparation. Response time for all of the potentiometric measurements with the fluoroborate electrode is less than 2 min. The response time is only a few seconds for the more concentrated boron solutions.

After analysis all samples were covered with Petri dishes, to help control evaporation, and stored for later evaluation.

The NBS standards were analyzed first. At the end of 24 h, the standard samples were brought back to their original 25-ml volume with distilled water. A second set of potential measurements was then obtained. The Raschig ring samples were then analyzed. A 50-p.p.m. (by weight) boron standard solution was used for restandardization. The calibration control on the Ionalyzer digital pH meter was set so that the original millivolt reading was obtained on the 50-ppm standard. Potential measurements were then obtained on the Raschig ring samples. At the end of 7 days, the Raschig ring samples were brought back to their original 25-ml volume with distilled water. A second set of potential measurements was then obtained.

All operations were conducted at room temperature ($25 \pm 2°C$). Both the NBS standard samples and the Corning Raschig ring samples were run in a random sequence, required for evaluation of the results by an analysis of variance.

RESULTS

A calibration graph for the ion-exchange–potentiometric determination of boron was plotted with the data obtained from the National Bureau of Standards Glasses (NBS 92 and 93) given in Table I. On semilogarithmic graph paper, the plot was a straight line. Since no standards were available above 12.76 wt% B_2O_3, the curve was extrapolated above this value so that it could be used on Raschig ring samples that contained up to 23 wt% B_2O_3. With this curve, the boron concentrations in the Corning Raschig ring glasses were determined by the

TABLE I

DATA FOR STANDARD CURVE

NBS Standard[a] *(% B_2O_3)*	*E.m.f. (mV) (Mean ± s)*[b]	*B content of solutions*	
		(p.p.m.)	*(mg/25 ml)*
5	173.3 ± 2.6	25.0	0.625
10	153.0 ± 1.8	50.0	1.250
12.76	145.2 ± 1.5	63.8	1.595

[a] Prepared by mixing required amounts of NBS Standards No. 92 (0.70 wt% B_2O_3) and No. 93 (12.76 wt% B_2O_3) or using No. 93 by itself.

[b] 5 determinations on each standard.

described method. These results are summarized in Table II, which also includes mean values for the Corning results.

The experiments for both the NBS standards and the Raschig rings were designed so that the data obtained could be evaluated by an analysis of variance. There was no statistically significant difference in the results of the NBS standards between the three concentrations or between the same solutions analyzed within 24 h. For the Raschig rings, the only significant difference observed was between results obtained on the same sample solution analyzed after 7 days; this difference is attributed to hydrolysis of the tetrafluoroborate ion.

The pooled standard deviation of the potentiometric measurements on the NBS standards obtained on the same day was ± 2.0 mV. When the measurements obtained on two days were combined, the pooled standard deviation was ± 2.2 mV. Comparable precision was obtained on the Raschig rings.

TABLE II

ANALYSES OF RASCHIG RINGS

Sample No.	*Wet chemical*[a] *results (% B_2O_3)*	*E.m.f. (mV) (mean ±s)*[b]	*% B_2O_3 (mean ±s)*[b]	*Error*	
				Mean (% B_2O_3)	*Relative %*
ML-2139	9.54	152.9±1.8	9.92±0.60	−0.38	−3.98
ML-2143	15.59	136.0±1.2	17.48±0.74	−1.89	−12.12
ML-2144	22.32	126.7±2.0	23.87±1.6	−1.56	−6.99

[a] Data supplied by Corning Glass Works. A potentiometric titration of the boron–mannitol complex was used for the analyses.
[b] 9 determinations on each sample.

The sensitivity of the potentiometric method is shown with determinations down to 0.625 mg boron/25 ml ($5.78 \cdot 10^{-5}$ *M*) (Table I). The average percent of difference between values of the Corning Glass Works and those of the potentiometric method is −7.7%. The results are shown in Table II.

DISCUSSION

Dissolution of the borosilicate glasses and formation of the tetrafluoroborate ion are believed to proceed in the following manner. First, the silicate glass is dissolved by the concentrated (48 wt%) hydrofluoric acid[6];

$$SiO_2 + 6\ HF \rightarrow H_2SiF_6 + H_2O$$

With the silicate glass structure dissolved, the boric oxide hydrates rapidly to the metaboric and orthoboric acids[7];

$$B_2O_3 + H_2O \rightarrow 2\ HBO_2$$

$$B_2O_3 + 3\ H_2O \rightarrow 2\ H_3BO_3$$

These then react with the concentrated hydrofluoric acid to form tetrafluoroboric acid[7];

$$HBO_2 + 4\ HF \rightarrow HBF_4 + 2\ H_2O$$

$$H_3BO_3 + 4\ HF \rightarrow HBF_4 + 3\ H_2O$$

The borosilicate solutions contained from 25.0 to 119.4 mg B l^{-1}. Since a 25-ml aliquot from each of the 1-l solutions was used, only 1/40 of the total boron concentration was present for detection by the fluoroborate electrode. Therefore, only 0.625–2.98 mg of boron was detected as the tetrafluoroborate ion. The 0.625 mg ($5.78 \cdot 10^{-5}$ *M*) of boron in 25 ml was well within the lower detection limits of the fluoroborate electrode. The Ionalyzer fluoroborate electrode detects the tetrafluoroborate ion down to 0.11 p.p.m. boron ($1.02 \cdot 10^{-5}$ *M*) (ref. 8). At the low boron concentrations (10^{-5} *M* boron), Carlson and Paul[5] have shown that the response of the fluoroborate electrode to the tetrafluoroborate ion was masked by 0.28 *M* hydrofluoric acid, but not masked by 0.028 *M* hydrofluoric acid, provided that the solutions were stirred.

Amberlite XE-243 resin was used to remove the tetrafluoroborate ion selectively from the 0.2 *M* hydrofluoric acid solutions. All cations present in the glass silicate solutions were also removed from the tetrafluoroborate ion. The tetrafluoroborate was removed from the Amberlite XE-243 resin as the sodium salt. Dowex 50W-X8 resin was used to convert the sodium tetrafluoroborate back to the tetrafluoroboric acid.

The Ionalyzer fluoroborate electrode operates within the pH range 2–12 (ref. 8). Each sample solution was adjusted to a pH in the range 6–7 with 0.5 *M* ammonia solution, which allowed for a more stable fluoroborate solution. The tetrafluoroborate ion has the property of hydrolyzing to form such ions as $BF_3(OH)^-$, $BF_2(OH)_2^-$, and $BF(OH)_3^-$. Hydrolysis of the tetrafluoroborate ion would cause serious error in a boron analysis since the fluoroborate electrode detects boron only as the tetrafluoroborate ion. Neutral fluoroborate solutions hydrolyze very slowly and are stable for periods of several weeks. However, fluoroborate solutions at high or low pH hydrolyze rapidly and are stable for only short periods of time[8]. The pH of the solutions should not be allowed to go much above 7 since basic solutions would contain excessive amounts of the hydroxyl ion. The fluoroborate electrode responds to certain other anions (Table III)[8]. Since the hydroxide ion is an interfering ion, there would be some error associated with a solution. The error could be very substantial in a 10^{-4}–10^{-5} *M* fluoroborate solution.

If the standard and sample solutions are maintained at a constant temperature in an air-conditioned laboratory, a precision of ± 0.2 mV can be achieved on replicate direct electrode measurements of the same sample[9]. A 0.2-

TABLE III

APPROXIMATE ANION SELECTIVITY CONSTANTS

Anion	*Selectivity constant*[a]
BF_4^-	1.0
NO_3^-	0.1
Br^-	$4 \cdot 10^{-2}$
OAc^-, HCO_3^-	$4 \cdot 10^{-3}$
F^-, Cl^-, OH^-, SO_4^{2-}	10^{-3}

[a] Electrode response to interfering ion, in proportion to electrode response to fluoroborate ion.

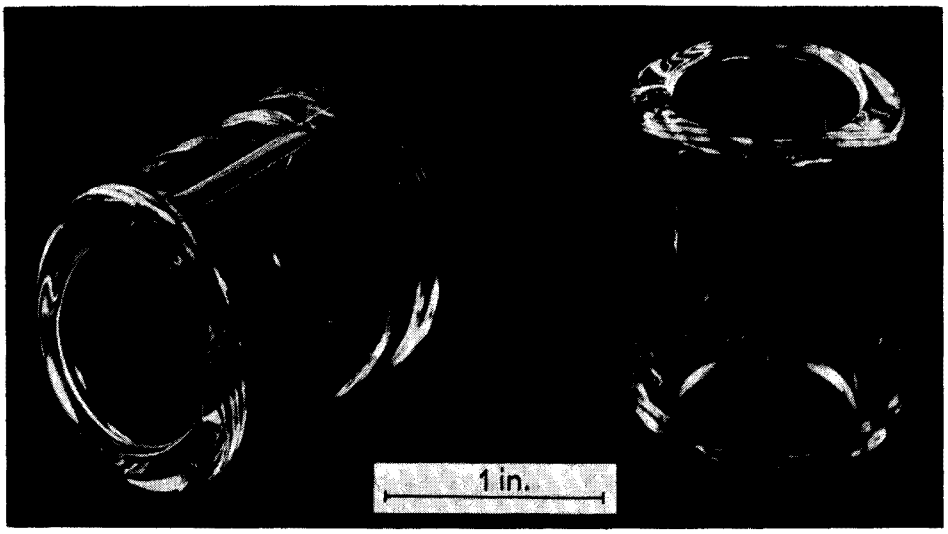

Fig. 1. Borosilicate glass Raschig rings.

mV change in potential is theoretically equivalent to a 0.4% uncertainty (relative error) with monovalent ions. However, under average laboratory conditions, the precision is approximately ± 2 mV which is equivalent to a 7.5% uncertainty (relative error). This is in close agreement with the results obtained with the ion electrodes, used in this boron study under average laboratory conditions. These results were a ± 2 mV precision and a 7.7% average relative error as shown in Table II. With special emphasis placed on a constant temperature environment, a ± 0.2 mV precision could possibly be attained.

The author is grateful to Dr. F. J. Miner for his valuable suggestions and to Y. Ferris for assistance with the statistical design and calculations.

SUMMARY

Raschig rings used as a safety mechanism, to avoid critical reactions in solutions containing radioactive materials, are usually made of borosilicate glass. Since boron is the active neutron absorbing ingredient, it is important to determine the boron content in the Raschig rings at any given time. A method has been developed to determine rapidly the boron content of borosilicate glasses. Ion exchange and potentiometric measurement are used to determine boron as the tetrafluoroborate ion. The precision of the method is ± 2.0 mV. The average difference between values of a wet chemical analysis and those of the potentiometric method is 7.7%.

REFERENCES

1 W. E. Schunter and R. W. Woodard, *USAEC Report RFP-329*, 1963.
2 S. Glasstone, *Sourcebook on Atomic Energy*, Van Nostrand, New Jersey, 2nd edn., 1958, p. 320.

3 King Towell, *USAEC Spec. No. A-11729*, 1969.
4 J. P. Nichols, C. L. Schuske and D. W. Magnuson, *USAEC Report Y-CDC-8*, 1971.
5 R. M. Carlson and J. L. Paul, *Anal. Chem.*, 40, (1968) 1292.
6 J. R. Partington, *A Text Book of Inorganic Chemistry*, McMillan, London, 6th edn., 1950, p. 667.
7 T. Moeller, *Inorganic Chemistry*, Wiley, New York, 1952, p. 752.
8 *Orion Fluoroborate Electrode Instruction Manual.*
9 J. W. Ross, Jr. in R. A. Durst (Ed.), *Ion-Selective Electrodes*, Spec. Publ. 314, National Bureau of Standards, Washington, D.C., 1969, pp. 60, 61.

Analytica Chimica Acta, 71 (1974) 458–460

SHORT COMMUNICATION

The use of an argon–hydrogen flame for the atomic absorption and atomic fluorescence spectrometry of antimony

J. D. NORRIS and T. S. WEST

Chemistry Department, Imperial College of Science and Technology, London SW7 2AY (England)

(Received 2nd January 1974)

Antimony has similar detection limits by atomic absorption (a.a.s.) or atomic fluorescence (a.f.s.) spectrometry. Kolihova and Sychra[1] examined the a.f.s. of antimony in premixed flames, obtaining a detection limit of 0.03 p.p.m. in an argon–hydrogen flame at 217.6 nm. The best a.a.s. detection limit reported for antimony is 0.1 p.p.m. in an air–hydrogen flame[2], which is the same limit as that obtained by a.f.s. in this flame[1], Despite superior detection limits, interference effects in the argon–hydrogen flame would be expected to be greater, owing to the lower temperature. The effects of 19 elements, most of which gave significant interferences, on the a.a.s. of tin in an argon–hydrogen flame have been reported[3]. However, these flames may well be useful for determinations in fairly constant matrices.

The determination of antimony by a.a.s. in technical materials often requires a preliminary separation. Yanagisawa *et al.*[4] found that only arsenic, germanium, gold, iron and tin were partially extracted with antimony into methyl isobutyl ketone from a 6 *M* hydrochloric acid solution. This communication describes the use of this extraction for the a.f.s. determination of antimony in copper-base alloys, with an argon–hydrogen flame.

Experimental

Apparatus. A modified Southern Analytical A1740 flame spectrometer, as described previously[5], was used for a.f.s. measurements, together with an antimony electrodeless discharge lamp[6]. A.a.s. measurements were made with a Techtron AA4 spectrometer and an antimony hollow-cathode lamp.

Reagents. An aqueous 100 p.p.m. antimony solution was prepared from A.R. grade potassium antimony tartrate.. Acids and salts for solutions of diverse ions were also A.R. grade materials.

Procedure for the analysis of copper-base alloys. Weigh 0.1–0.2 g of the alloy into a 100-cm^3 beaker. Add 6 cm^3 of hydrochloric acid and 2 cm^3 of nitric acid, and warm the sample to dissolve in the usual manner. Transfer the solution to a 100-cm^3 volumetric flask and dilute to volume. Pipette a 10-cm^3 aliquot into a 100-cm^3 volumetric flask, add 60 cm^3 of hydrochloric acid and dilute to volume. Transfer 20 cm^3 of this solution to a separating funnel, add 0.5 cm^3 of

aqueous 5% (w/v) sodium nitrite solution and shake for 1 min. Add 5 cm^3 of methyl isobutyl ketone and shake for 2 min. Discard the aqueous layer and nebulize the organic layer into the argon–hydrogen flame. The atomic fluorescence was compared with that of extracts of standard solutions containing between 0.1 and 1 p.p.m. of antimony.

Results and discussion

The a.a.s. sensitivities and a.f.s. detection limits for antimony in various flames are given in Table I. In both cases the argon–hydrogen was doubly superior to the air–hydrogen flame.

The effects of 100-fold (weight) amounts of sixteen elements on the a.a.s. of an aqueous 10-p.p.m. antimony solution in argon–hydrogen and air–hydrogen flames are given in Table II. Most of the elements showed significant interferences, which

TABLE I

A.A.S. SENSITIVITIES AND A.F.S. DETECTION LIMITS FOR ANTIMONY

Flame	*A.a.s. sensitivity (p.p.m.)*	*A.f.s. detection limit (p.p.m.)*
Air–C_2H_2	0.6	0.1
Air–C_3H_8	0.5	0.05
Air–H_2	0.45	0.05
N_2–H_2	0.3	0.03
Ar–H_2	0.2	0.02

TABLE II

INTERFERENCES IN A.A.S. OF ANTIMONY

Element	*% Interference*		*Element*	*% Interference*	
	Air–H_2	*Ar–H_2*		*Air-H_2*	*Ar-H_2*
Al	−10	−60	Pb	NI	NI
Ba	−12	−55	Mg	−10	−20
Cd	NI[a]	NI	Ni	−20	−60
Ca	−45	−80	Si	NI	NI
Co	−5	−15	Na	−5	−10
Cu	−3	−70	Sr	−18	−40
Ga	NI	−3	Tl	−5	−25
La	NI	−6	Zn	NI	NI

[a] NI represents less than ±3%.

were greater in the argon–hydrogen flame. The effects of 100- or 1000-fold (weight) amounts of As, Bi, Cu, Fe, Pb, Ni, Sn and Zn on the a.f.s. of 0.5 p.p.m. of antimony, after solvent extraction, in an argon–hydrogen flame were also determined. The only interferences which exceeded an error of ±1% were 1000-fold amounts of copper (+4%) and 100-fold amounts of iron (−2%) or tin (−1%).

TABLE III

A.F.S. DETERMINATION OF ANTIMONY IN COPPER-BASE ALLOYS

Sample	*Certificate value (%)*	*A.f.s. value (%)*
BCS 183/3 Leaded gunmetal	0.25	0.26
BCS 207/1 Bronze	0.084	0.090
BCS 364 Leaded bronze	0.18	0.18

Analysis of copper-base alloys. Results for the a.f.s. determination of antimony in three copper-base alloys are compared, in Table III, with the B.C.S. certificate values. Two samples of each alloy were weighed, dissolved and extracted. The a.f.s. results are the average of three separate readings taken for each extract.

The results indicate that advantage may be taken of the sensitivity obtainable with argon–hydrogen flames if extraction procedures are employed.

REFERENCES

1 D. Kolihova and V. Sychra, *Anal. Chim. Acta*, 59 (1972) 477.
2 H. L. Kahn, *Advan. Chem. Ser.*, 73 (1968) 183.
3 I. Rubeska and M. Miksovsky, *At. Absorption Newslett.*, 11 (1972) 57.
4 M. Yanagisawa, M. Suzuki and T. Takeuchi, *Anal. Chim. Acta*, 47 (1969) 121.
5 J. D. Norris and T. S. West, *Anal. Chim. Acta*, 55 (1971) 359.
6 R. M. Dagnall, K. C. Thompson and T. S. West, *Talanta*, 14 (1967) 1151.

Analytica Chimica Acta, 71 (1974) 461–463

SHORT COMMUNICATION

Rapid extractive spectrophotometric determination of gold(III) with 4-(2-pyridylazo)-resorcinol

S. G. NAGARKAR and M. C. ESHWAR

Department of Chemistry, Indian Institute of Technology, Bombay-400076 (India)

(Received 24th December 1973)

The extraction of gold(III) generally involves chloroaurate and bromoaurate species. The chloroaurate complex can be extracted with ethyl acetate from 10% hydrochloric acid[1], or as the ferroin complex into nitrobenzene[2]. Bromoaurate has been claimed to be the better extraction form, and can be extracted with isopropyl ether[3], butyl acetate[4] or trioctylphosphine oxide in chloroform[5]. The colour of the gold azide[6] complex, extracted with butanol, is unstable. The colloidal complex of gold with diethyldithiocarbamate[7] can be extracted with tributyl phosphate, and the gold–tetraphenylarsonium chloride complex with chloroform[8]. The complex with ethyl violet is extractable into benzene[9].

Even though 4-(2-pyridylazo)-resorcinol (PAR) and many of its metal chelates are water-soluble[10], gold(III) yields a sparingly soluble orange-red complex with PAR in acidic media. This is unstable in aqueous media, but can be stabilized by extraction into apolar solvents such as benzene, xylene and toluene.

Experimental

Reagents and apparatus. A stock solution of gold was prepared from gold(III) chloride (Johnson–Matthey, London), and standardized[11] gravimetrically. An aqueous 0.1% solution of PAR was prepared from the monosodium salt of 4-(2-pyridylazo)-resorcinol (E. Merck, p.a.). All other chemicals were of AnalaR grade (BDH).

Apparatus used included a type Cϕ-4 quartz spectrophotometer with matched 10-mm quartz cells, and a wrist-action flask shaker.

Procedure. Place an aliquot of gold solution containing less than 18 μg Au ml^{-1} in a 25-ml flask, and add 5 ml of 0.1 *M* nitric acid, 5 ml of 5% tartaric or citric acid solution and 1 ml of PAR solution. Leave for 5 min with intermittent shaking, and then add 5 ml of tert-butanol. Shake thoroughly, dilute the contents to the mark with distilled water, transfer to a separating funnel and shake with 10 ml of xylene for 2 min. Transfer the organic layer to a 25-ml measuring flask, dilute to the mark with tert-butanol, and measure the absorbance at 540 nm against a reagent blank prepared in the same way.

Results and discussion

Gold(III) forms a sparingly soluble orange-red complex with 4-(2-pyridylazo)-

resorcinol in acidic media (0.002–0.08 *M* nitric acid), in the presence of tartaric or citric acid, and this dissolves in tert-butanol.

Effect of reagent concentration and acidity. The amount of reagent (0.1% PAR) was varied from 0.1 to 5 ml with 240 μg of gold(III) taken per 25 ml. The absorbance was found to be constant with amounts of reagent greater than 0.3 ml. Hence, 1 ml of reagent was selected.

The nitric acid concentration was varied from 0.002 to 0.08 *M*. Constant absorbance was found for acid concentrations between 0.004 and 0.04 *M*; the absorbance decreased outside this range. Hence, the acidity was maintained in all measurements at 0.02 *M*.

Effect of tartaric or citric acid. The absorbance of the complex increased in the presence of tartaric or citric acid. When the acid concentration was varied, constant absorbance was recorded on addition of 1–10 ml of a 5% acid solution. Hence, 5 ml of 5% acid solution was selected.

Effect of nonaqueous solvent and stability. The complex formation was studied at different intervals of time. The absorbance remained constant when the time allowed for complexation was between 3 and 7 min; 5 min was therefore allowed. As the complex was unstable beyond 7–8 min in aqueous media, it was extracted into apolar solvents such as benzene, xylene and toluene. The complex extracted into xylene was stable for at least 90 min.

Absorption spectra and Beer's law. The absorption spectrum of the gold(III)–PAR complex, extracted into xylene, was recorded (Fig. 1) against a reagent blank produced under the same conditions. The complex showed maximal absorbance at 540 nm. Beer's law was obeyed in the concentration range 3.5–18 μg Au(III)

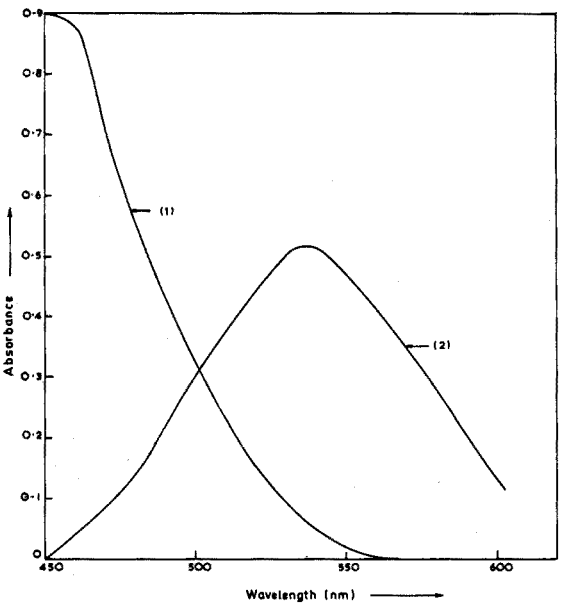

Fig. 1. Absorption spectra. (1) Reagent blank *vs.* water, (2) gold(III)–PAR complex *vs.* reagent blank. $[Au(III)] = 2.4 \cdot 10^{-3}$ *M*, $[PAR] = 2.4 \cdot 10^{-3}$ *M*.

ml^{-1}. The molar absorptivity is 8295 and the Sandell sensitivity index is 0.051 μg Au(III) cm^{-2}.

Composition and formation constant. The composition of the complex was studied by the Job and mole ratio methods. Both methods gave the ratio of the complex as 1:1. The formation constant (log K), calculated from the above curves, was found to be 5.7008 ± 0.20, and 5.6970 ± 0.20, respectively.

Effect of diverse ions. The interference of about 40 ions was studied for solutions containing 9–60 μg Au ml^{-1}. The tolerance limits for various ions are shown in Table I.

TABLE I

EFFECT OF DIVERSE IONS

(Amount of Gold(III) taken, 240 μg/25 ml)

Ion added	*Tolerance limit*[a] *(μg)*
Se(IV), Te(IV)	5000
F^-, malonate, acetate	2500
Al(III), Zn(II), Hg(II), Cd(II), Mn(II), Mo(VI), W(VI)	2000
Zr(IV), Th(IV)	1000
Re(VII),Be(II),Cr(III),Ni(II),V(V),U(VI), Pb(II), Ti(IV), Pt(IV)	500
Bi(III), Ag(I)	250

[a] Amount causing an error of less than 2%.

The relative standard deviation, calculated from ten determinations with 240 μg of gold(III) in 25 ml, was found to be $\pm 1.10\%$. The method compares favourably in accuracy and sensitivity with other methods, and takes less than 20 min for extraction and determination.

REFERENCES

1 S. Hirano, A. Mizuike and K. Yamoeda, *Jap. Anal.*, 9 (1960) 64.
2 Y. Yamamoto, M. Tsubouchi and I. Okimura, *Jap. Anal.*, 16 (1967) 176.
3 W. A. McBryde and J. H. Yoe, *Anal. Chem.*, 20 (1948) 1094.
4 V. Petrovsky, *Collect. Czech. Chem. Commun.*, 27 (1962) 1705.
5 W. B. Holbrook and J. E. Rein, *Anal. Chem.*, 36 (1964) 2451.
6 R. G. Clem and E. H. Huffman, *Anal. Chem.*, 37 (1965) 1155.
7 S. Komatsu, T. Nomura and T. Oguchi, *J. Chem. Soc. Japan, Pure Chem. Sect.*, 87 (1966) 1137.
8 J. W. Murphy and H. E. Affsprung, *Anal. Chem.*, 33 (1961) 1658.
9 Huikai Lin and Ju Chin Yu, *Chem. Bull. (Peiping)*, (1965) 244.
10 F. H. Pollard, P. Hanson and W. J. Geary, *Anal. Chim. Acta*, 20 (1959) 26.
11 A. I. Vogel, *A Textbook of Quantitative Inorganic Analysis*, Longmans Green, London, 3rd edn., 1961, p. 513.

Analytica Chimica Acta, 71 (1974) 464–467

SHORT COMMUNICATION

The use of auxiliary complexing agents in the differential complexiметric titration of zinc and cadmium with thermometric end-points

KUNIO DOI* and MOTOHARU TANAKA**

Laboratory of Analytical Chemistry, Faculty of Science, Nagoya University, Nagoya 464 (Japan)

(Received 27th November 1973)

EDTA and its homologues have been widely used in the determination of various metals, and some examples have been given for the thermometric titration with solutions of the tetrasodium salt of EDTA[1]. Differential thermometric titration of calcium and magnesium[2] constitutes a typical example of the advantages of thermometric end-point detection in complexiметric titrations. The thermometric titration curves of these two metals consist of an exothermic portion for calcium, followed by an endothermic portion for magnesium. For differential thermometric titration of two components, it is highly desirable, though not indispensable, that one reaction should be exothermic and the other endothermic.

A survey of the available thermometric data for the complexation of metal ions[3] indicates that only magnesium and aluminum give endothermic reactions with aminocarboxylates. Hitherto only the complexation of aquo metal ions has been utilized for the complexiметric titration of metals with thermometric end-points. The use of the following ligand substitution reaction would offer possibilities for the differential titration of various metals:

$$MA_n + Y \rightleftharpoons (MY)' + n\,A \qquad (1)$$

where M refers to a metal, Y an aminocarboxylate anion, A an auxiliary complexing agent, and (MY)′ all the 1:1 species involving M and Y, *i.e.* MY, MHY, MYOH, *etc.* The heat of the reaction (1) is given by the difference between the enthalpies of formation of (MY)′ and MA_n.

In the present communication, the use of auxiliary complexing agents in the differential complexiметric titration of metals with a thermometric end-point is discussed. The differential thermometric determination of mixtures of zinc and cadmium is given as an example.

Experimental

Reagents. Zinc or cadmium solution ($5 \cdot 10^{-2}$ *M*) was prepared from the pure (99.999%) metal by dissolution in a small excess of nitric acid, and dilution with water.

* Present address: Nagoya Institute of Technology, Nagoya 466, Japan.

** To whom correspondence should be addressed.

EGTA solution (0.4 *M*) was prepared by dissolution of 70.468g of ethylene glycol-bis(2-aminoethylether)-N,N N′,N′-tetraacetic acid (G. R., Dojinco Co., Kumamoto, Japan) in 100 ml of distilled water containing four equivalents of sodium hydroxide, and dilution to 500 ml with water. The solution was standardized against a standard solution of cadmium with eriochrome black T as indicator.

Apparatus. An automatic recording titrator (Hirama Rika Kenkyujo, Kawasaki, Japan), and a radiometer pH Meter Model PHM22 (Copenhagen, Denmark) were used.

Recommended procedure. Place about 100 ml of a weakly acidic sample solution containing 10–50 mg of zinc and 20–100 mg of cadmium in a 200-ml Dewar vessel covered with a block of polystyrene foam. Adjust the pH of the solution to 9.3–9.8 with (1 + 1) 1 *M* ammonia–1 *M* ammonium nitrate buffer solution. Then titrate with the standard EGTA solution delivered from an automatic titrator.

Results and discussion

In Table I, thermodynamic quantities of some complexes of zinc and cadmium are tabulated. As can be seen, these metals tend to form complexes of similar stability. However, for the EGTA and tetraammine complexes, the differences in the formation constants are appreciable, and differential titrations of these metals are possible with amperometric and photometric end-points[4,5].

TABLE I

FORMATION CONSTANTS AND ENTHALPIES OF FORMATION OF SOME COMPLEXES OF ZINC AND CADMIUM[1,3,6]

Complex	*Ligand A*	Zn^{2+}		Cd^{2+}	
		log βn^a	$-\Delta H^b$ *(kcal mole*$^{-1}$*)*	*log* $\beta_n{}^a$	$-\Delta H^b$ *(kcal mole*$^{-1}$*)*
MA	EDTA	16.3	5.6	16.3	10.1
MA	DTPA	18.8	10.6	18.9	12.4
MA	EGTA	14.4	5.0	16.6	14.1
MA	Ammonia	2.35	2.6	2.66	3.5
MA_2	Ammonia	4.80	5.7	4.75	7.0
MA_3	Ammonia	7.31	9.6	6.18	10.5
MA_4	Ammonia	9.46	14.8	7.11	14.0
MA_5	Ammonia	—	—	6.82	17.5
MA_6	Ammonia	—	—	4.40	21.0

[a] $\beta_n = [MA_n{}^{2+}]/[M^{2+}][A]^n$.
[b] Enthalpy for the reaction $M^{2+} + nA \rightleftharpoons MA_n{}^{2+}$.

As can be seen from Table I, the formation of the cadmium–EGTA complex involves a much more exothermic process than that which produces the zinc–EGTA complex; the formation of the ammine complexes, however, is almost equally exothermic for both metals. Moreover, the enthalpies of formation of the cadmium–EGTA complex and the cadmium tetraammine complex are about the same.

The effective enthalpy of formation of the metal complexes MA_n is now denoted as $\Sigma\Delta H_{MA_n}$ and defined as follows:

$$\Sigma\Delta H_{MA_n} = \frac{1}{[M']}\sum_{1}^{N}\Delta H_{MA_n}[MA_n]$$

$$= \frac{\Delta H_{MA}\beta_1[A]+\Delta H_{MA_2}\beta_2[A]^2+\Delta H_{MA_3}\beta_3[A]^3+\ldots}{1+\beta_1[A]+\beta_2[A]^2+\beta_3[A]^3+\ldots} \quad (2)$$

This value was calculated as a function of pH for the zinc and cadmium ammine complexes (Figs. 1 and 2); in these figures, the heats of formation of the relevant EGTA complexes are also given. It can be seen that, under ordinary experimental conditions, *e.g.* with $c_{NH_3}=[NH_3]+[NH_4^+]=0.3$ in excess, the titration with EGTA is endothermic for zinc above about pH 8 and exothermic for cadmium over the entire pH range shown.

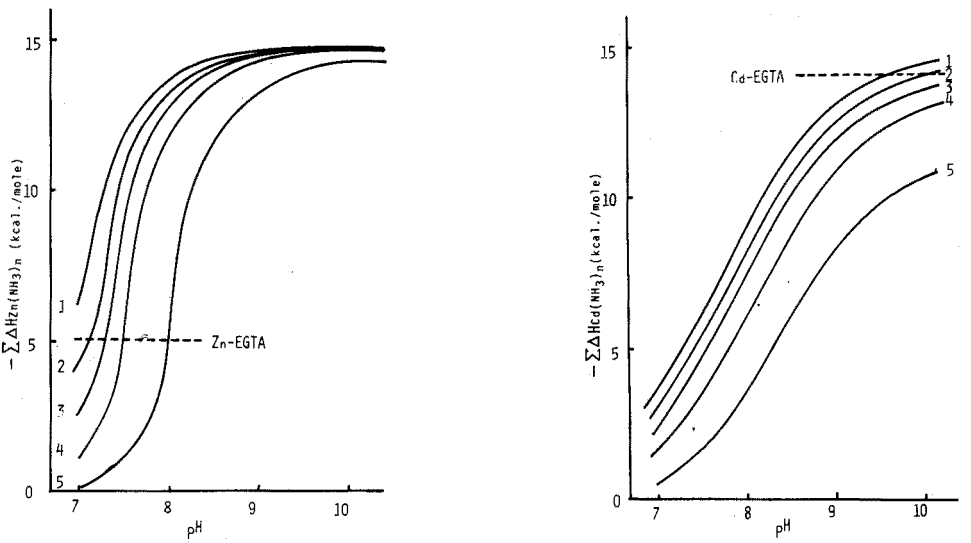

Fig. 1. Enthalpy of formation of zinc complexes as a function of pH. c_{NH_3}=(1) 1.0 *M*, (2) 0.7 *M*, (3) 0.5 *M*, (4) 0.3 *M*, (5) 0.1 *M*.

Fig. 2. Enthalpy of formation of cadmium complexes as a function of pH. Curves (1)–(5) as for Fig. 1.

During the titration, the pH of the solution increases, as a result of the following equilibria:

$$M(NH_3)_n + Y \rightleftharpoons MY + n\ NH_3 \quad (3)$$

$$NH_3 + H_2O \rightleftharpoons NH_4^+ + OH^- \quad (4)$$

The buffer capacity of the solution being large, *e.g.* for an ammonia–ammonium buffer solution of pH 9.3–9.8 with $c_{NH_3}=0.3$, the pH change on titration is less than about 0.2. Therefore the heat of reaction for eqn. (4) is small compared with ΔH_{MY} and $\Sigma\Delta H_{MA_n}$, and the overall heats of reactions for the titration are nearly equal to $-(\Delta H_{MY}-\Sigma\Delta H_{MA_n})$, so that the thermogram is a straight line.

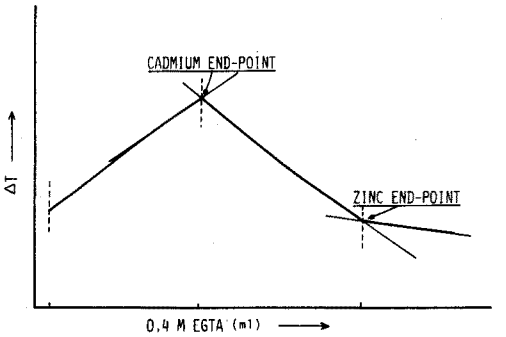

Fig. 3. Thermometric titration of Cd(II) and Zn(II) with EGTA. Conditions: c_{NH_3} 0.3 *M*, pH 9.7, titration speed 1.5 ml min^{-1}, temperature 24.4°C.

TABLE II

DETERMINATION OF ZINC AND CADMIUM IN MIXTURES

Sample no.	*Cd taken (mg)*	*Cd found (mg)*	*Zn taken (mg)*	*Zn found (mg)*
1	30.2	30.5	80.5	79.8
2	107.3	106.3	20.7	20.4
	107.3	106.7	20.7	20.8
3	50.6	50.1	34.1	33.7

Though the precipitation of zinc hydroxide was expected under the experimental conditions, no precipitate was observed at pH 9.3–9.8 with $c_{NH_3}=0.3$. This pH range is therefore recommended.

Under the optimal conditions thus determined, the cadmium–ammine complexes are titrated first with EGTA in an exothermic reaction and the zinc–ammine complexes subsequently react endothermically. The end-point for cadmium is easily determined at the intersection of the extrapolated exothermic and endothermic portions of the thermometric titration curves (Fig. 3), as in the thermometric titration of a mixture of calcium and magnesium[2]. Both zinc and cadmium give exothermic reactions in the absence of ammonia. Thus, the differential determination of zinc and cadmium is possible by means of thermometric titration.

Some mixtures of these metal ions were titrated by the recommended procedure—with the results as shown in Table II. These results are considered to be satisfactory.

REFERENCES

1 H. J. V. Tyrrell and A. E. Beezer, *Thermometric Titrimetry*, Chapman and Hall, London, 1968, p. 107.
2 J. Jordan and T. G. Alleman, *Anal. Chem.*, 29 (1957) 9.
3 J. J. Christensen and R. M. Izatt, *Handbook of Metal Ligand Heats and Related Thermodynamic Quantities*, Dekker, New York, 1970.
4 H. Flaschka and J. Ganchoff, *Talanta*, 9 (1962) 76.
5 H. Flaschka and R. Speights, *Anal. Chim. Acta*, 28 (1963) 403.
6 L. G. Sillén and A. E. Martell, *Stability Constants of Metal-Ion Complexes*, The Chemical Society, London, 1964.

Analytica Chimica Acta, 71 (1974) 468–471

SHORT COMMUNICATION

Analytical uses of some N-nitroso-N-alkyl (or -N-cycloalkyl)-hydroxylamines

Part III. N-Nitroso-N-cyclooctylhydroxylamine, N-nitroso-N-cyclododecylhydroxylamine and N-nitroso-N-isopropylhydroxylamine

F. BUSCARONS and J. CANELA

Department of Analytical Chemistry, Faculty of Sciences, University of Barcelona, Barcelona (Spain)

(Received 10th December 1973)

In recent papers[1,2], the reactions, properties and analytical uses of hexahydrocupferron (sodium salt of N-nitroso-N-cyclohexylhydroxylamine) have been described. In order to establish the effect of molecular weight on the behaviour of the N-nitrosohydroxylamine group, the sodium salts of the N-cyclooctyl-(octyl) (I) and N-cyclododecyl-(dodecyl) (II), and the ammonium salt of the N-isopropyl-(isopropyl) (III) derivatives have now been examined.

These substances, in the solid state and in aqueous solution, show the same good stability as hexahydrocupferron, and they also offer the advantage of giving colourless decomposition products; only the dodecyl derivative is insoluble in water and so requires alcoholic solutions.

The reactions with metal ions involve precipitation, like those of hexahydrocupferron, with similar pH conditions and extraction possibilities, and the same stoichiometries of the metal complexes. Because of molecular weight effects, the isopropyl derivative reacts with fewer ions; the octyl and dodecyl derivatives react with most tetra-, tri- and divalent metals. The sensitivities of the dodecyl derivative are the highest of all these reagents, including hexahydrocupferron. For example, the dodecyl derivative gives dilution limits of 1:200,000 and 1:300,000 with calcium and magnesium, respectively; these reactions are of qualitative interest and may be used for turbidimetric or heterometric determinations, as well as for recovery or concentration purposes.

The preparation of these reagents has already been described[3].

Experimental

Solubilities. The solubilities were determined at 20°C as described by Wittenberger[4]; they were found to be 24.35 g (I), 1.04 g (II) and 25.58 g (III) per 100 ml of water, and 4.13 g (I), 5.31 g (II) and 6.77 g (III) per 100 ml of ethanol. All three reagents are sparingly soluble in apolar solvents; aqueous solutions of (II) tend to be colloidal, so that alcoholic solutions must be used.

Ultraviolet absorption spectra. Spectra were measured with a Perkin–Elmer M 124 spectrophotometer in 0.1 *M* hydrochloric acid and 0.1 *M* sodium hydroxide solutions (with 1% ethanol for (II)).

In acidic medium, each of the three reagents shows a single absorption maximum: (I) at 224.5–226.0 nm ($\varepsilon = 4{,}794$), (II) at 225.0–227.0 nm ($\varepsilon = 5{,}832$), and (III) at 224.0–226.0 nm ($\varepsilon = 6{,}883$). In neutral or alkaline medium, the maxima appear at 245.0–246.5 nm ($\varepsilon = 6{,}372$) for (I), 246.0–247.0 nm ($\varepsilon = 7{,}065$) for (II), and 245.0–247.0 nm ($\varepsilon = 9{,}044$) for (III). The absorptivities can be used to distinguish between the three reagents.

Determination of pK values. The pK values were determined as described by Albert and Sergeant[5], at a wavelength (260 nm) at which only the anionic forms of the reagents absorb. The pK values were found to be 5.65 ± 0.02 for (I), 5.47 ± 0.04 for (II) and 5.64 ± 0.04 for (III), which is in good agreement with the value of 5.58 ± 0.04 for hexahydrocupferron[1], and very different from the analogous reagents with aromatic groups, such as cupferron[6] (pK 4.28), neocupferron[7] (pK 4.28) and *p*-phenylcupferron[7] (pK 4.00).

Infrared spectra. The spectra were recorded in KBr discs on a Beckman 20A spectrophotometer. Like hexahydrocupferron, the reagents are characterized by four stretching vibrations: two bands of low intensity at 1300–1320 and 1440–1450 cm^{-1} assigned to the N=O group in its dimeric and monomeric forms, one of high intensity at 1040–1070 cm^{-1} ascribed to the N–N bond, and one of medium intensity at 930–940 cm^{-1} ascribed to the N–O bond.

Stabilities in 6 M hydrochloric acid media. The stabilities of 10^{-4} M reagent solutions in 6 M hydrochloric acid were determined by plotting their absorbances at the u.v. maxima (224 nm) against time. Concentrations decreased by 50% after 5.6 days for (I), 13 for (II) and 5.3 for (III). Neutral aqueous solutions were stable for at least three months.

Reactions with metal ions

Reactions of the three reagents with 50 inorganic ions were studied with aqueous 1% (w/v) solutions of (I) and (III) and an ethanolic 1% solution of (II). The reactions and their sensitivities were determined by the same semimicro procedure as for hexahydrocupferron[1]. The reactions, colour formations and extraction possibilities were very similar to those found with hexahydrocupferron, but the sensitivities were generally much greater, particularly with the dodecyl compound (II).

Recovery or concentration of calcium and magnesium by precipitation with the dodecyl derivative

The high sensitivities obtained with the dodecyl derivative (II) for calcium and magnesium, suggested the possibility of gravimetric or turbidimetric determinations of these elements. The solubilities of the precipitates, determined by atomic absorption spectrometry on aqueous saturated solutions at 20°C, were found to be 17.53 and 26.97 mg l^{-1} for, respectively, the calcium and magnesium compounds. Gravimetric determinations were impossible, since all solvents tested to remove the excess reagent from the precipitate (acetone, dioxane, water–alcohol mixtures, *etc.*) also dissolved the calcium and magnesium compounds. Nevertheless, a satisfactory recovery or concentration of 5–40 mg of calcium or magnesium in 500 ml of solution was possible; the precipitates could be ignited at 700°C, dissolved in hydrochloric acid and titrated with EDTA, the relative errors being

less than 0.9%. Even for 1–2 mg of calcium or magnesium, the relative errors were only in the range 1–2%.

Turbidimetric determinations

Measurements were made at 420 nm with a Metrohm E 1009 spectrocolorimeter with 1-cm cells. A 1% (w/v) solution of polyvinyl alcohol was used as protective colloid. The reagent was added slowly with continuous magnetic stirring, to avoid local precipitations which led to irreproducible results; the absorbances of samples containing 5–10% (v/v) of the polyvinyl alcohol solution and stirred for 20 min, remained constant for the next 15 min and then decreased quickly. The turbidity depended on pH and, for both metals, reached a constant value between 7.10 and 8.73.

Procedure. Place the samples containing 0.375–3.0 mg of calcium or 0.10–0.65 mg of magnesium in 50-ml volumetric flasks, and add 5 ml of a pH 7.30 buffer and 5 ml of a 1% (w/v) polyvinyl alcohol solution. Dilute with distilled water to 35 ml, and slowly add 10 ml (or 5 ml for magnesium) of a 0.02 *M* solution of the dodecyl derivative in ethanol, while stirring electromagnetically for 20 min. In the next 15 min, dilute to volume and measure the absorbance at 420 nm.

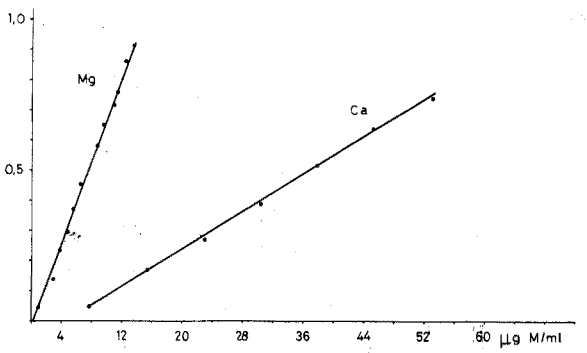

Fig. 1. Calibration graphs for calcium and magnesium.

Results. Beer's law was followed over the ranges 7.5–60 μg Ca ml^{-1} and 2–13 μg Mg ml^{-1}. The slopes of the calibration graphs (Fig. 1) depended on the stirring speed so that, as usual in turbidimetric methods, reference standard samples were necessary in each determination. Relative errors were better than 2%. The accuracy and sensitivity of this determination of calcium were much better than those for the determination with oxalate[8–10].

Heterometric titrations

Titrations were conducted under the same optical conditions as for the turbidimetric determinations, but in mechanically stirred 60-ml cells. Polyvinyl alcohol or gelatin was used as the protective colloid.

Procedure. In a 60-ml titration vessel, take 0.2–0.8 mg of calcium or 0.10–0.35 mg of magnesium, add 5 ml of a pH 7.30 buffer, and dilute with water to 50 ml. Heat the sample to 60°C, add 3 ml of 1% (w/v) polyvinyl alcohol solution,

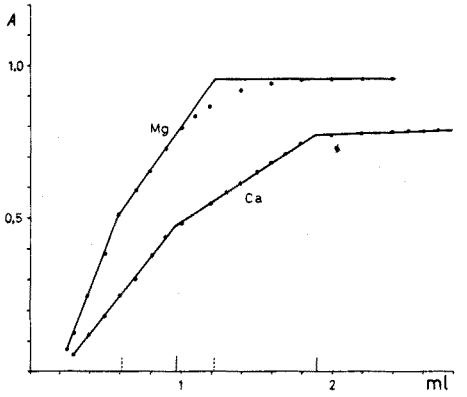

Fig. 2. Heterometric titration curves for calcium and magnesium.

and titrate slowly with a 0.02 *M* solution of the dodecyl derivative in 60% (v/v) ethanol, stirring for 15 min before each measurement to obtain constant turbidity.

Results. Typical titration curves are shown in Fig. 2; the curves show two inflexions, which can be assigned to compounds with stoichiometries of one metal atom to one or two molecules of reagent. Results, calculated from the 1:2 stoichiometries for the above metal concentration ranges, showed relative errors of ± 0.2–2.4%.

Attempts to accelerate the titrations by using automatic equipment (Radiometer SBR-2C; pH meter 28; autoburette ABU 12) were unsuccessful; the end-points were badly defined and the relative errors were about 5%.

REFERENCES

1 F. Buscarons and J. Canela, *Anal. Chim. Acta*, 67 (1973) 349.
2 F. Buscarons and J. Canela, *Anal. Chim. Acta*, in press.
3 H. Metzer, B.A.S.F. A.G., *D.A.S.* 1,019,657 Kl 12q from 18.8.56.
4 W. Wittenberger, *Chemisches Laboratoriums Technik*, Springer, Vienna, 1950, p. 101.
5 A. Albert and E. Sergeant, *Ionization Constants of Acids and Bases*, Methuen, London, 1962, p. 69.
6 I. V. Pyatnitokii, *Zh. Anal. Khim.*, 1 (1946) 135.
7 P. J. Elving and E. C. Olson, *J. Amer. Chem. Soc.*, 78 (1946) 4206.
8 J. Grant, *Met. Ind. (London)*, 44 (1934) 459.
9 J. G. Hunter and A. Hall, *Analyst (London)*, 78 (1953) 106.
10 A. I. Polinkowskaja, *Trans. Inst. Test., Build. Mat. Glass*, 27 (1930) 11.

Analytica Chimica Acta, 71 (1974) 472–476

SHORT COMMUNICATION

Anion-exchange behaviour of indium(III) in citrate and tartrate solutions: separation from mixtures

R. SITARAM and S. M. KHOPKAR

Department of Chemistry, Indian Institute of Technology, Bombay 400076 (India)

(Received 3rd December 1973)

A study of the anion-exchange behaviour of indium(III) in organic acid solutions[1] showed that indium(III) forms negatively charged complexes with 3% citric or tartaric acid at pH 2.5–3.0. The complex can be sorbed on anion-exchange resins such as Dowex 21K. It is possible to separate indium(III) from many elements by anion-exchange chromatography, in either acid medium by selective sorption or selective and gradient elution.

Anion-exchange studies of indium(III) in chloride[2,3] bromide[4] and iodide[5] media have already been reported. Indium has been separated from zinc in sulphuric acid media[6]. Carbonate[7] and thiocyanate[8] complexes have been explored for its separation from aluminium and iron. Alimarin *et al.*[9] studied the complexes of indium in acetate, formate and propionate solutions. The present communication reports systematic studies of the behaviour of indium on Dowex 21K resin in citrate and tartrate solutions. Various mineral acid and neutral salt solutions were tested as eluents. Methods are described for the separation of indium from various other elements.

Experimental

Apparatus and reagents. The ion-exchange column (1.4 × 20 cm) was similar to that described earlier[10]. An automatic fraction collector (Tower's type) with a 10-ml syphon, and a Cambridge pH meter with glass and calomel electrodes were used.

A stock solution of indium(III), prepared by dissolving 1.78 g of indium trichloride trihydrate (BDH AnalaR) in 250 ml of distilled water, was standardized with EDTA[11]; the solution contained 3.014 mg In ml^{-1}.

Dowex 21K resin (50–100 mesh; Cl^- form) was converted to the citrate or tartrate form by passing 200 ml of a 5% solution of the corresponding acid buffered at pH 2.5–3.0. The excess of acid in the column was thoroughly washed out with distilled water.

General procedure. To an aliquot of indium chloride solution, 2 g of citric acid, or about 1.5 g of tartaric acid, was added, and the pH was adjusted to 2.5–3.0 with 0.1 *M* ammonia solution or 0.1 *M* citric or tartaric acid. The solution was then sorbed on the column at a flow rate of 1 ml min^{-1}. After the column had

TABLE I

ANION EXCHANGE STUDIES OF INDIUM(III) IN CITRATE OR TARTRATE MEDIA

(Indium(III), 15.5 mg)

		Citrate medium					*Tartrate medium*				
Eluant(M)		V_{max} *(ml)*[a]	V_t *(ml)*[b]	*Recovery (%)*	E[c]	D_v[c]	V_{max} *(ml)*[a]	V_t *(ml)*[b]	*Recovery (%)*	E[c]	D_v[c]
HNO_3	0.25	80	110	99.6	0.65	1.54	70	130	99.6	0.52	1.90
	0.50	50	80	99.9	0.85	1.18	50	90	98.5	0.85	1.18
	1.0	30	60	99.9	2.20	0.35	40	90	99.0	1.22	0.82
H_2SO_4	0.25	100	120	99.9	0.38	2.61	90	120	98.4	0.38	2.62
	0.50	60	90	101.0	0.65	1.54	50	90	99.7	0.85	1.18
	1.00	40	70	101.0	1.22	0.81	30	100	99.9	2.20	0.35
HCl	0.25	130	160	99.5	0.24	4.06	90	140	99.3	0.38	2.62
	0.50	60	120	99.2	0.65	1.54	70	90	99.2	0.52	1.90
	1.00	40	100	99.4	1.22	0.82	50	80	99.4	0.85	1.18
NH_4NO_3	0.50	90	160	99.0	0.38	2.62	80	200	68.1	—	—
	1.00	50	120	99.0	0.85	1.18	50	140	84.8	0.85	1.18
$NaNO_3$	0.50	80	200	92.4			80	150	99.1	0.44	2.26
	1.00	40	90	100.0	1.22	0.82	50	140	100.0	1.22	0.82
NH_4Br	0.50	70	170	98.8	0.52	1.90	—	200	—	—	—
	1.0	50	110	98.7	0.85	1.18	—	—	—	—	—

[a] Peak elution volume.

[b] Total volume.

[c] E is the elution constant, and D_v the volume distribution coefficient.

been washed with 25 ml of water, indium was eluted with 200 ml of various eluents (Table I). The effluent was collected in 10-ml fractions. Each fraction was evaporated to dryness with a mixture of nitric and perchloric acids to destroy the organic matter. It was then extracted with water and the indium content was determined by titration with EDTA with PAN as indicator[11]. On the basis of the elution constants (E) and the volume distribution coefficients (D_v)[10], the efficiency of the eluents was evaluated.

Ion exchange in citrate solutions

From the data given in Table I, the eluents tested can be arranged in order of decreasing efficiency:

$$HNO_3 > H_2SO_4 > HCl > NH_4Br > NH_4NO_3$$

Sodium chloride, ammonium chloride and ammonium acetate were found to be poor eluents for indium in any concentration range from 0.25 to 1.0 M.

Separation of alkali and alkaline earth metals. These elements do not form citrate complexes[12,13] at pH 2.5–3.0 and hence are not adsorbed. Therefore, after sorption of indium, the column was washed out with distilled water, and then indium was eluted with 200 ml of 1.0 M hydrochloric acid and determined as described above.

Separation from Zn, Cd, Mn(II), Co, Ni, Fe(III), Al, Bi(III) and Cu(II). These metals form weak complexes with citric acid, compared to that formed with indium at pH 2.5[12,14]. Mineral acid salts are good eluents for these metals, although they are poor for indium. Hence, zinc, cobalt and nickel were first eluted with 0.25 M sodium chloride, and indium was then eluted with 1.0 M nitric acid. Similarly, iron(III) and bismuth(III) were eluted first with 1.0 M sodium chloride, aluminium with 0.25 M ammonium nitrate, and copper(II) or cadmium with 1.0 M ammonium sulphate, before the elution of indium with 1.0 M nitric acid or 1.0 M hydrochloric acid.

Separation from titanium(IV). Titanium(IV) forms a very stable complex[15] with citric acid under the conditions for the separation of indium. Therefore, after sorption of the mixture, indium was first eluted with 1.0 M hydrochloric acid, and then titanium(IV) was eluted with 3.0 M hydrochloric acid.

The results of the various separations are shown in Table II.

Ion exchange in tartrate media

From the results given in Table I, the eluents can be arranged in the following order of decreasing efficiency

$$H_2SO_4 > HNO_3 > HCl > NH_4NO_3 > NaNO_3 > NH_4Br$$

Sodium chloride, ammonium chloride and ammonium acetate were poor eluents in any concentration range from 0.25 to 2.0 M.

Separation from alkali metals. These metals do not form negatively charged complexes[16,17] at pH 2.5 and are not retained by the column. After the column had been washed with distilled water, indium was desorbed with 1.0 M nitric acid and determined in the usual manner.

Separation from Zn, Cd, Mn(II), Co, Ni, Mg, Sr, Ba, Tl(I). Zinc, cadmium,

TABLE II

ION EXCHANGE SEPARATIONS

(Indium(III), 15.5 mg)

Foreign ions	*Amount added (mg)*	*Indium found*			
		Citrate media		*Tartrate media*	
		(mg)	*(%)*	*(mg)*	*(%)*
Li	65.2	15.50	100.0	15.50	100.0
Na	65.2	15.50	100.0	15.50	100.0
K	76.3	15.50	100.0	15.50	100.0
Rb	76.3	15.50	100.0	15.50	100.0
Cs	76.3	15.40	99.4	15.50	100.0
Mg	45.3	15.32	98.9	15.40	99.4
Sr	47.9	15.41	99.5	15.50	100.0
Ba	47.9	15.50	100.0	15.40	99.4
Be	45.0	15.35	99.1	15.50	100.0
Ca	51.1	15.41	99.4	15.30	98.7
Al(III)	31.0	15.41	99.4	15.41	99.4
Fe(III)	45.5	15.47	99.8	15.40	99.4
Bi(III)	45.5	15.50	100.0	15.32	99.0
Co(II)	52.2	15.30	98.7	15.50	100.0
Ni(II)	52.2	15.50	100.0	15.40	99.4
Cu(II)	53.3	15.42	99.6	15.35	99.0
Zn(II)	55.2	15.47	99.8	15.41	99.4
Cd(II)	52.5	15.50	100.0	15.50	100.0
Mn(II)	45.9	15.50	100.0	15.40	99.4
Ti(IV)	45.6	15.50	100.0	15.45	99.5
Zr(IV)	40.5	15.40	99.4	15.42	99.5
V(IV)	42.2	15.50	100.0	15.43	99.5
Th(IV)	46.1	15.43	99.5	15.43	99.5
U(VI)	51.5	15.35	99.0	15.38	98.0

manganese, cobalt, nickel, magnesium, strontium, barium and thallium(I) form very weak unstable tartrate complexes[16,18] at pH 2.5–3. Therefore, the weak or partially formed tartrate complexes were first removed by washing with distilled water, and indium was then eluted in 1.0 *M* nitric acid.

Separation from Cu(II), Fe(III), Al, V(IV), Th(IV) and U(VI). These metals form very weak tartrate complexes[16] while indium forms a reasonably strong complex at pH 2.5–3.0. Also the salts of mineral acids are good eluents for these elements but not for indium. Hence copper(II) was first eluted with 0.25 *M* sodium chloride, iron(III), uranium(VI) or aluminium with 0.25 *M* sodium nitrate, and vanadium(IV) or thorium(IV) with 1.0 *M* sodium chloride. Indium was subsequently eluted with 200 ml of 1 *M* nitric acid.

Separation from zirconium(IV). Zirconium(IV) forms a more stable complex[16,18] with tartaric acid than indium(III), at pH 2.5. Hence indium was first eluted with 0.25 *M* nitric acid, and zirconium(IV) was later eluted with 2.0 *M* nitric acid.

Separation from vanadate, molybdate and chromate. For this separation, indium

was first eluted with 1.0 *M* nitric acid, followed by the elution of vanadate or molybdate with 10% sodium carbonate, or chromate with 1.0 *M* potassium chloride.

Results for these separations are shown in Table II. From ten runs with 15.5 mg of indium in citrate and tartrate media, 15.5 ± 1 mg of indium was recovered. The accuracy is within 2%. The proposed method is very simple and rapid, and facilitates the separation of indium from a number of other elements, since selective sorption and selective elution are possible.

REFERENCES

1 R. Sitaram and S. M. Khopkar, *Chromatographia*, 6 (1973) 198.
2 K. A. Kraus, F. Nelson and G. W. Smith, *J. Phy. Chem.*, 58 (1954) 11.
3 D. N. Sunderman, I. B. Ackermann and W. W. Meinke, *Anal. Chem.*, 31 (1959) 40.
4 J. Korkisch and I. Hazan, *Anal. Chem.*, 37 (1965) 707.
5 L. L. Kotschera, *C.R. Acad. Bulg. Sci.*, 22 (1969) 447.
6 S. Stancheva, I. P. Alimarin and E. P. Tsintsevich, *Zavod. Lab.*, 28 (1962) 156.
7 I. P. Alimarin, E. P. Tsintsevich and V. P. Burlaka, *Zavod. Lab.*, 25 (1959) 1287.
8 J. Korkisch and F. Hecht, *Mikrochim. Acta*, (1956) 1230.
9 I. P. Alimarin, V. P. Tsintsevich and T. N. Leonova, *Vestn. Mosk. Univ., Khim.*, 6 (1960) 33.
10 R. Sitaram and S. M. Khopkar, *Chromatographia*, 5 (1972) 408.
11 F. J. Welcher, *The Analytical uses of Ethylenediamine tetracetic acid*, Van Nostrand, London, 1958.
12 E. R. Tompkins, J. X. Khym and W. E. Cohn, *J. Amer. Chem. Soc.*, 69 (1947) 2769.
13 F. Nelson and K. A. Kraus, *J. Amer. Chem. Soc.*, 77 (1955) 801.
14 N. C. Li and J. M. White, *J. Inorg. Nucl. Chem.*, 16 (1960) 131.
15 N. E. Brown and W. Rieman III, *J. Amer. Chem. Soc.*, 74 (1952) 1278.
16 A. E. Martell and M. Calvin, *Chemistry of the Metal Chelate Compounds*, Prentice Hall, 1956.
17 J. Inczedy, *Analytical Applications of Ion Exchangers*, Pergamon, 1966.
18 G. P. Pitstick, R. Sweet and G. P. Morie, *Anal. Chem.*, 35 (1963) 995.

Analytica Chimica Acta, 71 (1974) 477–481

SHORT COMMUNICATION

Determination of Th–U and U–Zr alloy composition with a fluoride-selective electrode

FU CHUNG CHANG, HUI-TUH TSAI and SHAW-CHII WU

Institute of Nuclear Energy Research, Atomic Energy Council, Lung-Tan, Taiwan (Republic of China)

(Received 9th October 1973)

Even though uranium has several valence states, the uranyl ion is the only stable species in solution in contact with air. Various species, UO_2F^+, UO_2F_2, $UO_2F_3^-$ and $UO_2F_4^{2-}$ are formed in the presence of fluoride. If the concentration of fluoride in solution is kept constant, a linear relationship exists between the logarithmic fluoride concentration, increased by the release of fluoride from the uranium–fluoride complexes, and the logarithmic uranium(VI) ion concentration, so that the latter can be measured indirectly. Thorium and zirconium form thorium tetrafluoride and zirconium tetrafluoride quantitatively with fluoride ion under appropriate conditions. Thus thorium and zirconium can be determined by measuring the difference between the fluoride ion concentration before and after it reacts with zirconium or thorium. The relationship of uranium(VI), thorium-(IV) and fluoride is shown in Fig. 1, when a known amount of fluoride ion is added to a solution containing a mixture of uranyl and thorium ions. $[F^-]_E$ can be measured directly with a fluoride selective electrode, after introducing a suitable masking agent[1] to liberate the fluoride ion from its U–F complexes. $[F^-]_C$ can

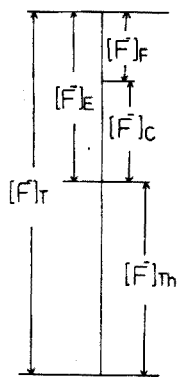

Fig. 1. The relationship of fluoride, uranyl and thorium ions in mixtures. $[F^-]_T$, Total amount of fluoride added to solution; $[F^-]_E$, effective fluoride ion concentration reacting with UO_2^{2+}; $[F^-]_F$, free fluoride ion concentration after forming ThF_4 and UO_2^{2+}–F^- complexes; $[F^-]_C$, amount of fluoride forming complex with UO_2^{2+}; $[F^-]_{Th}$, amount of fluoride forming complex with thorium.

then be obtained by subtracting $[F^-]_E$. The amount of thorium can be calculated from the difference of $[F^-]_T$ and $[F^-]_E$.

In the present work, different concentrations of uranium, thorium, zirconium, U(VI)–Th and U(VI)–Zr mixtures have been studied. The sensitivity and relative error have been estimated. Other methods for the determination of uranium–zirconium and uranium–thorium alloys[2] are rather complicated and time-consuming in comparison with the proposed method.

Experimental

Apparatus. An Orion Model 94-09 fluoride-selective electrode and a Model 90-01 reference electrode coupled with a Sargent recorder were employed. Solutions were stirred magnetically during measurements.

Reagents. A solution of $7.1 \cdot 10^{-3}$ *M* uranium was prepared from primary standard U_3O_8, and less concentrated solutions were prepared by dilution. Thorium ($4.0 \cdot 10^{-2}$ *M*) and zirconium ($1.0 \cdot 10^{-3}$ *M*) solutions were prepared from extra-pure $Th(NO_3)_4 \cdot 4H_2O$ and $ZrOCl_6 \cdot 8H_2O$. Stock solutions of sodium fluoride were prepared from the reagent-grade salt after drying at 100°C for 24 h. Triethanol-amine buffer solution was prepared by dissolving 240 g of reagent-grade tri-ethanolamine in distilled water, introducing sufficient hydrochloric acid to bring the pH to 5.5, and diluting to exactly 1 l. All other reagents were prepared from reagent-grade substances without further purification.

Determination of uranium. Uranium solutions of different concentrations were added to buffer solutions containing fluoride. The residual fluoride concentrations of the solutions were measured with the fluoride electrode. Measurements were repeated after 100 mg of ammonium carbonate, as masking agent, had been intro-duced to release fluoride from its complex with uranium.

Determination of thorium and zirconium. A known amount of fluoride was added to the buffer solution containing either thorium or zirconium. The residual fluoride concentration of the solution was measured, and the measurement was repeated after sodium salicylate had been added to the zirconium solution and sodium acetate to the thorium solution as masking agent, to determine the con-centration of fluoride released from its corresponding complexes.

Determination of Th–U(VI) or U(VI)–Zr mixtures. A known amount of fluoride in buffer solution was added to the Th–U(VI) mixture. The fluoride ion concentration of the resulting solution was measured, and the measurement was repeated after 50 mg of ammonium carbonate had been added as masking agent, to determine the concentration of fluoride released from its complexes. The same procedure was used for U(VI)–Zr mixture, sodium salicylate being used instead of ammonium carbonate.

Results and discussion

Determination of thorium and zirconium. Table I gives the fluoride, thorium and zirconium concentrations and the complexing ratio of thorium and zirconium with fluoride. Thorium forms thorium tetrafluoride easily, and no special care is needed. But in the determination of zirconium, the amount of fluoride added should be at least 20 times larger than that of zirconium to achieve a 1:4 ratio; other-wise, zirconium may form $ZrOF_2$ or other cationic species such as ZrF^{3+},

TABLE I

DETERMINATION OF THORIUM AND ZIRCONIUM WITH FLUORIDE

F^- added (M)	Th^{4+} added (M)	Zr^{4+} added (M)	F^- released (M)	Ratio	
				F^-/Th^{4+}	F^-/Zr^{4+}
$5.0 \cdot 10^{-4}$	$2.0 \cdot 10^{-5}$		$8.0 \cdot 10^{-5}$	4.0	
$2.0 \cdot 10^{-3}$	$4.0 \cdot 10^{-5}$		$2.0 \cdot 10^{-4}$	4.0	
$2.0 \cdot 10^{-3}$	$1.0 \cdot 10^{-4}$		$4.0 \cdot 10^{-4}$	4.0	
$4.0 \cdot 10^{-3}$	$9.0 \cdot 10^{-4}$		$3.6 \cdot 10^{-3}$	4.0	
$5.0 \cdot 10^{-4}$		$3.0 \cdot 10^{-5}$	$1.2 \cdot 10^{-4}$		4.0
$2.0 \cdot 10^{-3}$		$5.0 \cdot 10^{-5}$	$2.0 \cdot 10^{-4}$		4.0
$2.0 \cdot 10^{-3}$		$7.0 \cdot 10^{-5}$	$2.7 \cdot 10^{-4}$		3.9
$2.0 \cdot 10^{-3}$		$1.0 \cdot 10^{-4}$	$3.9 \cdot 10^{-4}$		3.9
$2.0 \cdot 10^{-3}$		$2.4 \cdot 10^{-4}$	$7.5 \cdot 10^{-4}$		3.8
$2.0 \cdot 10^{-3}$		$4.0 \cdot 10^{-4}$	$8.4 \cdot 10^{-4}$		2.1

ZrF_2^{2+}, ZrF_3^+, $ZrOF^+$, *etc.* The advantage of using sodium salicylate or sodium acetate as a masking agent to release fluoride from the zirconium or thorium complex is that no prior sample separation is necessary if other ions which form complexes with fluoride but not with sodium salicylate or sodium acetate are also present. For instance, hafnium, titanium, uranium, molybdenum, iron, chromium, thorium and zirconium all form complexes with fluoride, but only zirconium can be masked by salicylate. Hence, separation will not be necessary in the determination of zirconium in presence of those ions. Tedious and time-consuming procedures such as separation and filtration can thus be eliminated.

Determination of uranium. A series of calibration lines (Fig. 2) was obtained by plotting the logarithmic concentration of the fluoride in the complex form against the logarithmic concentration of uranium. The Figure indicates that the

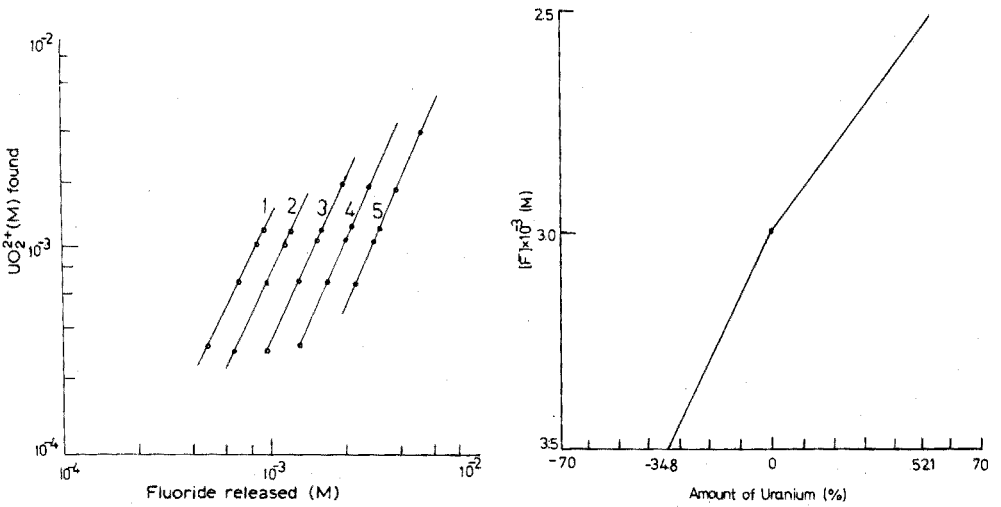

Fig. 2. Calibration curve for uranyl ion at different concentrations of fluoride. Lines 1–5 represent $2.0 \cdot 10^{-3}$, $2.5 \cdot 10^{-3}$, $3.0 \cdot 10^{-3}$ and $4.0 \cdot 10^{-3}$ M fluoride, respectively.

Fig. 3. Correction curve for uranium(VI).

TABLE II

COMPARISON OF URANYL ION CONCENTRATION FOR A GIVEN AMOUNT OF FLUORIDE RELEASE

F^- released (M)	*F^- added (M)*	*UO_2^{2+} found (M)*	*Difference (%)*
$1.30 \cdot 10^{-3}$	$2.50 \cdot 10^{-3}$	$8.15 \cdot 10^{-4}$	52.3
$1.30 \cdot 10^{-3}$	$3.00 \cdot 10^{-3}$	$5.35 \cdot 10^{-4}$	
$1.70 \cdot 10^{-3}$	$2.50 \cdot 10^{-3}$	$1.47 \cdot 10^{-3}$	52.1
$1.70 \cdot 10^{-3}$	$3.00 \cdot 10^{-3}$	$9.70 \cdot 10^{-4}$	
$2.00 \cdot 10^{-3}$	$2.50 \cdot 10^{-3}$	$2.13 \cdot 10^{-3}$	52.1
$2.00 \cdot 10^{-3}$	$3.00 \cdot 10^{-3}$	$1.40 \cdot 10^{-3}$	
$1.30 \cdot 10^{-3}$	$3.00 \cdot 10^{-3}$	$5.35 \cdot 10^{-4}$	34.8
$1.30 \cdot 10^{-3}$	$3.50 \cdot 10^{-3}$	$3.48 \cdot 10^{-4}$	
$1.70 \cdot 10^{-3}$	$3.00 \cdot 10^{-3}$	$9.70 \cdot 10^{-4}$	34.9
$1.70 \cdot 10^{-3}$	$3.50 \cdot 10^{-3}$	$6.35 \cdot 10^{-4}$	
$2.00 \cdot 10^{-3}$	$3.00 \cdot 10^{-3}$	$1.40 \cdot 10^{-3}$	34.3
$2.00 \cdot 10^{-3}$	$3.50 \cdot 10^{-3}$	$9.20 \cdot 10^{-4}$	

complexing ratio of fluoride–uranium is proportional to the fluoride concentration in solution, and inversely proportional to the uranium concentration.

In the sample mixture, since the fluoride complex of thorium or zirconium is much more stable than that of uranium (Fig. 1), the effective fluoride concentration, $[F^-]_E$, in the formation of uranium–fluoride complexes is less than the total fluoride ion concentration, $[F^-]_T$, which is originally present in the solution. Correction is necessary if the effective fluoride ion concentration cannot be found from the calibration lines in Fig. 2. The principle of the correction is based on the parallel and equal distance between calibration lines in Fig. 2. For example, in each calibration line, the amount of uranium which forms complexes with the same amount of fluoride is always 52.1% less than the lines on the left and 34.7% more than the lines on the right (Table II). A correction curve can then be obtained (Fig. 3) by plotting the percentage differences of uranium in Fig. 2, between the calibration lines of different fluoride concentrations when these calibration lines provide the same amount of fluoride in uranium–fluoride complexes, *vs.* concentration of total fluoride. The amount of fluoride in mixed solution can be found from the nearest calibration lines in Fig. 2. and then a correction can be made according to Fig. 3. The amount of thorium can be calculated from the difference of the total fluoride concentration and the free fluoride concentration after addition of masking agent. The results for the determination of Th–U(VI) and U(VI)–Zr mixed solution are shown in Table III.

Effect of pH and ionic strength. Fluoride ion forms HF and HF_2^- below pH 5 so that the effective concentration of fluoride ion decreases; above pH 8.5, interference by hydroxide becomes significant. Thus, fluoride ion should be measured in the pH range 5–8.5. Since thorium and zirconium hydrolyze easily in basic solution, the optimal pH value for the fluoride measurement is 5.0–5.5.

Since the fluoride-selective electrode was used here to measure the fluoride concentration, the ionic strength must be kept constant in order to maintain the same activity coefficient[3,4]. Triethanolamine was used to keep the ionic strength

TABLE III

DETERMINATION OF URANIUM(VI), THORIUM(IV) AND ZIRCONIUM(IV) IN MIXTURES

F^- added ($\cdot 10^{-2}$ M)	Th^{4+} ($\cdot 10^{-3}$ M)		UO_2^{2+} ($\cdot 10^{-4}$ M)		Zr^{4+} ($\cdot 10^{-5}$ M)		Relative error (%)		
	Added	Found	Added	Found	Added	Found	Th^{4+}	UO_2^{2+}	Zr^{4+}
1.90	4.0		6.5	6.4		4.0	0	3.0	
1.90	4.0		7.1	6.9		4.1	2.5	2.3	
1.90	3.9		3.6	3.5		4.0	2.0	1.4	
0.30			9.0	8.9	3.5	3.5		1.1	0
0.30			9.0	8.8	4.5	4.4		1.7	2.2
0.30			9.0	8.9	5.5	5.3		1.1	3.6
						Mean	1.5	1.8	1.9

at about 0.5 *M* and the pH at 5.5. Inert electrolyte such as potassium nitrate, can also be added to the solution to increase the ionic strength to 1 *M*.

Detection limit and precision. The concentrations of different ions can be determined down to $2 \cdot 10^{-5}$ *M* for thorium, $3 \cdot 10^{-5}$ *M* for zirconium, and 10^{-4} *M* for uranium. The relative error for each element is under 2%, as shown in Table III.

REFERENCES

1 D. D. Perrin, *Masking and Demasking of Chemical Reactions*, Wiley, New York, 1970, p. 44.
2 I. M. Kolthoff and P. J. Elving, *Treatise on Analytical Chemistry*, Vol. 9, Wiley, New York, 1962, p. 151.
3 R. A. Durst, *Ion selective electrodes*, NBS Spec. Publ. No. 314, 1969.
4 M. Frant and J. W. Ross, *Anal. Chem.*, 40 (1968) 1169.

ERRATUM

J. E. Going and S. J. Eisenreich, Spectrophotometric studies of reduced molybdoantimonylphosphoric acid, *Anal. Chim. Acta*, 70 (1974) 95–106.

On page 105, the third line of the paragraph *Mixed reagent*, "add 0.668 g of potassium antimony tartrate" should read "add 0.0668 g of potassium antimony tartrate".

ANALYTICA CHIMICA ACTA, VOL. 71 (1974)

AUTHOR INDEX

Adams, F. 67
Afghan, B. K. 355
Aomura, K. 349

Bala Bhaskara Rao, G. 202
Belcher, R. 255
Belliveau, P. E. 355
Bhattacharyya, K. 107
Blanc, B. 97
Block, C. 53
Bobbitt, J. M. 222
Bosset, J. 97
Braun, T. 133
Budesinsky, B. W. 333, 343
Buscarons, F. 468

Canela, J. 468
Chakraborti, D. 196
Chang, F. C. 477
Colaruotolo, J. F. 222
Collins, L. W. 411

Dake, J. D. 277
Dams, R. 53
De Corte, F. 263
Dickerson, R. L. 433
Doi, K. 464
Doležal, J. 35

Edrissi, M. 215
Eisenreich, S. J. 393
Ejaz, M. 383
Eshwar, M. C. 461

Fano, V. 218
Farag, A. B. 133
Fehér, Zs. 425
Filho, H. B. 225
Fujinaga, T. 141
Furukawa, M. 85

Geckeler, K. 79
Ghonaim, S. A. 255
Gödl, L. 113
Going, J. E. 393
Goto, K. 85
Griffiths, T. R. 1
Guest, R. J. 233
Guilbault, G. G. 419

Hansen, E. H. 225
Hanssen, J. E. 35
Hayes, W. P. 210
Hogberg, K. 157
Hoshino, H. 349
Hoste, J. 67, 263

Jacobsen, E. 157, 175
Jäger, H. 43

Kamada, H. 303
Karmarkar, K. H. 419
Khopkar, S. M. 472
Kiriyama, T. 375
Kochen, R. L. 451
Koh, T. 367
Korkisch, J. 113
Krishna Rao, P. V. 202
Kuroda, R. 375
Kuwamoto, T. 141

Langmyhr, F. J. 35, 205
Larose, R. H. 355
Licci, F. 218

Macpherson, D. R. 233
Mairesse-Ducarmois, C. A. 165
Massoumi, A. 205, 215
Miura, Y. 367
Mottola, H. A. 443
Murai, S. 141
Murata, M. 295
Murthy, T. K. S. 107
Murti, P. S. 202

Nagarkar, S. G. 461
Noguchi, M. 295
Norris, J. D. 289, 458

Overvoll, P. 205

Patriarche, G. J. 165
Pearson, K. H. 405
Plattner, E. 97
Porthault, M. 185
Potts, P. J. 1
Pungor, E. 151, 425

Ramirez-Muñoz, J. 311, 321
Rezazadeh, M. 215
Robinson, J. W. 277
Rogers, J. W. 433
Rohrbaugh, D. G. 311
Růžička, J. 225
Ryan, J. F. 355

Sapio, J. P. 222
Sasa, A. H. 210
Schmidt, K. 79
Schöning, A. G. 17
Shibata, S. 85
Shiek Fareed, V. 210
Sitaram, R. 472
Street, K. W. 405
Strelow, F. W. E. 123
Stubergh, J. R. 35

Tanaka, M. 464
Terasawa, M. 303
Thomassen, Y. 35
Thorburn Burns, D. 210
Thorgersen, K. B. 175
Tóth, K. 151
Townshend, A. 255
Tsai, H.-T. 477
Tu An, T. 151

Vandecasteele, C. 67
Vandenbalck, J. L. 165
Van der Linden, R. 263
Van der Walt, T. N. 123
Vernon, F. 192
Vittori, O. 185
Volaire, M. 185

Wagai, A. 367
Weinert, C. H. S. W. 123
Wendlandt, W. W. 411
West, T. S. 289, 458
Wu, S.-C. 477

Yotsuyanagi, T. 349

Zanotti, L. 218

ANALYTICA CHIMICA ACTA, Vol. 71 (1974)

SUBJECT INDEX

Air pollutants,
remote sensing of — by laser-induced infrared fluorescence—a review (Robinson, Dake) 277
Alkaline earth metals,
a simple microtitrimetric method for — (Fano *et al.*) 218
Alpha activation analysis,
the determination of oxygen in silicon by — and helium-3 activation analysis (Vandecasteele *et al.*) 67
Amine oxides,
the extraction of trace amounts of tungsten(VI) from different mineral acid solutions by — (Ejaz) 383
Amino groups,
rapid determination of primary — on soluble polymers (Schmidt, Geckeler) 79
Analgesics,
the identification of non-prescription internal — by thermal analysis (Wendlandt, Collins) 411
Antimony,
the use of an argon–hydrogen flame for the atomic absorption and atomic fluorescence spectrometry of — (Norris, West) 458
Antipyrylazo III,
photometric determination of calcium with — (Budesinsky) 343
Argon,
the use of an — –hydrogen flame for the atomic absorption and atomic fluorescence spectrometry of antimony (Norris, West) 458
Arsenazo III,
ion-exchange separation and spectrophotometric determination of zirconium, thorium and uranium in silicate rocks with — (Kiriyama, Kuroda) 375
Automatic materials analyzer,
analytical applications of an — (Rohrbaugh, Ramírez-Muñoz) 311

Beryllium,
separation of lithium from sodium, — and other elements by cation-exchange chromatography in nitric acid–methanol (Strelow *et al.*) 123
Biological material,
activation analysis of — with ruthenium as a multiisotopic comparator (van der Linden *et al.*) 263
Boron,
molecular emission cavity analysis (MECA) — a new flame analytical technique. Part III. The determination of — (Belcher *et al.*) 255
potentiometric determination of — in borosilicate glasses (Kochen) 451
Borosilicate glasses,
potentiometric determination of boron in — (Kochen) 451

Cadmium,
atomic absorption spectrometric determination of —, lead, silver, thallium and zinc in silicate rocks by direct atomization from the solid state (Langmyhr *et al.*) 35
the use of auxiliary complexing agents in the differential complexiметric titration of zinc and — with thermometric end-points (Doi, Tanaka) 464
Calcium,
photometric determination of — with antipyrylazo III (Budesinsky) 343
Chlorpheniramine maleate,
polarographic determination of — in pharmaceuticals (Jacobsen, Hogberg) 157
Citrate,
anion-exchange behaviour of indium(III) in — and tartrate solutions: separation from mixtures (Sitaram, Khopkar) 472
Coal,
determination of silicon and oxygen in — and coal ash by 14-MeV neutron activation (Block, Dams) 53
Coal ash,
determination of silicon and oxygen in coal and — by 14-MeV neutron activation (Block, Dams) 53
Cobalt,
spectrophotometric studies on the reaction of — with 4-(2-pyridylazo)-1,3-diaminobenzene and its halogen derivatives (Shibata *et al.*) 85
Complexiметric titration,
the use of auxiliary complexing agents in the differential — of zinc and cadmium with thermometric end-points (Doi, Tanaka) 464
Copper,
some observations on the determination of — with thiocyanate (Hayes *et al.*) 210

Cysteine,
a contribution to the electrochemistry of thiols and disulfides. Part I. — and cystine (Mairesse-Ducarmois *et al.*) 165
Cystine,
a contribution to the electrochemistry of thiols and disulfides. Part I. Cysteine and — (Mairesse-Ducarmois *et al.*) 165

Dibasic acids,
electrochemical investigations in non-aqueous media. Part I. Investigation of the dissociation of — (Tu An *et al.*) 151
Diethyldithiocarbamate foam,
plasticized open-cell polyurethane foam as a universal matrix for organic reagents in trace element preconcentration. Part II. Collection of mercury traces on dithizone foam and — (Braun, Farag) 133
Di(2-ethylhexyl)phosphoric acid,
extraction–spectrophotometric determination of — with rhodamine B (Bhattacharyya, Murthy) 107
Disulfides,
a contribution to the electrochemistry of thiols and —. Part I. Cysteine and cystine (Mairesse-Ducarmois *et al.*) 165
Dithizone foam,
plasticized open-cell polyurethane foam as a universal matrix for organic reagents in trace element preconcentration. Part II. Collection of mercury traces on — and diethyldithiocarbamate foam (Braun, Farag) 133

Electrode,
a universal ion-selective — based on graphite paste (Sapio *et al.*) 222
determination of the hydrogensulphite content in wine by means of the air-gap — (Hansen *et al.*) 225
determination of thorium–uranium and uranium–zirconium alloy composition with a fluoride-selective — (Chang *et al.*) 477
Electronic absorption spectra,
a computer-based storage and retrieval system for — (Schöning) 17
a computer-based study of the effect of pH and temperature on the — of acid–base indicator solutions (Griffiths, Potts) 1
Epoxy resin,
an ion exchanger– — pelletization method for sample preparation in x-ray fluorescence analysis. Microanalysis of metal ions in industrial waste water (Murata, Noguchi) 295

Ferron,
complex formation of indium(III) or thallium(III) with 8-hydroxy-7-iodoquinoline-5-sulphonic acid (—) (Massoumi *et al.*) 205
Full milk,
a new method for the automatic determination of proteins in —. Part II. Linearity, selectivity, specificity (Bossett, Blanc) 97

Gold,
further investigations of the spectrometric analysis of raw — by glow discharge excitation (Jäger) 43
Gold(III),
rapid extractive spectrophotometric determination of — with 4-(2-pyridylazo)-resorcinol (Nagarkar, Eshwar) 461
Graphite paste,
a universal ion-selective electrode based on — (Sapio *et al.*) 222

Helium-3 activation analysis,
the determination of oxygen in silicon by alpha and — (Vandecasteele *et al.*) 67
Hydrazides,
a spot test for the detection of some aromatic — (Murti *et al.*) 202
Hydrogen,
the use of an argon– — flame for the atomic absorption and atomic fluorescence spectrometry of antimony (Norris, West) 458
Hydrogensulphite,
determination of the — content in wine by means of the air-gap electrode (Hansen *et al.*) 225
3-Hydroxy-1,3-diphenyltriazene,
— and its substituted derivatives as spectrophotometric reagents for vanadium(V) (Chakraborti) 196
8-Hydroxy-7-iodoquinoline-5-sulphonic acid,
complex formation of indium(III) or thallium(III) with — (ferron) (Massoumi *et al.*) 205

Indicator,
a computer-based study of the effect of pH and temperature on the electronic absorption spectra of acid–base — solutions (Griffiths, Potts) 1
Indium(III),
anion-exchange behaviour of — in citrate and tartrate solutions: separation from mixtures (Sitaram, Khopkar) 472
complex formation of — or thallium(III) with 8-hydroxy-7-iodoquinoline-5-sulphonic acid (ferron) (Massoumi *et al.*) 205
Infrared fluorescence,
remote sensing of air pollutants by laser-induced — —a review (Robinson, Dake) 277
Ion exchanger,
an — –epoxy resin pelletization method for sample preparation in x-ray fluorescence analysis.

Microanalysis of metal ions in industrial waste water (Murata, Noguchi) 295

Lanthanum(III),
the determination of micro amounts of polythionates. Part VIII. Cyanolysis of trithionate by catalysis with — and photometric determination of trithionate (Koh *et al.*) 367
Lead,
atomic absorption spectrometric determination of cadmium, —, silver, thallium and zinc in silicate rocks by direct atomization from the solid state (Langmyhr *et al.*) 35
Ligands,
some considerations on reaction rate methods—the analytical use of modifying effects of — in some electron-transfer reactions (Mottola) 443
Ligand vapour,
gas chromatography of metal chelates with carrier gas containing —. Thorium(IV) trifluoroacetylacetonate (Fujinaga *et al.*) 141
Lithium,
separation of — from sodium, beryllium and other elements by cation-exchange chromatography in nitric acid–methanol (Strelow *et al.*) 123

Mercury,
plasticized open-cell polyurethane foam as a universal matrix for organic reagents in trace element preconcentration. Part II. Collection of — traces on dithizone and diethyldithiocarbamate foams (Braun, Farag) 133
Metal chelates,
gas chromatography of — with carrier gas containing ligand vapour. Thorium(IV) trifluoroacetylacetonate (Fujinaga *et al.*) 141
Metal ions,
an ion exchanger–epoxy resin pelletization method for sample preparation in x-ray fluorescence analysis. Microanalysis of — in industrial waste water (Murata, Noguchi) 295
Methanol,
separation of lithium from sodium, beryllium and other elements by cation-exchange chromatography in nitric acid– — (Strelow *et al.*) 123
Molecular emission cavity analysis (MECA),
— —a new flame analytical technique. Part III. The determination of boron (Belcher *et al.*) 255
Molybdoantimonylphosphoric acid,
extraction of reduced molybdophosphoric acid and — with oxygenated solvents (Eisenreich, Going) 393
Molybdophosphoric acid,
extraction of reduced — and molybdoantimonylphosphoric acid with oxygenated solvents (Eisenreich, Going) 393
Multivitamin tablets,
electroreduction and pulse-polarographic determination of nicotinamide in — (Jacobsen, Thorgersen) 175

Niacin,
determination of — and niacinamide in pharmaceutical products by automatic discrete-sample analysis (Ramírez-Muñoz) 321
Niacinamide,
determination of niacin and — in pharmaceutical products by automatic discrete-sample analysis (Ramírez-Muñoz) 321
Nicotinamide,
electroreduction and pulse-polarographic determination of — in multivitamin tablets (Jacobsen, Thorgersen) 175
Nitric acid,
separation of lithium from sodium, beryllium and other elements by cation-exchange chromatography in — –methanol (Strelow *et al.*) 123
N-Nitroso-N-cyclododecylhydroxylamine,
analytical uses of some N-nitroso-N-alkyl (or N-cycloalkyl) hydroxylamines. Part III. N-Nitroso-N-cyclooctylhydroxylamine, — and N-nitroso-N-isopropylhydroxylamine (Buscarons, Canela) 468
N-Nitroso-N-cyclooctylhydroxylamine,
analytical uses of some N-nitroso-N-alkyl (or N-cycloalkyl) hydroxylamines. Part III. —, N-nitroso-N-cyclododecylhydroxylamine and N-nitroso-N-isopropylhydroxylamine (Buscarons, Canela) 468
N-Nitroso-N-isopropylhydroxylamine,
analytical uses of some N-nitroso-N-alkyl (or N-cycloalkyl) hydroxylamines. Part III. N-Nitroso-N-cyclooctylhydroxylamine, N-nitroso-N-cyclododecylhydroxylamine and — (Buscarons, Canela) 468
Non-aqueous media,
electrochemical investigations in —. Part I. Investigation of the dissociation of dibasic acids (Tu An *et al.*) 151
Non-ferrous metal alloys,
the use of a non-dispersive atomic fluorescence spectrometer for the determination of zinc in soils and —.(Norris, West) 289

Oxygen,
determination of — in silicon by alpha and helium-3 activation analysis (Vandecasteele *et al.*) 67
determination of silicon and — in coal and coal ash by 14-MeV neutron activation (Block, Dams) 53
Oxygenated solvents,
extraction of reduced molybdophosphoric acid

and molybdoantimonylphosphoric acid with — (Eisenreich, Going) 393

Palladium(II),
the direct spectropolarimetric titration of — ion with D-(−)-1,2-propylenediaminetetraacetic acid (Street, Pearson) 405
Palladium-4-(2-pyridylazo)-resorcinol,
acid dissociation reaction of — complexes (Yotsuyanagi *et al.*) 349
Pharmaceutical products,
determination of niacin and niacinamide in — by automatic discrete-sample analysis (Ramírez-Muñoz) 321
Phenols,
an improved method for determination of trace quantities of — in natural waters (Afghan *et al.*) 355
Piezoelectric crystals,
a new design and coatings for — in measurement of trace amounts of sulfur dioxide (Karmarkar, Guilbault) 419
Polydentate ligands,
photometric investigation of systems of two complexes with — (Budesinsky) 333
Polymers,
rapid determination of primary amino groups on soluble — (Schmidt, Geckeler) 79
Polythionates,
the determination of micro amounts of —. Part VIII. Cyanolysis of trithionate by catalysis with lanthanum(III) and photometric determination of trithionate (Koh *et al.*) 367
Polyurethane foam,
plasticized open-cell — as a universal matrix for organic reagents in trace element preconcentration. Part II. Collection of mercury traces on dithizone and diethyldithiocarbamate foams (Braun, Farag) 133
D-(−)-1,2-Propylenediaminetetraacetic acid,
the direct spectropolarimetric titration of palladium(II) ion with — (Street, Pearson) 405
Proteins,
a new method for the automatic determination of — in full milk. Part II. Linearity, selectivity, specificity (Bosset, Blanc) 97
4-(2-Pyridylazo)-1,3-diaminobenzene,
spectrophotometric studies on the reaction of cobalt with — and its halogen derivatives (Shibata *et al.*) 85
4-(2-Pyridylazo)-resorcinol,
rapid extractive spectrophotometric determination of gold(III) with — (Nagarkar, Eshwar) 461
Rhodamine B,
extraction–spectrophotometric determination of di-(2-ethylhexyl)phosphoric acid with — (Bhattacharyya, Murthy) 107
Ruthenium,
activation analysis of biological material with — as a multi-isotopic comparator (van der Linden *et al.*) 263

Silicate,
atomic absorption spectrometric determination of cadmium, lead, silver, thallium and zinc in — rocks by direct atomization from the solid state (Langmyhr *et al.*) 35
ion-exchange separation and spectrophotometric determination of zirconium, thorium and uranium in — rocks with arsenazo III (Kiriyama, Kuroda) 375
the use of flame procedures in metallurgical analysis. Part I. Determination of silicon in sulphide and — minerals (Guest, Macpherson) 233
Silicon,
determination of oxygen in — by alpha and helium-3 activation analysis (Vandecasteele *et al.*) 67
determination of — and oxygen in coal and coal ash by 14-MeV neutron activation (Block, Dams) 53
the use of flame procedures in metallurgical analysis. Part I. Determination of — in sulphide and silicate minerals (Guest, Macpherson) 233
Silver,
atomic absorption spectrometric determination of cadmium, lead, —, thallium and zinc in silicate rocks by direct atomization from the solid state (Langmyhr *et al.*) 35
gravimetric and turbidimetric determination of — with thione reagent (Edrissi *et al.*) 215
Sodium,
separation of lithium from —, beryllium and other elements by cation-exchange chromatography in nitric acid–methanol (Strelow *et al.*) 123
Soils,
the use of a non-dispersive atomic fluorescence spectrometer for the determination of zinc in — and non-ferrous metal alloys (Norris, West) 289
Sulfur dioxide,
a new design and coatings for piezoelectric crystals in measurement of trace amounts of — (Karmarkar, Guilbault) 419
Sulphide minerals,
the use of flame procedures in metallurgical analysis. Part I. Determination of silicon in — and silicate minerals (Guest, Macpherson) 233

Tartrate,
anion-exchange behaviour of indium(III) in citrate and — solutions: separation from mix-

tures (Sitaram, Khopkar) 472
Tellurium(II)
determination of — in acidic media by alternative pulsed voltage and linear-sweep voltammetry (Volaire *et al.*) 185
Thallium,
atomic absorption spectrometric determination of cadmium, lead, silver, — and zinc in silicate rocks by direct atomization from the solid state (Langmyhr *et al.*) 35
Thallium(III),
complex formation of indium(III) or — with 8-hydroxy-7-iodoquinoline-5-sulphonic acid (ferron) (Massoumi *et al.*) 205
Thiocyanate,
some observations on the determination of copper with — (Hayes *et al.*) 210
Thiols,
a contribution to the electrochemistry of — and disulfides. Part I. Cysteine and cystine (Mairesse-Ducarmois *et al.*) 165
Thione,
gravimetric and turbidimetric determination of silver with — reagent (Edrissi *et al.*) 215
Thorium,
determination of — –uranium and uranium–zirconium alloy composition with a fluoride-selective electrode (Chang *et al.*) 477
ion-exchange separation and spectrophotometric determination of zirconium, — and uranium in silicate rocks with arsenazo III (Kiriyama, Kuroda) 375
Thorium(IV) trifluoroacetylacetonate,
gas chromatography of metal chelates with carrier gas containing ligand vapour. — (Fujinaga *et al.*) 141
Trifluoromethylnitrosobenzene intermediates,
electroanalytical study of isomeric — (Dickerson, Rogers) 433
Triphenyltin,
the fluorimetric determination of — compounds (Vernon) 192
Trithionate,
the determination of micro amounts of polythionates. Part VIII. Cyanolysis of — by catalysis with lanthanum(III) and photometric determination of — (Koh *et al.*) 367
Tungsten(VI),
the extraction of trace amounts of — from different mineral acid solutions by amine oxides (Ejaz) 383

Uranium,
determination of thorium– — and — –zirconium alloy composition with a fluoride-selective electrode (Chang *et al.*) 477
determination of — in natural waters after anion-exchange separation (Korkisch, Gödl) 113
ion-exchange separation and spectrophotometric determination of zirconium, thorium and — in silicate rocks with arsenazo III (Kiriyama, Kuroda) 375

Vanadium(V),
3-Hydroxy-1,3-diphenyltriazene and its substituted derivatives as spectrophotometric reagents for — (Chakraborti) 196
Voltammetry,
the application of hydrodynamic — in chemical analysis (Fehér, Pungor) 425

Water,
an improved method for determination of trace quantities of phenols in natural — (Afghan *et al.*) 355
an ion exchanger–epoxy resin pelletization method for sample preparation in x-ray fluorescence analysis. Microanalysis of metal ions in industrial waste — (Murata, Noguchi) 295
determination of uranium in natural — after anion-exchange separation (Korkisch, Gödl) 113
Wine,
determination of the hydrogensulphite content in — by means of the air-gap electrode (Hansen *et al.*) 225

X-rays,
the use of ion-induced — for spectrochemical analysis (Kamada, Terasawa) 303
Zinc,
atomic absorption spectrometric determination of cadmium, lead, silver, thallium and — in silicate rocks by direct atomization from the solid state (Langmyhr *et al.*) 35
the use of auxiliary complexing agents in the differential complexiметric titration of — and cadmium with thermometric end-points (Doi, Tanaka) 464
the use of a non-dispersive atomic fluorescence spectrometer for the determination of — in soils and non-ferrous metal alloys (Norris, West) 289
Zirconium,
determination of thorium–uranium and uranium– — alloy composition with a fluoride-selective electrode (Chang *et al.*) 477
ion-exchange separation and spectrophotometric determination of —, thorium and uranium in silicate rocks with arsenazo III (Kiriyama, Kuroda) 375